FIELD OBSERVATIONS OF THE BEHAVIOUR OF THE UPPER LIAS CLAY AT THE EMPINGHAM DAM SITE

by

MAURO LUCIO GUEDES WERNECK

B.Sc. (Civ. Eng.), Fed. Univ. Rio de Janeiro, Brazil, 1958
B.Sc. (Physics), Guanabara University, Rio de Janeiro, Brazil, 1959
Licentiate (Physics), Guanabara University, Rio de Janeiro, Brasil, 1964
M.Sc. (Eng.), Fed. Univ. Rio de Janeiro, Brazil, 1971

A Thesis submitted to the

University of London

for the degree of

Doctor of Philosophy in the Faculty of Engineering

November 1974
Department of Civil Engineering
Imperial College of Science and Technology
London

CIVIL ENGINEERING LIBRARY
IMPERIAL COLLEGE

To my wife Regina

To my parents Joaquim and Zilda

To my parents-in-law Dejalma and Iza

To my children Eliane, Ricardo and Claudio

To two great friends Coimbra and Medina

ABSTRACT

The main features of the Empingham Pumped-Storage Scheme are summarized and the geology of the region described, special emphasis being placed on the soil disturbance caused by superficial geological structures such as cambering, valley-bulging, etc.

The basic engineering problems associated with the construction of a 37 m high embankment on a thick layer of brecciated Upper Lias Clay are discussed. The results of the site investigation are briefly analysed and details of the initial design adopted are presented and justified.

The reasons for the construction of an instrumented trial bank and the adoption of the design-as-build criterion are discussed, with special reference to the solution adopted of making the trial bank a part of the final configuration of the main dam.

The trial bank experiment is presented, its aims listed, the instrumentation installed described and its performance detailed. Results are analysed, conclusions compared to the initial design assumptions and some decisions concerning the final design explained.

Constant head and falling head in-situ permeability tests are performed on twin-tube hydraulic piezometers in the fill of the trial bank, under high excess heads, aiming at inducing hydraulic fracturing of the ground. Difficulties associated with

this new technique of determining stresses in partly saturated media are shown as a result of the tests carried out. In particular, the possibility of a crack not closing up is examined in the light of increase in the apparent permeability of the fill after fracturing is achieved.

ACKNOWLEDGEMENTS

A thesis is dependent upon the interest and support of many people. Some of those who were particularly helpful throughout the research are acknowledged below.

The work was carried out in the Department of Civil Engineering of Imperial College of Science and Technology, at the Soil Mechanics section headed by Professor A.W. Bishop. The project was supervised by Dr. P.R. Vaughan to whom the Author is indebted for his permanent encouragement and advice, proper guidance and assistance, and helpful discussions and comments.

The research was supported by CAPES, an Agency of the Brazilian Ministry for Education and Culture, by the Federal University of Rio de Janeiro through its Postgraduate (COPPE) and Graduate (EE) Schools of Engineering, and also, in the last months, by the Brazilian firm of geotechnical engineering Romani-Gouvêa Engenharia de Solos Ltda.. To them all the Author wishes to express his gratitude.

The field work was carried out at the site of the Empingham Dam, constructed for the Welland and Nene River Authority by Gleeson (Civil Engineering) Ltd.. The consulting engineers were T. and C. Hawksley and Professor A.W. Bishop, Dr. P.R. Vaughan, Mr. J.M. McKenna and Prof. J.L. Knill acted as special advisors. The site investigation was carried out by Soil Mechanics Ltd. and Terresearch

Ltd.. Instrumentation equipment was provided by Soil Instruments Ltd. and Nuttal Geotechnical Services Ltd..

The site work on the trial bank was performed under the direction of the Resident Engineer, Mr. J.H. Winder, and Messrs. R.C. Bridle, P.S. Horswill, C.J. Sammons, G.A.F. Miller, H.J. Walbancke and J.J.M. Powell assisted with the observations. Much of this thesis is due to their efforts, made under difficult circumstances.

Frequent useful discussions were held by the Author with his fellow postgraduate research students, particularly Messrs. H.J. Walbancke, R. Pugh, M.M.A.F. Hamza and M. Maguire, engaged in the same project or in similar research. They have been helpful, cooperative and friendly, and to them the Author extends his thanks.

And last but by no means least, I wish to thank my wife, Regina, not only for her having been dedicatedly responsible for the total typing of this thesis but, above all, for her continuous encouragement and patient forbearance at all times during the research and the writing.

NOMENCLATURE

a: radius of spheric piezometer tip (or r)

a: Henkel's pore pressure parameter (or α)

a: Kondner's parameter in hyperbolic plot

A: central area of the dam foundation

A: type of fill utilized in the trial bank and also in the main dam upstream of the core and downstream of the sand drain area

A: Skempton's pore pressure parameter

A: area of the standpipe cross section

Al: type of fill including granular material and used as general fill

b: Kondner's parameter in hyperbolic plot

B: area of the dam foundation adjacent to the central area A

B: Skempton's pore pressure parameter equal to $\Delta u/\Delta\sigma_3$

$\bar{B}$: pore pressure parameter equal to $\Delta u/\Delta\sigma_1$

c: coefficient of swelling or consolidation

c': cohesion intercept

c_v: coefficient of consolidation

c_s: coefficient of swelling

c_u: undrained strength

C: type of fill utilized in centre of the main dam

C and C': foundation areas on the valley sides

Ch or CH: chainage

d: depth

Di (i = 1,2,3): reference datum points in the trial bank

e: void ratio

E: Young's modulus

E: eastings

el or El: elevation

F: intake (or shape) factor of piezometers

F_s: factor of safety

h: height of fill (or H)

h: excess head of water in permeability and fracture tests

H: height of fill (or h)

HiX; HiA to HiF (i = 1,2,3): horizontal movement points in foundation

HiY; HiG to HiJ (i = 1,2,3): Horizontal movement points in fill

Ii or ITBi (i = 1,2,3,4): inclinometers

I_p: plasticity index

J: rate of horizontal strain increase, $d\epsilon_x/d(\log_{10}t)$

J': rate of horizontal strain increase, $d\epsilon_x/d(\log_e t)$

k: coefficient of permeability

K_o: coefficient of earth pressure at rest

K_{ac}: coefficient of earth pressure at active state

K_p: coefficient of earth pressure at passive state

l or L: length

m: coefficient of volume change; compressibility

m: slope of the trial bank

m_v: coefficient of compressibility

m_s: coefficient of swelling

M: magnet used as settlement points

n: porosity

p_s: isostatic stresses after sampling

PiB (i = 1,2,3,4): piezometer in the fill

PiF (i = 1,2, etc): piezometer in the foundation

P: resultant of lateral forces

P_{av}: available force, due to shear stresses

q: flow

q: maximum shear stress; one-half of stress difference

r: radius of spheric piezometer tip (or a)

r: radial direction

r_u: pore pressure ratio, equal to $u/\gamma.h$

R_f: ratio between $(\sigma_1 - \sigma_3)_f$ and $(\sigma_1 - \sigma_3)_{ult}$

S: degree of saturation

Si, SiX, SiY (i = 1, 2, etc): surface reference points

t: time

T: time factor, equal to ct/a^2

u: pore pressure

u_s: suction after sampling

v: variation of pore pressure parameter A with depth

ViB (i = 1,2, etc): settlement points in the fill

ViF (i = 1.2, etc): settlement points in the foundation

w: moisture content

w_l: liquid limit

w_p: plastic limit

x: horizontal direction (across axis)

y: horizontal direction (along axis)

z: vertical direction

α : Henkel's pore pressure parameter (or a)

α : one of the angular coordinates of inclinometer

α : factor used by BJERRUM et al (1972) to describe reduction of tangential stress in the ground induced by piezometer driving: $\sigma'_\theta = (1-\alpha)\, K'_o\, \sigma'_z$

β : angle of major pricipal strain with the vertical

β : one of the angular coordinates of inclinometer

β : tilting angle measured by inclinometer

β : factor used by BJERRUM et al (1972) to describe increase in radial stresses caused by piezometer driving: $\sigma'_r = (1+\beta) K'_o \sigma'_z$

γ : bulk unit weight

γ : angular distorsion

γ' : apparent unit weight of soil skeleton

δ : horizontal displacement

Δ : increment

ϵ : linear strain

$\dot{\epsilon}$: variation of linear strain with time

ϕ : angle of shear resistance (friction) at peak

ϕ_r : residual friction angle (large deformations)

μ : factor used by GIBSON (1966), equal to $4 \cdot \pi \cdot a^3 \cdot m \cdot \gamma_w \cdot A$

ν : Poisson's ratio

τ : shear stress

Ω : initial inclinometer casing inclination with the vertical

Ψ : incremental inclination of inclinometer casing

σ : normal stress

Subscripts

o: initial

1: major principal direction

1: one-dimensional

2: intermediate principal direction

2: two-dimensional

3: minor principal direction

3: three-dimensional

∞ : at infinite time

a: allowable

av: available

b: at 'blow-off' pressure

b: in the fill (bank)

c: at a constant head condition

c: in triaxial compression

d: drained

ec: at end of construction

exp: indefinite expansion of a cavity in the ground

f: final

f: at failure

f: at fracturing (cracking)

f: foundation

in: initial

m (or mean): mean

max: maximum

mim: minimum

mob: mobilized

pc: post-construction

pl: initiation of plasticity

ps: plane-strain

r: in radial direction

r: residual

s: swelling

s: after sampling

t: tensile

u: undrained

ult: ultimate; assymptotic value in Kondner's hyperbole

v: volumetric

v: consolidation

w: relative to the pore fluid

x: in horizontal, across-axis direction

xz: relative to an upright soil element of sides parallel to directions x and z

y: in horizontal, along-axis direction

z: in vertical direction

θ: in circumferential direction

Index

': referring to effective stresses (no-indexed quantities are generally total stresses or parameters related to total stresses)

CONTENTS

		Page No.
DEDICATORY		(i)
ABSTRACT		(ii)
ACKNOWLEDGEMENTS		(iv)
CONTENTS		(xii)
CHAPTER 1:	INTRODUCTION	1
1.1	Scope of the Study	2
1.2	Outline of the Thesis	3
1.3	Main Features of the Empingham Pumped-Storage Scheme	4
CHAPTER 2:	GEOLOGY OF THE SITE	7
2.1	General Features	8
2.2	Local Stratigraphy	10
2.3	Geological Structure	13
2.4	Superficial Structures	15
2.5	The Brecciation of the Upper Lias Clay	17
CHAPTER 3:	THE DESIGN OF THE EMBANKMENT SECTION	19
3.1	Basic Engineering Problems	20
3.2	Dam Section Adopted	25
3.2.1	External configuration	25
3.2.2	Internal drainage facilities	27
3.2.3	Core	28
3.2.4	Filter	29
3.2.5	Fill zoning	29
3.2.6	Cut-off trench	30
3.2.7	Initial design calculations	30
3.2.8	Final design	32
3.3	Soil Parameters Required in Engineering Analysis	32
3.3.1	Undrained strength of the foundation	32
3.3.2	Foundation strength in terms of effective stresses	34
3.3.3	Foundation coefficient of consolidation	35

		Page No.
3.3.4	Fill properties	36
3.3.5	Initial stresses in the foundation	37
3.3.6	Stress-strain-time characteristics	40
3.3.7	Pore pressure parameters	41
3.4	Summary of Findings in the Site Investigation	42
3.4.1	General	42
3.4.2	Site investigation programme	43
3.4.3	Boreholes	44
3.4.4	Sampling	44
3.4.5	Index properties	45
3.4.6	Foundation undrained strength	46
	(i) Laboratory tests	46
	(ii) Plate tests	48
3.4.7	Foundation strength in terms of effective stresses	49
3.4.8	Foundation consolidation parameters	51
	(i) Coefficient of consolidation	51
	(ii) Compressibility	53
	(iii) Permeability	53
3.4.9	Fill properties	54
3.5	The Adoption of a 'Design-As-You-Build' Approach	55
3.6	Initial Design Assumptions	57
CHAPTER 4:	THE DESIGN OF THE TRIAL BANK	60
4.1	Reasons for the Construction of the Trial Bank	61
4.2	Advantages and Disadvantages of the Approach	63
4.3	The Characteristics of the Trial Bank	65
4.4	Instrumented Sections	67
4.5	Aims of the Trial Bank Experiment	67
CHAPTER 5:	THE TRIAL BANK INSTRUMENTATION	71
5.1	Instrumentation Installed	72
5.2	Inclinometers	74
5.3	Settlement Magnets	78
5.4	Hydraulic Settlement Gauge	80
5.5	Horizontal Movement Magnets	83
5.6	Wire Extensometer (Rod Gauges)	86
5.7	Surface Reference Points	88
5.8	Piezometers	89
CHAPTER 6:	DETAILED PERFORMANCE OF THE TRIAL BANK	91
6.1	Horizontal Displacements	92

		Page No.
6.1.1	Inclinometer measurements	92
	(i) Operation procedures	92
	(ii) Calculations	96
	(iii) Face errors	98
	(iv) Angle measurement repeatability	103
	(v) Influence of casing distorsion	106
	(vi) Measurements	111
	(vii) Horizontal displacements	115
	(viii) Equipment performance	116
	(ix) Comments on the accuracy of the measurements	119
6.1.2	Foundation wire extensometer (rod gauges)	121
	(i) Operation procedures	121
	(ii) Initial adjustment	123
	(iii) Measurements repeatability	124
	(iv) Results	125
	(v) Equipment performance	127
	(vi) Measurement accuracy	130
6.1.3	Fill wire extensometers (rod gauges)	132
	(i) Measurements - Zero corrections	132
	(ii) Corrected horizontal displacements	135
	(iii) Accuracy of the results	138
6.1.4	Surface reference points - EDM surveys	139
	(i) Operation	139
	(ii) Measurement results	140
	(iii) Accuracy	142
6.2	Vertical Displacements	142
6.2.1	Inclinometer settlement magnets	142
	(i) Operation	142
	(ii) Measurements	144
	(iii) Zero-corrections	145
	(iv) Grout stiffness correction	146
	(v) Sand compressibility correction	148
	(vi) Corrected settlements	150
	(vii) Equipment performance	152
	(viii) Measurement accuracy	153
6.2.2	Hydraulic settlement gauge	156
	(i) Operation and performance of the apparatus	156
	(ii) Results	158
	(iii) Comments on the accuracy of the measurements	159
6.2.3	Levelling of surface monuments	159
6.3	Overall Pattern of Displacements	161
6.4	Horizontal Strains	162
6.4.1	Foundation wire extensometers	162
6.4.2	Fill wire extensometers	169
6.4.3	Inclinometers	171
6.5	Vertical Strains	172
6.6	Shear Strains	175

		Page No.
6.7	Principal Strains	179
6.8	Pore Pressures in the Foundation	184
6.8.1	Installation and operation procedures	184
6.8.2	Measurements	185
6.8.3	Response time	190
6.8.4	Pore pressure dissipation	191
6.8.5	Precision and accuracy	192
6.9	Pore Pressure in the Fill	192
CHAPTER 7:	CONCLUSIONS DRAWN FROM THE TRIAL BANK EXPERIMENT	193
7.1	Brief Description of the Experiment	194
7.2	Appreciation of the Approach Adopted	195
7.3	Total Stress Stability Analysis	199
7.4	Stability Analysis in Terms of Effective Stresses	202
7.4.1	Methods applied	202
7.4.2	Strength parameters utilized	203
7.4.3	Pore pressure assumptions	203
7.4.4	Results of the analysis	204
7.5	Interpretation of the Measured Horizontal movement	207
7.5.1	The mechanism of horizontal deformations	207
7.5.2	The basis of the deformation analysis	207
7.5.3	Application of the approximate model	209
	(i) Basic theory and expressions	209
	(ii) The raising of the embankment - Numerical application	212
7.5.4	Comparison between model and prototype	214
7.6	Pore Pressure Parameters in Foundation	216
7.6.1	Data utilized in the analysis	216
7.6.2	Pore pressure parameters 'A' and 'a'	218
7.6.3	Parameter $\bar{B}$	220
7.6.4	Parameter B	224
7.7	Deformation Parameters for the Foundation	224
7.7.1	Method of analysis applied	224
7.7.2	Initial stress - Determination of K_o	225
7.7.3	Stress-strain curves	233
7.8	Fill Properties	236
7.9	Comparison of Trial Bank Findings with Design Assumptions	238
7.9.1	Undrained strength	238
7.9.2	Strength in terms of effective stresses	240
7.9.3	Consolidation parameters	241
7.9.4	Fill properties	243
CHAPTER 8:	HYDRAULIC FRACTURE	246
8.1	In-situ Permeability Tests	247

8.1.1	Piezometer tests	247
8.1.2	Constant head tests	247
8.1.3	Variable head tests	250
8.2	Allowable Applied Pressures in Permeability Tests on Piezometers	253
8.2.1	Brief review of literature	253
8.2.2	Recent evidences of hydraulic fracture in soils	254
8.3	The Use of Hydraulic Fracture in Assessing Stresses in Soil Media	256
8.3.1	Saturated masses	256
8.3.2	Partly saturated soils	257
8.4	Some Theoretical Considerations about Hydraulic Fracture	258
8.4.1	Drainage impeded	259
8.4.2	Full drainage	266
8.5	Hydraulic Fracture Tests at the Empingham Trial Bank	268
8.5.1	Main objectives	268
8.5.2	'Blow-off' and fracturing pressures	269
8.5.3	'Shut-in' pressures	270
8.5.4	'Close-up' pressures	271
8.5.5	Variation of apparent permeability	271
8.5.6	Summary of the results obtained	274
CHAPTER 9:	CONCLUSIONS AND RECOMMENDATIONS	277
9.1	General	278
9.2	Performance of the Instrumentation	278
9.2.1	Horizontal movements	279
9.2.2	Vertical movements	282
9.2.3	Pore pressures	283
9.3	Properties of the Brecciated Upper Lias Clay	284
9.4	Hydraulic Fracture Tests	287
9.5	Suggestion of Further Work	288
9.5.1	Instrumentation	288
9.5.2	Soil properties	289
9.5.3	Hydraulic fracture	290
REFERENCES		292

C H A P T E R _ O N E

INTRODUCTION

1.1 Scope of the Study

1.2 Outline of the Thesis

1.3 Main Features of the Empingham Pumped-Storage Scheme

C H A P T E R _ O N E

INTRODUCTION

1.1 SCOPE OF THE STUDY

The purpose of this thesis is to describe the field observations carried out at Empingham Dam site aiming at a better understanding of the engineering properties of the Upper Lias Clay under the particular geological conditions encountered at that site.

Most of the data and informations presented here derive from frequent visits paid by the Author to the Empingham Dam works from 1972 to 1974, during which period he was in charge of various field tests and in-situ measurements and also became involved with other tests and observations carried out by the consultant's personnel under the supervision of the special advisors to the project.

The Author's main tasks were the installation and operation of the field instrumentation as well as the interpretation of the data, great emphasis having been put on the trial bank experiment, where deformations and pore pressures were intensive and extensively measured under controlled fill geometries. The overall picture of the research on the Lias Clay properties at the Empingham Dam site is completed by the comprehensive series of

special laboratory tests performed at Imperial College by Mr. M. Maguire, and by finite element analyses carried out by Mr. M.M.A.F. Hamza, also at Imperial College; their studies, both of them supervised by Dr. P.R. Vaughan, one of the special advisors to the Empingham Project, are described in forthcoming theses (MAGUIRE, 1974; HAMZA, 1974).

1.2 OUTLINE OF THE THESIS

In the present chapter, in addition to the description of the main objectives of the research and the summary of the thesis, the main features of the Empingham water supply scheme are briefly delineated.

Chapter Two discusses the regional and local geology, with special attention to the effects of geological structures on the engineering properties of the foundation.

Chapter Three sets the scene for the research. The basic embankment section is presented along with the reasons which led to its adoption; the soil investigation findings are discussed and the remaining uncertainties emphasized; the original design assumptions are summarized and the decision to construct a trial embankment as part of the main design justified.

In Chapter Four the design of the trial bank is described, whereas its instrumentation is detailed in Chapter Five.

The performance of the trial bank is set forth

in Chapter Six, where all field observations and subsequent calculations are shown in detail. The conclusions drawn from these results are listed in Chapter Seven together with a critical review of the approach adopted and the equipment utilized; a comparison is also made of the values of some parameters found in the analysis of the trial bank with the assumptions used in design.

Chapter Eight describes the attempts made to establish a reliable technique for assessment of stresses in the fill by means of hydraulic fracture tests. The theories of in-situ permeability tests and hydraulic fracturing are summarized and briefly discussed. Both successful and unseccessful attempts to open and close cracks in the fill are reported, together with results of permeability tests carried out before and after fracturing had been induced.

Finally, Chapter Nine presents the conclusions drawn from the research. They refer to the approach adopted, the instrumentation utilized, the techniques employed and the parameters studied. Also in this chapter are included suggestions for future works.

1.3 MAIN FEATURES OF THE EMPINGHAM PUMPED-STORAGE SCHEME

In order to meet the rapidly growing demand of water supply in expansion areas of East Midlands, the Welland and Nene River Authority and the Mid-Northamptonshire Water Board put

forward a joint enterprise consisting chiefly of the construction of a large pumped-storage reservoir, on the valley of the small river Gwash, a tributary of the Welland, to be fed with water diverted from the rivers Welland and Nene, some 150 kilometres North of London, England (figure 1.1).

The Empingham Project received parliamentary approval in 1970 and the works started in the following year, their final completion being expected to occur in 1976.

The whole project is described in detail elsewhere (WELLAND AND NENE RIVER AUTHORITY, 1972 and 1973) and its main features are shown in figure 1.2 where it can be seen that two Intakes and Pumping Stations - at Wansford, by the river Nene, and at Tinwell, by the Welland - are used to divert and pump water from these rivers into the Empingham Reservoir through tunnels and large diameter pipelines. The construction of an embankment dam just upstream of the village of Empingham, in Rutland, creates a reservoir over 8 km long, the yield of which, assessed as 3.4 cubic metres per second, will be partially (about 60%) delivered to the Treatment Works at Wing and further conducted to Service Reservoirs at Corby and Hannington, near Wellingborough, while the remainder will be discharged downstream of the dam to be further abstracted by the South Lincolnshire Water Board.

The most important parts of the Project are the reservoir and the dam, shown in greater detail in figure 1.3. Although every effort is being made to promote the amenity potential

of the reservoir, for which purpose facilities for sailing, fishing, rambling, etc, have been planned, its primary objective is the water supply of fast expanding areas in that neighbourhood. To cope with this task, a maximum volume of 124 million cubic metres of water will be stored under a total horizontal surface of 1,260 hectares corresponding to a perimeter of 39 km, really impressive figures of what will be the largest man-made lake in Britain with a size comparable to lake Windermere, the biggest fresh water surface in England. The depth of water will average just under 11 metres, reaching a maximum of 34 metres near the dam, above the present channel of river Gwash.

The dam, presently under construction, is a 1200 m long rolled earth-fill structure, the crest of which will lie about 40 metres above the lowest point of the fill. The most extensively employed material in the embankment is the Upper Lias Clay, extracted from the area to be flooded.

C H A P T E R _ T W O

GEOLOGY OF THE SITE

2.1 General Features

2.2 Local Stratigraphy

2.3 Geological Structure

2.4 Superficial Structures

2.5 The Brecciation of the Upper Lias Clay

C H A P T E R _ T W O

GEOLOGY OF THE SITE

2.1 GENERAL FEATURES

For geological description purposes, Rutland is often included in an arbitrarily delimited area denominated Central England Region, together with the counties of Northamptonshire, Leicestershire, Warwickshire and Staffordshire and parts of Derbyshire, Nottinghamshire, Worcestershire, Cheshire, Flintshire and Shropshire (HAINS and HORTON, 1969), of approximately the same physical features, scenery and underlying rock characteristics. Southwestern Lincolnshire presents also many common features with the Central England Region.

In the eastern part of the region, where Rutland lies, the geological scene is dominated by Jurassic deposits and, to a much lesser extent, by some other Mesozoic and recent sediments. Alluvia, fen deposits, river gravels, boulder clays and other Quaternary sediments are found resting directly on Jurassic rocks (a term here used with the meaning it has for geologists), as Cretaceous and Tertiary strata are totally unknown in the area.

The predominantly argillaceous and calcareous formations of the earliest Jurassic strata are generally named Lias, after an old quarryman's terminology from Western England. They were

deposited under marine environment during sea trangressions that took place at the end of Keuper times. The Lower and Upper Lias depositions occurred when the height of water was large enough to cause predominance of clay fraction sedimentation, while in Middle Lias, a shallowing of the sea created conditions for deposition of silts and thin calcareous sandstones and later produced ferruginous and calcareous shelly sediments that formed the Marlstone Rock Bed.

After the Lower Jurassic, conditions under which deposition occurred oscilated between shallow sea and deltaic or estuarine areas. The calcareous sediments corresponding to marine deposition in the Midlands during the Middle Jurassic are the Northampton Sand, the Lincolnshire Limestone, the Great Oolite Limestone and Cornbrash, while the Upper Estuarine Limestone and parts of the Blisworth Clay were formed under a more restricted environment. Deltaic or coastal conditions led to formation of the Estuarine series. The Kellaways Beds, consisting of fine sand and silt, may have resulted of a slight land uplift after Cornbrash times, but the overlying stratum of Oxford Clay suggests the early reestablishment of previous conditions of argillaceous deposition.

Jurassic rocks are in general abundant in fossils, the ammonites being the most important of them owing to their rapid evolution and complete replacing of a species by the newly developed forms, a circumstance that has proved very useful in the identification of the various strata. Roughly 20 characteristic ammonite zones have been recognized in the Lias, 6 of which are in

the Upper Lias; many more sub-zones have been identified and most of these are named after species of ammonites.

2.2 LOCAL STRATIGRAPHY

The wider outcrop of the Upper Lias Clay in the Central England Region occurs in Northamptonshire and Rutland; elsewhere it only appears in narrow and discontinuous bands in valleys cut in the more resistant Middle Jurassic sediments. The thickness of the Upper Lias stratum decreases towards London, in the south, as this city was part of the Anglo-Belgian Island during the sea transgression that governed the marine deposition in the Midlands during Jurassic times; the thickness of the Upper Lias ranges in general between 40 m and 60 m, but a maximum 76 m has been recorded in Northamptonshire and smaller thicknesses are found in places where cambering is present.

The Upper Lias Clay (Black Jura for German geologists) is a highly folliliferous dark grey soil of medium plasticity containing calcareous and ferruginous nodules. Its fauna is rich in cephalopods and lamellibranchs; among the former, the ammonites are the most easily found, including many species of Dactylioceras, Harpoceras and Hildoceras, but belemnites are also very common; as for the lamellibranchs, the most common are Inoceramus Dubius, Nuculana Ovum and Steinmannia Bronni. In the Upper Lias Clay excavated from locations close to Empingham Dam and employed as fill for the embankment, the Hildoceras Bifrons is the most abundant fossil.

Resting unconformably on the uniform deposits of the Upper Lias is the Northampton Sand, the earliest of the strata enclosed in the broad denomination of Inferior Oolite Series. It was deposited under shallow sea conditions after the higher Liassic layers had undergone some erosion. In some places, chemical precipitation of iron compounds gave origin to bedded ironstones, an extraordinary feature for iron-ore bodies, usually found cutting across and replacing the 'country' rocks and not in regular beds as occurs with normal sedimentary deposits. In present times, no marine deposition of iron compounds is known to be going on, which makes the formation of these ironstones a rather mysterious geological phenomenon. Massive yellow and orange brown sandstones and calcareous fissile sandstones, sometimes called the Variable Beds, are also encountered at places in the Northampton Sand, overlying the ironstone. The total thickness of Northampton Sand, ranges generally from 4 m to 8 m and its fauna consists chiefly of lamellibranchs, few ammonites being found.

Pale grey and white sands, grey to lilac tinted silts, carbonaceous clays and occasionally calcareous sandstones, normally united under the common classification of Lower Estuarine Series, generally overlie the Northampton Sand, although in some places they rest directly on the Upper Lias Clay. The maximum total thickness is under 8 m and the fossils encountered are almost entirely plant fragments. These sediments accumulated when shallowing of the sea, initiated after Lias times, led to the formation of a series

of deltas and estuarine strand-flats. The Estuarine Series are still part of the Inferior Oolite Series.

The last division of the Inferior Oolite Series is the Lincolnshire Limestone, formed when favourable conditions for carbonate deposition were created by further marine regression. It is commonly divided into two strata: the Lower and Upper Lincolnshire Limestone. The total thickness varies widely, the maximum value of 40 m having been recorded in Lincolnshire. The Lower Lincolnshire Limestone, encountered in the region of Empingham Dam, is highly fossiliferous, many molluscs being present.

In the neighbourhood of the Empingham Dam site, the various geological horizons herein described have been analysed by KNILL(1968) and are schematically shown in figure 2.2. Their most important characteristics are as follows:

a) The Middle Lias is represented by stiff grey sandy mudstones with occasional fossiliferous or calcareous band.

b) The Marlstone Rock Bed is a hard grey-green fossiliferous chamositic sandy limestone, just over 2.0 m thick.

c) The Upper Lias is represented by a thick layer of dark grey shelly silty clay with occasional discontinuous thin bands of limestones or septarian nodules ('claystones'), at times assuming the appearance of a mudstone. In the middle of the valley, the total thickness is around 20 metres but this unusually low value for the Upper Lias Clay reflects the influence of bulging and camber-

ing, as elsewhere it exhibits rather greater thicknesses. Some parts of the stratum are shaley clays.

d) The Northampton Sand is represented by fine- to coarse-grained well cemented sandstones, limestones, bands of ironstones and clay seams. Apart from the clay, the remainder are hard rocks occurring in fractured or broken conditions. They are reddish or orange-stained when weathered, as in general they are, but otherwise buff or grey in colour. Thicknesses vary from 4 to 7 metres.

e) The Lower Estuarine Series are generally represented by a thin layer of dark, red or orange-stained, weathered silty clays and more rarely silty sands and clays, but thin ironstone layers are occasionally present. The total thickness ranges from 0.5 to 2.5 m.

f) The Lower Lincolnshire Limestone is present on the hillside of Empingham valley but only half of its full thickness can be found there. It is a massive, thickly bedded rock, white or silvery when fresh but cream in colour if weathered. Both harder bands and clayey infillings are encountered in the limestone, a rock generally broken, fragmented by the effect of cambering, exhibiting localized disintegration by weathering into gravelly sandy clay. Up to 10 m of such a stratum has been recorded on site.

2.3 GEOLOGICAL STRUCTURE

The major structural pattern of the region is

relatively simple; a gentle dip of a few degrees, at an east-south-eastern direction is a little disturbed, here and there, by some folds and faults.

At Empingham Dam site, the site investigation results show that the Upper Lias/Middle Lias contact (the easily identified maker horizon formed by the upper surface of the Marlstone Rock Bed) is an approximately plane surface dipping 0.6° eastwards from a strike direction of about N 15° W, which accords with the regional dip and strike pattern. A line of boreholes put down in the valley bottom revealed that the Marlstone levels at that location were up to 2.2 m above the suggested plane surface; this was interpreted as a valley bulging phenomenon (see next section, 2.4) taking the form of a gentle anticlinal structure whose axis lies centrally beneath the valley bottom.

The Geological Survey maps (1":1mile, sheet 157; 6":1mile, sheet SK 90 NW, and the Geologist's Field Map, KELLAWAY, 1941) show a NW-SE trending fault crossing the Gwash valley just downstream of the dam axis with a westwards downthrow of about 1 metre. Shallow borings put down in the vicinity of the fault during the site investigation confirmed the existence of the fault but suggested that it might have a hinged structure with small throws to both the east and the west. Deeper boreholes in lines along and across the dam axis, however, showed a 4 to 6 m eastwards downthrow at the Marlstone level; it is suggested that this fault and the superficial fault structure are related in some way, the apparent

changes in throw magnitude and direction being attributed to accomodation in the intervening Upper Lias Clay strata. The extension of the fault has not been precisely determined, but it possibly dies out laterally not far beyond the valley bulging.

In one of the deep boreholes, numbered DG-4 (figure 3.4), some 250 m north of the river, the Marlstone level was found 2 to 3 metres below expected. This anomaly might be attributed to a local downdrag near the fault or, perhaps, to a small fault trending along the line of the valley bulging and defining its northern margin.

Although there is no definitive conclusion about the hydraulic continuity between the parts of the Marlstone located at opposing sides of the fault, some evidences from pore pressure observations on piezometres installed in the Marlstone seem to indicate that there is some sort of communication from one side to the other; if it is actually so, the two most likely justifications may be: (1) one or both edges of the Marlstone stratum is (are) bent in the vicinity of the fault, or (2) instead of a fault, there is a fold.

2.4 SUPERFICIAL STRUCTURES

From the engineering standpoint, important features of the area are the superficial geological structures, which are well displayed in the Jurassic regions of England and have been specially investigated in the Northampton Sand Ironfield

(HOLLINGWORTH et al, 1944; HOLLINGWORTH and TAYLOR, 1946 and 1951). In that area, a network of valleys appears to follow synclinal troughs in the resistant flat-bedded capping plateaux; it is been demonstrated, however, by Hollingworth and his collaborators, that these apparent synclines were the result of local superficial structures such as cambering, valley bulging, 'gulls' and dip-and-fault, the most important of which can be identified in figure 2.2.

Cambering basically consists of valley-ward bending down of resistant beds lying above weaker strata, generally clays, and appears to be associated to non-uniformity in overburden pressure acting on the plastic layer, which leads to its squeezing into the less stressed zones. It is been advocated by Hollingworth and Taylor that the process began by the progressive down cutting of valleys by streams and was followed by clay flow under the weight of the nearby superincumbent rocks, which bent down to give place to the formation of cambering. The clay out- and upflow is called valley bulging and the 'bulge peak' is in general gradually removed by erosion. During the whole process, tension zones near the hard bed top, induced by the bending, causes the formation of nearly vertical small faults later filled with material from higher sediments or detritus falling down from the fault walls; they are usually called 'gulls' after an old quarryman's terminology. Another possible structure in cases like this is named 'dip-and-fault' structure, characterized by small vertical displacement and tilting of blocks of the harder beds within the gashes formed as a

consequence of cambering.

Although these mechanisms are not fully understood yet, it appears that they took place during and immediately after the Pleistocene Ice Age, finished some 10,000 years ago, when alternating freeze-and-thaw cycles resulting from the extremely cold tundra-like environment may have softened the stratum, thus making it more plastic and more prone to mass movements.

2,5 THE BRECCIATION OF THE UPPER LIAS CLAY

The Upper Lias Clay, basically a heavily overconsolidated plastic clay which may have been subjected to an overburden thickness in excess of 1000 metres, is encountered at the Empingham Dam site (and in other places where cambering and valley bulging can be observed) in the form of rounded lumps of more or less intact soil, closely packed, frequently tilted with regard to their original bedding planes, spaces between 'clay pebbles' being filled with rather wetter and softer matrix of disturbed material.

This severe disturbance of the soil fabric, for which the term 'brecciation' has been used (CHANDLER, 1973), is associated with the shattering effect of the above mentioned superficial geological structures, but, in addition to their influence, there are considerable grounds for conjecture about the importance of permafrost conditions during the Pleistocene in the disturbance of the Upper Lias Clay, caused or augmented by the formation and subsequent melting of ground ice lenses (CHANDLER, 1972) or by the

forces developed in the mass when a zero isotherm generates the formation of ice in the larger pores before the phenomenon takes place in the smaller ones (NICHOLLS, 1973), both interpretation being aggravated by successive freezing-thawing cycles.

Soil oxidation, visually detected in samples from shallower layers, particularly in the surroundings of fissures and weak zones, provides a basis for the evaluation of the extent to which weathering has acted upon the Upper Lias Clay. The oxidation has been confirmed for similar geological conditions at Wothorpe, near Stamford, by chemical measurements of the ratio Fe_2O_3/FeO (CHANDLER, 1972).

The weathering is also associated with an increase in water content and, therefore, with a drop in undrained strength, its effect being interrelated with and superimposed on the influence of superficial structures, permafrost conditions and the like, contributing thus to an even lower shear strength (undrained and, perhaps, to a lesser extent, drained) of the shallower layers of the Upper Lias Clay.

Other alternative or associated explanations have been offered to justify the observed brecciation of the Upper Lias Clay, namely creep movements, artesian groundwater conditions at depth, etc. (KNILL, 1968), but whatever the origins of such a strong disturbance, the consequences for the engineering properties of this soil are clear enough and will be dealt with in detail further on in this thesis and elsewhere in forthcoming publications (MAGUIRE, 1974, for example).

C H A P T E R _ T H R E E

THE DESIGN OF THE EMBANKMENT SECTION

3.1 Basic Engineering Problems

3.2 Dam Section Adopted
- 3.2.1 External configuration
- 3.2.2 Internal drainage facilities
- 3.2.3 Core
- 3.2.4 Filter
- 3.2.5 Fill zoning
- 3.2.6 Cut-off trench
- 3.2.7 Initial design calculations
- 3.2.8 Final design

3.3 Soil Parameters Required in Engineering Analysis
- 3.3.1 Undrained strength of the foundation
- 3.3.2 Foundation strength in terms of effective stresses
- 3.3.3 Foundation coefficient of consolidation
- 3.3.4 Fill properties
- 3.3.5 Initial stresses in the foundation
- 3.3.6 Stress-strain-time characteristics
- 3.3.7 Pore pressure parameters

3.4 Summary of Findings in the Site Investigation
- 3.4.1 General
- 3.4.2 Site investigation programme
- 3.4.3 Boreholes
- 3.4.4 Sampling
- 3.4.5 Index properties
- 3.4.6 Foundation undrained strength
- 3.4.7 Foundation strength in terms of effective stresses
- 3.4.8 Foundation consolidation parameters
- 3.4.9 Fill properties

3.5 The Adoption of a 'Design-as-you-build' Approach

3.6 Initial Design Assumptions

CHAPTER THREE

THE DESIGN OF THE EMBANKMENT SECTION

3.1 BASIC ENGINEERING PROBLEMS

During the preliminary site investigation, it became clear that the main engineering problem related to the design of the embankment section was the existence of a poor and uncertain foundation.

Coefficients of consolidation in the order of 0.5 m^2/year (1.4 x 10^{-2} mm^2/sec) obtained in some oedometer tests on foundation samples (BISHOP, 1969) showed that, unless expensive internal drainage facilities were provided in the design to accelerate pore pressure dissipation, the undrained strength of the upper layers of the foundation would be the critical factor to control the embankment geometry.

Political as well as economical reasons led to the decision to use the Upper Lias Clay excavated from the area to be flooded as fill material. Prior to the works commencement, the only available tests on which it was possible to base an estimate for the undrained strength of the fill were some quick triaxial, tests on laboratory compacted specimens. These results, open to criticism as the soil structure attained in the field compaction by means of vibrating sheepfoot roller differ from the dynamic technique

utilized in the laboratory, suggested an increase in undrained strength after compaction, probably as a result of the destruction of fissures and the reduction in the degree of saturation during sample preparation and compaction. The undrained strength of the rolled embankment, although a not so important factor as that of the foundation, was one of the parameters to be taken into account in conventional limit equilibrium analyses.

Figure 3.1 shows how the height and the slope of the embankment depend on the soil undrained strength. For the configuration shown in 3.1.b, the use of the 'Stability Number Charts' (TAYLOR, 1948), built for the case of uniform undrained strength throughout the fill and the foundation, led to the full line (figure 3.1.b) when the bank height H is made equal to 40 m and a 'hard' horizon is assumed at the depth of 20 m (approximately the conditions of Empingham Dam design). According to this curve, the circular limit analysis for a factor of safety equal to the unity relates undrained strengths and slope inclinations in such a way that, for a factor of safety equal to the unity, while a c_u of 40 kN/m^2 requires the adoption of an extraordinarily flat 25:1 slope, another value twice as high (80 kN/m^2) would only necessitate a 6:1 slope. The consequences of such a variation are emphasized in figure 3.1.c, where the embankment geometries for various values of undrained strength are compared, and also in figure 3.1.a, where the volume of earth fill is seen to decrease from about 40,000 m^3/m run in the case of c_u = 40 kN/m^2 to 10,000 m^3/m run for c_u = 80 kN/m^2.

The real problem of Empingham Dam is not exactly the same as that depicted in figure 3.1, as the increase of the foundation undrained strength with depth somewhat alters the stability analysis. Besides, the stress-dependency of the fill undrained strength, the differences in stress-strain characteristics of the fill as compared to the foundation, anisotropy, time effects and progressive failure make the analysis much more complicated and difficult. A good indication of what order of magnitude should be expected for the overall undrained strength of overconsolidated plastic clays is provided in Table 3.1, reproduced from VAUGHAN and CHANDLER (1974) where results of back-analyses of collapsed cuts on different clay masses are compared. It is seen that notwithstanding the variety in geological history and geometry, all 9 cuts failed when average mobilized shear stresses were within the narrow range of 23 - 54 kN/m^2. Going back to figure 3.1, it is visualized that values like these would require a slope flatter than 12:1 (for a factor of safety equal to the unity) and whose angle is extremely sensitive to small changes in strength.

With so great an influence of the undrained strength on the geometry and the cost of the embankment, the accurate assessment of the parameters involved was of utmost importance.

Any improvement in the foundation as well as in the fill strength would be certainly beneficial to the economy and the safety of the earth structure. In the case of sand drains being designed (as indeed they were in part of the foundation) a

sound estimate of the overall coefficient of consolidation would be essential for a reasonable assessment of the gain of soil strength with time and its correlation to the planned construction rate. For this purpose a good knowledge of the Upper Lias Clay strength parameters in terms of effective stress was also required.

TABLE 3.1

(reproduced from Vaugham and Chandler, 1974)

Back-analyses of cuts in overconsolidated clays

Material	Site	w_l (%)	w_p (%)	Slope + height (m)	Ave. C_r (kN/m^2)	Time to failure (days)	Reference
Leda Clay	Messena, Canada	45	27	4.5 6.5 6.5	23 32 28	0	Bazett et al, 1961
London Clay	Wraysbury, England	73	28	9 x	35	3	Simons, 1967
Upper Lias Clay	Tinwell, England	62	28	9	31	0	Vaughan, Chandler 1974
Boom Clay	Antwerp, Belgium	81	29	10.7	42	50	De Beer, 1969
Upper Lias Clay	Empingham, England	63	29	14	47	3	Vaughan, Chandler 1974
London Clay	Bradwell, England	95	30	15 15	54 50	5 19	Skempton, La Rochelle 1965

+ : Average slope angles between 45° and 85°, higher slopes being, in general, less steep.

x : 6 m of this slope was in gravel; the strength calculated is for the clay below.

The results of the site investigation will be presented in greater detail further on in this chapter but, for a better understanding of the engineering problem involved in the choice of the embankment section and the establishment of dimensions, a brief description of the site conditions and the order of magnitude of some soil parameters are listed below. These were provisional values subject to a possible future revision, but they represented the best estimate available at the time the first decision was taken about the dam geometry in 1971 or thereabouts.

i) Foundation: Upper Lias Clay from the top (at the valley floor) down to about 20 to 25 metres below ground level, followed by a 2 to 3 m thick permeable Marlstone Bed Rock and a thick layer of Middle Lias Clays and Silts. The undrained strength of the Upper Lias Clay as measured in quick triaxial tests averaged 50 kN/m^2 at the top, increasing downwards at a rate of 5 kN/m^3; the scatter of test results was quite pronounced and a 'lower bound' straight line was defined by the equation c_u (kN/m^2) = 35 + 3.5z (metres). Plate tests, however, resulted in higher values, ranging from 50 to 80 kN/m^2 at the top and from 120 to 280 kN/m^2 around 18 metres below. Effective stress envelopes derived from drained and undrained tests were characterized by cohesion intercepts c' between 0 and 20 kN/m^2 and peak friction angles ϕ' ranging from 18° to 30°. Residual friction angles from reversing shear box tests were around 11°, but the lower-limit angle for box-samples containing known shear planes was 16° at the end of one travel. Coefficients of consolid-

ation obtained from oedometer tests and triaxial consolidation tests averaged 0.5 m^2/year (1.4 x 10^{-2}/sec).

ii) Fill: Prior to any placing of fill, laboratory compacted samples and also undisturbed samples taken from the river diversion embankment were subjected to quick undrained triaxial tests under cell pressure of 250 kN/m^2 (VAUGHAN, 1973), resulting in average c_u = 94 kN/m^2. No effective stress parameters were determined at that time, but there is no reason to suppose they should exhibit any important difference from values obtained in tests on undisturbed samples.

Four triaxial consolidation tests on laboratory compacted specimens subject to a cell pressure of 500 kN/m^2 resulted in an average c_v = 0.2 m^2/year = 0.63 x 10^{-2} mm^2/sec.

3.2 DAM SECTION ADOPTED

3.2.1 External Configuration

In the top of figure 3.2, the most important features of the dam section in the valley floor are schematically shown. Each particular aspect of that drawing will be discussed and explained in the present chapter and the reasons which led to their inclusion in the design thoroughly scrutinized.

As already pointed out in previous comments small variations in the foundation undrained strength in the range 30 - 100 kN/m^2 has an enormous influence on the section dimensions.

As the rapid completion of design for the early letting of contracts was required, the scope of the pre-contract investigation was limited and some important uncertainties about soil parameters and embankment dimensions still existed at the time the contract was let. For this reason, a flexible design was made and the contract allowed for geometry and quantities to be altered during construction, as new and more precise information was acquired.

Figure 3.3, depicting the most important features of the dam in its highest section, shows that in lieu of a unique slope linking toe to crest, two comparatively steeper slopes, one on the toe and the other by the crest, are connected by a gentle platform. This solution, apart from bringing saving in compacted fill, separates almost entirely the two slip zones, each acting on a different foundation area.

It is worthy to mention that the fill can withstand those much steeper slopes at the berm ends not only because their effective height is less than half the total dam height but also because the rolled clay undrained strength is considerably higher than the foundation one, owing to the lowering of water content and the destruction of original soil discontinuities during excavation and compaction.

Figure 3.3 also shows the initial design configuration, with shorter berms, used as a basis for the contract, and the extension to be added to the design if further investigations

indicated that the initial assumptions were optimistic. The length of such a berm is mainly a function of the foundation strength, whereas its thickness depends on the magnitude of horizontal active thrust exerted by the fill centre and the passive resistance offered to failure by the berm itself.

3.2.2 Internal Drainage Facilities

An alternative to flattening the slopes could be the acceleration of foundation consolidation, but extremely low rates of pore pressure dissipation were anticipated and to rely upon sand drains alone as a means of increasing strength all over the dam area would be uneconomical and could delay construction. As an increase in embankment volume cost less than sand drains, it was decided to limit their use to the central part of the dam foundation (figure 3.3), where larger total stresses develop. Their spacing was designed to give a pore pressure ratio r_u of 0.7 at the end of construction, if a conservatice c_v of only 0.25 m^2/year (0.79 x 10^{-2} mm^2/sec) were actually representative of the foundation, or of the order 0.4 if values of c_v obtained from trial sand drains were correct. The accelerated consolidation due to the sand drains provides a certain increase in factor of safety between completion and impounding and this relatively rapid improvement in stability with time after completion also guards against undrained creep.

As fill properties were difficult to predict beforehand, provisional fill drainage blankets were provided for in the design, and fill zones were defined with the aim of making the

central part of the fill drier and stronger. During the construction, however, an average c_u of 160 kN/m^2 obtained from quick triacial tests on samples taken from the fill showed that placing conditions in that zone were good enough to provide low pore pressures and high strength, and the internal drainage blankets were discontinued after the height of the embankment had reached 10 metres.

3.2.3 Core

Although the dam is homogeneous in that, apart from the filter, it is all built with basically the same material, an inclined more flexible core of wetter material was incorporated into the design as a protection against cracking and to avoid possible initially high permeabilities due to compaction at water contents below optimum.

Reasons for the preference of this core configuration to an alternative vertical core (VAUGHAN, 1973) included (i) the fear that reservoir would drain downstream through a path formed by sand drains located upstream of the vertical central core, the Marlstone Rock Bed and downstream sand drains, (ii) the advantage of having drainage of the foundation fully operational during and after impounding, (iii) the reduction of the thrust exerted by central zones upon the shoulders when drier stronger material is employed, (iv) the reduction of the thrust exerted upon the berms by a very flat core, despite its weakness, as compared to one inclined 45° (v) the reduction in post-construction settlements, both absolute and differential.

3.2.4 Filter

The Upper Lias Clay consists almost entirely of clay and silt size particles. The finest particles which could be lost through internal erosion (piping) was found to be 'clay flocs' when water with the probable chemistry of the future reservoir was utilized in the studies. To prevent the loss of such particles, an adequate filter protection was designed.

Instead of an inclined filter immediately adjacent to the core, a vertical central one was adopted; it is simpler to construct, reveals externally any settlement and maintains its continuity if loss of material occurs.

3.2.5 Fill Zoning

Figure 3.2 shows that three different sorts of fill, denoted 'A', 'B' and 'C', were used in the dam design. They were all of them basically the same Upper Lias Clay excavated from borrow pits in the reservoir area, but differences in degree of saturation contributed to lend some particularity to the behaviour of each type.

The so-called 'C-fill', to be utilized in the centre of the section (figure 3.2) was drier and therefore stronger. During initial fill placing in 1972, quick undrained triaxial tests on samples taken from the embankment averaged 160 kN/m^2 for a mean moisture content of 21%.

The 'A-fill, employed upstream of the core-foundation contact and downstream of the sand drain area, was a

material of poorer quality, for which average results of tests mentioned above were c_u = 140 kN/m^2 and w = 22%.

For the wetter, weaker, more flexible 'B-fill' used in the core, mean values were, in the same tests, c_u = 75 kN/m^2 and w = 25%.

Sandy clay from head deposits, weathered Lias Clay and some granular material from excavations in the 'cap' materials were named 'A1-fill' and employed as general fill in the least stressed central zones of the berms. Average values for moisture content and undrained strength of the clay materials present were, respectively, 25% and 80 kN/m^2.

3.2.6 Cut-off Trench

Towards the top of valley sides, particularly in the south direction, an increasing thickness of permeable layers (Northampton Sand, Lower Estuarine Series, Head, Top Soil) overlies the Upper Lias Clay at elevations below the dam crest level. To prevent leakage of the stored water through these permeable layers outcropping below the water table, a cut-off trench was designed to provide a continuous contact of the clay foundation with the core by means of a backfill made of rolled Upper Lias Clay, types, 'A' and 'B'. The trench is not represented in figures 3.2 and 3.3 as it is non-existent at the bottom of the valley, where the core contacts directly the stripped ground.

3.2.7 Initial Design Calculations

Dimensions of the section were initially

established by means of multiple wedge analyses, in which the thrust exerted by the centre of the embankment was estimated from effective stress parameters $c' = 0$, $\phi' = 22^{\circ}$, $F_s = 1.5$ and mobilized $\phi' = 15^{\circ}$, and pore pressure ratio $r_u = 0.6$ for the highest section.

The length of the berm necessary to resist the thrust depends on the foundation superficial undrained strength, one of the most uncertain parameters at the time of the initial design. A c_u value of 30 kN/m^2 at the top of the Upper Lias Clay led to the conservative design of figure 3.3, whereas a more optimistic assumption (c_u = 45 kN/m^2) resulted in the shorter berm depicted in that drawing. In both cases, a gain in strength of 3.5 kN/m^2 per metre of depth was assumed from the stripped ground level down to the Marlstone, around 20 metres below.

In this sort of analysis, the berm depth at each point must be kept large enough to avoid the development of weaker path for the slip surface through the fill and not in the foundation.

Provisional as it was, the initial design did not allow for any deeper consideration concerning unequal stress-strain characteristics of the different materials involved, a subject which received careful attention during the final design. It was already realized at that time, however, that an even mobilization of foundation and fill strengths could hardly be expected and that this could become a difficult problem to solve if brittleness and progressive failure proved important.

Analyses were performed not only on the highest section but also on 6 other locations, berm lengths varying longitudinally so as to give the most efficient cross-section. Particularly important were the sections located just outside the sand drain area, where no significant improvement in the foundation strength could be expected at the end of construction.

3.2.8 Final Design

Most of the existing uncertainties still present at the initial design were later clarified by means of several sorts of tests and analyses, which include the trial bank experiment, field and laboratory tests, observation of the fill performance during the first year of construction, limit equilibrium analyses and non-linear finite element analyses of both the trial bank and the dam.

Some of the above cited elements will be subsequently described and commented in this thesis, whereas others are to be found in forthcoming publications (MAGUIRE, 1974; HAMZA, 1974; etc).

3.3 SOIL PARAMETERS REQUIRED IN ENGINEERING ANALYSIS

3.3.1 Undrained Strength of the Foundation

As already pointed out, the establishment of reliable values for the undrained strength of the Upper Lias Clay at various levels was the most important and difficult task faced by the designers.

The geological disturbance of the foundation make

it difficult to determine accurately such a parameter from small-scale laboratory and even in-situ tests. And yet, as demonstrated in section 3.1 and figure 3.1, the influence of its magnitude on the embankment dimensions is enormous.

Besides the geological problem, mechanical disturbance during boring, sampling and handling operations may considerably affect the laboratory-measured undrained strength, mainly because of their effect on the suction in the specimen pores. Similar type of error source is likely to occur during boring for the performance of plate tests.

In addition, anisotropy in undrained strength, originated either from anisotropy in terms of effective stresses, or from anisotropic pore pressure parameters, or from both, makes the c_u values to be used in limit equilibrium analyses dependent on the angles of potential slip surfaces at each point. The circumstance certainly adds to the difficulty of choosing conventional values for c_u capable of correctly representing the soil strength in the type of analysis selected and the shape of surface on trial.

Spacial variations of c_u are also expected, not only owing to changes in disturbance from point to point across the valley but also because the existence of a soil mantle of variable thickness overlying the Upper Lias Clay inevitably leads to higher effective stresses and therefore greater c_u values (for a same depth below the top of the stripped ground level) at locations where larger

removals of superficial layers were necessary.

3.3.2 Foundation Strength in Terms of Effective Stresses

Reliable values for cohesion intercept c' and shearing resistance angle ϕ' are required in analyses in terms of effective stresses. In the sand drain area, where partial dissipation of pore pressure is certain to occur during construction, the analysis cannot be carried out in terms of undrained strength, an assessment of gain of strength with increasing mean effective stress being required. For this purpose, a good knowledge of effective stress parameters and also of the coefficient of consolidation is essential.

Geological disturbance may also affect the values of strength parameters in terms of effective stresses, more strikingly at low normal stresses where a decrease in the cohesion intercept, and in the friction angle has a proportionally greater effect on the overall strength.

Mechanical disturbance too, albeit not so influential as in the case of undrained strength, may introduce errors in effective stress envelopes derived from laboratory tests.

The effect of cambering and valley bulging combined caused considerable movement of soil elements towards the zone of the 'bulge', during which the direction of bedding planes change from approximately horizontal to nearly vertical in extreme cases. These displacements and the bending of the layers create condition for the development of shearing between successive beds.

This shearing is expectedly accompanied by a reduction in shear strength towards residual values. Therefore, anisotropic strength in terms of effective stresses is predictable, the direction of minimum values being likely to vary from place to place; while away from the valley bottom the minimum strength should roughly correspond to horizontal shear places, it may drastically change in the 'bulge' zone, where even the vertical direction might be the weakest.

3.3.3 Foundation Coefficient of Consolidation

The coefficient of consolidation c_v is known to depend on the soil permeability and compressibility. The former factor is usually strongly anisotropic, the coefficient of permeability in the direction of bedding planes being normally many times greater than across it, whereas the compressibility, although variable, generally ranges between much closer limits. As a consequence, the coefficient of consolidation exhibits in general a degree of anisotropy of the same order of magnitude as that of the permeability.

Oedometer tests and triaxial consolidation tests in which side drains are either absent or ineffective measure coefficients of consolidation in the specimen vertical direction, although the parameter may be also determined in other directions if inclined and horizontal specimens are tested.

In the case of the Empingham Dam foundation, superficial geological structures may have had a very great influence on the consolidation characteristics of the Upper Lias Clay, particularly at the 'bulge' zone, increasing the overall perability by soil

softening and opening of discontinuities, augmenting the compressibility by similar means, inducing or exaggerating anisotropy, rotating directions of maximum and minimum coefficient of consolidation, etc. Laboratory tests can be hardly expected to accurately represent the spacial and directional variations of the parameters involved or provide data for a reliable model of the global pore pressure dissipation pattern in the foundation. In-situ tests embrace much larger volumes of soil, are less damaged by mechanical disturbance and their results are thus considerably more trustworthy in assessment of spacial variation of the permeability (specially where its horizontal component is the most significant), but they require a number of installations spread over the foundation and good judgement in interpretation of results and the establishement of design values.

Nevertheless, the determination of reliable values for the coefficient of consolidation is essential to a good estimate of the pore pressure ratio r_u in the sand drain area at the end of the construction, a very important factor in the stability analysis of the embankment. A $c_v = 0.25$ m^2/year, for example, would result in a r_u value around 0.7 in the sand drain at the end of construction, whereas a c_v value of 1.5 m^2/year would bring r_u down to around 0.2. This uncertainty corresponds to a difference of over 300 kN/m^2 in mean effective stresses and more than 100 kN/m^2 in mobilized shear stresses; changes of this sort might mean considerable economy in the design.

3.3.4 Fill Properties

The determination of fill properties from laboratory compacted specimens utilizing conventional dynamic techniques is certainly open to criticism, as these have a different structure from the fill material subjected to field rolling compaction. As placing moisture contents are also difficult to predict in advance of construction, an accurate assessment of fill properties can only be made after construction starts.

The strength of the fill influences the stability of the embankment in two main ways. Firstly, it controls the active thrust exerted by the central zone of the dam upon its shoulders. Secondly, it governs the passive resistance offered by the berms, a factor which ensures that potential slip surfaces pass through the foundation and do not emerge at the slope.

For both aspects mentioned above, the development of strains to achieve full mobilization of the fill strength must be considered, since the development of high shear stresses in both the active and passive cases may imply unacceptable foundation displacements.

3.3.5 Initial Stresses in the Foundation

Soil properties considered in items 3.3.1 through 3.3.4 are the most directly linked to the stability problem. There are, however, other parameters and soil characteristics that must be taken into account in an engineering analysis intended to be as complete as circumstances permit. Among these factors, which will be discussed in this and subsequent items, is the determination of

stresses acting upon the soil elements in the foundation prior to the loading due to the embankment construction.

The strength reserve available at each point of an earth mass depends not only on the failure envelope in terms of effective stresses and the shape of the effective stress path but also on the point this path starts from, i.e the state of initial stresses. This is conveniently expressed by means of the coefficient of lateral stresses at rest K_o', defined as $K_o' = \sigma_x' / \sigma_z'$, where σ_z' is the vertical effective stress and σ_x' is the lateral effective stress assumed constant in any horizontal direction.

Beneath a triangular or trapezoidal strip load, incremental horizontal stresses in the toe region are greater than vertical ones. If it happens that $K_o' > 1$, the strength reserve at this zone is smaller than generally assumed from conventional laboratory triaxial tests, started from isotropic initial stresses. In the middle of the section width, on the contrary, incremental vertical stresses supersede horizontal ones and, therefore, the most unfavourable case, as far as strength reserve is concerned, corresponds to $K_o' < 1$.

In heavily overconsolidated soils or overcompacted fills, it may happen that K_o' comfortably exceeds the unity and even approaches the passive failure value K_p'; in this case, shear stresses are very likely to equal the available strength in the vicinity of the toe in early stages of the construction; local yield develops then in a progressive fashion, from toe to centre, follow-

ing the constructional sequence. This pattern is more pronounced if the fill is considerably stronger than the foundation and the central region of the earth structure still possesses a strength reserve while the foundation is already failing.

A flat slope obviously diminishes the magnitude of shear stresses by the toe but, on the other hand, causes the extension of the region where major principal incremental stresses are approximately horizontal seen above to correspond to the most unfavourable condition for $K_o' >> 1$.

At Empingham Dam, designed slopes are exceptionally flat and the active thrust exerted upon the shoulders by the fill centre are likely to generate larger lateral incremental stresses along the top of the foundation outside the sand drain area and, as the strength reserve is a function of the K_o' value, a correct determination of such a parameter becomes important, particularly in face of the enormous influence on the dam geometry exerted by the magnitude of the available undrained strength.

An aspect to be considered refers to the uniqueness of the K_o' value. In an inclined ground there is no reason to assume that K_o has a single value in any horizontal direction; the steeper the ground is the greater the departure of the initial state of stresses from the condition of K_o' uniqueness. At Empingham, in addition to gently sloped valley sides (average 5^o, but approaching 10^o near the bottom of the valley), there is the influence of geological disturbance on the original initial stresses. The intensive

earth movement towards the middle of the valley, the shearing along this direction and the upwards movement in the 'bulge' zone may quite probably induce anisotropy to initial stresses in the soil medium; across the valley K_o' might have increased towards the passive value K_p', whereas parallel to the stream, it might have, if anything, decreased towards normally consolidated figures.

3.3.6 Stress-strain-time Characteristics

It is been previously commented that, beneath the slopes of an embankment, shear stresses may locally exceed the foundation strength; in this case as construction proceeds, the yielded zone extends towards the centre in a progressive way. If the soil exhibits a certain degree of brittleness under undrained conditions, this pattern is aggravated and accelerated, the propagation of the failure surface (or zone) depending on the rate of strength drop with increasing shear strain. If undrained creep movements are important, soil distorsion may still take place after the loading is discontinued and the mechanism of progressive failure may thus proceed.

Another important aspect to be considered refers to the compatibility of strains developed in the various materials. Differences in volumetric deformation and distortion resistance moduli from zone to zone of the earth structure greatly affects stress distribution and deformation patterns. This is not easy to take into account unless finite element techniques are employed, but even in this case analytical modelling difficulties (three-dimensional

effects, inelasticity, non-linearity) adds to computing problems. The even greater experimental difficulties in the reliable determination of the parameters required in the analysis makes stress and strain predictions mere approximations, still at a tentative stage.

In the face of the magnitude of the task and the approximations involved, simplified analyses are perfectly justified. Isotropic elasticity is often based on the linear deformation modulus E (Young's modulus, in terms of total or effective stresses, according to the problem) and Poisson's ratio ν (also in terms of total or effective stresses). A refinement of growing use consists of adopting non-linear expressions for relationships between stress difference , strains and, when necessary, stress level and Poisson's ratio.

3.3.7 Pore Pressure Parameters

For partly saturated materials and also for saturated soils subjected to shear stresses, pore pressures developed under undrained loading depend on deviatoric as well as mean total normal stresses. The knowledge of such pore pressures is important in stability analyses in terms of effective stresses in which steady-state seepage does not occur and also in the estimate of starting points for consolidation.

The Empingham Dam foundation is saturated and the pore pressure parameter B (SKEMPTON, 1954; BISHOP, 1954) is, for practical purposes, assumed equal to the unity. That is certainly

not the case of the fill, where B strongly depends on the degree of saturation at placing conditions, the compressibility of the compacted material and stress level; furthermore, pore pressures may be negative (suction) for quite large a range of mean stresses and the anticipation of their magnitude in the fill is very difficulty to achieve from laboratory tests or even from field measurements carried out in advance of construction.

Pore pressure parameters A (SKEMPTON, 1954; BISHOP, 1954) or α (HENKEL, 1960), expressing the influence of deviatoric stresses on pore pressures set up under undrained loading, are not so unfluential as B, unless in extreme cases of heavily overconsolidated or sensitive normally consolidated soils. In any event, if its accurate evaluation is possible, analyses become more refined and correct.

If analysis is carried out in terms of effective stresses and the pore pressure ratio r_u is utilized, its value may be approximately calculated from values of A, B and estimated shear stresses.

3.4 SUMMARY OF FINDINGS IN THE SITE INVESTIGATION

3.4.1 General

Under the above heading, the most important findings obtained from the site investigation carried out before the initial design are presented in a summarized form. The project

programme required that the main embankment construction contract should start less than a year after the commencement of site investigation. Thus, time for a major assessment of foundation properties was limited and it was decided to produce a preliminary design for tendering purposes in which allowance was made for subsequent alterations during construction as additional informations were obtained and more refined analyses performed.

Conclusions arisen from the trial bank experiment and from other sources, added to the initial site investigation results herein quoted, will be dealt with in subsequent chapters where all the available information will be considered together and analysed to produce the best picture of the Upper Lias Clay behaviour at the Empingham Dam site.

3.4.2 Site Investigation Programme

A preliminary feasability site investigation was carried out in 1967 at the proposed site for Empingham Dam (TERRESEARCH LTD., 1967), but only few boreholes were put down and a few soil tests performed at that time.

Later, in 1970 and 1971, after parliamentary approval for the scheme, a larger number of borings were sunk and laboratory and field tests were carried out (SOIL MECHANICS LTD., 1971), but the required rapid completion of design limited the scope of the pre-contract site investigation.

More borings and soil tests were carried out

during construction, but they will not be considered in this chapter, their presentation and discussion being deferred to further chapters where all available informations will be jointly discussed and interpreted.

3.4.3 Boreholes

The boreholes put down for the general site investigation of the foundation are shown in figure 3.4, some other holes bored in neighbour locations being also depicted in that drawing.

A longigudinal profile as emerged from the simplified soil classification of samples from a line parallel to the dam crest is portrayed in figure 3.5. As the layers of alluvium, head and top soil were stripped before the banking commenced, the engineering properties of these strata are unimportant, the Upper Lias Clay remaining the most relevant earth deposit as far as the embankment foundation behaviour is concerned.

3.4.4 Sampling

The vast majority of samples were taken with U.100 sampler, generally driven by percussion methods using a trip hammer. Two kinds of samplers were utilized: the standard type, recommended in the British Standard Code of Practice C.P. 2001 (BRITISH STANDARDS INSTITUTION, 1957), and the Soil Mechanics Ltd. sampler with a liner; undrained strength measurements on samples obtained by means of either sampler did not appear to differ.

Some of the samples were tested on site, in a

small laboratory, after a storage period of 22 to 61 days, while others were sent to London to be tested in the central laboratory of the Site Investigation Contractor after a dalay of 9 to 16 days from sampling date. Undrained strength as measured on site, were 20 to 50% higher than London results; this discrepancy has been attributed to disturbance caused by transportation of the samples.

3.4.5 Index Properties

The index properties of the Upper Lias Clay for the arbitrarily chosen Area A (figure 3.4) of the dam site are plotted in figure 3.6, based on laboratory tests carried out by Soil Mechanics Ltd. It is possible to see that the particle size distribution and the Atterberg limits exhibit a remarkable uniformity with depth and do not appear to vary horizontally more than would be expected from a normal scatter that certainly includes human factors as a major influence. 45% clay, 45% silt and 10% fine sand are approximate figures which consistently describe the results of grain-size analysis by sedimentation using 25 to 30 g of soil in 1000 ml of distilled water treated with hydrogen peroxide. Plastic limit 25% and liquid limit 60% appear to be representative of the upper 6 - 7 metres, with a tendency towards lower liquid limits at greater depths, values of 50% or so having been measured around 20 m below the top of Lias. This may be partly associated with weathering.

Unit weights are virtually constant for practical purposes, averaging 20.3 kN/m^2, while water contents exhibit a slight

decrease from 25% near the top (just over the plastic limit) to about 19% at a depth of 20 metres (well below the plastic limit).

A Plasticity Chart (figure 3.7) shows that practically all Atterberg limit test results led to points above the so called 'A' line, with an average for the liquid limit quite close to Oxford Clay's value (also a Jurassic deposit), somewhere between Weald Clay and London Clay, both of them being plastic clays but belonging to the Tertiary Era. According to the well known Unified Soil Classification System, the Upper Lias Clay is classified as CH, some points falling in the CL range.

The activity of the clay, defined as the ratio of plasticity index to Clay faction (SKEMPTON, 1953) varies from 0.5 to 0.9, most values falling close the average number of 0.7, here again an intermediate figure between Weald Clay and London Clay, typical activities of which are, respectively, 0.63 and 0.95 (SKEMPTON, 1953).

3.4.6 Foundation Undrained Strength

(i) Laboratory tests

The basic test generally employed in the site investigation to assess the strength of the foundation material under undrained loading consisted in subjecting cylindrical undisturbed samples, 100 mm dia. x 200 mm height, to a vertical strain-controlled aplication of stress difference, up to failure, at a rate of 2% of the original sample height per minute, the specimen having been

previously stressed by an all-round hydraulic pressure of 400 kN/m^2 in a triaxial cell. This pressure, which exceeded the overburden pressure for a large range of samples of importance, was selected taking also into account practical reasons: it corresponded to the full-height of a single self-compensating mercury equipment for stress control (BISHOP and HENKEL, 1962).

The results for Area A, in terms of half the peak value for the stress-difference, are plotted in figure 3.6 against depth of sampling below the top of the Upper Lias Clay. A linear regression by the method of least squares led to the establishment of the average line shown in the figure. The wide scattering of results is probably due to the severe shearing and reworking of the overconsolidated Upper Lias Clay, induced by the combined effects of cambering, valley bulging and frost action, associated with the known effects of sample size, rate-of-loading and anisotropy.

Similar graphs are presented for Area B as well as Areas C and C' (combined) of the dam foundation (figure 3.8). The width of bands enclosing 90% of test results are of the same order for the plots of undrained strength of samples from the three areas (figures 3.6 and 3.8), namely 60 to 75 kN/m^2, but there is a clear shift in the 'lower bound' and 'average' lines, increased of about 40 kN/cm^2 from Area A to the others. This may have partly resulted from the valley-bulging as area 'A' is the most affected by such a structure, but the fact that the deposits overlying the the Lias are 2 to 3 metres thicker at Areas 'B' and 'C' than at

Area 'A' may have contributed with some 10 to 20 kN/m^2 increase in undrained strength.

(ii) Plate tests

In the influence areas of borings nos. DF-14 and DF-35 (figure 3.4), 25 constant rate-of-penetration plate bearing tests were carried at 1.5 m depth intervals in 254 mm (10 in) dia. boreholes, utilizing 152 (6 in) plates, and 18 other tests were performed using larger boreholes (305 mm = 12 dia.) and plates (267 mm = 10.5 in) . In both sort of tests, the borings were advanced using cable tool methods, unlined in the Upper Lias Clay, the final 200 mm above each test level being hand-augered so that to avoid greater ground disturbance and ensure a smoother test surface. The load was applied through a steel column of 152 mm (6 in) dia. by means of a hand-operated hydraulic jack reacting against an anchored beam, the force being measured with a load cell and the penetration worked out from precise levelling of a scale fixed to the column. A rate of 10 mm per minute was adopted up to 300 mm penetration with load readings taken every minute.

The load at failure was taken from the load x penetration curves, but in some cases this point was hard to define as the curve appeared to reach a peak value but the load still increased beyond such a point although slowly; when this was the case, two values were considered as possible failure loads: the first peak and the maximum load reached (WALBANCKE, 1971).

The undrained strength c_u, corrected for depth (SKEMPTON, 1951) was further reduced by 7% for tests performed with the smaller plate to account for the effect of possible friction of the straight sided plunger employed in these tests against boring walls. Both the reduced and unreduced values are plotted together in figure 3.9, where scatter is seen to be comparable to that obtained in laboratory tests on small samples.

The plate tests showed higher strengths than the laboratory tests, particularly at depth, suggesting that brecciation effects die out about 15 m, and that the undrained tests on U.100 samples may have given unrealistically low values owing to shattering of the hard clay during sampling.

3.4.7 Foundation Strength in Terms of Effective Stresses

A few drained tests and undrained tests with pore pressure measurements were carried out during the preliminary site investigation (TERRESEARCH LTD., 1967) or in testing that followed the parliamentary approval for the scheme (SOIL MECHANICS LTD., 1971). Their results are separately plotted in figures 3.10 and, 3.11, in which a considerable scatter of effective stress parameters is present. Cohesion intercepts ranging from 0 to 20 kN/m^2 and friction angles from 18.5° (for $c' = 0$) to 30° can be obtained, with best fitting average lines yielding cohesion intercept around 10 kN/m^2 and friction angle of 24°, for Terresearch tests, and, correspondingly, 20 kN/m^2 and 18.5° for those of Soil Mechanics Ltd.

Measurements of residual friction angles at large displacements were made at Imperial College. In repeatedly reversing shear box tests an angle of 11° was found (BISHOP, 1969), whereas tests in the ring shear apparatus jointly developed by Imperial College and the Norwegian Geotechnical Institute (GARGA, 1970; BISHOP et al, 1971) on an undisturbed sample taken from a location immediately below the Lias top at Empingham (DAVIES, 1972), resulted in a residual angle of 8.5°. The lower bound of shear box tests on samples containing actual shear planes corresponded to a friction angle of 16° for zero cohesion intercept.

It is relevant to note that the 'lower-limit' and the 'pre-cut-specimens' envelopes do not differ by more than 2 or 3 degrees, suggesting that the lower values encountered in some triaxial tests might have corresponded to failure surfaces partly or totally developed along existing discontinuities, what could well be the dominant behaviour in real slope slips. Bulging must have produced substantial shearing towards valley and such shear planes may not have necessarily been represented in laboratory samples. Possible movements along such planes needed to be considered in establishing design parameters for the dam.

Hollowell Dam is a 12 m high puddle-cored embankment founded on the Upper Lias Clay at a site exhibiting similar disturbance to that observed at Empingham. The back-analisis of its upstream section, carried out for end-of-construction conditions utilizing the best estimation of pore pressure developed in the found-

ion, resulted in an average mobilized friction angle of 16^{o} for $c' = 0$.

3.4.8 Foundation Consolidation Parameters

(i) Coefficient of consolidation

During the site investigation a series of oedometer and triaxial consolidation tests were carried out at various effective stresses (SOIL MECHANICS LTD., 1971; DAVIES, 1972, etc.) and the coefficients of consolidation obtained from them are plotted in figure 3.13.

Measurements of c_v were also performed through four sand drain trials in the zone to be consolidated by means of internal drainage. These experiments, reported by MOYA (1971) and SOIL MECHANICS LTD. (1971), were of two sorts; in the conventional sand drain trials, initial pore pressure increase was achieved through the construction of a small embankment with spoil excavated from the tunnel, whereas in the special trials, pore pressure was lowered and consolidation induced by de-watering the sand drains by bailing through special plastic casings installed in them. Pore pressure observations were made on piezometers located between the sand drains. Results of calculations, pictured in figure 3.13, show a sharp variation of c_v with effective stresses, contrasting with the tendency observed in laboratory tests, where the decrease in c_v was much less pronounced.

Practically all measurement which resulted in c_v values over 1 m^3/year (3.2×10^{-2} mm^2/sec) corresponded to laboratory or in-situ tests on soil of the bulged zone in the valley

bottom and it was feared that the clay might have been atypically influenced by the valley bulge. Outside the bulge zone, most c_v determinatios ranged from 0.15 to 1.0 m^2/year (0.48 to 3.2 x 10^{-2} mm^2/sec).

Throughout this chapter the coefficient of consolidation was treated as though its tridimensional version had the same physical meaning as the one-dimentional one, but it must be emphasized that it is not so. If the soil skeleton is isotropically elastic their mathematical expressions are:

$$c_{v,1} = \frac{k}{\gamma_w} \cdot \frac{E'(1-\nu')}{(1-2\nu')(1+\nu')} \tag{3.1}$$

$$c_{v,3} = \frac{k}{\gamma_w} \cdot \frac{E'}{3(1-2\nu')} \tag{3.2}$$

where E' and ν' are, respectively, Young's modulus and Poisson's ratio, and γ_w is the pore fluid unit weight.

The same remarks apply for the coefficient of volume change, discussed in next item. For the case of isotropic elasticity, it is expressed as follows:

$$m_{v,1} = \frac{(1-2\nu')(1+\nu')}{E'(1-\nu')} \tag{3.3}$$

$$m_{v,3} = \frac{3(1-2\nu')}{E'} \tag{3.4}$$

For $\nu' = 0.5$, both compressibility parameters are equal to zero and both consolidation coefficients tend to

infinity, but for the rather more realistic value of 0.25, for example, the tridimensional volume change coefficient is about 80% higher and, the tridimensional consolidation coefficient is roughly 40% lower than their corresponding one-dimensional versions.

(ii) Compressibility

Coefficients of volume compressibility, as obtained from oedometer tests (DAVIES, 1972) and triaxial consolidation tests (SOIL MECHANICS LTD. 1971), have been plotted in figure 3.14. Their values vary between 0.45 and 0.03 m^2/MN, decreasing with depth and with increasing average effective stresses. The unexpected increase in m_v shown in figure 3.14 at low stress levels has been attributed to a structural breakdown provided by the presence of ironstone inclusions in the samples (DAVIES, 1972), taken from shallow levels; another possible mechanism capable of explaining such a behaviour would be: at very low stress levels, volume changes are mainly due to consolidation of individual lumps, whereas at stresses which induced higher compressibility coefficients, shear distorsions associated with local collapse of inter-lump contacts might have added their effect to volume change due to consolidation.

(iii) Permeability

Triaxial consolidation tests (SOIL MECHANICS LTD., 1971), performed under cell pressure of 400 kN/m^2, resulted in coefficients of permeability of just over 1.0×10^{-10} m/sec between 10 and 20 metres.

Consolidation tests (DAVIES, 1972) under vertical stresses of 25 to 200 kN/m^2 resulted in permeabilities diminishing from 5 to 1 x 10^{-11} m /sec, in good agreement with triaxial results.

A series of in-situ permeability tests were carried out before construction started and their results are shown in figure 3.15. They were of two types: constant head tests and rising head tests. In the constant head tests, the water pressure applied was always positive, inducing a reduction in effective stresses and, therefore, soil swelling. Rising head tests, on the other hand, were characterized by negative water pressure, increase in effective stresses and consolidation. Consistently, rising head tests resulted in lower coefficients of permeability than in the case of constant head tests, an indication of a significant reduction in permeability with increasing effective stresses. In figure 3.15, results of various in-situ permeability measurements are plotted against depth; they show considerable reduction in permeability with depth, but this variation may be the consequence of either increasing effective stresses or differential soil disturbance due to geological causes, or more likely, both effects combined. The figures involved vary from 10^{-10} to 10^{-9} m/sec near the top of the Lias and from 10^{-12} to 10^{-11} m/sec twenty metres below, in general agreement with laboratory test results above quoted.

3.4.9 Fill Properties

At the contract design stage, the likely properties of the fill were uncertain, and parameters used in the initial

design were based on the results of a few laboratory tests on samples dynamically compacted in laboratory or taken from the embankment built for river diversion.

Quick undrained tests ($\dot{\epsilon}_1$ = 2% per min.) on laboratory compacted samples and also on undisturbed samples taken from the river diversion embankment, under cell pressures of 250 kN/m^2 (VAUGHAN, 1972), resulted in an average c_u of 94 kN/m^2.

Drained triaxial tests on samples recompacted to Proctor effort (SOIL MECHANICS LTD., 1971) led, as expected, to strength parameters similar to those found for undisturbed soil: c_d = 10 to 20 kN/m^2 and ϕ_d = 20 to 24°.

Combination of above mentioned parameters for undrained and drained strength, together with assumed A_f values of 0.3 to 0.5, leads to pore pressure ratios r_u between 0.6 to 0.8 under all-round conditions. In the dam, mean normal stresses are expected to be lower than apparent overburden pressures and, therefore, a lower r_u value is predictable. Some all-round pressure tests were carried out (SOIL MECHANICS LTD., 1971) and resulted in B = 0.7 to 0.9, but the samples tested exhibited exceptionally high water contents and approached full saturation, more severe conditions than forseen for the real embankment.

3.5 THE ADOPTION OF A 'DESIGN-AS-YOU-BUILD' APPROACH

BISHOP and GREEN (1973) list a series of problems

faced by a dam designer which are not amenable to standard procedures of testing and analysis, and whose further clarification and solution require the adoption of expensive and time-consuming techniques of special sampling and laboratory or in-situ testing as alternatives to very conservative design.

Among the problems cited by those authors are those relating to sampling and testing of brecciated or fissured overconsolidated plastic clays, the possibility of progressive failure involving a soil of high brittleness index, the interaction of two or more soils of different stress-strain characteristics, etc. These sorts of problems were present at Emgingham and, in addition to them, the time available for the design did not leave room for a programme of large in-situ tests and laboratory tests on large-scale specimens of various orientations.

Constructing an instrumented trial bank may be a useful option in cases such as these, but this solution too is in general costly and causes delays to construction.

At Empingham, the designers resorted to the adoption of a provisional design based on optimistic assumptions,

trial bank (figure 3.3). During the first year of construction, the works would follow this provisional design and, at the same time, the trial embankment would be built, observed and analyzed. The results of the trial bank measurements and the observation of the initial behaviour of the dam itself along the first year of construction

would be coupled with laboratory and in-situ tests and several forms of analysis (non-linear limit equilibrium, non-linear finite element, etc.), to produce the final version of the design.

The advantages of such an approach are self-evident. Cost increase brought about by the trial bank was kept to a minimum by enclosing it in the dam section. Total cost and safety were better preserved by sophistication in analysis, special testing and observations of prototype and model behaviour. Delay was averted. Opportunity for applied research and the consequent improvement in the knowledge of the Upper Lias Clay properties was also to be included among the advantageous aspects of the approach adopted.

Details of the trial bank design and the description of its instrumentation will be presented in subsequent chapters, along with the description of its performance, analyses of the results and conclusions arisen from these and other measurements performed during the two initial years of the Empingham Dam construction.

3.6 INITIAL DESIGN ASSUMPTIONS

With basis on the findings of the site investigation, the more conservative preliminary design was drawn with short berms (figure 3.3), corresponding to optimistic assumptions, and the contract let accordingly; provisional berms were included, but their extent was to be decided four months after the completion of the trial embankment.

The assumptions adopted in the initial design are summarized as follows:

(i) Foundation undrained strength

An undrained strength c_u of 30 kN/m^2 was assumed for the top of the Upper Lias Clay, increasing with depth at a rate of 3.5 kN/m^3 so that at 20 metres it would be 100 kN/m^2.

(ii) Foundation strength in terms of effective stresses

Zero cohesion intercept and a friction angle of 18° characterize the failure envelope adopted in the preliminary design. A factor of safety of 1.3 gave a mobilized strength of $c' = 0$ and $\phi' = 14°$. This was subsequently reduced to $c' = 0$, $\phi' = 14°$ and mobilized $\phi' = 11°$ for part of the foundation where numerous emergent shears were noticed when the foundation was stripped.

(iii) Consolidation of the sand drain area

A coefficient of consolidation $c_v = 0.25$ m^2/year (0.79×10^{-2} mm^2/sec) was adopted and the sand drains designed to give a pore pressure ratio ($r_u = u/\gamma.h$) of 0.7 at the end of construction. An average value of c_v of 1.5 m^2/year (4.8×10^{-2} mm^2/sec) would give 80% consolidation during construction, and, since the design could be revised to take advantage of more rapid consolidation, the sand drain installation would only become innefficient if this value were substantially exceeded.

(iv) Fill properties

In view of large uncertainties about the predictable fill properties existing at the time of the provisional design, conservative assumptions were adopted for calculating the active thrust exerted upon the shoulders and the maximum section: $\phi' = 22^{\circ}$, $F_s = 1.5$, mobilized $\phi' = 15^{\circ}$, $r_u = 0.6$. This is equivalent to a mobilized shear strength of approximately 40 kN/m^2. Elsewhere and in the berms, a mobilized stress of 50 kN/m^2 was assumed.

Drainage blankets were designed for the central fill to ensure that the design assumptions were met regardless of the properties of the fill as placed.

C H A P T E R _ F O U R

THE DESIGN OF THE TRIAL BANK

4.1 Reasons for the Construction of the Trial Bank

4.2 Advantages and Disadvantages of the Approach

4.3 The Characteristics of the Trial Bank

4.4 Instrumented Sections

4.5 Aims of the Trial Bank Experiment

CHAPTER FOUR

THE DESIGN OF THE TRIAL BANK

4.1 REASONS FOR THE CONSTRUCTION OF THE TRIAL BANK

The basic features of the dam design are discussed in Chapter Three. Limit equilibrium methods were used to analyse this section and to determine the required dimensions. The principal soil parameters required for these analyses were:

(1) the reliable bulk undrained strength of the foundation;

(2) the reliable bulk drained strength of the foundation;

(3) the rate of consolidation of the foundation, and

(4) the strength and other properties of the fill.

In addition, the application of limit analysis was subjected to the uncertain effects of progressive failure.

The solution adopted to allow the contract to be let on schedule was as follows. Two designs were prepared, one based on pessimistically assumed soil properties and the other on more optimistic ones. The difference between the two sections was restricted to the extent and thickness of the berms (figure 3.3). Provisional internal drainage blankets were also included.

The contract was let on the basis of the more optimistic design, with provisional items covering the extension of the berms and the internal drainage blanket. It was stated in the contract that the final berm size and number of drainage blankets could be decided after the first year of construction.

Under normal circumstances, during the first year's construction, observations could be carried out of (1) the pore pressure developed in the limited fill height and the rate of its dissipation during the winter stoppage, and (2) the early rate of consolidation in the foundation due to sand drains.

It has been shown (SODHA, 1974) that properties of compacted clay fills cannot be predicted from tests on laboratory compacted specimens but can be predicted from tests on samples taken from field compacted material. Thus, samples could be taken and tested during the first year's placing.

There was limited evidence concerning the properties of the Upper Lias Clay from previous engineering works, and the programme for completion of the scheme did not allow further time for more detailed site investigation. There was scarce and somewhat conflicting informations on the undrained and the drained strength of the foundation. No information was available on the possible influence of progressive failure.

Accordingly, it was decided to build a trial bank within the upstream berm of the dam, so that, whatever design

alternative was adopted, it would form a part of the main embankment

4.2 ADVANTAGES AND DISADVANTAGES OF THE APPROACH

The approach chosen has advantages and disadvantages (VAUGHAN, WERNECK and HAMZA, 1973) which can be summarized as follows:

(i) Advantages

a) By building a very steep temporary bank within the upstream berm, a relatively large volume of clay could be subjected to shear stresses higher than those beneath the eventual structure.

b) This could be done at slightly extra cost, as the fill would form part of the final embankment.

c) Since only a small proportion of the final foundation embankment would be weakened by post-failure movements, failure of the trial bank foundation could be tolerated.

d) The reliable bulk undrained strength of the foundation could be deduced from total stress analyses and, using observed pore pressures, reliable bulk drained strengths could be deduced from effective stress analyses. While a further programme of large in-situ tests could have been used to examine undrained strength, the volumes of clay tested would still have been relatively small, and reliable bulk drained strength could not be determined from in-situ tests.

e) The behaviour of the trial bank could indicate the significance of the progressive failure mechanism.

f) The performance of the embankment would provide data from which the bulk stress-strain behaviour of the fill and foundation could be inferred.

g) Instrumentation techniques could be tested and experience gained at an early stage of construction.

(ii) Disadvantages

a) The base of the valley was narrow, and thus it was not possible to build a trial bank of sufficient length for conditions to be two-dimensional.

b) The bulge zone in the valley floor, over which the trial bank would have to be built, had properties unrepresentative of the general foundation.

c) The restricted area of foundation tested by the trial bank might not be representative.

d) The trial bank had to be much steeper than the main dam for it to impose comparable shear stresses. Thus conditions in the trial embankment would be not directly comparable to those in the dam. The shape and length of potential failure surfaces, and the effects of anisotropy, etc., could be different.

e) Analysis would be complicated by the major difference between the undrained strengths of the fill and the

foundation.

f) The measurements required represented an additional heavy load on the site staff at a time when foundation treatment, the installation of sand drains, etc., were going on. The programme for the construction of the trial bank was controlled by general construction requirements and there was little freedom to adjust it to suit the needs of accurate measurement. Thus it had to be accepted that the number and the accuracy of measurements which could be made would be limited.

4.3 THE CHARACTERISTICS OF THE TRIAL BANK

The design of the trial bank was adjusted as ground stripping disclosed the foundation conditions. Its configuration, as constructed, is shown in figures 4.1 through 4.4. The principal features are:

(1) The bank was shifted to the South, to avoid the bulge zone, which ran slightly to the North of the valley centre at this point.

(2) A trench was cut into the south slope and the crest of the bank was formed with a longitudinal slope, so that the height from trench base to crest was approximately constant for a length about three times the bank height. While the section of the bank was not constant, it was hoped that this would give behaviour sufficiently close to two dimensional plane strain conditions for

two dimensional methods of analysis to be valid.

(3) The outer slope was originally intended to be 2:1. When the initial behaviour showed very large strains restricted to the outside of the embankment a berm was formed to ensure that early failure was avoided and that yield occurred further from the bank toe.

(4) The inner (downstream) slope was made flatter and was progressively supported by the main embankment fill. Thus downstream movement was effectively prevented.

With the undrained strength of the fill and foundation assumed equal to the initial design assumptions, limit analyses showed that the factor of safety of a trial bank 20 m high was approximately one. Linear finite element analyses (NAYLOR, 1972; HAMZA, 1973) showed that the design strength of the foundation could be exceeded (no limit strength values were imposed to the stress-strain models used in such analyses).

During the early stages of construction it was found that the fill was rather stronger than originally assumed. However, the finite element analyses confirmed that the design foundation strength would be reached over the full width of the embankment foundation.

A drainage blanket of gravel 200 mm thick was placed on the foundation beneath the trial bank.

Since the trial bank was not uniform along its

length it was decided to spread the instrumentation over three cross-sections as shown in figures 4.1 to 4.4.

4.4 INSTRUMENTED SECTIONS

Figure 4.1 pictures the highest of the three instrumented sections, at Chainage 537. Its crest lies over 22 metres above the lowest point of the stripped ground level.

The inclination of the lower slope is 45% (i.e 24° or 1:2.2), but the average overall inclination, from toe to crest, is only 33% (18° or 1:3.0).

Figure 4.2 portrays the instrumented section at Chainage 514, where the trench excavated as an extension to the fill slope can be seen. Its final height was roughly 21 metres above the trench base. Inclinations were 45% (24° or 1:2.2) for the lower part and 36% (20° or 1:2.8) for the whole slope.

In figure 4.3, section at Chainage 487 is depicted. On completion, its crest lay 17 m above the lowest fill level and 20 m above the trench bottom. Lower slope was 37% (20.5° or 1:2.7) and average inclination 32% (17.5° or 1:3.1).

4.5 AIMS OF THE TRIAL BANK EXPERIMENT

The trial bank experiment as a whole represented a large-scale test for the brecciated Upper Lias Clay, both as foundation material and as compacted fill. It would therefore be a

combined check for the reliability of design parameters, analyses employed and constructional procedures, all factors put together.

Separate examination of some parameters and analysis techniques were also possible and, this way, interpretation of results and their use in prediction of the main dam behaviour were facilitated.

The trial was intended to furnish directly the following data:

(1) horizontal and vertical movements of some selected points within the foundation and the fill as well as on the slope, at various stages of the trial bank construction and after final completion;

(2) pore pressure developed within the foundation and the fill, throughout trial bank construction, and its rate of dissipation during stoppages.

From measured quantities, straighforward calculations would lead to other useful additional data:

a) linear strains;

b) shear strains;

c) pore pressure ratio $r_u = u/(\gamma.h)$;

d) coefficient of consolidation c_v;

e) fill undrained compressibility in terms of vertical stress $m_v = \epsilon_v/(\gamma.h)$.

Use of measured and calculated parameters combined

with conventional techniques of limit equilibrium analyses would permit the establishment of a lower limit for reliable average undrained strengths of both fill and foundation. Limit analyses in terms of effective stresses would allow an estimative of the reliable drained strength of the foundation.

It was hoped that pore pressure measurements coupled to finite element predictions of total stresses would allow approximate determination of:

a) pore pressure parameters A and B;

b) effective stress paths;

c) strength envelope parameters in terms of effective stresses: c' and ϕ'.

The use of finite element predictions for displacements and strains could be compared to observed profiles; elastic parameters and initial stresses in computational procedures could be adjusted so as to result in a reasonable agreement of both sorts of curves. Such a technique would allow an indication of:

a) deformation moduli for fill and foundation and its variation with stress level, strain magnitude and spacial location;

b) coefficients of horizontal earth pressure at rest K_o;

c) Poisson's coefficients for fill material ν_b;

d) stress-strain curves for materials involved.

Piezometers installed could be used for in-situ permeability and hydraulic fracture tests, in order to determine:

a) coefficient of permeability k;

b) minimum total stresses, both in the fill and the foundation, a check for finite element predictions.

Measurement of displacements and calculation of strains corresponding to various fill heights could be coupled to values for factors of safety obtained from some limit equilibrium stability analysis method and therefore provide a means of monitoring the behaviour of the final works.

Last, but by no means least, installation and operation of various sorts of instrument would permit cross-checks of their performance, resulting in gain of real experience with their use and better assessment of amount and type of instrumentation to be designed for the main dam and similar jobs.

C H A P T E R _ F I V E

THE TRIAL BANK INSTRUMENTATION

5.1 Instrumentation Installed

5.2 Inclinometers

5.3 Settlement Magnets

5.4 Hydraulic Settlement Gauge

5.5 Horizontal Movement Magnets

5.6 Wire Extensometer (Rod Gauges)

5.7 Surface Reference Points

5.8 Piezometers

C H A P T E R F I V E

THE TRIAL BANK INSTRUMENTATION

5.1 INSTRUMENTATION INSTALLED

Figures 4.1 to 4.3 show the devices installed at the three instrumented sections. Table 5.1 summarizes the amount of each at every particular cross-section and includes the surface reference points installed on the fill slope and trench; these are seen in figure 4.4 and, some of them, also in figures 4.1 through 4.3.

TABLE 5.1

Amount of Instrumentation Installed

DEVICE	LOCATION	CHAINAGE (m)				TOTAL
		487	514	537	Others	
Inclinometer	found. fill	56 m 21 m	- -	44 m 22 m	- -	100 m 43 m 143 m
Settlement magnets (inclinometer tube)	found. fill	17 6	- -	14 6	- -	31 12 43
Wire extensometer plates	found. fill	7 4	7 4	7 4	- -	21 12 33
Horiz. movt. magnets	found.	4	-	5	-	9
Hydr. settlement gauge	found.	100 m	-	110 m	-	210 m
Surface reference points	slope trench	2 -	3 1	3 -	5 2	13 3 16
Survey reference data	outside	1	1	1	-	3
Hydr. piezometers	found. fill	8 -	- -	4 4	- -	12 4 16

At Chainage 487, portrayed in figure 4.3, a scaffolding was built across the trench in order to carry extensometer wires and hydraulic settlement ducts, to the reference datum located on the opposite side to the trial bank.

Detailed descriptions of devices used in the observation of pore pressures and displacements in the trial bank as well as of those instruments employed in field measurements of soil properties are included in this chapter. They may be briefly summarised as follows:

Inclinometer tubes were metallic, in sections 3 metres long, surveyed by a Wilson's Slope Indicator series 200 B.

Twin-tube hydraulic piezometers had coarse tips, in general, but those in the fill or near the foundation top were supplied with high air entry value ceramic tips.

Settlement magnets, externally attached to inclinometer tubes, had their levels periodically surveyed by means of a probe containing reed switch sensors.

Wire extensometer steel plates were buried in the foundation top and connected to outside through wires running freely inside plastic ducts; saw cuts on each wire were periodically compared to reference marks on a concrete slab.

The hydraulic settlement probe was a sealed system capable of measuring settlements from the variation of pressure caused by increase in level difference between surveyed points

and a reference level outside the bank.

Surface reference points were surveyed by conventional methods as well as by Tellurometer MA-100, a short-range Electronic Distance Measuring (EDM) device.

Horizontal movement points were plates embedded in the foundation, around the tube used for the hydraulic settlement probe, detectable by an inductance coil probe, coupled to the hydraulic one and connected to outside through the same cable. These were used to check the location of the settlement probe within the tube.

5.2 INCLINOMETERS

Nowadays, these devices are extensively used in precise determinations of horizontal movements of foundations, natural slopes, excavations, embankments and even concrete or steel structures.

Various sorts of inclinometers have been described in recent years (e.g. WARD, 1965; WILSON, 1959, 1962; KALLSTENIUS and BERGAU, 1961; SHANNON et al, 1962; SIMON et al, 1968; GREEN 1969, 1973; MURRAY and IRWIN, 1970; BROMWELL et al, 1971; PEIGNAUD and PERRIN, 1973; PHILIPS and JAMES, 1973) and by now there is quite a considerable literature on the subject. Most of these apparatuses consist essentially of plastic or metallic casings coupled on site and backfilled into boreholes put down in earth masses (or built up as placing of fill proceeds), their interior being period-

ically surveyed by means of a tilt measuring probe lowered into the ducts guided by grooves or rails in the casing while hanging from cables connected to a read-out unit outside the hole. Inclinations measured at convenient intervals are integrated to produce inclinometer profiles. Repetition of the procedure from time to time enables horizontal movements to be calculated by difference.

At Empingham Dam trial bank casings consisted of epoxy-coated extruded aluminium alloy tubes, 3.05 m (10 ft) long and 76 mm (3 in) dia., gap-jointed by means of wider couplings weakly riveted to the main ducts, so as to allow for vertical sliding of the tubes inside the couplings after soil vertical movement had caused the rivets to shear.

Inclinometer tubes were placed in purpose-made boreholes, sunk to levels around 20 m below stripped ground surface and then backfilled with a mixture of cement and bentonite via a tremie pipe. As fill was placed the tubes were protected by short steel tubes, 250 mm dia., which were progressively withdrawn, the space around the inclinometer tubes being filled with coarse dry sand.

To prevent grout or sand entering the tubes and thus creating obstacles to free lowering of the torpedo, all joints were sealed with greased tape prior to backfilling.

To make sure that the probe always kept the same orientation as it was lowered inside the well, the tubes had four grooves, 90 degrees apart, used in guiding the torpedo wheels during

operation. The slightly wider couplings had also similar grooves, kept parallel to the others, so that the probe could easily track across the joints.

The angle measuring device utilized was a Wilson's Slope Indicator, series 200 B, manufactured by Slope Indicator co., Seattle, Wash., USA, maker's number 200 B/59, owned by Imperial College. This apparatus was submitted to an extensive testing in laboratory environment a few years ago (GREEN, 1969, 1973) and has been described earlier in some papers (e.g. SHANNON et al, 1961; WILSON, 1962; WILSON and HANCOCK, 1965). It consists of a water-tight torpedo, machined from solid aluminium alloy, enclosing a pendulum whose inclination with respect to the probe axis is measured by means of a contact, mounted in the pendulum tip, which divides a curved resistance element into two portions of length proportional to the tilting angle. These two resistances, together with other two enclosed in the read-out unit outside the hole, form a Wheatstone bridge circuit, whose balance is ensured by a manually adjustable rotary potentiometer fitted with a three-figured dial. The system is energized by four 6-volt dry-cell batteries contained in the instrument box.

The pendulum, enclosed in an oil-filled chamber, is allowed to swing in a ± 15 degrees range, on a unique plane, protected by rubber stops. Its contact with the resistance element is ordinarily open, the circuit being only actuated by a remote-controlled relay, what prevents any friction before the pendulum

comes to rest, provided that brinelling of the contact does not occur. Another possible source of friction is the support, where contamination of the two ball bearing pivots can cause erratic readings.

The torpedo is guided along the well grooves by two fixed wheels, 305 mm (12 in) apart, running on sealed, oil-filled ball bearings, while another pair of wheels, just opposite to them are forced by springs to maintain contact with the opposing slots.

The probe is connected to the read-out unit by a specially fabricated robust electrical cable with a stranded steel core and a neoprene rubber cover. Coloured markings at 305 mm (12 in) intervals on the cable enable the probe to be always positioned at the same level, if vertical movements of inclinometer ducts are controlled or absent. Provided that the torpedo does not stick in the hole, when a great effort would be necessary to pull it up, axial forces due to the probe's and cable's weight do not appear to cause any important stretch in the cable.

On the top of the inclinometer a pulley-wheel guides the cable and makes it hang approximately in the centre of the well. A jam-cleat attached to the pulley-wheell acts as a safety device against fall of the probe inside the hole and permits the readings to be taken by a single operator, in addition to providing a reasonable reference for control of the depth at which measurements are to be taken.

Measurements are usually the result of averag-

ing two paired readings taken in opposing grooves in order to annul face errors. This technique minimizes errors due to imperfections in the casing surfaces when positioning of the apparatus at identical level of previous measurements proves impossible and immediately detects any gross errors caused by instrument defects or human fault.

The sensitivity of the instrument is of one dial unit, the correspondence being 35 units to 1 degree, approximately, what leads to a precision, in each individual reading, of less than 2 minutes of arc, i.e 5.5×10^{-4} rd of 0.05%. The manufacturers, however, quote more conservative values in their promotional literature: 3 minutes of arc, corresponding to nearly 1×10^{-3} rd or 0.1%.

5.3 SETTLEMENT MAGNETS

Around inclinometer ducts, both in the foundation and in the fill, magnetic rings loosely attached to them at intervals of approximately 3 metres, could move vertically in conjuction with the surrounding material, their levels being periodically surveyed by means of a probe containing a reed switch sensitive to a magnetic field, lowered inside the tubes while hanging from the end of a graduated steel tape (BURLAND et al, 1972; BURLAND and MOORE 1973), thus permiting the calculation of absolute settlements with respect to a fixed reference and the determination of average linear strains between two neighbouring magnets.

Relative movements of a settlement ring with

respect to the others were partly due to the ability they had to slide along inclinometer tube walls and partly to closure of gaps between consecutive duct lengths after coupling rivets were sheared.

The probe utilized to survey magnet levels, manufactured by Soil Instruments Ltd., London, was covered by a hard plastic co-axial weight, designed to keep the steel tape straight and to force the probe axis to be permanently centred in the inclinometer wells during operation.

Precision of settlement measurements carried out in the conventional way is claimed by the makers to be 2.5 mm; if required, much greater accuracy may be achieved, by lowering the probe on rods attached to a vernier winding mechanism at the top of the borehole, when movements as small as 0.25 mm can be measured, again according to maker's promotional literature. GOULD and DUNNICLIFF (1971) have pointed out that although the electrical sensitivity of such a system is only in the order of 0.5 mm, accuracy in real distance measurements drops to ± 3 to 6 mm; if steel tape stretch occurs, it obviously worsens even further. BURLAND and MOORE (1973) and BURLAND et al (1972) have stated that magnet locations may be detected to an accuracy of 1 to 2 mm, which would give to each individual distance measurement, obtained by difference between two successive level observation, an accuracy of 2 to 4 mm.

BURLAND et al (1972), claim, however, that by keeping a permanent datum rod or tape in the access tube with a reed

switch mounted opposite each magnet and using precise measurement of the small axial datum movements required to reestablish the balance broken by displacement of the magnet, accuracy of 0.05 mm can be achieved.

5.4 HYDRAULIC SETTLEMENT GAUGE

After the ground surface had been stripped by some 3 metres, three square-sectioned trenches, approximately 1 metre deep, were excavated along the full width of the planned trial embankment at chainages 487, 514 and 537; systems of both horizontal and vertical displacement measurements were then installed in them and, finally, the trenches were backfilled with dry coarse sand.

Among the instrumentation embedded in these purpose-made trenches were two flexible polythene tubes, at chainages 487 and 537, designed to function as access tubes for the hydraulic settlement gauge schematically seen in figure 5.1.

The hydraulic settlement probe consisted basically of a chamber where a rubber ballon was externally in contact with atmosphere through a PVC tubing, called the 'air line' in figure 5.1, while internally linked to a pressure transducer, placed outside the bank, by means of a sealed nylon conduit permanently filled with deaired water; variations in level of the probe induced changes in negative water pressure along the 'water line', measured by the transducer, comparison of suction recorded on different occasions for a

same point gave the settlement experienced by it during the time elapsed between the readings.

Both 'air' and 'water' lines were contained in a cable that connected the probe to a drum outside the bank, around which it was reeled. Every time a set of measurements was to be taken, the drum was located at the reference datum spot, where it rested on a frequently surveyed concrete slab. The probe was inserted in the access tube, being pulled by an operator at the opposite side of the embankment by means of a terrylene cord attached to the probe. Movement was interrupted at selected points so that water pressure measurements could be made. Knowledge of reference datum elevation and of differences in level between it and chosen points at the foundation top enabled horizontal profiles to be drawn and corresponding settlements calculated for various fill heights.

To ensure that positions of observed points were correctly recorded in each set of measurements so that settlements could be properly worked out, two systems of control were provided. Firstly, a graduated steel tape, reeled around a drum coaxially attached to the cable reel (figure 5.1), was connected to the probe as it was inserted in the access tube; every time a measurement was made, distance from the datum, as given by reading of the tape, was also recorded. Secondly, there were some magnetic plates beforehand placed around the ducts, detectable by a second probe, of inductance coil type, acting adjacently to the hydraulic one; this system, which will be described later, was primarily designed as a horizontal move-

ment measuring device, but it was solely used as a means of controlling the location of each individual settlement measurement point on different occasions even when this point had experienced lateral displacement.

The maximum difference in level between a measuring point and the pressure transducer is limited by cavitation problems, but an adaptation to the system that would avoid this difficulty would consist of adding to the scheme a source of constant air pressure to be connected to the probe chamber; this air pressure should be chosen so as to keep the entire 'water line' under positive pressure, thus avoiding cavitation and the undesirable negative range for the pressure transducer.

The makers, Soil Instruments Ltd., London, claim a sensitivity of 3 mm for each individual observation with the normal version of the instrument and a total range of settlement measurements of 3 metres.

DUNNICLIFF (1971) classifies this sort of device as a 'full profile' settlement gauge, but the particular type he names 'balloon type' differs considerably from the Soil Instrument's apparatus, inasmuch as that instrument (BERGDAHL and BROMS, 1967) uses air under slowly increasing pressure inside the balloon and relies upon the change in level of the open 'water line' to detect the moment when expansion of the balloon signs the establishment of equilibrium between air and water pressures. Both sorts of equipment,

however, present some common problems, such as the variation of water density with temperature, what implies the need for correction of each individual reading, and the impossibility of taking measurements below freezing point unless water is replaced by some other fluid. For a revised version of the 'air-inside-the-balloon' apparatus, GOULD and DUNNICLIFF (1971) found an accuracy of 5 mm in cases when difference between ambient and subsurface temperatures does not exceed 20°F (11°C), but in hot weather, differential temperatures coupled to insufficient time allowed for equalization may cause precision to drop to up to ± 50 mm for severe temperature differences of 80°F (44°C). Comparisons with settlements measured by other means have shown an accuracy of ± 25 mm in observed settlements at a site in Massachussets, USA, according still to the same source, and this is also the upper limit quoted by DUNNICLIFF (1971) in his Table 6.

5.5 HORIZONTAL MOVEMENT MAGNETS

As mentioned in previous item, aluminium plates containing magnetic rings were buried in two purpose-made trenches, at chainages 487 and 537, around ducts to be used for the hydraulic settlement gauge. These magnets could be detected by an inductance coil probe (figure 5.1), contiguous to the hydraulic settlement one, and the reading of the graduated steel tape gave the horizontal position of every plate at each particular time; successive sets of readings were planned at different fill heights, so that curves of horizontal displacements versus fill heights could be plotted for

each individual plate.

The sensing unit consisted of a coil forming the active arm of an inductance bridge, thrown out of balance every time the probe approached a steel plate's magnetic field; at the read-out box, placed at the reference datum spot, by the cable reel, a needle deflected as a result of the imbalance, and the position corresponding to maximum deflection was recorded as representative of the plate position.

Precision quoted by the makers, Soil Instruments Ltd., London, was 8 mm, but PENMAN (1969) claims to have achieved far better accuracy, in the order of 2 mm, by averaging readings of a similar device taken at 50% maximum deflection as it both rose and fall.

GOULD and DUNNICLIFF (1971) point out that, although the electrical sensitivity of such a system is the same as in settlement gauges, as low as 0.6 mm, the real overall accuracy in distance measurement to each plate is significantly less in horizontal tubes than in vertical ones, a maximum of 25 mm having been quoted by DUNNICLIFF (1971). This is possibly due to larger lengths in general involved, greater difficulties in keeping the tape straight and the use of different traction forces in various readings.

At Empingham site, access tubes ran along the entire length of the embankment and cords attached to the probes were used to pull them from an observation point to the next. This

system can be employed in most road embankments, but in dams, quite apart from difficulties arising from large dimensions normally encountered, this two-open-ends scheme obviously cannot be employed during impounding and operation, and it is not advisable to create a preferential path for a possible leakage from the reservoir; in cases like this, a blank ended tube is installed, accessible only from downstream, and a system for insertion and removal of the probes has to be devised. At Scammondem Dam, north of England, (PENMAN and MITCHELL, 1970), for instance, lateral displacements were measured by means of a horizontal magnetic gauge coupled to a hydraulic settlement 'overflow type' gauge, based on a similar instrument used at Gepatsch Dam (LAUFFER and SCHOBER, 1964), but the probes were driven to the inner end of the access tunnel by a duct motor, actuated by compressed air, an apparatus originally developed by British Post Office for threading telephone wires along ducts (DEADMAN and SLIGHT, 1965). An experiment was carried out at Empingham in which a pulley was placed at the end of a tube and the attempt was made to pull the probe through by a cord passing round the pulley and back to the open end of the tube. This was unsuccessful as the cords became twisted in the tube.

To insert the probe in the tubes the following procedure was adopted: initially, a rag attached to fishing line was blown through the ducts; the fishing line was then used to pull the terrylene cord through.

As the main embankment fill was raised, the

inside (downstream) ends of the settlement tubes had to be bent up so that access to them could be maintained.

5.6 WIRE EXTENSOMETER (ROD GAUGES)

Other instruments buried in the trenches mentioned in the two previous intems, were wire extensometers, devices also called 'rod gauges' throughout this thesis.

They consisted of six conveniently spaced vertical square steel plates (305 mm x 305 mm x 25 mm) in each of the three instrumented sections, connected to outside through high tensile steel wires, 6 mm dia., capable of sliding freely within telescopic plastic pipes (VAUGHAN, 1974); saw cuts near the free ends were usually once or twice a day compared with frequently surveyed reference points cast in concrete slabs, the same used as bases for the hydraulic settlement cable reel.

In addition to steel plates, numbered H1A through H1F, at chainage 537 (figure 4.1), H2A through H2F at chainage 514 (figure 4.2) and H3A through H3F at chainage 487 (figure 4.3), three concrete blocks (H1X, H2X and H3X) were placed at junctions of the bank slope with the stripped ground surface, one at each instrumented section, and linked through steel wires to the reference concrete bases; they were so incorporated to the rod gauges system and their tops (S1X, S2X and S3X) could also be surveyed by conventional and EDM methods to provide a check for both sort of measurements.

By difference, average horizontal strains could be calculated for each pair of adjacent plates (or plate-block).

When the fill reached approximately one-half of the planned bank height, three new lines of wire extensometers were added to the instrumentation scheme. Each set comprised three plates (H1G to H1J, H2G to H2J and H3G to H3J, figures 4.1 through 4.3) plus a reference point cast in concrete (H1Y $\equiv$ S1Y, H2Y $\equiv$ S2Y and H3Y $\equiv$ S3Y), used as a target for levelling and EDM surveying.

A system of rod gauges similar to that herein described has been successfully used at Kainji Dam, Nigeria (as mentioned by PENMAN and CHARLES, 1973) and also Backwater Dam, in Scotland; in the latter, it has been mentioned (GEDDES et al, 1972) that, although crude, observations of such devices were clear enough to indicate upstream and downstream core movements depending on which side earth filling was taking place. Neither of the two papers cited any information on precision or accuracy of the system, but, the most important sources of errors in this sort of instrumentation are: initial misleading movement observations due to initial adjustment of steel plates in the sand trench; changes in wire paths during construction due to embankment and foundation movements; damage or displacement of reference marks on concrete slabs; temperature effects causing wire length change; difference in tension used to pull the rods at various readings, and arching of the sand in the trench. It may be noted that when the system is extending the wires are self-tensioning. Vertical movements cause only small errors, provided the settlement profile is uniform. A discontinuity may

produce a 'kink' in the system and cause a major error; this occurred in the trial bank at Ch. 537. Apart from this, experience at Empingham suggested a repeatability of the order of 5 mm if readings were taken at approximately the same hour every time.

5.7 SURFACE REFERENCE POINTS

Figure 4.4 portrays a plan of the surface reference targets located on the trial bank slope, the trench slope and the trench bottom. These targets comprise the standard reference points S1 to S10, whose sole purpose was to assist the monitoring of superficial settlements and horizontal displacements, the reference datum points D1, D2 and D3, the tops of concrete blocks associated to the rod gauge system, named S1X, S2X, S3X, S1Y, S2Y and S3Y, and the tops of four inclinometer tubes I1 through I4.

These points were frequently levelled and surveyed by both conventional and EDM procedures from benchmarks located outside the influence area of the embankment.

The EDM equipment used was the Tellurometer MA-100, a short-range instrument, capable of measuring distances up to 2 km with an accuracy claimed by its manufacturers to be characterized by a standard error of 1.5 mm at short ranges, increasing to 5 mm at 2 km. PENMAN and CHARLES (1971) attributes to this apparatus an expected accuracy of 3 p.p.m. $\pm$ 0.1 mm.

The Tellurometer MA-100 consists essentially of

a single tripod-mounted package containing the optics, the associated electronics and the read-out, whereas passive reflectors, mounted on targets whose movements are meant to be measured, complete the system. The source of radiation is a gallium arsenide diode emitting in the near infra-red which is modulated by measuring frequencies of about 75 MHZ. Prism reflectors at the targets reflect the beam, which returns to the instrument to be detected by a silicon photo diode. The distance measurement between the tripod and the various surface reference points are obtained by comparing the modulation phase of the transmitted signal with that of the received signal and is displayed under digital form at the read-out. Detailed description of Tellurometer MA-100's main features and achievements may be found in promotional literature or in some written works (e.g. HOLSCHER, 1969; JAAKKOLA, 1971).

As for the conventional levelling, usual procedures adopted at Empingham, should ensure a precision of ± 10 mm, although careful surveying coupled to the adoption of a closed circuit and distribution of errors in proportion to square root of distance might have cut it to half or one-third.

5.8 PIEZOMETERS

Piezometers locations at Empingham trial bank are shown in figures 4.1 and 4.3. They were hydraulic twin-tube water pressure cells in general with coarse porous tip surrounded by cylindrical sand pocket, but those placed in the fill or in upper

layers of the foundation, where negative pore pressures were expected - and in fact recorded - as a consequence of partial saturation (fill) or swelling due to stress relief (foundation), had high-air-entry-value Bishop-type conical ceramic tip buried in small quantities of plaster of Paris so as to prevent the trapping of air voids between cells and bore walls, which would cause delays in response time.

All piezometers were linked to an instrument-house, located a few metres from Datum D-1, through nylon tubings coated with a polythene sleeve. In the piezometer chamber, tubing ends were connected to a hydraulically rigid panel where pore pressures were measured by means of a pressure transducer and an electronic digital read-out, a mercury-manometer being also available for periodic checks of the electronic system. Deairing facilities for piezometer flushing consisted of a portable three-cylinder deairing unit and a paraffin volume gauge (devices that could also be used for in-situ permeability and hydraulic fracture tests), a foot-pump being used to increase air pressure in the deairing unit.

The equipment described was supplied by Soil Instruments Ltd., London.

C H A P T E R S I X

DETAILED PERFORMANCE OF THE TRIAL BANK

6.1 Horizontal Displacements

6.1.1 Inclinometer measurements

6.1.2 Foundation wire extensometer (rod gauges)

6.1.3 Fill wire extensometers (rod gauges)

6.1.4 Surface reference points - EDM surveys

6.2 Vertical Displacements

6.2.1 Inclinometer settlement magnets

6.2.2 Hydraulic settlement gauge

6.2.3 Levelling of surface monuments

6.3 Overall Patterns of Displacements

6.4 Horizontal Strains

6.4.1 Foundation wire extensometers

6.4.2 Fill wire extensometers

6.4.3 Inclinometers

6.5 Vertical Strains

6.6 Shear Strains

6.7 Principal Strains

6.8 Pore Pressure in the Foundation

6.8.1 Installation and operation procedures

6.8.2 Measurements

6.8.3 Response time

6.8.4 Pore pressure dissipation

6.8.5 Precision and accuracy

6.9 Pore Pressures in the Fill

C H A P T E R _ S I X

DETAILED PERFORMANCE OF THE TRIAL BANK

6.1 HORIZONTAL DISPLACEMENTS

6.1.1 Inclinometer Measurements

(i) Operation procedures

From the initial readings, taken 10 to 20 days before construction started, to the final set of measurements, 4 to 5 months later, 8 to 10 surveys were carried out on each inclinometer in the E-W direction corresponding to movements across the embankment axis. They totalled 36 surveys in that direction, performed by 3 different operators as many as 26 having been carried out by the Author himself. In the N-S direction, parallel to the axis, only 2 or 3 sets of measurements were taken on each inclinometer; out of a total of 10 surveys, 6 were performed by the Author and the remainder by another single operator.

Since the beginning, it was appreciated that positioning the inclinometer torpedo at exactly equal levels or at the very same point of each tube length was an impossible task owing to the following factors:

a) three years before the trial bank experiment, spacings between coloured bands on the electrical cable were found to vary erratically within a range of ± 3 mm and one of the markings

was misplaced by over 3 mm (GREEN, 1969). At the time these findings took place, this particular instrument was practically unused, but in a similar device, numbered 200 B/37, borrowed from Nuttall Geotechnical Services, errors were considerably greater, generally in the order of 6 mm, but reaching values over 12 mm near the torpedo (GREEN, 1969). If the inclinometer top were kept at a fixed or controlled level, difference in marking intervals would be unimportant, but with new lengths being added as the embankment was raised, a perfect account of true levels would represent an enormous amount of work, incompatible with time and personnel availability, unneccessary in face of the precision required and, above all, a useless effort since other sources of error would not be removed.

b) there is no refined system of reference in the apparatus; the most precise means of trying to take measurements at repeatable levels consists of positioning the top or the base of each marking corresponding to the casing end or the jaws of the jam-cleat; either method is likely to introduce errors of up to 5 mm.

c) survey of inclinometer tops, by conventional methods could provide a control for levels of measurements, but its precision was not better than 5 mm, perhaps worse.

d) inclinometer bases were expected to settle, owing to their relative shallowness as compared to the extension of loaded area and the possible partial consolidation of the clay into the Marlstone.

e) vertical movements of several magnetic rings loosely attached around inclinometer pipes were periodically measured through an inductance coil probe, but an uncertainty remained about which proportions of the measured settlement were due to the ralative displacement of the ring with respect to the ducts or, alternatively, to the closing of gaps between two successive casing lengths.

All these difficulties having been realized, a simplified operation scheme was devised in order to compromise between the limitations of staff and time on the one hand, and the desirability of taking as many complete sets of readings as advisable for such a research work, on the other. It was appreciated that, by doing so, a lot more of work would be required in calculations and analyses, but the procedure adopted was judged worthwhile. During the observational period, measured horizontal displacements reached such high values that greater refinement in calculations proved unnecessary for the efficient control of trial bank movements, although from a scientific standpoint they are useful and, accordingly, they were carried out.

The operational procedures consisted of first lowering the torpedo down to the well base and leaving it there for some 2 or 3 minutes to allow for temperature equalization; then, the probe was raised until a cable marking coincided with the jam-cleat jaws, the distance between the bottom and this point being recorded; a first reading was taken and the torpedo raised up to the top, new measurements being made at each marking spacing (305 mm). When

the probe reached the top, it was reversed, lowered again into the well and the whole procedure repeated. Each individual measurement took an average half-minute; 10 seconds after the probe was brought to a new position, a reading of the micro-dial was made, interpolation by eye to the decimal between two whole digits being attempted; at every 10 seconds, new readings were taken until two successive numbers did not differ by more than 0.2 or 0.3 of a dial unit, when the probe was displaced to next point. Convergence in general occurred in the second or third readings.

The criterion of always having a cable marking coinciding with the jaws in the first reading, used as origin for 305 mm-spaced measuring points, introduces errors, as it corresponds to purposely adopting different positions for the measurements in each set. This procedure may be unacceptable for some special jobs where great accuracy is essential, as the observation of tiny displacements in rock, concrete or steel structures aiming at the determination of moments, for example, but for the trial bank experiment, the influence of such a technique was not important as shown further in this chapter.

When, owing to large horizontal movements of upper layers of the foundation, the inclinometers became so distorted that the torpedo could not reach the base, procedures had to be somewhat altered; the probe was lowered to the blocked point and then raised until a marking coincided with the jam-cleat jaws, when a first reading was taken. In that case, since the horizontal move-

ment at the point of lowest measurement was not known, in reverse to what occurred with the inclinometer bottom (assumed to be zero), displacements were worked out from horizontal movements at foundation level obtained from wire extensometer measurements, checked in some cases by EDM observations.

(ii) Calculations

Measurements being made at 305 mm intervals, after each set of 8 or 9 readings taken along a tube length there were one or two consecutive observations in which one or both pairs of the torpedo wheels were positioned in the coupling or close to it. Situations like this were easily detected as sudden and erratic change in angle were recorded and the sum of opposing readings, which should be around 1000 dial units with no more than a few digits scattering, showed in general great discrepancies, in the order of 50 units or so. It was decided to discard always two readings taken in the coupling region, even if one or both appeared to be normal in some set of readings; it was understood that this irregular behaviour was a consequence of the technique employed (different torpedo positions, according to the distance from the bottom to the probe at the first reading) and of the shortening of the ducts due to the closing of coupling gaps, and that the most correct approach in calculations would be to discount always two readings in the suspicious region, replacing them by the two neighbouring measurements, certainly taken outside the joint influence.

It was intended that, in every set of readings, each individual measurement should correspond to horizontal displacements of the same point of the inclinometer well, regardless of the vertical movement it might have experienced. Shorter gauge lengths for the measurements taken immediately above each joint could have been adopted as a compensation for the partial closure of the coupling gaps, but this was an incovenient and difficult task, as it complicated considerably the operation and vertical movements at the joints were not accurately known. The gauge length of 1 ft (305 mm) was thus maintained. The errors arising from such a procedure are discussed below.

In the lower half of the foundation, displacements were small. As the casing was almost perfectly straight, tilting angles at the points where the measurement should be taken practically equalled those actually measured.

In the fill, settlements were quite large but the casing still tended to remain straight, sharp variations in slope only occurring at the joints. In this case, important errors would only arise if the shortening was of such a magnitude that the number of readings in a same length decreased (in general, from 9 to 8). To cope with this, an extra fictitious reading was added (made equal to the average along that length), re-establishing the previous number. This had roughly the same effect as reducing each individual measurement length by 1/9 of its original value.

The most critical situation took place in the upper half of the foundation, where settlements were small but the inclinometer casings bent considerably, giving place to great variations in angle within the lengths in addition to those at the couplings; no

correction was introduced, but an estimate of the errors involved is presented further in this chapter.

(iii) Face errors

Ideally, with inclinometer casings being really cylindrical, with no irregularities occurring in internal surfaces, with no horizontal movement taking place during the time elapsed between opposing readings of a same set, with the torpedo being placed at exactly symmetrical positions in opposing measurements, with no moisture having entered the probe and with the electrical circuit working properly, tilt angles recorded in two reversed set of readings should perfectly compensate each other, their sum being zero. Any departure from such a condition means a violation of one or more or the cited prerequisites or, less probably, a zero shift in the time interval between two opposing observations.

In the device utilized, zero angle roughly corresponded to a dial reading of 500 and, therefore, perfectly symmetrical readings were expected to sum up 1000. In laboratory conditions at Imperial College (GREEN, 1969), two series of 40 readings, one started from the bottom and the other from the top, led to somewhat different statistical distributions, but mean sums were approximately the same: 999.6 and 999.7 (figure 6.1.a); nearly 75% of the 80 pairs of measurements added up between 998 and 1002, while 95% of the values were in the 993-1004 range (for sum figures, 70 units correspond to 1° or 0.0175 rd).

Figures 6.1.b,c,d,e show frequency distribution

of face errors for initial readings of the four inclinometers, in terms of summation of opposing readings in dial units. By comparing the shape of these histograms with that corresponding to laboratory testing (figure 6.1.a), it is possible to see that readings of inclinometer I3 (East-West) taken on 23-6-72 were dissimilar to the remainder. Its mean sum value was around 997 whereas all the others fell in the 998.6-999.7 range; its standard deviation was 3.1 against 1.0 to 1.8 of the others; only 65% of its sums were comprised in the 5 central most frequent classes, whereas values between 85 and 98% were recorded for the rest. In fact, as it will be seen further in this chapter, this set of readings herein referred to was one of the few measurements proved to have given wrong results.

In figure 6.2, face errors of all sets of readings taken at Empingham Dam Trial Bank are analysed together with Green's laboratory observations and 7 measurements made by two different operators (four of them, made by the Author himself), at the Wansford Intake, with the same apparatus and at about the same time. Among over 50 observations, only 3 proved totally inconsistent with companion results and they are signed by arrows. It is shown in figure 6.2 that two of them were the only ones to have exhibited a mean sum above 1000 units. The three were among the four sets possessing standard deviations above 3 units (7.5×10^{-4} rd). The three were also among the four measurements for which the 5 central most frequent classes were below 65%

It seems that the three sorts of face error

control described above can be used in a combined way to ascertain whether a given set of readings may be trusted.

During the complete period of observations, entirely absurd results twice happened, sums of readings having been erratically well above or below 1000, with dial readings not becoming constant even after the torpedo was occupying a new position for many minutes, angles exhibiting striking inconsistency with regard to previous measurements, etc. On the first occasion, 18-9-72, batteries were replaced and following readings, restarted 3 days later, showed average sums closer to 999, standard deviations smaller and greater concentration of results in the central histogram classes. Forty days later, however, new absurd readings again took place and, this time, batteries could not be blamed. It was decided then to open the torpedo and leave it overnight in a warm atmosphere. From that day onwards, results were good, standard deviations reasonable, concentration of results in central histogram classes fairly good, but, inexplicably enough, mean sums dropped to values never recorded before, around 995.

The reason for absurd results and also for those readings which, without being clearly silly, led to wrong measurements, appears to have been the ingress of moisture in the torpedo through its top gland, owing probably to an insufficient tightening of the nut, but exposure of its interior tc a warm dry atmosphere seems to represent an adequate remedy. As for the change in face error after the torpedo was opened and dried, it could have been a

consequence of any other undetected cause, such as inadvertent drop or shock, lower temperature, etc.

Figures 6.3 to 6.5 display mean opposing reading sums for each casing length of inclinometers I3 and I4, corresponding to measurements taken on different occasions, from 23-6-72 to 26-9-72. Most individual values fall between 995 and 1000 and the width of scatter band is in general not greater than 3 dial units, less than 10^{-3} rd therefore. Some exceptions to this general trend can be visualized, however. The lowest and the highest lengths at times departed considerably from the overall pattern, which can be attributed, in the former, to a possibly insufficient temperature equalization time, and, in the latter, to slight changes in casing position between opposing readings taken in looser lengths as was the case of highest sections. Most important differences in behaviour were observed in measurements made on 23-6-72 for I3 (figure 4.3) and 29-8-72 for I4 (figure 4.5), when some of the dial sums averaged well over 1000 units and the scatter band were as wide as 8 units or so; these two sets of readings were those whose results were found to be inconsistent with previous and further measurements; these anomallies provide additional criteria for discarding results or putting them under suspicion. A final sort of discrepancy can be seen in figures 6.3 (I3, 5-9-72) and 6.5 (I4, 26-9-72), where a sharp deviation in pattern occurred about elevation 48 m AOD, and sums unexpectedly rose to values above 1000; in both cases, they were the last set of readings before inclinometer wells

had become so distorted that the measuring probe could not pass through and, furthermore, protuberances coincided exactly with parts of the ducts where shear distorsions were maximum ($\gamma > 5\%$) and individual inclinometer lengths were bent (see digures 6.15 and 6.16). This shows that while distorsions were kept below 5%, face errors did not appear to have been affected and the technique used in positioning the torpedo inside the pipes was successfull in spite of the operator never being sure to have opposing readings exactly at the same level. Only when individual lengths began to depart from straight line conditions were the consequences of a basically inaccurate procedure felt.

Figure 6.6 portrays average face errors for 10 individual lengths of inclinometer I4 corresponding to 8 sets of readings, including the anomallous record of 29-8-72 and the last full-depth measurement taken on 26-9-72. As for the 29-8-72 set, it is noteworthy that, while a 'shoot-up' is always present, from the bottom to the top, it is visibly more prominent in lower sections, gradually decreasing with height; whether or not this decreasing anomallous face error is accompanied by a diminishing error in angle measurement remains a matter for speculation, but it could well be that lower water pressures in higher elevations gave place to less moisture ingress and to reduced errors. With respect to 26-9-72 set, a discrepancy in face error is only observed at the length between couplings at elevations 46.9 and 50.3 m AOD, just below trench base level, the zone of maximum distorsion. Otherwise, scatter in face

error for each individual length is in general 3 dial units or, approximately, 8×10^{-4} rd.

(iv) Angle measurement repeatability

The power of resolution in the read-out dial is one digit in each reading, i.e 5×10^{-4} rd; if an error like this occurs in every measurement taken at each 305 mm, in a 30 metres deep inclinometer, accumulated deviation at the top will amount 15 mm (figure 6.7). If the operator succeeds in eye-approximating readings to half-unit, errors are obviously halved.

Overall individual errors, however, are expected to be higher than that, as they include not only the apparatus sensitivity but also irregularities of inclinometer's internal surfaces, the accuracy of mechanical as well as electronical parts, human errors, environmental factors (pressure, temperature, moisture), etc. Slope Indicator's manufacturers quote conservative figures in their promotional literature: 8.7×10^{-4} rd, corresponding to 26 mm horizontal displacement in 30 metres of casing.

Extreme errors are not expected however to act in full in every reading and always at the same direction; on the contrary, they are likely to vary at random and, therefore, errors at higher deviations, although greater in absolute values tend to become proportionally less important. CORNFORTH (1973) studied statistically 3 sites where a total of 80 sets of readings were made by a number of different operators at inclinometers that were after-

wards found not to have moved; the results of the survey are expressed in two curves defining the 'average' and the 'outer bound' values for maximum deviation of individual profiles with regard to the mean profile; according to this study, reproduced in figure 6.7, errors of up to 2 mm can be expected at 3 metres from the bottom (roughly 6×10^{-4} rd), but the curve slope rapidly varies, only 4 mm being predicted for a 12 metre high point (3×10^{-4} rd) and 5 mm for a 27 metre high elevation (approximately 2×10^{-4} rd).

DUNNICLIFF (1968) compared Wilson's inclinometer measurements with known inclinations of a 7.5 metre long calibration frame and concluded that overall accuracy was around 2×10^{-4} rd. GREEN (1969) carried out a more complete series of tests and deviation from the mean profile obtained for 2 sets of readings in the 24 metre high casing is shown in figure 6.7: at the height of 6 metres, the maximum deviation was 2 mm (3×10^{-4} rd) but at 21 metres it was less than 4 mm, i.e below 2×10^{-4} rd.

At Empingham Trial Bank, various inclinometer surveys were carried out before any movement could be detected, particularly at lower elevations and at inclinometers I2 and I4, located far away from the slope toe. As an example of the statistical treatment given to such readings, the maximum deviation curve for 5 different sets of measurements at I4 is displayed in figure 6.7, showing a maximum error of less than 5 mm at a 9 metres height (about 5×10^{-4} rd), dropping to 4 mm at 13 metres (3×10^{-4} rd) and just over 3 mm at 27 metres (1×10^{-4} rd). Also in figure 6.7 it

is possible to visualize the sudden departure of the curve corresponding to readings taken on 5-9-72, a clear evidence that the well had started to move above elevation 42 m AOD. Another strikingly different behaviour is exhibited by the 29-8-72 line, also depicted in figure 6.7, but in this case the reason for the flat curve was not the inclinometer deformation, as further observations demonstrated, but anomallous results, strongly disagreeing with the remainder, already referred to in previous items, possibly caused by moisture ingress into the torpedo chamber.

The maximum deviation curve for inclinometer I4 is possibly too steep in its lower portion and this might be due to insufficient equalization time prior to beginning of observations or, maybe, some distorsion in lowest inclinometer lengths induced by consolidation of layers close to the bottom into the Marlstone; the overall maximum error of 5 mm, however, is indeed quite small as compared to the magnitude of the recorded horizontal displacements.

Some points of maximum deviation curves for inclinometers I1 through I3 are also displayed in figure 6.7 and they show a good agreement with I4's pattern and Cornforth's curves. These points correspond to 9, 6 and 5 sets of observations in the case of I1, I2 and I3, respectively; the only measurement discarded was that made on 23-6-72 for I3, found to be wrong much in the same way as I4's taken on 29-8-72.

Cornforth's curves having been found to represent a safe limit for measurement repeatability, conditions not being

altered and evidently wrong readings discounted, the maximum error in horizontal displacement would be less than 5 mm at the foundation top. It must be emphasized, however, that precision limits arising from the above comments and from the curves of figure 6.7 refer to cases where no deformation occurred and little if any settlement was present. Where displacements take place and lengths bend, errors are certainly greater as the basic inaccuracy in positioning the torpedo within the well magnifies its effects.

(v) Influence of casing distorsion

As mentioned before, provided that individual inclinometer lengths remain straight and bends only occur at couplings, no significant error arises from not positioning the measuring probe at exactly the same levels in each set of readings. In the trial bank experiment, however, casing sections did not remain straight throughout construction and important changes in angle occurred in intervals between joints in two or three lengths, corresponding to zones of large shear strains (figures 6.13 to 6.16).

Figure 6.8 exemplifies how recorded angles varied along an extremely distorted portion of inclinometer I3 surveyed on 5-9-72, and similar behaviour was also observed at the other three wells. The base-curve in figure 6.8 was obtained on 11-7-72, 8 days after construction commenced, and it possibly already contains the effects of some horizontal movement, although small; in it, tilting angles are very consistent within each length, not varying more than

few tenths of a degree. On 5-9-72, however, distorsion was so pronounced that changes in tilting angles reached values between 3 and 5^{o} in two casing sections comprised between elevations 43 and 49 m AOD, where maximum shear strains were recorded. Angle changes with height in the critical zone oscilated from 2.5 degrees/metre to 13.5 degrees/metre, average lying between 6 and 7 degrees/metre.

Under these circumstances, inaccuracy in locating the torpedo always at the same position induces much larger errors. If tilting angles β_i are assumed to vary linearly between successive measuring points, an expression for the difference between 'correct' and 'wrong' horizontal displacements $(\Delta \delta_x)_i$ can be derived as a function of the vertical distance Δl_i between reading points adopted in 'correct' and 'wrong surveys:

$$(\Delta \delta_x)_i = \frac{\Delta l}{2}(\beta_i - \beta_{i-2}) \qquad (6.1)$$

If angles continue to vary in the same direction and torpedo positioning error is maintained, displacement errors increase with elevation. Assuming n reading points and $\Delta l_i = \Delta l =$ constant, cumulative errors between readings i and $i+n$ will be:

$$(\Delta \delta_x)_{i,n} = \frac{\Delta l}{2}\left[(\beta_{i+n} - \beta_{i-1}) + (\beta_{i+n-1} - \beta_{i-2})\right] \qquad (6.2)$$

Angle differences $(\beta_{i+n} - \beta_{i-1})$ and $(\beta_{i+n-1} - \beta_{i-2})$ may reaonably be assumed to equal. In this case, (6.2) would be simplified into:

$$(\Delta\delta_x)_{i,n} = \Delta l\,(\beta_{i+n} - \beta_{i-1}) \qquad (6.3)$$

With basis on equation (6.3), Table 6.1 was constructed, giving values for $(\Delta\delta_x)_{i,n}$, in millimetres, for various selected values of Δl and $(\beta_{i+n} - \beta_{i-1})$.

TABLE 6.1

Errors in horizontal displacements (in mm) due to torpedo misplacing

Δl	$(\beta_{i+n} - \beta_{i-1})$ in degrees					
(mm)	0.5	1	2	3	5	10
1	0.008	0.016	0.033	0.049	0.082	0.164
5	0.04	0.08	0.16	0.24	0.41	0.82
10	0.08	0.16	0.33	0.49	0.82	1.63
50	0.41	0.82	1.63	2.45	4.00	8.17
100	0.8	1.6	3.3	4.9	8.2	16.3
200	1.6	3.3	6.5	9.8	16.3	32.7
300	2.5	4.9	9.8	14.7	24.5	49.0

At Empingham Trial Bank, casing vertical movements as measured by means of settlement magnets never exceeded 50 mm in the foundation and maximum angle variation was never greater than 7°; maximum expected error in foundation horizontal displacements caused by inaccurate torpedo positioning was therefore kept below 5 mm, less than 1% of the measured total movement.

In the fill, settlements were much higher but tilting angle changes were considerably less than in the foundation and the criterion of adding a fictitious reading every time any casing length was shortened by more than 305 mm, limits the error in

horizontal movement to more or less 5 mm, the same order of magnitude as in the foundation.

When apparatus repeatability and torpedo positioning effects are superimposed, the overall precision of inclinometer measurements is within ± 10 mm.

Another source of error in inclinometer measurements is the fact that this sort of device measures angles, and displacements are usually worked out as integrations of $(L \times \beta)$, where L is the gauge length and β is the tilting angle in radians.

In fact, difference in level between two successive readings is not L, as normally assumed, but

$$\rho = \frac{1}{\sqrt{1 + \tan^2\alpha + \tan^2\beta}} \qquad (6.4)$$

where α and β are torpedo inclinations with respect to the vertical, measured in two orthogonal directions. For situations in which inclinometer ducts are initially very inclined ($\alpha = \beta = 20^\circ$, say), errors in elevations reach 12.5%, but for moderate inclination ($\alpha = \beta = 5^\circ$, say), it drops to only 0.8%.

More important than this is the effect of using $(L.\beta)$ to calculate displacements. If inclinometer pipes are initially close to vertical and further movements are moderate, the error introduced is negligible, but it may assume important proportions in severe inclinometer distorsions. It must be emphasized, however, that errors in this case lead to overestimation of horizontal

TABLE 6.2

Percent correction in horizontal displacements

(according to equation 6.5)

Ψ (°)	Initial casing inclination Ω(°)												
	-20	-10	-7	-4	-2	-1	0	+1	+2	+4	+7	+10	+20
1	94.0	98.5	99.4	100.0	100.0	100.0	100.0	100.0	100.0	99.7	99.1	98.5	93.7
2	94.5	98.6	99.4	100.0	100.0	100.0	100.0	100.0	100.0	99.6	98.9	98.2	93.1
3	94.7	98.8	99.5	100.0	100.0	100.0	99.9	100.0	99.9	99.5	98.8	97.9	92.8
4	95.1	99.0	99.7	100.0	100.0	100.0	99.9	99.9	99.8	99.4	98.7	97.6	92.4
5	95.3	99.1	99.7	100.0	100.0	100.0	99.9	99.8	99.7	99.2	98.5	97.4	92.1
7	95.8	99.3	99.8	99.9	99.9	99.8	99.8	99.6	99.4	99.0	98.2	97.0	91.4
10	96.2	99.5	99.8	99.9	99.8	99.6	99.5	99.3	99.1	98.6	97.7	96.2	90.3

displacements. Correction factors are presented in Table 6.2.

Denoting by Ω initial casing inclination and by Ψ further angle changes, always positive, percent corrections shown in Table 6.2 are calculated through the expression

$$\left(\Delta\delta_{\infty}\right)_{\Omega,\Psi} = \frac{\sin(\Omega+\Psi) - \sin\Omega}{\Psi\,(rd)} \times 100 \qquad (6.5)$$

It is possible to see that where initial casing position is 7° or less from the vertical, and further distorsions do not reach 7°, correction will always be over 98%, i.e, the error will be less than 2%; in fact, it will hardly exceed 1% in most cases.

(vi) Measurements

Prior to banking commencement, all four inclinometers were surveyed, both in the East-West (downstream-upstream) and the North-South directions. Owing to a defect in installation, inclinometer I3 at Ch. 487 had its grooves some 30 degrees twisted clockwise. A correct measurement of horizontal movement components in the bank-axis and across-axis directions would require, in this case, observations of both pairs of opposing grooves in each set of readings, but shortage of time and personnel prevented such a procedure and surveys of the direction closer to E-W alone were normally carried out, few N-S measurements having been made.

Figures 6.9 through 6.12 portray a total of 36 E-W surveys of inclinomerers I1 to I4 (in these drawings denoted ITB-1 to ITB-4), carried out from 15-6-72 to 15-11-72.

In nine of these observation sets, taken towards the end of the construction period, inclinometer distorsion was already so large that the measuring probe could not reach the well base and, therefore, the surveys were initiated at the lowest level possibe and proceeded upwards. In figures 6.9 to 6.12, horizontal displacements are presented without any correction and those corresponing to surveys which did not commence from the bottom are pictured on the basis of arbitrary starting lowest points, the profiles having been built up according to relative displacements as measured in the slope indicator device.

Out of these 36 surveys two clearly resulted in wrong calculated displacements, owing probably to ingress of moisture in the probe. They were the initial I3 profile (figure 6.11), measured on 23-6-72, and the fifth I4 record, on 29-8-72 (figure 6.12).

In figures 6.13 through 6.16, inclinometer profiles are again reproduced, but this time three corrections were introduced. Firstly, the two above mentioned discrepant observations were corrected by the addition of a constant increment to every angle measured, in such a way that the lower part of the profiles were made to coincide with those obtained in previous and further reading sets; values added were 1.3×10^{-3} rd (0.075^{o}) for I3 and 2.0×10^{-3} rd (0.115^{o}) for I4. The second correction consisted of discarding displacements smaller than $\pm$ 5 mm with regard to the initial profile, as this value has been shown to be within the confidence limits of the measurements. In these drawings, profiles

corresponding to readings in which the torpedo could not pass through distorted zone were not initiated from a arbitrary point; instead, horizontal displacements measured through wire extensometers at stripped ground level were taken as references and the profiles then drawn up- and down-wards. The third correction referred to the first survey of each inclinometer length; when the initial profile of a recently added casing length was first measured, it had already probably experienced some movement, approximately zero at the fill level but equal to the displacement of the next length top, immediately below it; the correction introduced consisted in assuming that initial movements varied linearly between these two limits.

Few N-S inclinometer readings were taken, the last complete surveys in this direction having been performed between 19-7-72 and 24-7-72, when fill elevation was nearly 58 m AOD (11 metres above toe level at Ch. 537). At this stage, inclinometer I3 had moved about 15 mm towards the North and I2 around 8 mm in the same direction; in both cases, displacements were concentrated in the higher 4 metres below ground surface. At chainage 487, measurements were less conclusive; I4 appeared to exhibit small displacement (maximum 8 mm) towards the South, but the very uniform pattern of this profile, departing linearly from initial reference readings in a very regular way from the bottom upwards is possibly attributed to the normal scatter of inclinometer measurements and not to real movement; interpretation of I3 readings are even more difficult in view of the twisted casings; on 19-7-72, N-S observations (in fact,

NNE-SSW) showed about 37 mm displacement towards SSW at foundation level, but this was mostly due to accoss-the-axis movement, whose ESE-WNW component was, at that time, around 30 mm. The twist being approximately 30 degrees, the above figures lead to components of 44 mm across-the-axis and 17 mm along the axis, towards the South, but it is noteworthy that the twist angle measurement was not precise and an error of up to 10^{o} might have been present; if a 40 degress angle had been used in calculations, the components would have been 47 mm and 9 mm (South); in either calculation two aspects deserve attention: firstly, movement along the axis seems to have been towards the South and not downhill as expected, and, secondly, across-the-axis displacements appear to have been well above values obtained in ESE-WNW measurements.

After well distorsion prevented complete inclinometer surveys, readings of upper angles of I3 were once made in the quasi-transverse direction; it was on 2-11-72, and a total deviation of over 50 mm was found between elevations 47.6 and 49.2 m AOD with respect to 19-7-72's survey, here again, towards the South. If deviation from the bottom is assumed to be twice as much as that and the 37 mm previously measured is added, around 150 mm NNE-SSW displacement matches 600 mm movement in ESE-WNW direction to result in components across and along the bank axis amounting to 595 mm and 170 mm (North), figures that demonstrate how insufficient the data were to provide a reliable estimate of N-S movement. The only findings concerning this particular aspect of horizontal movement were

that, until the fill reached 11 metres of height, Ch. 537 section appeared to have slightly moved towards the North, whereas Ch. 487 section seemed to be either stationary or perhaps, in its part closer to the trench, displacing towards the South; combination of these factors shows the possibility of an extension straining of the bank axis between the two extreme instrumented sections.

(vii) Horizontal displacements

Filling operations were not carried out in a regular pattern as far as bank height is concerned; during the first days of construction crest elevations were raised very fast; nearly 7 m of soil were compacted above ground level at Ch. 537 in the first 5 days and by the 14th. day fill height at that section was already 11 m (figure 6.17); there was then a work stoppage and for 25 days there was practically no filling operation; works restarted on the 39th. day with a slower rhythm; on the 93rd. day banking was completed, but, later on, the construction of the main dam core, adjacent to the downstream slope of the trial bank, may have contributed to further lateral movement of the embankment.

Figures 6.13 to 6.16 depict displacements profiles measured on several occasions, showing that final horizontal movements were in the order of 700-800 mm at ground level in inclinometers near the slope toe (I1 and I3) and around 400-500 in inner inclinometer wells (I2 and I4). Between 1 and 2 metres below the toe (or the trench base) level, displacements of toe-inclinometers rapidly decreased downwards, becoming negligible at elevations 8 m

below toe (or trench) level. At I2 and I4 locations, the pattern was similar, rapid decrease in displacement starting some 2 to 4 metres below toe-trench level and finishing 5 to 10 metres below it.

In figures 6.18 and 6.20, horizontal movements of I1 and I3 at foundation level are plotted against fill elevations. In figure 6.21, these data are combined with wire extensometer and surface point measurements to produce curves of horizontal displacement as functions of fill height, the reference chosen having been the trench base level at each instrumented section (toe level at Ch. 537). Patterns shown in these figures are fairly similar, a more or less parabolic shape being clearly indicated. In figure 6.22, horizontal movements at trench base level are plotted against fill height on a logarithmic scale, and it is possible to see that points corresponding to inclinometers I1 and I3, close to slope toe, lie approximately on a straight line for heights of fill above 6 metres, the same pattern being observed with regard to the inner inclinometers I2 and I4 for fill heights in excess of 11 metres, a circumstance that proves useful in the control of lateral movements during construction. Extrapolation of straight lines in figure 6.22 would lead to displacements over 1 metre at 24 metres fill height had construction proceeded to this level.

(viii) Equipment performance

Apart from those absurd readings referred to in section 6.1.1(iii) and the two sets of measurements which had to be

corrected in view of their showing a systematic drift from values obtained in previous and further observations, both anomalies probably caused by moisture in the pendulum chamber, the slope indicator device behaved quite satisfactorily, within a precision of ± 5 mm.

Aluminium casings exhibited a tendency to a dog-legged type of deformation profile, but each individual length was also capable of bending when displacements were high and average tilting angles exceeded 1 or 2 degrees with respect to initial profiles.

Temperature shock might have been responsible for a wider scatter in angle measurements in the lowest parts of inclinometer wells, but even if it was so, the error caused was not important.

Beyond average tilting angles of 4 or 5 degrees in an individual length, inclinometer tube bottoms were very likely to become inaccessible to the torpedo. More than once, as the probe was being lowered inside the pipes and the distorted zone was reached, the probe jammed in the casing and its release required great effort in tugging and pulling the cable, what might have caused some stretch to it.

During the inclinometer surveys, it was observed that a thick white foam existed in the top of the water column, forming so dense a crust that the settlement magnetic probe tended to float on it and it always took some time until it sank. This lather,

that usually covered the slope indicator probe when it was drawn out of the ducts, was probably the result of chemical reactions involving water seeping through the grout column, the grout and the aluminium alloy casing. At about the same time of the Empingham Trial Bank experiment, a portion of inclimometer tube was extracted from another job in this country, after 7 months buried in the ground, and chemically analysed together with the 3:1 bentonite-cement mixture utilized in grouting (FRASER, 1972); results of the analysis show that although treated with Alocrom 100, a rapid non-electrolitic dip process made by ICI and said to create a protective coating against corrosion, external surface of the tube revealed various degrees of corrosion, from very slight in some places to complete desintegration in others. Deficiency in cement in the grout mixture examined might have created favourable conditions for the sodium emanating from the bentonite (in fact, a treated fullers' earth, i.e a calcium-montmorillonite, often called non-swelling bentonite) to attack the metal, but it is possible that even with properly balanced and hardened grout, as must have been the case at Empingham where a 1:1 mixture was employed, some of the sodium alkalinity might be available for the metal attack. Stray current electrolysis or removal of protective aluminium oxide films by ammonium compounds derived from organic material in soils under alkaline environment are also possible factors causing or aggravating the corrosion.

Inclinometer casings protruding out of the fill

always face the risk of being damaged by the plant. Visual signals made of coloured flags were used to limit an area outside of which machines were allowed to operate, compaction around inclinometer ducts being done manually. In spite of this protection and recommendations to operators and inspectors, it once happened that an inclinometer was hit by a tractor and bent some metres below fill level, two complete lengths having to be removed by digging around it, replacing the damaged parts, refilling and recompacting.

(ix) Comments on the accuracy of the measurements

In order to correctly evaluate the accuracy of a measurement, not only its precision must be taken into account but also an appreciation should be made of the loss in correctness induced by the insertion, the presence and the operation of the measuring system within the ground and its influence on quantities measured.

In the case of inclinometers, the question to be answered in this context is: how much will an inclinometer profile depart from the profile that a vertical line of soil at the inclinometer's location would experience had it not been installed? Apart from soil disturbance and consequent softening and weakening during the inclinometer's installation, the presence of an inclusion of different stiffness in the earth mass may represent an important resistance to soil movement, both horizontal displacements and, more probably, shear distorsion tending to be underevaluated in measurements.

The stiffness of the inclinometer column may be considered constant along an individual length, but at couplings it practically drops to zero. The grout cover, however, may be regarded as a uniform continuous piece, provided that grouting operation has been properly carried out by means of pumping via tremie pipes, as was the case at Empingham. The resulting inclinometer stiffness should be represented by a basically constant value throughout the well, coupled to constant reductions at each joint. The ratio between inclinometer's and soil's stiffness is a more complicated issue, as earth masses are known to have variable deformation moduli with depth, effective stress level and strain level. Analysis too is not simple to make, since a typically axi-symmetrical structure (the inclinometer) is subjected to a sort of loading approximated to plane-strain conditions under irregular geometric boundaries; an exact analysis would necessarilly include a three-dimensional approach, non-linear spacially variable stiffness and even time effects, represented by consolidation process and creep deformation.

Not even an approximate analysis has ever been published for such a problem and no stiffness correction was introduced in the calculations at Empingham. The most likely effect of this inclinometer's stiffness influence is qualitatively easy to assess; measured displacements are probably smaller than real ones, although only to a very small extent over a long length, and observed deformation profiles are probably smoother than expected in an

inclinometer-free medium; measured shear strains particularly in potential slip zones, are likely to be considerably lower than real values; chances of inclinometer columns being sheared, as happened to Interstate Route 95, in New Hampshire, USA (LADD, 1972), probably decrease, it being worthwhile to comment that while no mention to backfilling material was made by LADD (1972), the system utilized in another American test embankment controlled by M.I.T., in Massachussets (WOLFSKILL and SOYDEMIR, 1971), consisted of filling the annular space between inclinometer casing and borehole walls with sand or peastone and not grout, a factor that might have facilitated the casing shearing.

6.1.2 Foundation Wire Extensometer (Rod Gauges)

(i) Operation procedures

By the time the filling of the trial bank started, the wire extensometer system was not completed. Initial readings were only taken on day 4, when fill height was already 5 metres at Chainage 537. The second set of readings took place 5 days later, when fill elevation had risen to 56 m AOD, representing a height of 9 metres for Ch. 537 and 3 metres for Ch. 487. From this date onwards, measurements were made once or twice a day until day 130, over a month after fill completion. Some measuring points had their initial readings taken later than the general pattern, as their installations occurred later too; that was the case of H1X, H2X and H3X, for which zero-readings were on day 11 (day 16 for Ch. 487),

and also H1F and H2F, first observed on day 7.

Every time a measurement was to be made, a spring scale, luggage-type, was used to pull the wire with a 54 N (10 lb) constant force, while the saw-cuts were compared to reference points in the concrete slab.

At Ch. 487, the datum slab was across the trench and wire extensometers were, within the flexible pipes, extended to it on the floor of the scaffolding platform.

If only one set of readings was taken on a given day, it took place in the morning, shortly after 7 a.m.; in the case of a second group of observations being made, it occurred at about 5 o'clock in the afternoon.

Figures 6.23 through 6.28 include all measurements made, without any correction, from the beginning until day 241, five months after the end of trial bank construction. In figure 6.28, it is seen that from approximately day 50 onwards horizontal displacements of steel plates H1A, H1B and H1C were practically stationary, contrasting with H1X movement; at the same time, displacements of H1D, H1E and H1F, towards the West, appeared too exaggerated; it was suspected that a kink might have been formed in the pipes, somewhere between H1A and H1X as all steel plates had been affected; between day 120 and 130 an excavation was made, the kink actually found and corrected, the cable stretched and readings reinitiated, as seen in figure 6.28.

(ii) Initial adjustment

Under ideal conditions, the whole system should have been installed well in advance of filling commencement, so that successive zero-readings could be taken and their variation examined. Looseness of steel plates in the sand back-filled trench, curvatures of wires and cable and the like, would probably cause apparent displacements prior to loading. Even if pre-construction readins are carried out, accommodation might not be completely achieved by the weak pull of a spring-scale. Initial observed movements would therefore include an unknown proportion due to part of the adjustments mentioned above.

At Empingham, installation were only concluded after filling operations had been initiated and, therefore, there was no check for initial adjustments, apparent displacements due to accommodation thus overlapping actual movement. A symptom of this is seen if figure 6.25, where displacements of all plates are seen to point westwards, when at least H2F should have moved eastwards and H2D was expected to remain more or less stationary. Plates at Ch. 537 exhibit the most normal behaviour, whereas at Ch. 487, strangely enough, the plates appeared to be initially moving downstream. An approximated quantification of these adjustment errors would be: 20 mm eastwards for Ch. 487, 60 mm westwards for Ch. 514 and 10 mm eastwards for Ch 537. In the case of Ch. 487 and Ch. 537, the existence of a basically more accurate means of horizontal movement measurement - the inclinometers - permitted periodical cross-examin-

ation of rod gauge data and a more precise estimate of initial adjustment errors, but that was not the case of Ch. 514, where no inclinometers were located.

(iii) Measurements repeatability

The way how readings oscilated can be observed in figure 6.23 for the period of work stoppage between days 13 and 31 and also for the measurements daken twice a day immediately before day 40, for Ch. 487, and in figures 4.25 and 4.27, at corresponding periods, for Ch. 514 and Ch 537. While at Ch. 537 and Ch. 514, the maximum amplitude of fluctuations were always within $\pm$ 3 mm and $\pm$ 5 mm, respectively, it rose to $\pm$ 10 mm in the case of Ch. 487, a possible explanation being the fact that lengths of cable between the fill and reference datum slabs were different in each case (13 m at Ch. 537, 20 m at Ch. 514 and 33 m at Ch. 487) and, obviously, the longer the portion outside the bank, the greater the temperature effect and the possibility of the rods being offset from their previous position. Besides, in the case of Ch. 487, variation in temperatures on the scaffolding platform floor might have been more severe than on the ground where cables lay at Ch. 514 and 537.

To illustrate the possible effect of temperature change to a material of coefficient of linear expansion around 11×10^{-6} per ^{o}C (steel), it must be said that a temperature change of 10 ^{o}C can cause an extension of 1 to 4 mm for lengths between 10 and 40 metres. As steel is a good thermal conductor, temperature

changes outside the embankment may well propagate inwards in a rapid fashion, expanding even further the exposed wire length.

When readings were always taken early in the morning and not twice a day, oscilations were considerably smaller and repeatability improved to just few millimetres (see figures 6.24, 6.26 and 6.28, between days 100 and 120, for example). If morning readings alone are taken into account, a precision of $\pm$ 3 mm can be regarded as perfectly possible and this value is certainly acceptable for the magnitude of displacements involved.

(iv) Results

As already mentioned, uncorrected results of horizontal displacement measurements by means of wire extensometers are shown against time in figures 6.23 through 6.28. In figures 6.29 to 6.31, horizontal movements were plotted against fill elevations, but, this time, displacements had been corrected in the case of Chainages 487 and 537, as described below.

The first correction applied was intended to annul the effects of initial adjustment and consisted of assuming that central plates (HiC and HiD, i = 1,3) were stationary until fill heights around 10 metres above trench base level had been attained, and supposing that relative distances between plates remained unchanged; this sort of correction was not used in the graph for Ch. 514 (figure 6.30), but if it had been, a deduction of up to 100 mm would have resulted in measured displacements.

The second correction referred only to slope measuring points (concrete blocks) denoted HiX (i = 1,2,3). There are strong grounds to believe that these points were the first to move, since they were at one end of the slope, and, as they were not installed at the banking commencement, a portion of their movement could not have been measured. It was then decided to superimpose the plots for HiX plates and inclinometers located near the toe, attempting to make them coincide and thus obtaining a correction for rod gauge observations. Plots concerning Ch. 487 and Ch. 537 can be seen in figures 6.18 and 6.20; in the case of Ch 487, 50 mm were added to cope with the missing movement; for Ch. 537, at which more fill have been placed, this correction reached 70 mm. As there was no inclinometer at Ch. 514 section, its correction was arbitrarily fixed in 50 mm (figure 6.19).

A third sort of correction was necessary in the case of Ch. 537, where a kink in the rod gauge pipes was uncovered. It consisted of assuming that the distance between H1X and H1A was kept practically constant throughout the constructional period, decreasing only slightly towards the full completion, and accepting as correct measured distances between remaining plates. In fact, when the kink was removed and the ducts again stretched, H1X was found to have moved 30 to 100 mm less than H1A, but the 70 mm adding correction cited in the previous paragraph made it -30 to 40 mm larger than H1A's displacement on day 120. The adoption of a solution where H1A was supposed to have moved less than H1X was justified on

on the following grounds:

a) this was the behaviour observed at Ch. 514 and Ch. 487;

b) it was taken for granted that relative movements among plates were correct even during and after the kink formation; the correction adopted gave resulting movements of H1E and H1F that approximately followed the same pattern observed at Ch. 514 and Ch. 487 (see figures 6.29 through 6.31).

Having applied the above quoted corrections, the best estimates for horizontal movements of rod gauge plates are those contained in figures 6.29 to 6.31, where it can be seen that displacements between 500 and 900 mm were measured during the construction period at foundation level, near the slope. Figures 6.24, 6.26 and 6.28 show that after fill completion movement still went on, although, as expected, the slope of the curves decreased with time; between day 93 and day 240, during the first five months elapsed after fill completion, displacements were as large as 200 to 300 mm, an increase of 30% to 40% on the top of measured values during construction. These time-dependent movements might have been a consequence of increase in shear stress due to horizontal stress reduction during consolidation or to undrained creep movement or, most probably, to the two effects combined.

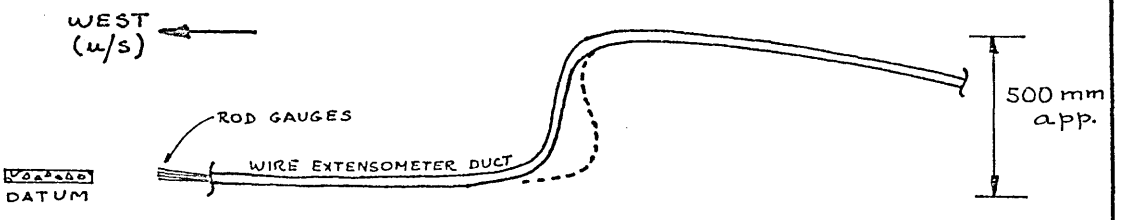
(v) Equipment performance

Rod gauges are very simple and inexpensive

devices, no sophisticated technique being essential in their installation and operation. Moreover, the rapidity with which readings are taken enables horizontal desplacements to be measured so often that a practically continuous record can be established.

Their precision is not as good as that of inclinometers, but for the magnitude of movement involved at Empingham they proved to be quite useful.

The only serious setback occurred during the observational period was the kink formed in the cable between plates H1A and H1X, at Ch. 537, from a date around 19-8-72 (day 47), more or less in the shape shown in figure 6.32 (next page), at a stage when fill height had reached nearly 14 metres and horizontal displacements were 200 mm at the toe. The kink was definitely a consequence of upwards heave in the toe-region and the development of a zone of high shear strains at that end of the potential slip surface. The formation of a shear plane just outside the trial embankment toe was observed at Ch. 537; since it did not rupture the inclinometer I1, it is assumed to have been a local effect, possibly due to softening by water ponding at the nearby low point. Even under these inconvenient conditions, however, relative movements between various adjacent plates are believed to have behaved properly and indeed, when the kink was removed and cables stretched, the distance between plates did not change by more than 2 to 33 mm, (averaging 14 mm) what represented 2 to 15% (averaging 8%) of previous measured lengths.



NOTE: If the duct was actually in position shown by dotted lines before excavation, it may have sprung as it was dug out.

Figure 6.32 - Shape of wire extensometer duct at Ch. 537 when dug out.

A very simple facility installed at Empingham but that, fortunately or not, never had a chance to work was a 'rupture signal', consisting of two leads attached to the wires of extreme plates, everyday reset in such a way that if movement exceeded a certain amount in twenty-four hours, which would mean an iminent danger of collapse, an electrical circuit would close and a visual signal, strategically placed on a higher part of the site, would switch on, giving a warning to plant operators and other personnel to leave the site as quickly as possible. This system requires a permanently working generator to energize it and can also be linked to sound signals, telephone line or, as at Mucking. Essex, to photographic camera prepared to automatically take

periodical photographs of the failing earth-structure (PUGH, 1974).

(vi) Measurement accuracy

As very often happens with field observations, there is no direct means of accurately assessing the degree of correctness of a measurement, as no way is available to precisely ascertain the real behaviour of the medium had the measuring system not been installed and operated. In general, accuracy can only be estimated by comparing independent measurements, at various points, and observing which differences exist among them.

In the case of Empingham Trial Bank, wire extensometer readings could be compared to inclinometer results and surface reference point surveys. Neither of them produced a complete overlapping span, as EDM surveys only provided acceptable data from day 38 and the useful life of inclinometers as totally independent measuring systems was shortened by excessive distorsion of the wells, which prevented the probe reaching the unmoved bottom towards the end of construction.

Figures 6.18 and 6.20 depict graphs for inclinometers located close to the slope and concrete blocks placed at the fill toe and incorporated to the rod gauge systems. In the overlapping portion of the plot, it is seen that they do not differ by more than 40 mm at Ch. 487 and practically nothing at Ch. 537, or, in proportional terms, less than 10% of final displacements, it being worthy of mention that not only the compared points were not

located at exactly the same eastings but also the chainage varied. H3X coordinates were (7794, 487, 53), the point V31B of I3 was (7801, 491, 55); corresponding figures of H1X and V16F - I1 were, respectively, (7780, 537, 48) and (7782, 540, 46).

Figures 6.18 and 6.20 also show displacements obtained through EDM surveys of the tops of concrete blocks H1X and H3X, denoted S1X and S3X. They corresponded to observations taken between days 38 and 99 and also revealed a good agreement with rod gauge readings differences ranging from 30 to 70 mm, 10% or less of final measured movements. Such differences may be explained by inaccuracies of both systems that include tilting of the concrete blocks during movement. They are, however, within perfectly acceptable limits.

Comparisons for Ch. 514 became much less effective as initial rod gauge readings were either absent or not trustworthy and, in addition, there was no EDM or inclinometer observations to match them. Figure 6.19 shows the wire extensometer curve for H2X, starting from an arbitrarily chosen point (based on displacements experienced by sections at Ch. 487 and Ch. 537 at the same fill elevation) and a plot for S2X survey starting too from an arbitrary point. Differences between both curves, although greater than for Ch. 487 and Ch. 537, were not substantial, never exceeding 100 mm, i.e 12% of the final movement.

A combined analysis of horizontal displacements

experienced by rod gauge and EDM points on the slope at foundation level, shown in figure 6.21, reveals that the three curves corresponding to each instrumented section were practically coincident until the height of fill crest was 10 metres above trench base level; from this point onwards, they started to depart and at 20 metres they differed by up to 200 mm, over 20% of the final maximum movement.

6.1.3 Fill Wire Extensometers (Rod Gauges)

(i) Measurements - Zero corrections

The sets of wire extensometers embedded in the fill, at around its mid-height (figures 4.1 through 4.3), were basically equivalent to those of the foundation, an important difference being, however, that their reference datum points SiY ≡ HiY (i = 1, 2,3) were not even approximately unmovable, frequent independent surveys of rod gauge locations being necessary for a correct evaluation of absolute movements; two systems were utilized to achieve such an aim: inclinometers and the EDM.

Figures 6.33 to 6.35 show relative movements undergone by the various rod gauge plates located at chainages 487, 514 and 537 with respect to datum spots H1Y, H2Y and H3Y. It must be noted, however, that, as installation went on, placing of fill proceeded and, of course, lateral displacements were already occuring; therefore, when readings enentually started, initial portions of real movements remained unrecorded; figures shown in the drawings are thus lower-limit estimates of actual movements and ways to correct

them and make them more realistic are detailed in this as well as in the next section of this chapter.

Also in figures 6.33, 6.34 and 6.35 are parts of inclinometer and EDM plots corresponding to the same time intervals of the wire extensometer measurements. It is possible to see that I2's and I4's curves for absolute movements follow H1J-H1Y's and H3J-H3Y's patterns in a very approximate fashion, indicating that HiJ (i = 1,3) points have experienced little if any horizontal displacement. This was confirmed by comparison with EDM observations, also pictured in drawings 6.33 to 6.35.

In figure 6.36, HiG-HiJ (i = 1,2,3) curves are put together and jointly compared to real absolute movements as measured at two different elevations (57 and 63 m AOD) of inclinometers I2 and I4, some interesting conclusions being drawn from them. Firstly, inclinometer displacements of I2 and I4 for both elevations appear not to differ considerably on corresponding days, a difference of less than 50 mm (around 10% of final movements) having been recorded. Secondly, from the day when displacements of both elevations could be observed, inclinometer graphs revealed a gradual difference in movement patterns, upper points having been displaced some 70 - 100 mm less than lower ones. Thirdly, rod gauge readings for HiH-HiJ (i = 1,2) resembled each other closely and agreed quite well with the curve for absolute movement of inclinometer I2, if initially unrecorded displacements amounting between 30 and 60 mm are added. The curve for H3G-H3J fits well with the inclinometers' plots, if

20 - 50 mm are added as correction for missing observations at the beginning. It must be noted that differences in extensometer plate displacements as recorded for Ch. 487 on one hand and Ch. 514 and Ch. 537 on the other, are most clearly due to differences in elevations where the sets of rod gauges were located, rather than to any extraordinary behaviour at Ch. 487 section, at least if time is taken as an independent variable and not height of fill.

Figure 6.37 too produces comparisons between horizontal movements as measured at various locations by means of different devices and techniques. This time, EDM observations were put together with relative movements of HiY (i = 1,2,3) plates with respect to HiJ (i = 1,2,3), which more or less corresponds to absolute displacements of HiY, as there are strong indications of HiJ having remained approximately stationary during the entire observational period. HiJ-HiY (i = 1,2)'s plots, initiated at about the same day, quite consistently agree with SiY (i = 1,2)'s EDM curves, differences having been less than 50 mm at any time; the same sort of comparison between S3Y and H3J-H3Y produces equivalent results, differences here being even smaller, never higher than 30 mm. EDM observations, however, started a considerable time after fill elevations had reached target levels and, therefore, proportions of missing records are much greater than in the case of rod gauges; in this context, comparisons to measurements taken for somewhat lower targets may be very useful in the assessment of zero-corrections to be introduced; that is provided for in figure 6.37 in which recorded dis-

placements for slope points at elevations 54-56 m AOD have also been drawn. The group comprising S3, S4 and S5 exhibited movements between 550 and 600 mm from day 52 until day 123, whereas HiJ-HiY (i = 1,2)'s measured changes were around 500 mm, an acceptable difference, particularly if it is taken into account the fact that wire extensometer sets were positioned 2.5 to 5.0 metres above the EDM targets. Comparisons of S3X and (S5 + S6)/2 against H3J-H3Y, between days 64 and 123 result in 380-400 mm for for EDM points 320 mm for rod gauges, a 7.5 m level difference being noteworthy.

A third group of cross-checks is displayed in figure 6.38, where relative movements of I1 and I3 with regard to I2 and I4, just above foundation levels at chainages 487 and 537, are compared to observations of outer portions of wire extensometers HiY-HiG (i = 1,2,3). Rod gauge readings commenced when fill elevations were between 1.5 and 3.5 metres higher than plate levels and this initial period was certainly characterized by a more pronounced spread than afterwards, as can gathered from both independent curves drawn for I1-I2 (49 m AOD) and I3-I4 (57 m AOD). Even taking into consideration the fact that the higher the fill elevation the smaller the movement, zero-corrections around 100 mm for Ch. 487 and Ch. 514 and 70 mm for Ch. 487 are evidently necessary.

(ii) Corrected horizontal displacements

In addition to zero-corrections described in the preceding item, account must be taken of the circumstance that points

HiJ (i = 1,2,3) were all of them located in between the positions of foundation rod gauge plates HiE and HiF (i = 1,2,3), for which mean absolute movements were only in the order of 30 mm eastwards from the date fill level reached fill wire extensometer elevation up to the day of banking completion. Thus, HiJ (i = 1.2,3) are not to be considered totally stationary points but, on the contrary, as points that actually experienced some movement downstream although small.

Figures 6.39 through 6.41 take into account a combination of all corrections and cross-checks mentioned above. For the cases of Ch. 537 (figure 6.39) and Ch. 487 (figure 6.41), curves corresponding to inclinometer displacements were used as bases for the plots, as these measurements were believed to be the most accurate of the techniques employed. Assuming that inclinometers and HiG plates coincided in space, relative movements between adjacent plates were then added after the folowing zero-corrections had been introduced:

a) Ch. 537 - Non observed interval: 58.0 - 61.5 m AOD

$(H1G - H1Y)_{61.5} = + 90$ mm

$(H1G - H1H)_{61.5} = - 40$ mm

$(H1H - H1J)_{61.5} = -10$ mm

b) Ch. 487 - Non-observed interval: 62.0 - 64.5 m AOD

$(H3G - H3Y)_{64.5} = + 50$ mm

$(H3G - H3H)_{64.5} = - 30$ mm

$(H3H - H3J)_{64.5} = - 10$ mm

In the same figures, absolute movements of the EDM targets S1Y and S3Y, corresponding to points cast in concrete slabs named H1Y and H3Y, were also drawn as a means of cross-examination of the combined inclinometer-rod gauge plots. A zero correction of 250 mm at elevation 63.5 m AOD was applied for S1Y, whereas 160 mm were added to S3Y's reading at elevation 65.8 m AOD. Resulting curves agreed quite well, the maximum difference between both kinds of graphs never having exceeded 30 mm on the dates of measurements.

Having obtained the confirmation of the reliability of EDM results, they were zero-corrected by the addition of 170 mm and used as a guide for the calculation of displacements in the section at Ch. 514 (figure 6.40), whose general trends very much agree with those of Ch. 537. An independent check was provided by the known horizontal movement endured by the foundation rod gauge plate H2C (figure 6.30), situated at roughly the same easting as H2G; both curves are compared in figure 6.40 and show a very pronounced resemblance in shape as well as in magnitude. Here too, relative movements between adjacent plates were zero-corrected before they were added to EDM's base line, values adopted being state below.

Ch. 514 - Non-observed interval: 60.0 - 62.5 m AOD

$(H2Y - H2G)_{62.5} = - 70$ mm

$(H2G - H2H)_{62.5} = - 20$ mm

$(H2H - H2J)_{62.5} = - 10$ mm

The various plots displayed in figures 6.39 to

6.41 were put together in figure 6.42, where the independent variable used in x-axis was not fill elevation, as in the previous drawings, but the difference in level between fill crest at any given day and the elevation of each particular wire extensometer set. The agreement between curves corresponding to Ch. 537 and Ch. 514 is quite remarkable and the plots for Ch. 487, although not so coincident, still exhibit a reasonably good fit in the case of slope points (S3Y and H3Y). Extreme differences never exceeded 80 mm at any stage.

An interesting check for the movements of slope points during construction is provided by the comparison of figures 6.21 and 6.42. In the former, the rate of lateral displacement with increasing bank height, for the last 10 metres, fluctuated between 45 and 57 mm/m of fill, according to the different curves there pictured, whereas in figure 6.42 average values for SiY and HiY (i = 1,2,3) in 10 metres of fill (7 metres in the case of Ch. 487) ranged from 48 to 53 mm/m of fill.

(iii) Accuracy of the results

Although the individual precision of the three different sorts of instrumentation employed was quite good when compared to the magnitude of displacements measured, overall accuracy was greatly spoilt by the fact that long time intervals had elapsed when first readings were taken, which have required the use of large zero-corrections, not only for rod-gauge relative movement measurements but also for EDM results, essential in the calculation or check

of absolute displacements.

A careful balance of all observations was done, however, as described in preceding sections and it clearly appears that maximum errors were never greater than 80 mm and, probably, were considerably less, around 50 mm perhaps. In terms of proportion of maximum movement, the accuracy was quite probably around 10% and, certainly, better than 20%.

6.1.4 Surface Reference Points - EDM Surveys

(i) Operation

The short-range EDM instrument employed in periodical surveys of reference points located on the slope of the trial embankment and on the trench parallel to the bank axis was the Tellurometer MA-100, an equipment manufactured by Plessey S.A., with basis on a project developed at the National Institute for Telecommunications Research of the South African Council for Scientific and Industrial Research, and marketed by the Plessey Group.

The apparatus was set up over reference benchmarks, remotely located with respect to the trial bank, by means of a tripod, a telescope being used to line up the instrument on the reflectors placed on the slope, at the various points whose movements it was intended to measure.

Following a fifteen minute warm-up period when starting from cold, the equipment was switched to 'automatic' and readings were then taken, the operator switching in sequence through

the various pattern frequencies to obtain finally an uncorrected slope distance measurement. Corrections for change in refractive index were calculated with basis on atmospheric pressure and temperature and applied to the readings. Every point was shot from two independent bench-marks and calculations, carried out by trilateration, were further corrected for level variations of targets measured by conventional levelling.

In the first sets of observations, it is believed that the number of reflectors in use was excessive and this may well have been a cause for abnormal readings, a possibility suggested by HOLSCHER (1969). The fact is that results were somewhat erratic in the beginning and became much more consistent when reflectors were reduced in number. Initial measurements were then discarded and the first set of reliable readings were taken on day 38, when fill elevations were 58.3 m AOD at Ch. 537, 58.4 m AOD at Ch. 514 and 59.4 m AOD at Ch. 487.

(ii) Measurement results

Horizontal displacements calculated with basis on initial reliable readings taken on day 38 are presented in figure 6.43, where the location in plan of every surface reference point is shown.

In figure 6.44, the points situated at elevations between 54 and 56 m AOD have been put together so that it became easier to compare them and observe the similitude of horizontal movement experienced by points of chainages 500 to 550. These displace-

ments slightly decrease in a steady way towards both abutments.

Neither figure, however, included any correction for the non-observed period between the time fill elevation reached the level at which monuments were put and the day number 38. Nor did figure 6.37 where lateral displacements of some selected points were plotted against time in days and also compared to wire extensometer curves.

Zero-corrections were introduced in drawings number 6.18 through 6.21 and 6.39 through 6.42, where movements of EDM targets were plotted against fill elevations or height of fill above the given points and compared to rod gauge readings and inclinometer observations. In general, these comparisons provided quite good agreement, particularly if the possibility of tilting of the concrete blocks SiX ($i = 1,2,3$), on the top of which the reflectors were installed, is taken into consideration.

Another aspect of horizontal movements as measured by EDM equipment refers to their components along the bank axis. Both figures 6.43 and 6.44 show that displacements of surface monuments occurred in a fan-like fashion, points moving towards the valley sides instead of its bottom. This was probably due to the convexity of the earth-structure and it is quite possible that the pattern in the central zones of the fill was different. According to the measurements, the distance between chainages 487 and 514 stretched nearly 200 mm, or 0.8%, at the outside of the bank.

(iii) Accuracy

As mentioned earlier, the accuracy of a measurement system can only be approximately evaluated by comparison to the results obtained from other independent systems. This was done with respect to horizontal movements as measured by surveys of inclinometer wells, readings of rod gauge displacements and surveys of surface monuments by EDM device. Results attained have already been quoted in previous items.

6.2 VERTICAL DISPLACEMENTS

6.2.1 Inclinometer Settlement Magnets

(i) Operation

Detection of levels of settlement magnets attached around inclinometer ducts was a very simple and rapid operation. The reed-switch probe was slowly lowered inside the pipes while hanging from an electrical cable and a graduated steel tape. As soon as it reached the zone of influence of a magnetic ring a whistle was heard outside the well and the tape marking coinciding with the inclinometer top recorded. To ensure that the measurement had been properly carried out, the probe was raised some 200-300 mm, again lowered more slowly, and the previous reading checked. Usual operation consisted of approaching magnets from top to bottom, but once or twice this procedure was reversed without any difference in results being observed.

After inclinometer tubes had become so distorted that the probe could not pass and thus reach the base, its 3 in (76 mm) dia. cover was removed and replaced by a thinner one (2 in = 51 mm dia.); this proved successful for a period of time but, as inclinometer distorsion proceeded, even this thinner cover had to be abandoned and the bare probe, around 1 in = 25 mm dia., was then utilized. With the 2 in. probe, accuracy of measurements decreased but it was still perfectly acceptable; the bare probe, however, produced erratic readings that had to be eventually discarded.

As the fill rose, new inclinometer lengths were added and settlements went on, the reference used for magnet level measurements frequently changed and only a very accurate independent means of assessing the elevation of inclinometer tops would allow a precise estimate of magnet collar levels. As for the measurement of shortening (or extension) of each individual length between adjacent plates, from which average linear strains can be worked out, it is entirely independent of the well top elevation on a particular date and is obtained by straight difference between successive readings. At the Empingham Trial Bank experiement, as inclinometer tops were neither frequently nor accurately surveyed, greater emphasis was placed on the measurement of strains rather than on settlements; when vertical movements are referred to in connection with magnetic ring surveys, they actually represent relative displacements with respect to the lowest magnet of each inclinometer, assumed unmoved. This approach is justifiable as far as undrained settlements are

concerned, since with no horizontal movement having been recorded in a fully saturated material, no vertical displacement could occur either; consolidation of lower clayey layers into the Marlstone, however, may well have induced unrecorded movement in the vertical direction.

(ii) Measurements

With basis on the assumption that lowest rings were fixed, vertical movements undergone by the various magnetic collars, both in the fill and in the foundation, were calculated and plotted in figures 6.45 through 6.48. In these drawings the results of measurements are presented exactly as they were recorded, without any of the corrections further described in this chapter.

Including the initial sets of readings, 44 surveys took place, from day -10 (23-6-72), before placing of fill started, until day 121, about a month after construction ended. The only points to exhibit heave instead of settlement were the two upper points of I1 (figure 6.45), shallowly located with respect to the stripped ground level, close to the embankment toe, where up to 250 mm vertical movement upwards was recorded. As expected, deformation of fill material was much more pronounced than in the foundation; while maximum fill settlements were in the order of 350 and 450 mm, for I4 and I2 respectively, the greatest displacement measured for foundation points neared 60 and 90 mm at those same inclinometers (here again, uncorrected figures).

(iii) Zero-corrections

In the foundation, no zero-correction was necessary, as the magnets were inserted in the boreholes well in advance of the commencement of the banking operation. In the fill, however, zero-corrections could only be dispensed with if magnet levels were determined at the time the fill crest elevation coincided with it, which in general did not happen at Empingham.

An attempt to determine zero-corrections for the various collars in the fill is shown in figures 6.49 and 6.50. In the case of I4 (figure 6.50), corrections were small (unless, perhaps, for the ring denoted V44B), as the surveys shortly followed the moment magnet and fill levels were equivalent. Unfortunately, the damage caused to I2, accidentally hit by a tractor, forced the removal and replacement of the two upper inclinometer lengths, whose rings had already been initially surveyed; when new zero-levels were measured, fill was considerably higher than the collars (6.6 metres for V22B and 3.6 metres for V23B) and this resulted in very high corrections of doubtful accuracy.

As displayed in figures 6.49 and 6.50, zero-corrections consisted of plotting displacements versus fill elevations and back-extrapolating the curves in order to estimate what the initial magnet elevation would have been, had the graphs behaved in a similar way before and just after observations started. This procedure obviously involves a great deal of uncertainty and the

values attained can only be regarded as gross estimates in the case of large corrections being necessary, as occurred to I2, when up to 261 mm additional movement was obtained.

(iv) Grout stiffness correction

After inclinometer ducts and magnetic rings had been inserted in the borehole put down in the foundation, annular spaces were backfilled with an 1:1 cement-bentonite grout, believed to have been stiffer than the surrounding soil. As fill proceeded and new inclinometer casing lengths were added, they were surrounded with loose dry sand, probably more compressible than the undrained rolled fill.

An example of the sort of errors that may arise from the differences in stiffness above pointed out is pictured in figure 6.51. If the grout column stiffness matched with that of the foundation soil, vertical displacements experienced by magnet M_o would equal those of the soil, similar behaviour being expected of the other rings, placed in the fill. If, however, grout stiffness were much higher than that of the surroundings, arching effects would not be able to balance the difference and M_o level would remain practically stationary while soil particles remotely placed with regard to it would behave normally.

If, at the same time, the sand involving the porion of the inclinometer situated in the fill were less stiffer than the compacted soil, magnets M_i (i = 1,2, etc.) would either

accompany soil movement or endure an even larger settlement in the case of the sand not withstanding the arching required to sustain the difference in vertical stress.

Hypothesizing that (a) there was actually a 'punching' of the grout column into the fill and ring M_o did not move at all, and (b) correct soil movements were recorded through fill magnets M_i (i = 1,2,etc.), the apparent shortening of length L_1 after the n-th lift was placed would be:

$$\rho'_{1,n} = \text{elev.}(1;1) - \text{elev.}(1;n) \qquad (6.6)$$

whereas the correct decrease in the layer thickness would equal:

$$\rho_{1,n} = \text{elev}(1;1) + \text{elev.}(0;0) - \text{elev.}(1;n) - \text{elev.}(0;n) \qquad (6.7)$$

The error committed is the difference between (6.6) and (6.7):

$$\Delta\rho_{1,n} = \text{elev.}(0;0) - \text{elev.}(0;n) \qquad (6.8)$$

or, in terms of average linear strain:

$$\Delta\epsilon_{1,n} = \frac{\Delta\rho_{1,n}}{L_1} = \frac{\text{elev}(0;0) - \text{elev.}(0;n)}{L_1} \qquad (6.9)$$

In practice, unless if the grout were too stiff, some vertical movement would take place at M_o and real errors would lie between zero and the values expressed by (6.8) and (6.9); in the case of observed fill magnet settlements being greater than those

of real soil, however, the errors involved could exceed them.

Evidences that errors of the kind herein mentioned did occur at Empingham Trial Bank can be seen in figures 6.52 to 6.55, where apparent average linear strains obtained from settlement magnet readings are presented for I2 and I4. In every graph, one of the two lowest lengths appeared to have experienced abnormally high strains, a fact probably due to an aggregation of real strains within the layer plus the effect of the foundation settlement resisted by the grout column. In those drawings, a correction was attempted by supposing that a linear relationship between elevations and strains should apply and by attributing to the foundation the difference found between extrapolated and measured strains.

(v) Sand compressibility correction

The loose dry sand surrounding inclinometer ducts in the fill was probably more compressible than the rolled fill under undrained conditions and moderate stress. Arching effects, however, might have caused a redistribution of stresses in such a way that vertical displacements undergone by magnetic collars involved by sand could have correctly reproduced real movements in the embankment. A means of verifying as to whether or not this happened is below described.

Under undrained conditions, reduction in volume of partly saturated materials is due to compression of air voids. The measurement of the degrees of saturation at the time the fill

was compacted (S_{in}) and after banking completion (S_f) allows the determination of volumetric strain (ϵ_v) through the following approximate expression where the porosity (n) is, for simplicity, assumed not to vary:

$$\epsilon_v = (S_f - S_{in}) \cdot n \qquad (6.10)$$

At Empingham, initial saturations were measured on samples taken from the field soon after compaction; their values were consistently around 90%. Final saturations, obtained from undisturbed samples taken from a borehole put down through the fill after banking had reached its end, were approximately 96% in lower layers of the embankment. Porosity being 40%, ϵ_v would be around 2.5%.

At high degrees of saturation, air in soil exists as trapped bubbles not connected to the atmosphere. If the air voids are assumed to be initially subjected to atmospheric pressure, the construction of about 20 m of fill above a soil element causes air pressure to be multiplied 3 to 5 times. Isothermal air compression and solubility of air into water would reduce voids to 1/4 to 1/8 of initial volume. At Empingham Trial Bank this would mean a volumetric strain of 3.0% to 3.5%.

Under plane strain conditions, vertical strains (ϵ_z) are expressed by

$$\epsilon_z = \epsilon_v - \epsilon_x \qquad (6.11)$$

where ϵ_x are transversal (across the bank) strains.

Transversal linear strains in the regions of I2 and I4 were, at the end, between -1.5 and -2.0% (extension). Vertical strains amounting 4 to 6% were, therefore, to be considered an evidence of the backfilling sand having behaved similarly to the fill. In figures 6.52 through 6.55, after the 'excess' strain was discarded, maximum values of 4.5% and 7.5% still remained for I4 and I2, respectively. The first figure is possibly acceptable while the second appears to be somewhat excessive. No alteration was introduced in the results as a consequence of such a finding, but it is considered that corrected fill settlements might be 20% to 50% higher than real ones.

(vi) Corrected settlements

Vertical displacements shown in figures 6.56 and 6.57 incorporate two sorts of corrections: zero-corrections, to cope with unrecorded movements in the fill before readings were first taken, and a grout stiffness correction, to balance the 'punching' of the grout column into the fill and annul the error induced by it in the computation of foundation settlements. The sand compressibility correction described in previous section, was not applied to calculations.

Application of either type of correction to I1 and I3 was considered unimportant as, in both cases, heights of fill were small and no time gap had occurred prior to initial set of readings. Futhermore, in the case of I1, the movement of upper magnetic rings had been upwards, in which case the influence of grout stiffness

in tension was even more difficult to evaluate. Figures 6.45 and 6.47 represent thus the best estimates for movements undergone by settlement magnets in those locations; if any correction should be made, this would consist of adding some 10 mm as zero-correction for point V31B of I3.

Figures 6.58 and 6.59 depict uncorrected displacements experienced by the highest foundation magnets of I2 and I4, denoted V26F and V47F, respectively, as well as the values obtained after zero-correction and grout stiffness correction. Movements of the lowest fill collars (V21B and V41B) are also shown, both without and with corrections. While maximum corrected foundation movements were 100 to 150 mm, fill ones reached 250 mm at I4 and 350 mm at I2.

Still in figures 6.58 and 6.59 are plotted the results of hydraulic settlement probe observations corresponding to points located at intersections with I2 and I4. Maximum figures were around 200 mm, between the values obtained for foundation and fill magnets, as might be expected.

A comparison was made between the volume of soil displaced horizontally (as measured by means of inclinometers) and that displaced vertically (as measured by the hydraulic gauge). Under plane strain conditions and no drainage occurring, both quantities should equal. At Ch. 487, calculations resulted in 1.1 m^3/m run of horizontal flow and 4.2 m^3/m run of vertical flow. At Ch. 537, corresponding figures were 1.5 and 6.2 m^3/run. In both

cases vertical flows were approximately 4 times larger than horizontal ones; this difference is probably due to consolidation of upper layers of the foundation, where overall permeability was much higher than a few metres below foundation level, and also to consolidation of bottom of the Upper Lias Clay into the Marlstone.

In figures 6.60 and 6.62, movements of collars V16F (Ch. 537), V38F and V31F (Ch. 487) are plotted against time in days and compared with measurements taken by other devices, namely the conventional levelling of surface reference points and the survey of horizontal ducts at the foundation top by means of the hydraulic settlement probe. The point V16F, at I1, some 5 metres from the toe, underwent a displacement above 200 mm upwards, whereas V16F and V31B, both at I3, located nearly 20 metres from the trench base, moved downwards 15 and 60 mm, respectively. Observation of data contained in figures 6.60 through 6.63 shows that, although values differ quite considerably from one instrumented section to the other, there is a general agreement between displacements of points located close, even when measured through different systems.

Figure 6.63 emphasizes particularly the general trend of vertical movements in the region around slope toes; while the toe and a part of the unloaded ground at its left moved upwards, this tendency is reversed somewhere between 8 and 20 m from the toe towards the bank centre, displacements then becoming downwards.

(vii) Equipment performance

As already mentioned, the detection of magnet levels by means of the reed-switch probe was quite an easy, simple, rapid and precise operation while inclinometer tubes were not distorted enough to impede the access of the probe with its original plastic cover. Even after the cover had to be replaced by a thinner one, measurements were still precise enough for the purposes in hand and the other aspects of the apparatus performance continued as before. When covers had to be totally removed, which only happened for final readings at two of the four inclinometer ducts, erratic behaviour became so pronounced that the measurements proved useless.

The buzzer sound was very clear, easily heard by the operator even when heavy plant was working nearby and the wind blowing strongly.

The need of using a steel tape to obtain precise level measurements makes operation a little awkward particularly when the probe jammed inside distorted pipes and had to be pulled up using the weak and strectchable electrical cable or, as was the case, using the brittle steel tape that once broke during the tugging. It also happenend sometimes that the tape and the cable were not advanced jointly and eventually tangled together with risk of damaging either line and causing wrong readings.

Carefully operated, however, the measuring system proved very reliable, simple and precise.

(viii) Measurement accuracy

The precision achieved in measuring magnet levels is certainly within ± 2 mm and the repeatability found in the vast majority of readings was in a even narrower band, comprised between ± 1 mm with respect to the average.

The overall accuracy, however, depends on how perfectly the transference of soil settlements to magnetic collar movements occurs, a factor affected by the grout column stiffness, the ease with which the rings slide on the ducts, the force necessary to shear coupling rivets, etc.

An independent check for the accuracy of settlement magnet surveys would be provided by the hydraulic settlement gauge inserted in horizontal tubes just below stripped ground level. Figures 6.60 and 6.61 show that hydraulic gauge data lies, as expected, between corrected movements for the top foundation ring and the bottom fill one, but, as the curves differ by quite large an amount, the check is inconclusive as means of providing an idea of the accuracy of the measurement.

Another independent way of assessing the accuracy of the magnetic system is provided by the comparison of their readings with conventional levelling of surface reference points. This is done in figure 6.62, where movements of surface monument S1X and foundation magnet V16F are put together; the curves agree reasonablywell over most of their paths, but the fact that the points do not coincide spacially, aggravated by the large gradient shown in

figure 6.63 for settlement plots against distances from slope toes, makes it impossible to draw any definitive conclusion, particularly because the example herein quoted refers to a case of heave where the accuracy does not necessary equal the one for positive settlements. An even better evidence of accuracy of the system in the case of heave arises from the same figure by the comparison between the movements undergone by V16F and the top of inclinometer I1; from days 24 to 144, the maximum difference between the two curves is around 10 mm, part or all of which could be attributed to partial closing of the gap at the highest coupling, slide of the V16F magnet along the pipe or settlement of the lowest collar assumed fixed.

A good comparison of vertical settlements as measured by different systems is provided by the plots corresponding to magnet V38F and point A of the hydraulic gauge profile, at figure 6.60. Both points are at the same distance from the trench base and, even though their elevation differs by some 2.5 metres and their chainages by roughly 4.5 metres, their movements follow an approximately equal pattern, the greatest discrepancy between them having been 40 mm; whether this difference is due to basic inaccuracy of either system or to the fact that they were not at exactly the same location remains of course open to question. Another cross-check is provided by conventional levelling of the top of inclinometer I3, whose results are also displayed in figure 5.16; the difference between this curve and that corresponding to V31B never exceeded 10 mm, a low figure that can be partly or totally discarded by

consideration of closing of the coupling gap, magnet sliding or settlement of the inclinometer base.

6.2.2 Hydraulic Settlement Gauge

(i) Operation and performance of the apparatus

With the cable drum resting on the concrete slab datum points D1 or D3, the probe was pulled all its way by an operator situated at the opposing end of the tunnel by means of a rope attached to the probe, the cable and the graduated steel tape being gradually unreeled. Then, reversing the movement, cable and tape were reeled back and the probe slowly brought to its original place, the operation being periodically interrupted so that levels displayed in the readout unit and distances measured at the tape could be recorded. It was a time-consuming procedure that always required a minimum of two operators, frequently more.

The principal of the apparatus requires that the water remain permanently deaired, as changes in fluid density caused by the presence of expansible air bubbles greatly affects the pressure at the transducer in the reel centre and obviously generates errors in the measurement. The possibility of air entering the system and coming from the water is greater the greater the differences in level between the point to be surveyed and the transducer, since suctions are higher in these cases. As settlements proceed, the situation is obviously aggravated. Changes in temperature are also matter for concern owing to the resulting variation of density

and pressure.

After the first readings taken with the instrument, various abnormalities were observed. Measurements changed with time, even though the probe was not being displaced and readings taken with the probe lying on the datum slab, before and after the set of observations, differed by up to 50 mm. Air bubbles and temperature effects were first thought to be responsible for such odd behaviour and, as a consequence, the sealed line was emptied, some air bubbles in fact found and the fluid entirely replaced by deaired water. Calibrations were then carried out, showing an improvement in results, although unexplained time-dependency of readings and zero-shifts still occurred. The apparatus was then returned to the manufacturers who found the pressure transducer to be defective, replaced it and returned the instrument to the site. From this date, its behaviour was much more consistent but not perfect, temperature and air bubbles being believed to be the cause of the remaining inaccuracy.

Apart from the measurements themselves, some operational difficulties limited the usefulness of the device. As banking proceeded and the earth mass distorted, insertion of the probe into the tube became harder and harder, two or more people being necessary to pull it from the inside end. The effort required to displace the probe inside the distorted pipes was so great that the probe was once severed from the cable. It at times also happened that the steel tape twisted on the cable making the correspond-

ence between vertical displacements and distance from the datum somewhat uncertain.

Figures displayed in the readout represented differences in level between the concrete datum and the desired point. In order to have correct settlement values, elevations of the spot where the drum rested had to be periodically surveyed. This was done by means of conventional levelling, whose precision was of few millimetres, probably better than the overall accuracy of measurements taken with the hydraulic probe. A deep bench-mark consisting of a sleeved rod founded in the Marlstone outside the bank was used as reference.

As reliable readings were only taken from day 44 onwards, initial horizontal profiles used in the calculation of settlements were those obtained by conventional levelling of the pipes at the time they were laid down in the instrument trench.

(ii) Results

In figures 6.64 and 6.65 the results of settlement measurements made with the hydraulic probe are presented.

At Ch. 487 maximum settlement was little over 200 mm, whereas at Ch. 537 it reached 300 mm. A basic difference between the two sets of profiles is that while maximum movement occurred beneath the final crest at Ch. 537, in the case of Ch. 487 it corresponded to the location of inclinometer I4, at the inner end of the berm. This suggests the development of two distinct types of earth movement, more restrict in area and closer to circular

shape at Ch. 487, more extensive and flatter at Ch. 537

In both sections, maximum settlements in each set of readings gradually shift from the toe eastwards following the displacement of the slope top towards downstream. This is a characteristic of undrained deformation, imposed by high shear stresses underneath the slopes, as opposed to settlements induced by consolidation, where the magnitude of the vertical stress is the governing factor.

Another noteworthy aspect of the curves refers to the direction of movement in the region by the toe. The findings of conventional levelling and the settlement magnet system are confirmed and it is possible to see how steep the profiles are close to the western end of the fill, with heave clearly developing even at early stages of the constructional period.

(iii) Comments on the accuracy of the measurements

As already pointed out in this chapter a precise definition of how accurate settlement measurements were is made very difficult by non-coincidence of measuring points, absence or unreliability of readings during certain periods, etc. Laboratory calibration, scatter observed during operation and comparison to values obtained independently, however, suggests an overall accuracy of ± 30 mm, certainly not a satisfactory figure in principle but reasonable for the magnitude of displacements involved at Empinham.

6.2.3 Levelling of Surface Monuments

Surface reference points depicted in figure 4.4 had their levels frequently surveyed through conventional methods. Some of the results have already been presented in figures 6.60 to 6.63 but they are again comprehensively displayed in figures 6.66 and 6.47, in which the only missing records are those of the monument S9, whose behaviour completely differed from the general pattern.

Much in the same way as before noted for hydraulic probe and magnetc ring surveys, upward movements predomimated at points on trench base, trench slope and fill toe, i.e points at lower elevations, a common trend in every instrumented section being a decrease in heave from west to east, eventually transformed into settlement. This is clearly pictured in figure 6.68, where vertical movements were plotted against monument elevations.

The repeatability of measurements, as seen in figure 6.66, was within a band 10 mm wide at early stages of fill placing, particularly in the period from day 16 to 38 when little if any soil was added to the bank.

Except for S9, all surface monuments behaved well, their levels agreeing quite reasonably one with another as well as with other forms of vertical movement measurement. In figure 6.60, for example, S3X's records are seen practically to coincide with the average between S5's and S6's, points symmetrically located with respect to S3X. Levels of I3 Top from day 24 onwards are seen in the same figure to run parallel to V3lB's ones. In figure 6.62, the

V16F curve and that corresponding to the I1 Top are similar and the plot for S1X, despite not being at the same location, largely follows the common trend.

6.3 OVERALL PATTERN OF DISPLACEMENTS

It was emphasized in section 6.1 that horizontal movements as measured by means of the various independent systems agreed quite well and that the pattern followed in the three instrumented sections were practically coincident.

As for the vertical movements, dealt with in section 6.2, the results of different sorts of measurements did not agree to the same extent and several corrections were necessary.

Nevertheless, as the horizontal displacements predominated over the vertical ones for most of the observational period, whatever the values of settlements used in calculations (within the range of uncertainty), the direction and magnitude of displacement vectors do not vary much, particularly at the points which experienced larger movements.

Figures 6.69 through 6.72 show displacement vectors corresponding to 4 stages of construction. For the sake of clarity, points within the fill were pictured separately from those in the foundation, but those on the boundary appear in both sort of drawings. These figures were based on the best estimates for vertical displacements but, as already pointed out, their overall pattern is not as much influenced by the magnitude of settlement as it is by

the values of horizontal movements, particularly in the foundation.

In figures 6.69 and 6.71 it is seen that, while at Ch. 487 the foundation movement appears to have followed an approximately cylindrical surface, at Ch. 537 a non-circular, nearly horizontal surface seems to have preponderated along most of the foundation top zone affected by undrained shear movement. This has been possibly caused by differences in geometry between the two sections and/or by the presence of atypical foundation soil at Ch. 537 (the 'bulge' area).

Post-constructional movements are not depicted in figures 6.69 to 6.72.

6.4 HORIZONTAL STRAINS

6.4.1 Foundation Wire Extensometers

From horizontal displacements as measured through wire extensometers (rod gauges) installed in the foundation, average horizontal linear strains were worked out.

In figures 6.73 through 6.75, average horizontal strains, calculated for each individual length between adjacent plates, are plotted against time, in days, since the day of the installation (day 3) until 5 months after banking completion. They were calculated on the basis of measured displacements, no correction having been applied to compensate for movements before initial readings, adjustment of the plates in the sand of the instrument

trench, stretching of the wires, etc.

Initial distances between adjacent plates varied from 10 to 30 metres and, for such lengths, the repeatability of measurements, in terms of strains, was generally of the order of ± 0.02%. Initial adjustments gave place to errors of about 0.1% in general, exceptionally rising to 0.2%.

Figure 6.75 corresponds to Ch. 537, where a 'kink' was formed on the rod gauge tubes from days 40-50 onwards. As a consequence of it, apparent strains at length H1X-H1A were abnormally high. After the ground was excavated near the bank toe and the 'kink' undone (days 123-126), values of strains at all lengths but that particular one remained approximately the same. At H1X-H1A, as expected, they returned to values around zero; scatter after that, however, ranged from -0.25% to +0.20%, much larger than at the other sections; this might have resulted of movement of the tubes laid down outside the embankment between the toe and the reference concrete slab, caused by plant or labour working at that spot.

In figures 6.76 to 6.78, horizontal strains developed during the constructional period are plotted against fill elevations, after the application of corrections described in section 6.1.3.

Observation of drawings numbered 6.73 through 6.78 show some common trends which can be summarized as follows:

a) at each particular length, horizontal strains increased more rapidly as the embankment slope was approaching the

first plate to the West, during the time the slope was being constructed above the length and shortly after it;

b) at a given instant, for points located beneath the embankment slope, the greater the height of fill above them the larger the strains.

c) as a consequence of (a) and (b), the development of horizontal strains with time followed a characteristic pattern described as follows: at the beginning, strains were greater by the bank toe, decreasing towards the axis; as construction proceeded and the slope advanced inwards, higher strains developed in subsequent lengths; at each particular moment, the largest strains approximately corresponded to lengths beneath the junction of the crest with the slope;

d) post-constructional horizontal strains were greater at inner lengths, both in absolute values and proportionally to values of strains during construction;

e) post-constructional horizontal strains were higher at those lengths which had experienced greater rate of strain increase immediately before banking completion.

In each of the curves in figures 6.73 to 6.78, 4 well characterized portions of the final horizontal strains can be visualized: (i) initial strains, prior to the rapid increase phase, (ii) strains developed during the steep parts of the curves, (iii) strains developed between the end of the steep part and the completion of the embankment, and (iv) post-construction strains.

In Table 6.3, among other data, the values of these 4 portions of strains are presented for the four central lengths of each instrumented section, and the characteristics described in items (a) to (e), above, are perhaps more easily demonstrated. Taking the length CD of Ch. 487, for example, one observes that from the construction beginning up to the moment fill reached elevation 62.5 m AOD, the horizontal strain at that length had been only 0.1%; from this elevation to 69.5 m AOD, it rose to 1.7%, at a rate of 0.23%/metre, the limits of such steep a portion of the curve corresponding approximately to final fill elevations above the length of 63.0-67.3 m AOD; this high rate of strain increase, close to the end of construction, was followed by considerable post-construction strains, amounting 0.7% or 41% of the total strain during construction.

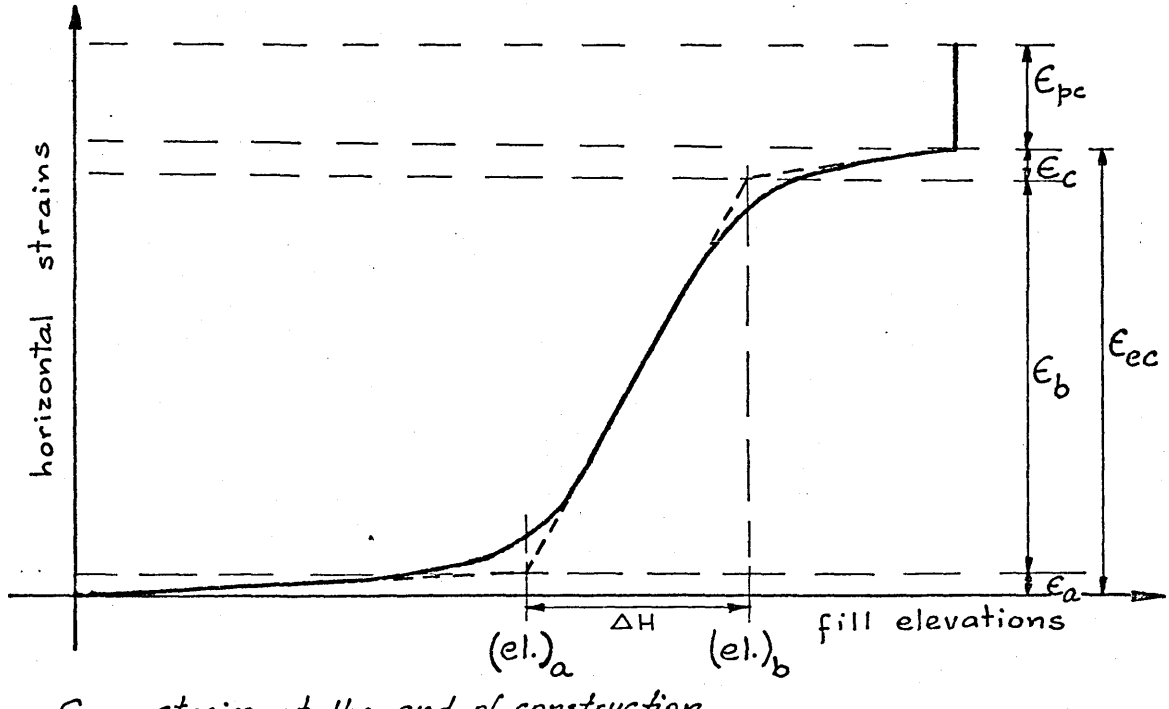
Figures 6.79 through 6.84 depict total and incremental strain distributions at 6 stages of the construction period in each of the 3 instrumented sections. In those drawings, the 'horizontal strain ripple' pattern is conveniently exposed. As construction goes on, the height of fill increases and the junction between the crest and the slope displaces towards the centre. While this happens, the zones of maximum strains also moves inwards until the final configuration, where they are located in the centre. Post-construction strains, not shown in those figures, do not alter the shape of final strain distributions but they magnify the difference between central and extreme strains.

TABLE 6.3

Average Horizontal Strains in the Foundation

Wire Extensometers

Ch.	Pts.	Final fill el. above points (m AOD)	Horiz. Strains (%)					El. limits steep part $(el)_a$-$(el)_b$ (m AOD)	$\frac{\epsilon_b}{\Delta H}$ (%/m)	$\frac{\epsilon_{pc}}{\epsilon_{ec}}$ (%)
			ϵ_a	ϵ_b	ϵ_c	ϵ_{ec}	ϵ_{pc}			
487	A–B	59.5–62.8	0.1	0.5	0.1	0.7	0.1	60.0–64.0	0.12	14
	B–C	62.8–63.0	0.1	0.8	0.2	1.1	0.3	60.1–66.0	0.13	27
	C–D	63.0–67.3	0.1	1.6	0.0	1.7	0.7	62.5–69.5	0.23	41
	D–E	67.3–70.2	0.1	0.8	–	0.9	0.6	66.0–70.2	0.13	67
514	A–B	61.7–63.6	0.0	1.1	0.0	1.1	0.0	56.0–63.0	L.16	0
	B–C	63.6–65.3	0.1	1.2	0.0	1.3	0.0	59.0–65.0	0.20	0
	C–D	65.3–69.9	0.2	1.4	–	1.6	0.6	62.0–70.0	0.17	38
	D–E	69.9–68.5	0.2	1.2	–	1.4	0.8	64.5–+0.0	0.22	57
537	A–B	56.0–60.8	0.1	0.7	0.0	0.8	0.1	57.0–61.0	0.17	12
	B–C	60.8–64.2	0.1	1.0	0.2	1.3	0.3	58.0–65.0	0.14	23
	C–D	64.2–68.3	0.1	1.4	–	1.5	0.5	60.0–68.6	0.16	33
	D–E	68.3–68.6	0.2	1.2	–	1.4	0.7	64.0–68.6	0.26	50



ϵ_{ec} : strain at the end of construction.

ϵ_{pc} : post-construction strain.

Post-construction strains at the 3 most strained lengths of chainages 487 and 514 are pictured against time, in logarithmic scale, in figure 6.85. Those corresponding to Ch. 537 were not included in the face of their atypical behaviour due to the formation of the 'kink' on the rod gauge tube. The lengths C-D and D-E, located underneath the highest zone of the embankment, showed pronounced strain increases, approximately parallel, whereas the B-C lengths, situated at outer positions, experienced much less post-construction horizontal strains. This is possibly explained by the fact that strains during construction at the length B-C were tapering down since day 55, an indication that creep strains might have been developing at that zone a long time before construction ended. All 6 curves are approximately straight lines, with some convexity at both ends. The period of time between days 95 and 135, when all graphs follow more closely the straight line patterns, corresponded to the rates of horizontal strain increase shown in Table 6.4.

TABLE 6.4

Rate of Post-Constructional Horizontal Strains

Foundation Wire Extensometers

Chainage	Points	$J = \frac{d\epsilon_x}{d(\log_{10} t)}$	$J' = \frac{d\epsilon_x}{d(\log_e t)}$
487	B-C	0.0015	0.0007
	C-D	0.0030	0.0013
	D-E	0.0024	0.0011
514	B-C	0.0003	0.0001
	C-D	0.0026	0.0011
	D-E	0.0034	0.0015

The horizontal strain in a particular length at a given time t, after the end of construction, can be approximately calculated by the expression:

$$\epsilon_{x,t} = \epsilon_{x,(t_{ec}+1)} + \log_e (t-t_{ec})^{J'} = \epsilon_{x,(t_{ec}+1)} + \log_{10} (t-t_{ec})^{J} \qquad (6.12)$$

where $\epsilon_{x,t}$ is the horizontal strain at the time t, t_{ec} is the time at the end of construction and J and J' are defined in the headings of the two columns at the right of Table 6.4.

If time is expressed in days, $\epsilon_{x,(t_{ec}+1)}$ can be replaced by 1.05 x ϵ_{ec} and (6.12) becomes:

$$\epsilon_{x,t} = 1.05\,\epsilon_{ec} + \log_e (t-t_{ec})^{J'} = 1.05\,\epsilon_{ec} + \log_{10} (t-t_{ec})^{J} \qquad (6.13)$$

where ϵ_{ec} is the horizontal strain at the end of construction.

The values of J shown in Table 6.4 (0.0003 to 0.0034; average 0.0022) are of the same order of magnitude of those of $d\epsilon_1/d\,(\log_{10} t)$, calculated for undisturbed brown London Clay in drained creep tests (BISHOP, 1966, fig. 34) under various stress levels: 0.0008 to 0.0020; average 0.0015. They are also intermediate between figures quoted by LADD (1967) for rates of secondary compression in oedometer tests on overconsolidated clays exhibiting overconsolidation ratio in excess of 2 ($d\epsilon_z/d\log_{10} < 0.001$) and on normally consolidated clays ($d\epsilon_z/d\log_{10} t > 0.05$). Two points must be emphasized, however. Firstly, both cases differ from that of Empinham Trial Bank inasmuch as they were drained laboratory tests,

no rotation of principal axes occurred and their results refer to major principal strains. Secondly, as already pointed out, the lowest recorded post-construction strains, corresponding to lengths B-C, are believed to represent underestimations of actual creep strains, and, therefore, maximum post-construction strain rates are more likely to describe the real behaviour of the soil than average figures.

6.4.2 Fill Wire Extensometers

Average horizontal strains, calculated from the displacements experienced by the wire extensometer plates in the fill, are plotted in figures 6.86 to 6.88 against time in days. They follow approximately the same pattern of the foundation rod gauges but the strains are considerably smaller (around one-third less). In the three instrumented sections, the initial readings were taken 10 to 20 days after the fill had reached the rod gauges level, but the non-recorded initial strains can be estimated from the records of corresponding foundation strains (shown in dotted line in those drawings); maximum errors for HiG-HiH and HiH-HiJ ($i = 1,2,3$) are less than 0.2% in the case of Ch. 537, 0.25% in Ch. 514 and 0.3% in Ch. 487.

Post-construction strains are presented in Table 6.5 as well as in figures 6.86 through 6.89. In the latter, they are plotted against logarithm of time elapsed from the end of construction (day 92.5). In Table 6.5, strains at the time of banking completion include a zero-correction to compensate for missing

readings at the beginning of the records. As in the case of foundation rod gauges, the log plot of post-construction strains follows a straight line with convexity at both ends. Rates of strain increase J, calculated for the portions of the graphs between days 95 and 135, are seen in Table 6.5 to range from 0.0005 to 0.0025; figures corresponding to the two inner lengths were between 0.0008 and 0.0025, averaging 0.0015, about one-third less than in the foundation.

TABLE 6.5

Post-Construction Horizontal Strains in the Fill

Wire Extensometers

Ch.	Pts.	Hor.strains (%)		$\frac{\epsilon_{pc}}{\epsilon_{ec}}$ (%)	$J = \frac{d\epsilon_x}{d(\log_{10} t)}$	$J' = \frac{d\epsilon_x}{d(\log_e t)}$
		ϵ_{ec}	ϵ_{pc}			
487	Y-G	0.40	0.20	50	0.0015	0.0007
	G-H	0.75	0.25	33	0.0012	0.0005
	H-J	0.45	0.20	44	0.0008	0.0003
514	Y-G	0.50	0.20	40	0.0010	0.0004
	G-H	0.75	0.25	33	0.0011	0.0005
	H-J	0.90	0.35	39	0.0017	0.0008
537	Y-G	0.25	0.10	40	0.0005	0.0002
	G-H	1.50	0.65	43	0.0025	0.0011
	H-J	0.90	0.30	33	0.0016	0.0007

ϵ_{ec}: Horizontal strain at the end of construction

ϵ_{ec}: post-construction horizontal strains

't' in J and J' expressions stands for time elapsed after banking completion (day 92 1/2).

In figures 6.90 to 6.92, horizontal strains are

plotted against fill elevations; also in those drawings are estimates for zero-corrections based on corresponding foundation strains reduced by one-third. Corrected strains are shown in figure 6.93 for the two inner lengths HiG-HiH and HiH-HiJ (i = 1,2,3). The average rate of strain increase with height of fill varied between 0.06 and 0.15%/m, most curves falling in the 0.075-0.095 range; these figures are slightly in excess of the average rate for central lengths in foundation wire extensometers (HiB-HiC, HiC-HiD and HiD-HiE, i = 1,2,3), for which the values were between 0.04 and 0.09, averaging around 0.07.

6.4.3 Inclinometers

In sections at chainages 487 and 537, the average horizontal strains between the two pairs of inclinometer tubes can be calculate at various levels. As compared to strains worked out from wire extensometer data, they have the advantage of greater precision and of the fact that they can be obtained for levels where there was no alternative means of measuring horizontal deformations and strains. Two disadvantages are: (i) inclinometer measurements were not made so often as rod gauge ones, and (ii) there were only two wide lengths between inclinometers and thus only a few average strains can be obtained, no evaluation of their horizontal variations being possible.

Average horizontal strains between inclinometers I1 and I2 (Ch. 537) and I3 and I4 (Ch. 487) are shown in figures 6.94 and 6.95. Final values between -0.6% and -1.0% were measured at the

top of the foundation and lower elevations of the fill, whereas values around -0.1% were recorded at elevation 42 m AOD; below elevation 39 m AOD, there was practically no horizontal strain.

Figures 6.94 and 6.95 also show horizontal strains calculated from wire extensometers for the length between inclinometers; they agree considerably well with the curves drawn from inclinometer data at the top of the foundation, particularly if it is taken into account that rod gauge plates do not coincide spacially with inclinometer wells (and thus interpolations were necessary in calculations) and that the two sorts of equipment were not installed at exactly the same chainage.

6.5 VERTICAL STRAINS

The only available sources for vertical strain calculations were the data from settlement magnetic collars placed around inclinometer ducts, both in the foundation and in the fill. Comparisons of vertical displacements at the foundation top worked out from them, however, showed large discrepancies with respect to the figures obtained by means of the hydraulic settlement probe and, therefore, strains calculated from such movements are not reliable. Furthermore, in some inclinometers, tube distorsion was so pronounced that the settlement probe could not reach lower levels of the wells towards the end of the experiment and, thus, even if the measurements were reliable, some of the final records were missing.

Apparent vertical strains in the foundation, as

measured through settlement magnets, never exceeded 0.2% in the case of I4 and 0.6% in the case of I2, much lower figures than recorded for horizontal strains at the same location (1.0% to 1.5%); undrained loading of saturated soil under plane strain conditions should, obviously, result in horizontal and vertical strains numerically equal.

As for vertical strains in the fill, the problem is opposite to the one in the foundation: a possibly greater compressbility of the sand placed around inclinometer tubes as compared to the surrounding fill might have led to exaggerated measured values of strains, chiefly near the base of the embankment, as already discussed in section 6.2.1. Figures 6.52 through 6.55 show observed vertical strains in the fill on 8 different occasions, both before and after the correction for the 'punching' effect of the grout column was applied. Graphs of both uncorrected and corrected vertical strains are plotted against fill elevations, in figures 6.96 and 6.97. Maximum gradients of the curves corresponding to lengths located in the lower half of the embankment ranged from 0.3 to 0.9%/metre, after correction for the 'punching' of the grout column, final average values varied between 0.2 and 0.4%/metre but, if only the records taken before the fill reached its maximum level at the inclinometer tops are accounted for, average slopes are between 0.25 and 0.55%/m.

Post-construction observations of the magnetic ring levels were made twice on inclinometer I2 at Ch. 537 (days 102

and 121) and once on I4 at Ch. 487 (day 121). Post-construction vertical strains in the foundation calculated from these measurements were always smaller than 0.1% for 28 days, but this is within the precision limits of the system employed and no definitive conclusion therefore arises from the data collected, although the fact that all records consistently showed shortening of the lengths seems indicative of real strains and not normal scatter alone; an average rate $d\epsilon_z/d\ (\log_{10}t)$ of 0.0004 was found for the upper lengths of both inclinometers.

In the fill, post-construction strains were much larger; they varied from 0.09% to 0.79% in 28 days (average 0.33%), rates of vertical strain increase $d\epsilon_z/d\ (\log_{10}t)$ ranging from 0.0005 to 0.0045 (average 0.0018). Measured post-construction vertical strains in the fill are plotted against logarithm of time in figure 6.98 and also included in Table 6.6.

TABLE 6.6

Post-construction Vertical Strains in the Fill Settlement Magnets

Ch.	Points	Vert. strains (%)		$\frac{(\epsilon_z)_{pc}}{(\epsilon_z)_{ec}}$ %	$\frac{d\epsilon_z}{d(\log_{10}t)}$	$\frac{d\epsilon_z}{d(\log_e t)}$
		$(\epsilon_z)_{ec}$	$(\epsilon_z)_{pc}$			
487	V41B/V42B	4.5	0.79	18	0.0045	0.0020
	V42B/V43B	3.3	0.15	5	0.0009	0.0004
	V43B/V44B	1.6	0.19	12	0.0011	0.0005
	V44B/V45B	0.4	0.23	57	0.0013	0.0006
537	V21B/V22B	7.8	0.58	7	0.0033	0.0014
	V22B/V23B	5.5	0.24	4	0.0014	0.0006
	V23B/V24B	2.9	0.32	11	0.0014	0.0008
	V24B/V25B	0.5	0.09	18	0.0005	0.0002

6.6 SHEAR STRAINS

From deformation profiles obtained by means of the slope indicator, lower bounds for shear strains can be calculated. They are named 'horizontal shear strains' throughout this thesis and they represent the angular distorsion of a plane upon which horizontal stresses act. In points where settlements are uniform, these 'horizontal shear strains' equal the engineering shear strains γ_{xz} experienced by a square soil element of sides originally coinciding with the vertical and horizontal directions. In points where vertical displacements vary, however, γ_{xz} is the result of inclinometer distorsion added to settlement gradient. At Empingham, the greatest recorded variations in settlement were in the region of inclinometers I1 and I3, near the trial embankment toe (see figures 6.64 and 6.65) where gradients of up to 1.5% (Ch. 487) and 3.0% (Ch. 537) were measured. These values are considerably lower than those obtained in inclinometer observations and, accordingly, they have not been taken into account in calculations of shear strains and principal strains. Therefore, figures quoted for such quantities are to be understood as lower bounds for them, acceptable for practical purposes and believed not to include larger errors than those inherent to the techniques employed in observations and analyses.

Inclinometer profiles are not perfectly smooth curves owing to the relative stiffnesses of the casings and of the grout columns as compared with those of the couplings and the soil and, therefore, measured shear strains cannot be calculated at each

point of the inclinometer but only estimated as an average value along a certain length. This too contributes to underestimation of maximum shear strains and principal strains.

In figures 6.99 through 6.102 horizontal shear strains corresponding to various inclinometer profiles are presented. They were calculated with basis on lengths of approximately 3 metres, so as to minimize the influence of differential stiffness along the tubes. If shorter lengths were adopted in calculations, the values of maximum shear strains would have been greater and the curves would have not exhibited the same smooth appearance; figures 6.103 and 6.104 are examples in which lengths of 1.2 m were adopted; if they are compared with figures 6.99 and 6.101, the point put above is demonstrated.

Figures 6.105 and 6.106 show the variation of horizontal shear strains with fill elevations. In both instrumented sections considered there, the pattern was approximately the same; at early stages of the construction the inclinometers located near the embankment toe distorted considerably, whereas the inner ones showed small horizontal shear strain; as time went on and the slope advanced inwards, the inner inclinometers too exhibited large horizontal shear strains and, eventually, the slope indicator torpedo could not pass the most bent points as had already occurred to the inclinometers by the bank toe. The reason for such a behaviour is two-fold: firstly, shear stresses are larger beneath slopes and the inner inclinometers were far from the slope at the early stages of

the construction; secondly, inclinometers only detect shear strains when one of the directions of principal strains do not coincide with the well axis.

As horizontal shear strains could not be measured throughout the entire length of the inclinometers towards the end of the construction period, an attempt to obtain them by extrapolation was made in figures 6.107 to 6.110, where it was assumed that the trend followed before the blockage of the ducts in the horizontal shear strain-horizontal displacement plots would continue the same until the end of construction.

The procedures outlined above led to the determination of maximum horizontal shear strains at each inclinometer The values found were as follows:

a) Chainage 487

a.1) Inclinometer I3: $(\gamma_{xz})_{max}$ = 10-12%, at elevations 46-49 m AOD.

a.2) Inclinometer I4: $(\gamma_{xz})_{max}$ = 7-8%, at elevations 47-50 m AOD.

b) Chainage 537

b.1) Inclinometer I1: $(\gamma_{xz})_{max}$ = 13-18%, at elevations 42-45 m AOD.

b.2) Inclinometer I2: $(\quad_{xz})_{max}$ = 8-12%, at elevations 42-44 m AOD.

Post-construction horizontal shear strains can be estimated from inclinometer profiles measured after the end of

construction, even though difficulties with access of the torpedo prevent great accuracy in such a calculation. Estimates for increase of γ_{xz} in the foundation after banking completion are presented in Table 6.7; they were based on figures 6.13 to 6.16 and 6.107 to 6.110.

TABLE 6.7

Post-Construction Shear Strains γ_{xz} in the Foundation Inclinometers

Chainage	Inclin.	Shear strains (%)		$\frac{\gamma_{pc}}{\gamma_{ec}}$ (%)	$\frac{d\gamma_{xz}}{d(\log_{10} t)}$	$\frac{d\gamma_{xz}}{d(\log_e t)}$
		γ_{ec}	γ_{pc}			
487	I3	9.0	2.1	23	0.0164	0.0071
	I4	5.0	2.2	44	0.0152	0.0066
537	I1	15.5	2.2	14	0.0172	0.0075
	I2	11.0	1.1	10	0.0076	0.0033

γ_{ec}: horizontal shear strain at the end of construction

γ_{pc}: post-construction horizontal shear strains

't' in the two last columns stands for time after banking completion (day 92 1/2).

Another way of estimating creep shear strains consists of assuming that no rotation of principal strins take place after construction and, hence, the ratio between shear and horizontal strains remains equal to that at the end of construction: $\gamma_{xz} = \tan 2\beta.(\epsilon_z - \epsilon_x)$. In figures 6.113 and 6.114 β is seen to be between 28° and 37° for inner inclinometers I2 and I4. These values

combined with maximum post-construction rates for horizontal strains (assumed numerically equal to vertical ones) shown in Table. 6.4 (J = 0.0026 to 0.0034), result in estimate rates for creep shear strains of 0.004 to 0.012. These figures are lower than those shown in Table 6.7, but it should be taken into account that angles β were calculated with basis on underestimated shear strains γ_{xz} and, consequently, they too must have been underestimated. An angle β of 40° would lead to rates of creep shear strain J of 0.015 to 0.020, approximately equal to the figures of Table 6.7.

6.7 PRINCIPAL STRAINS

In some points of the foundation and the fill, horizontal, vertical and shear strains were known with a reasonable accuracy. This allows the determination of the magnitudes of major and minor principal strains as well as their directions, by using the following expressions.

$$\left.\begin{matrix}\epsilon_1 \\ \epsilon_3\end{matrix}\right\} = \frac{\epsilon_x + \epsilon_z}{2} \pm \frac{1}{2}\sqrt{(\epsilon_z - \epsilon_x)^2 + \gamma_{xz}^2} \qquad (6.14)$$

$$\tan 2\beta = \frac{\gamma_{xz}}{\epsilon_z - \epsilon_x} \qquad (6.15)$$

where ϵ_1 and ϵ_3 are, respectively, major and minor principal strains; ϵ_z and ϵ_x are, respectively, vertical and horizontal strains; γ_{xz} is shear strain corresponding to the x and z directions and β is the angle made by the direction of the major principal

strain with the vertical.

In the foundation, vertical strain measurements were not reliable, but under undrained loading and plane strain conditions, $\epsilon_z = -\epsilon_x$ and (6.14) and (6.15) can be transformed so as not to include ϵ_z:

$$\left.\begin{matrix}\epsilon_1 \\ \epsilon_3\end{matrix}\right\} = \pm \frac{1}{2} \sqrt{4\epsilon_x^2 + \gamma_{xz}^2} \qquad (6.16)$$

$$\tan 2\beta = -\frac{\gamma_{xz}}{2\epsilon_x} \qquad (6.17)$$

Above equations were used to calculate the values presented in figures 6.111 and 6.112, where principal linear strains at two points of the foundation top are plotted against fill elevations, and in figures 6.113 and 6.114, where angles are plotted as the variable on y-axis. In figures 6.115 and 6.116, data from both instrumented sections are drawn together, fill elevations being replaced on the x-axis by height of fill above trench (or toe) level. Figure 6.117 shows the rotation of principal strain. Through these drawings it is seen that, near the embankment toe, the major principal strain had its direction rapidly rotated to approximately 45° (plane of maximum shear strain horizontal) and its value raised to about 1% at a height of fill H of 10 metres, 2% for H = 12 m, 5% for H = 17 m, and so forth. Away from the toe, principal strain rotation was slower and smaller and the major principal strain also presented lower values: 1% for H = 16 m, 2% for H = 18 m, etc.

Figure 6.117 shows that, in all of the 4 curves, when ϵ_1 reached 1%, the directions of principal strains were already approximately those of the end of the construction.

In the fill, the largest strains are the vertical ones which reached, at the end of construction, values of up to 8%. Horizontal strains never exceeded 1.5% (extension) and horizontal shear strains were always less than 1%, in either direction, unless at the bottom of the embankment, close to the foundation level. Therefore, the principal strains practically coincided with vertical and horizontal linear strains, both in magnitude and direction; towards the top of the fill, the direction of the major principal strain ϵ_1 pointed inwards some 10° at the banking completion; on the other end, 3 metres above the stripped ground level, it pointed outwards a few degrees; in the middle, it pointed vertically downwards.

Figures 6.118 through 6.122 show the variation, at various levels, of the maximum shear strain $\gamma_{max} = (\epsilon_1 - \epsilon_3)$ and of the angle β formed by the major principal strain ϵ_1 with the vertical. At the inner inclinometers, the behaviour of the fill with respect to magnitude and direction of strains was considerably different from that of the foundation horizon 3 to 5 metres below the embankment.

Strains in the trial bank fill developed more or less linearly with the rise of the embankment, whereas, in the foundation, the curves exhibit an approximately parabolic shape. As for

the directions of principal strains, while a large rotation occurred in the foundation, even when strains were still very low, there was little change in strain directions in the fill throughout the whole period of construction.

In the fill, principal strains approximately coincided with vertical and horizontal ones and post-construction changes in principal strains or in maximum shear strains can be worked out by the use of the following expressions.

$$\frac{d\epsilon_1}{d(\log t)} \doteqdot \frac{d\epsilon_z}{d(\log t)} \qquad (6.18)$$

$$\frac{d\gamma_{max}}{d(\log t)} \doteqdot \frac{d\epsilon_z}{d(\log t)} - \frac{d\epsilon_x}{d(\log t)} \qquad (6.19)$$

The variations of vertical strains and horizontal strains with time have been discussed in sections 6.4 and 6.5. Adding the values quoted for $d\epsilon_z/d(\log_{10} t)$ and $d\epsilon_x/d(\log_{10} t)$, taking into account that they have opposite signs, rates of γ_{max} increase are found to range from 0.0016 to 0.0070 (averaging 0.0040) in the fill.

In the foundation, at the end of construction, principal strains were inclined between 30° and 45° with respect to the vertical. In this case, the evaluation of the increase in γ_{max} depends on the knowledge of the variations of ϵ_x and ϵ_z as well as γ_{xz}. Punching of the grout column invalidated the measured vertical strains, but under plane strain and undrained loading

conditions $\epsilon_z = -\epsilon_x$.

Using values of ϵ_x from Table 6.3 and γ_{xz} from Table 6.7, Table 6.8 was constructed. It shows that the rate of principal strain increase in the foundation after construction, $d\epsilon_1/d(\log_{10}t)$ ranged from 0.005 to 0.01, approximately, at a level some 3 to 5 metres below the foundation surface where shear strains were a maximum.

TABLE 6.8

Principal Strains in the Foundation after Fill Completion

Ch.	Inclin.	Fill el. (m AOD)	ϵ_1 (%)		$\frac{(\epsilon_1)_{pc}}{(\epsilon_1)_{ec}}$ (%)	$\frac{d\epsilon_1}{d(\log_{10}t)}$	$\frac{d\epsilon_1}{d(\log_e t)}$
			$(\epsilon_1)_{ec}$	$(\epsilon_1)_{pc}$			
537	I1	43	7.8	1.1	14	0.0086	0.0037
	I2	43	5.7	0.7	12	0.0048	0.0021
487	I3	47	4.6	1.0	22	0.0078	0.0037
	I4	47	3.0	1.3	43	0.0090	0.0039

Figure 6.123 depicts, in log scale, the increase with time of major principal strains after the end of construction at the points of the foundation referred to in Table 6.8. In the same drawing, post-construction principal strains corresponding to points of the fill located some 3 metres above the stripped ground level are also presented. The rates of post-construction strain increase in the fill appear to be lower than in the foundation (about one-half); this is probably due to lower stress levels in the fill as compared to those in the foundation.

6.8 PORE PRESSURES IN THE FOUNDATION

6.8.1 Installation and Operation Procedures

All 12 piezometers installed in the foundation at the sections located at chainages 487 and 537 (figures 4.1 and 4.3) were twin-tube hydraulic piezometers, in which the tip cavity was connected to the measuring board in the instrument-house outside the bank by means of two water-filled Nylon 11 tubes sleeved with 'Polythene' so as to minimize the entry of air into the tubing.

The piezometers numbered P2F, P3F, P5F, P6F, P8F, P10F and P11F had low air-entry-value porous ceramic tip surrounded by a sand filter. They were inserted in 100 mm dia. boreholes, back-filled, above the sand pocket, with a cement-bentonite mixture. A few days before installation of the piezometers, the original ground level was stripped some 3 to 7 metres and this undrained unloading obviously reduced the pore pressures, but no pressure below atmospheric was ever recorded on the cavities of these piezometers; however, as the manometer datum in the piezometer chamber was situated at elevation 51.0 m AOD, in parts of the tubing pressures were initially lower than atmospheric, although by not more than 5 metres in terms of head of water.

At piezometers number P1F, P4F, P7F, P9F and P12F, located at shallow depths, it was feared that pressures could be initially lower than atmospheric and, accordingly, the tips employed were high air-entry-value ones, inserted in extension to boreholes made with mandrels of a conical shape the same size of the Bishop-

type tips. A small amount of plaster of Paris was placed in the conical hole, prior to the insertion of the cell, in order to ensure an intimate contact between the probe and the soil and the exclusion of air bubbles.

The installation of piezometers and the pore pressure measuring system was completed shortly before the banking commencement and there was no time available to observe fluctuations, equalization tendencies, discrepancies between measurements and the like.

De-airing was possible by using a portable de-airing unit which enabled the flushing of air-free water, under moderate excess pressure, through the lines of the piezometer. A criterion was adopted of carrying out the de-airing of a particular cell when the measurement of pressure on either limb disagreed by more than 0.3 metres of water, as this is indicative of the presence of air in one or both tubes; it should be noted, however, that the existence of air in the piezometer cavity will not cause this difference and yet, it may lead to a wrong recorded of the pore pressure.

The measurement of pore pressures were made by means of a pressure transducer linked to an eletronic digital read-out unit. A mercury manometer was also available and was used to check the measurements, but its response time was obviously much larger.

6.8.2 Measurements

Figures 6.124 through 6.126 show pore pressures, in terms of elevation of water, observed from the first day of fill placing until 4 months after the bank completion. In the same drawings, a day-to-day record of fill elevations above each piezometer tip is also depicted.

In figures 6.127 to 6.129, total vertical stresses (assumed to equal overburden pressures) and pore water pressures are plotted against fill elevations. These drawings show that there was practically no pore pressure response to loading during the first days of the bank construction. This might have resulted of the deairing carried out just prior to the construction or the soil disturbance during drilling and installation operations, but for whatever reason the fact is that pore pressures recorded during these early stages of the banking were not reliable.

The ratios between pore pressures and overburden stresses, named pore pressure ratios (r_u), are pictured in figures 6.130 and 6.131. The graphs show increasing values towards the end of construction, a maximum of 0.7 having been recorded.

Discarding the initial portions of all curves on drawings 6.127 to 6.129, values of $\Delta u/\Delta(\gamma.h)$ were calculated and are presented in Table 6.9, in next page.

The values of $\Delta u/\Delta(\gamma.h)$ are well below those predicted by one-dimensional theory ($\Delta u = \Delta\sigma_z$), except for piezometers P6F, P9F and P11F, located at deep levels beneath the central

region of the trial embankment (P10, at approximately the same situation unexpectedly behaved quite differently, but it should be noted that de-airing of this piezometer after banking completion resulted in a rise of nearly 10 m of water in pore pressure, an evidence of its previous misbehaviour). Those points at shallower elevations and closer to the bank toe might have been strongly affected by horizontal stress relief induced by lateral movements, development of high shear stress levels and partial pore pressure dissipation through discontinuities in a certainly more weathered, reworked, relatively permeable material.

TABLE 6.9

Values of $\Delta u/\Delta(\gamma.h)$

Chainage	Piezometer	$\Delta u/\Delta(\gamma.h)$
487	P1F	0.38
	P2F	0.49
	P3F	0.71
	P4F	0.80
	P5F	0.86
	P6F	0.95
	P11F	0.99
537	P7F	0.35
	P8F	0.60
	P9F	0.95
	P10F	0.48

If dissipation is neglected and the undrained pore pressure response is assumed to equal the incremental mean normal stress (elastic material), an approximate analysis can be

produced to relate the pore water response with the values of $K' = \sigma'_x / \sigma'_z$ at each point. In this analysis, expressions below are assumed to hold.

$$\Delta u = u - u_o = \Delta\sigma_{mean} \tag{6.20}$$

$$\Delta\sigma_{mean} = \frac{\Delta\sigma_x + \Delta\sigma_y + \Delta\sigma_z}{3} = \frac{1}{3}\left[(\sigma_x - \sigma_{x_o}) + (\sigma_y - \sigma_{y_o}) + (\sigma_z - \sigma_{z_o})\right] \tag{6.21}$$

$$\sigma_{x_o} = \sigma_{y_o} = K'_o \sigma_{z_o} + (1 - K'_o) u_o \tag{6.22}$$

$$\sigma_x = K' \sigma_z + u (1 - K') \tag{6.23}$$

$$\sigma_y = \left(\frac{1 + K'}{2}\right)\sigma_z + u\left(\frac{1 - K'}{2}\right) \tag{6.24}$$

$$\sigma_z = \gamma . h \tag{6.25}$$

The combination of formulae (6.20) to (6.25) result in

$$K' = 2\,\frac{\gamma h_o - u_o}{\gamma h - u} \cdot \frac{1 + 2K'_o}{3} - 1 \tag{6.26}$$

where subscript 'o' refers to conditions at fill elevation of 50.9 m AOD for Ch. 537 and of 53.8 for Ch. 487 and symbols without subscript refers to the time when fill levels became stationary above any given piexometer; u is pore pressure, σ_{mean} is mean normal total stress, σ_x, σ_y, and σ_z are normal total stresses in 3

orthogonal directions, σ'_x, σ'_y and σ'_z are the corresponding effective stresses, K' is the ratio between σ'_x and σ'_z, h is the vertical distance between the piezometer tip and the top of the fill above it and γ is the total unit weight of the soil assumed not to vary.

Using equations 6.25 and 6.26 and taking into account the records of pore pressure and fill height presented in figures 6.124 to 6.127, Table 6.10 was constructed. In it, values of K' which would have led to the pore pressures equivalent to those effectively measured are shown for several values of K'_o arbitrarily chosen.

TABLE 6.10

Values of $K' = \sigma'_x / \sigma'_z$

Piezo.	σ'_{z_o} kN/m^2	σ'_z kN/m^2	K' values for K'_o =					
			0.6	0.8	1.0	1.2	1.5	2.0
P 1F	89	139	-0.06	0.11	0.28	0.45	0.71	1.26
P 2F	141	200	0.03	0.22	0.41	0.60	0.88	1.49
P 3F	176	216	0.20	0.41	0.63	0.85	1.17	1.88
P 4F	105	160	-0.04	0.14	0.31	0.49	0.75	1.32
P 5F	135	169	0.17	0.38	0.60	0.81	1.13	1.82
P 6F	174	185	0.38	0.63	0.88	1.13	1.51	2.32
P 7F	149	246	-0.11	0.05	0.21	0.37	0.61	1.14
P 8F	136	212	-0.06	0.11	0.28	0.45	0.71	1.27
P 9F	152	165	0.35	0.60	0.84	1.09	1.46	2.25
P10F	162	306	-0.22	-0.08	0.06	0.21	0.41	0.87
P11F	195	196	0.46	0.72	0.99	1.26	1.65	2.52

For K'_o equalling 0.6, 0.8 and 1.0, most values of K' fall below 0.45, which corresponds to the active state of a soil characterized by a friction angle of 22^o, and some of them are even negative, what implies an absurd development of tension zones in the foundation. K'_o values of 1.5 and 2.0 lead in many cases to K' greater than K'_o, what is not expected beneath the centre of the embankment. With $K'_o = 1.2$, neither of the above defects are present (except for P10F already seen to have behaved unreliably). Moreover, with $K'_o = 1.2$, final K' equals 0.37 at P7F, 0.45 at P1F and 0.49 at P4F; these were piezometers located at zones of large shear strains, where local failure is thought to have been reached or closely approached. Piezometers P6F, P9F and P11F, deeper and further from the toe, show very little drop in K', as would be expected. At piezometer P8F K is 0.45; this is an unexpected value as its level, 38 m AOD, appears to be just outside the zone affected by the horizontal flow of the soil (see inclinometer I1's profiles, figures 6.9 and 6.13).

6.8.3 Response Time

On 1-7-72, 7th. day of construction, after a very rapid loading at Ch. 537 in which the fill level was raised from 46.9 to 55.9 m AOD in only 7 days, the placing of fill stopped for 2 days. The average change in pore pressure during these days was -0.025 m for the 4 piezometers of that section, suggesting that no practical problems existed with respect to time lag in pore pressure response and measurement.

From day 14 to 26, the trial bank works stopped completely. In that period, the average increase in pore pressure records was less than 0.2 m. After banking completion, from day 93 onwards, the tendency was to stabilization or a slight decrease in pore pressure, no continuation of the fastly increasing trend observed before stoppage having occurred, save at P7F where an unusual increase took place shortly before and after day 93. Both examples seem to corroborate the belief that the response time of the system was fully satisfactory.

6.8.4 Pore Pressure Dissipation

During the four months that folowed banking completion, observed pore pressure decrease averaged 0.2 m. During construction, effective stresses were lower and, if c_v were approximately the same, dissipation would have been necessarily lower.

In the sand drain trials, however, coefficients of consolidation were seen to be strongly dependent on effective stresses at low stress levels, probably due to closing up of fissures in the soil. This might explain the feeble pore pressure response measured at initial stages of the loading, although this is a less likely explanation for deep piezometers than for those located at shallower depths, in more disturbed and weathered ground.

It may be stated, however, that, except for low stress increments occurring at the beginning of the construction, pore pressure dissipation appears to have been unimportant and conditions

were close to completely impeded drainage. This is in great part confirmed by the measured final values of r_u (Table 6.9).

6.8.5 Precision and Accuracy

The overall precision of the system employed was of the order of 0.1–0.2 m, but there was no independent system of measurement capable of providing any basis for the assessment of the accuracy with which observations were taken.

6.9 PORE PRESSURES IN THE FILL

At Ch. 537, 4 fine tip piezometers, Bishop type, were installed during the placing of the fill, at elevations 51 and 55 m AOD. They were also connected to the instrument houses by two water-filled nylon tubes sleeved with 'Polythene'.

Their records, shown in figure 6.132, reveal that pore pressures remained below atmospheric throughout the whole period of the experiment. At the end of construction, they were between -4 and -7 metres of water. Four months later, they had decreased even further, ranging then from -5 to -8 metres of water. This could mean that the fill was drying out or that creep movements had a dilatant component.

Pore pressure ratios $r_u = u/\gamma.h$ were, at the end of construction, between -0.15 and -0.40.

C H A P T E R _ S E V E N

CONCLUSIONS DRAWN FROM THE TRIAL BANK EXPERIMENT

7.1 Brief Description of the Experiment

7.2 Appreciation of the Approach Adopted

7.3 Total Stress Stability Analysis

7.4 Stability Analysis in Terms of Effective Stresses

7.4.1 Methods applied

7.4.2 Strength parameters utilized

7.4.3 Pore pressure assumptions

7.4.4 Results of the analysis

7.5 Interpretation of the Measured Horizontal Movements

7.5.1 The mechanism of horizontal deformation

7.5.2 The basis of the deformation analysis

7.5.3 Application of the approximate model

7.5.4 Comparison between model and prototype

7.6 Pore Pressure Parameters in Foundation

7.6.1 Data utilized in the analysis

7.6.2 Pore pressure parameters 'A' and 'a'

7.6.3 Parameter $\bar{B}$

7.6.4 Parameter B

7.7 Deformation Parameters for the Foundation

7.7.1 Method of analysis applied

7.7.2 Initial Stresses - Determination of K_o

7.7.3 Stress-strain curves

7.8 Fill Properties

7.9 Comparison of Trial Bank Findings with Design Assumptions

7.9.1 Undrained strength

7.9.2 Strength in terms of effective stresses

7.9.3 Consolidation parameters

7.9.4 Fill properties -

C H A P T E R _ S E V E N

CONCLUSIONS DRAWN FROM THE TRIAL BANK EXPERIMENT

7.1 BRIEF DESCRIPTION OF THE EXPERIMENT

After the ground had been stripped of some 5 metres, the installation of inclinometers, piezometers, and horizontal and vertical extensometers took place at the same time the trench was excavated. These operations were carried out in the second half of June 1972.

On 3rd. July 1972 the placing of fill started, but at that date a part of the instrumentation was still to be installed, calibrated or checked. The initial rate of fill placing was very fast, particularly at the lowest section where, in 6 days, the crest level had risen around 9 metres. Owing to this, some of the initial records were either missing or of doubtful quality.

On the 8th. day of the experiment inclinometer readings showed a maximum horizontal displacement in excess of 40 mm at the bank toe and the development of average shear strains around 1% in the region comprised between 42.5 and 46 m AOD (1 to 4.5 m below stripped ground level).

The premature failure of the outside part of the embankment was then feared and in the case of this actually occurring the equipment installed in the inner zones of the bank (inclinometer,

piezometers, extensometers, settlement points) would have been ineffective. It was accordingly decided to introduce a berm in the trial bank so as to delay or prevent failure and displace inwardly the zone of major movements and strains.

Before the bank was completed, several slips occurred in temporary borrow pit slopes and their back-analyses resulted in an average undrained strength of 50 kN/m^2 for the upper 10–15 m of the Upper Lias Clay layer, giving partial confirmation of the undrained strength assumed in the dam design. This lessened the need to reach failure of the trial embankment and the construction was terminated when the average height of fill was around 20 metres and horizontal movements of up to 800 mm had been recorded. This enabled four months of creep measurements to be made.

In an attempt to give a sufficient length of embankment at the same height and impose conditions near plane strain, a trench was excavated into the side of the valley. During construction, as lateral displacements were larger in the lowest section and the level of the trench bottom was actually higher than the toe of the lowest section, it was decided to keep the fill crest at Ch. 487 some 1.5 m above the one at Ch. 537. In the end, the variation of maximum horizontal movement in the three instrumented sections was ± 15% with respect to the average.

7.2 APPRECIATION OF THE APPROACH ADOPTED

The trial bank did not fail but the instrumentation installed in it permitted the measurement of displacements and strains, whose final magnitudes were so large that the earth structure can be analysed as though its factor of safety was actually at unity or slightly above it. The fact of the average undrained strength of the fill being two to three times greater than the bulk value for the higher horizons of the foundations poses a major difficulty in the analysis of the trial bank, but apart from probable values for the soil parameters, which were determined and are presented in next sections, some valuable qualitative information also resulted from the experiment.

While distortion of the inclinometer tubes during the later stage of construction prevented the instrument from passing, the casings could always be plumbed, showing that while large strains had occurred, there was no evidence of significant displacement along shear discontinuities. Two general conclusion follow. Firstly, progressive failure seems unimportant in this material, despite brittle behaviour indicated by large post-failure displacements of the borrow pit slips. Secondly, as failure is preceded by large displacements, the monitoring of the movements of the main dam could be done with sufficient accuracy for potentially dangerous conditions to be detected well before complete collapse occurs.

The measurement of displacements and distorsions allowed the approximate calculation of the complete state of strains

in some selected points of the fill as well as of the foundation. This permitted a better appreciation of the material properties and useful comparisons with values found in laboratory tests, computer modelling and approximate analytical calculations. These comparisons led to a better understanding of the mechanisms controlling deformation and failure and to a more accurate knowledge of the stress-strain-strength relationships governing the soil behaviour.

The approach adopted had a number of disadvantages, among which the most important are mentioned here. The trial bank was constructed during the initial stage of the main contract when there were many other calls on the site staff. The programme for its construction had to be controlled by the needs of the job as a whole and not by the need of obtaining information. These problems were appreciated at the outset and, because of them, the instrumentation was kept to a minimum. In the event, insufficient time was available for installing the equipment, checking and calibrating it, taking and confirming initial readings and gaining experience in their operation. Installation and operation of the equipment was performed by the resident engineers staff, with assistance of Imperial College. Different people became responsible for the operation of different parts of the equipment, and this added to organizational difficulties in the desirable consideration of all informations together soon after they were obtained.

Had there been more time available before the construction started and also more personnel engaged in the field

observations, the quality of the data obtained would have certainly been much improved. If, in addition, more instrumentation had been installed (for example, a third inclinometer in each section between the two existing ones), more attention had been paid to ensuring that the equipment was mutually self checking, and greater coordination had existed between the surveying team and the instrumentation crew, most of the gaps in the records would have been closed, the uncertainties and the need for corrections and extrapolations greatly reduced and the accuracy of measurements and calculations certainly improved.

The influence of the stiffness of the inclinometer casings and of the material surrounding it in the measurement of shear strains and, mainly, vertical strains is another item to deserve attention. The adoption of shorter lengths of tubes and their anchoring to the borehole walls would lead to more trustworthy measurements of vertical strains and displacements, provided that a recognizedly more compressible protective material (grout, sand, pea gravel) were used around the wells.

It must be emphasized, however, that in view of the large displacements and strains actually recorded and of the amount of careful scrutiny employed in the analysis and interpretation of the observations, almost all the information that would have resulted from a more sophisticated design of the experiment were in fact obtained and the aims of the trial bank successfully achieved.

7.3 TOTAL STRESS STABILITY ANALYSIS

The trial bank did not fail. Shear strains in excess of 10% were however measured and horizontal displacements neared 1 metre in the region close to the embankment toe. A plot of horizontal displacements against height of fill in log scale (figure 6.22) suggests that if the bank had been raised some 2 or 3 metres more, the displacements would have reached the improbable value of 2 metres. Figures 6.111 and 6.112 indicated values of major principal strain ϵ_1 over 5%, rising rapidly and spreading over the whole foundation. It is thus considered that the factor of safety of the final configuration of the trial bank sections should have been slightly above one, around 1.05 perhaps.

A limit equilibrium stability analysis in terms of total stresses was carried out for the three instrumented sections at the end of construction. Two sorts of slip surfaces were assumed: cylindrical and multiple wedge. In both cases the surfaces were forced to pass through the region of the foundation where maximum shear strains were measured. Two hypotheses were adopted with respect to the average mobilized shear stress in the fill; firstly, it was assumed to equal the average mobilized shear stress in the foundation; secondly, it was fixed as 80 kN/m^2, a value corresponding to the mean peak strength of the fill throughout its highest central portion, calculated with basis on the following parameters: $\gamma = 20\ kN/m^3$, $c' = 20\ kN/m^2$, $\phi' = 22^o$, $r_u = -0.3$, $\sigma_z = \sigma_1 = \gamma.h$; this latter assumption means the mobilization of equal stress levels

$(\sigma_1 - \sigma_3)/(\sigma_1 - \sigma_3)_f$ both in the fill and the foundation.

The minimum values for the foundation undrained strength resulting from curves passing through the crest were 24 kN/m^2 for τ_b = 80 kN/m^2 and 44 kN/m^2 for $\tau_b = \tau_f$. Values a little lower were obtained for slip surfaces starting from a vertical crack at the toe of the upper slope: τ_f = 20 kN/m^2 for τ_b = 80 kN/m^2 and 25 kN/m^2 for $\tau_b = \tau_f$. These minimum values were obtained at Ch. 487, where the most distorted region was some 4 to 6 metres below the stripped ground level and they obviously already include all allowances for brittleness, anisotropy, size effect and creep movement.

The assumptions of τ_b = 80 kN/m^2 and slip surfaces starting with a deep tension crack (8 metres) were almost certainly exaggerated and, therefore, the resulting values for the bulk c_u of the foundation were too low. Even at surface number 3, where a crack actually developed during the experiment, attempts to reach its bottom by means of thin rods did not pass the depth of 2 metres. A more realistic prediction for c_u is likely to lie between the two limits represented by the ($\tau_b = \tau_f$) curves and the τ_b = 80 kN/m^2 'cracked' slip surfaces, i.e between 20 kN/m^2 and 43 kN/m^2, 5 metres below the stripped ground level. The provisional dam design was based on a line defined by the expression c_u(kN/m^2) = 30 + 3.5z(m), which results in c_u = 47 kN/m^2 at the depth of 5 metres. It seems that even this value, corresponding to the lower bound of all undrained and in situ tests, is probably higher than the real

overall undrained strength of the foundation. It is advocated here that more pessimistic equations as $c_u(kN/m^2) = 20 + 3.0z(m)$ or $c_u(kN/m^2) = 25 + 2.5z(m)$, for example, should better represent the undrained strength of the upper 5 to 10 metres of the Upper Lias Clay at the Empingham Dam site. Such values are some 20% less than the average figure obtained in the back-analyses of the borrow pit cut slips, but they correspond to slip surface in the foundation much closer to the horizontal than in the case of the failed cuts and anisotropy could well have caused this difference.

Another series of limit equilibrium analyses was carried out investigating the position of the critical circular slip surface (not necessarily passing through the most strained zones as detected in inclinometer measurements). The simplified version of Bishop's method was utilized and the combination of soil parameters which led to a factor of safety equal to one were:

i) Ch. 537

a) foundation $c_u(kN/m^2) = 23 + 2.7z(m)$

b) fill $c_u(kN/m^2) = 50 + 2.2h(m)$

ii) Ch. 487

a) foundation $c_u(kN/m^2) = 20 + 2.3z(m)$

b) fill $c_u = 43 + 1.9h(m)$

These results are similar to those obtained from the analyses based on slip surfaces passing through the regions where the largest shear strains were measured, although the circles were

deeper (see curve 4 in figure 7.3 and curve 5 in figure 7.1). The average assumed mobilized shear stress in the fill were roughly the same in both sorts of analysis.

7.4 STABILITY ANALYSIS IN TERMS OF EFFECTIVE STRESSES

7.4.1 Methods Applied

The appriximate shape and location of the critical slip surfaces at Ch. 487 and Ch. 537 can be reconstructed from the direction of the displacement vectors at the end of construction and from the records of maximum shear strains developed in the foundation as well as in the fill. The circular surfaces that most closely conforms to the critical ones are those numbered 1 in figures 7.1 and 7.3 and, accordingly, they were used in the limit equilibrium analyses carried out according to the Swedish Fellenius' Method of Slices (FELLENIUS, 1936) and also to the simplified version of the Bishop's Method of Slices (BISHOP, 1955).

In either method, the parameters necessary to the evaluation of the factor of safety are: the cohesion intercept c' and the friction angle ϕ', the unit weight γ, and the spacial distribution of pore pressure. In the analysis, both the fill and the foundation were assumed to have the same strength parameters (c' and ϕ') and also the same unit weight γ. As for the pore pressures, use was made of the pore pressure ratio $r_u = u/\gamma.h$, but two different values were employed, one for the fill and other for the foundation.

The unit weight adopted in the analysis was 20 kN/m^3. The values of the remaining parameters are presented and discussed in the following sections.

7.4.2 Strength Parameters Utilized

From laboratory tests carried out during the preliminary site investigation, from other published results (CHANDLER, 1974, for example) and from recent tests carried out at Imperial College (MAGUIRE, 1974), a ϕ' value of 22^o was chosen to be used in the analysis. Another more conservative value, $\phi' = 18^o$, was also tested, its choice being justified by lower results obtained in laboratory tests on pre-cut specimens and in the back-analysis of Hollowell Dam.

Determinations of the cohesion intercept c' from all sources known to the Author always resulted in values ranging from 0 to 20 kN/m^2. Recent tests at Imperial College (MAGUIRE, 1974) appear to indicate that c' may be anisotropic varying with the direction of principal stresses between 0 and 10 kN/m^2. Five values were used in the analysis: 0, 5, 10, 15 and 20 kN/m^2.

7.4.3 Pore Pressure Assumptions

The final r_u measured at the highest piezometers in the foundation were 0.35 at P1F, 0.61 at P4F, 0.39 at P7F and 0.63 at P9F (average 0.50). If the stripping of the ground were taken into account and a $\Delta u / \Delta \sigma_z$ ratio of 1 were assumed (saturated material, no lateral movement), a final r_u of 0.70 to 0.85 would have

resulted.

It was appreciated that a value of $r_u = 0.5$ or, at most, 0.6 would be appropriate for the analysis, but it was decided to investigate the influence on the factor of safety exercized by the variation of r_u within the range 0.4 - 0.8.

The final measured pore pressure ratios in the fill, were -0.23 at P1B, -0.21 at P2B, -0.42 at P3B and -0.25 at P4B (average -0.28), based on the assumption that the measured pore water pressure correctly represented the resulting pore pressure of the air-water phase. These values and the fact that they were nearly unaltered during the whole experiment appears to indicate that there was continuity of the air in the fill and connection to the outside atmosphere. If this was so, the resulting pore pressure to be used in the analysis should lie between the value above quoted, -0.3 approximately, and 0. In the analysis actually performed these two values were used together with $r_u = +0.3$. The reason for the choice of this third value was that the pore pressure measurements in the fill were faced with some suspicion and the development of positive pore pressures was a possibility worth taking into consideration.

7.4.4 Results of the Analysis

In figures 7.4 and 7.5, factors of safety are plotted against pore pressure ratios in foundation for several combinations of c' and fill r_u values.

The analyses were in fact performed by using

the Swedish Method of Slices, but a couple of calculations were also made by the Bishop's Simplified Method of Slices and they showed a difference of around 0.10 in the factor of safety with respect to that obtained from the Swedish Method.

The straight use of the parameters found in the trial bank experiment (foundation $r_u = 0.5$; fill $r_u = -0.3$) coupled to the lowest strength parameters ($c' = 0$, $\phi' = 18^\circ$) leads to factors of safety of 0.97 and 0.99 (Fellenius) and 1.07 to 1.09 (Bishop). The use of fill $r_u = 0$ lowers the factors of safety to 0.92 to 0.94 (Bishop), if ϕ' is kept equal to 18°; for $\phi' = 22^\circ$ and fill $r_u = 0$, the factors of safety are between 1.12 and 1.14 (Bishop).

Interpolation between above results gave the following effective stress parameters, according to Bishop's Method: $c' = 0$, $\phi' = 18^\circ$ (for foundation $r_u = 0.5$, fill $r_u = -0.15$, $F_s = 1.0$). If Fellenius' Method were applied instead, the mobilized friction angle obtained would be 20° for $c' = 0$.

Investigations were also performed to obtain the location of the critical slip circle according to Bishop's method, assuming the strength of the fill to be given by an expression derived from the results of undrained tests on samples taken from the fill during construction: $(c_u)_b(kN/m^2) = 64 + 2.86h(m)$. The resulting circles were deeper and the values found for the angle of shearing resistance in the foundation considerably lower: 13.5° in the case of Ch. 357 and 11.5° in the case of Ch. 487. Such a difference is

probably explained by the different location of the critical slip surface (seen in figures 7.1 and 7.3) and perhaps by the exaggerated mobilization of shear stresses in the fill assumed in the analysis.

An accurate evaluation of the effective stress parameters from the back-analysis of the trial bank was impossible to achieve. Considerable variations in the factor of safety derived from relatively small changes in the method of analysis employed, in the shape and location of critical slip surfaces, in the values of pore pressure ratios in the fill and the foundation, and in the cohesion intercept adopted.

The above is illustrated in figures 7.4 and 7.5 where, for example, the factor of safety is seen to drop: some 0.10 to 0.15 when r_u in the foundation increases by 0.10, between 0.15 and 0.20 when r_u in the fill rises from -0.3 to 0, around 0.10 when Fellenius' method replaces Bishop's one, 0.10 to 0.15 for each drop of 5 kN/m^2 in cohesion, and around 0.20 when ϕ' decreases from 22° to 18°. An analysis by Fellenius' method with $(r_u)_f = 0.6$, $(r_u)_b = 0$, $c' = 0$ and $\phi' = 18°$, results in $F_s = 0.72$, whereas Bishop's method, with $(r_u)_f = 0.5$, $(r_u)_b = -0.3$, $c' = 5$ kN/m^2 and $\phi' = 22°$, leads to $F_s = 1.42$. All values used in this comparison are quite close to mean values obtained from laboratory tests and field observations and yet the results in terms of factor of safety are so discrepant that no definitive conclusions can be drawn about the foundation strength parameters in terms of effective stresses.

7.5 INTERPRETATION OF THE MEASURED HORIZONTAL MOVEMENT

7.5.1 The Mechanism of Horizontal Deformations

The measurement of horizontal displacements and strains by means of wire extensometers and inclinometers showed an interesting trend which was initially unappreciated. As placed, clay fill compacted by heavy plant has high horizontal stresses. If the embankment slope is steep, these stresses try to impose a high shear stress on the foundation. If its shear strength is exceeded, yield of the foundation may occur, accompanied with spreading of the fill. As spread takes place, there is a relief of the horizontal stresses and, provided that loss of strength with increasing strain is unimportant and progressive failure does not occur, the earth structure remains stable.

A mechanism of this sort seems to have operated in the trial bank, giving place to large horizontal movements while the embankment remained stable.

A simple approximate analysis that reproduces this behaviour was set up and is described in next section.

7.5.2 The Basis of the Deformation Analysis

In the approximate analysis herein described, the embankment and the foundation are replaced with a simpler model, whose overall behaviour is expected to be similar to that of the actual earth structure and whose main characteristics are as follows:

a) the foundation is assumed to behave as a rigid-plastic material, i.e, no elastic deformation is experienced

before yielding and no strain hardening, or strain softening occurs after it;

b) horizontal stresses in any point of the fill are functions of the fill unit weight, the height of the fill above the point and a coefficient K expressing the ratio between horizontal and vertical total stresses;

c) the initial value for the coefficient K, denoted K_o, corresponding to a condition of no horizontal extension in the fill, is assumed constant throughout the embankment, although it is recognized that its value depends not only on the material itself and the effort applied to compact it but also on the height of fill at each point;

d) the resultant P_o of the horizontal forces initially acting on vertical section of the embankment varies along the bank width with the square of the height of fill;

e) the first derivative of such a force with respect to x (horizontal length) is assumed to equal the shear stress acting on vertical-horizontal elements of the interface between bank and foundation;

f) this shear stress cannot exceed the interface shear strength, defined as a unique value along the embankment base;

g) the excess shear stress, equal to the difference between the shear stress imposed by the bank under no-lateral-yield conditions and the available strength has to be matched by a reduction in horizontal stresses in the fill, i.e a reduction in the

value of the coefficient K;

h) this reduction in the K value is related to horizontal strains by constant parameters on the basis of linear isotropic elasticity; and

i) in this model, horizontal strains at each section of the bank base develop in full during the period of construction when the slope is being set up right above the given section.

7.5.3 Application of the Approximate Model

(i) Basic theory and expressions

In this model, the foundation is assumed to remain unmoved during the whole construction. The spread of the fill causes shearing on the interface between the bank and the foundation or on a weaker place parallel to it.

Figure 7.6 depicts the main features of this model. Prior to any lateral movement, vertical and horizontal stresses acting on the interface are assumed to be given by expressions (7.1) and (7.2).

$$(\sigma_z)_i = \gamma_b \cdot h \qquad (7.1)$$

$$(\sigma_x)_i = K_o \cdot \gamma_b \cdot h \qquad (7.2)$$

At any point of the x-axis, the horizontal force per unit length resulting from horizontal stresses acting on the height of the fill is expressed by:

$$P_o = \frac{1}{2} K_o (\sigma_z)_i h = \frac{1}{2} K_o \gamma_b h^2 \qquad (7.3)$$

As the height of fill is variable, the force P_o is a function of x and its first derivative is:

$$\frac{dP_o}{dx} = K_o \gamma_b h \frac{dh}{dx} = K_o \gamma_b m h \qquad (7.4)$$

where m is the slope of the fill above the given point.

The change in horizontal force, expressed by (7.4), is resisted by shear stresses developed on the horizontal base.

$$\tau_{xz} = \frac{dP_o}{dx} = K_o \gamma_b m h \qquad (7.5)$$

In this model, no lateral displacement is assumed to take place until and unless the shear strength of the material τ_f is exceeded, in which case the bank spreads over the foundation. As the fill spreads, horizontal strains cause the earth pressure ratio K_o to drop to an intermediate value between K_o and the active ratio K_{ac} corresponding to the yield of the bank material. Simple linear isotropic elasticity and plane strain conditions may be used to establish a relationship between horizontal strains and the drop in the K value:

$$K = K_o + \frac{E_b}{\gamma_b h (1 - \nu_b^2)} (\epsilon_x)_b \qquad (7.6)$$

The available force provided by the interface

shear strength τ_f is, at any point located at the distance x from the toe:

$$P_{av} = \tau_f \cdot x \tag{7.7}$$

If the embankment slope m is constant from toe to crest, the acting horizontal force P under K-conditions (different from K_o-conditions), would be at a point situated at the distance x from the toe:

$$P = \frac{1}{2} K \gamma_b m^2 x^2 = \frac{1}{2} K \gamma_b h^2 \tag{7.8}$$

As P cannot exceed P_{av}, the K-value of equation (7.8) must be such that P equals P_{av} and (7.7) equals (7.8):

$$P - P_{av} = \frac{1}{2} K \gamma_b m^2 x^2 - \tau_f x = 0 \tag{7.9}$$

$$K = \frac{2 \tau_f}{\gamma_b m^2 x} \tag{7.9}$$

Putting (7.10) into (7.6), an expression for the horizontal strains results at each point.

$$(\epsilon_x)_b = \frac{(K - K_o) \gamma_b h (1 - \nu_b^2)}{E_b} \tag{7.10}$$

or

$$(\epsilon_x)_b = \frac{\left(\frac{2 \tau_f}{\gamma_b m^2 x} - K_o \right) \gamma_b h (1 - \nu_b^2)}{E_b} \tag{7.11}$$

According to this model, expressed by equation (7.12), $(\epsilon_x)_b$ will assume increasingly negative values (extension) for $x > 2 \tau_f / K_o \gamma_b m^2$. For lower values of x, close to the bank toe,

the bank experiences compression and elevation of its K from K_o towards the passive ratio K_p.

Horizontal displacements only develop outside the crest zone, where the bank is sloped. In the crest, formula (7.8) does not apply and all equation derived from them are also not applicable.

(ii) The raising of the embankment- Numerical application

At the first stages of a bank construction, the interim crest occupies most of the width. According to this model, horizontal strains only develop beneath the slope and therefore, at early phases of construction strains are concentrated in the region near the toe. As construction proceeds, the slope advances inwards and so do the points affected by horizontal strains; since the strains increase with the distance x from the toe, the retarded extension of inner points becomes eventually greater than that of outer positions.

Three numerical applications of this model are shown in figures 7.7 to 7.9. The three embankments analyzed approximately correspond to the three instrumented sections of the Empingham trial bank, but a single slope from toe to crest substitutes in each case the real configuration of two different slopes separated by a berm. Average inclinations and bank heights were maintained though.

In order to allow a more suitable comparison

with the measured horizontal shear strains, the sections of the model for which strains were predicted were made approximately coincident with the real positions of the wire extensometer plates.

The same sort of analysis was applied to the three sections, regardless of the depth of the trench at each one. The heights of the embankment were calculated on the basis of the level of the trench bottom.

The Poisson's ratio used was 0.4 and the fill unit weight was taken as 20 kN/m^3. These are not however the most inportant factors in calculations. The most critical parameters are the initial stress ratio in the fill K_o, the Young's modulus of the fill E_b and the shear strength τ_f of the foundation. To study their influence on the horizontal strain distribution, five different values of K_o were examined (1.0, 1.1, 1.2, 1.5 and 2.0) and, in each case, an E_b value was chosen so as to give the best overall agreement with the measured strains. The value of τ_f adopted was, on the basis of the findings of section 7.3, taken as 25 kN/m^2, save for the analysis of the Ch. 487 section in which the interface, taken at the elevation of the trench bottom, was some 3 metres below the foundation level; in this case, the τ_f adopted was 30 kN/m^2.

A minimum value for K of 0.45 was imposed in any case, corresponding to the active state for $\phi' = 22^o$, $c' = 0$ and $r_u = 0$. When a figure lower than this was required to keep shear stresses equal to the available strength, the zone of yield and

spread was extended a little beyond the junction between crest and slope so that a coincidence of P and P_{av} would be eventually reestablished. In the region near the toe where the available strength was high enough to cope with the shear stresses, no horizontal strain was assumed, either positive or negative.

7.5.4 Comparisons between Model and Prototype

In figures 7.7 to 7.9, predictions of horizontal strains are compared with measured values at every fill elevation. The initial state of total stresses in the fill was arbitrarily fixed by means of the coefficient $K_o = 1.5$, and a Young's modulus E_b was investigated so that the overall distributions of calculated horizontal strains approximately coincided with the observed values. This was accomplished with the use of roughly the same E_b for the three cases, ranging from 15 to 18 MN/m^2.

In order to look into the influence excercised on the value of E_b by the K_o chosen, calculations were also made with K_o values from 1.0 to 2.0 and their results are shown in figure 7.10, where E_b is seen to equal about 8 MN/m^2 for $K_o = 1.0$ and around 26 MN/m^2 for $K_o = 2.0$. Between these limits, an approximately linear trend was observed in all three analyses.

It is worth to comment at this stage that recent laboratory undrained tests carried out at Imperial College on 100 mm x 200 mm cylindrical samples extracted from the trial embankment (SODHA, 1974) led to Young's modulus E_b of 12 MN/m^2 for an axial

strain of 1%. In these tests, the confining pressure adopted was 414 kN/m^2, certainly greater than the average horizontal stresses in the real fill, which would tend to exaggerate the calculated value of the compression modulus. For axial strains corresponding to stress level of 0.5, the laboratory tests yielded even lower moduli, around 10 MN/m^2 for ϵ_1 = 1.35 to 1.50%.

As in the actual bank the confining stresses were lower than in the laboratory tests and the average measured vertical and horizontal strains were rather high in the field, two alternative conclusions arise from the relationships between K_o and E_b shown in figure 7.10:

a) either the initial earth pressure coefficient in the fill K_o was low, around 1.0 or less,

b)or, alternatively, the actual fill was stiffer than implied by laboratory triaxial tests.

There was a better agreement between measured horizontal strains and the values of horizontal strains calculated with higher values of E_b, but the rough approximation inherent in the analysis employed does not leave much margin for definitive conclusion in this respect.

The accuracy of the prediction, by the model, of the pattern of horizontal strains developed as the fill rises is reasonable. Absolute strains strongly depended on the values selected for the various parameters, particularly E_b and K_o, but

the relations between the strain magnitudes at each section of the bank base did not vary considerably within plausible limits for K_o and the calculated distribution of horizontal strains agreed fairly well with the observed pattern.

7.6 PORE PRESSURE PARAMETERS IN FOUNDATION

7.6.1 Data Utilized in the Analysis

An attempt was made to determine the values of the pore pressure parameters A and B (SKEMPTON, 1954; BISHOP, 1954) from analyses of the observed pore pressures on piezometers of Ch. 487 coupled with predictions of stresses obtained from finite element analysis of the trial bank.

The finite element analysis (HAMZA, 1974) was based on a non-linear stress-strain relationship for the foundation and an undrained strength increasing from 30 kN/m^2 at the top to 100 kN/m^2 20 metres below. The Poisson's ratio adopted was 0.49 and the initial deformation modulus (for zero-strain conditions) increased from 39 MN/m^2 at the top to 76.5 MN/m^2 15 metres below, both parameters defined in terms of total stresses. The strength of the fill was made equal to $90 + 0.24\ \sigma_3$ (kN/m^2) and the deformat- modulus, assumed not to vary with strains, equal to $13800\ (1 + 0.00267\ \sigma_3)$, in kN/m^2. The Poisson's ratio of the fill material was 0.45 and the initial stresses in foundation defined by $K_o = 1.0$.

The observed pore water pressure changes on the

7 piezometers of Ch. 487 are plotted against fill elevations in figures 7.11 and 7.12 together with finite element predictions for $\Delta\sigma_1$, $\Delta\sigma_3$ and $(\Delta\sigma_1 - \Delta\sigma_3)/2$. It is seen in those drawings that there was little or no response in pore pressure to the first stages of loading, but it seems, from the shape of the curves, that there was a further recovery and that final pore pressures were representative of the zone where the piezometers were located. This anomaly, common to all 7 piezometers may have been caused by soil disturbance and/or presence of air trapped around piezometer tips, installed shortly before the placing of fill started, these effects being eventually annulled by further compression and pore pressure equalization with time. An alternative explanation for the sudden increase in Δu observed as the fill elevation was around 62 m AOD would be the development of some movement along the axis direction, leading to a rise in the intermediate stress σ_2 and, obviously, in the mean stress σ_m. On piezometers P1 and P2, near the toe and located at relatively shallow depths, such a 'jump' did not occur and this might have been a consequence of the fan-like movement experienced by outer points of the embankment and measured through the survey of surface monuments.

Calculated values for A_{ps} (parameter A for plane strain conditions) varied from 0 to 1.2, but, except for piezometers P6 and P11, A_{ps} was always below 0.6. The piezometers P6 and P11 were located below the region where lateral movement of foundation was recorded by means of inclinometers and it is possible that shear

stresses and minor principal stresses were not correctly predicted in that zone.

7.6.2 Pore Pressure Parameters 'A' and 'a'

Figure 7.13 shows that A_{ps} tended to rise with increasing mean total stresses and that the mean value of calculated A_{ps} was 0.51, practically the value that would be expected for an isotropically elastic material.

If the unexpectedly high values of 0.75 and 1.20 measured on Piezometers P11 and P6 are discarded, the average A_{ps} drops to 0.33, typical value for slightly overconsolidated soils.

In order to appreciate better the significance of the range of values for A_{ps}, a relationship must be established between A_c, measured on conventional triaxial compression tests, and A_{ps}, corresponding to plane strain conditions. This can be accomplished by using a formula expressing Δu as a function of the three principal stresses (HENKEL, 1960), shown below for the case of a saturated material with B = 1:

$$\Delta u = \frac{\Delta\sigma_1 + \Delta\sigma_2 + \Delta\sigma_3}{3} + a\sqrt{(\Delta\sigma_1 - \Delta\sigma_2)^2 + (\Delta\sigma_2 - \Delta\sigma_3)^2 + (\Delta\sigma_3 - \Delta\sigma_1)^2} \qquad (7.13)$$

For the case of triaxial compression, $\Delta\sigma_2 = \Delta\sigma_3 = 0$, and (7.13) becomes:

$$\Delta u = \frac{1 + 3a\sqrt{2}}{3}\Delta\sigma_1 \qquad (7.14)$$

If parameter A is used (SKEMPTON, 1954; BISHOP, 1954), the expression equivalent to (7.14) is

$$\Delta u = A_c \cdot \Delta \sigma_1 \qquad (7.15)$$

Consequently, for triaxial compression:

$$A_c = \frac{1 + 3a\sqrt{2}}{3} \qquad (7.16)$$

For an elastic material, u does not vary with changes in the deviatoric stress, a = 0, and A = 1/3.

In plane strain, assuming Poisson's ratio of 0.5, $\Delta \sigma_2 = 0.5\ \Delta \sigma_1$ in case σ_3 is kept constant. Formula (7.13) becomes then:

$$\Delta u = \frac{1 + 2a\sqrt{1.5}}{2} \Delta \sigma_1 \qquad (7.17)$$

Using parameter A,

$$\Delta u = A_{ps} \cdot \Delta \sigma_1 \qquad (7.18)$$

Comparing, (7.17) with (7.18)

$$A_{ps} = \frac{1 + 2a\sqrt{1.5}}{2} \qquad (7.19)$$

For a = 0 (elastic materials), $A_{ps} = 0.5$.

If parameter a is assumed not to depend on the state of stresses the element of soil is subject to, expressions derived from (7.16) or (7.19) must be equivalent:

$$a = \frac{3A_c - 1}{3\sqrt{2}} = \frac{2A_{ps} - 1}{2\sqrt{1.5}} \qquad (7.20)$$

And, finally,

$$A_{ps} = 0.866\ A_c + 0.211 \qquad (7.21)$$

Expressions (7.19) and (7.21) were utilized in figure 7.13 to build the y-axis where A_c and a are related to A_{ps}.

7.6.3 Parameter $\bar{B}$

With basis on observed pore water pressures in foundation and finite element predictions for the major total principal stresses at the points of the piezometer tips, the parameter $\bar{B}$, defined below was calculated for each piezometer.

$$\bar{B} = \frac{\Delta u}{\Delta \sigma_1} \qquad (7.22)$$

Values ecountered varied from 0.35-0.45 on P2 to 1.10 on P6, the average being 0.75. If the only value above the unity is discarded, the average drops to 0.69.

Using the overburden pressure before construction σz_o and the pore pressure measured then, u_o, values of K_o (coefficient of earth pressure at rest, in terms of total stresses), can be related to K_o' (the same coefficient in effective stresses) by the following equation:

$$K_o = \frac{\sigma_x}{\sigma_z} = \frac{\sigma'_x + u}{\sigma'_z + u} = \frac{K_o' + \frac{u}{\sigma_z'}}{1 + \frac{u}{\sigma_z'}} \qquad (7.23)$$

Selecting arbitrarily 4 values for K'_o (0.8, 1.0, 1.5 and 2.0), Table 7.1 was constructed, according to equation (7.23), to determine values of K_o for each K'_o chosen.

Also on the basis of finite element predictions and pore pressure observations, major principal effective stresses were calculated for the end of construction, as seen in Table 7.2. Assuming that peak strength had been mobilized in the regions of every piezometer and using a coefficient of active pressure $K'_{ac} = (\sigma'_{3_f} / \sigma'_{1_f}) = 0.45$ (corresponding to $c' = 0$, $\phi' = 22^o$), the same coefficient in terms of total stresses was worked out for each piezometer and its values are presented in Table 7.2.

TABLE 7.1

Coefficient of Earth Pressure At Rest in Total Stresses (K_o)

(from pwp observations and overburden pressure)

Piezo.	σ_{z_o} kN/m^2	u_o kN/m^2	σ'_{z_o} kN/m^2	$\frac{u_o}{\sigma'_{z_o}}$	Values of K_o for K'_o =			
					0.8	1.0	1.5	2.0
P1	102	22	80	0.275	0.84	1.00	1.39	1.78
P2	190	64	126	0.508	0.87	1.00	1.33	1.66
P3	264	97	167	0.581	0.87	1.00	1.32	1.63
P4	81	11	70	0.157	0.83	1.00	1.43	1.86
P5	156	48	108	0.444	0.86	1.00	1.35	1.69
P6	267	106	161	0.658	0.88	1.00	1.30	1.60
P11	253	68	185	0.368	0.85	1.00	1.37	1.73

TABLE 7.2

Coefficients of Active Pressure in Total Stresses K_{ac}

(from pwp observations and finite element predictions)

Piezo.	σ_1 kN/m^2	u kN/m^2	σ_1' kN/m^2	$\sigma_{3_{ac}}'$ kN/m^2	$\sigma_{3_{ac}}$ kN/m^2	K_{ac}
P1	216	78	138	62	140	0.65
P2	355	131	224	101	234	0.66
P3	458	229	229	103	332	0.73
P4	378	259	119	54	313	0.83
P5	438	306	132	59	365	0.83
P6	555	394	161	72	466	0.84
P11	508	297	211	95	392	0.77

Parameter $\bar{B}$ can be estimated by means of the equations derived below:

$$B = \frac{\Delta u}{\Delta \sigma_{mean}} = \frac{3\,\Delta u}{\Delta\sigma_1 + \Delta\sigma_2 + \Delta\sigma_3} = 1 \text{ (for saturated soils)} \qquad (7.24)$$

If $\Delta\sigma_3 = (1 - \Delta K)\,\Delta\sigma_1$ and $\Delta\sigma_2 = (1 - \Delta K/2)\,\Delta\sigma_1$ (for plane strain, $\nu = 0.5$),

$$B = \frac{\Delta u}{\Delta\sigma_1 (1 - 0.5\,\Delta K)} = \frac{\bar{B}}{(1 - 0.5\,\Delta K)} \qquad (7.25)$$

Hence, for B = 1,

$$\bar{B} = 1 - 0.5\,\Delta K \qquad (7.26)$$

In Table 7.3, the various estimated values of K_o were combined with K_{ac} to produce ΔK and predictions for $\bar{B}$ which are compared with calculated $\bar{B}$. Interpolation gives values of K_o

1.0 and 1.5.

7.6.4 Parameter B

Average A_{ps} based on a parameter B equal to the unity was 0.5, a value corresponding to an elastic material. Slow undrained triaxial tests on samples of various sizes and orientations (MAGUIRE, 1974) confirm such a trend, and this is an evidence of the adequacy of taking B = 1 in foundation for all practical purposes, at least at levels where piezometers were installed.

Accordingly this was the value used in the theory applied in previous section to predict values for the parameter $\bar{B}$.

7.7 DEFORMATION PARAMETERS FOR THE FOUNDATION

7.7.1 Method of Analysis Applied

As frequently mentioned throughout this thesis, non-linear finite element analysis have been applied to the trial bank and to the main dam in order to determine stress distributions as well as displacement patterns (VAUGHAN, WERNECK and HAMZA, 1973; HAMZA and VAUGHAN, 1974; HAMZA, 1974). Prior to the trial bank construction, linear finite element analyses were carried out (NAYLOR, 1972; HAMZA, 1972), two different assumptions having been made of values for deformation moduli of the foundation and three different K_o having been adopted: K_o = 0.75, 1.0 and 1.25, corresponding to K'_o = 0.5, 1.0 and 1.5 for coinciding ground and water levels and γ = 20 kN/m^3.

Stress distributions are known not to vary considerably with the stress-strain relationships adopted, particularly in the case of the major principal stress; minor principal stresses are more dependent on the correctness of the peak strength imposed and on the brittleness of the material. Predicted finite element stresses can be coupled with measured strains to produce stress-strain curves to be compared with those obtained from laboratory or in-situ tests.

This method of analysis will not be extensively dealt with here, but some brief comparisons will be presented.

This sort of analysis requires, as a first step, the assessment of initial stresses in the ground, as the soil behaviour is stress path dependent and deformations and local failure are affected by the strength reserve at each point, a function of initial lateral stresses.

7.7.2 Initial Stresses - Determination of K_o'

Where the surface ground is horizontal, no directional earth movement has taken place in geological or recent times, bedding places are horizontal and horizontal uniformity exists, soil can be expected to exhibit cross anisotropy with respect to various physical properties, inclusive of stresses acting upon any element of the earth mass. In other words, in any horizontal direction, stresses are defined by:

$$\sigma_x' = \sigma_y' = K_o' \sigma_z' = K_o' \int_o^z \gamma . dz \qquad (7.27)$$

$$\sigma_x = \sigma_y = K_o' \sigma_z' + u_z \qquad (7.28)$$

where σ_x', σ_y' and σ_z' are effective stresses at depth z; σ_x, σ_y and σ_z are total stresses at the same depth; u_z is the pressure in the pore fluid at depth z; γ is the unit weitht of overburden soil, and K_o' is the coefficient of horizontal stresses at rest, a parameter depending on the soil nature and varying largely with the stress and deformation history of the soil.

At Empingham Dam site, where hill side inclinations, although gentle, are known to coincide in direction with earth movements associated to valley bulging-cambering structures, there are no reasonable grounds to assume that across-the-valley stresses should equal the stresses prevailing along directions parallel to the stream channel. Nevertheless, as the construction of an embankment is approximately a plane-strain problem (if three-dimensional effects are unimportant), engineering analysis can be carried out by adopting, as a starting point, a state of stresses where across-the-bank effective stresses are related to vertical effective stresses by a constant ratio that, for sake of simplicity, will be herein noted K_o' as though it were a unique horizontal ratio for horizontal effective stresses.

During the phases of site investigation and trial bank construction, no attempt was made to estimate horizontal stresses in the ground, either by laboratory tests or field measurements. The knowledge of existing initial stresses before applicat-

ion of the embankment load is nevertheless essential for a good understanding of stress-deformation-strength patterns followed by an earth structure. A theoretical analysis, developed as means of predicting the approximate state of initial stresses, is presented in the following paragraphs.

Attempts have been made in the past to relate the total stresses relieved by sampling operations with the consequential pore pressure changes in the sample measured in laboratory (SKEMPTON, 1961; BISHOP et al., 1965; KNIGHT and BLIGHT, 1965; BLIGHT, 1967; and SOM, 1968, for example). If shape distorsion induced by stress relief is supposed not to generate any variation in pore pressure, the lattter will be a function of in-situ stresses alone:

$$p'_s = -u_s = \frac{1+2K'_o}{3}\sigma'_z = \frac{1+2K'_o}{3}(\sigma_z - u_z) \qquad (7.29)$$

where p'_s is the isostatic effective stress acting on a soil element after a perfect sampling (numerically equal to suction u_s).

If no suction change occurred from the moment the sample was in the ground, before drilling started, up to the instant when suction was measured in laboratory, this method of calculating K_o would be reliable. However, mechanical disturbance moisture content changes during drilling, sampling, transporting, handling, trimming and testing can cause large errors in laboratory suction measurements and these effects are likely to push the results consistently in one single direction if techniques employed are unvaried, which makes such methods imprecise even when averaging of

a great many 'good' tests are carried out.

The improvement of such a technique proposed here consists of considering the variation of measured suction with depth rather than absolute values; systemmatic shifts would disappear then, provided that errors did not vary from elevation to elevation. Wide scatter, a usual pattern in suction measurements, is still a problem but, in this case, the performance of a large number of tests and the use of average, upper-limit or lower-limit lines would minimize errors.

At Empingham, few suction measurements were carried out and the straight application of principles above outlined is not possible. Nowadays, however, effective strength parameters and pore pressure parameters for the Upper Lias Clay are reasonably well known and the results of hundreds of undrained triaxial tests can be used for an indirect evaluation of suction and, therefore, its variation with depth. The derivation of mathematical expressions to cope with this problem is presented in the following paragraphs.

If a unique coefficient of horizontal stresses holds for any direction contained in a plane parallel to ground surface, (7.29) is valid. Specimens characterized by a initial isostatic effictive stress p'_s and pore pressure parameters $B = 1$ and A_f, follow, in conventional undrained triaxial tests, an effective stress path defined by:

$$\frac{\sigma_1 - \sigma_3}{2} = \frac{1}{1-2A_f}\left(\frac{\sigma_1 + \sigma_3}{2} - p'_s\right) \qquad (7.30)$$

or

$$q = \frac{1}{1 - 2A_f}(p' - p'_s) \qquad (7.31)$$

This path intercepts the effective stress envelope:

$$\frac{\sigma_1 - \sigma_3}{2} = \frac{c'}{\cos \phi'} + \frac{\sigma_1' + \sigma_3'}{2} \sin \phi' \qquad (7.32)$$

or

$$q = \frac{c}{\cos \phi'} + p' \sin \phi' \qquad (7.33)$$

The value of q at failure (interception of the two straight lines), denoted q_f, is the undrained strength corresponging to a specimen displaying an after-sampling suction of $u_s = -p'_s$:

$$c_u = q_f = \frac{c' \sec \phi' + p_s' \sin \phi'}{1 - \sin \phi' (1 - 2A_f)} \qquad (7.34)$$

or

$$c_u = q_f = \frac{c' \sec \phi' + 1/3 (1 + 2K_o') \sin \phi' \int (\gamma - \gamma_w) dz}{1 - \sin \phi' (1 - 2A_f)} \qquad (7.35)$$

In cases where c', ϕ', K_o', A_f, γ and γ_w do not vary with depth, derivation of (7.35) with respect to z leads to:

$$\frac{dc_u}{dz} = \frac{dq_f}{dz} = \frac{(1 + 2K_o') \sin \phi' (\gamma - \gamma_w)}{3 [1 - \sin \phi' (1 - 2A_f)]} \qquad (7.36)$$

For the Upper Lias Clay at Empingham, ϕ' was found to be around 23° (for zero cohesion intercept), $(\gamma - \gamma_w)$ approximately 10 kN/m^3 and A_f ranging from 0.3 to 0.5 under triaxial

conditions corresponding to equation (7.36). Variation of undrained strength with depth is depicted in figures 3.6, 3.8 and 3.9 a 'lower-limit' line showing a gain of 3.5 kN/m^3 for triaxial tests and 4.5 kN/m^3 for plate bearing tests. Use of these and some other numbers yield the values for K_o' presented in Table 7.4.

TABLE 7.4

Theoretical Values for K_o' at Empingham

$\frac{dqf}{dz}$ (kN/m^3)	Triaxial Compression A_f			
	0.3	0.33	0.4	0.5
3.5	0.64	0.67	0.74	0.84
4.0	0.80	0.83	0.92	1.03
4.5	0.96	1.00	1.10	1.23

Although a large variation in K_o values is seen to stem from relatively small changes in (dqf/dz) and A_f, it is important to note that figures between 0.64 and 1.23, which form the extreme limits for cases treated in Table 7.4, are well below what is typical of other overconsolidated clays, even when strongly fissured. Lower K_o as well as higher A_f values characterize the Upper Lias Clay, an unusual feature for a material that has been subjected to more than 1,000 m of overburden deposits in its geological past. It appears that combined action of superficial strucures, permafrost and weathering has dissipated overconsolidation effects, reducing lateral stresses and decreasing tendency to

dilatancy.

It is worthwhile mentioning at this point that for similar angles of shearing resistance and unit weights, other well known overconsolidated clays exhibit rather larger gains in undrained strength with depth, an evidence of higher K_o and lower A_f values. That is, for instance, the case of London Clay (BISHOP and LITTLE, 1967), Barton Clay (MARSLAND and BUTLER, 1967) and Oxford Clay (PARRY, 1972), although an exception to this trend have been reported for Boom Clay, in Belgium (DE BEER, 1967, for which a gain of 3.5 kN/m^3 is associated to A values of 0.38, both figures similar to those of Empingham's Upper Lias Clay.

Similarly, the normally consolidated clay of low sensitivity encountered at Drammen, Norway (KJAERNSLI and SIMONS, 1962) exhibits a gain of 1.3 kN/m^3, a result that can be also reached by the application of equation (7.36) for $A_f = 1.0$, $K'_o = 0.5$, $(\gamma - \gamma_w) = 8$ kN/m^3, ϕ' 19°, values quite close to typical figures commonly attributed to such a sort of soil. Quick clays, whose parameters A at failure in general exceed unity, are expected to display an undrained strength increase of less than 1 kN/m^3; indeed, 5 Norwegian quick clays cited by AAS (1967) presented gains ranging from 0.5 to 1.0 kN/m^3.

Examples of normally consolidated clays exhibiting undrained strength gains between 0.7 and 1.5 kN/m^3 include, among others, Göta River Clay (BRINK, 1967), the sensitive clay at Interstate Route 95 trial bank, Portsmouth, New Hampshire, USA (LADD,

1972), Bangkok Clay (EIDE and HOLMBERG, 1972) and a marine clay near Ottawa, Canada (BOZOZUK, and LEONARDS, 1972). A gain of only 0.74 kN/m^3 could correspond, for instance, to a parameter set such as $\phi' = 14^o$, $K_o' = 0.5$, $A_f = 1.2$, $(\gamma - \gamma_w) = 6$ kN/m^3, common values for very sensitive or organic clays.

Laboratory undrained triaxial tests on Empingham samples have shown an increase of A_f with initial suction p_s' at an approximate rate of 0.1 per 100 kN/m^2 (MAGUIRE, 1974). Assuming a linear variation v with depth,

$$A_f = A_{f_o} + v.z \tag{7.37}$$

Putting (7.37) into (7.35), derivating and re-arranging terms leads to:

$$\frac{dc_u}{dz} = \frac{\frac{1+2K_o'}{3}(\gamma-\gamma_w)\sin\phi'\left[1+2\sin\phi'(A_{f_o}-0.5)\right]-2\,c'v\tan\phi'}{\left[1+2\sin\phi'(A_{f_o}+vz-0.5)\right]^2} \tag{7.38}$$

According to expression (7.38), the gain in strength dc_u/dz varies with depth and, unlike equation (7.36), it also depends on the cohesion intercept. Table 7.5 was constructed on the basis of the following parameters: $c' = 0$, $\phi' = 23^o$, and $v = 0.01$ m^{-1}. K_o was assumed 0.7, 1.0 and 1.3, and three values for A_{f_o} were examined: 0.3, 0.4 and 0.5. Rates of strength gain were calculated for 4 depths: 0, 5, 10 and 15 metres. A cohesion intercept of 10 kN/m^2 would reduce the strength rate by only 0.07 to 0.12 kN/m^3 and, therefore, its influence is small.

TABLE 7.5

Predicted Strength Rate for Increasing A_f

K_o	z (m)	$\frac{dq_f}{dz}$ (kN/m^3) for A =		
		0.3	0.4	0.5
0.7	0	3.71	3.39	3.13
	5	3.39	3.12	2.90
	10	3.11	2.88	2.69
	15	2.86	2.67	2.51
1.0	0	4.64	4.24	3.91
	5	4.24	3.90	3.62
	10	3.89	3.60	3.36
	15	3.57	3.34	3.13
1.3	0	5.56	5.08	4.69
	5	5.08	4.68	4.35
	10	4.66	4.32	4.03
	15	4.29	4.00	3.76

Values in Table 7.5 do not differ much from those in Table 7.4. They confirm the finding that strength gains in the order of magnitude found in field and laboratory tests (3 to 5 kN/m^3), coupled to A_f values between 0.3 and 0.5 (in terms of triaxial compression), correspond to K_o around one and perhaps less, certainly not a typical value for overconsolidated clays.

7.7.3 Stress-Strain Curves

Adopting $K_o = 1$, non-linear finite element analyses were carried out (HAMZA, 1974) for the section of Ch. 487.

Combining shear stresses predicted in these analyses with measured strains recorded in certain zones of the foundation, 3 to 5 metres below stripped ground level, stress-strain curves were obtained and are shown in figure 7.14.

Linear finite element analyses performed before construction (NAYLOR, 1972; HAMZA, 1972) used the two sets of assumed foundation secant moduli shown in Table 7.6.

TABLE 7.6

Moduli Used in F.E. Analysis

Depths (m)	E (MN/m^2)	
	Low	High
0 - 5	13.5	45.0
5 - 10	17.0	57.0
10 - 15	21.0	70.0
15 - 20	105.0	350.0

The assumption of high E gave place to predictions of maximum lateral movements of 40 to 50 mm at I3 and I4, whereas low E resulted in predicted displacements of 140 to 160 mm at the same locations. Measured horizontal movements at the end of construction were 400 to 600 mm at Ch. 487 and extrapolation of above results would lead to an overall deformation modulus of 4 MN/m^2 for the upper 5 metres of the foundation. This corresponds to secant moduli determined for I4 and I3 (figure 7.14) at stress levels of 75% to 90%.

Hyperboles have been suggested as functions to represent the relationships between stress differences and major principal strains, (KONDNER, 1963; KONDNER and ZELASKO, 1963 a,b; KONDNER and HORNER, 1965) and their use has given good results (KULHAWY et al, 1969, and WERNECK, 1971, for example). Using stress difference levels instead of deviatoric stresses, Kondner's hyperbole is expressed under normalized form:

$$\frac{2\epsilon c_u}{\sigma_1 - \sigma_3} = (2a\,c_u) + (2b\,c_u)\epsilon_1 \qquad (7.38a)$$

where

$$a = \frac{1}{E_{in}} \qquad (7.39)$$

$$b = \frac{1}{(\sigma_1 - \sigma_3)_{ult}} \qquad (7.40)$$

and

$$(\sigma_1 - \sigma_3)_{ult} = \frac{(\sigma_1 - \sigma_3)_f}{R_f} = \frac{2c_u}{R_f} \qquad (7.41)$$

where E_{in} is the tangent modulus for $\epsilon_1 = 0$, $(\sigma_1 - \sigma_3)_{ult}$ is the asymptote of the hyperbole, and R_f is the ratio between the peak strength $(\sigma_1 - \sigma_3)_f$ and the asymptote.

Stress-strain curves derived from field measurements are plotted, under the modified form suggested by Kondner, in figure 7.15, where parameters a and b were determined as functions of the undrained strength c_u. Averaging both results, the stress-strain relationship found was:

$$\frac{\sigma_1 - \sigma_3}{2 c_u} = \frac{\epsilon_1}{0.0041 + 0.93\,\epsilon_1} \qquad (7.42)$$

It must be noted in figure 7.15 that the first point of the plot for I4 is below the straight line. This departure from the hyperbole modified plot means that actual initial deformation moduli are higher than that obtained in the hyperbolic plot, i.e expression (7.42) leads to flatter plots than effectively recorded. This difference is not significant, however, in the face of the other approximations involved, both in the strain measurements and in the finite element predictions for stress differences.

7.8 FILL PROPERTIES

Pore pressure measurements in the fill never resulted in positive values. If the air-water phase is assumed to be at atmospheric pressure, total stresses in fill equal effective ones.

Figures 6.96, 6.97, 6.118 and 6.119 show that strains in the fill increased with fill heights in an approximately linear fashion and, therefore, constant deformation moduli are expected to efficiently describe the behaviour of the fill as far as deformation is concerned.

Assuming effective and total stresses to equal overburden pressure, the moduli defined by the ratios between vertical stress and strains were found to be between 3.6 and 8.4 MN/m^2

(average 5.3 MN/m^2). As there was lateral yield of the soil, such a modulus is intermediate between oedometric and Young's moduli.

Vertical and horizontal strains were measured in the fill. Assuming vertical stresses to equal overburden pressure $\gamma.h$, an equation of elastic theory for plane strain can be used to assess the Young's modulus of the fill.

$$E_b = \frac{\gamma_b . h \, (1 - \nu_b - 2\nu_b^2)}{\nu_b \epsilon_x + (1-\nu_b)\epsilon_z} \qquad (7.43)$$

The expression above, for a Poisson's ratio ν_b of 0.4, led to $E_b = 4.2$ MN/m^2 for Ch. 487 and $E_b = 2.2$ for Ch. 537. As vertical strains are suspected to have been overmeasured, owing to the high compressibility of the sand surrounding inclinometer ducts, these values must be regarded as lower bounds for Young's Modulus.

Combination of E_b value found from measured linear strains with the curves of figure 7.10 suggests that initial stresses in the fill were characterized by a coefficient $K_o = \sigma_x / \sigma_z$ below one, around 0.8 perhaps. It must be taken into account however, that in the analysis, K_o did not refer to the conditions immediately following the placing of the fill but to those occurring as the embankment slope started to be built above the considered point, a situation in which the effects of 'built in' horizontal stresses imposed by compaction might have been greatly reduced.

No clear indications can be obtained from the

field measurements about reliable values of Poisson's ratio to be used in analysis, but from laboratory tests on samples taken from the fill (SODHA, 1974) and from some indirect observations, values bwtween 0.4 and 0.45 appear to represent well the material employed in the trial embankment.

7.9 COMPARISON OF TRIAL BANK FINDINGS WITH DESIGN ASSUMPTIONS

7.9.1 Undrained Strength

In a soil mass where shear strength increases substantially with depth, the critical slip surface developed under loading imposed by an embankment tends to be flat in its part contained in the foundation, often departing from circular shape to become nearly horizontal. This tendency is aggravated where embankment slopes are gentle and, even more, where anisotropic foundation shear strength has its minimum value corresponding to shear planes which are approximately horizontal.

At Empingham main dam, fill slopes are flat and the foundation shear strength is known to experience an important gain with depth. In addition, the Upper Lias Clay is thought to exhibit anisotropic properties, its undrained strength and cohesion intercept reaching a minimum in directions near horizontal (MAGUIRE, 1974).

As a result, the critical slip surface of the main embankment was expected to be nearly horizontal in the foundation, and one of the possible disadvantages of the trial bank approach

originally considered was that its critical slip surface might differ from that of the main dam, making analysis more difficult and uncertain. Fortunately, the measurement of deformations of the trial bank and the relatively easy identification of the strain pattern in the foundation, showed the shape of the potential slip surface in the trial bank to be close enough to that predicted for the main embankment to make trial bank findings satisfactorily applicable to the main dam design.

In the most conservative of the two provisional designs initially drawn, the foundation undrained strength was assumed to be 30 kN/m^2 at the top, increasing steadily with depth to 100 kN/m^2 at a level 20 metres below the ground surface. These figures correspond to an average c_u of 47 to 56 kN/m^2 for the upper 10 to 15 metres of the foundation, approximately the same average value obtained from back-analyses of failed cuts at borrow pits.

Back analyses of the trial bank assuming that its factor of safety was between 1.0 and 1.05 have, however, resulted in lower values, around 20 to 25 kN/m^2 at the top and a gain with depth of 2.5 to 3.0 kN/m^3. A more precise definition of the foundation undrained strength through the trial bank back-analysis is made difficult owing to uncertainties concerning the mobilized shear stresses in the fill, and above figures quoted for the foundation strength are believed to be safe enough for use in design. Furthermore, since measured strains were much higher in the trial bank than predicted for the main dam and creep movements were allowed over a

long period under probably high stress levels, the calculated strength is likely to include some combined effects of brittleness and time dependent loss of strength not likely to occurr to the same degree in the main dam.

The main dam was designed with a factor of safety of 1.5, which brings the assumed strength to $c_u(kN/m^2) = 20 + 2.33\ z(m)$, more or less the most pessimistic result of the trial bank back-analysis.

An important aspect to be considered in the dam design is that its deformations are being accurately controlled by means of different cross-checking systems. With the experience gained with the trial bank, excessive deformations and strains are easily identifiable during construction and in the case of their occurring, remedial works could be done safely in time. The dam is nearing completion now and, as expected, this has proved to be unnecessary, an indication of the suitability of the design assumptions.

7.9.2 Strength in Terms of Effective Stresses

Bishop's method of slope stability analysis applied to slip surface configuration obtained from the trial bank deformation measurements and to average measured values for r_u in the fill and in the foundation, led to a friction angle of 18^o for a zero cohesion intercept. However, these parameters are very sensitive to small variations in r_u and even to the method of analysis employed.

In the design, $c' = 0$ and $\phi' = 18^o$ were initially adopted, a factor of safety of 1.3 bringing the mobilized friction

angle down to 14°. For the part of the foundation where emergent shears were noticed after stripping, lower values were later chosen: $c' = 0$ and $\phi' = 14^{\circ}$ (with $F_s = 1.3$, the mobilozed ϕ' was 11°).

The value of 14° for ϕ' would correspond, in the trial bank back-analysis, to a foundation pore pressure ratio r_u around 0.65, between the measured average, 0.50, and the predicted values for no-lateral-yield r_u, 0.70 to 0.85.

7.9.3 Consolidation Parameters

No direct measurement of c_v was planned as part of the trial bank experiment as this parameter would be better evaluated through sand drain trials and observation of the prototype behaviour during winter stoppages. Nevertheless, an indication of its overall value can be indirectly obtained from permeability measurements combined with the compressibility of the soil skeleton predicted from laboratory tests.

In 1973, in-situ permeability tests were carried out by the Author on piezometers located at the sand drain area of the main dam. These measurements are not described in this thesis but their results, summarized in Table 7.7, show that permeabilities varied from about 1×10^{-10} m/sec at 5 m below the top of Lias to just over 1×10^{-11} m/sec at the depth of 20 m, for vertical effective stresses generally between 200 and 300 kN/m^2.

Falling head stages of hydraulic fracture tests led to fill permeabilities of the order of 1×10^{-11} m/sec, close to

TABLE 7.7

In-situ Permeability Tests - Sand Drain Area

Piezo.	Position (m)				u	σ'_z	k
	Ch.	E.	El.	d(+)	kN/m^2	kN/m^2	10^{-11} x m/sec
SD-1	398.4	7979.4	53.5	5.8	135	200	10.0
SD-2	389.4	7979.4	42.5	16.8	200	240	7.5
SD-5	451.4	7964.0	51.3	5.7	105	315	13.2
SD-6	451.4	7964.0	46.1	10.9	220	245	1.7
SD-8	451.4	8040.0	49.8	6.4	155	235	10.2
SD-9	451.4	8040.0	44.2	12.0	260	240	4.4
SD-10	451.4	8040.0	35.5	20.7	255	305	1.2
SD-11	499.0	7964.0	45.8	4.7	205	280	9.8
SD-12	499.0	7964.0	42.2	8.3	300	255	7.5
SD-14	499.0	8040.0	46.8	3.2	175	255	3.5
SD-15	499.0	8040.0	41.3	8.7	265	275	1.6
SD-16	499.0	8040.0	33.6	16.4	335	355	1.2
SD-17	516.0	7947.5	43.8	4.7	215	290	3.5
SD-18	516.0	7947.5	39.8	8.7	250	275	2.8
SD-26	619.0	7970.0	48.5	4.4	140	210	1.9
SD-30	640.0	8033.0	49.5	5.0	150	120	1.3
SD-31	640.0	8033.0	44.0	10.5	175	195	4.9

(+): d - depth of piezo. tip below top of Lias.

the lower bound of foundation values.

Coefficients of volume change for σ'_z around 300 kN/m^2 were found in laboratory tests to be approximately 0.1 m2/MN. Combination of this figure with the measured in-situ permeabilities gives coefficients of consolidation of the order of 3 m^2/year at the depth of 5 metres and 0.3 m^2/year 15 metres below. Above the depth of 5 metres, c_v is likely to be even higher, due to greater disturbance.

The contract design was based on c_v = 0.25 m^2/year, but in its revision c_v was made variable with effective stresses, dropping from 3 m^2/year, for σ'_z between 0 and 180 kN/m^2, to 0.25 m^2/year at $\sigma'_z \geq$ 250 kN/m^2. In the bulge area, the revised design allowed higher c_v, around 5 m^2/year for σ'_z = 200 kN/m^2, decreasing to 0.25 m^2/year for $\sigma'_z \geq$ 420 kN/m^2. This modification was made after observations during the first winter stoppage of pore pressure dissipation in piezometers located in the sand drain area resulted in c_v values considerably higher than previously predicted and strongly dependent on effective stresses.

7.9.4 Fill Properties

Undrained triaxial tests on samples taken from the trial bank were carried out during construction. Specimens subjected to cell pressures of 250 kN/m^2 presented an average undrained strength of 140 kN/m^2, considerably higher than initially predicted. No tests performed in normal conditions resulted in c_u

lower than 90 kN/m^2.

Combination of above figures with failure envelopes characterized by $c' = 0$ to 20 kN/m^2 and $\phi' = 18^o$ to 24^o and with pore pressure parameter A of 0.3 to 0.5 led to calculated suctions between 0 and 100 kN/m^2, in the same order of magnitude of suctions measured in the fill by means of piezometers.

The active thrust of the dam centre on the berms was calculated in the initial design on the basis of a mobilized shear stress of 40 kN/m^2, corresponding to $c' = 0$, $\phi' = 22^o$, $F_s = 1.5$ ($\phi'_{mob} = 15^o$) and $r_u = 0.6$. With the results of the trial bank experiment and also of the observations taken during the placing of fill of the first 10 metres of the main dam, the fill was found to be stronger than initially forecast. Accordingly, the active thrust was reassessed for the final design, a mobilized shear stress of 80 kN/m^2 being then used. This value, based on stress ratios obtained at horizontal strains of 0.5% in compression tests on fill samples, corresponds to $r_u = 0.3$, $c' = 0$, $\phi'_{mob} = 10^o$. A horizontal strain of the order of that used in calculations is likely to cause horizontal deformations under the berms of about 100 mm, an acceptable value as seen in the trial bank experiment.

Another modification introduced in the final design refers to the thickness of the berms. As most of the shear stresses imposed on the foundation take place as the central part of the embankment is built, in order to avoid local overstressing it

was desirable to transmit the central thrust as uniformly as possible towards the toes. For this purpose, the stiffness of the berms should be increased and this was accomplished by assuming a lower level of mobilized shear stresses in the berms ($\tau_{mob} = 15$ kN/m^2), which made greater berm depths required.

CHAPTER EIGHT

HYDRAULIC FRACTURE

8.1 In-situ Permeability Tests

8.1.1 Piezometer tests

8.1.2 Constant head tests

8.1.3 Variable head tests

8.2 Allowable Applied Pressures in Permeability Tests on Piezometers

8.2.1 Brief review of literature

8.2.2 Recent evidences of hydraulic fracture in soils

8.3 The Use of Hydraulic Fracture in Assessing Stresses in Soil Media

8.3.1 Saturated masses

8.3.2 Partly saturated soils

8.4 Some Theoretical Considerations about Hydraulic Fracture

8.4.1 Drainage impeded

8.4.2 Full drainage

8.5 Hydraulic Fracture Tests at the Empingham Trial Bank

8.5.1 Main objectives

8.5.2 'Blow-off' and fracturing pressures

8.5.3 'Shut in' pressures

8.5.4 'Close up' pressures

8.5.5 Variation of apparent permeability

8.5.6 Summary of the results obtained

CHAPTER EIGHT

HYDRAULIC FRACTURE

8.1 IN-SITU PERMEABILITY TESTS

8.1.1 Piezometer Tests

The most recent development of in-situ tests to determine the bulk permeability of a soil deposit is the piezometer test. It consists of imposing an excess head to a piezometer installed in the ground and, by observing the resulting flow, to deduce analytically the overall coefficient of permeability. The excess head may be positive or negative, either constant or variable with time.

8.1.2 Constant Head Tests

In the constant excess head tests (constant head tests, in short), a static pressure h_c (in terms of head of water), in general positive, is added to the original piezometric level and kept constant, the inflow being measured.

In saturated incompressible soils, steady state is practically instantaneously reached and the permeability k is calculated through the equation:

$$k = \frac{q_c}{F \cdot h_c} \qquad (8.1)$$

where q_c is the inflow and F, named shape factor, is a constant, with the dimension of length, which depends on the geometries of the piezo-

meter cavity and of the soil mass. Shape factors for different cavity geometries buried in infinite, homogeneous, isotropic soil media are listed by HVORSLEV (1951).

In compressible soils, consolidation or swelling may considerably delay the establishment of steady state seepage. The shape factor varies during the time necessary to reach a stable flow and its determination at any given instant is very complicated and inconvenient. This difficulty can be averted by allowing the test to run for a long time until final flow is reached or closely approached; formula (8.1) is applicable then and shape factors to use are those corresponding to steady state. Alternatively, as will be demonstrated in this chapter, a cavity of small intake (shape) factor can be used to minimize the error in assessing the stable flow; this is undesirable, however, inasmuch as it causes the permeability to be measured in a more localized way than otherwise.

In partly saturated soils, it may be noted that additional effects occur, due to the compressibility of the pore fluid, the effect of a compressible pore fluid being similar to that of a compressible soil skeleton.

The basic theory for the in-situ measurement of soil permeability of compressible media by means of constant head tests (GIBSON, 1963) on spherical piezometers is expressed by the equation:

$$q = 4 \cdot \pi \cdot r \cdot h_c \cdot k \cdot \left(1 + \frac{1}{\sqrt{\pi T}}\right) \qquad (8.2)$$

where q is the flow at any time t from the start of tests, r is the radius of the piezometer tip, k is the soil permeability, h_c is the excess head (positive or negative), and T is the time factor defined as follows:

$$T = \frac{c.t}{r^2} \qquad (8.3)$$

where c represents either the consolidation coefficient c_v, in the case of a negative excess head being applied, or the swelling coefficient c_s for positive heads.

In practice, piezometers are generally cylindrical and not spherical. Expression (8.2) has been transformed in such cases by equating the value $4\pi r$ to the shape factor F for cylindrical cavities, generalizing the fact that, for spheres, F actually equals $4\pi r$.

$$q = F\,k\,h_c\left(1 + \frac{1}{\sqrt{\pi T}}\right) \qquad (8.4)$$

Substituting (8.3) for T in (8.4), this becomes:

$$q = F\,k\,h_c\left(1 + \frac{r}{\sqrt{\pi c}} \cdot \frac{1}{\sqrt{t}}\right) \qquad (8.5)$$

Making $t \to \infty$ in (8.5) steady flow q_∞ is obtained:

$$q_\infty = F\,k\,h_c = 4\pi r\,k\,h_c \qquad (8.6)$$

Formula (8.5) may thus be rewritten:

$$q = q_\infty + \frac{4\pi r^2 k\,h_c}{\sqrt{\pi c}} \cdot \frac{1}{\sqrt{t}} \qquad (8.7)$$

Dividing (8.7) by (8.6):

$$\frac{q_t}{q_\infty} = 1 + \frac{r}{\sqrt{\pi c}} \cdot \frac{1}{\sqrt{t}} \qquad (8.8)$$

Equation (8.8) demonstrates the point previously made. Small piezometer intake factors (small r) reduce the error in assessing steady state flow q_∞ which arises from wrongly taking the flow at any finite time t instead. A more convenient way of obtaining q_∞, however, was devised by GIBSON (1963). It consists of plotting measured flows q against the inverse of the square root of time, $t^{-1/2}$, and determining by extrapolation the point the straight line expressed by (8.7) intersects the q-axis for $t^{-1/2} = 0$. i.e $t \to \infty$. The final flow q_∞ having been estimated, the permeability is directly calculated by means of (8.6).

Some more recent developments in the theory of in-situ determination of permeability by constant head piezometer tests include contributions by GIBSON (1966; 1970) and WILKINSON (1968). However, they are not as yet supported by definitive experimental evidences and k values have been satisfactorily determined by means of the original Gibson's theory in many cases (as those quoted by BISHOP and ALDHAIR, 1969; AL DHAIR et al, 1969; WILKINSON et al, 1969; RAYMOND and AZZOUZ, 1969, etc.). Accordingly, the recent refinements in theory above mentioned will not be dealt with here.

8.1.3 Variable Head Tests

All methods of in-situ measurements of the coefficient of permeability by means of varying (increasing or decreasing) head tests make use of the time lag in equalization to the piezometric level existing prior to the test, which is, of course, a function of the flow pattern developed in the surroundings of the piezometer cavity.

For the case of a standpipe piezometer in an incompressible deposit, the intake factor F may be regarded as a non-time dependent quantity and the permeability is calculated through the equation:

$$k = \frac{A}{F\,(t_2 - t_1)} \log_e \frac{h_1}{h_2} \qquad (8.9)$$

where heads h_1 and h_2 correspond to times t_1 and t_2, and A is the area of the standpipe cross section.

The use of varying head tests in connection with compressible media is more complicated. If two constant head tests were performed under excess heads h_1 and h_2, the plots of flow against the inverse of square root of time would be given by two straight lines. However, if a variable head tests were performed instead, the part of the curve in the time interval (t_1, t_2) would be intermediate between the two lines corresponding to constant head tests and the graph using the inverse of the square root of time in z-axis would by no means be a straight line. Because intake factors vary with time in compressible media and extrapolation to infinite time is meaningless in this case (as $h_\infty = 0$ and $q_\infty = 0$), accurate analyt-

ical expressions are much more complicated, except for soils of high coefficient of consolidation, or very small piezometer tips, where steady state is quickly approached and Hvorslev's equation for incompressible media provides a good approximate solution. Reasonably precise measurements are also obtained from very slow tests with standpipes of large cross sections, where the drop in excess head is small enough to allow the test to be treated as a constant head one.

An exact solution for variable head tests on spherical piezometers in homogeneous, isotropic, compressible soils were obtained by GIBSON (1963) on the basis of Terzaghi's consolidation theory. It requires complicated calculations or the use of graphs or tables, for eventually obtaining the dimensionless quantity $\mu = 4\pi a^3 m\ \gamma_w/A$, where a is the piezometer tip radius, A is the area of the standpipe cross section, m is the coefficient of volume change of the soil in three-dimensional terms and γ_w is the fluid unit weight. However, to obtain μ and, from it, to determine $k = m.\ \gamma_w/c$, one must know first the value of c, which corresponds to the coefficient of swelling c_s or of consolidation c_v. Apart from the normal difficulties in determining such a pressure dependent parameter, the fact that initial consolidation in the surroundings of the piezometer tip gives place to further swelling (or vice-versa), challenges the use of Gibson's expression, derived as though c were constant throughout the test. It may be noted that the results of Gibson's theory are similar to those of equation (8.9) at high degrees

of equalisation. Variable head tests are adequate to give an approximate guide to in-situ permeability.

8.2 ALLOWABLE APPLIED PRESSURES IN PERMEABLY TESTS ON PIEZOMETERS

8.2.1 Brief Review of Literature

There have been, in the past, few references in the Soil Mechanics bibliography to the amount of hydraulic pressure that can be applied within soils without causing reversible or irreversible changes in the permeability of the medium and temporary or permanent damage to the soil structure.

Undesirable effects of fracturing induced by excessive hydraulic pressure, however, have been sporadically considered and mentioned by specialists in the fields of Rock Mechanics, Grouting and Dams, and the technique of purposely inducing fracture in the surroundings of boreholes in oil well drilling has often been utilized as a means of increasing the oil output.

Prior to 1970, information on hydraulic fracture and rules concerning pressures to force (or avoid, depending on each specific engineering problem) cracking on rock or soil masses can be found, for example in CREAGER et al, (1945), CLARK (1949), AHRENS and BARLOW (1951), SCOTT et al (1953), GRUNDY (1955), VAN POOLEN (1957), LIPPOLD (1958), U.S. CORPS OF ENGINEERS (1960), NONVEILLER and ANAGNOSTI (1961), and MORGENSTERN and VAUGHAN (1963).

Rules suggested in above mentioned literature

vary quite considerably according to the material they were devised to apply to (rocks or soils), to the importance of the engineering works (dams, grouting, etc) and to the standpoint of the designer as to the desirability or otherwise of having hydraulic fracture induced (oil industry or civil engineering). For soil deposits where water levels coincide with ground surfaces and initial vertical effective stresses approximately equal initial pore pressures, the proposed rules put in terms of the ratio $(\Delta u)_a / \sigma_{z_o}'$, between the allowable excess hydraulic pressure and the initial vertical effective stress, lie within the wide range limited by the values 1.0 and 6.0, a range which certainly includes figures which are too optimistic for a great variety of soils.

An exception to the high allowable ratios quoted above is found in a paper by HUBBERT and WILLIS (1957), analysing conditions of incipient normal faulting such as may exist in parts of the Gulf Coast of America. It was found that for saturated strata where $K_o' = 1/3$ a ratio $(\Delta u)_a / \sigma_{z_o}'$ equal to 1/3 may initiate fracture, whereas in masses where $K_o' > 1$ the allowable ratio rises to 1.

8.2.2 Recent Evidences of Hydraulic Fracture in Soils

In recent years, leakage of two newly built embankment dams during the first impounding have been attributed to cracking resulting from hydraulic fracture in the clay core, induced by the increasing reservoir water pressure on a zone where arching might have caused reduction in vertical stresses: Hyttejuvet Dam (KJAERNSLI and TORBLAA, 1968) and Balderhead Dam (VAUGHAN *et al*,

1970; VAUGHAN, 1970).

Another recent reported field case of hydraulic fracturing refers to in-situ permeability tests on piezometers installed in the impervious core of a dyke at the Dead Sea in Israel (BJERRUM et al, 1972). More than 1000 constant head tests carried out with excess head ratios $\Delta u / \sigma_{z_o}'$ just below one led to consistent calculated permeabilities of the order of 10^{-6} m/sec, whereas tests in which lower ratios were used (0.5 or less) gave place to values of k roughly 1000 times less. Analogous behaviour was found in similar tests at Fornebu, Oslo, in a natural deposit of normally consolidated clay, under conditions where the possibility of arching effects was non-existent (BJERRUM et al, 1972); in this example, the large 'jump' in apparent permeabilities, also from 10^{-9} to 10^{-6} m/sec, occurred between ratios of 0.8 and 1.1.

As part of a laboratory investigation at King's College, London (KENNARD, 1970), fracture was imposed to saturated masses of remoulded brickearth by carrying out constant head tests, at various ratios $\Delta u / \sigma_{z_o}'$, on piezometers embedded in the sample. There was considerable scatter in the results, but the ratio $\Delta u / \sigma_{z_o}'$ was consistently above the unity, even though the ratio K' between horizontal and vertical effective stresses was only 0.4. Two aspects of those tests were particularly noteworthy. Firstly, observed vertical fracture planes, corresponding to the direction of minimum stresses, only developed after effective stresses were negative, both in horizontal and vertical directions, tensile stresses of

50 kN/m^2 or more having been withstood by the samples. Secondly, in short duration tests, where conditions were closer to undrained loading, ratios $\Delta u / \sigma_{z_o}'$ were higher than in tests approaching full drainage, suggesting that soil masses can sustain high hydraulic pressures for a short period without cracking and that significant time effects may affect the fracture mechanisms.

8.3 THE USE OF HYDRAULIC FRACTURE IN ASSESSING STRESSES IN SOIL MEDIA

8.3.1 Saturated Masses

The use of hydraulic fracturing as a means of assessing horizontal stresses in the ground was pioneered in the Rock Mechanics world (see, for instance, KEHLE, 1964; FAIRHURST, 1964. HAIMSON, 1968, and HAIMSON and FAIRHURST, 1970).

In Soil Mechanics, the first attempt to determine K_o' in natural deposits by hydraulic fracture tests was performed on a saturated mass of soft normally consolidated marine clay in Southern Norway (BJERRUM and ANDERSEN, 1972). It was found then that the influence of the soil tensile strength, of stress changes induced during testing and of inevitable disturbance due to piezometer installation, made impossible estimation of minimum stress from the excess heads causing sudden increase in inflow during permeability tests. It was advocated instead that the least total stress is more reliably evaluated by assuming it to equal the excess head capable of reversing the inflow to values around those observed prior to crack format-

ion. Accordingly, a test technique was developed whereby hydraulic pressures were first increased until crack formation was evident and then allowed to drop to values where 'close up' was attained. The knowledge of minimum total stresses and pore pressures enables K_o' to be determined in the case of deposits exhibiting K_o' below unity. For heavily, overconsolidated materials, exhibiting $K_o' > 1$, minimum stresses equal overburden pressures and the cracking plane is expected to be horizontal.

8.3.2 Partly Saturated Soils

A type of test similar to that described by BJERRUM and ANDERSEN, (1972) has been used in the United Kingdom to examine in-situ stresses in partly saturated clay cores of embankment dams (VAUGHAN, 1972; PENMAN, 1972).

At Balderhead Dam (VAUGHAN et al, 1970), measurements of flow were made for each step of a series of increasing constant head in-situ permeability tests on borehole piezometers as well as on twin-tube piezometers. When inflow suddenly increased by some orders of magnitude, fracture was assumed to have occurred and a falling head test immediately followed. The pressures at which sudden inflow changes occurred as heads were raised were named 'fracture pressures' and those which reversed the previous situation, during falling head tests, were called 'close up pressures'. While a large scatter in fracture pressures was observed (in some tests they were not even reached despite pressures greater than overburden pressures), 'close-up' stresses showed a much more consistent trend,

ratios u_{cl}/σ_{z_o} between 'close-up pressures' and total overburden pressures, at piezometer tips, varying from 0.38 to 0.89 (average 0.58).

At Cow Green Dam (VAUGHAN, 1972), 'closing up' of cracks were achieved either by steps of constant head tests or by falling head tests, no variation having been found in 'close up' pressures, which showed consistency with the likely minor stresses in the core.

Comparisons of results of fracture tests with values of major, intermediate and minor stresses recorded by means of load cells (PENMAN, 1972) showed that 'close up' pressures were closer to mean stresses rather than to the minor ones.

Evidences of fracture planes being nearly vertical in dam cores (where minor stresses are actually expected to act in horizontal across-the-axis direction) were found at Balderhead Dam.

Constant head permeability tests, performed at Cow Green Dam before and after fracture tests had been carried out, did not appear to reveal any important influence on the coefficient of permeability.

At Balderhead Dam, although no direct evidence of delayed fracture was found, this is thought to have occurred in some of the tests.

8.4 SOME THEORETICAL CONSIDERATIONS ABOUT HYDRAULIC FRACTURE

8.4.1 Drainage Impeded

Analyses by KENNARD (1970) distinguished between 'blow off' pressures and fracture pressures, the former corresponding to a situation where the soil is pushed away from the piezometer and the latter representing the pressure at which the mass cracks following a plane perpendicular to the direction of the minor principal stress.

Ignoring any possibility of tensile stresses being sustained by the soil or at the soil-piezometer interface, Kennard found the 'blow-off' pressure to be governed by the equation:

$$(u_b - u_o) = K'_o \sigma'_{z_o} \qquad (8.10)$$

where K'_o is not necessarily the coefficient of earth pressure at rest of the undisturbed medium, as borehole drilling or pushing of piezometer into the ground during installation may lower or raise horizontal stresses and make them different in radial and tangential directions.

As for the fracture pressure, the same Author derived an equation that, for the case of an infinite mass, reduces to

$$(u_f - u_o) = K'_o \sigma'_{z_o} \left(1 + \frac{1}{2A}\right) \qquad (8.11)$$

where A is Skempton's pore pressure parameter.

A simple elastic analysis can be made by assuming the piezometer to be a continuous infinite cylindrical cavity and

applying the equations for stresses developed in a thick-walled cylinder subject to internal pressure. Assuming no vertical restraint, the expressions for incremental stresses (plane stress conditions) are:

$$\Delta\sigma_z = 0 \tag{8.12}$$

$$\Delta\sigma_r = -\Delta\sigma_\theta = \frac{(u - u_o)\, a^2}{r^2} \tag{8.13}$$

$$(\Delta u)_u = \frac{\Delta\sigma_z + \Delta\sigma_r + \Delta\sigma_\theta}{3} = 0 \tag{8.14}$$

where $\Delta\sigma_z$, $\Delta\sigma_r$, and $\Delta\sigma_\theta$ are the vertical, radial and circumferencial components of incremental total stresses developed in the mass, under undrained conditions, as a consequence of the excess head $(u - u_o)$ inside the piezometer, a is the radius of the cylindrical piezometer, r is radial distance from the piezometer axis and $(\Delta u)_u$ is the pore pressure increment in the mass due to undrained loading.

If 'blow off' occurs as the radial effective stress vanishes at r = a and fracture takes place as the minimum tangential effective stress also equals zero, the resulting equations are:

$$\sigma_\theta' = K_o' \sigma_{z_o}' + \Delta\sigma_\theta - (\Delta u)_u = K_o' \sigma_{z_o}' - (u_f - u_o) = 0 \tag{8.15}$$

and

$$(u_f - u_o) = K_o' \sigma_{z_o}' = (u_b - u_o) \tag{8.16}$$

BJERRUM et al (1972) also presented an analysis for hydraulic fracture under undrained conditions, including in it the effects on initial horizontal stresses induced by the driving of a piezometer into the ground. Horizontal stresses, initially axi-symmetric and equal to $K_o' \sigma_{z_o}'$, are assumed to become $(1 + \beta) K_o' \sigma_{z_o}'$ in the radial direction and $(1 - \alpha) K_o' \sigma_{z_o}'$ in the circumferencial one. For an infinite mass of saturated, homogeneous, isotropic soil, the resulting equations are:

$$\frac{(\Delta u)_b}{\sigma_{z_o}'} = (1 + \beta) K_o' \qquad (8.18)$$

and

$$\frac{(\Delta u)_f}{\sigma_{z_o}'} = \left(\frac{1}{\nu'} - 1\right)\left[(1-\alpha) K_o' + \frac{\sigma_t'}{\sigma_{z_o}'}\right] \qquad (8.19)$$

where $(\Delta u)_b$ and $(\Delta u)_f$ are excess heads at conditions of, respectively, 'blow off' and fracture, ν' is the Poisson's ratio of the soil skeleton, σ_t' is the tensile strength of the material, K_o' is the coefficient of earth pressure at rest in terms of effective stresses, σ_{z_o}' is the vertical effective stress, and α and β have been defined in the previous paragraph.

Equation (8.19) has been derived as though the fracture pressure preceded the 'blow off' one. If the opposite is true,

$$\frac{(\Delta u)_f}{\sigma_{z_o}'} = (1 - \nu')\left[(2 + \beta - \alpha) K_o' + \frac{\sigma_t'}{\sigma_{z_o}'}\right] \qquad (8.20)$$

A brief examination of expressions (8.10), (8.11), (8.16), (8.18), (8.19) and (8.20) is now made for the case of elastic soil with no disturbance in piezometer installation, $\sigma_{z_o} = 2u_o = 2\,\sigma'_{z_o}$, and $\sigma'_t = 0$.

The three analyses mentioned result in the same value of 'blow off' pressure for this case. The equations give directly the coefficient of earth pressure at rest and it would be the most convenient way of assessing K'_o if soil disturbance during installation and tensile strength at the interface were insignificant or could be accurately quantified.

The equations for fracture pressure show different results. Equation (8.11), due to Kennard, leads to $\Delta u/\,\sigma'_{z_o} = 2\,K'_o$ for A = 0.5, which makes the limit of $\Delta u/\,\sigma'_{z_o} = 1$, corresponding to horizontal fracture, to be attained first for all values of K'_o above 0.5, which does not seem to be backed by experimental evidence. Equation (8.19) also leads to high values of $\Delta u/\,\sigma'_{z_o}$, between 1.5 and 3.0 times K'_o for ν' ranging from 0.25 to 0.40; it is not applicable, however, where 'blow-off' precedes fracture, and this seems to be always the case in ideal installation (no soil disturbance). Equation (8.20) is less affected by ν' values and $\Delta u/\,\sigma'_{z_o}$ ranges from 1.2 to 1.5 K'_o for ν' varying between 0.25 and 0.40. Equation (8.16) results in $\Delta u/\,\sigma'_{z_o} = K'_o$, the same ratio for 'blow off'.

All analyses above mentioned and briefly summarized ignore the effects of plastic yield around the borehole before fracture, as pointed out by VAUGHAN (1971).

GIBSON and ANDERSON (1961), studying the pressuremeter tests, presented the following expressions for an elastic-plastic material:

a) initiation of plasticity

$$\frac{(\Delta u)_{pl}}{\sigma'_{z_o}} = K'_o + \frac{c_u}{\sigma'_{z_o}} \qquad (8.21)$$

b) indefinite expansion of the cylindrical cavity

$$\frac{(\Delta u)_{exp}}{\sigma'_{z_o}} = K'_o + \frac{c_u}{\sigma'_{z_o}}\left[1 + 2.3 \log_{10}\left(\frac{1}{2(1+\nu)} \cdot \frac{E}{c_u}\right)\right] \qquad (8.22)$$

where $(\Delta u)_{pl}$ and $(\Delta u)_{exp}$ are the excess pressures necessary to cause yield to a material characterized by the Young's Modulus E and the Poisson's ratio ν in the elastic phase and by an ultimate strength c_u.

For $\nu = 0.5$ and E/c_u ranging from 100 to 500, equation (8.22) becomes:

$$\frac{(\Delta u)_{exp}}{\sigma'_{z_o}} = K'_o + (3.5 \text{ to } 5.1)\frac{c_u}{\sigma'_{z_o}} \qquad (8.23)$$

LADANYI (1963) compares the pressure necessary to expand a spherical cavity at depth with the bearing capacity of a pile point and presents the equation:

$$\frac{(\Delta u)_{exp}}{\sigma'_{z_o}} = K'_o + N_c \frac{c_u}{\sigma'_{z_o}} \qquad (8.24)$$

where N_c is the bearing capacity factor, of the order of 9 for a spherical cavity and 7 for a cylindrical one.

The right hand sides of formulae (8.21) through (8.24) give values between 1 and 9 times c_u/σ'_z to be added to K'_o. At reasonable depths, c_u/σ'_z varies between 0.1 and 1.0 for most clayey soils and these values result in ratios $\Delta u/\sigma'_{z_o}$ greater than those predicted in elastic analyses. This is an indication that plastic yield may raise the allowable excess head to be applied to undrained saturated soil masses. The above analyses assume uniform stresses and symetrical behaviour. In practice, local unevenesses or corners in piezometer sand pockets and piezometers may cause stress concentrations which influence the initiation of fracture and 'blow off'.

Theoretical analyses and numerical applications provide a useful framework within which predictions can be reasonably made for lower bounds of excess heads capable of causing hydraulic fracture during, for example, in-situ permeability tests, grout injections or the filling of a reservoir. However, approximations involved in the analyses and major uncertainties concerning soil parameters, such as E, ν', A, σ'_t, c_u, etc, make the prospects of using cavity expansion or opening of cracks as a means of assessing in-situ stresses quite doubtful in the present state of knowledge.

Although not interfering directly with the determination of stress, it is a matter for speculation whether a vertical crack in a soil of $K'_o < 1$ propagates upwards or downwards. Clarification of this point might help in interpretation of test results where the piezometer tip is located near the boundary of

another material possessing different properties.

The gradient of water pressure along a vertical crack with zero flow is given by

$$\frac{du}{dz} = \gamma_w \tag{8.25}$$

whereas the gradient of the horizontal total stress, in a saturated mass, is expressed by

$$\frac{d\sigma_x}{dz} = K_o' \gamma' + \gamma_w \tag{8.26}$$

Crack propagation can only take place if

$$\frac{du}{dz} = \gamma_w > \frac{d\sigma_x}{dz} = K_o' \gamma' + \gamma_w \tag{8.27}$$

Equation (8.27) holds for any values of K_o', and γ', for negative values of z. That is, cracks should propagate upwards in saturated masses.

In fills and other partly saturated masses, analysis is more conveniently expressed in terms of coefficients of earth pressure for total stresses, K_o, and in this case, (8.26) becomes

$$\frac{d\sigma_x}{dz} = K_o \gamma \tag{8.28}$$

Fracture will propagate downwards if

$$\gamma_w > K_o \gamma \tag{8.29}$$

For the case of $\gamma = 2\gamma_w$, crack will propagate downwardly if $K_o < 0.5$ and upwardly if $K_o > 0.5$.

In the face of the difficulties in correctly relating the 'blow off' and the fracture pressures to the initial stresses in the ground, it has been advocated (BJERRUM and ANDERSEN, 1972; VAUGHAN, 1972) that the hydraulic pressure at which a pre-open crack closes again provides a more accurate measurement of the disturbed zone around the piezometer tip. This method, an extension to soils of a technique proposed for rocks by HAIMSON (1968), is based on a number of assumptions of which the most important, as emphasized by VAUGHAN (1971), are:

a) the crack propagates along the place upon which the minor principal stress acts;

b) the occurrence of fracture does not change the total stress across it, and

c) the properties of the surrounding soil are not strongly time dependent.

8.4.2 Full Drainage

Investigating the case whereby 'blow off' and cracking occur when the soil surrounding the piezometer tip is in a fully drained condition, KENNARD (1970) derived the following expressions for an infinite cylindrical rigid piezometer of radius a installed in a much larger saturated mass of homogeneous isotropic soil where initial vertical and horizontal effective stresses were,

respectively, σ_{z_o}' and $K_o' \sigma_{z_o}'$:

$$\frac{(\Delta u)_b}{\sigma_{z_o}'} = K_o' \qquad (8.30)$$

$$\frac{(\Delta u)_f}{\sigma_{z_o}'} = \frac{2K_o'}{1+\nu'} \qquad (8.31)$$

Equation (8.31) refers to vertical cracking. If the limit established by $(\Delta u)_f = \sigma_{z_o}'$ is attained first, horizontal fracture is expected to occur.

Both (8.30) and (8.31) were derived on the basis of a complete freedom of soil movement in the vertical direction (place stress), no tensile strength in the soil or on the soil/piezometer interface and radial drainage. The analysis did not take into account the possible development of plastic yield and, at the moment, there is not any available analysis by which these effects may be estimated for conditions of full drainage.

For $\nu' = 0.25$ to 0.40, (8.31) becomes

$$\frac{(\Delta u)_f}{\sigma_{z_o}'} = (1.25 \text{ to } 1.43)\, K_o' \qquad (8.32)$$

Above values are of the same order of those found for the undrained case by BJERRUM et al (1972) and are lower than those obtained by Kennard himself in his analysis for hydraulic fracture with drainage prevented. This means that there is the possibility of long term development of hydraulic fracture at excess heads unable to crack the soil in undrained conditions. Such a

theoretical finding was confirmed in laboratory experiements carried out by Kennard. No field definitive evidence of delayed hydraulic fracture has as yet been obtained, but this is thought to have occurred in some of the tests at Balderhead Dam (VAUGHAN, 1971).

8.5 HYDRAULIC FRACTURE TESTS AT THE EMPINGHAM TRIAL BANK

8.5.1 Main Objectives

Despite the shortage of time, equipment and personnel, attempts were made to clarify some uncertainties concerning the performance of hydraulic fracture tests on twin-tube hydraulic piezometers embedded in partly saturated fills, as was the case with the Empingham Trial Bank.

It was hoped that this work would provide answers to the following questions:

a) Was there a repeatable 'blow-off' pressure?

b) Was there a repeatable fracturing pressure?

c) Having achieved the 'blow-off' pressure, was it possible to identify, in a falling head test, a 'shut in' pressure?

d) Having achieved fracturing of the ground, was it possible to have the crack 'closed up' at a well defined pressure?

e) Was it possible to relate in any way one of above pressures ('blow-off', 'shut in', cracking or 'close up') to total stresses in the fill so that the thrust exerted by centre of the main embankments upon the berms could be more accurately predicted?

f) Was it possible to establish a lower limit hydraulic pressure, under undrained conditions, below which hydraulic fracture was not to be feared?

g) Was 'blow-off' of soil around piezometer reflected in any apparent increase in overall permeability?

h) Was there any increase in the apparent bulk permeability of the ground after fracturing had been achieved, indicating that the crack might have not closed up completely?

Some of these questions were successfully answered in the course of the trial bank experiment, whereas others could not be conveniently tackled owing to insufficiency or inadequacy of the equipment or to the already mentioned shortage of time and personnel available.

8.5.2 'Blow-off' and Fracturing Pressures

Figures 8.1 through 8.3 depict flows obtained in constant head tests on piezometers P1B, P2B and P3B plotted against ratios $u/\gamma.h$. It is seen in all three drawings that, in the range of $u/\gamma.h$ between 0.6 and 0.8, there was a sudden increase in the flow, indicating an apparent rise in permeability or, more probably, the formation of a cavity around the piezometer. The flow of too much water into the fill was in general feared as it might cause irreversible damage to the soil structure and, therefore, tests were discontinued after proportionally high flows were measured over a short period (0.5 to 1.5 min.). In one test, however, carried out on P1B at a

ratio u/ γ.h = 0.83, the inflow was kept for 10 minutes and the flow was seen to decrease from 68 mm^3/sec in the first 30 seconds to 15 mm^3/sec at the 10th minute. At the same test, but at the considerably higher ratio of 1.30, the flow dropped from 30 mm^3/sec, average over the 1st. minute, to 2 mm^3/sec over the fourth. This demonstrated that despite the sudden increase in flow, there was no continuous expansion of the cavity and, therefore, 'blow-off' had not been followed by fracturing of the ground.

The safe capacity of the portable deairing unit used to increase pressures only allowed high ratios u/ γ.h on piezometer P1B, where the overburden pressure was least. Constant head tests were accordingly carried out on P1B at ratios of up to 1.7 and their results are shown in figure 8.1. Flows nearing 500 mm^3/sec were attained and they did not appear to decrease over the period of observation (1.5 to 4 minutes), indicating a continuous expansion of a cavity or, most probably, the propagation of a crack, which appears from the drawing to have been formed at about u/ γ.h = 1.4.

8.5.3 'Shut in' Pressures

'Blow-off' consistently occurred at ratios u/ γ.h between 0.6 and 0.8 for three different piezometers. Falling head tests invariably followed 'blow-off', starting from higher ratios, and the measured flows at each ratio u/ γ.h in this stage are seen in figures 8.3 to 8.6. In most of the graphs the flow neared zero at ratios of 0.7-0.8 at P1B, 0.5-0.6 at P2B, 0.5-0.6 at P3B and

0.45-0.55 at P4B.

Some tests, however, departed from above values and in none of them was a sudden decrease of flow or the occurrence of outflow, which would indicate an instant return of expanded cavities to their previous boundaries, adjacent to piezometer tips. It is thought that either the ground did not return to its initial position or it did in a slow manner, difficult to identify in the falling head tests carried out.

8.5.4 'Close up' Pressures

The mercury manometer available for the falling head tests was not long enough to allow tests to start from ratios $u/\gamma.h$ above 1.5 in the case of P1B, 1.3 for P3B and lower values for the other two piezometers.

In addition to this difficulty, it appears that once fracturing was first achieved some damage, either permanent or of long duration, was caused to the fill and 'closing up' of cracks were not successfully achieved. If these findings, based so far on limited evidence, are confirmed by further observations, the usefulness of the hydraulic fracture test with relation to the monitoring of stresses in fills of dry compacted clay as that of the Empingham Trial Bank will be seriously questioned.

8.5.5 Variation of Apparent Permeability

Figure 8.7 shows the values of the apparent fill permeability as measured during several hydraulic fracture tests.

They were calculated as though the intake factor F after 30 minutes of test equalled that corresponding to steady state. Formulae for constant head tests were used and this is thought not to have introduced any important error, as heads were varying quite slowly and the shape factor was very small.

Results of tests on P2B and P4B agree quite well, showing a gentle decrease of permeability with time (and height of fill) from 8×10^{-11} m/sec to 2×10^{-11} m/sec. This decrease was to be expected in the face of the increase in effective stresses and the reduction in porosity. Values found must be regarded as upper limits for the real overall permeability, as the ratios q/h from which they were calculated were still decreasing.

The two initial tests on P1B resulted in an apparent permeability of 3×10^{-11} m/sec. After fracturing was induced on the afternoon of 7-9-72, however, the next test, on 20-10-72, showed a value about 10 times greater, just below 30×10^{-11} m/sec. Subsequent tests revealed a decrease in such figures to around 11×10^{-11} m/sec, still much higher than initially observed. Whether this was due to a partial 'close up' of the fracture or to a real decrease in the ground permeability is difficult to clarify completely, but judging from the decrease observed for P2B it is believed that both things happened. The partial 'close up' of fractures is likely to have been facilitated by movement experienced by the fill as placing of material and compaction went on, or swelling of the fill.

Tests on P3B started from high apparent permeabilities, around 50 x 10^{-11} m/sec, decreasing to values between 10 and 14 x 10^{-11} m/sec after bank completion. No fracturing during the first tests was demonstrated but this might have been the case, as an initial ratio u/γ.h of over 1.3 was used (figure 8.3). If it was so, the abnormal results of tests number 1, 2 and 3 (figure 8.3) seem to indicate that no 'close up' occurred and a much increased intake factor led to high flows and a sluggish decrease, even at low ratios u/ γ.h. Tests 4 and 5 showed a more usual behaviour but there is no evidences of cracks having been reopened or closed up. Exceptionally high flows during constant head tests on 21-9-72 (figure 8.3) appear to be a consequence of a fracture which was still open, but the sudden increase at ratios u/ γ.h around 0.9 appear to be a sign of 'blow-off' superimposed to an open crack. This movement might have contributed to a further partial decrease in the extent of the fracture in a more pronounced fashion than observed at P1B; this possibility arises from the greater reduction in apparent permeability shown in figure 8.7.

If the increases in apparent permeability observed in tests on P1B were due to changes in the intake factor induced by ground fracturing and not by propagation of the cracks during the phases of the tests when flows were measured, the final shape factor was, at least, five times greater. The amount of water forced into the ground during the constant head tests was 318 cm^3, two to three times the piezometer tip volume, and this volume might well correspond

to a shape factor 5 to 10 times greater if the cavity created was thin and large in area.

Measurements of permeability based on flow measured after 9 minutes were made for various ratios $u/\gamma.h$ on P1B on 6 and 7-11-72. Calculations, made as though the shape factor after 9 minutes of test equalled that of steady state, resulted in upper limits for permeability between 0.8 and 1.4 x 10^{-10} m/sec for $u/\gamma.h$ ranging from 0.7 to 1.2 (below 'blow-off'). This means an increase in intake factor to 1.5 to 2.5 times its previous value. Assuming that the expanded cavity retained the original length, an increase in radius of 20 to 30 mm would multiply the initial intake factor by 1.45 to 1.75, an increase similar to the rise observed in apparent permeability.

8.5.6 Summary of the Results Obtained

The results obtained through the attempts to fracture the embankment fill are summarized as follows:

a) 'blow-off' appears to have occurred at ratios $u/\gamma.h$ around 0.7, even on piezometers previously already 'blown off' several times. On basis of analyses by KENNARD (1970) and BJERRUM et al (1972), for zero tensile strength at the soil/piezometer interface, this would mean that munimum stresses at the disturbed region around the piezometer tip equalled 0.7 times the overburden pressure from the beginning to the end of construction.

b) fracture seems to have taken place at ratios

$u/\gamma.h$ of approximately 1.4.

c) 'close up' of fracture was not achieved and irreversible fill fracturing increased the intake factor of the piezometer about 10 times.

d) there appears to have occurred some partial closing up of the cracks with continuation of the embankment construction but, at the end, the intake factor was still 5 times greater than initially.

e) the expanded cavity due to 'blow-off' appears not to have returned to its original position or, more probably, to have done it slowly.

f) the coefficient of permeability of the intact fill at the end of construction was of the order of 1×10^{-11} m/sec.

g) during the field experiment, there was no check as to whether one of the measured pressures ('blow-off', 'shut in', fracture or 'close up') actually corresponded to minimum stresses in the ground. Such a check is more likely to be achieved in laboratory research, although scaling effects and difficulties concerning the measurement of small flows may cause some problems, both experimental and analytical.

h) to the best of the Author's knowledge, the hydraulic fracture tests at Empingham represented the first attempt so far made on dry fill, of low degree of saturation, exhibiting negative pore pressures, capable of swelling considerably when wetted during the tests, and the doubts expressed in this chapter as to whether

hydraulic fracture may be successfully employed to determine in-situ stresses does not necessarily apply to other type of soils. It must be noted that at Cow Green Dam and Balderhead Dam, the fill consisted of boulder clay, a soil of low swelling characteristics, where high degrees of saturation and high pore pressures had been measured; at both embankments, hydraulic fracture tests presented considerably more encouraging results than at Empingham.

C H A P T E R _ N I N E

CONCLUSIONS AND RECOMMENDATIONS

9.1 General

9.2 Performance of the Instrumentation

9.2.1 Horizontal movements

9.2.2 Vertical movements

9.2.3 Pore pressures

9.3 Properties of the Brecciated Upper Lias Clay

9.4 Hydraulic Fracture Tests

9.5 Suggestion of Further Work

9.5.1 Instrumentation

9.5.2 Soil properties

9.5.3 Hydraulic fracture

C H A P T E R _ N I N E

CONCLUSIONS AND RECOMMENDATIONS

9.1 GENERAL

The research consisted primarily of the observation of the trial bank performance and of the instrumentation installed in it. Analyses of the data were carried out, including some newly proposed approximate methods of interpreting horizontal movements and predicting initial stresses in the ground. In-situ permeability tests were performed and various attempts were made to induce fracturing in the fill and to relate the pressures which caused 'blow-off', cracking or 'closing up' of fractures to stresses in the soil mass.

It was a diversified work, covering a wide area of various disciplines as Soil Mechanics, Dam Engineering and Field Instrumentation. The number of conclusions, of varied importance, had thus necessarily to be large; many have already been mentioned throughout this thesis, but the most relevant of them are summarized in following sections.

This chapter also presents some suggestions of theoretical and experimental work which would be useful in clarifying uncertainties still remaining after the research carried out and in widening the findings herein described.

9.2 PERFORMANCE OF THE INSTRUMENTATION

9.2.1 Horizontal Movements

A careful examination was made of measurements carried out by means of a Wilson Slope Indicator series B-200, a system of wire extensometers and a Telluromerer MA-100, and the following conclusions have arisen from such a study:

a) In the face of the amount of horizontal displacements involved and of the approximations characterizing the control of levels, the operation procedures adopted could not ensure that the torpedo was precisely positioned at the same points of the inclinometer wells every time a set of readings was to be taken. Nevertheless, as individual lengths remained approximately straight for average tilting angles of less than 1^{o}, this technique proved not to introduce any relevant error. The repeatability of measurements achieved was of such order that, for the time interval when the inclinometer tubes remained practically stationary, the maximum deviation with respect to the mean value was kept below 5 mm and the curves of variation of maximum deviation with depth approximately coincided with that established by CORNFORTH (1973); this represents a far better precision than stated in the maker's literature, particularly at high elevations.

b) Out of more than 50 sets of readings, three gave discrepant results when compared with the data obtained from the other measurements. Analysis of their statistical distribution provided some numerical bases for discarding suspicious measurements. The rules established were: (i) the sum of opposing readings should

sum up less than 1000 units (for the particular apparatus used), (ii) the standard deviation of face errors along the total inclinometer height had to be less than 3 dial units (7.5×10^{-4} rd), and (iii) the central most frequent classes (in dial units) of the face error histograms should include, at least, 65% of the readings.

c) Clearly, absurd readings occurred at times, preceding or following the three wrong sets mentioned above. They have been attributed to ingress of moisture in the pendulum chamber due to insufficient tightening of the top nut. Leaving the torpedo open overnight in a warm atmosphere reestablished the normal behaviour.

d) At moderate changes in inclinometer inclination (less than 1°), individual casing lengths remained straight, fluctuation of tilting angles within them not exceeding a few tenths of a degree. For average incremental inclinations of the order of 2° or more, variations in tilting angles become important (at Empingham, they reached values of up to 5° in a single length). In this case, misplacing of the torpedo may introduce great errors. At Empingham, for a maximum of 5° in angle fluctuation within a casing length and a maximum of 50 mm error in positioning the torpedo, the resulting error in horizontal displacement is kept below 5 mm. In the fill where the material was more compressible, greater differences in level of the readings might occur, although compensated by much smaller angle fluctuations; the criterion adopted of adding 'fictitious' reading every time shortening of the length exceeded 300 mm limited the maximum error due to torpedo misplacing to 5 mm, both in the fill

and in the foundation.

e) The overall precision of inclinometer measurements was therefore of ± 10 mm, corresponding to 1% to 2% of the total observed horizontal displacements.

f) Beyond average tilting angles of 4^{o} or 5^{o}, inclinometer tubes became so distorted that the torpedo could not reach the bottom. The tubes did not shear however, and, up to the end of the experiment, inclinometer bases could be plumbed with the bare settlement probe.

g) The relative stiffness of casings and grout columns probably contribute to smoothing recorded profiles and underestimating shear strains. The effects on the magnitude of displacement however, appears to be small, on the evidences obtained by comparing movements measured by means of inclinometers, rod gauges and EDM survey.

h) Errors in measurements with wire extensometers due to initial adjustment of plates in the sand trench and straightening of wires within the pipes and of the pipes thenselves reached up to 60 mm at Empingham.

i) Fluctuation of rod gauge readings taken in the morning and in the afternoon were of the order of ± 10 mm, mainly due to temperature effect. If morning measurements only were considered, variations dropped to ± 3 mm.

j) At the time the trial bank was around 14 m

high and the horizontal displacements was approximately 200 mm at the toe, a kink in the rod gauge pipes started to develop in the region near the bank toe where, afterwards, an excavation was made and a shear plane exposed. Although measured displacements then became totally wrong,average strains were still approximately correct, an evidence that wires could slide more or less freely inside the pipes, despite the kink.

k) In spite of the respective measuring points not coinciding exactly, comparison between rod gauge and inclinometer records show a reasonably good agreement, differences between them never exceeding 40 mm, or about 5% of the final movement. Similar comparisons between rod gauges and EDM surveys resulted in differences of 30 to 70 mm, 5% to 10% of final displacements.

l) EDM surveys initially gave discrepant results, but after the number of reflecting prisms was reduced, accuracy was much improved, matching those of inclinometers and rod gauges.

9.2.2 Vertical Movements

Vertical movement measurements proved not to have been as reliable as the horizontal ones, owing to some problems summarized below:

a) Greater stiffness of the grout columns surrounding inclinometer ducts and possible consolidation of lower layers of the clay foundation into the Marlstone, may have caused punching into the fill by foundation inclinometer tubes. This led to underestimated measured settlements in the foundation and exaggeration of vertical

strains in the lower parts of the fill.

b) In the fill, the compressibility of the dry sand used around inclinometer pipes was greater than that of the compacted soil and this resulted in overestimated observed settlements.

c) Operation of the hydraulic settlement gauge was cumbersome, time-consuming and demanded too great a labour force. Problems associated with air in the water line, temperature effects and defective pressure transducer made its records not very reliable. The system appears to be rather inappropiate for the size of the trial bank and the amount of movement involved.

d) Despite the shortcomings of both systems used in measuring vertical movements, they successfully recorded the sharp variation in settlement near the toe and the occurrence of heave close to the junction of the slope with the ground, facts confirmed by conventional levelling.

9.2.3 Pore Pressures

Twin-tube hydraulic piezometers, with either coarse tips or high air-entry-value ones worked in general properly. One of the coarse tip piezometers, however, although located 8 metres below ground surface, showed too low pore pressure response from a certain day; de-airing after the end of construction resulted in a rise in pore pressure of nearly 10 metres.

Unexpectedly, fill piezometers recorded pressures below atmosphere through out the experiment, but this is thought to

have faithfully portrayed the fill behaviour, as all four piezometers behaved accordingly and laboratory undrained tests on samples taken from the fill gave very high strength, as would be predicted for specimens exhibiting high initial effective stresses.

9.3 PROPERTIES OF THE BRECCIATED UPPER LIAS CLAY

Based on trial bank measurements and some other laboratory field testing, simple analyses were carried out, leading to estimates of the overall properties of the brecciated Upper Lias Clay presented below:

a) Back analyses of the trial bank utilizing conventional limit equilibrium techniques resulted in a bulk undrained strength around 20-25 kN/m^2 at the top of the foundation, and a gain with depth of 2.5 to 3.0 kN/m^3. This gives an average of about 40 kN/m^2 for the upper 10 to 15 m of the foundation. Back analyses of several failed provisional cuts in the borrow pits resulted in an average c_u of 50 kN/m^2, roughly 25% higher therefore. The lower limit of all laboratory and field tests gave a straight line defined by $c_u(kN/m^2) = 35 + 3.5\ z(m)$, corresponding to about 60 kN/m^2 for the upper 10-15 metres. The average lines of laboratory tests and plate tests were considerably higher, resulting in c_u of the order of 80 kN/m^2 or more for the upper 10 metres, but it must be noted that rapid rates of strain were employed in such tests and that no correction for rate of loading was applied in calculations. This comparison shows that lower limits of laboratory tests results should be used in design

and that even they might be slightly on the unsafe side. Plate tests also failed in correctly predicting the reliable undrained strength of the foundation, even when lower limits were selected, and these results too might reflect the influence of the rapid rate of loading, size effects and anisotropy. Discrepancy between back analyses of the failed cuts and the trial bank may be explained by anisotropy effects combined with difference in shape of slip surfaces, or by variation in degree of brecciation between the region the trial bank was built on and the borrow areas.

b) Back analyses in terms of effective stresses were not so accurate owing to the variety of factors involved. Use of average measurements from the trial bank led to an angle of shearing resistance of 18° for a cohesion intercept $c' = 0$. This roughly corresponds to the lower limit of laboratory tests, the results of triaxial tests on pre-cut specimens and the back analysis of Hollowell Dam.

c) Theoretical analysis based on the gain in undrained strength with depth resulted in a coefficient of earth pressure at rest around 0.7, a much lower value than expected for an overconsolidated material, subjected in the geological past to an overburden in excess of 1000 metres. This is probably a consequence of the same causes that led to brecciation of the soil: superficial geological structures (cambering, valley bulging, etc), weathering and the like. From pore pressure observation, assuming that active state developed at the locations of the piezometers and that parameter A was that of elastic materials, an average K'_o of 1.36 was found. This

disagrees with previous figure of 0.7 but is still well below values found for other overconsolidated clays.

d) High shear strains were observed since early stages of the trial bank construction and they eventually reached values over 10%. Nevertheless, there was no evidence of significant displacement along shear discontinuities, which seems to indicate that progressive failure is not important in such a material, for the amount of displacements involved (between 500 and 1000 mm at the toe).

e) Considerable undrained creep was measured after banking completion, increasing strains at the end of construction by between 40% and 70% in the central regions of the foundation and of the fill. Rates of creep movement, $d\epsilon_1/d(\log_{10}t)$, were of the order of 0.005 to 0.010.

f) Average pore pressure ratio r_u in the foundation was, for the amount of displacements involved, around one-third less than that predicted for K_o-conditions. In the fill, it was always found to be negative. Parameter B was found to be approximately one, $\bar{B}$ averaged 0.75 and Henkel's parameter a was around zero (elastic).

g) Horizontal strains, measured by means of wire extensometers, developed in a 'ripple' fashion. Each section experienced most of its final strains at the time the slope was being built above it. A simple approximate analysis was devised in such a way that isotropic elasticity was used to relate these horizontal strains to decreases in coefficients of lateral stresses in the fill and deformation parameters. Numerical application of this analysis to the instrumented sections of the trial bank showed that the observed

'strain ripple' shape was conveniently reproduced in the theoretical analysis and that predicted and measured strain magnitudes approximately coincided for $(K_o)_b = 1.5$ and $E_b = 15$ to 18 MN/m^2, for example, but also for $(K_o)_b = 1.0$ and $E_b = 8$ MN/m^2, $(K_o)_b = 2.0$ and $E_b = 26$ MN/m^2, etc. Calculations from vertical and horizontal strains in the fill led to E_b around 3 kN/m^2 and a $(K_o)_b$ below 1.0, but uncertainties about measured vertical strains make these figures likely to correspond to the lower bounds of the real parameters.

h) In-situ permeability tests showed that the coefficent of permeability of the foundation was around 1×10^{-10} m/sec at 5 m below the top of Lias, decreasing to 1×10^{-11} m/sec at the depth of 20 metres. In the upper 5 metres, it may be higher than 1×10^{-10} m/sec, due to presence of fissures. Combination of such figures with coefficients of compressibility measured in laboratory results in coefficients of consolidation of 3 m^2/year at the depth of 5 m and 0.3 m^3/year 15 metres below.

9.4 HYDRAULIC FRACTURE TESTS

Attempts were made to induce fracturing of the fill and observe pressures at which 'blow-off', 'shut-in', cracking and 'close-up' occurred, aiming at relating them to stresses in the fill. The attempts were not in general successful owing chiefly to premature interruption of tests caused by the limited capacity of pressure sources, insufficient length of the mercury manometer, shortage of time and also lack of experience with the technique. Some findings were important, however, and their presentation below illustrates some

of the difficulties involving fracture tests in partly saturated media as was the case of the Empingham trial bank.

a) 'Blow-off' occurred at ratios $u/\gamma.h$ of 0.6 to 0.8. If no tensile strength impeded the separation of the ground from the piezometer and disturbance around the tip is neglected, this means that minimum stressed equaled 0.6 to 0.8 times the overburden pressure.

b) Fracturing took place at ratios $u/\gamma.h$ over 1.4, 40% higher than the overburden pressure therefore.

c) Cracks were not totally 'closed up', causing an irreversible increase in intake factor that resulted in an apparent increase in permeability of 10 times. Further tests showed a reduction in such a figure to about 5 times the initial permeability, but it is not clear whether this was due to a real decrease in permeability due to increase in effective stresses and reduction in porosity, or to partial 'closing up' of the fracture due to swelling of the soil or rearrangement during movement.

d) 'Blown-off' cavities seem not to return to its previous position or, more probably, to do it slowly.

9.5 SUGGESTIONS OF FURTHER WORK

9.5.1 Instrumentation

Theoretical and experimental studies are required for the assessment of the influence of the stiffness of inclinometer casings and grout (or sand) on the measurement of horizontal

displacements and, more importantly, shear and vertical strains.

The hydraulic settlement gauge should be carefully examined in laboratory and improvements studied in its details so that operation can be simplified and results become more reliable. In order to minimize the possibility of air coming up out of the water or ingressing into the water line, it is herein suggested that a source of constant positive pressure could be used connected to the measuring chamber and the back of the transducer.

Some verifications are recommended of the accuracy of EDM surveys, particularly the influence of number of reflectors used, influence of atmospheric conditions, etc.

9.5.2 Soil Properties

Observation of an instrumented cut in brecciated Upper Lias Clay taken to failure could be very useful in assessing its bulk undrained strength to be compared with the findings of this thesis and results of in-situ and laboratory tests.

Studies should also be done of the variation of the strength and deformation characteristics of the Upper Lias Clay with the degree of brecciation and the distance from the bulge area.

Measurements of K_o', preferably by field tests but also by laboratory tests should be compared with the gain in undrained strength with depth and suction measurements to widen the experimental basis for the theoretical methods of assessing K_o' postulated in this thesis.

Undrained creep measurements might be made both in-situ and in laboratory, and its influence in the strength evaluated. Rates of creep strain should be compared with those recorded at Empingham.

Pore pressure developed in fills of Upper Lias Clay are to be examined and related to initial moisture contents and degrees of saturation.

In-situ permeability tests should be carried out at various depths of the sand drain area after a considerable dissipation of pore pressure, preferably at the same piezometers used by the Author, so as to evaluate which proportion of permeability decrease is due to increasing effective stresses and which one can be attributed to differential structural disturbance.

9.5.3 Hydraulic Fracture

A great amount of research is to be done before hydraulic fracturing becomes a standard technique of assessing stresses in the ground, particularly in fills.

The performance of hydraulic fracture tests on overconsolidated soils known to have $K'_o > 1$, should lead to a 'close up' pressure equal to the overburden pressure. It is recommended thus that such tests be carried out on London Clay or other overconsolidated soil to verify this assumption.

Tests on piezometers located near load cells, buried in soil masses or embedded in retaining walls, would be also useful in providing experimental field evidence for hydraulic fracture

tests.

All hydraulic tests should be preceded and followed by permeability tests so as to evaluate the irreversibility or otherwise of the damage caused to the soil.

'Blow-off' pressures are to be examined and compared to K_o measurements, aiming at establishing a correspondence between their values for various processes of piezometer installation. A series of consecutive 'blow off-shut in' pressures could be useful in eliminating the influence of tensile strength at the interface soil piezometer.

Fracturing pressures under both undrained and drained conditions should be examined, in situ or in large-scale laboratory models, so as to establish safe limits for permeability tests and first filling of reservoirs, particularly where settlement of clay cores are expected to exceed that of more rigid shoulders and arching effects associated with plastic yield may lower considerably minimum stresses in the fill.

REFERENCES

AAS, G. (1967) 'Vane tests for investigation of anisotropy of undrained shear strength of clays', Proc. Geotechnical Conf, Oslo, Vol. I, pp. 3-8.

AHRENS, T.P. and BARLOW, A.C. (1951) 'Permeability tests using drill holes and wells', Geol. Report G-97, U.S. Bur. Reclamation, p.45.

AL-DAHIR, Z.A.; KENNARD, M.F., and MORGENSTERN, N.R. (1969) 'Obserations on pore pressures beneath the ash lagoon embankments at Fidlers' Ferry Power Station', Conf. on In-situ Testing in Soils and Rocks, London, pp. 175-186.

BAZETT, D.J.; ADAMS, J.I, and MATYAS, E.L. (1961) 'An investigation of a slide in a test trench excavated in fissured sensitive marine clay', Proc. 5th. Int. Conf. S.M. and F.E., Paris, Vol. 1, pp. 431-435.

BERGDAHL, U. and BROMS, B.B. (1967) 'New method of measuring in-situ settlements', Journal of ASCE, S.M. and F.E. Div., Vol. 93, SM5, pp. 51-57.

BISHOP, A.W. (1954) 'The use of pore pressure coefficients in practice', Géotechnique, Vol. 4, No 4, pp. 148-152.

BISHOP, A.W. (1955) 'The use of the slip circle in the stability analysis of earth slopes', Géotechnique, Vol. 5, No. 1, pp. 7-17.

BISHOP, A.W. (1966) 'The strength of soils as engineering materials', 6th. Lecture, Géotechnique, Vol. 16, No. 2, pp. 91-130.

BISHOP, A.W. (1969) 'The Rutland Project: a feasibility study of dams at Empingham and Manton', Report to the Welland and Nene River Authority, unpublished.

BISHOP, A.W. and AL-DAHIR, Z.A. (1969) 'Some comparisons between laboratory tests, in-situ tests and full scale performance with special reference to permeability and coefficient of consolidation', Conf. on In-situ Testing in Soils and Rocks, London, pp. 161-174.

BISHOP, A.W.; GREEN, G.E; GARGA, V.K.; ANDRESEN, A. and BROWN, J.D. (1971) 'A new ring shear apparatus and its application to the measurement of residual strength', Géotechnique, Vol. 21, No. 4, pp. 273-318.

BISHOP, A.W., and GREEN, P.A. (1973) 'The development and use of trial embankments', Proc. Symp. on Field Instrumentation in Geotechnical Engineering, London, Part 1, pp. 13-37.

BISHOP, A.W. and HENKEL, D.J. (1962) 'The measurement of soil properties in the triaxial test', Arnold, London, 2nd. edition.

BISHOP, A.W. and LITTLE, A.L. (1967) 'The influence of the size and orientation of the sample on the apparent strength of the London clay at Maldon, Essex', Proc. Geotechnical Conf. Oslo, Vol. I, pp. 89-96.

BISHOP, A.W., WEBB, D.L., and LEWIN, P.I. (1965) 'Undisturbed samples of London clay from the Ashford Common shaft: strength-effective stress relationships', Géotechnique, Vol. 15, No.1 pp. 1-31.

BJERRUM, L. and ANDERSEN, K.H. (1972) 'In-situ measurement of lateral pressures in clay', Proc. 5th. European Conf. S.M. and F.E., Madrid, Vol. 1, pp. 11-20.

BJERRUM, L.; NASH, J.K.T.L.; KENNARD, R.M., and GIBSON, R.E. (1972) 'Hydraulic fracturing in field permeability testing', Géotechnique, Vol. 22, No. 2, pp. 319-332.

BLIGHT, G.E. (1967) 'Horizontal stresses in stiff and fissured lacustrine clays', Proc. 4th. African Conf. S.M. and F.E., Johannesburg, Vol. 1, pp. 95-99.

BOZOZUK, M. and LEONARDS, G.A. (1972) 'The Gloucester test fill', Proc. Specialty Conf. on Performance of Earth and Earth-supported Structures, ASCE, Lafayette, Indiana, USA, Vol, 1, Part 1, pp. 229-317.

BRINK, R. (1967) 'Effective angle of friction for a normally consolidated clay', Proc. Geotechnical Conf. Oslo, Vol. I, pp. 13-17.

BRITISH STANDARDS INSTITUTION (1957) 'Site investigations', British Standard Code of Practice CP 2001.

BROMWELL, L.G.; RYAN, C.R. and TOTH, W.E. (1971) 'Recording inclinometer for measuring soil movement ', Proc. 4th. Panamerican Conf. S.M. and F.E., San Juan, Puerto Rico, Vol. II, pp. 333-343.

BURLAND, J.B. and MOORE, J.F.A. (1973) 'The measurements of ground displacements around deep excavations', Proc. Symp. on Field Instrumentation in Geotechnical Engineering, London, Part I, pp. 70-84.

BURLAND, J.B.; MOORE, J.F.A., and SMITH, P.D.K. (1972) 'A simple and precise borehole extensometer', Géotechnique, Vol. 22, No. 1, pp. 174-177.

CHANDLER, R.J. (1970) 'The degradation of Lias clay slopes in an area of the East Midlands', Quart. J. Geol. Soc. London, Vol. 2, pp. 161-181.

CHANDLER, R.J. (1972) 'Lias clay: weathering processes and their effect on shear strength', Géotechnique, Vol. 22, No. 3, pp. 403-431.

CHANDLER, R.J. (1973) 'A study of structural discontinuities in stiff clays using a polarising microscope', Proc. Int. Symp. on Soil Structure, Gothenburg, Sweden, pp. 78-85.

CHANDLER, R.J. (1974) 'Lias clay: the long-term stability of cutting slopes', Géotechnique, Vol. 24, No. 1, pp. 21-38.

CLARK, J.B. (1949) 'An hydraulic process for increasing the productivity of wells', Trans. AIME, Vol. 186, p.1.

CORNFORTH, D.H. (1973) 'Performance characteristics of the Slope Indicator Series 200B inclinometer', Proc. Symp. on Field Instrumentation in Geotechnical Engineering, Part I, pp. 126-135.

CREAGER, W.P.; JUSTIN, J.D. and HINDS, J. 'Engineering for dams', Wiley, N. York. 3 Vols.

DAVIES, P. (1972) 'A laboratory investigation of the variation of the residual angle of shearing resistance and the compressibility values with effective normal stresses for clay from Empingham site', Imperial College, London, unpublished.

DE BEER, E. (1962) 'Shear strength characteristics of the Boom clay', Proc. Geotechnical Conf. Oslo, Vol. I, pp. 83-88.

DE BEER, E. (1969) 'Experimental data concerning clay slopes', Proc. 7th. Int. Conf. S.M. and F.E., Mexico City, Vol. 2, pp. 517-525.

DEADMAN, D.J. and SLIGHT, J.R. (1965) 'A new approach to the duct-rodding problem - Ductomotor No.1', Post Office Electrical Engineering Journal, London, Vol. 58, Part 2, pp. 91-92.

DUNNICLIFF, C.J. (1968) 'Instrumentation of the Plover Cove main dam', Géotechnique, Vol. 18, No. 3, pp. 283-300.

DUNNICLIFF, C.J. (1971) 'Equipment for field deformation measurements', Proc. 4th. Panamerican Conf. S.M. and F.E., San Juan, Puerto Rico, Vol ii, pp. 319-332.

EIDE, O. and HOLMBERG, S. (1972) 'Test fills to failure on the soft Bangkok clay', Proc. Specialty Conf. on Performance of Earth and Earth-supported structures, ASCE, Lafayette, Indiana, USA, Vol.1, Part 1, pp. 159-180.

FAIRHURST, C. (1964) 'Measurement of in-situ rock stresses with particular reference to hyfraulic facturing', Rock Mechanics and Engineering Geology, Vol. 2, p. 129.

FELLENIUS, W. (1936) 'Calculation of the stability of earth dams', Proc. 2nd. Cong. Large Dams, Washington, Vol. 4, p. 445.

FRASER, W.S. (1972) Certificate of analysis No. 1114, 8-8-72, for Ove Arup and Partners, unpublished.

GARGA, V.K. (1970) 'Residual shear strength under large strains and the effect of sample size on the consolidation of fissured clays', Ph.D. thesis, University of London.

GEDDES, W.G.N.; ROCKE, G., and SCRIMGEOUR, J. (1972) 'The Backwater Dam', Proc. Inst. Civ. Eng., London, Vol. 51, pp. 433-464.

GIBSON, R.E. (1963) 'An analysis of system flexibility and its effect on time lag in pore water pressure measurements', Géotechnique, Vol. 13, No. 1, pp. 1-11.

GIBSON, R.E. (1966) 'A note on the constant head test to measure soil permeability in-situ', Géotechnique, Vol. 16, No. 3, pp. 256-259.

GIBSON, R.E. (1970) 'An extension to the theory of the constant head in-situ permeability test', Géotechnique, Vol. 20, No. 2, pp. 193-197.

GIBSON, R.E. and ANDERSON, W.F. (1961) 'In-situ measurement of soil properties with the pressurometer', Civil Engineering and Public Works Review, London, Vol. 56, No. 658 (May), p. 615.

GOULD, J.P. and DUNNICLIFF, C.J. (1971) 'Accuracy of field deformation measurements', State-of-the-art Paper, Proc. 4th. Panamerican Conf. S.M. and F.E., San Juan, Puerto Rico, Vol. I, pp. 313-361.

GREEN, G.E. (1969) 'Report on tests on the performance of the Wilson Slope Indicator and the Soil Instruments Inclinometer', Imperial College, London, unpublished.

GREEN, G.E. (1973) 'Principles and performances of two inclinometers for measuring horizontal ground movements', Proc. Symp. on Field Instrumentation in Geotechnical Engineering, London, Part 1, pp. 166-179.

GRUNDY, C.F. (1955) 'The treatment by grouting of permeable foundations of dams', Proc. 5th. Int. Cong. Large Dams, Paris, Vol. 1, pp. 647-664.

HAIMSON, B. (1968) 'Hydraulic fracturing in porous and non-porous rock and its potential for determining in-situ stresses at great depth', Tech. Report No. 4-68 (July), U.S. Army Corps of Engineers, Missouri River Div., Omaha, Nebraska - Also Ph.D. thesis.

HAIMSON, B. and FAIRHURST, C. (1970) 'In-situ stress determination at great depth by means of hydraulic fracturing', Proc. Symp. on Rock Mechanics, Berkeley, Calif., USA, (1969), "Rock Mechanics; Theory and Practice", pp. 559-584.

HAINS, B.A. and HORTON, A. (1969) 'British regional geology - Central England', NERC-IGS, HMSO, 3rd. edition.

HAMZA, M.M.A.F. (1972) 'Certain problems with non-linear finite element method: I - Acceleration technique; II - Embankment dam', M.Sc. thesis, University of Wales.

HAMZA, M.M.A.F. and VAUGHAN, P.R. (1974) 'Empingham dam - Finite element analyses of the embankment section', Imperial College, London, unpublished.

HENKEL, D.J. (1960) 'The shear strength of saturated remoulded clays', Proc. Research Conf. on Shear Strength of Cohesive Soils, ASCE, Boulder, Colo., USA, pp. 533-554.

HOLLINGWORTH, S.E. and TAYLOR, J.H. (1946) 'An outline of the geology of the Kettering District', Proc. Geol. Assoc. London, Vol. 57, pp. 204-233.

HOLLINGWORTH, S.E. and TAYLOR, J.H. (1951) 'The Northampton Sand ironstone - Stratigraphy, structure and reserves', Mem. Geol. Survey of Great Britain, HMSO.

HOLLINGWORTH, S.E.; TAYLOR, J.H., and KELLAWAY, G.A. (1944) 'Large--scale superficial structures in the Northampton Ironstone field', Quart. J. Geol. Soc. London, Vol. 100, pp. 1-44.

HOLSCHER, H.D. (1969) 'A short range highly accurate electro--optical distance measuring equipment', National Institute for Telecommunication Research: CSIR.

HVORSLEV, M.J. (1951) 'Time lag and soil permeability in ground water observations', Bull. No. 36, W.E.S., U.S. Corps of Engineers, Vicksburg, Miss., USA.

HUBERT, M.K. and WILLIS, D.G. (1957) 'Mechanics of hydraulic fracturing', Petroleum Transactions AIME, Vol. 210, pp. 153-166.

JAAKKOLA, M. (1971) 'A survey with the Tellurometer MA-100', Survey Review, Vol. XXI, No. 159, pp. 29-34.

KALLSTENIUS, T. and BERGAU, W. (1961) 'In-situ determinations of horizontal ground movements', Proc. 5th. Int. Conf. S.M. and F.E., Paris, Vol. I, pp. 481-485.

KEHLE, R.O. (1964) 'Determination of tectonic stresses through analysis of hydraulic well fracturing', Journal of Geophysical Research, Vol. 69, p. 259.

KELLAWAY, G.A. (1941) Geological Survey, 6" to one mile Geologist's Field Map (County Sheets - Rutland 10 NW)

KENNARD, R.M. (1970) 'The measurement of soil permeability in situ by the constant head test', Ph.D. thesis, University of London.

KJAERNSLI, B. and SIMONS, N. (1962) 'Stability investigations of the north bank of the Drammen River', Géotechnique, Vol. 12, No. 2, pp. 147-167.

KJAERNSLI, B. and TORBLAA, I. (1968) 'Leakage through horizontal cracks in the core of Hyttejuvet Dam', Norwegian Geotechnical Institute, Pub. No. 80.

KNIGHT, K. and BLIGHT, G.E. (1965) 'Studies of some effects resulting from the unloading of soils', Proc. 6th. Int. Conf. S.M. and F.E., Montreal, Vol. 2, pp. 103-107.

KNILL, J.L. (1968) 'The geology of the proposed Empingham and Manton reservoirs', Imperial College, London, unpublished.

KONDNER, R.L. (1963) 'Hyperbolic stress-strain response: cohesive soils', Journal of ASCE, S.M. and F.E. Div., Vol. 89, SM1, pp. 115-141.

KONDNER, R.L. and HORNER, J.M. (1965) 'Triaxial compression of a cohesive soil with effective octahedral normal stress control', Canadian Geotechnical Journal, Vol. 2, pp. 40-52.

KONDNER, R.L. and ZELASKO, J.S. (1963a) 'Void ratio effects on the hyperbolic stress-strain response of a sand', Symp. on Laboratory Shear Testing of Soils, ASTM, STP No. 361, pp. 250-257.

KONDNER, R.L. and ZELASKO, J.S. (1963b) 'A hyperbolic stress-strain formulation for sands', Proc. 2nd. Panamerican Conf. on S.M. and F.E., Belo Horizonte, Brazil, Vol. 1. pp. 289-324.

KULHAWY, F.H.; DUNCAN, J.M., and SEED, H.B. (1969) 'Finite element analyses of stresses and embankments during construction', Univ. of California, Berkeley, Report No. TE-69-4.

LADANYI, B. (1963) 'Expansion of a cavity in a saturated clay medium', Journal of ASCE, S.M. and F.E. Div., Vol. 89, SM4, p. 127.

LADD, C.C. (1967) 'Strength and compressibility of saturated clays', Panamerican Soils Course, Univ. Catolica Andres Bello, Caracas.

LADD, C.C. (1972) 'Test embankment on sensitive clay', ASCE Specialty Conf. on Performance of Earth and Earth-supported Structures, ASCE, Lafayette, Indiana, USA, Vol. 1, Part 1, pp. 101-128.

LAUFFER, H. and SCHOBER, W. (1964) 'The Gepatsch Rockfill Dam in the Kauner Valley', Proc. 8th., Int. Cong. Large Dams, Edinburgh, Vol. 3, pp. 655-660.

LIPPOLD, F. M. (1958) 'Pressure grouting with packers', Journal ASCE, S.M. and F.E. Div., Vol. 84, SM1, pp

MAGUIRE, M. (1974) 'Undrained strength and stress-strain behaviour of the brecciated Upper Lias clay', Ph.D. thesis (in preparation), University of London.

MARSLAND, A. and BUTLER, M.E. (1967) 'Strength measurements on stiff fissured Barton clay from Fawley (Hampshire)', Proc. Geotechnical Conf. Oslo, Vol. 1, pp. 139-145.

MORGENSTERN, N.R. and VAUGHAN, P.R. (1963) 'Some observations on allowable grouting pressures', Symp. on Grouts and Drilling Muds, London, Butterworths.

MOYA, J. (1971) 'A review of precompression methods for improving foundation soils', M.Sc. thesis, Imperial College, Univ. London.

MURRAY, R.T and IRWIN, M.J. (1970) 'The performance of an inclinometer for measuring lateral movements in soil', RRL Report LR 332.

NAYLOR, D.J. (1972) 'Empingham trial embankment, finite element analysis', University of Wales, unpublished.

NICHOLLS, R.A. (1973) Discussion to R.J. Chandler's paper (1972), Géotechnique, Vol. 23, pp. 131-132.

NONVEILLER, E. and ANAGNOSTI, P. (1961) 'Stresses and deformations in cores of rockfill dams', Proc. 5th. Int. Conf. S.M. and F.E. Paris, Vol. 2, p. 673.

PARRY, R.H.G. (1972) 'Some properties of heavily overconsolidated Oxford clay at a site near Bedford', Géotechnique, Vol. 22, No.3, pp 485-507.

PEIGNAUD, M. and PERRIN, J. (1973) 'Inclinometers' in "Remblais sur sols compressibles", Special number of the "Bulletin de Liaison", Lab. Central des Ports et Chaussées, Paris, pp. 297-304.

PENMAN, A.D.M. (1969) 'Instrumentation for earth and rock fill dams', BNCOLD News and Views, May, pp. 7-10. Also BRS Current Paper 35/69.

PENMAN, A.D.M. (1972) Discussion, Proc. 5th. European Conf. S.M. and F.E., Madrid, Vol. 2, p. 87.

PENMAN, A.D.M. and CHARLES, J.A. (1971) 'Measuring movements of engineering structures', Proc. Congress of Surveyors, Commission 6, Wiesbaden, Paper 605.4. Also BRS Current Paper 32/71.

PENMAN, A.D.M. and CHARLES, J.A. (1973) 'Measuring movements of embankment dams', Proc. Symp. on Field Instrumentation in Geotechnical Engineering, London, Part 1, pp. 341-358.

PENMAN, A.D.M. and MITCHELL, P.B. (1970) 'Initial behaviour of Scammonden Dam', Proc. 10th. Int. Cong. Large Dams, Montreal, Vol. 1, pp. 723-747.

PHILIPS, S.H.E. and JAMES, E.L. (1973) 'An inclinometer for measuring the deformation of buried structures with reference to multi-tied diaphragm walls', Symp. on Field Instrumentation in Geotechnical Engineering, London, Part 1, pp. 359-369.

PUGH, R. (1974) Private communication.

RAYMOND, G.P. and AZZOUZ, M.M. (1969) 'Permeability determination for predicting rates of consolidation', Conf. on In-situ Testing in Soils and Rocks, London, pp. 195-203.

SCOTT Jr., P.P; BEARDEN, W.G. and HOWARD, G.C. (1953) 'Rock rupture as affected by fluid properties', Trans. AIME, Vol. 198, p.111.

SHANON, W.L.; WILSON, S.D. and MEESE, R.H. (1962) 'Field problems: field measurements', in "Foundation Engineering", G.A. Leonards ed., McGraw Hill, N. York, Ch. 13, pp. 1025-1080.

SIMON, I.; EMSLIE, A.G.; STRONG, P.F. and McCONNELL, R.K. (1968) 'Sensitive tiltmeter utilizing a diamagnetic suspension', Rev. Sci. Instr., Vol. 39, No. 11, pp. 1666-1671.

SIMONS, N.E. (1967) Discussion, Proc. Geotechnical Conf. Oslo, Vol. 2, pp. 159-160.

SKEMPTON, A.W. (1951) 'The bearing capacity of clays', Building Research Congress, Vol. 1, pp. 180-189.

SKEMPTON, A.W. (1953) 'The colloidal activity of clays', Proc. 3rd. Int. Conf. S.M. and F.E., Zurich, Vol. I, p. 57.

SKEMPTON, A.W. (1954) 'The pore pressure coefficients A and B', Géotechnique, Vol. 4, pp. 143-147.

SKEMPTON, A.W. (1961) 'Horizontal stresses in an overconsolidated Eocene clay', Proc. 5th. Int. Conf. S.M. and F.E., Paris, Vol, 1, pp. 351-357.

SKEMPTON, A.W. and LA ROCHELLE, P. (1965) 'The Bradwell slip: a short-term failure in London clay', Géotechnique, Vol. 15, No. 3, pp. 221-242.

SODHA, V.G. (1974) 'The stability of embankment dam fills of plastic clays', M.Phil thesis, University of London.

SOIL MECHANICS LTD. (1971) 'Site investigation for Empingham reservoir, Rutland', Reports Nos. 5633/1 to 5633/12 16 Vols., unpublished.

SOM, N.N. (1968) 'The effect of stress path on the deformation and consolidation of London clay', Ph.D. thesis, University of London.

TAYLOR, D.W. (1948) 'Fundamentals of Soil Mechanics', Wiley, N. York.

TERRESEARCH LTD. (1967) 'Site investigation of Empingham reservoir site', unpublished.

UNITED STATES CORPS OF ENGINEERS (1960) 'Geological investigations', Mannual EM. 1110-1-1801.

VAN POOLEN, H.K. (1957) 'Theories of hydraulic fracturing', Colo. Sch. Mines, Quart., Vol. 52, No. 3, pp. 114-127.

VAUGHAN, P.R. (1970) 'Introductory notes - British Geotechnical Society meeting on cracking of dam cores', Surveyor and Local Government Technology, Vol. 85, No. 4051.

VAUGHAN, P.R. (1971) 'The use of hydraulic fracture tests to detect crack formation in embankment dam cores', Interim Report, Imperial College, unpublished.

VAUGHAN, P.R. (1972) Discussion, Proc. 5th. European Conf. S.M. and F.E., Madrid, Vol. 2, pp. 72-75.

VAUGHAN, P.R. (1973) 'Notes on Soil Mechanics aspects of embankment design', Welland and Nene River Authority, unpublished.

VAUGHAN, P.R. (1974) General Report of Session 3 and Discussion to Session 2, Symp. on Field Instrumentation in Geotechnical Engineering, to be shortly published by Butterworths. London.

VAUGHAN, P.R. and CHANDLER, R.J. (1974) Introductory notes for a meeting of the British Geotechnical Society on 'The design of cutting slopes in overconsolidated clay', 29-5-74.

VAUGHAN, P.R.; KLUTH, D.J.; LEONARD, M.W., and PRADOURA, H. (1970) 'Cracking and erosion of the rolled clay core of Balderhead Dam and the remedial works adopted for its repair', Proc. 10th. Cong. Large Dams, Vol. 1, pp. 73-93.

VAUGHAN, P.R.; WERNECK, M.L.G., and HAMZA, M.M.A.F. (1973) - Discussion to sessions 3 and 4 Symp. on Field Instrumentation in Geotechnical Engineering, to be shortly published by Butterworths, London.

WALBANCKE, H.J. (1971) 'Site investigation at the Empingham Dam', Internal Report, Imperial College, unpublished.

WARD, W.A. (56) 'A remote reading inclinometer', Building Research Note E697.

WELLAND AND NENE RIVER AUTHORITY (1972) 'The Empingham reservoir project', Internal Distribution.

WELLAND AND NENE RIVER AUTHORITY (1973) 'The Empingham pumped-storage project', Internal Distribution.

WERNECK, M.L.G. (1971) 'Contribuição ao estudo de relações tensão--deformação em solos residuais compactados' (Contribution to the study of stress-deformation relationships for compacted residual soils), M.Sc. thesis, Fed. Univ. Rio de Janeiro.

WILKINSON, W.B. (1968) 'Constant head in situ permeability tests in clay strata', Géotechnique, Vol. 18, No. 2, pp. 172-194.

WILKINSON, W.B.; BARDEN, L., and ROCKE G. (1969) 'An assessment of in-situ and laboratory tests in predicting pore pressure in an earth dam'. Proc. Conf. on In-situ Testing in Soils and Rocks, London, pp. 187-194.

WILSON, S.D. (1959) 'Application of the principles of Soil Mechanics to open-pit mining', Quart. Colo. Sch. Mines, Symp. on Rock Mechanics, Golden, Colo., USA, Vol. 54, No. 3.

WILSON, S.D. (1962) 'The use of slope measuring devices to determine movements in earth masses. Symp. On Field Testing of Soils, ASTM STP 322, pp. 187-198.

WOLFSKILL, L.A. and SOYDEMIR, C. (1971) 'Soil instrumentation for the I-95 MIT-MDPW test embankment', MIT Dept. of Civ. Eng., Research Report R71-28, Soils Publication 283.

EMPINGHAM PUMPED STORAGE SCHEME

LOCATION IN THE COUNTRY

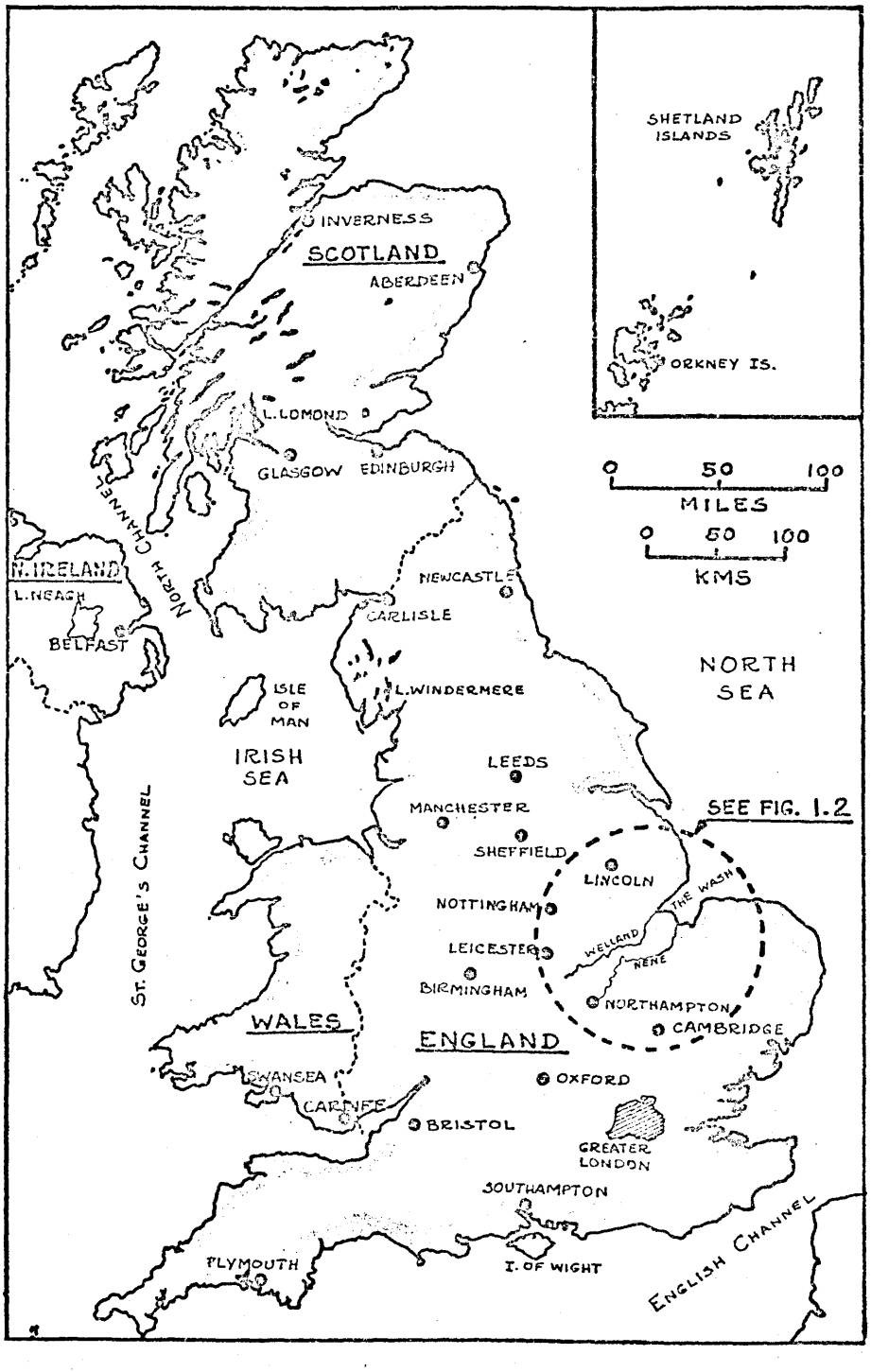


FIG. 1.1

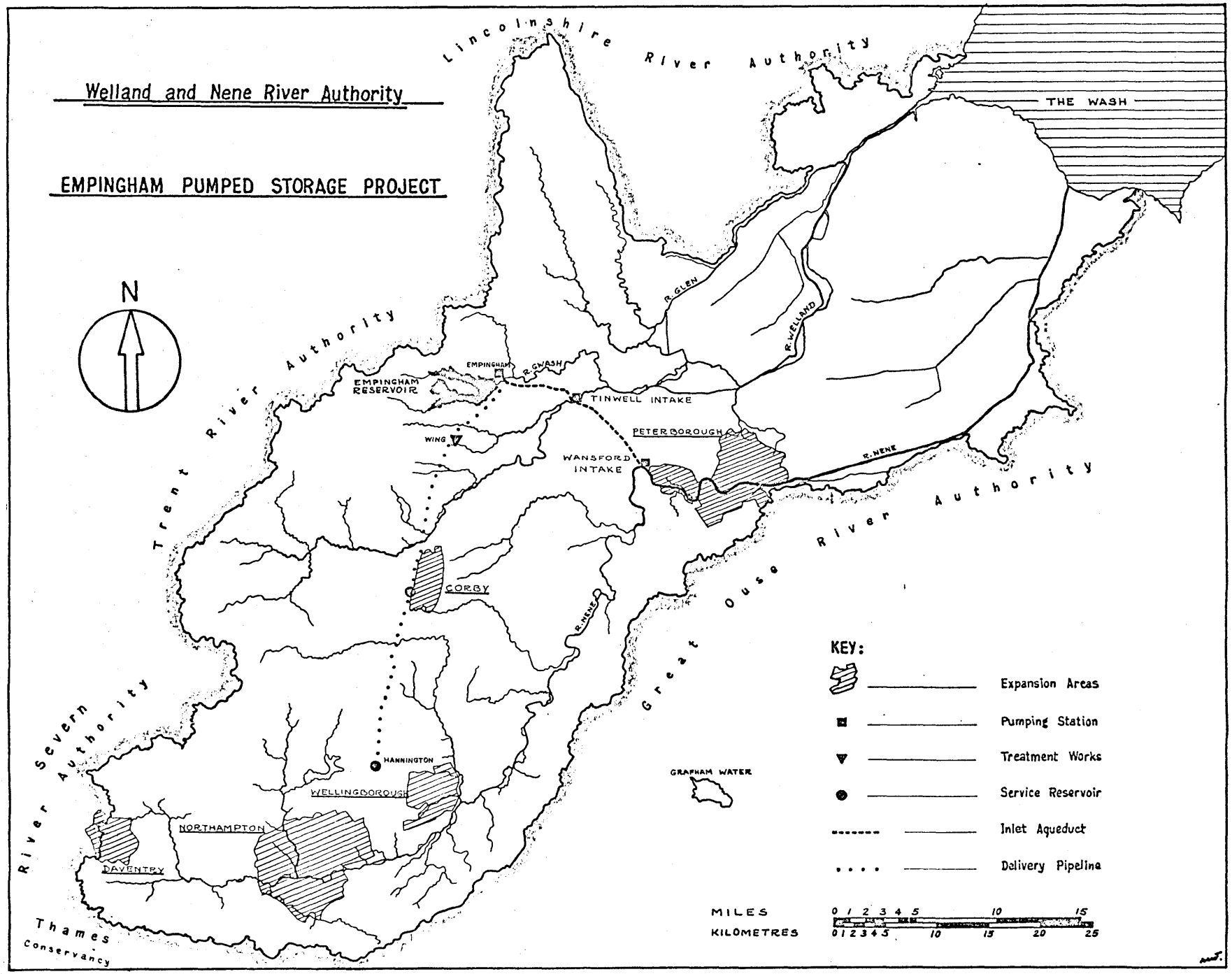
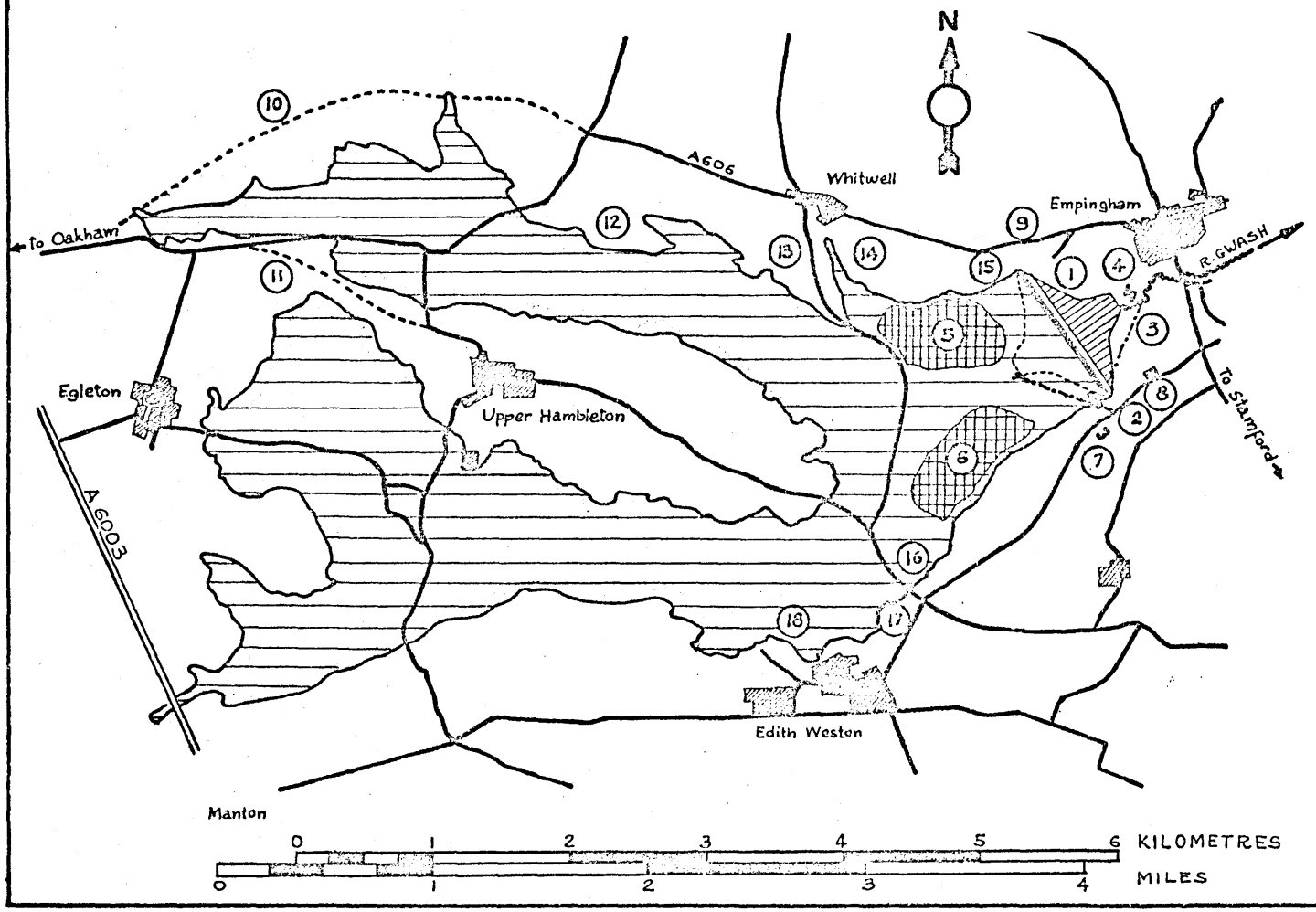

Welland and Nene River Authority
EMPINGHAM PUMPED STORAGE PROJECT
N
Lincolnshire River Authority
THE WASH
Trent River Authority
EMPINGHAM
R. WASH
EMPINGHAM RESERVOIR
TINWELL INTAKE
R. GLEN
R. WELLAND
PETERBOROUGH
WING
WANSFORD INTAKE
R. NENE
Great Ouse River Authority
CORBY
R. NENE
River Severn Authority
HANNINGTON
WELLINGBOROUGH
NORTHAMPTON
DAVENTRY
GRAFHAM WATER
Thames Conservancy
KEY:
Expansion Areas
Pumping Station
Treatment Works
Service Reservoir
Inlet Aqueduct
Delivery Pipeline
MILES
KILOMETRES
0 1 2 3 4 5 10 15
0 1 2 3 4 5 10 15 20 25

FIG. 1.2

FIG. 1.2

EMPINGHAM DAM

PLAN OF RESERVOIR



KEY:

1. Dam
2. Draw-off Tower and Overflow
3. Diversion Tunnel
4. Empingham Pumping Station
5. North Borrow Pit
6. South Borrow Pit
7. Resident Engineer's Site Office
8. Viewing Car Park
9. Viewing Car Park
10. Proposed Route of A606 Diversion
11. Proposed New Road to Upper Hambleton
12. Proposed Barnsdale Picnic Site
13. Proposed Whitwell Picnic Site
14. Proposed Sailing Centre, Fishing Lodge and Administration Block
15. Proposed Sykes Lane Picnic Site
16. Proposed Fishing Lodge
17. Proposed Normanton Picnic Site
18. Proposed Sailing Club

FIG. 1.3

FIG. 1.3

EMPINGHAM RESERVOIR

GEOLOGICAL MAP

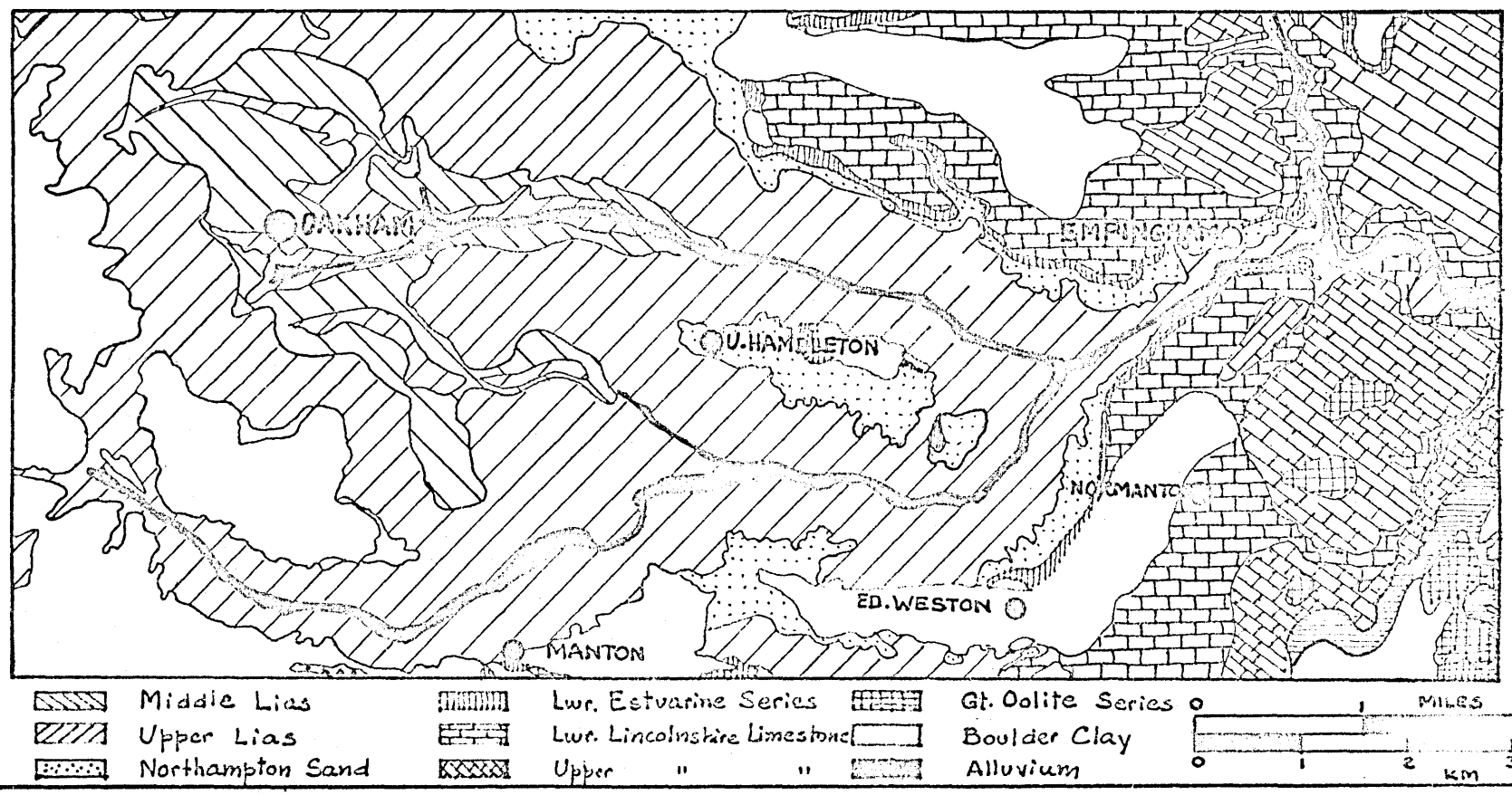


FIG. 2.1

FIG. 2.1.

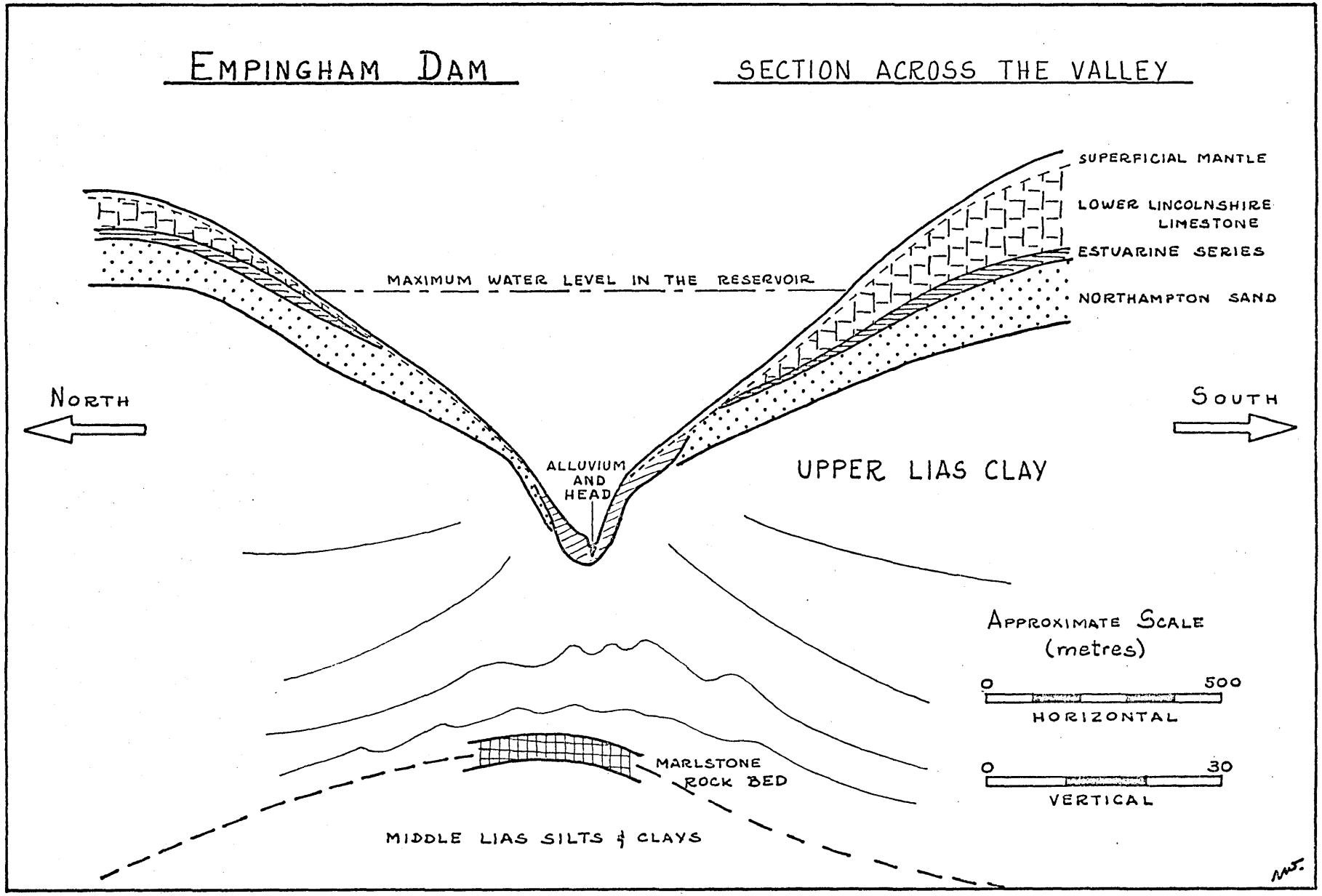

EMPINGHAM DAM
SECTION ACROSS THE VALLEY
SUPERFICIAL MANTLE
LOWER LINCOLNSHIRE LIMESTONE
ESTUARINE SERIES
NORTHAMPTON SAND
MAXIMUM WATER LEVEL IN THE RESERVOIR
NORTH
SOUTH
ALLUVIUM AND HEAD
UPPER LIAS CLAY
APPROXIMATE SCALE (metres)
0
500
HORIZONTAL
0
30
VERTICAL
MARLSTONE ROCK BED
MIDDLE LIAS SILTS & CLAYS

FIG. 2.2

FIG. 2.2

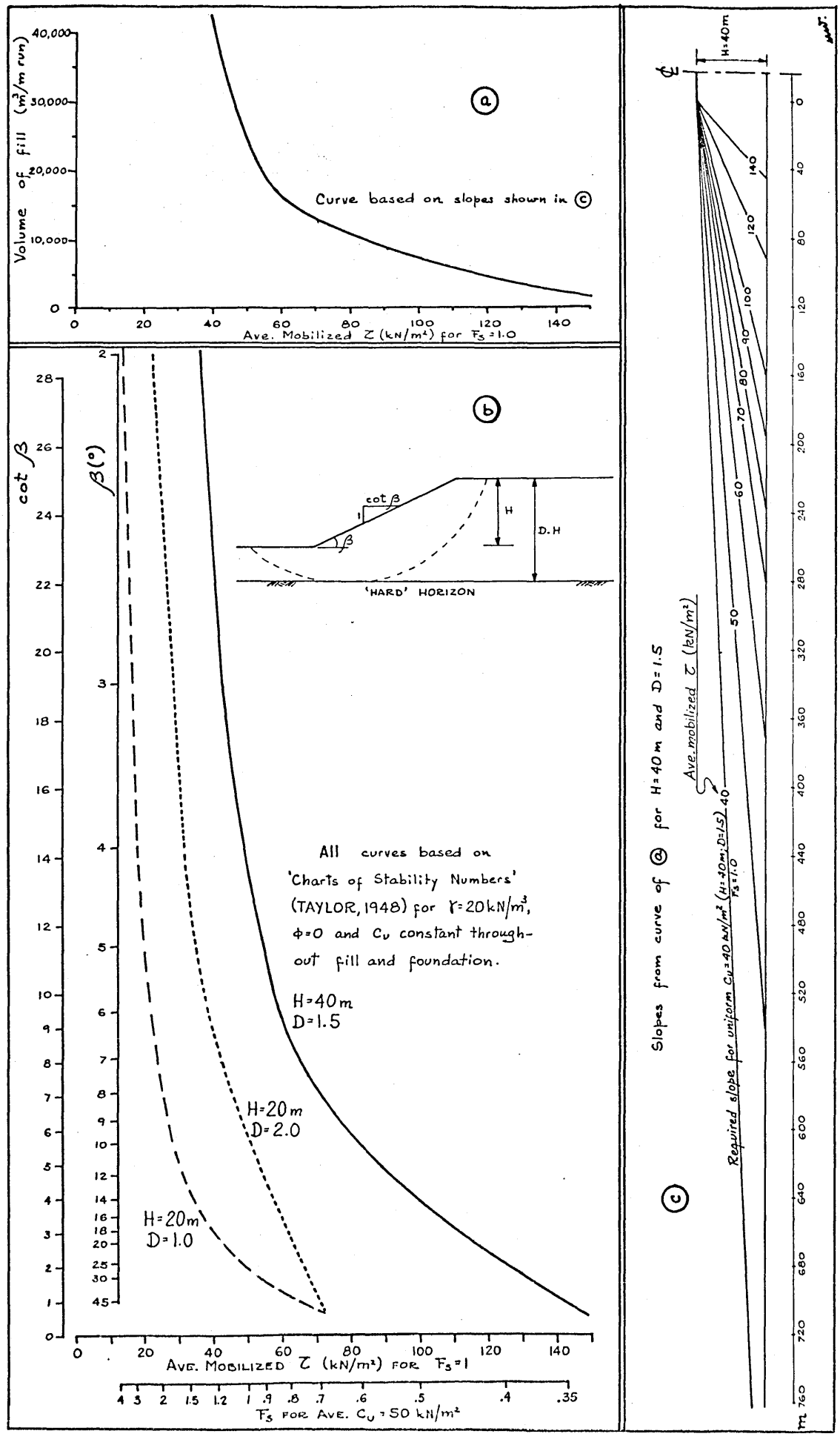
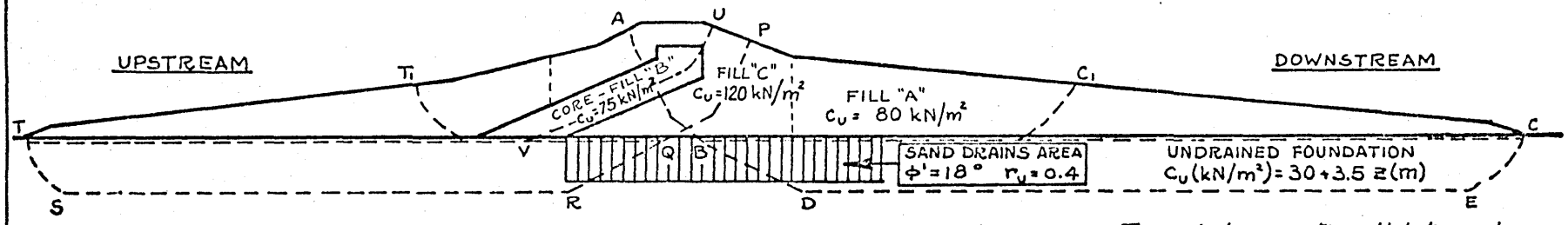

a
Volume of fill (m³/m run)
40,000
30,000
20,000
10,000
0
Curve based on slopes shown in ©
0 20 40 60 80 100 120 140
Ave. Mobilized Z (kN/m²) for Fs=1.0
b
cot β
β(°)
cot β
1
β
H
D.H
'HARD' HORIZON
All curves based on 'Charts of Stability Numbers' (TAYLOR, 1948) for γ=20kN/m³, φ=0 and Cu constant throughout fill and foundation.
H=40m
D=1.5
H=20m
D=2.0
H=20m
D=1.0
Ave. Mobilized Z (kN/m²) for Fs=1
4 3 2 1.5 1.2 1 .9 .8 .7 .6 .5 .4 .35
Fs for Ave. Cu=50 kN/m²
c
H=40m
Slopes from curve of @ for H=40m and D=1.5
Ave. mobilized Z (kN/m²)
Required slope for uniform Cu=40 kN/m² (H=40m; D=1.5) Fs=1.0
140
120
100
90
80
70
60
50
40
m

FIG. 3.1

FIG. 3.1

EMPINGHAM DAM

STABILITY ANALYSIS

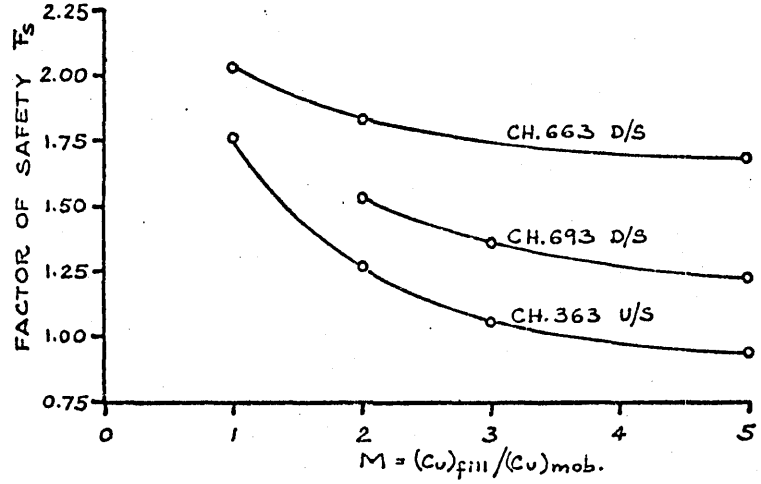


Typical dam section - Not to scale

Calculated Factors of Safety							
DOWNSTREAM				UPSTREAM			
Slip Surface	Chainage 543	453	363	Slip Surface	Chainage 543	663	693
ABC	1.64	1.67	1.21	PQT	1.56	1.66	1.11
ABC1	1.26	1.47	0.86	UVT	1.18	1.38	0.92
ADE	2.12	1.74	1.73	PQT1	1.31	1.41	1.03
ABE	2.24	2.11	1.75	PRS	1.97	2.20	1.50
ADC	1.91	1.69	1.62	PQS	1.90	2.14	1.50
				PRT	1.87	2.12	1.46

NOTE: All F_s calculated by Morgenstern's method for $f(x) = \frac{X}{\lambda \cdot E} = 1$ and $M = \frac{(C_u)_{fill}}{(C_u)_{mob}} = 5.0$

EFFECT ON F_s OF VARYING M



NOTE: All F_s for slip surfaces at the foundation Top, emerging at the Toe.

mvt.

FIG. 3.2

FIG. 3.2

EMPINGHAM DAM

LOCATION OF TRIAL BANK

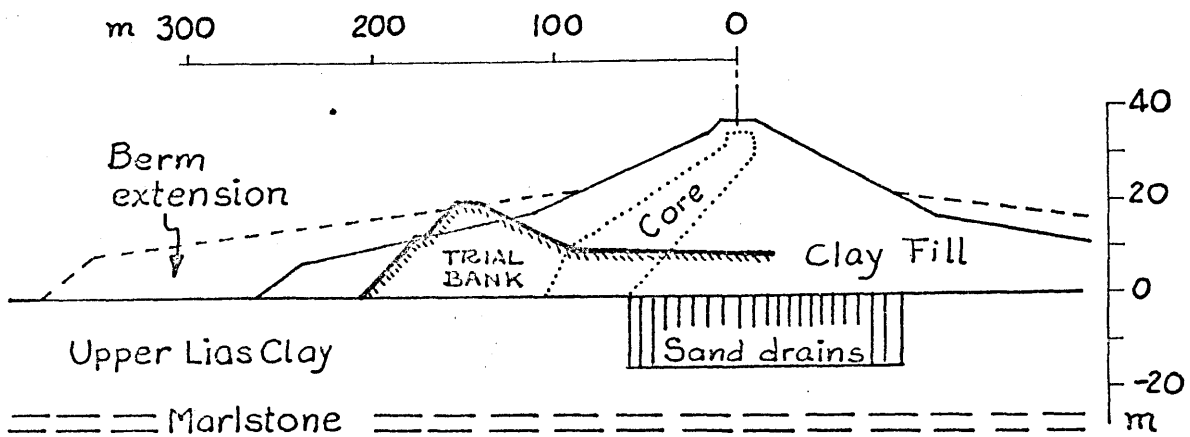


FIG. 3.3

FIG. 3.3

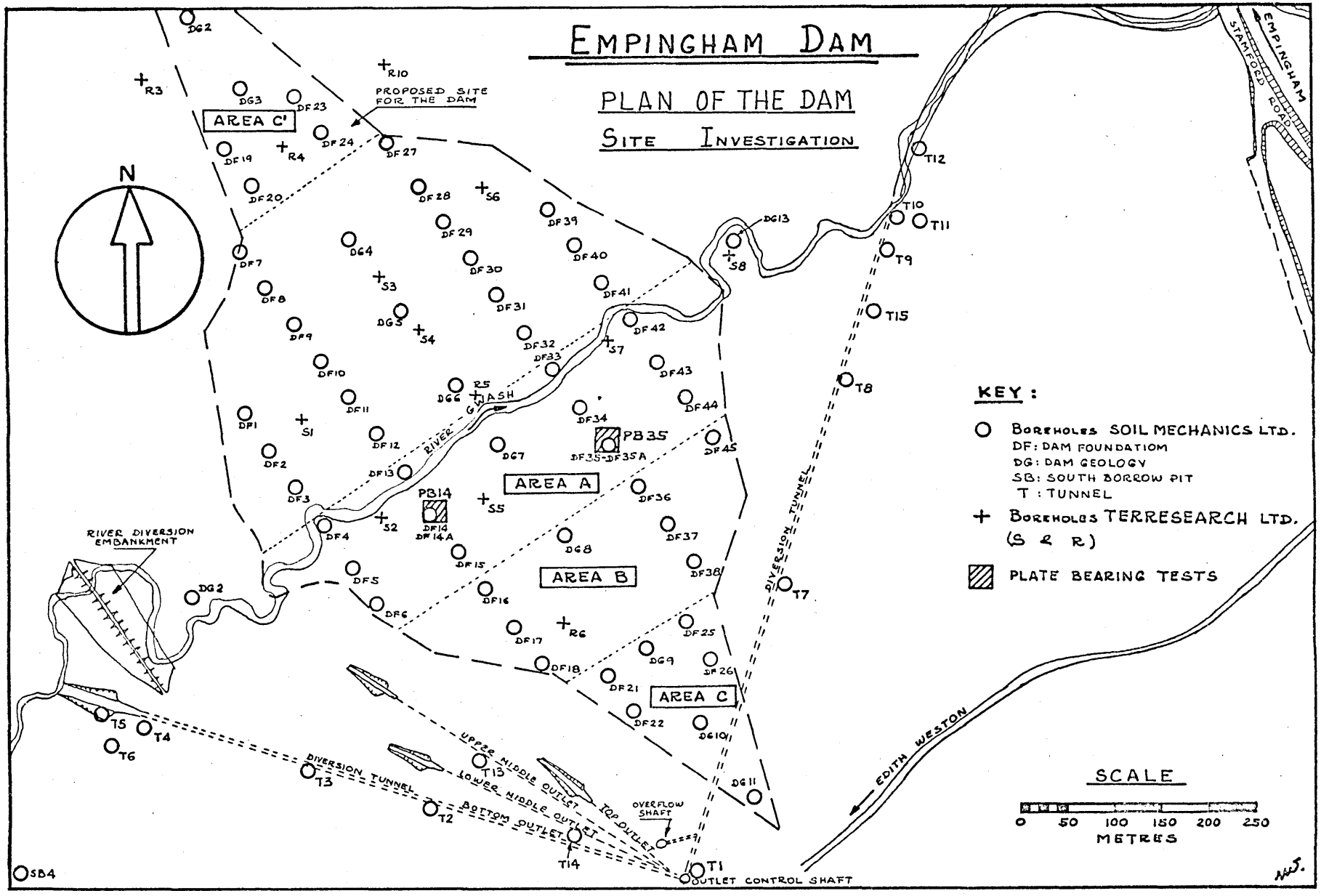

EMPINGHAM DAM
PLAN OF THE DAM
SITE INVESTIGATION
PROPOSED SITE FOR THE DAM
AREA C'
AREA A
AREA B
AREA C
N
KEY :
BOREHOLES SOIL MECHANICS LTD.
DF: DAM FOUNDATIOM
DG: DAM GEOLOGY
SB: SOUTH BORROW PIT
T : TUNNEL
BOREHOLES TERRESEARCH LTD. (S & R)
PLATE BEARING TESTS
SCALE
0 50 100 150 200 250
METRES
RIVER
WASH
RIVER DIVERSION EMBANKMENT
DIVERSION TUNNEL
UPPER MIDDLE OUTLET
LOWER MIDDLE OUTLET
TOP OUTLET
BOTTOM OUTLET
OVERFLOW SHAFT
OUTLET CONTROL SHAFT
EDITH WESTON
EMPINGHAM
STAMFORD ROAD
PB35
PB14
DF35-DF35A
DF14
DF14A

FIG. 3.4

FIG. 3.4

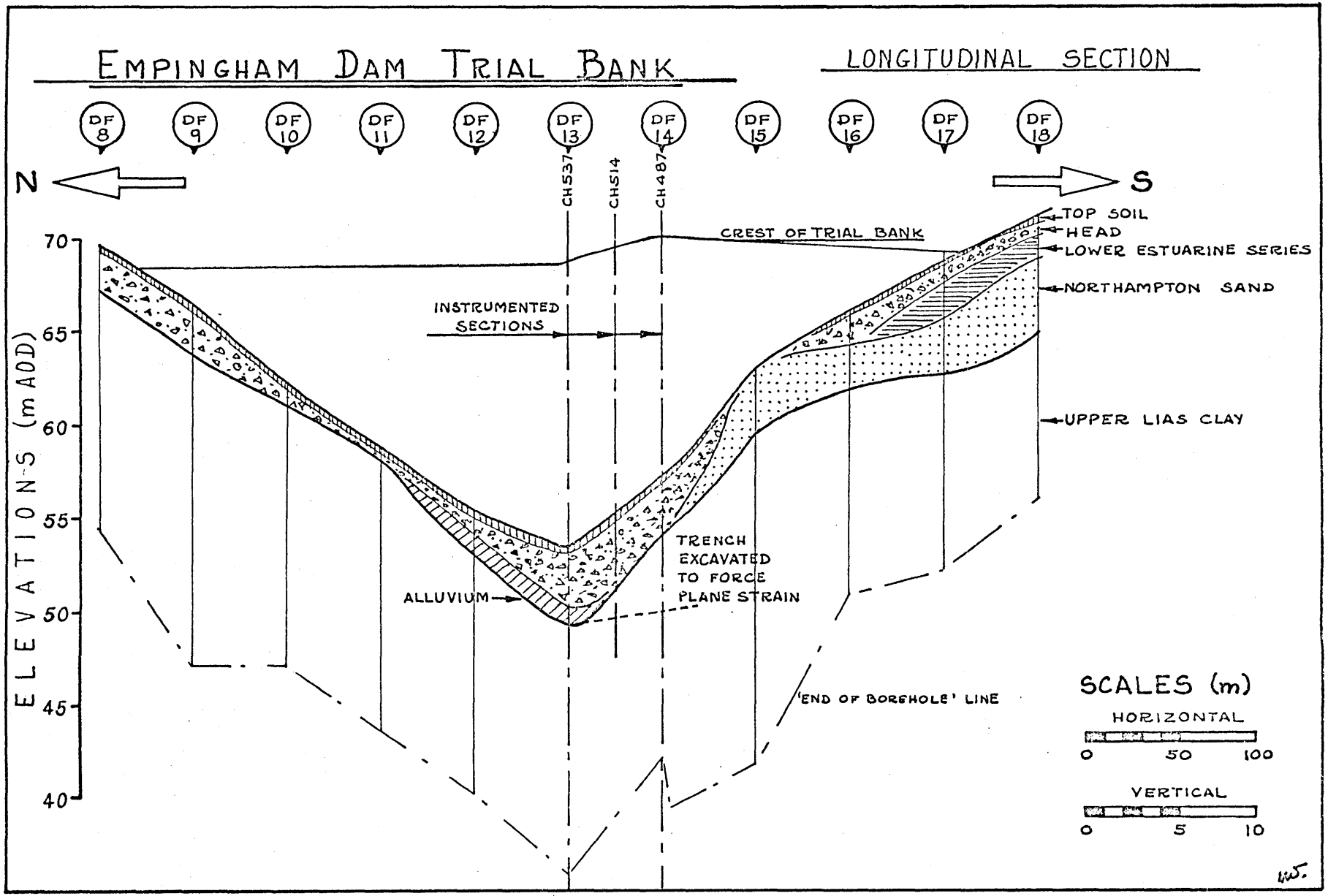

EMPINGHAM DAM TRIAL BANK
LONGITUDINAL SECTION
DF 8
DF 9
DF 10
DF 11
DF 12
DF 13
DF 14
DF 15
DF 16
DF 17
DF 18
N
S
CH537
CH514
CH487
CREST OF TRIAL BANK
INSTRUMENTED SECTIONS
TOP SOIL
HEAD
LOWER ESTUARINE SERIES
NORTHAMPTON SAND
UPPER LIAS CLAY
ALLUVIUM
TRENCH EXCAVATED TO FORCE PLANE STRAIN
'END OF BOREHOLE' LINE
ELEVATIONS (m AOD)
70
65
60
55
50
45
40
SCALES (m)
HORIZONTAL
0 50 100
VERTICAL
0 5 10
W.S.

FIG. 3.5

FIG. 3.5

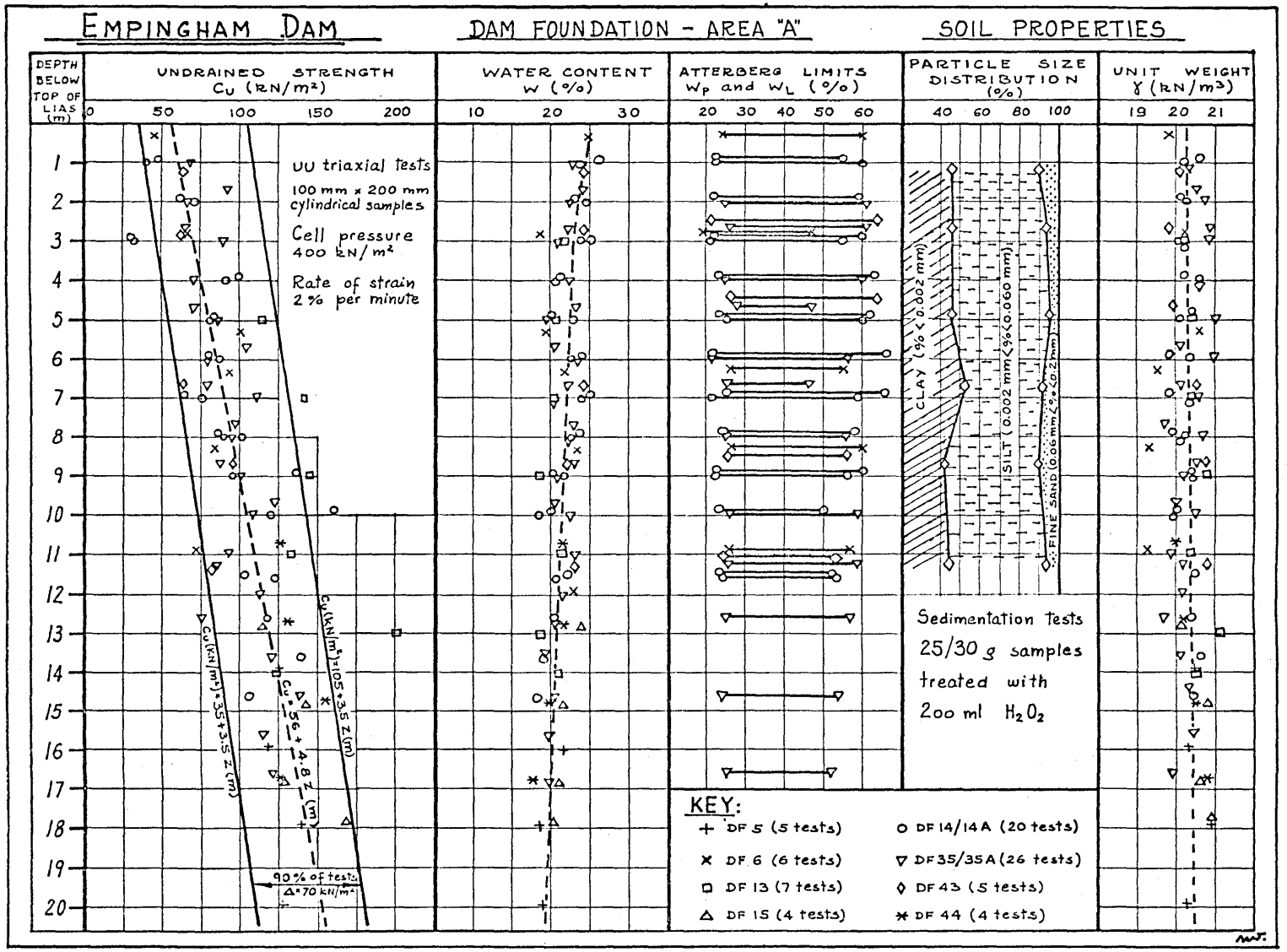

EMPINGHAM DAM
DAM FOUNDATION - AREA "A"
SOIL PROPERTIES
DEPTH BELOW TOP OF LIAS (m)
UNDRAINED STRENGTH Cu (kN/m²)
WATER CONTENT w (%)
ATTERBERG LIMITS Wp and WL (%)
PARTICLE SIZE DISTRIBUTION (%)
UNIT WEIGHT γ (kN/m³)
UU triaxial tests
100 mm x 200 mm cylindrical samples
Cell pressure 400 kN/m²
Rate of strain 2% per minute
Cu(kN/m²)=105+3.5 Z(m)
Cu(kN/m²)=35+3.5 Z(m)
Cu=56+4.8 Z(m)
90% of tests Δ=70 kN/m²
CLAY (% < 0.002 mm)
SILT (0.002 mm < % < 0.060 mm)
FINE SAND (0.06 mm < % < 0.2 mm)
Sedimentation Tests
25/30 g samples
treated with
200 ml H2O2
KEY:
DF 5 (5 tests)
DF 6 (6 tests)
DF 13 (7 tests)
DF 15 (4 tests)
DF 14/14A (20 tests)
DF 35/35A (26 tests)
DF 43 (5 tests)
DF 44 (4 tests)

FIG. 3.6

FIG. 3.6

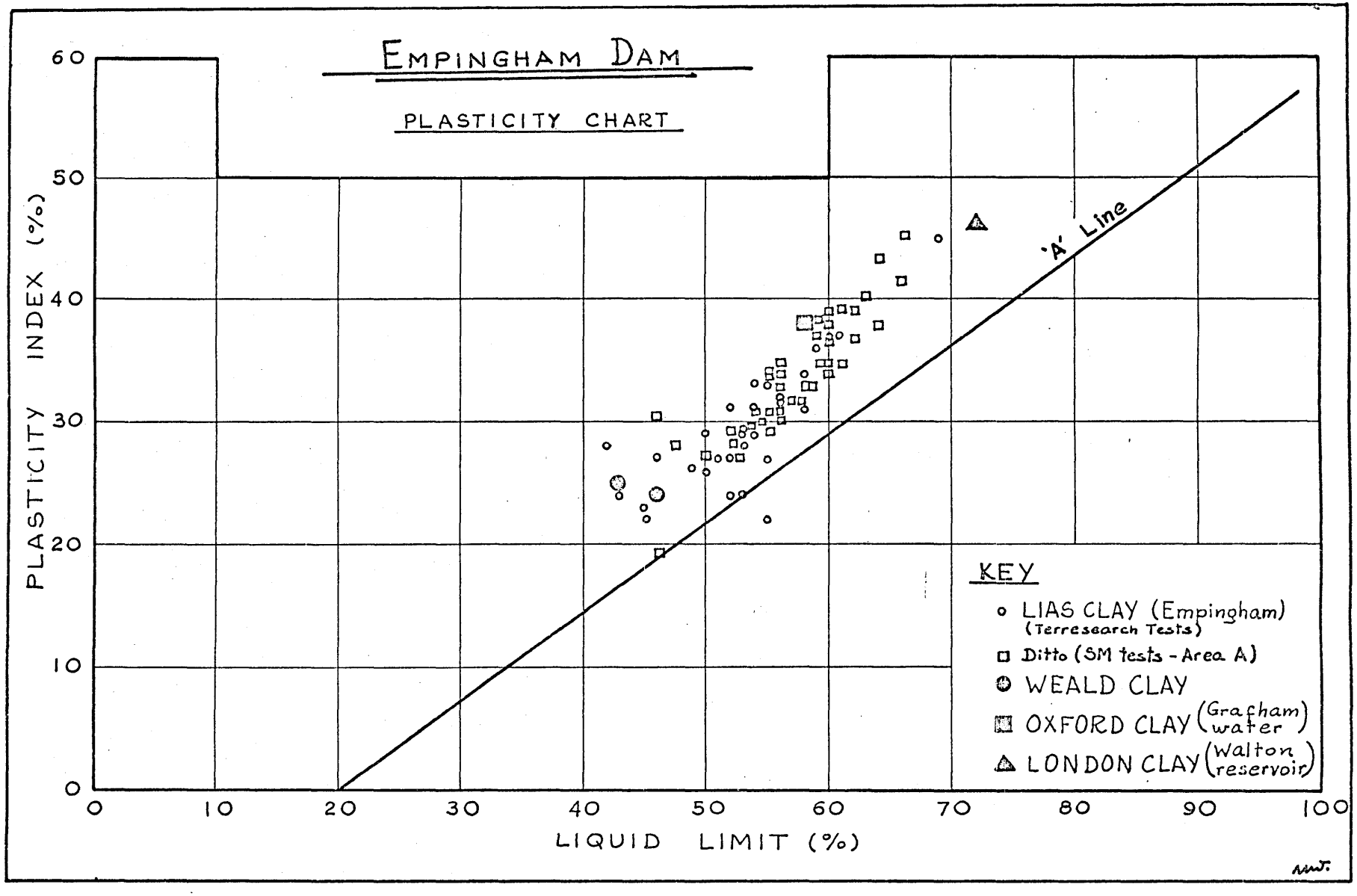

EMPINGHAM DAM
PLASTICITY CHART
PLASTICITY INDEX (%)
LIQUID LIMIT (%)
0
10
20
30
40
50
60
70
80
90
100
'A' Line
KEY
LIAS CLAY (Empingham) (Terresearch Tests)
Ditto (SM tests - Area A)
WEALD CLAY
OXFORD CLAY (Grafham water)
LONDON CLAY (Walton reservoir)

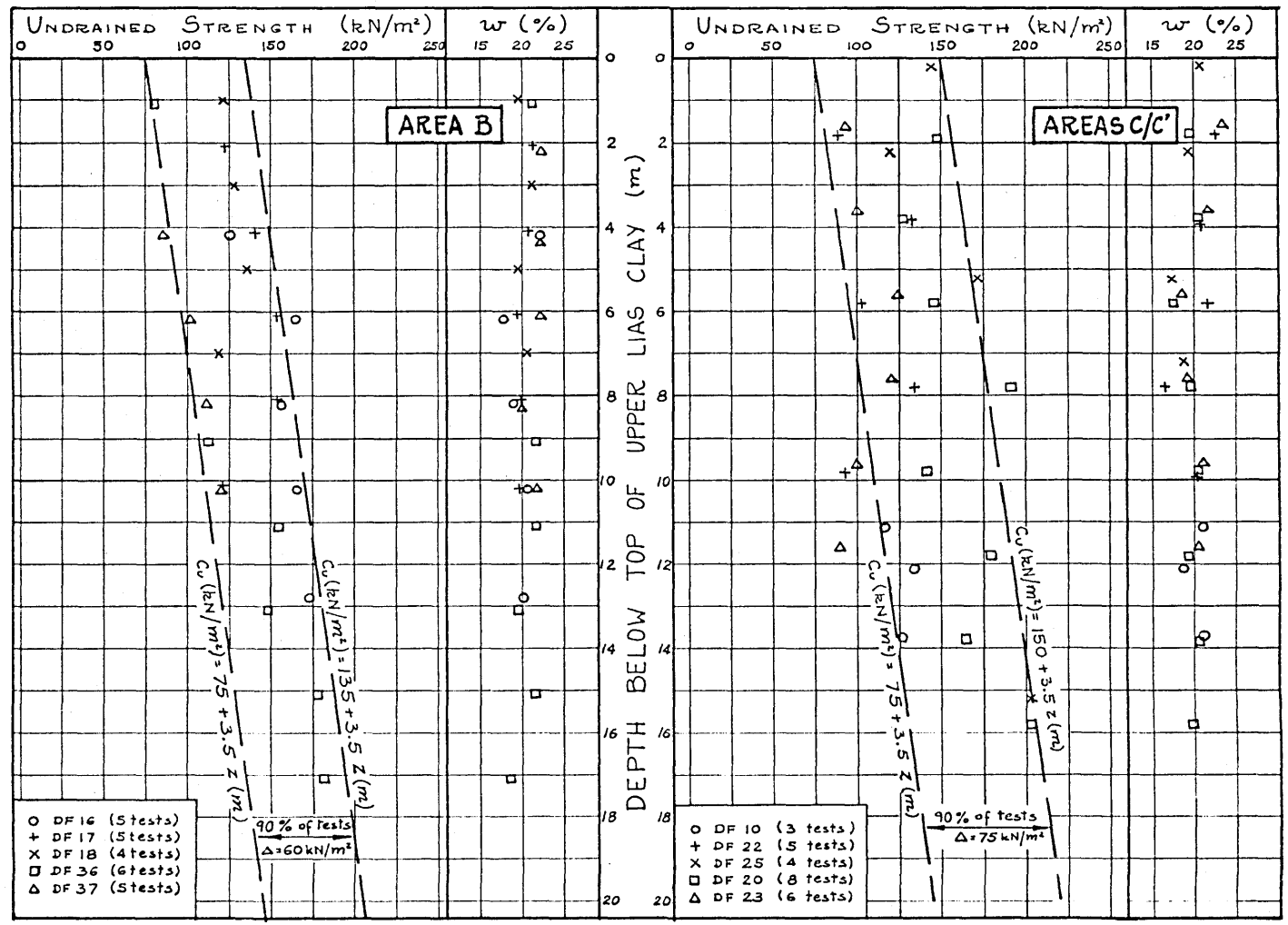
FIG. 3.7

FIG. 3.7

EMPINGHAM DAM FOUNDATION

AREAS "B" AND "C/C'"

SOIL PROPERTIES



NOTE: Undrained strength from UU triaxial tests on 100 mm × 200 m cyl. samples – σ_{cell} = 400 kN/m² – $\dot{\epsilon}_1$ = 2% per minute

mwr.

FIG. 3.8

FIG. 3.8

EMPINGHAM DAM

PLATE BEARING TESTS

(CONSTANT RATE OF PENETRATION)

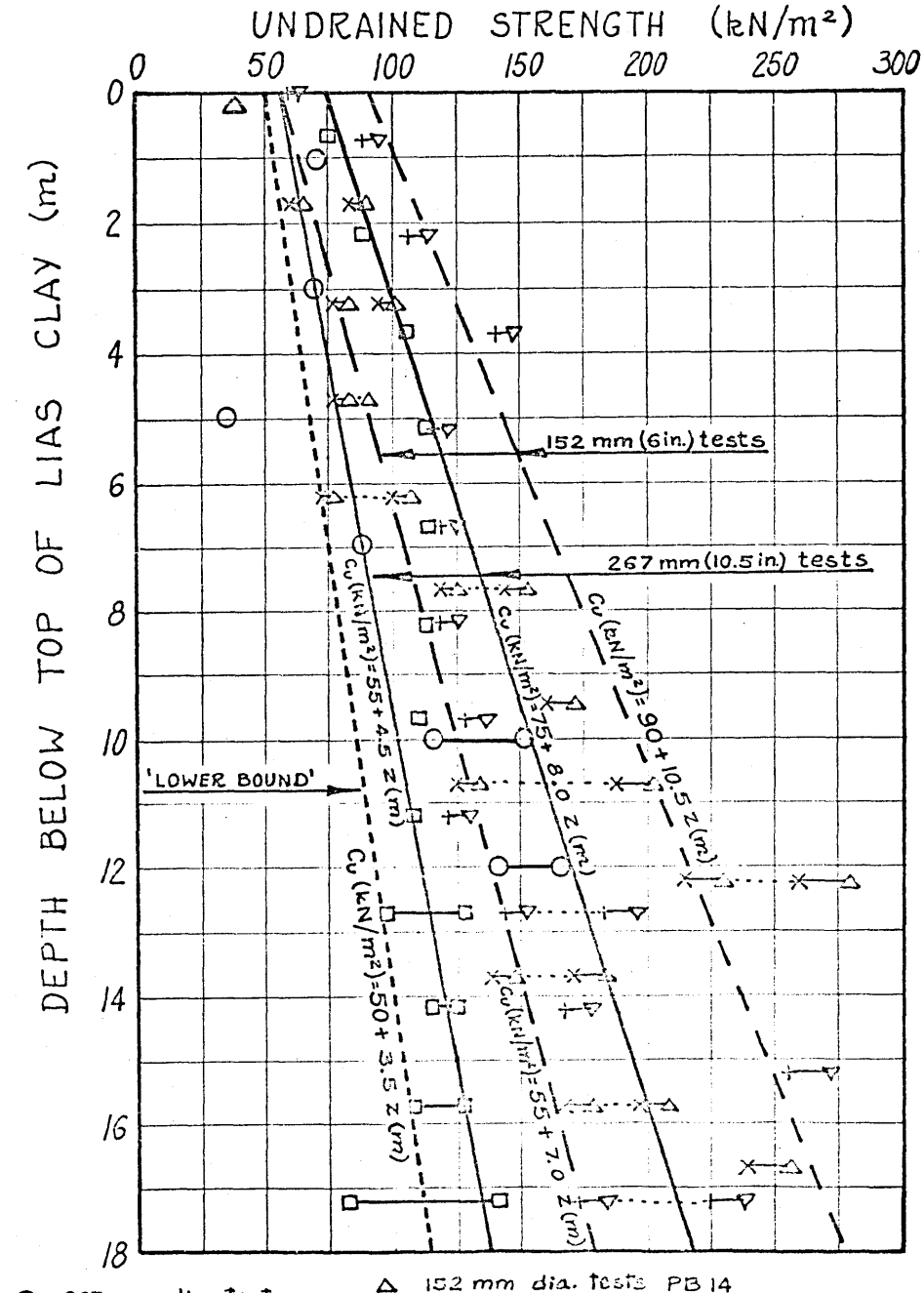


FIG. 3.9

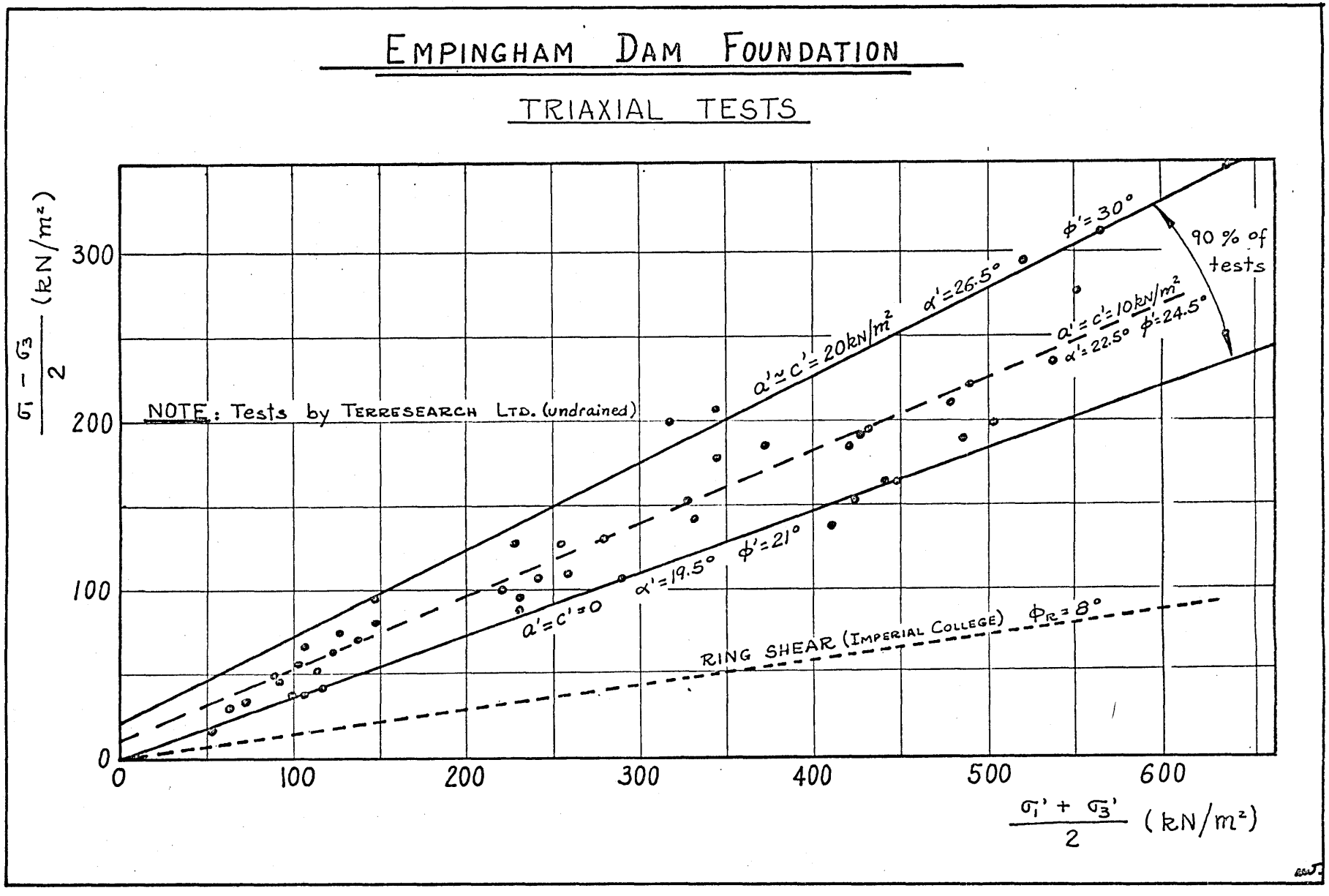


FIG. 3.10

FIG. 3.10

EMPINGHAM DAM FOUNDATION

TRIAXIAL TESTS

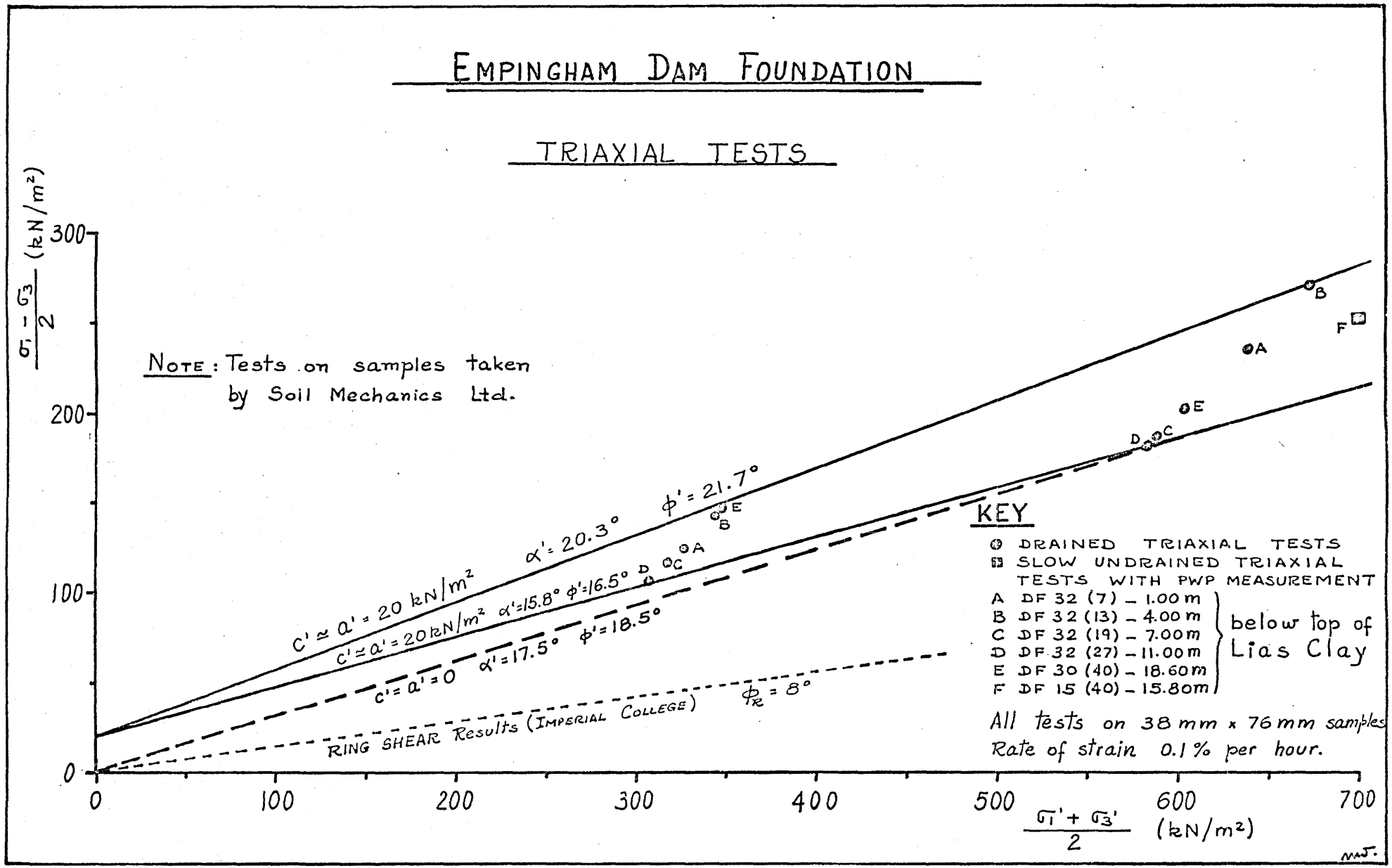


FIG. 3.11

FIG. 3.11

UPPER LIAS CLAY

SHEAR STRENGTH IN TERMS OF EFFECTIVE STRESSES

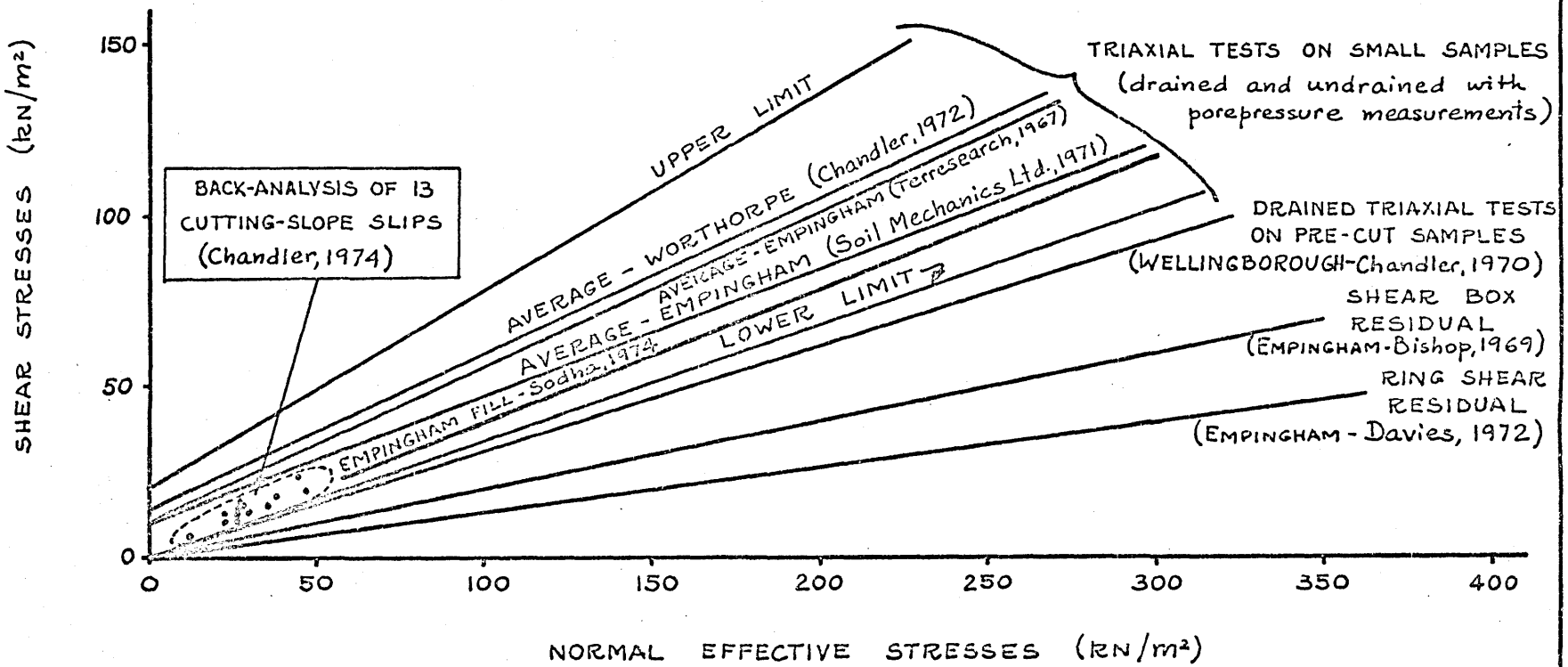


FIG. 3.12

FIG. 3.12

EMPINGHAM DAM

COEFFICIENT OF CONSOLIDATION

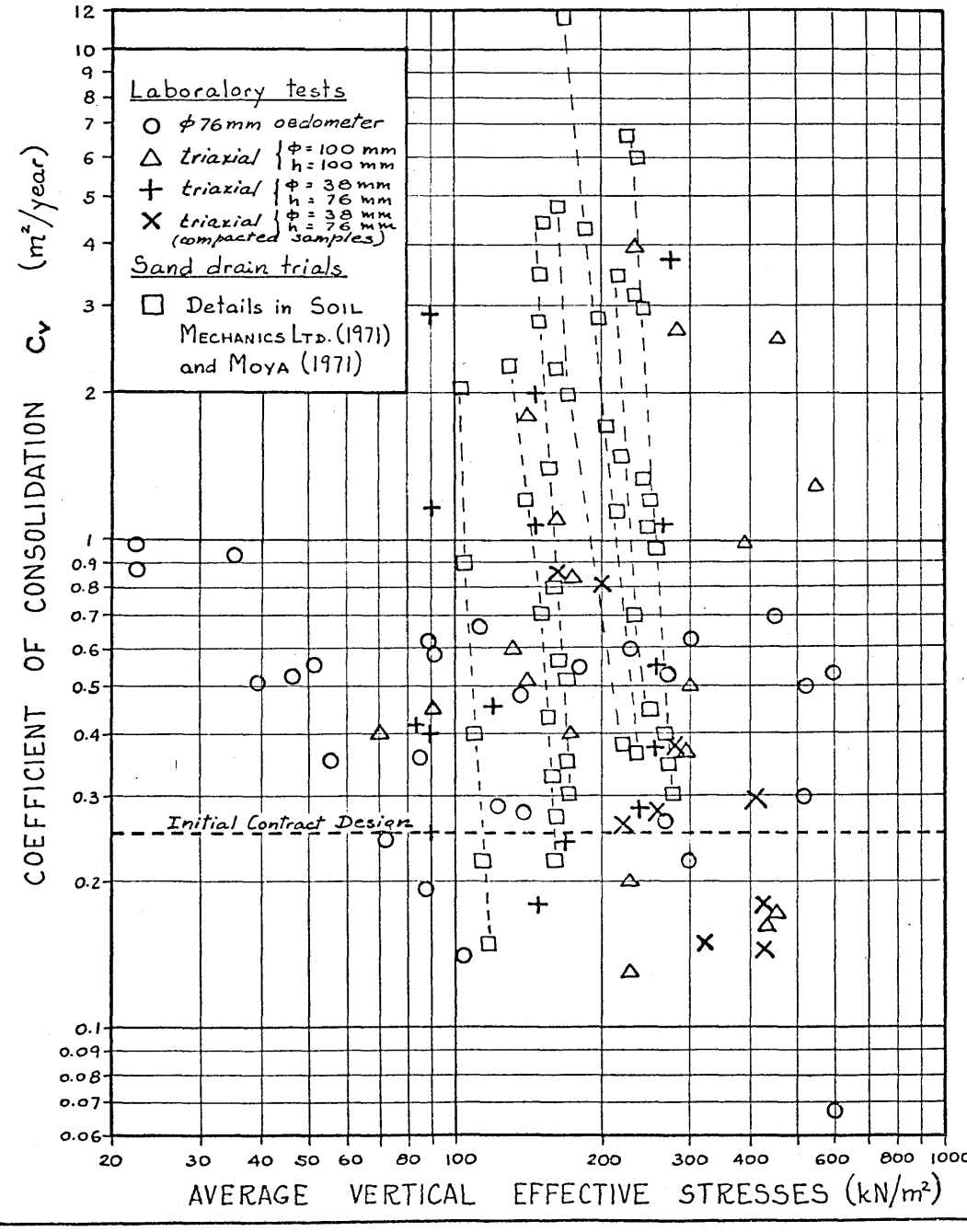


FIG. 3.13

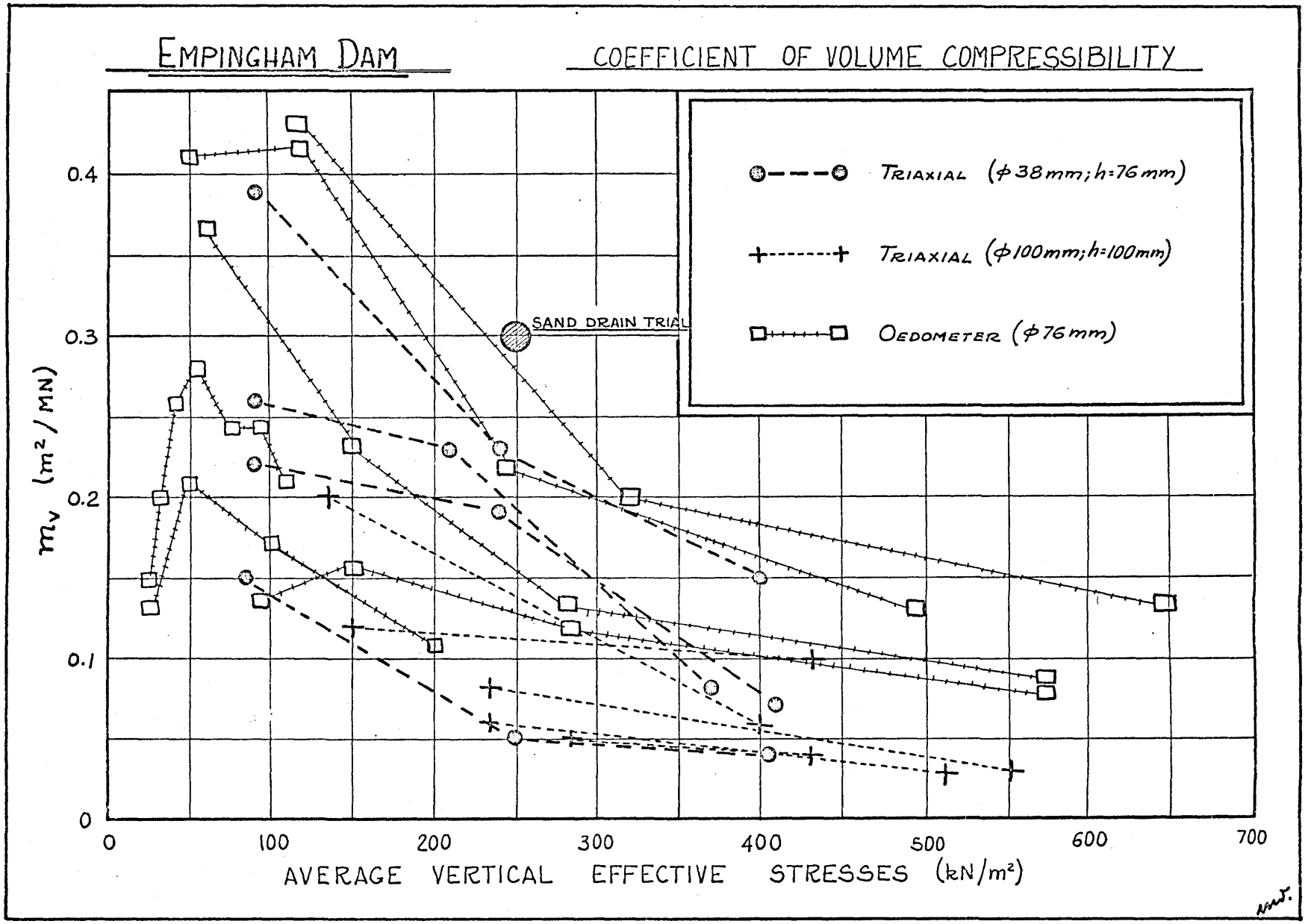


FIG. 3.14

FIG. 3.14

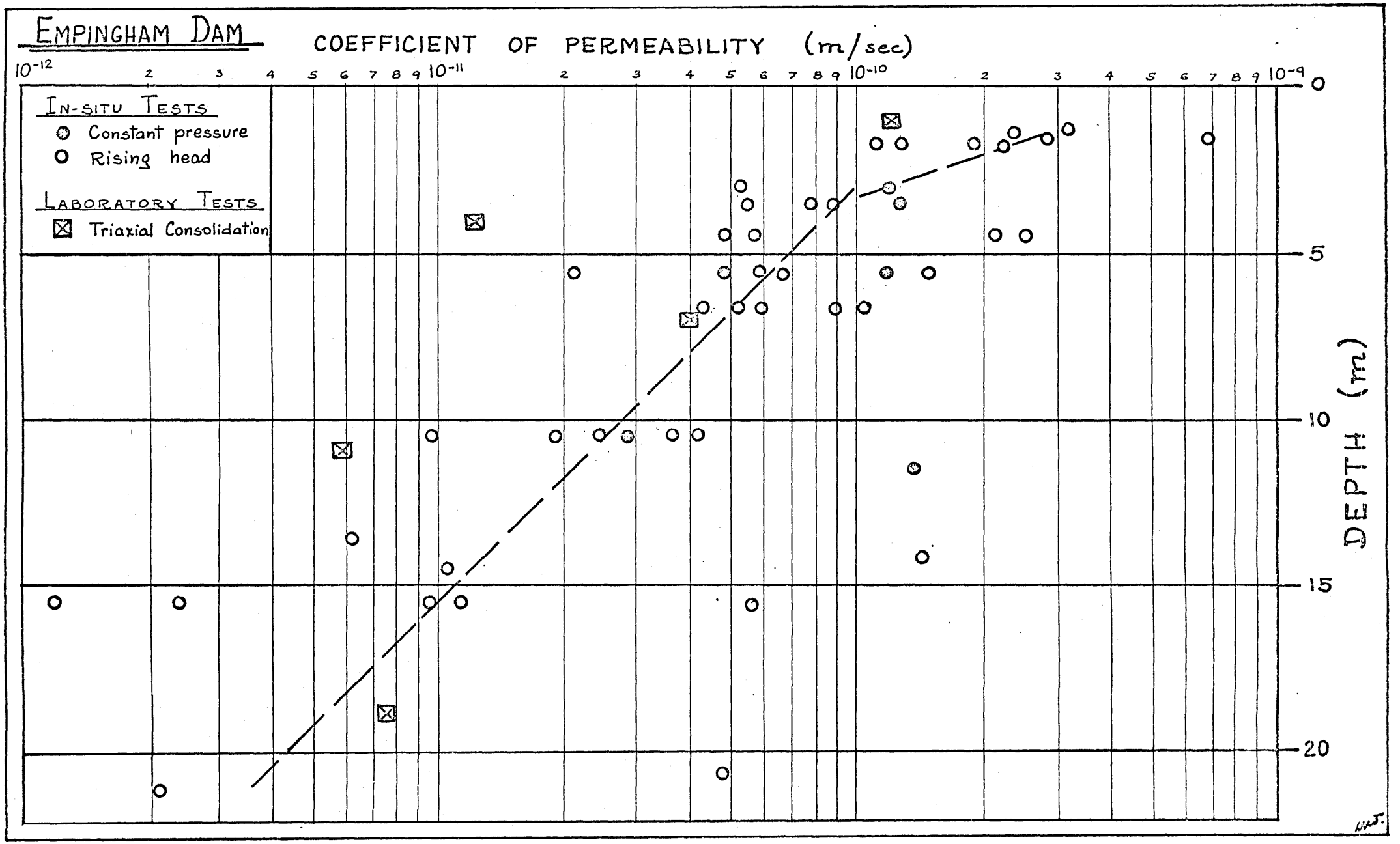


FIG. 3.15

FIG. 3.15

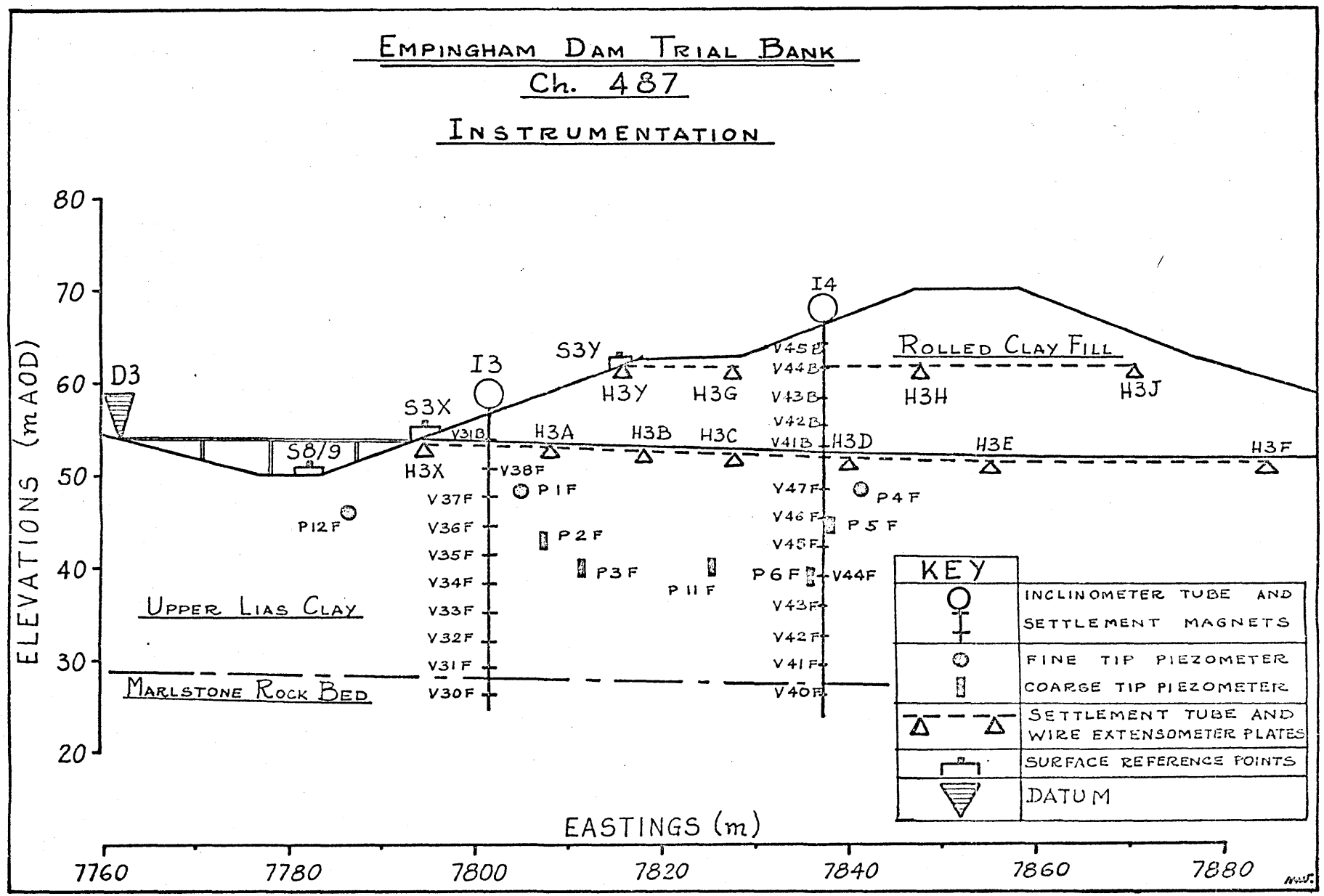

EMPINGHAM DAM TRIAL BANK
Ch. 487
INSTRUMENTATION
ELEVATIONS (mAOD)
80
70
60
50
40
30
20
EASTINGS (m)
7760
7780
7800
7820
7840
7860
7880
D3
S8/9
S3X
I3
S3Y
I4
H3X
H3Y
H3G
H3A
H3B
H3C
H3D
H3H
H3E
H3F
H3J
ROLLED CLAY FILL
UPPER LIAS CLAY
MARLSTONE ROCK BED
V31B
V38F
V37F
V36F
V35F
V34F
V33F
V32F
V31F
V30F
V45B
V44B
V43B
V42B
V41B
V47F
V46F
V45F
V44F
V43F
V42F
V41F
V40F
P1F
P2F
P3F
P11F
P6F
P4F
P5F
P12F
KEY
INCLINOMETER TUBE AND SETTLEMENT MAGNETS
FINE TIP PIEZOMETER
COARSE TIP PIEZOMETER
SETTLEMENT TUBE AND WIRE EXTENSOMETER PLATES
SURFACE REFERENCE POINTS
DATUM

FIG. 4.1

FIG. 4.1

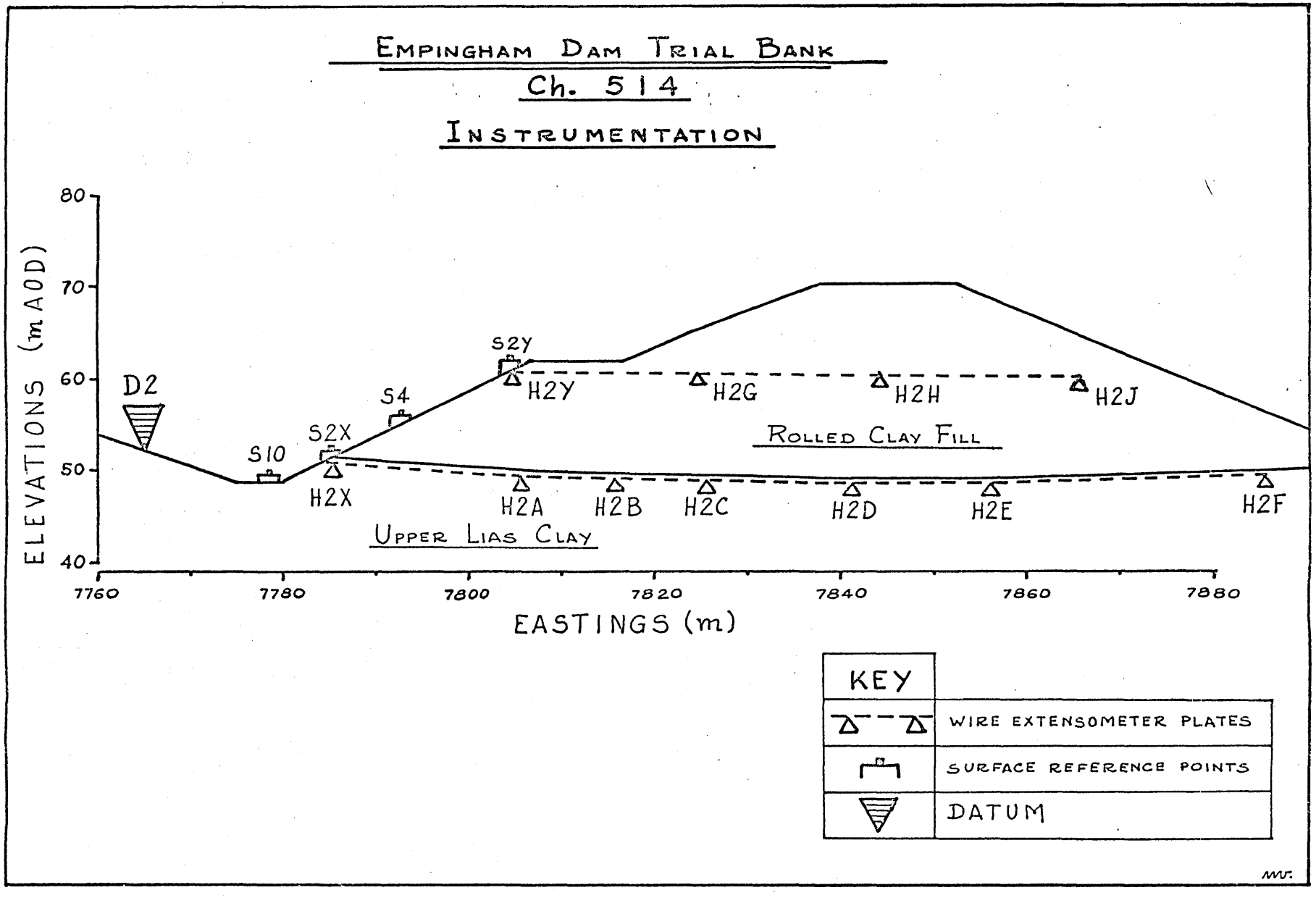

EMPINGHAM DAM TRIAL BANK
Ch. 514
INSTRUMENTATION
ELEVATIONS (mAOD)
80
70
60
50
40
D2
S10
S2X
S4
S2Y
H2X
H2Y
H2A
H2B
H2C
H2D
H2E
H2F
H2G
H2H
H2J
ROLLED CLAY FILL
UPPER LIAS CLAY
7760
7780
7800
7820
7840
7860
7880
EASTINGS (m)
KEY
WIRE EXTENSOMETER PLATES
SURFACE REFERENCE POINTS
DATUM
MV.

FIG. 4.2

FIG. 4.2

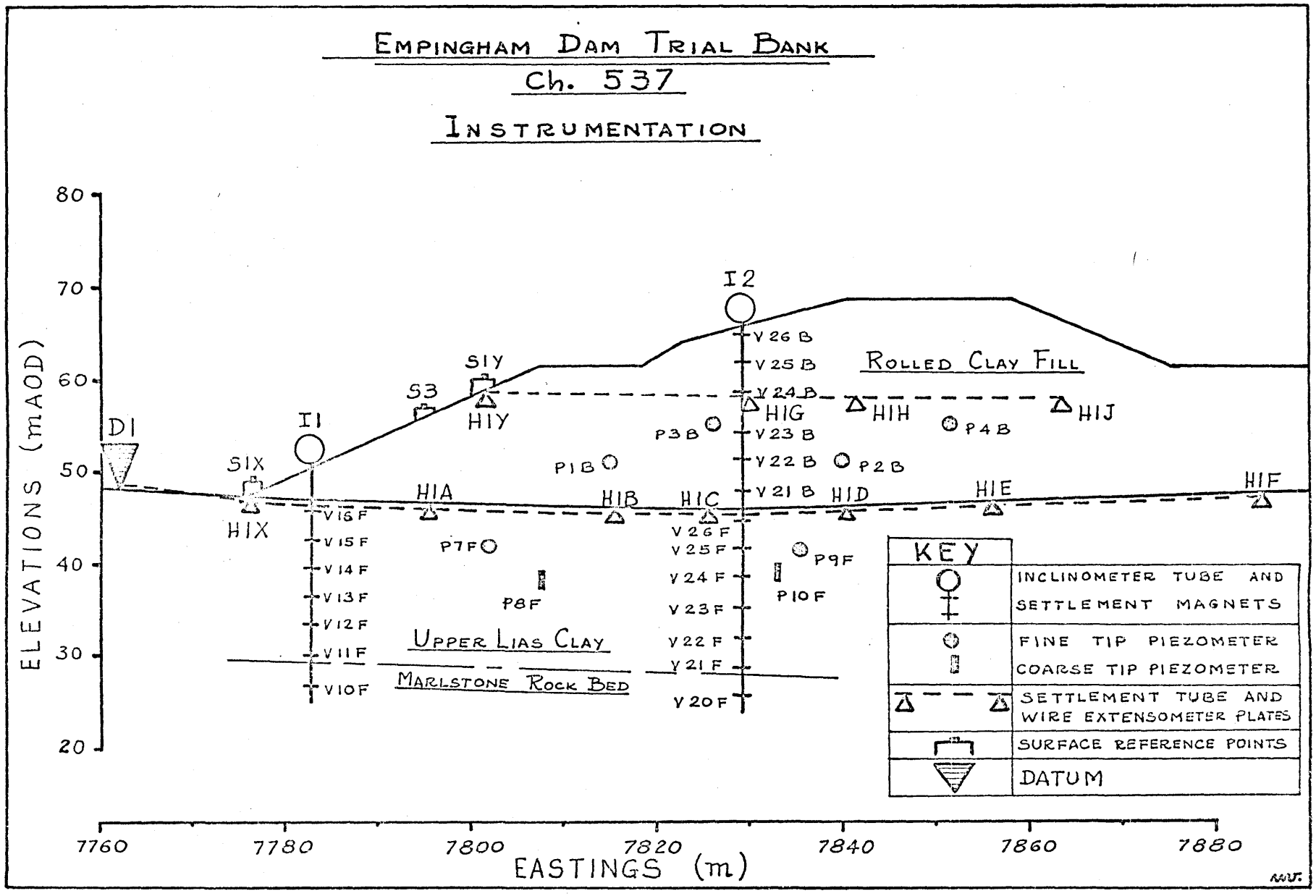

EMPINGHAM DAM TRIAL BANK
Ch. 537
INSTRUMENTATION
ELEVATIONS (mAOD)
80
70
60
50
40
30
20
EASTINGS (m)
7760
7780
7800
7820
7840
7860
7880
D1
I1
I2
S1X
S1Y
S3
H1X
H1Y
H1A
H1B
H1C
H1D
H1E
H1F
H1G
H1H
H1J
V16F
V15F
V14F
V13F
V12F
V11F
V10F
V26B
V25B
V24B
V23B
V22B
V21B
V26F
V25F
V24F
V23F
V22F
V21F
V20F
P1B
P2B
P3B
P4B
P7F
P8F
P9F
P10F
ROLLED CLAY FILL
UPPER LIAS CLAY
MARLSTONE ROCK BED
KEY
INCLINOMETER TUBE AND SETTLEMENT MAGNETS
FINE TIP PIEZOMETER
COARSE TIP PIEZOMETER
SETTLEMENT TUBE AND WIRE EXTENSOMETER PLATES
SURFACE REFERENCE POINTS
DATUM

FIG. 4.3

FIG. 4.3

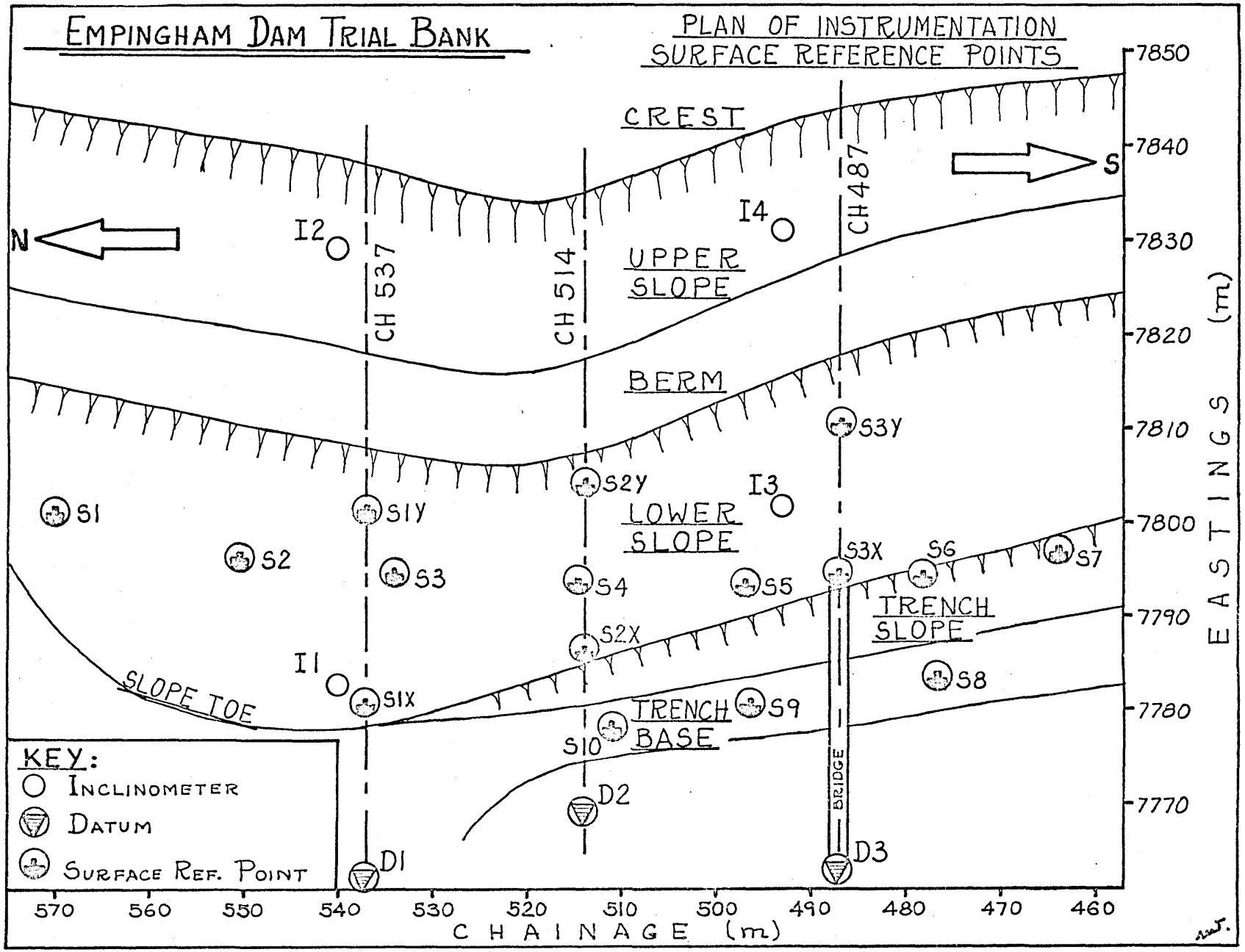

EMPINGHAM DAM TRIAL BANK
PLAN OF INSTRUMENTATION
SURFACE REFERENCE POINTS
CREST
UPPER SLOPE
BERM
LOWER SLOPE
TRENCH SLOPE
TRENCH BASE
SLOPE TOE
N
S
I1
I2
I3
I4
CH 537
CH 514
CH 487
S1
S1Y
S2
S2Y
S2X
S3
S3Y
S3X
S4
S5
S6
S7
S8
S9
S10
S1X
D1
D2
D3
BRIDGE
KEY:
INCLINOMETER
DATUM
SURFACE REF. POINT
7850
7840
7830
7820
7810
7800
7790
7780
7770
EASTINGS (m)
570
560
550
540
530
520
510
500
490
480
470
460
CHAINAGE (m)

FIG. 4.4

FIG. 4.4

HYDRAULIC SETTLEMENT GAUGE

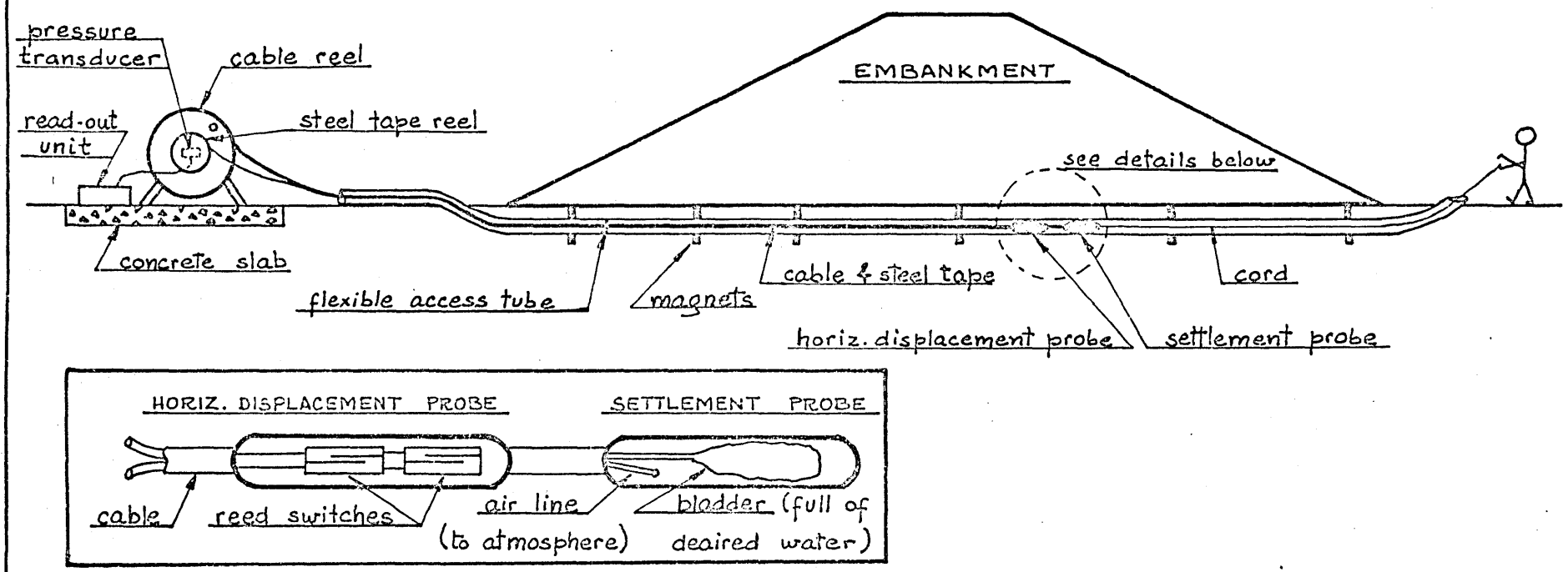


FIG. 5.1

FIG. 5.1

EMPINGHAM DAM TRIAL BANK

FACE ERROR DISTRIBUTIONS IN INITIAL READINGS

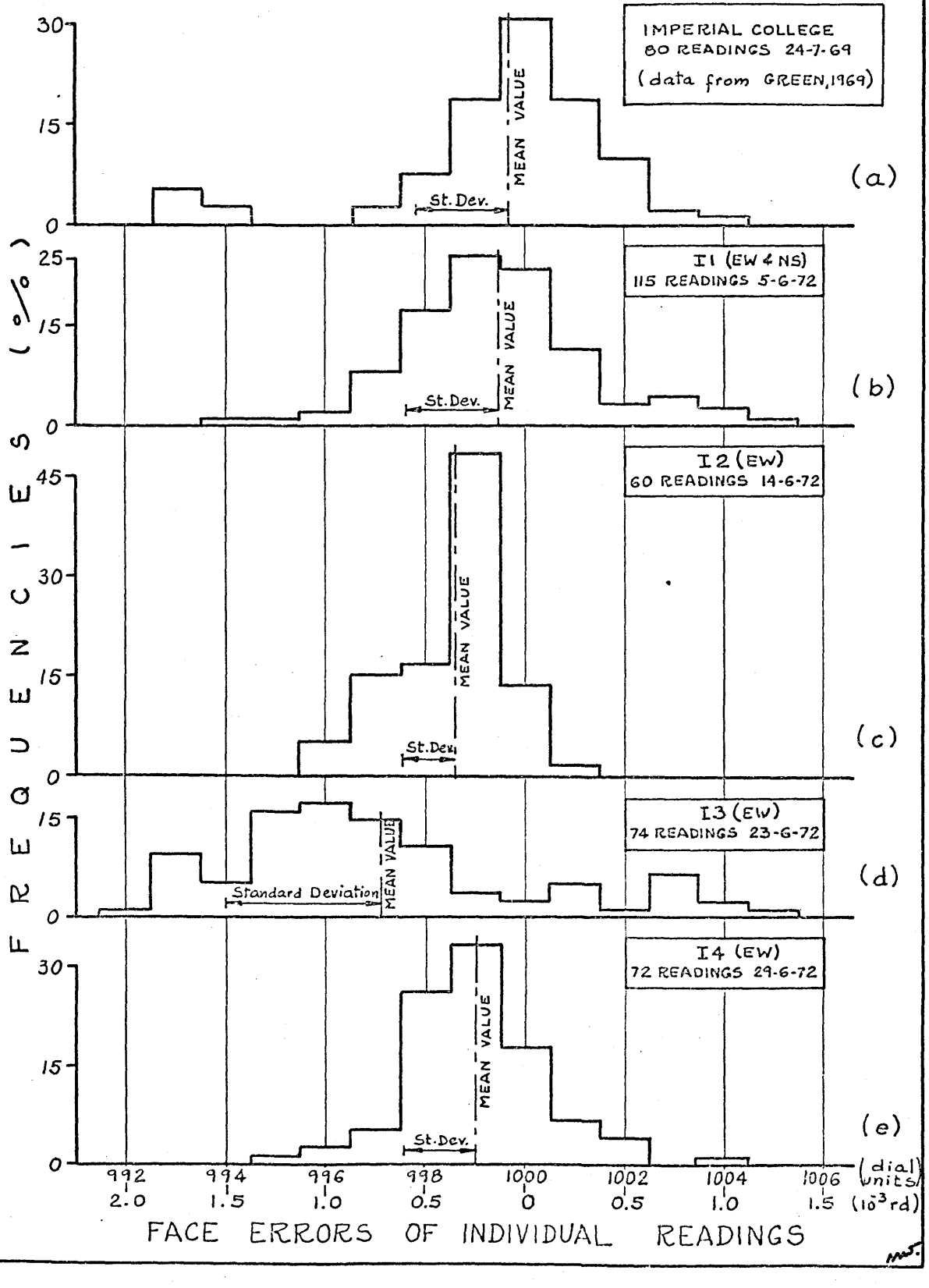


FIG. 6.1

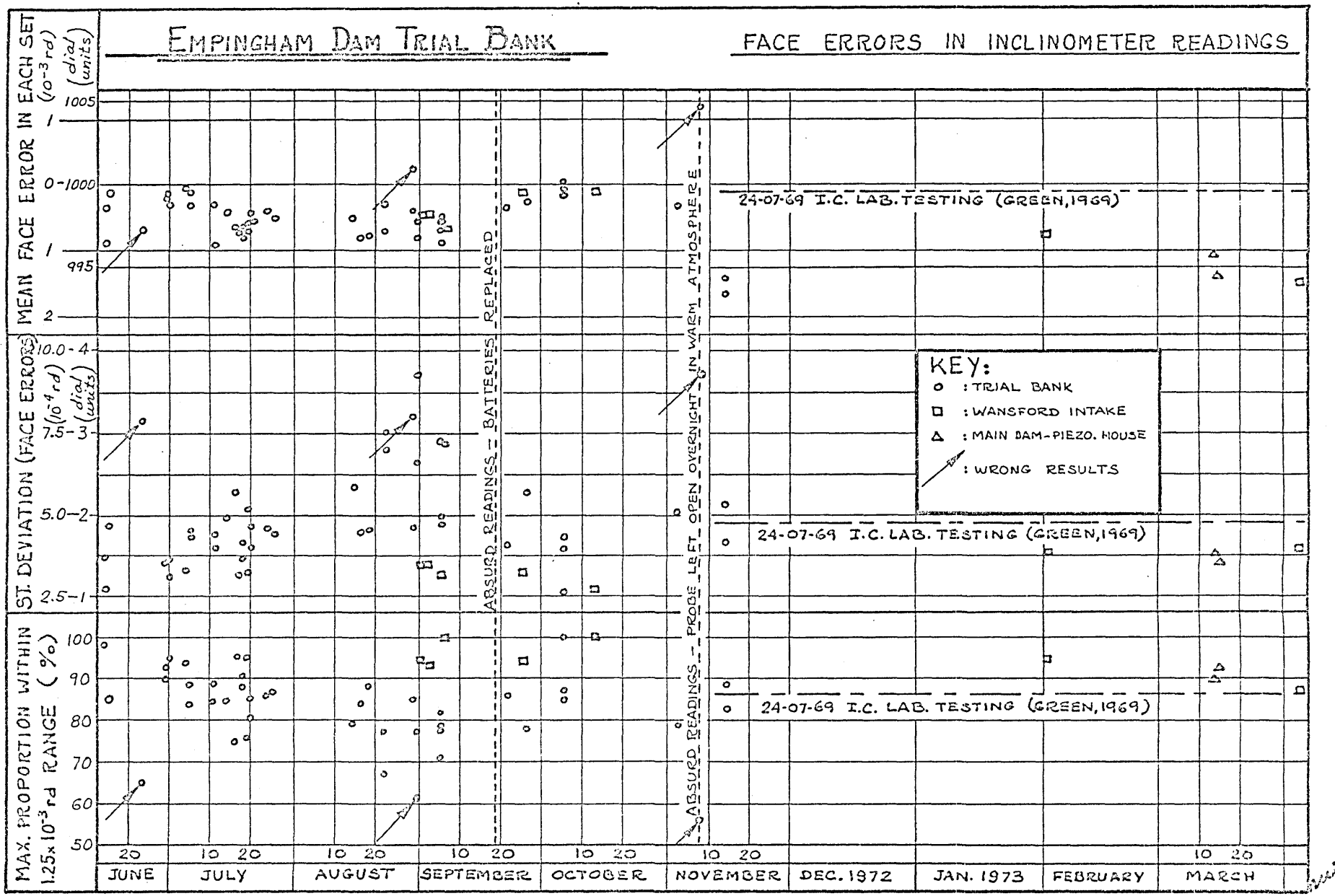

EMPINGHAM DAM TRIAL BANK
FACE ERRORS IN INCLINOMETER READINGS
MEAN FACE ERROR IN EACH SET (10^{-3} rd) (dial units)
1005
1
0-1000
1
995
2
ST. DEVIATION (FACE ERRORS) (10^{-4} rd) (dial units)
10.0 - 4
7.5 - 3
5.0 - 2
2.5 - 1
MAX. PROPORTION WITHIN 1.25 x 10^{-3} rd RANGE (%)
100
90
80
70
60
50
ABSURD READINGS - BATTERIES REPLACED
ABSURD READINGS - PROBE LEFT OPEN OVERNIGHT IN WARM ATMOSPHERE
24-07-69 I.C. LAB. TESTING (GREEN, 1969)
24-07-69 I.C. LAB. TESTING (GREEN, 1969)
24-07-69 I.C. LAB. TESTING (GREEN, 1969)
KEY:
o : TRIAL BANK
□ : WANSFORD INTAKE
△ : MAIN DAM-PIEZO. HOUSE
: WRONG RESULTS
20
10 20
10 20
10 20
10 20
10 20
JUNE
JULY
AUGUST
SEPTEMBER
OCTOBER
NOVEMBER
DEC. 1972
JAN. 1973
FEBRUARY
10 20
MARCH

FIG. 6.2

FIG. 6.2

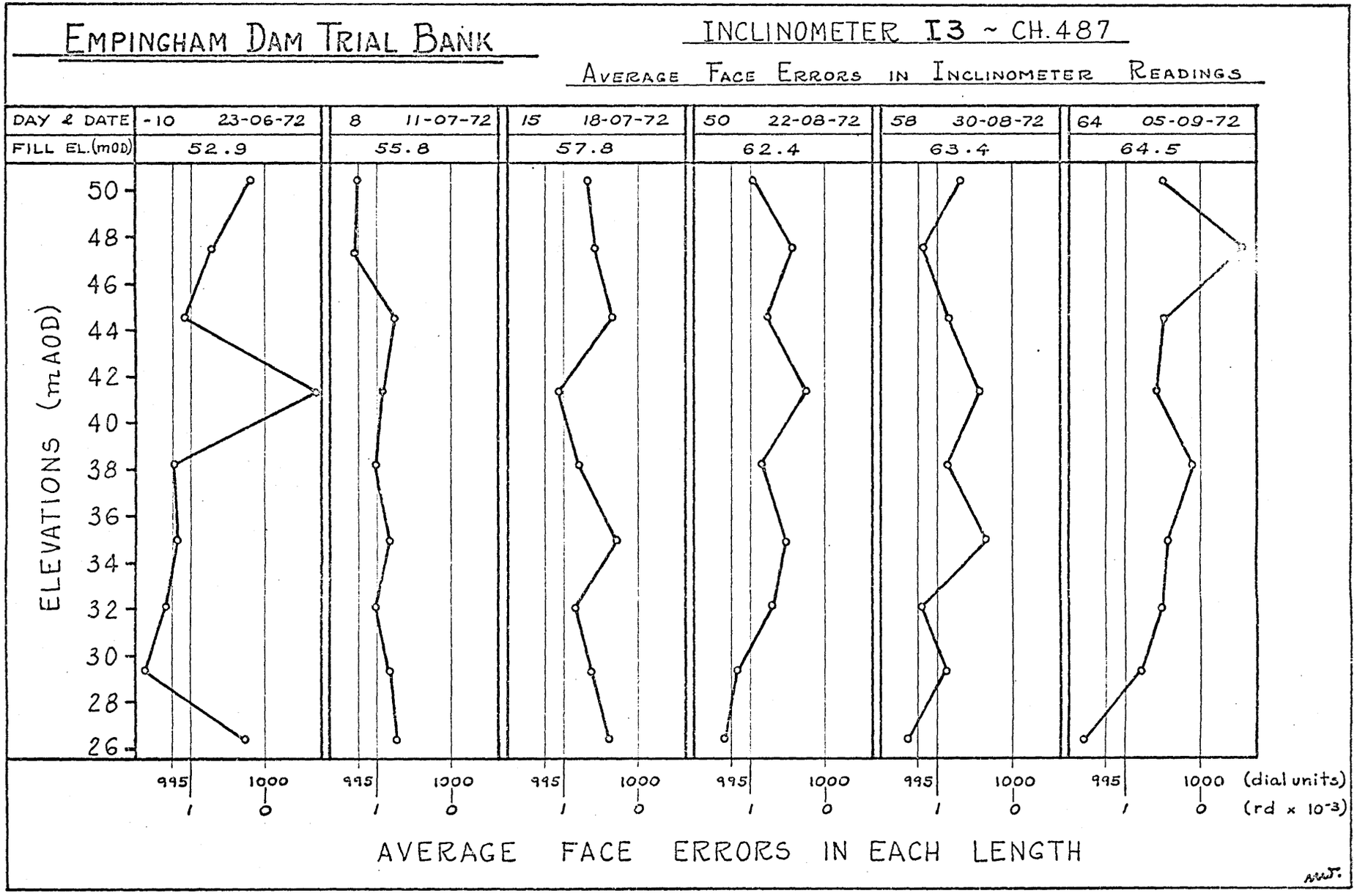

EMPINGHAM DAM TRIAL BANK
INCLINOMETER I3 ~ CH.487
AVERAGE FACE ERRORS IN INCLINOMETER READINGS
DAY & DATE
-10 23-06-72
8 11-07-72
15 18-07-72
50 22-08-72
58 30-08-72
64 05-09-72
FILL EL.(mOD)
52.9
55.8
57.8
62.4
63.4
64.5
ELEVATIONS (mAOD)
50
48
46
44
42
40
38
36
34
32
30
28
26
995
1000
(dial units)
(rd x 10⁻³)
AVERAGE FACE ERRORS IN EACH LENGTH

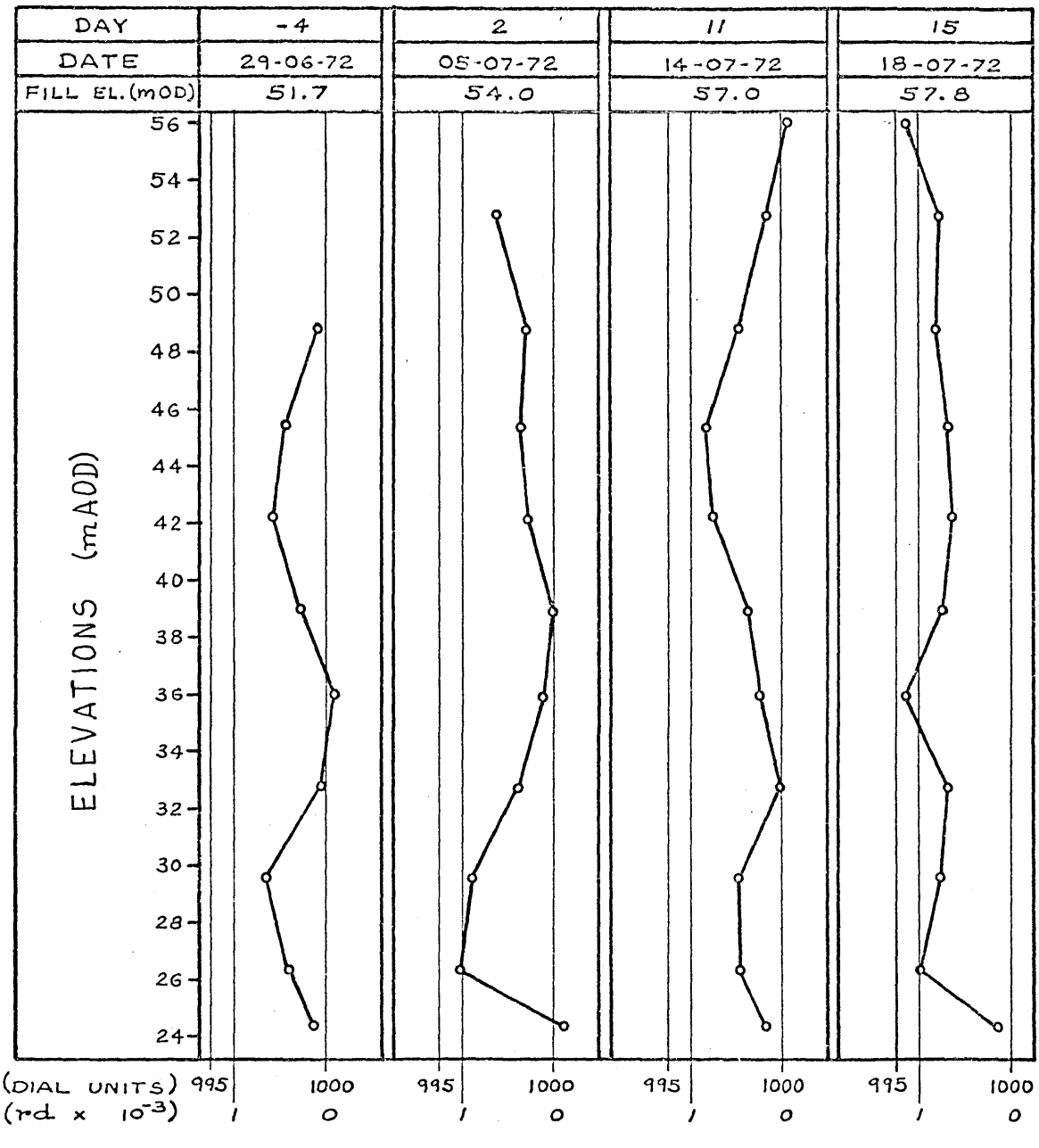
FIG. 6.3

FIG. 6.3

EMPINGHAM DAM TRIAL BANK

INCLINOMETER I4 ~ CH.487

AVERAGE FACE ERRORS IN INCLINOMETER READINGS



AVERAGE FACE ERRORS IN EACH LENGTH

FIG. 6.4

EMPINGHAM DAM TRIAL BANK

INCLINOMETER I4 ~ CH 487

AVERAGE FACE ERRORS IN INCLINOMETER READINGS

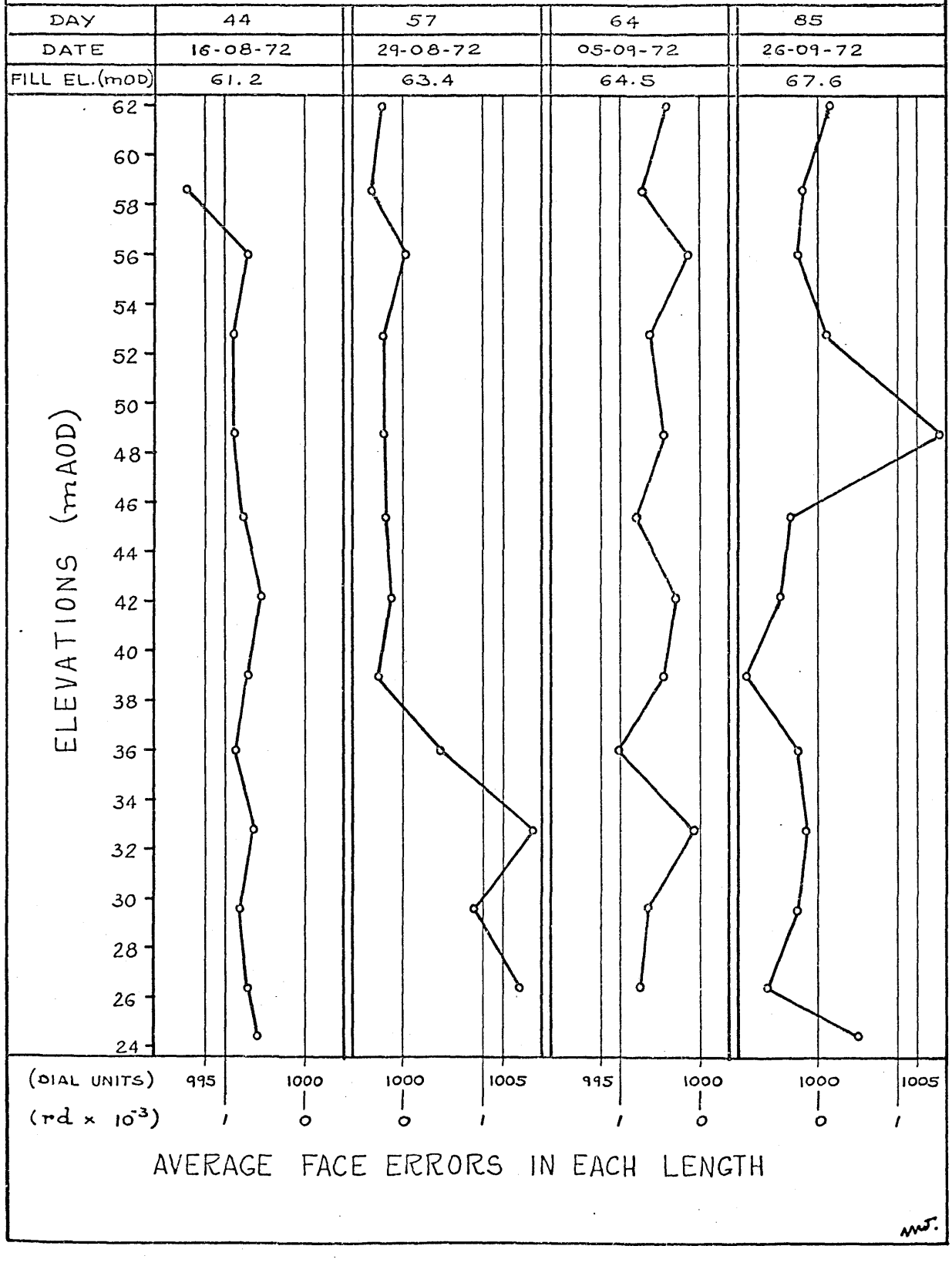


FIG. 6.5

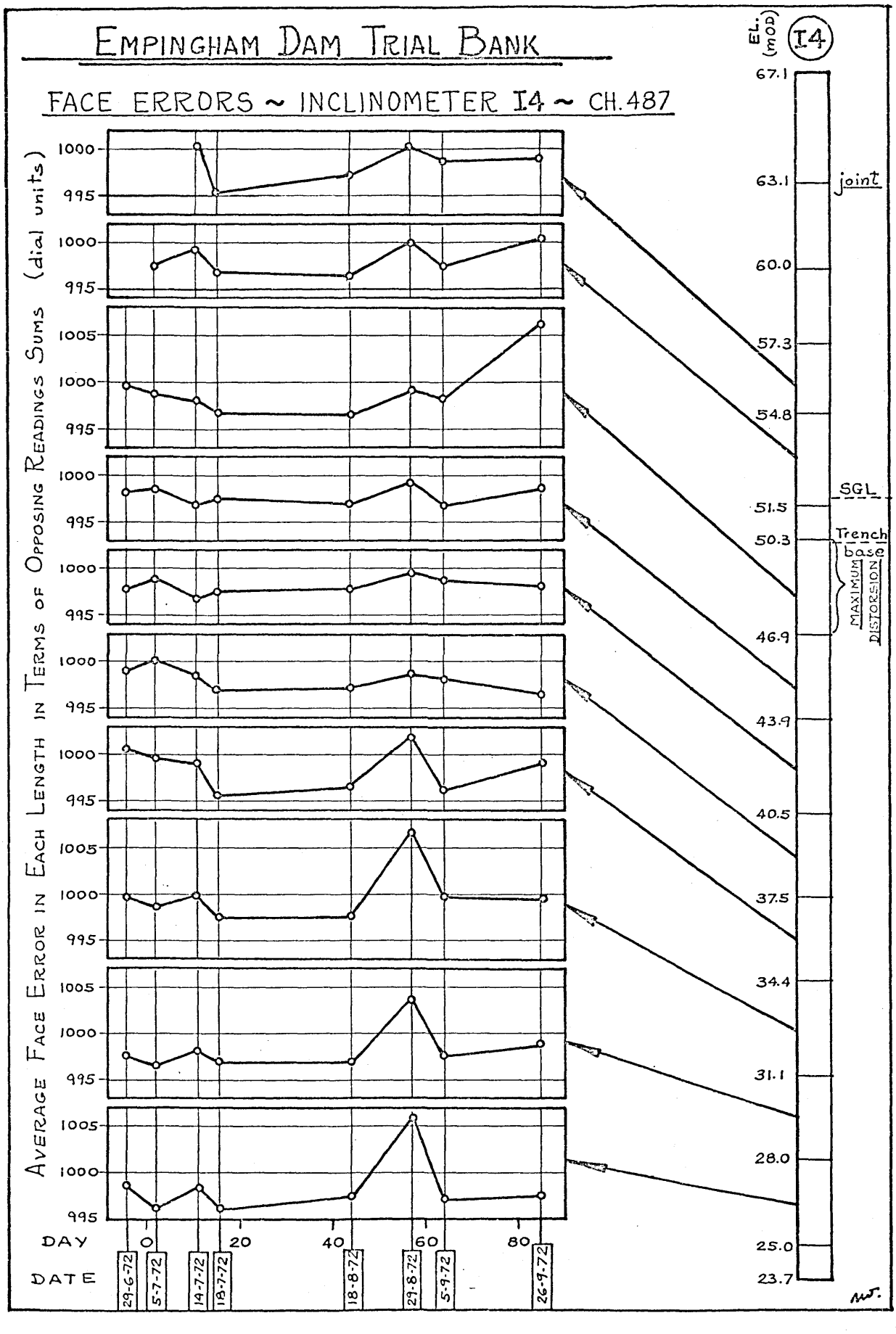

EMPINGHAM DAM TRIAL BANK
FACE ERRORS ~ INCLINOMETER I4 ~ CH.487
AVERAGE FACE ERROR IN EACH LENGTH IN TERMS OF OPPOSING READINGS SUMS (dial units)
1000
995
1005
DAY
0
20
40
60
80
DATE
29-6-72
5-7-72
14-7-72
18-7-72
18-8-72
29-8-72
5-9-72
26-9-72
EL. (mOD)
I4
67.1
63.1
joint
60.0
57.3
54.8
SGL
51.5
50.3
Trench
MAXIMUM OF DISTORSION
46.9
43.9
40.5
37.5
34.4
31.1
28.0
25.0
23.7

FIG. 6.6

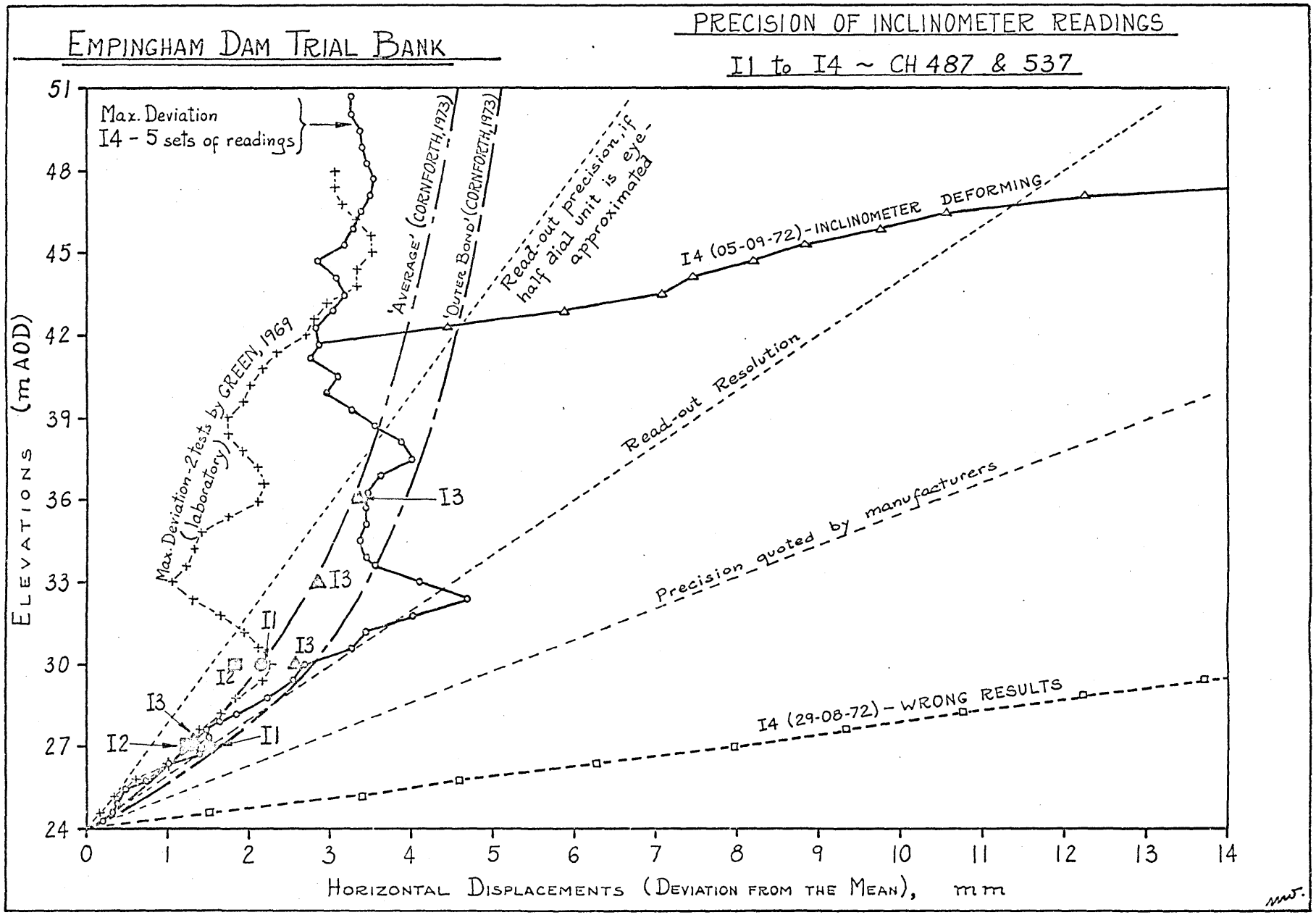

EMPINGHAM DAM TRIAL BANK
PRECISION OF INCLINOMETER READINGS
I1 to I4 ~ CH 487 & 537
Max. Deviation
I4 - 5 sets of readings
'AVERAGE' (CORNFORTH, 1973)
'OUTER BOND' (CORNFORTH, 1973)
Read-out precision, if half dial unit is eye-approximated
I4 (05-09-72) - INCLINOMETER DEFORMING
Max. Deviation - 2 tests by GREEN, 1969 (Laboratory)
Read-out Resolution
Precision quoted by manufacturers
I4 (29-08-72) - WRONG RESULTS
I1
I2
I3
ΔI3
ELEVATIONS (m AOD)
HORIZONTAL DISPLACEMENTS (DEVIATION FROM THE MEAN), mm
51
48
45
42
39
36
33
30
27
24
0
1
2
3
4
5
6
7
8
9
10
11
12
13
14

FIG. 6.7

FIG. 6.7

EMPINGHAM DAM TRIAL BANK

TILTING ANGLES

I3 ~ CH 487

(11-07-72 & 05-09-72)

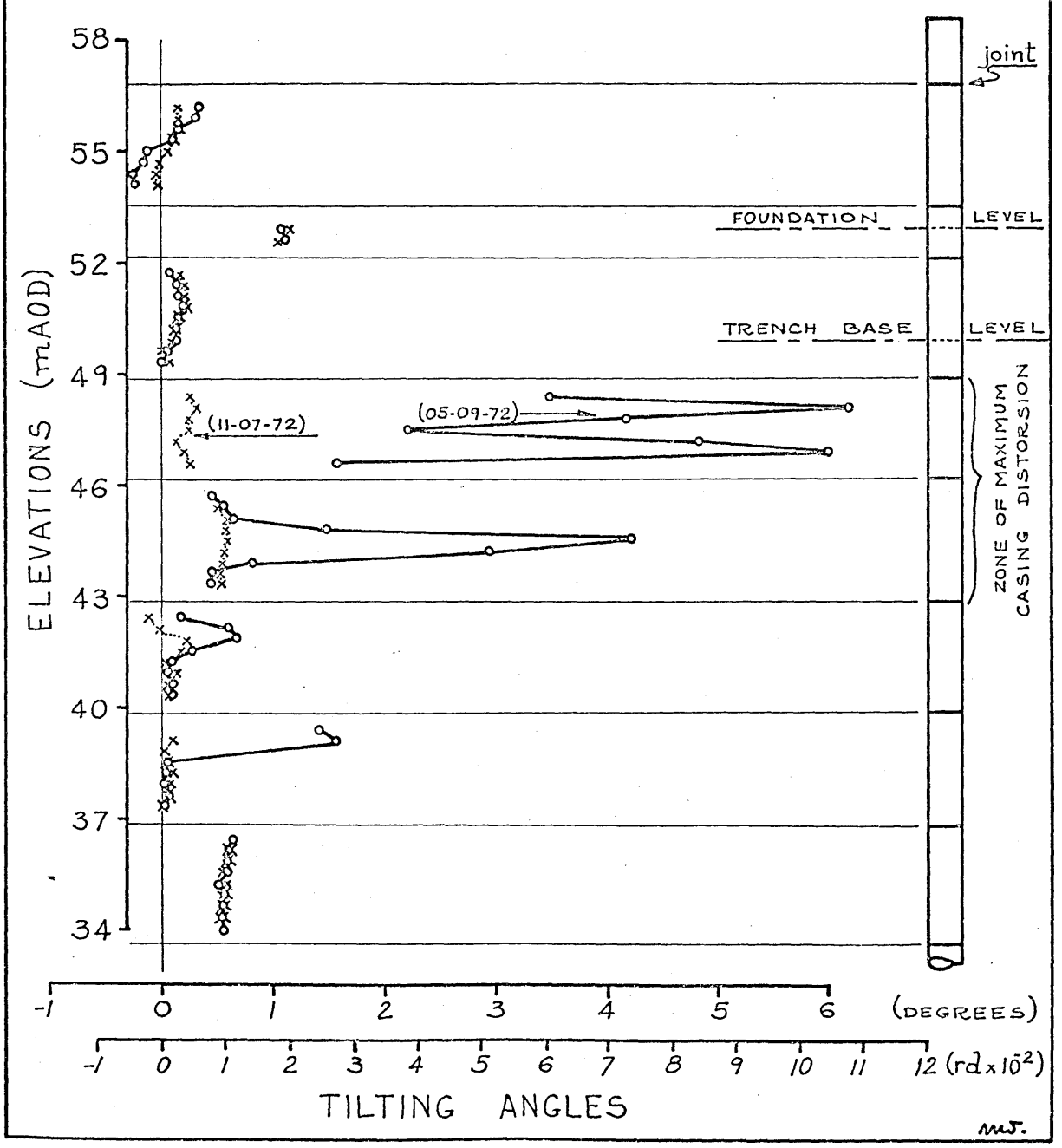
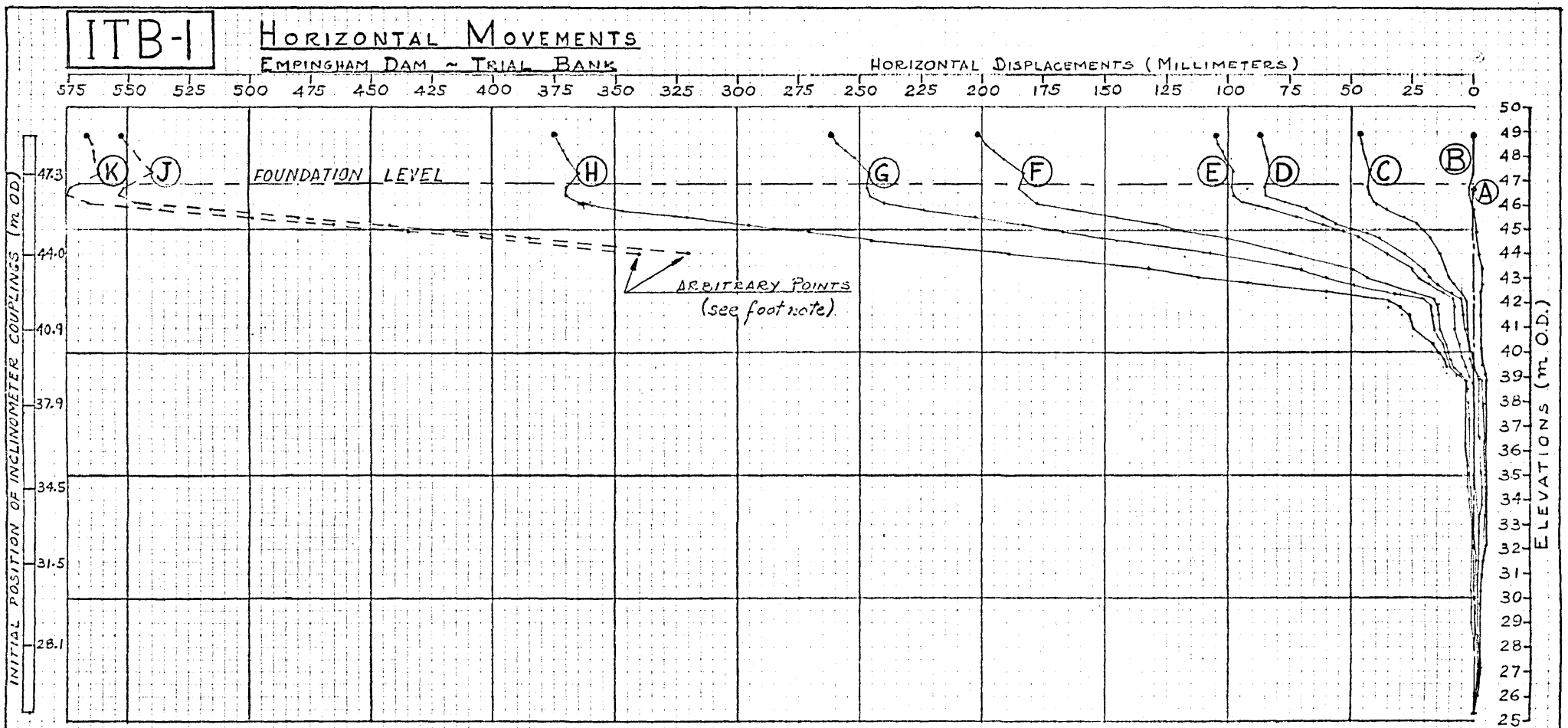


FIG. 6.8



CURVE	DATE	DAY	FILL ELEVATION (m OD)
A	15-06-72	-18	46.9
B	05-07-72	2	50.5
C	11-07-72	8	55.9
D	19-07-72	16	57.6
E	26-07-72	23	57.6

CURVE	DATE	DAY	FILL ELEVATION (m OD)
F	14-08-72	42	60.4
G	22-08-72	50	60.9
H	05-09-72	64	63.4
J	05-10-72	94	68.6
K	02-11-72	122	68.6

Note: Readings J and K were taken after casing had become so distorted that the inclinometer torpedo could not reach the bottom. Therefore, curves J and K are mere estimates based on arbitrarily chosen initial lower points at elevation 44 m OD

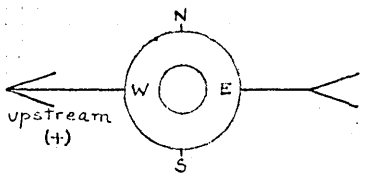


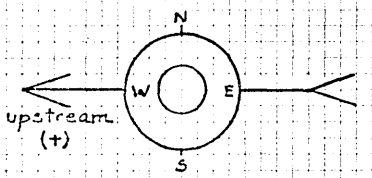
FIG. 6.9

FIG. 6.9

ITB-2

HORIZONTAL MOVEMENTS

EMPINGHAM DAM ~ TRIAL BANK



CURVE	DATE	DAY	FILL ELEVATION (m OD)
A	14-06-72	-19	46.2
B	04-07-72	1	48.2
C	17-07-72	14	57.6
D	18-08-72	46	60.4
E	29-08-72	57	62.6
F	05-09-72	64	63.4
G	21-09-72	80	65.2
H	05-10-72	94	68.6
J	15-11-72	135	68.6

HORIZONTAL DISPLACEMENTS (MILLIMETERS)

450 425 400 375 350 325 300 275 250 225 200 175 150 125 100 75 50 25 0

INITIAL POSITION OF INCLINOMETER COUPLINGS (m OD)

63.0 60.0 56.4 55.7 52.3 49.3 46.2 42.9 39.8 36.5 33.4 30.1 27.0

ELEVATIONS (m OD)

66 65 64 63 62 61 60 59 58 57 56 55 54 53 52 51 50 49 48 47 46 45 44 43 42 41 40 39 38 37 36 35 34 33 32 31 30 29 28 27 26 25 24

FOUNDATION LEVEL

ARBRITARY POINTS
(see Note)

Note: Readings G, H and J were taken after casing had become so distorted that the inclinometer torpedo could not reach the bottom. Therefore, curves G, H and J are mere estimates based on arbitrarily chosen initial lower points around elevations 42/43 m O.D.

FIG. 6.10

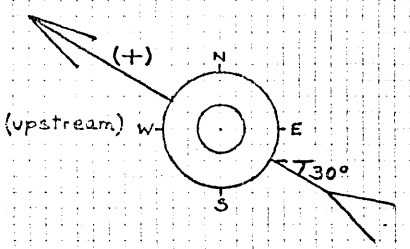
FIG. 6.10

ITB-3

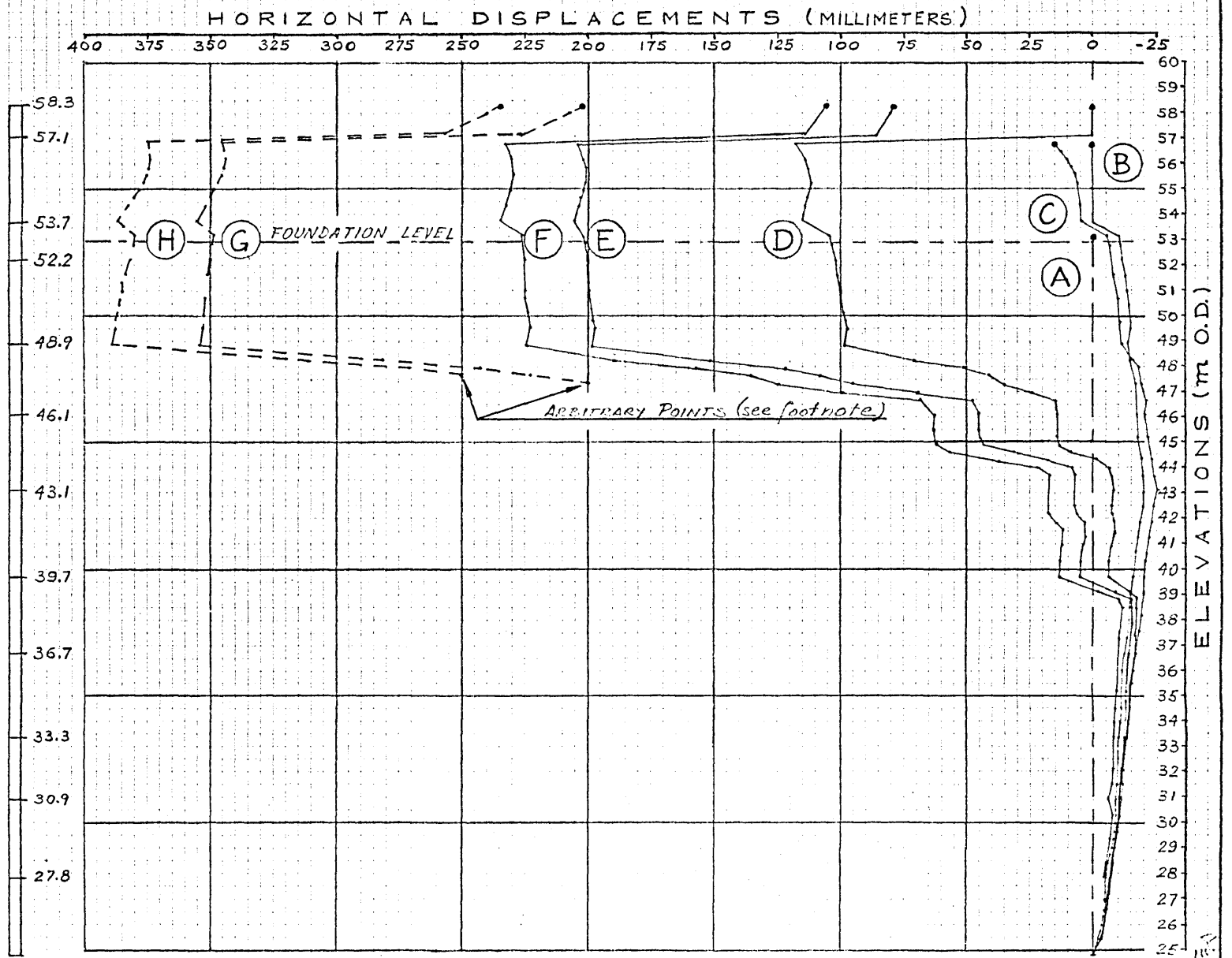
Horizontal Movements

Empingham Dam

Trial Bank



CURVE	DATE	DAY	FILL ELEVATION (m O.D.)
A	23-06-72	-10	52.9
B	11-07-72	8	55.8
C	18-07-72	15	57.8
D	22-08-72	50	62.4
E	30-08-72	58	63.4
F	05-09-72	64	64.5
G	05-10-72	94	70.2
H	02-11-72	122	70.2



NOTE: Readings G and H were taken after casing had become so distorted that the inclinometer torpedo could not reach the bottom. Therefore, curves G and H are mere estimates based on arbitrarily chosen lower points at elevation 47.5 m O.D.

FIG. 6.11

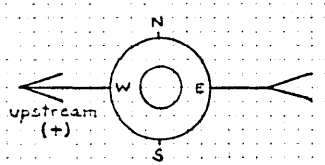
FIG. 6.11

ITB-4

HORIZONTAL MOVEMENTS

EMPINGHAM DAM

TRIAL BANK



CURVE	DATE	DAY	FILL ELEVATION (m O.D.)
A	29-06-72	-4	51.7
B	14-07-72	11	57.0
C	18-07-72	15	57.8
D	16-08-72	44	61.2
E	29-08-72	57	63.4
F	05-09-72	64	64.5
G	26-09-72	85	67.6
H	05-10-72	94	70.2
J	15-11-72	135	70.2

HORIZONTAL DISPLACEMENTS (MILLIMETERS)

400 350 300 250 200 150 100 50 0 -25

INITIAL POSITION OF INCLINOMETER COUPLINGS (m O.D.)

67.1 63.1 60.0 57.3 54.8 51.5 50.3 46.9 43.9 40.5 37.5 34.4 31.1 28.0 25.0 23.7

ELEVATIONS (m O.D.)

67 66 65 64 63 62 61 60 59 58 57 56 55 54 53 52 51 50 49 48 47 46 45 44 43 42 41 40 39 38 37 36 35 34 33 32 31 30 29 28 27 26 25 24

J H G F E D C B A

FOUNDATION LEVEL

ARBITRARY POINT (see footnote)

NOTE: Readings H and J were taken after casing had become so distorted that the inclinometer torpedo could not reach the bottom. Therefore, curves H and J are mere estimates based on arbitrarily chosen lower points around elevations 48.0/48.5 m O.D.

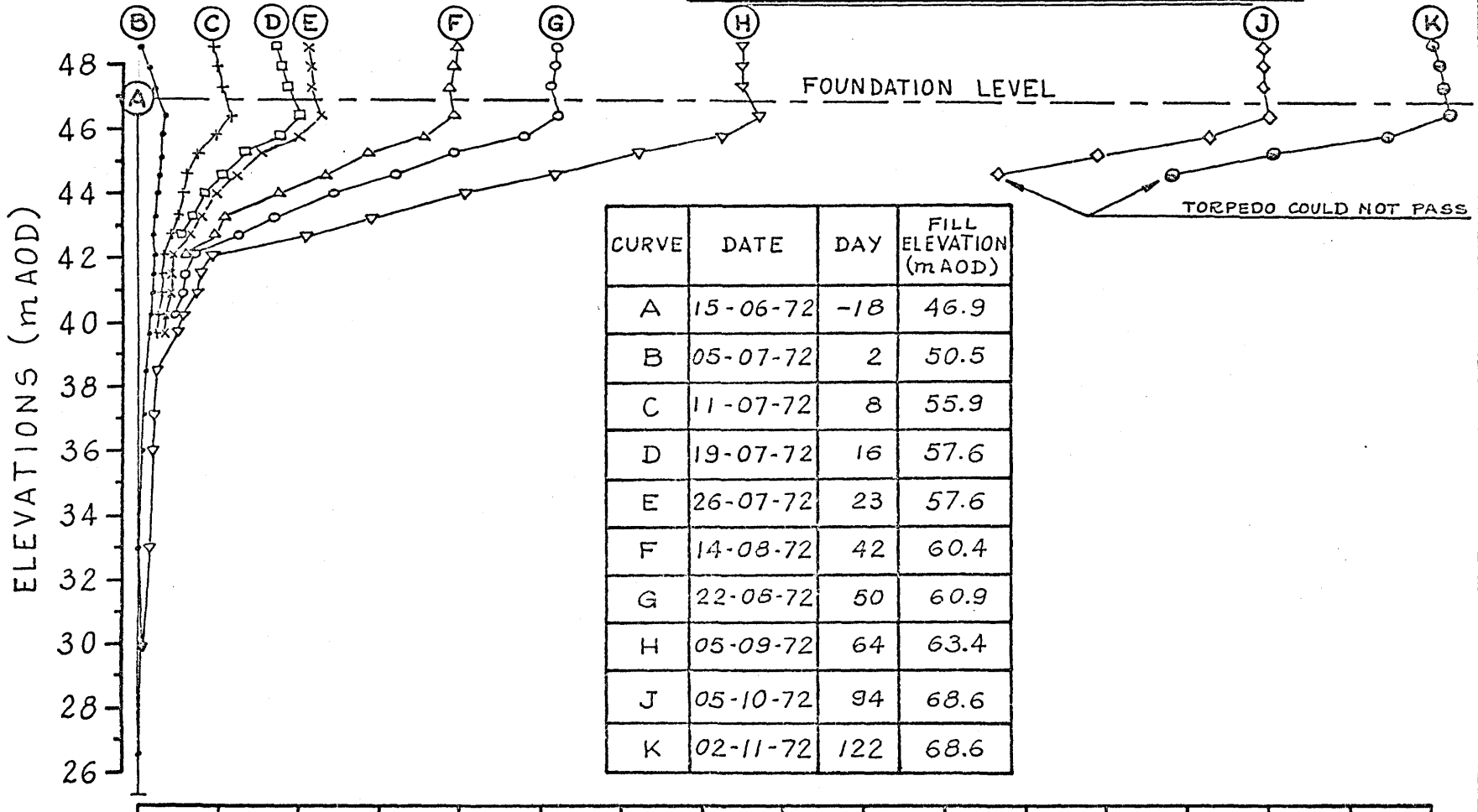
FIG. 6.12

FIG. 6.12

EMPINGHAM DAM TRIAL BANK

HORIZONTAL MOVEMENT

Ch.537 ~ INCLINOMETER I1



CURVE	DATE	DAY	FILL ELEVATION (m AOD)
A	15-06-72	-18	46.9
B	05-07-72	2	50.5
C	11-07-72	8	55.9
D	19-07-72	16	57.6
E	26-07-72	23	57.6
F	14-08-72	42	60.4
G	22-08-72	50	60.9
H	05-09-72	64	63.4
J	05-10-72	94	68.6
K	02-11-72	122	68.6

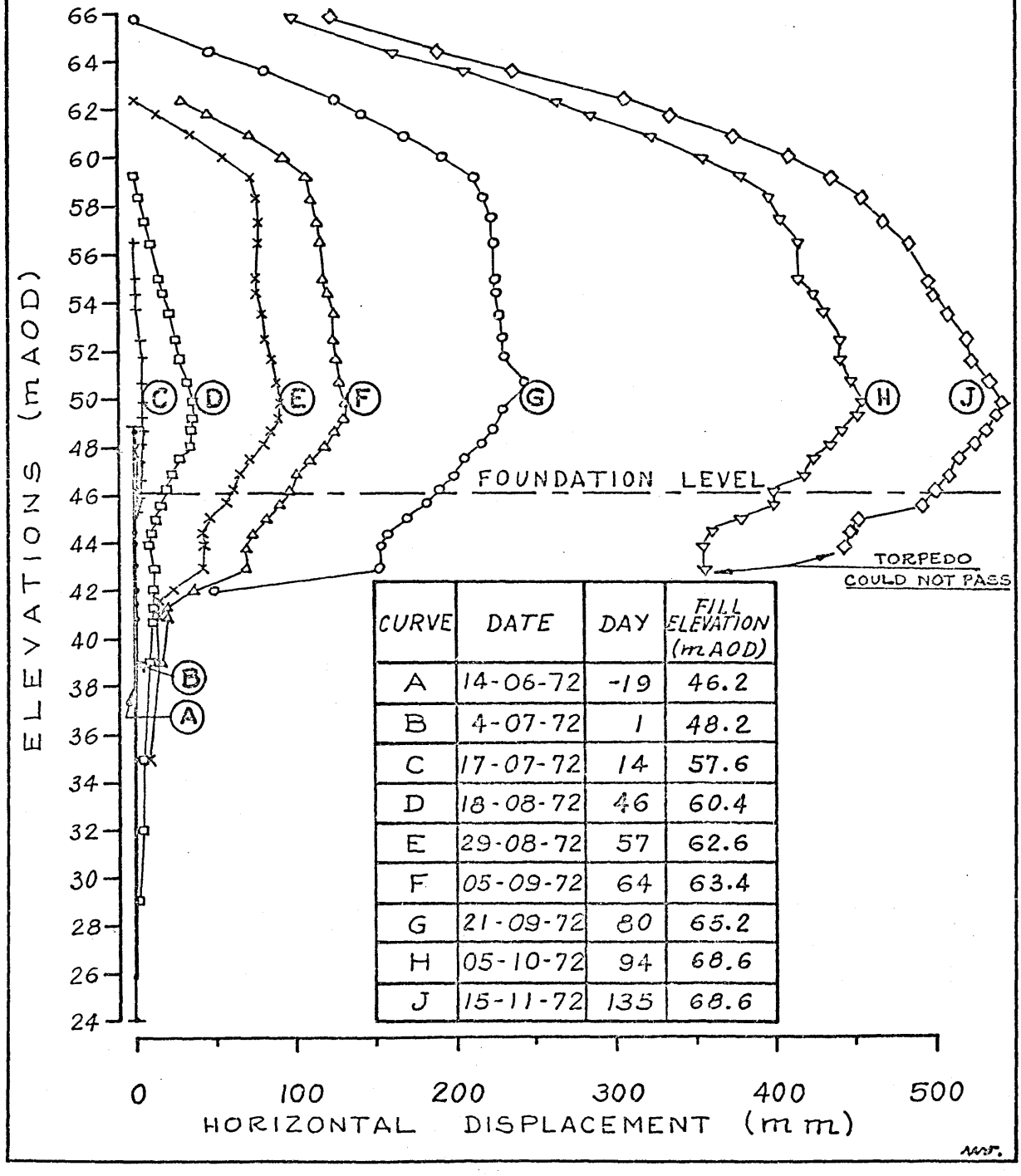
FIG. 6.13

FIG. 6.13

EMPINGHAM DAM TRIAL BANK

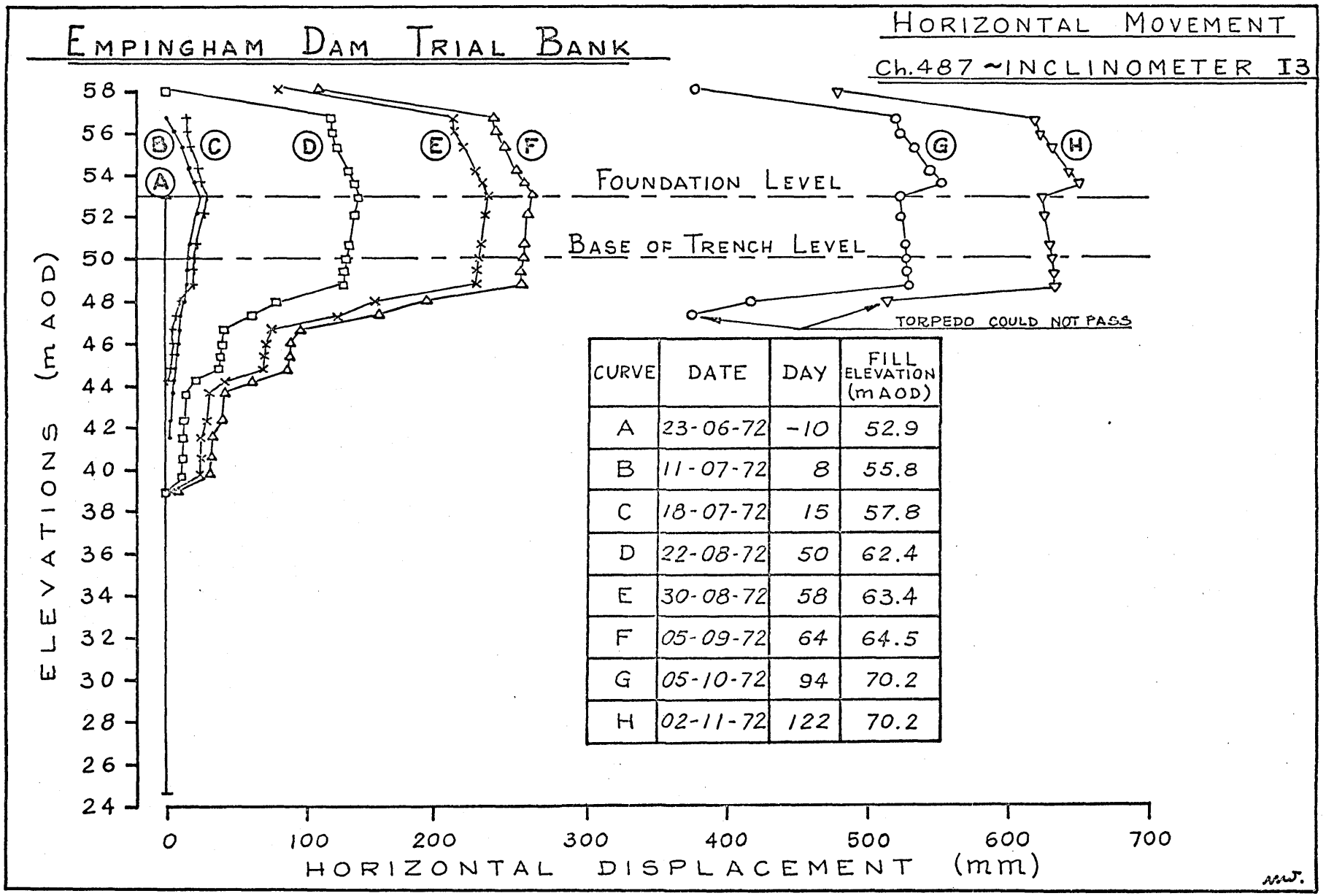
HORIZONTAL MOVEMENT

Ch.537 INCLINOMETER I2



CURVE	DATE	DAY	FILL ELEVATION (mAOD)
A	14-06-72	-19	46.2
B	4-07-72	1	48.2
C	17-07-72	14	57.6
D	18-08-72	46	60.4
E	29-08-72	57	62.6
F	05-09-72	64	63.4
G	21-09-72	80	65.2
H	05-10-72	94	68.6
J	15-11-72	135	68.6

FIG. 6.14



CURVE	DATE	DAY	FILL ELEVATION (mAOD)
A	23-06-72	-10	52.9
B	11-07-72	8	55.8
C	18-07-72	15	57.8
D	22-08-72	50	62.4
E	30-08-72	58	63.4
F	05-09-72	64	64.5
G	05-10-72	94	70.2
H	02-11-72	122	70.2

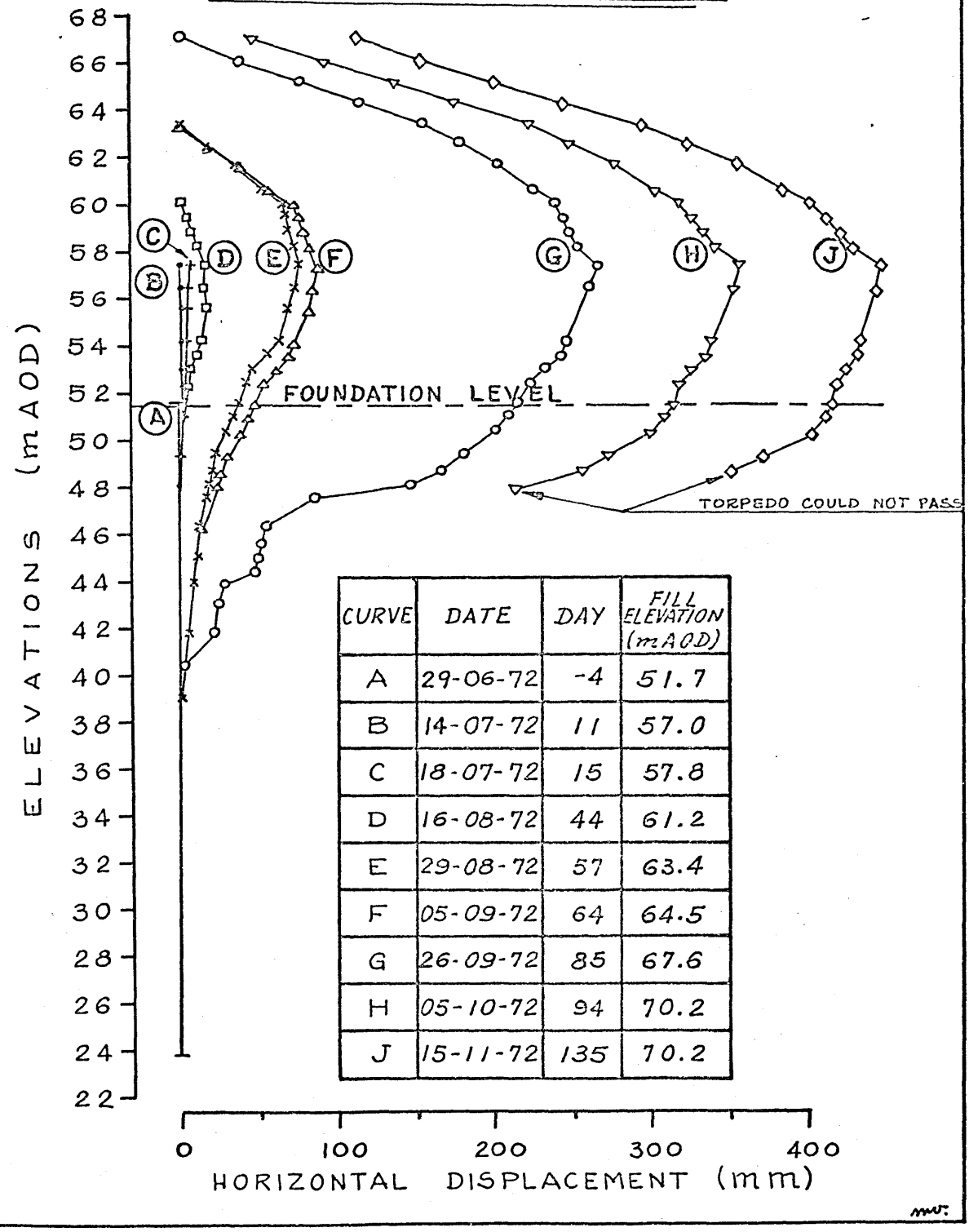
FIG. 6.15

FIG. 6.15

EMPINGHAM DAM TRIAL BANK

HORIZONTAL MOVEMENT

Ch. 487 INCLINOMETER I4



CURVE	DATE	DAY	FILL ELEVATION (mAOD)
A	29-06-72	-4	51.7
B	14-07-72	11	57.0
C	18-07-72	15	57.8
D	16-08-72	44	61.2
E	29-08-72	57	63.4
F	05-09-72	64	64.5
G	26-09-72	85	67.6
H	05-10-72	94	70.2
J	15-11-72	135	70.2

FIG. 6.16

EMPINGHAM DAM TRIAL BANK

FILL ELEVATIONS

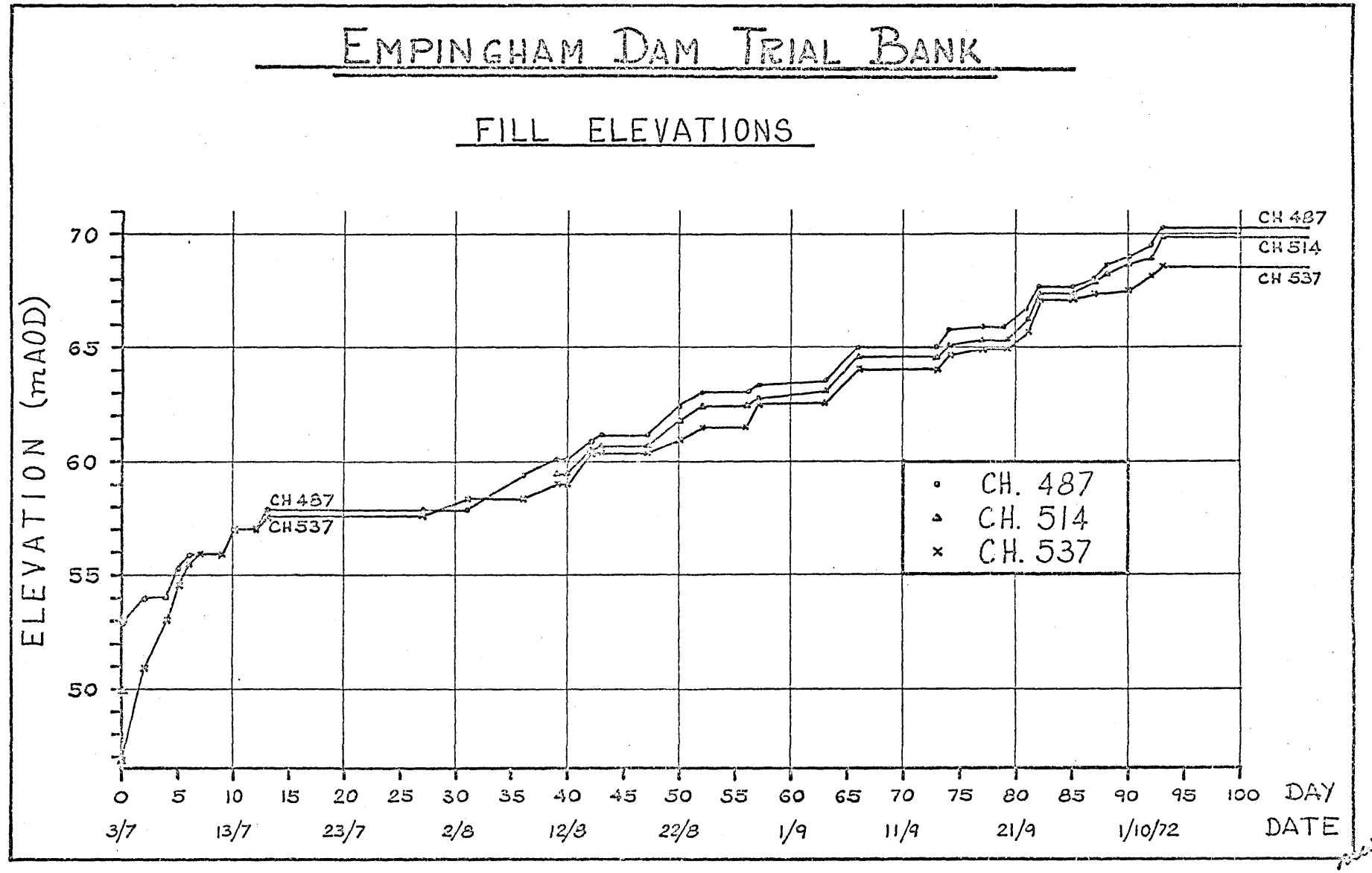


FIG. 6.17

FIG. 6.17

EMPINGHAM DAM TRIAL BANK

Ch. 487

HORIZONTAL MOVEMENT AT THE BANK TOE

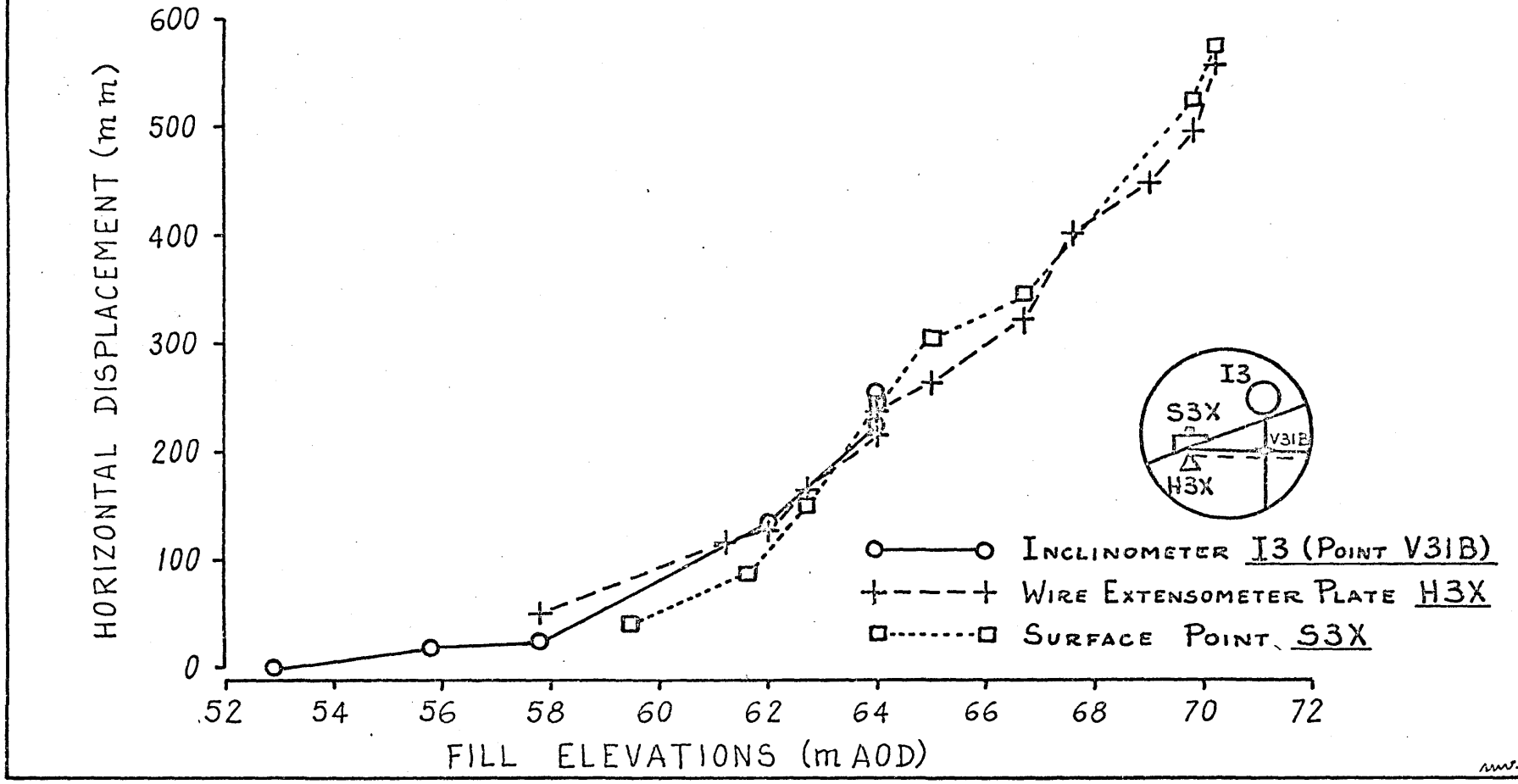


FIG. 6.18

FIG. 6.18

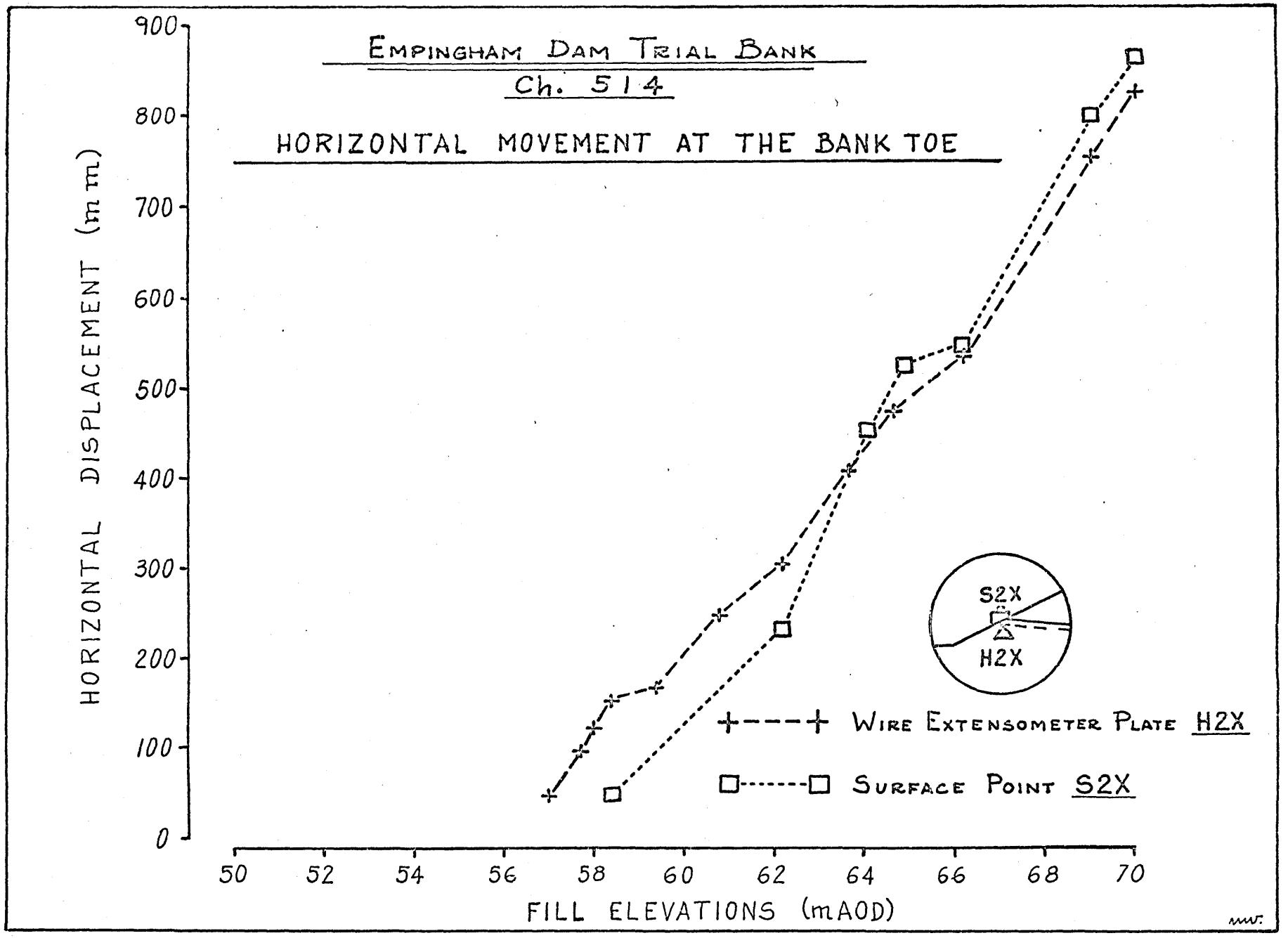


FIG. 6.19

FIG. 6.19

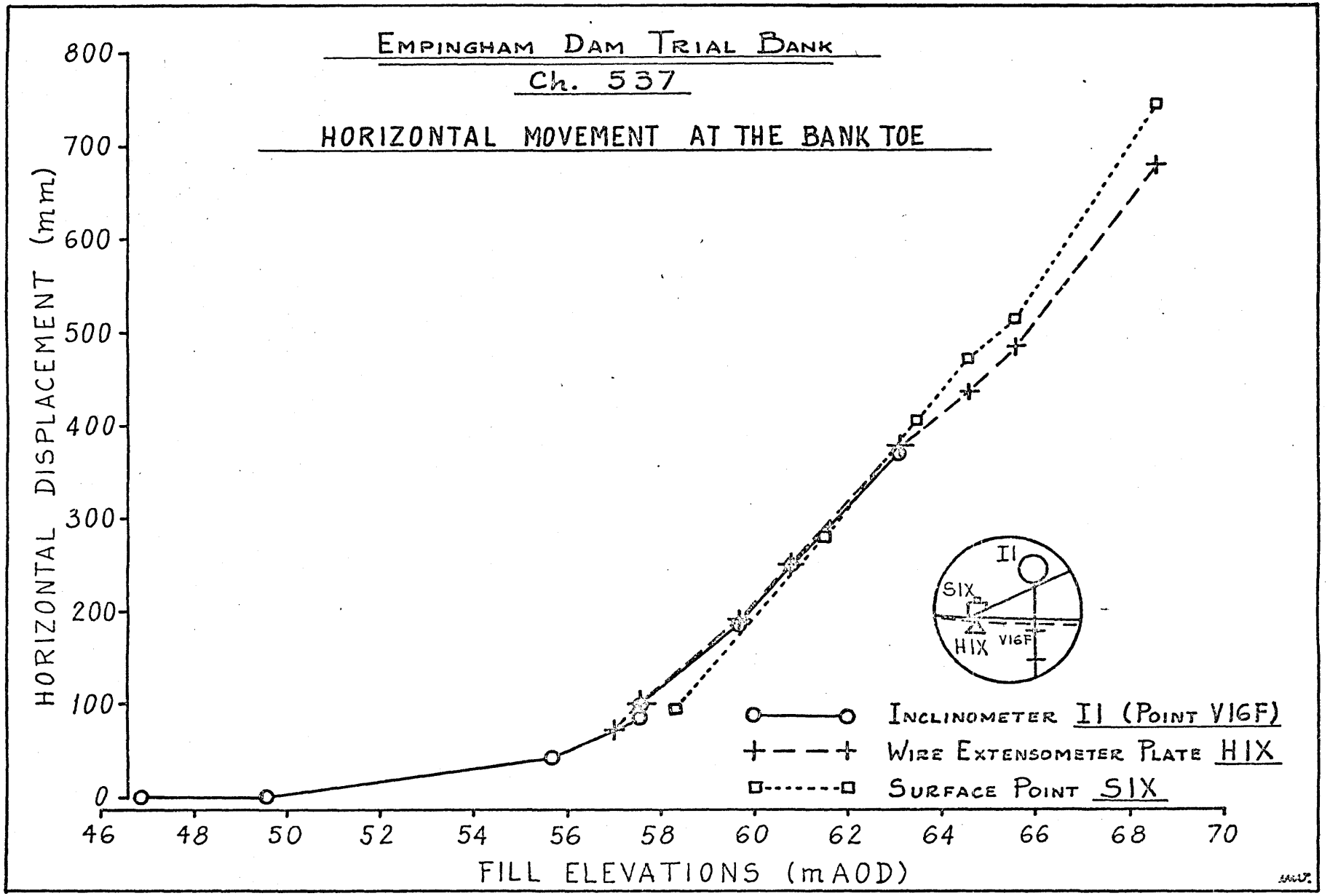


FIG. 6.20

FIG. 6.20

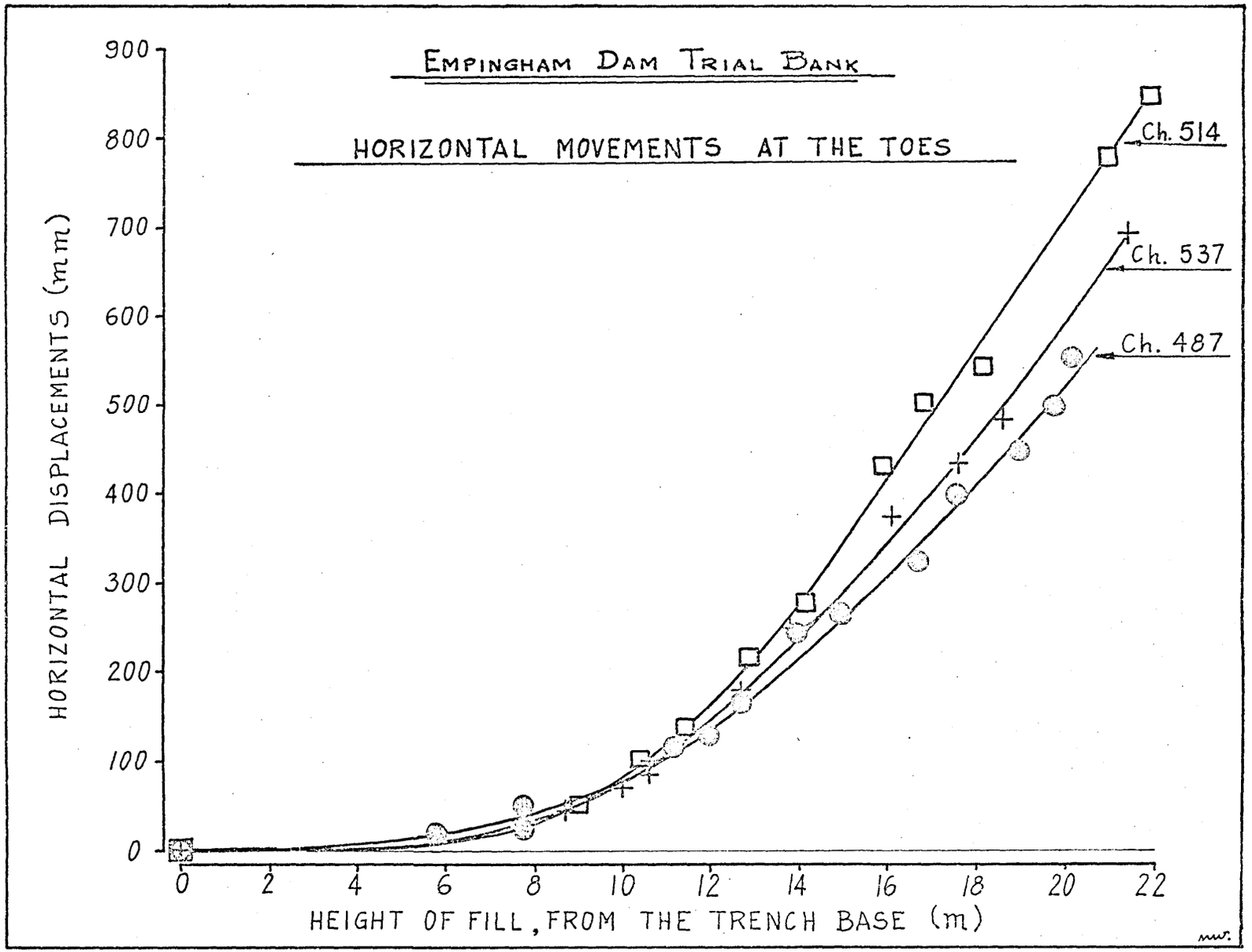


FIG. 6.21

FIG. 6.21

EMPINGHAM DAM TRIAL BANK

HORIZONTAL MOVEMENT AT TRENCH BASE LEVEL

INCLINOMETERS I1 TO I4 - CH. 487 & 537

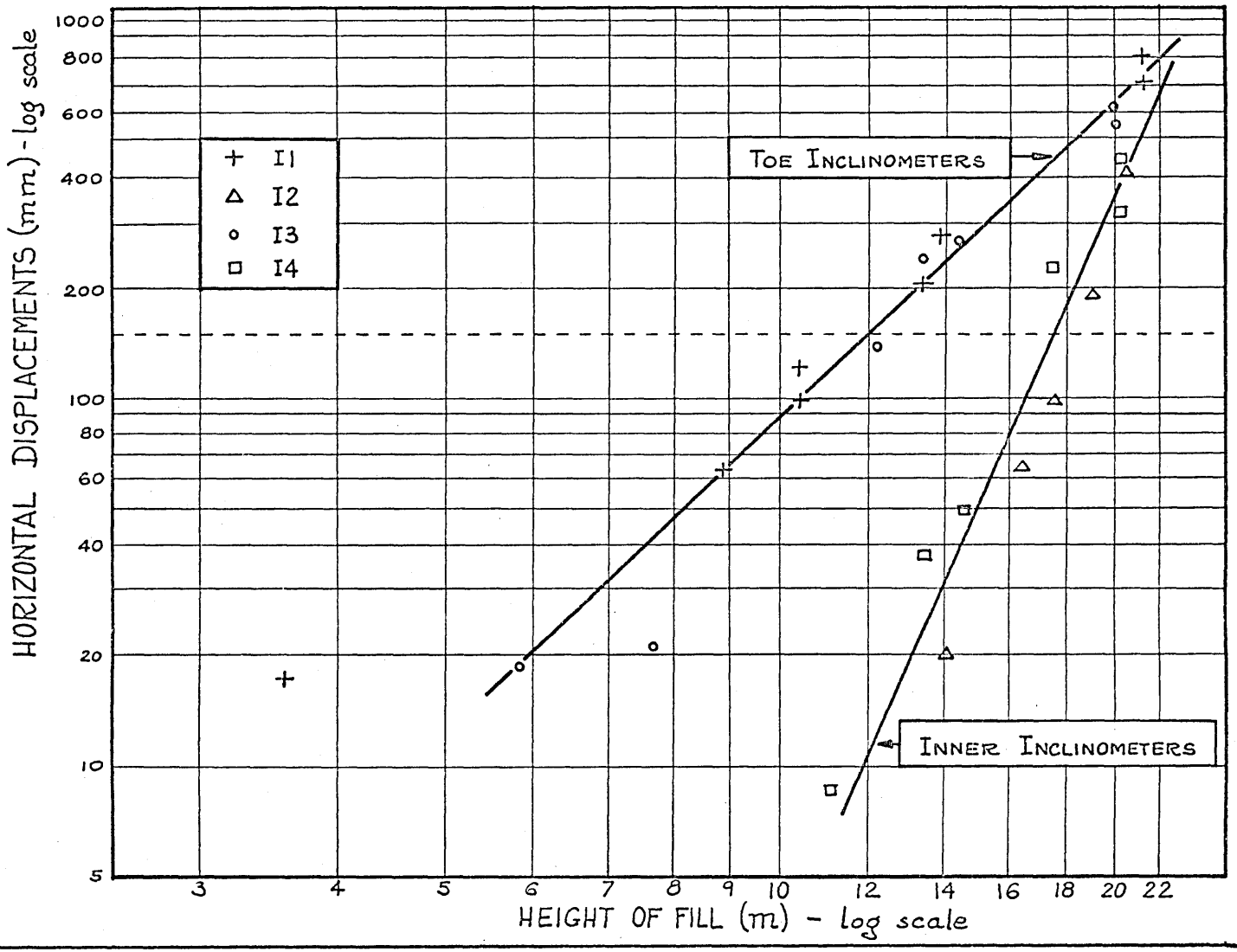


FIG. 6.22

FIG. 6.22

EMPINGHAM DAM TRIAL BANK

HORIZONTAL MOVEMENTS
WIRE EXTENSOMETER
CH 487

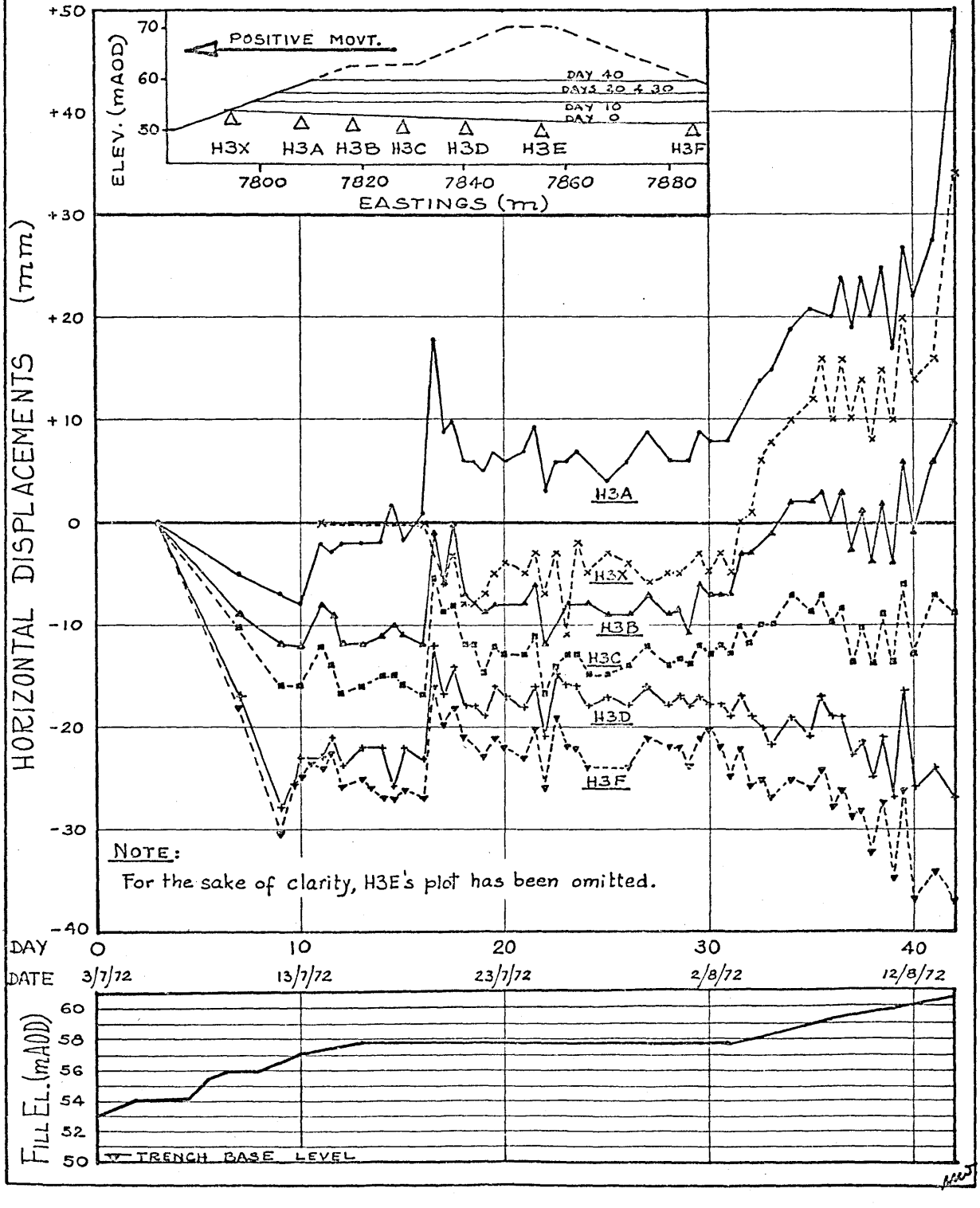


FIG. 6.23

EMPINGHAM DAM TRIAL BANK

HORIZONTAL MOVEMENTS - WIRE EXTENSOMETERS (ROD GAUGES)

CH 487

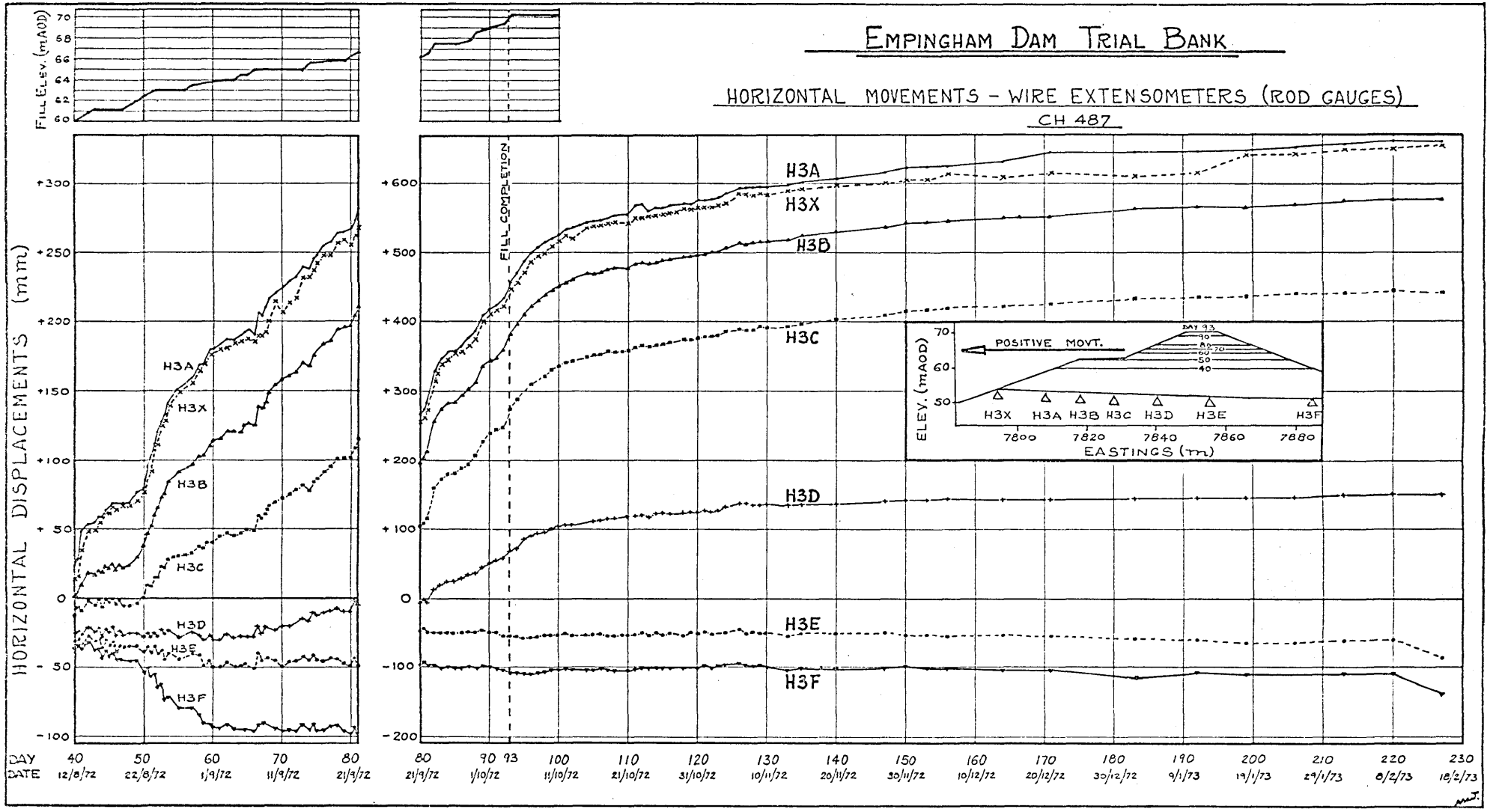


FIG. 6.24

EMPINGHAM DAM TRIAL BANK

HORIZONTAL MOVEMENTS

WIRE EXTENSOMETERS

CH 514

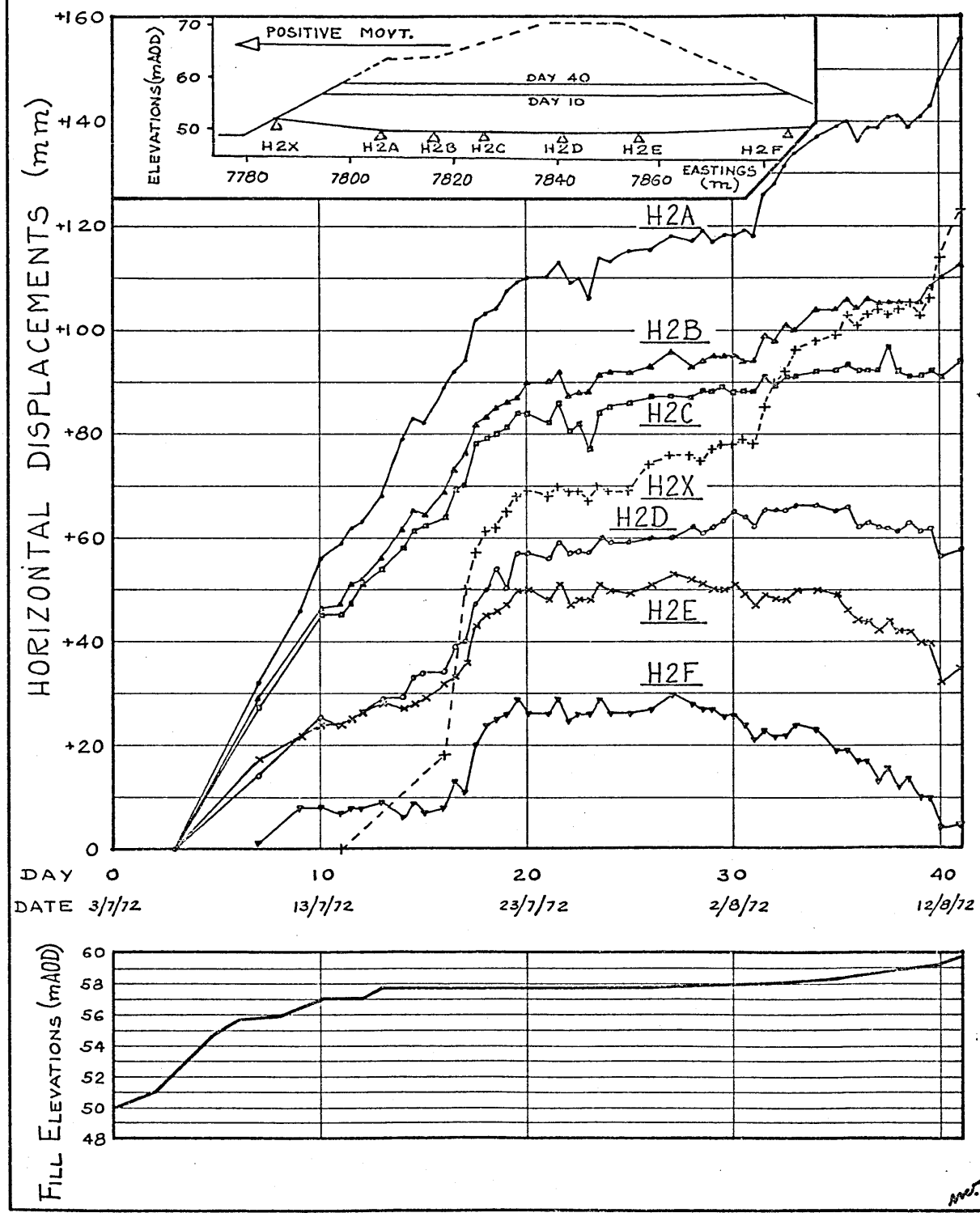


FIG. 6.25

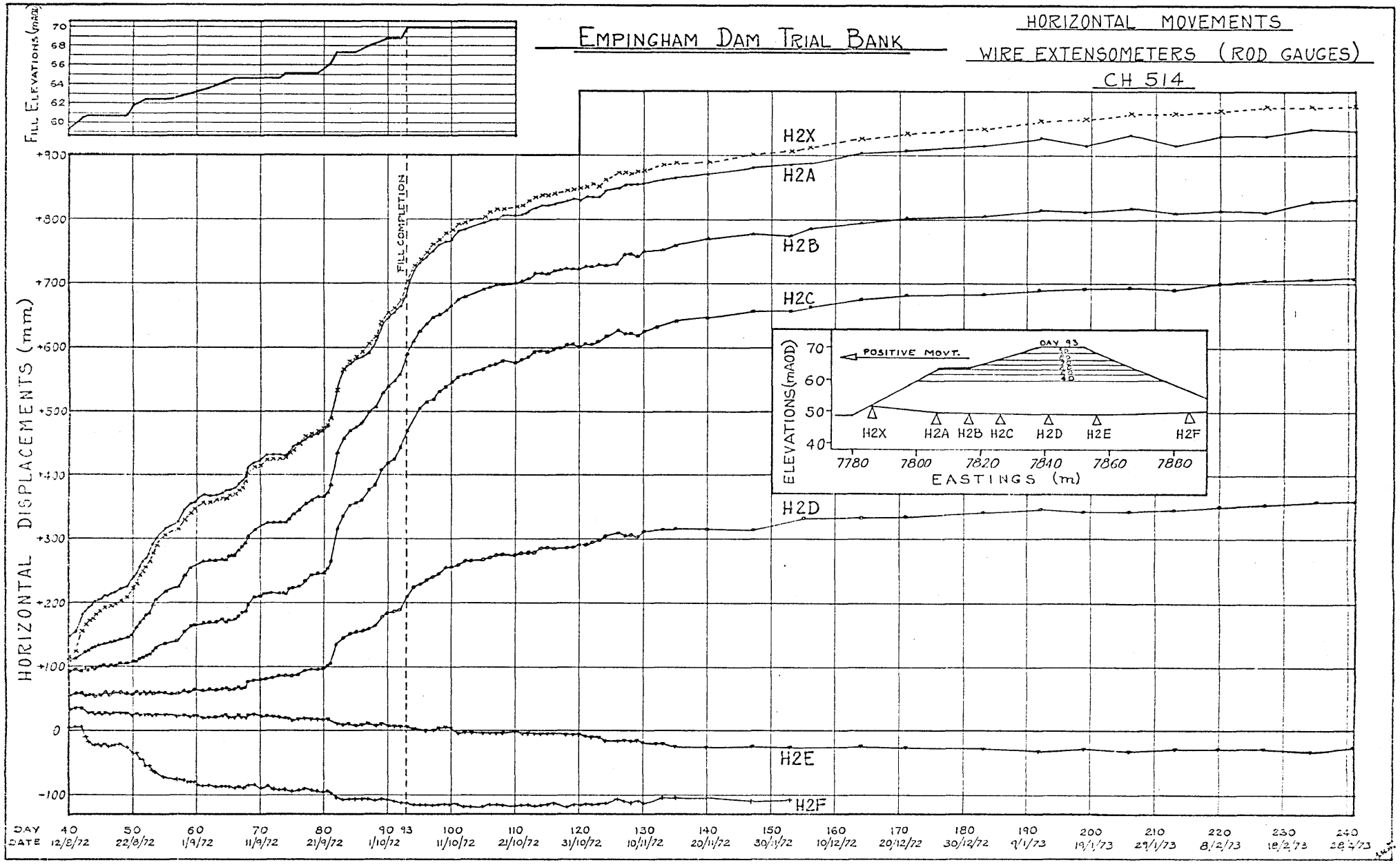

EMPINGHAM DAM TRIAL BANK
HORIZONTAL MOVEMENTS
WIRE EXTENSOMETERS (ROD GAUGES)
CH 514
FILL ELEVATIONS (mAD)
70
68
66
64
62
60
FILL COMPLETION
H2X
H2A
H2B
H2C
H2D
H2E
H2F
HORIZONTAL DISPLACEMENTS (mm)
+900
+800
+700
+600
+500
+400
+300
+200
+100
0
-100
POSITIVE MOVT.
DAY 93
ELEVATIONS (mAOD)
70
60
50
40
H2X H2A H2B H2C H2D H2E H2F
7780 7800 7820 7840 7860 7880
EASTINGS (m)
DAY 40 50 60 70 80 90 93 100 110 120 130 140 150 160 170 180 190 200 210 220 230 240
DATE 12/8/72 22/8/72 1/9/72 11/9/72 21/9/72 1/10/72 11/10/72 21/10/72 31/10/72 10/11/72 20/11/72 30/11/72 10/12/72 20/12/72 30/12/72 9/1/73 19/1/73 29/1/73 8/2/73 18/2/73 28/2/73

FIG. 6.26

EMPINGHAM DAM TRIAL BANK

HORIZONTAL MOVEMENTS
WIRE EXTENSOMETERS
CH 537

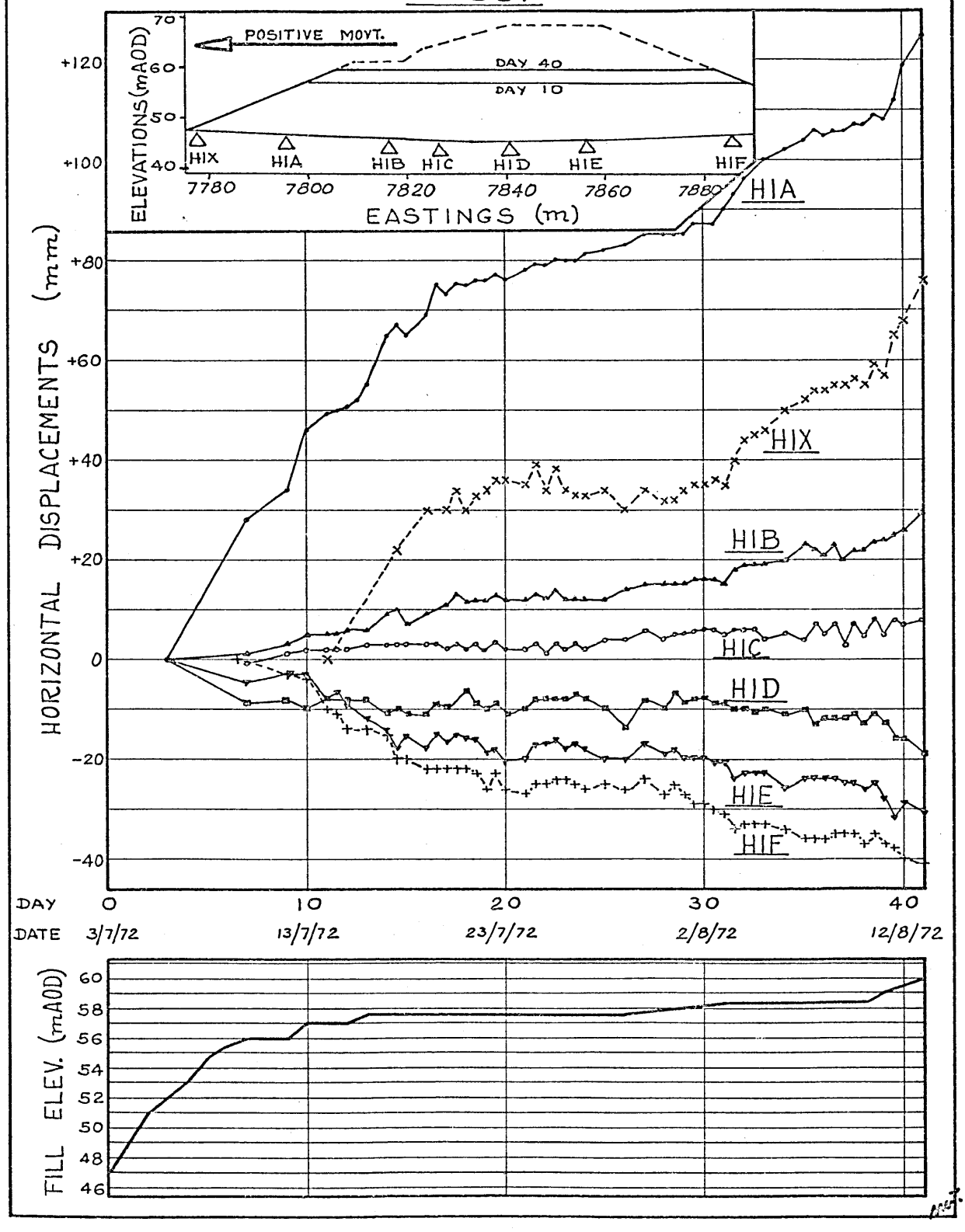
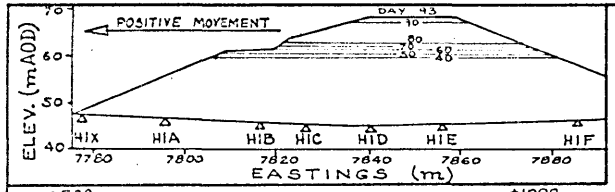


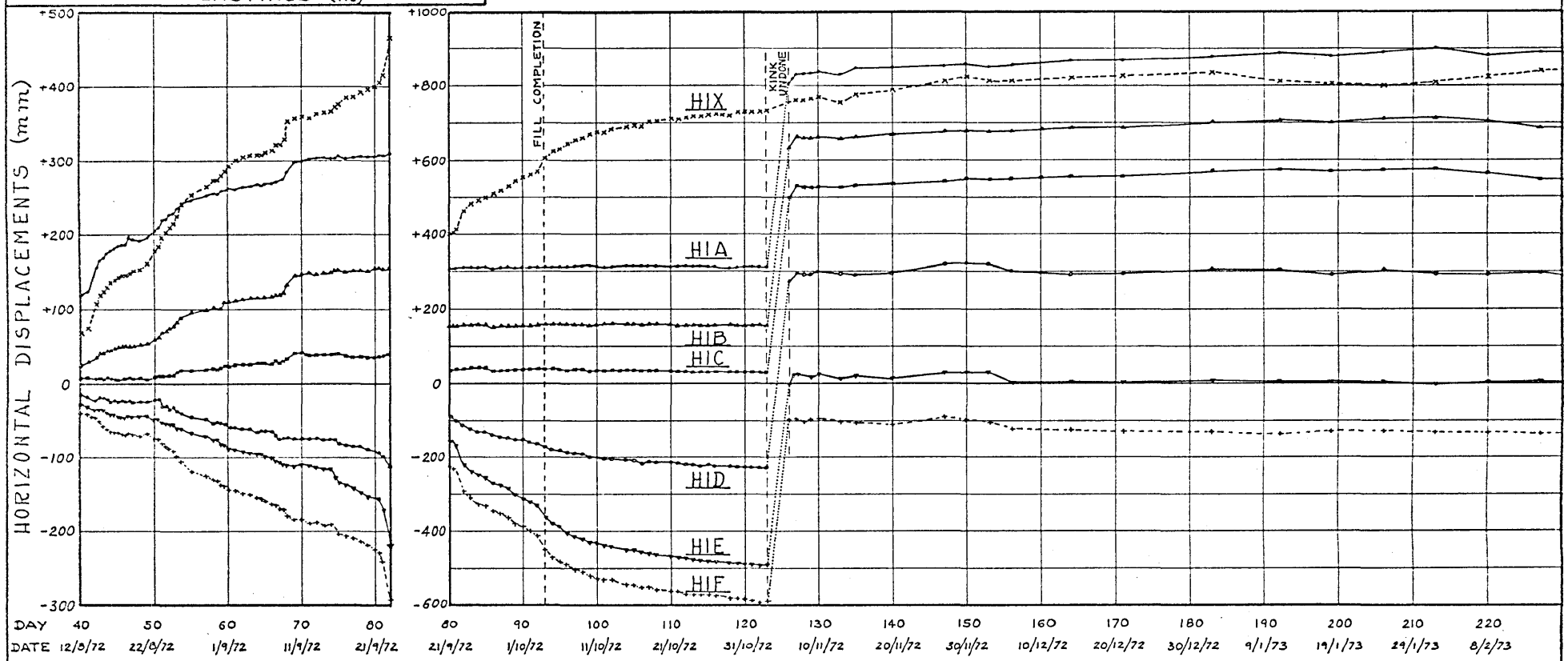
FIG. 6.27

EMPINGHAM DAM TRIAL BANK

HORIZONTAL MOVEMENTS – WIRE EXTENSOMETERS (ROD GAUGES)

CH 537





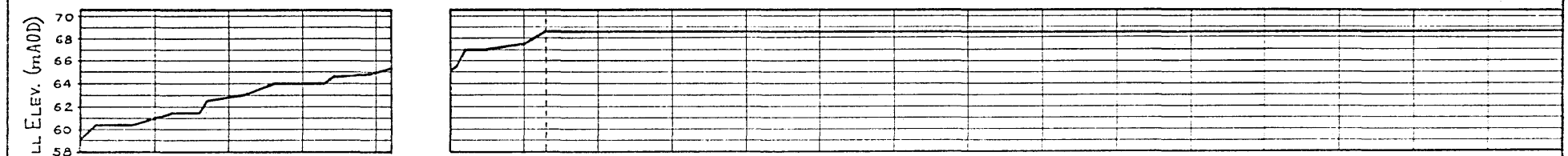


FIG. 6.28

FIG. 6.28

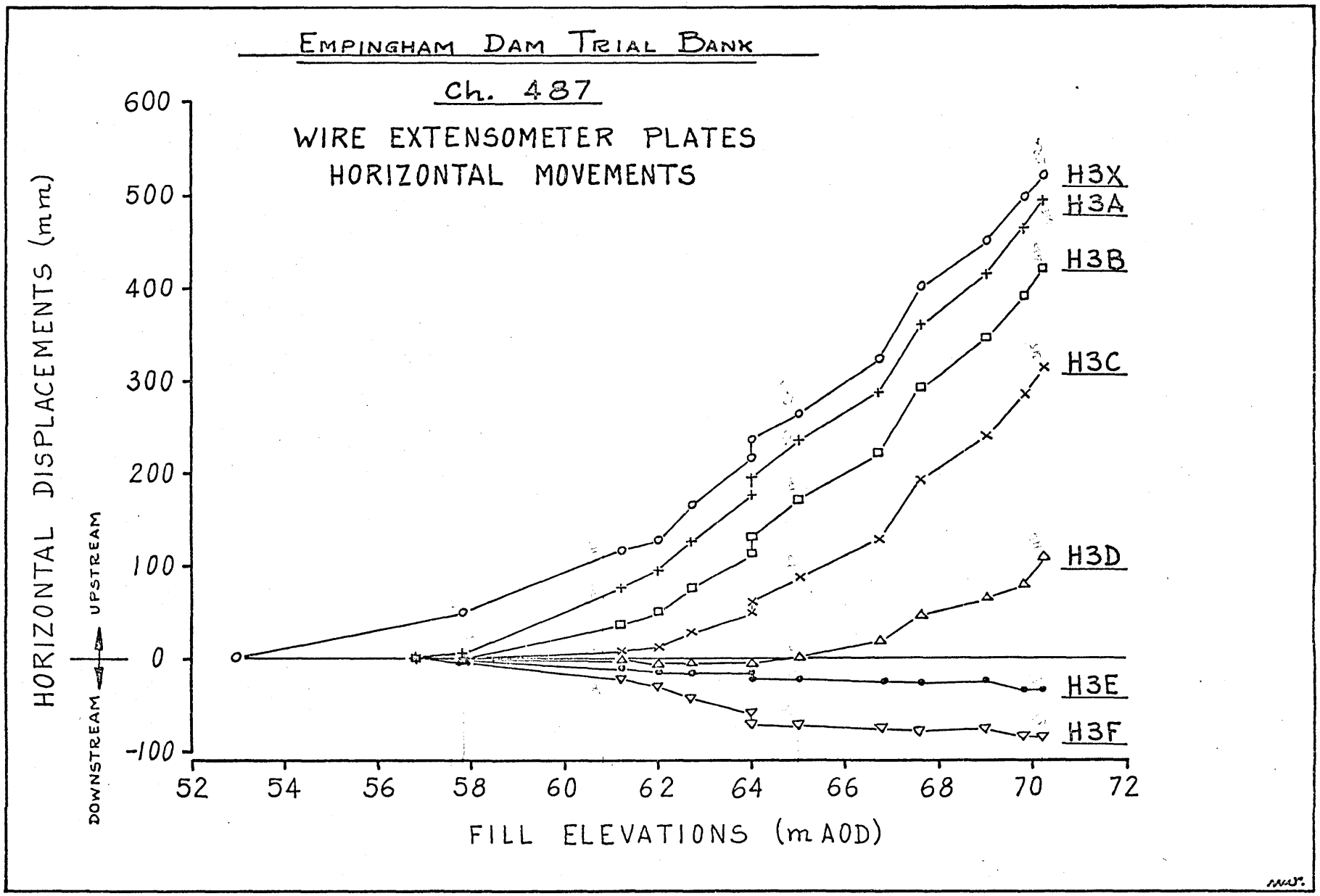


FIG. 6.29

FIG. 6.29

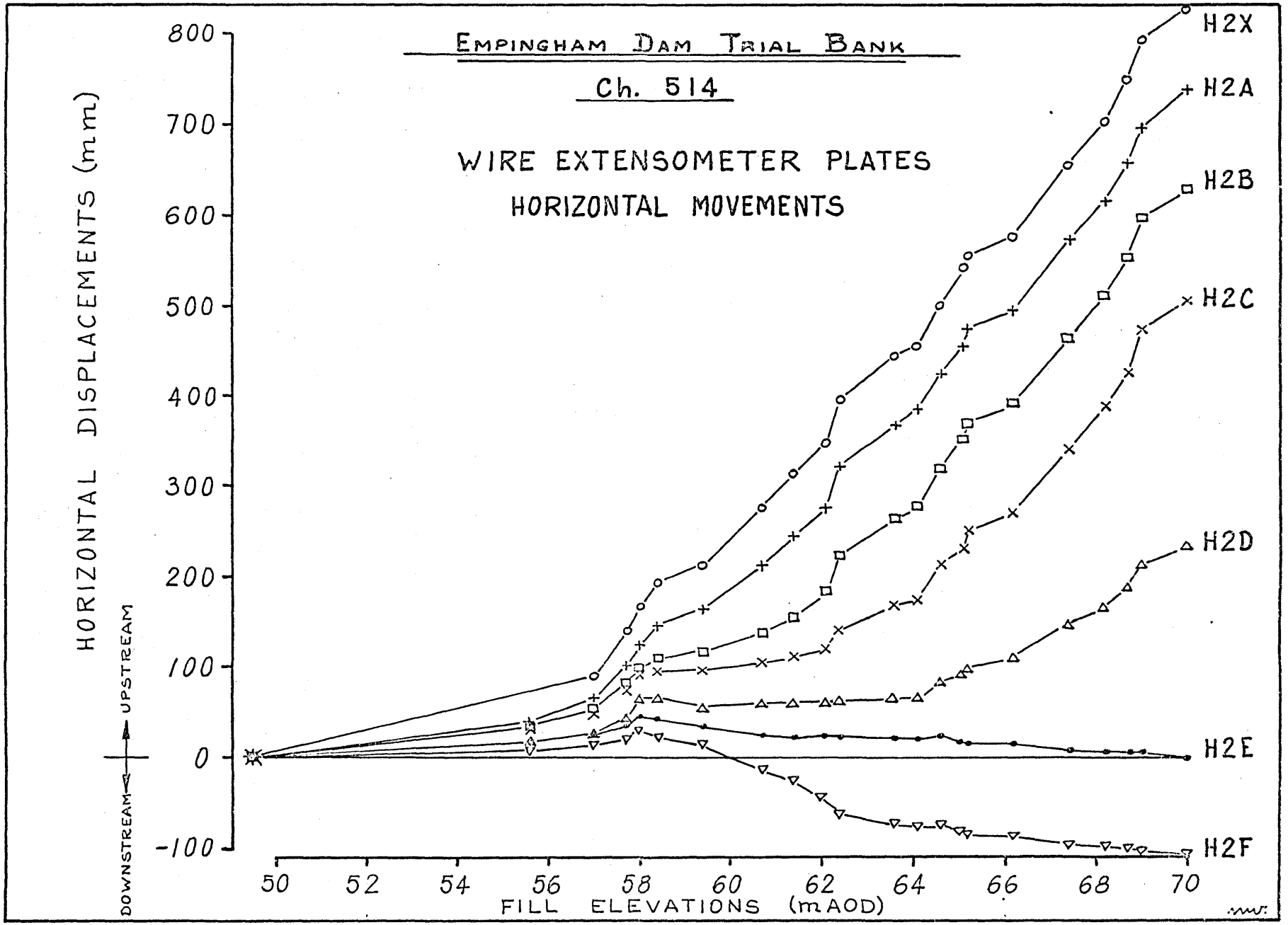


FIG. 6.30

FIG. 6.30

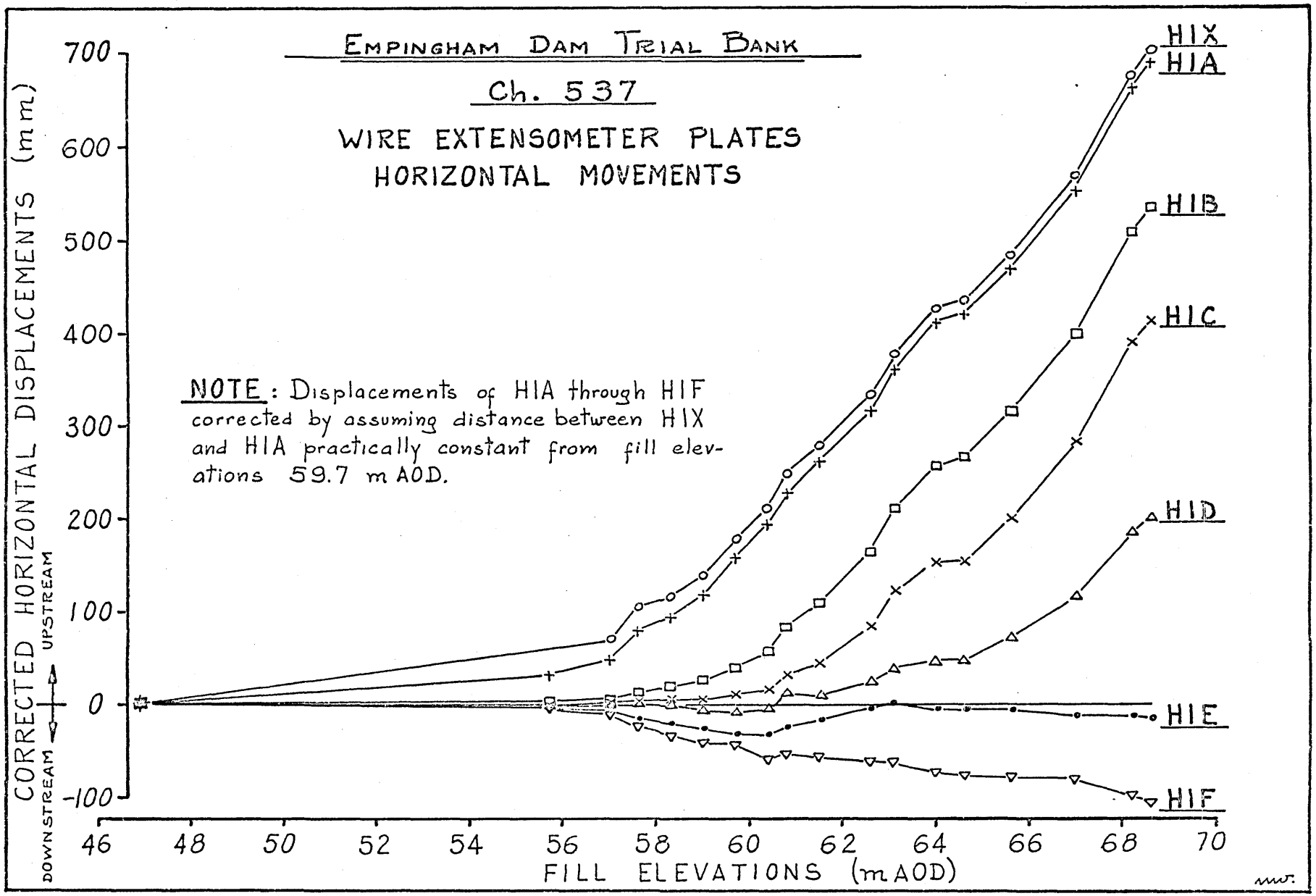


FIG. 6.31

FIG. 6.31

EMPINGHAM DAM TRIAL BANK

HORIZONTAL MOVEMENTS
FILL WIRE EXTENSOMETERS (ROD GAUGES)
CH 487

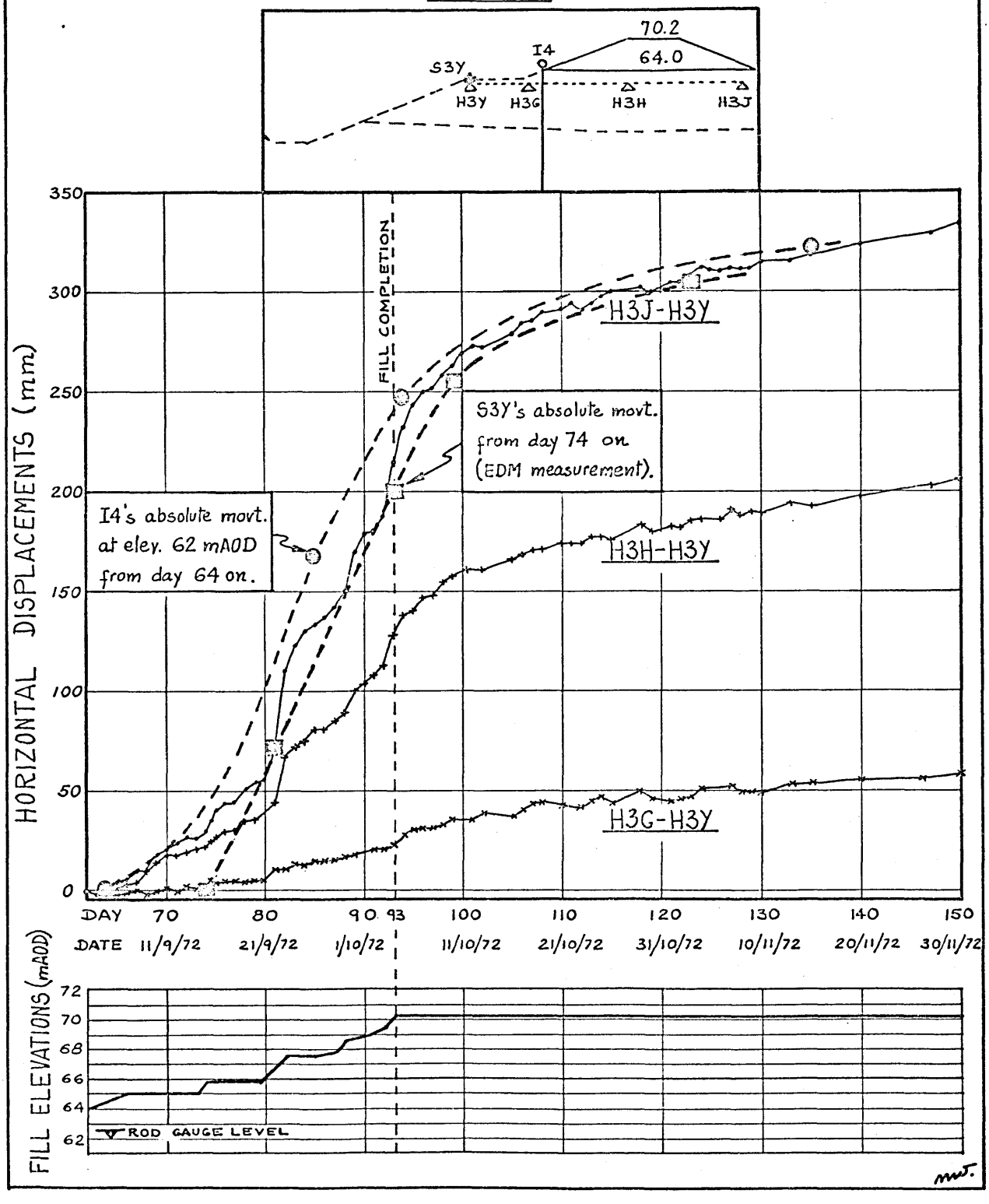


FIG. 6.33

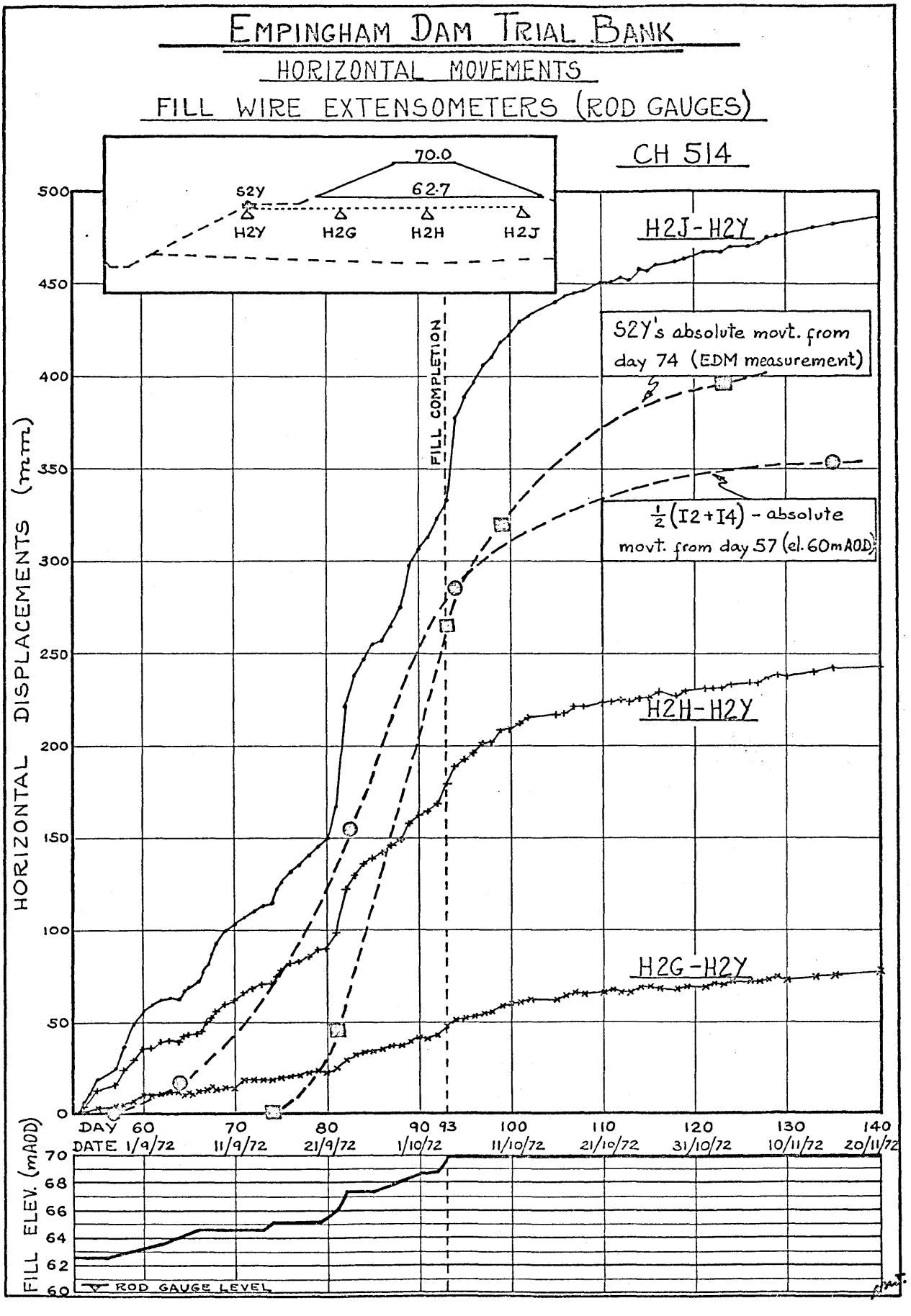

EMPINGHAM DAM TRIAL BANK
HORIZONTAL MOVEMENTS
FILL WIRE EXTENSOMETERS (ROD GAUGES)
CH 514
70.0
62.7
S2Y
H2Y
H2G
H2H
H2J
H2J-H2Y
S2Y's absolute movt. from day 74 (EDM measurement)
FILL COMPLETION
½(I2+I4) - absolute movt. from day 57 (el. 60mAOD)
H2H-H2Y
H2G-H2Y
HORIZONTAL DISPLACEMENTS (mm)
500
450
400
350
300
250
200
150
100
50
0
DAY 60 70 80 90 93 100 110 120 130 140
DATE 1/9/72 11/9/72 21/9/72 1/10/72 11/10/72 21/10/72 31/10/72 10/11/72 20/11/72
FILL ELEV. (mAOD)
70
68
66
64
62
60
ROD GAUGE LEVEL

FIG. 6.34

EMPINGHAM DAM TRIAL BANK

HORIZONTAL MOVEMENTS — FILL WIRE EXTENSOMETERS (ROD GAUGES)

CH 537

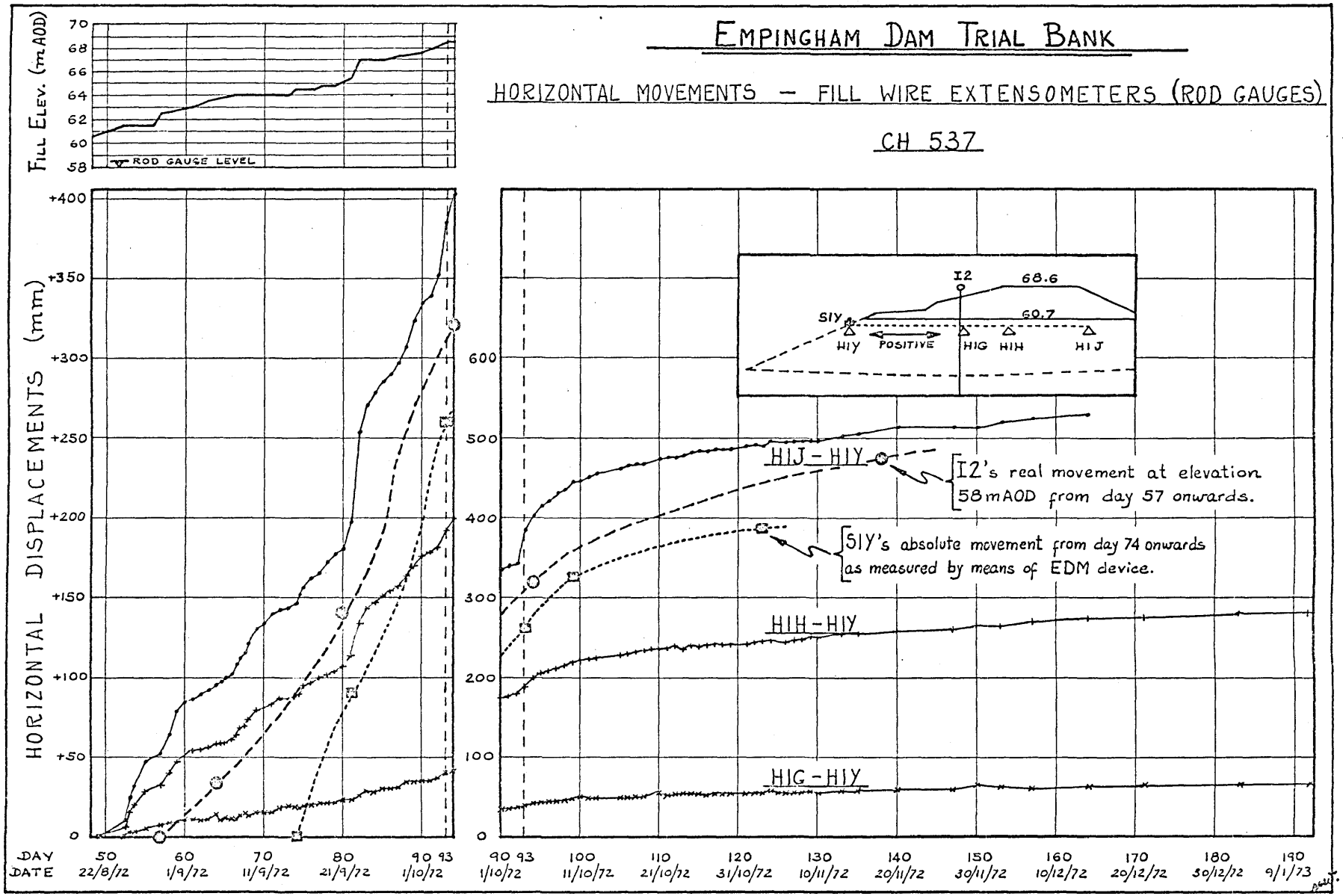
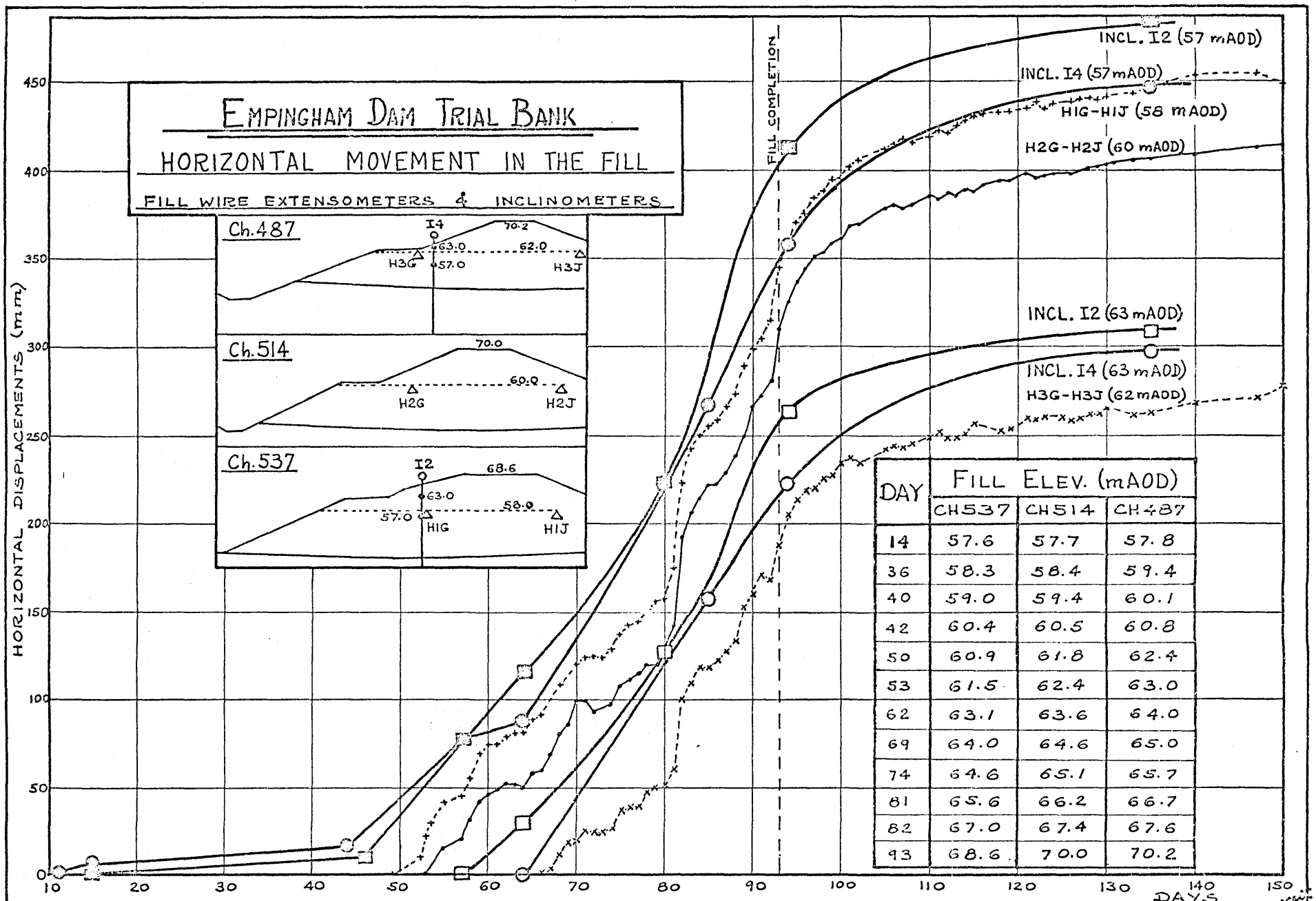


FIG. 6.35

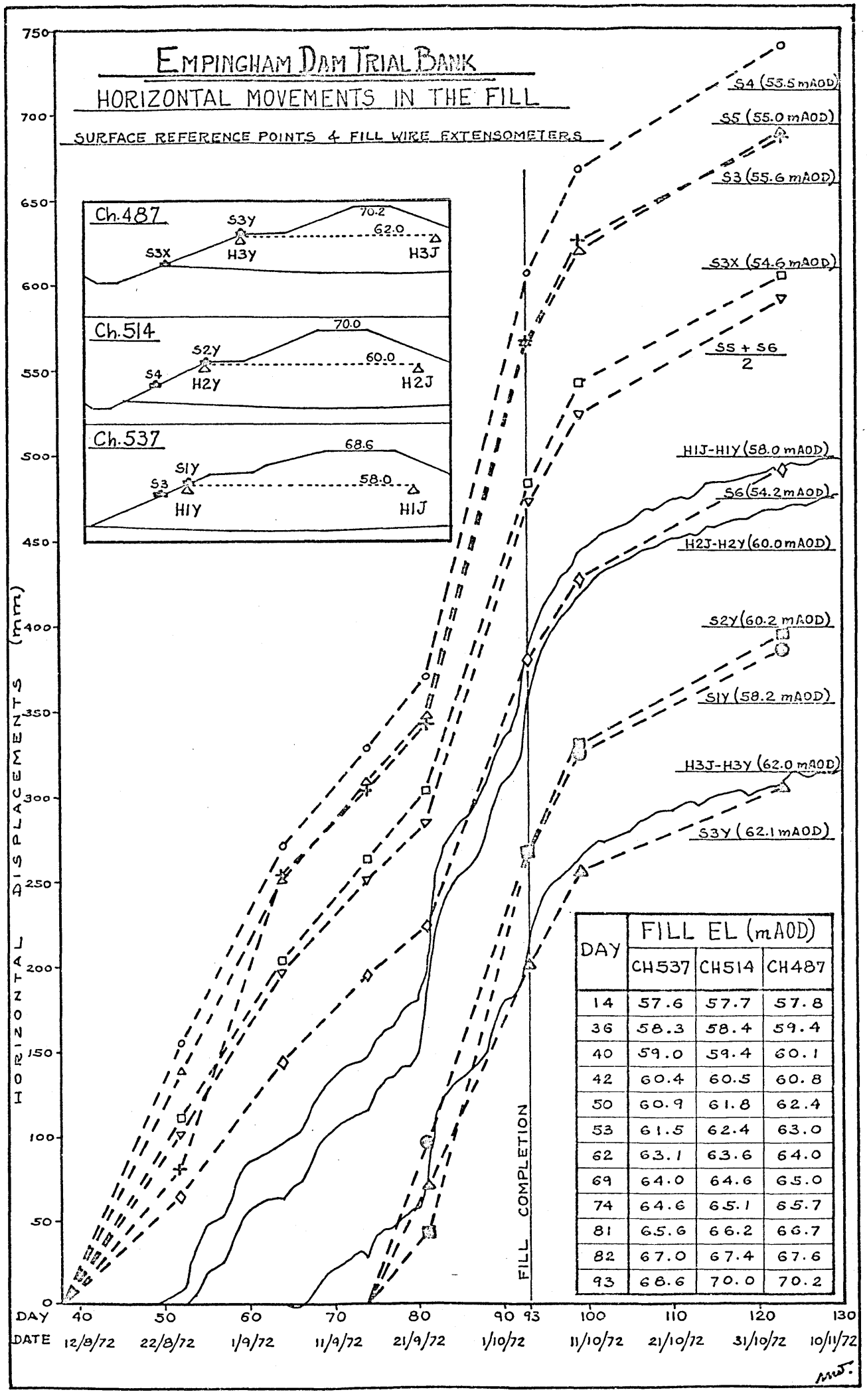
FIG. 6.35



DAY	FILL ELEV. (mAOD)		
	CH537	CH514	CH487
14	57.6	57.7	57.8
36	58.3	58.4	59.4
40	59.0	59.4	60.1
42	60.4	60.5	60.8
50	60.9	61.8	62.4
53	61.5	62.4	63.0
62	63.1	63.6	64.0
69	64.0	64.6	65.0
74	64.6	65.1	65.7
81	65.6	66.2	66.7
82	67.0	67.4	67.6
93	68.6	70.0	70.2

FIG. 6.36

FIG. 6.36



DAY	FILL EL (mAOD)		
	CH537	CH514	CH487
14	57.6	57.7	57.8
36	58.3	58.4	59.4
40	59.0	59.4	60.1
42	60.4	60.5	60.8
50	60.9	61.8	62.4
53	61.5	62.4	63.0
62	63.1	63.6	64.0
69	64.0	64.6	65.0
74	64.6	65.1	65.7
81	65.6	66.2	66.7
82	67.0	67.4	67.6
93	68.6	70.0	70.2

FIG. 6.37

EMPINGHAM DAM TRIAL BANK

RELATIVE HORIZONTAL MOVEMENTS

INCLINOMETERS & FILL WIRE EXTENSOMETERS

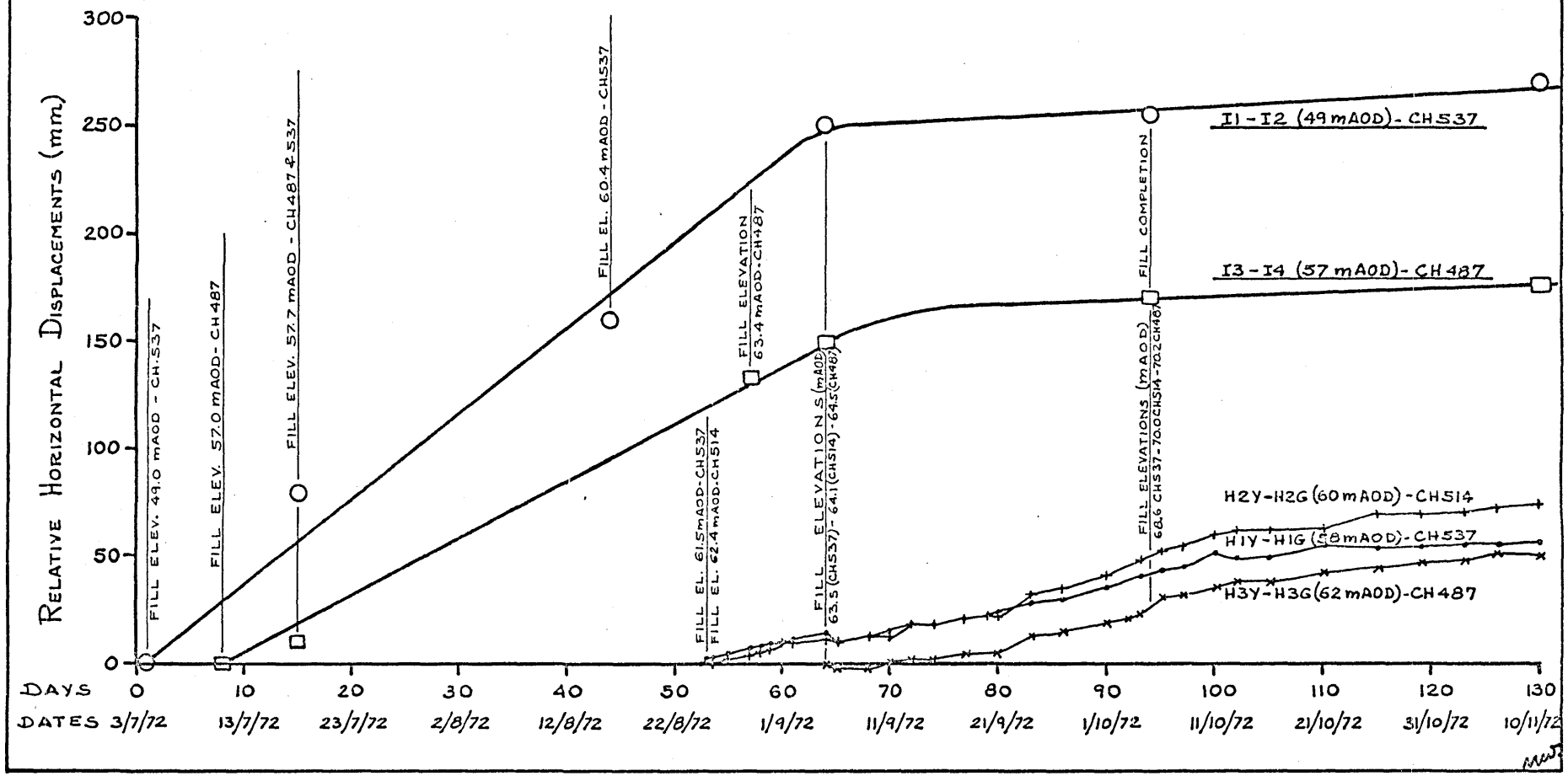


FIG. 6.38

FIG. 6.38

EMPINGHAM DAM TRIAL BANK

HORIZONTAL MOVEMENTS IN THE FILL

CH 537

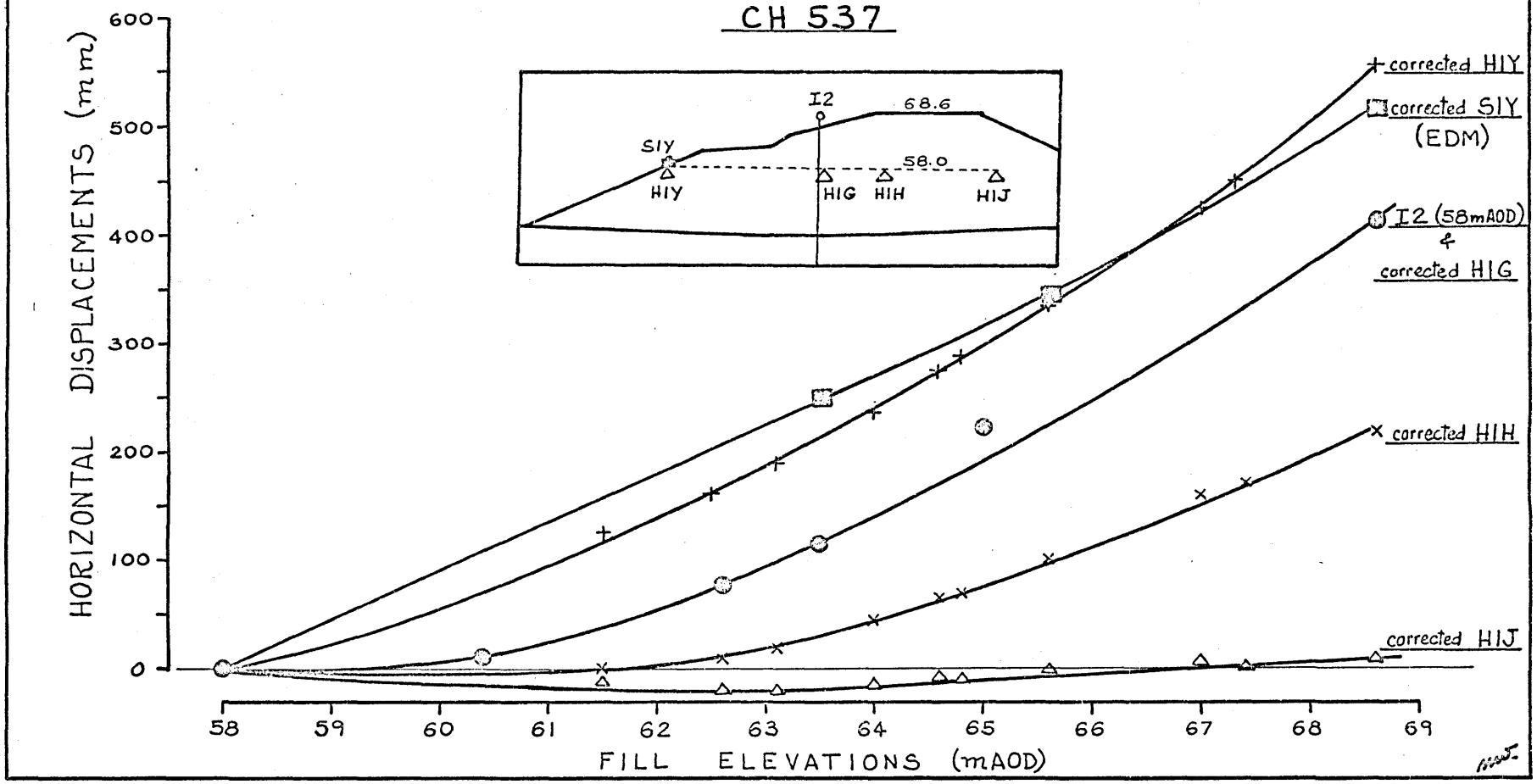


FIG. 6.39

FIG. 6.39

EMPINGHAM DAM TRIAL BANK

HORIZONTAL MOVEMENTS IN THE FILL

CH 514

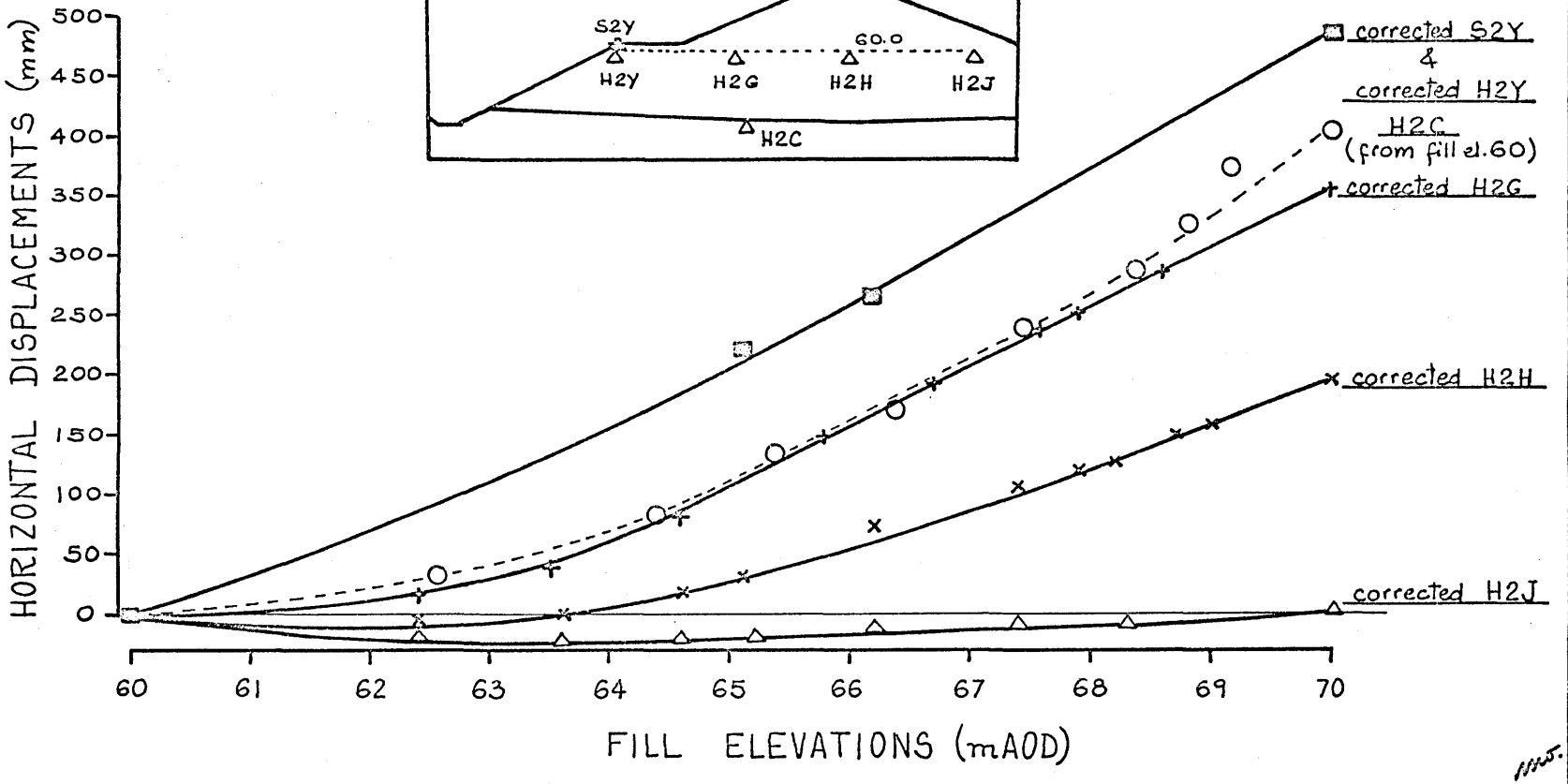


FIG. 6.40

FIG. 6.40

EMPINGHAM DAM TRIAL BANK

HORIZONTAL MOVEMENTS IN THE FILL

CH 487

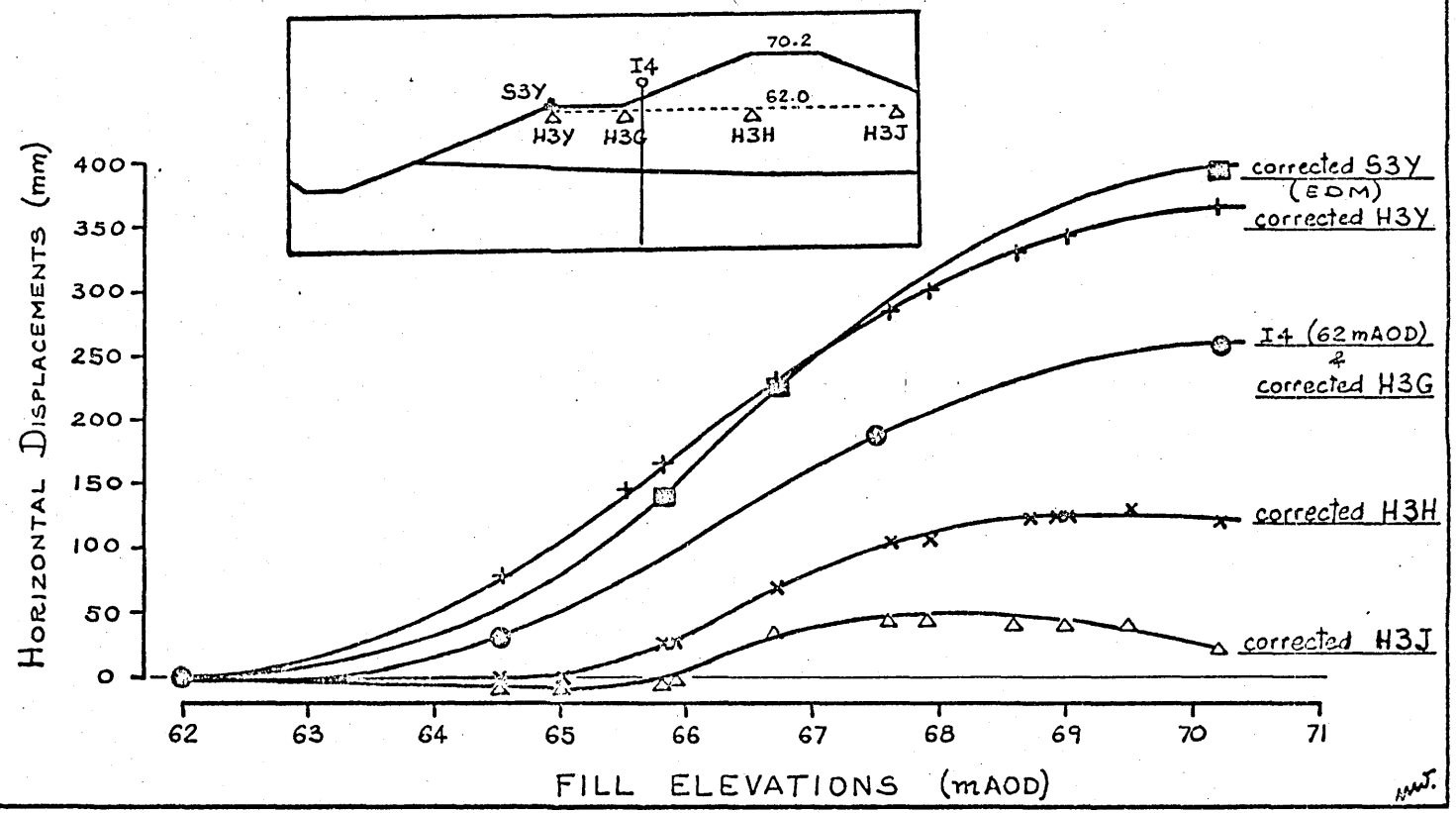


FIG. 6.41

FIG. 6.41

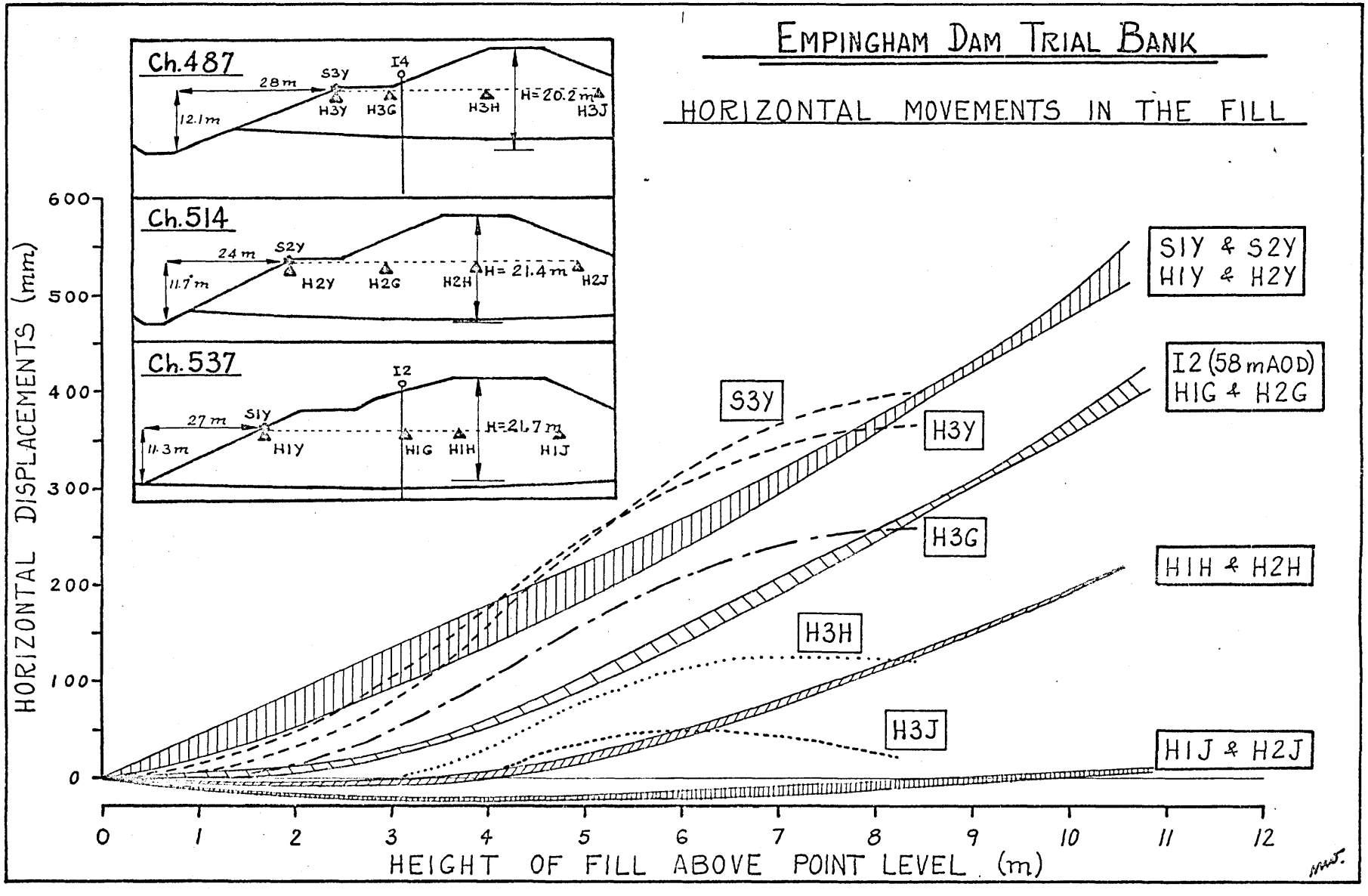


FIG. 6.42

FIG. 6.42

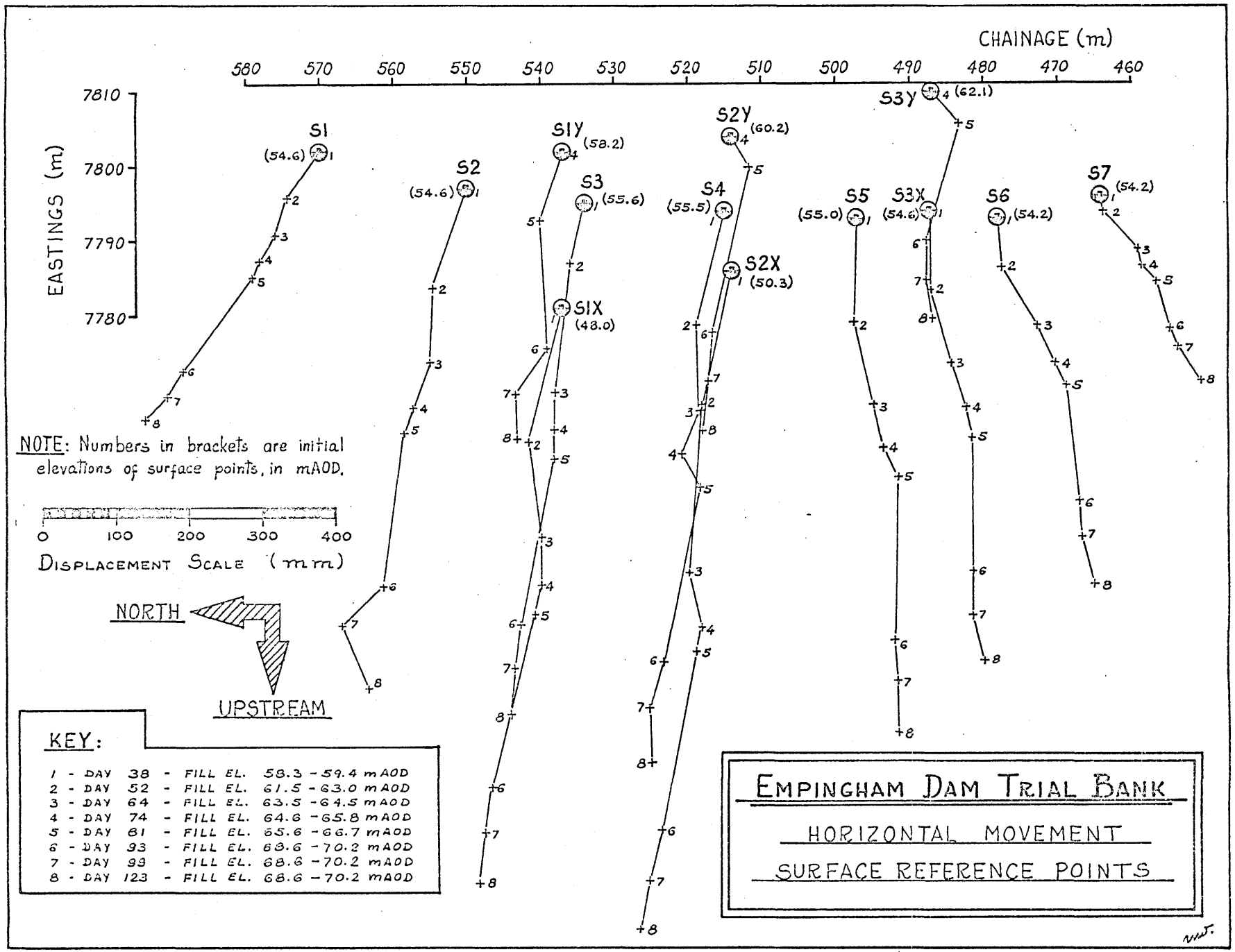


FIG. 6.43

FIG. 6.43

EMPINGHAM DAM TRIAL BANK

HORIZONTAL MOVEMENT SURFACE REFERENCE POINTS

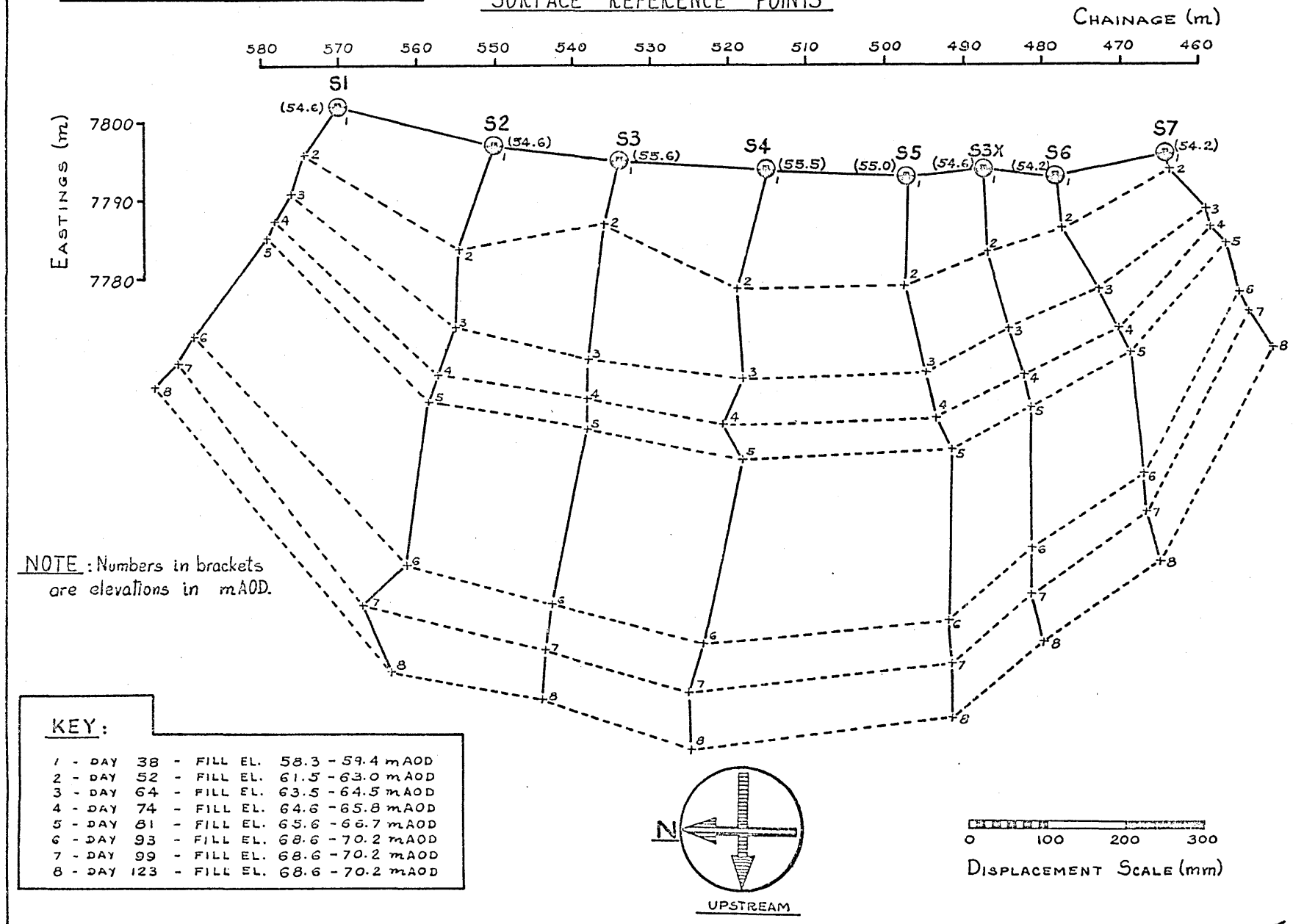


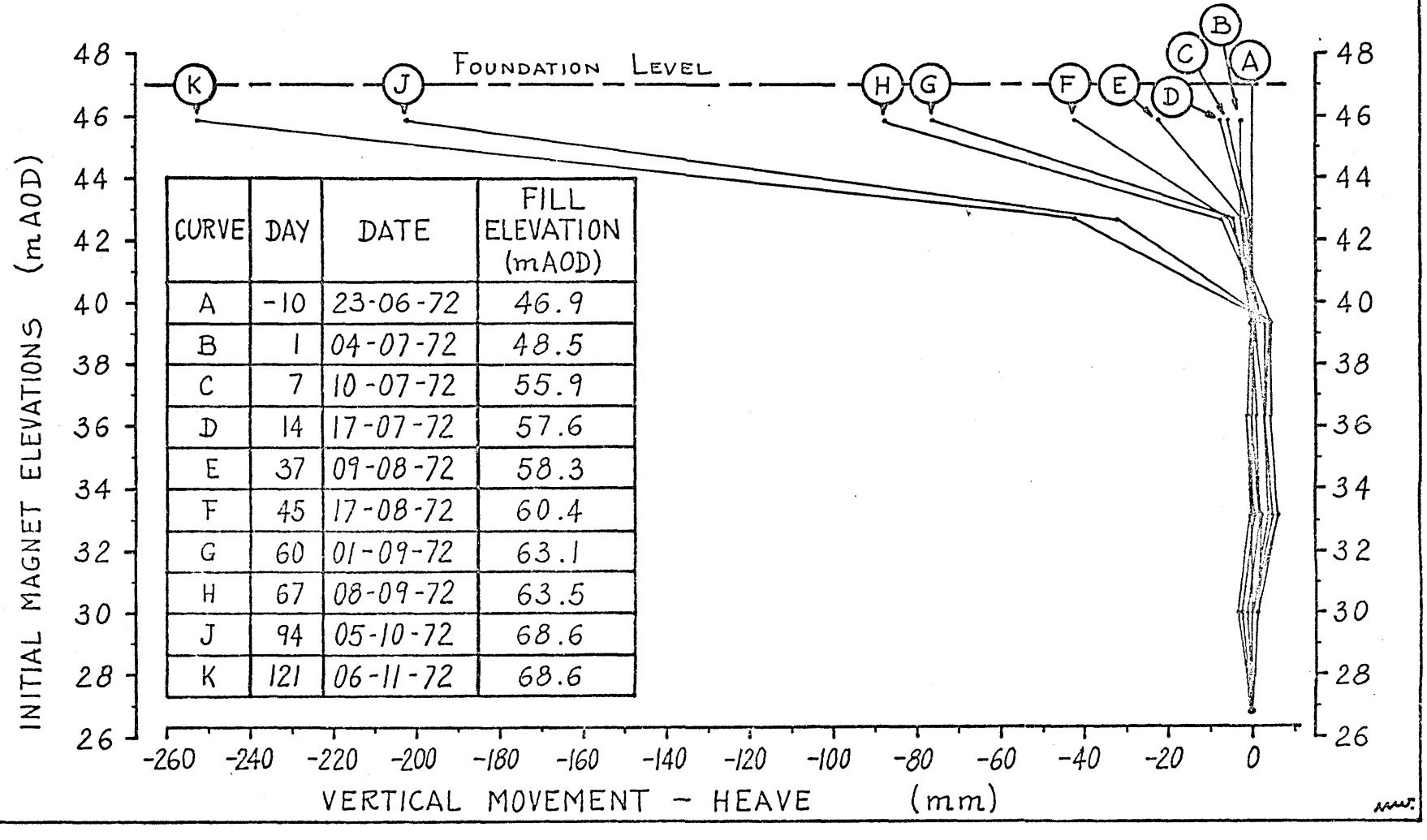
FIG. 6.44

FIG. 6.44

EMPINGHAM DAM TRIAL BANK

INCLINOMETER II ~ Ch.537

VERTICAL MOVEMENTS — SETTLEMENT MAGNETS



CURVE	DAY	DATE	FILL ELEVATION (mAOD)
A	-10	23-06-72	46.9
B	1	04-07-72	48.5
C	7	10-07-72	55.9
D	14	17-07-72	57.6
E	37	09-08-72	58.3
F	45	17-08-72	60.4
G	60	01-09-72	63.1
H	67	08-09-72	63.5
J	94	05-10-72	68.6
K	121	06-11-72	68.6

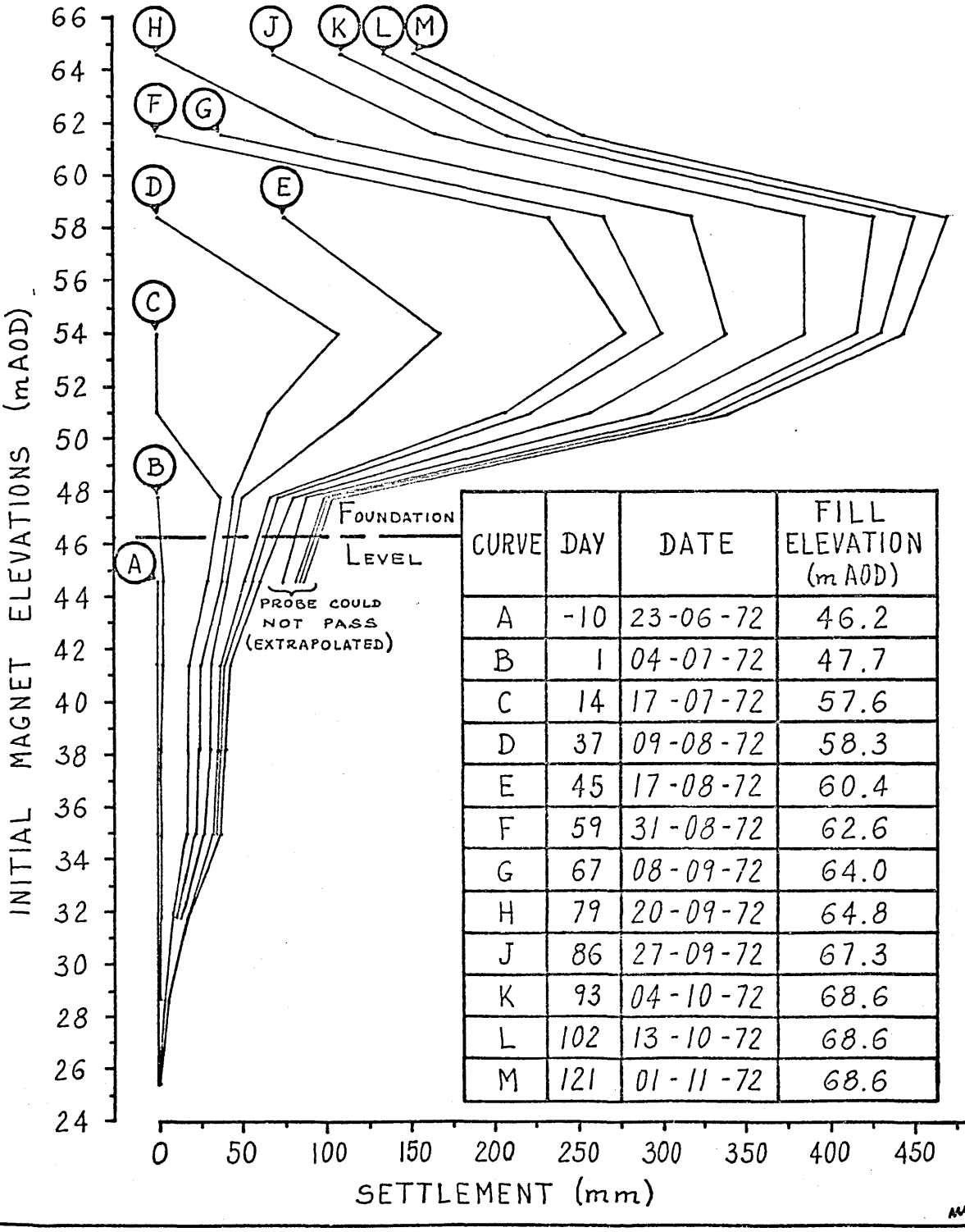
FIG. 6.45

FIG. 6.45

EMPINGHAM DAM TRIAL BANK

INCLINOMETER I2 ~ Ch.537

VERTICAL MOVEMENTS – SETTLEMENT MAGNETS

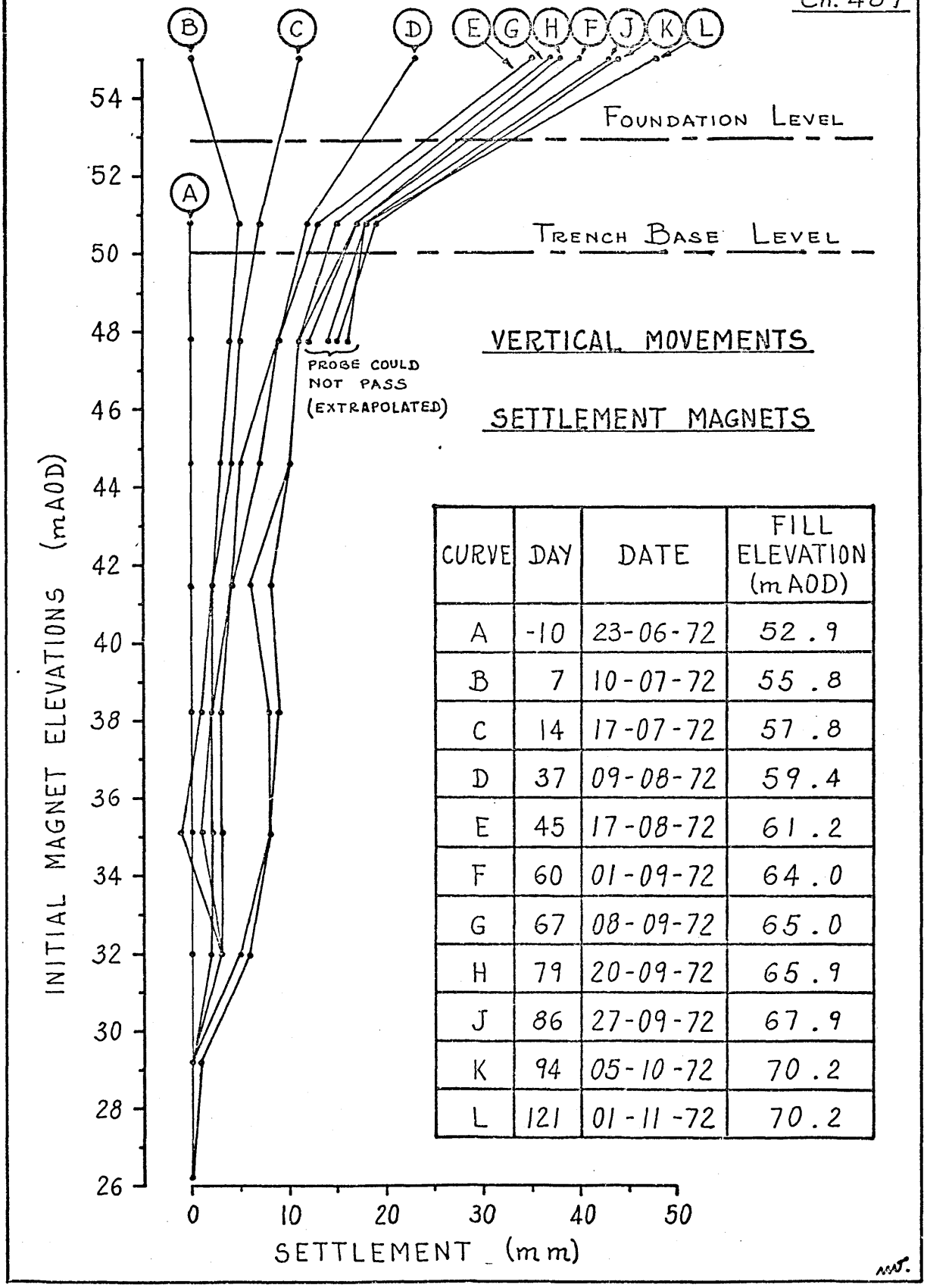


CURVE	DAY	DATE	FILL ELEVATION (m AOD)
A	-10	23-06-72	46.2
B	1	04-07-72	47.7
C	14	17-07-72	57.6
D	37	09-08-72	58.3
E	45	17-08-72	60.4
F	59	31-08-72	62.6
G	67	08-09-72	64.0
H	79	20-09-72	64.8
J	86	27-09-72	67.3
K	93	04-10-72	68.6
L	102	13-10-72	68.6
M	121	01-11-72	68.6

FIG. 6.46

EMPINGHAM DAM TRIAL BANK — INCLINOMETER I3

Ch. 487



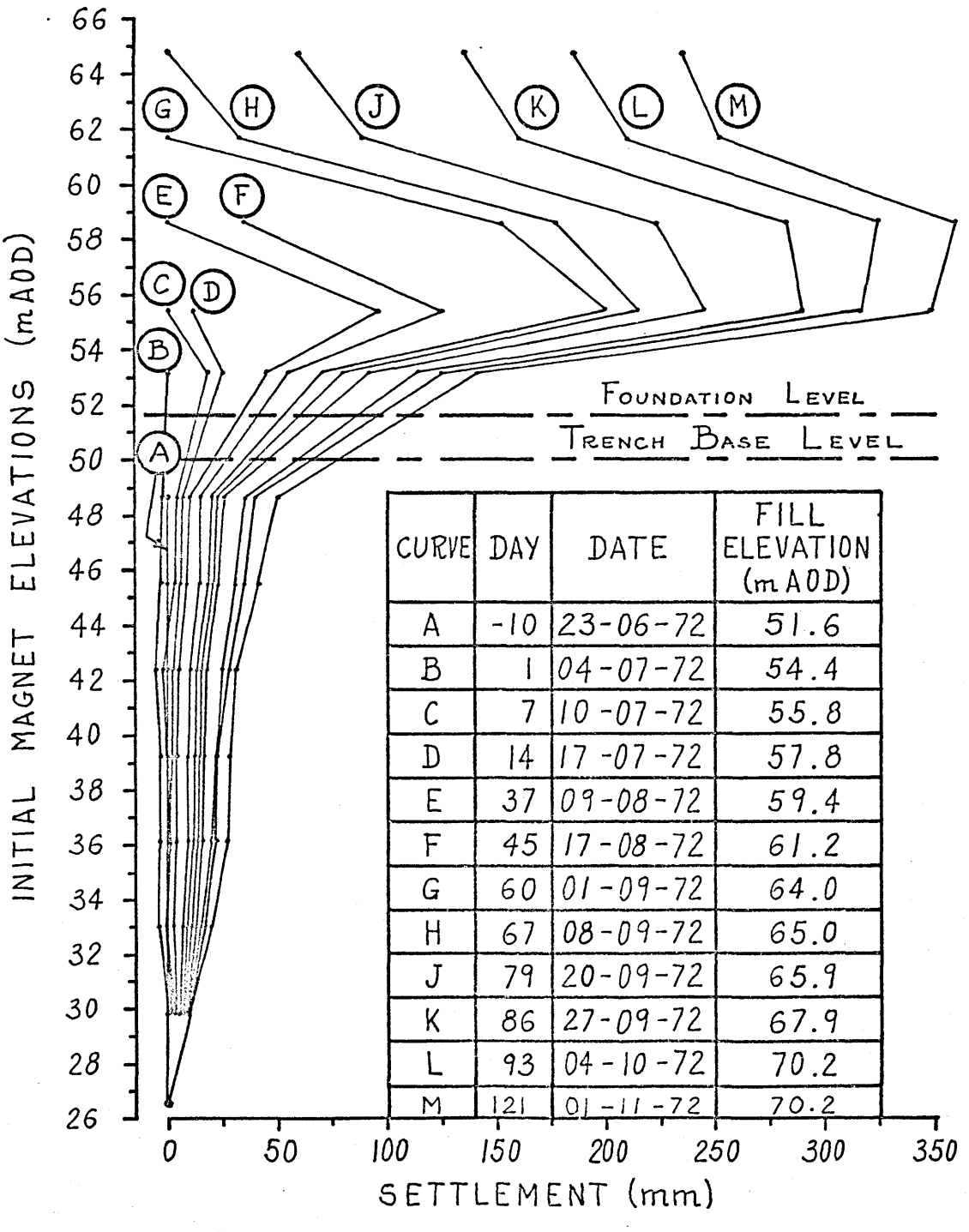
CURVE	DAY	DATE	FILL ELEVATION (mAOD)
A	-10	23-06-72	52.9
B	7	10-07-72	55.8
C	14	17-07-72	57.8
D	37	09-08-72	59.4
E	45	17-08-72	61.2
F	60	01-09-72	64.0
G	67	08-09-72	65.0
H	79	20-09-72	65.9
J	86	27-09-72	67.9
K	94	05-10-72	70.2
L	121	01-11-72	70.2

FIG. 6.47

EMPINGHAM DAM TRIAL BANK

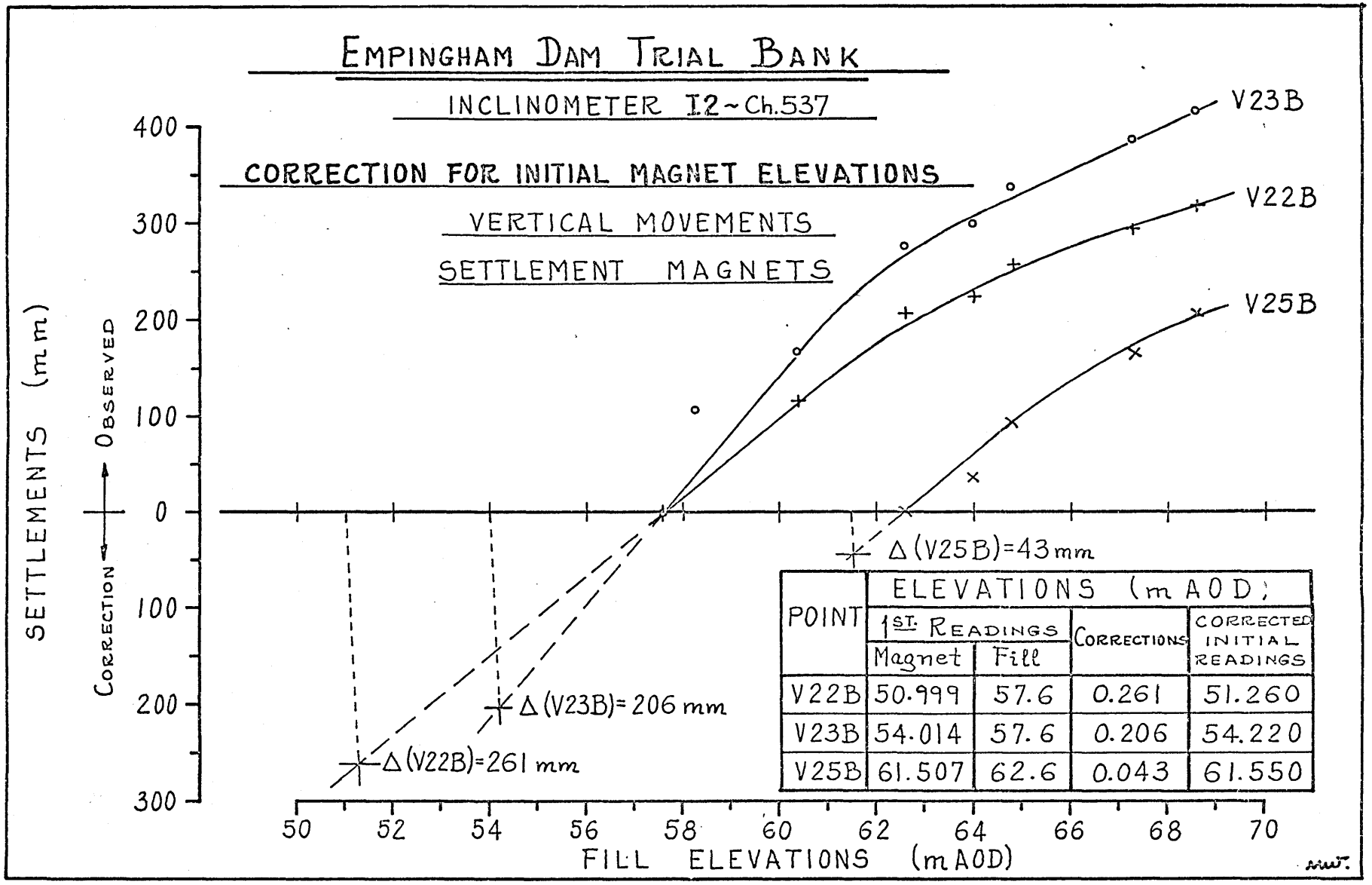
INCLINOMETER I4 ~ Ch. 487

VERTICAL MOVEMENTS — SETTLEMENT MAGNETS



CURVE	DAY	DATE	FILL ELEVATION (m AOD)
A	-10	23-06-72	51.6
B	1	04-07-72	54.4
C	7	10-07-72	55.8
D	14	17-07-72	57.8
E	37	09-08-72	59.4
F	45	17-08-72	61.2
G	60	01-09-72	64.0
H	67	08-09-72	65.0
J	79	20-09-72	65.9
K	86	27-09-72	67.9
L	93	04-10-72	70.2
M	121	01-11-72	70.2

FIG. 6.48



POINT	ELEVATIONS (m AOD)			
	1st. READINGS		CORRECTIONS	CORRECTED INITIAL READINGS
	Magnet	Fill		
V22B	50.999	57.6	0.261	51.260
V23B	54.014	57.6	0.206	54.220
V25B	61.507	62.6	0.043	61.550

FIG. 6.49

EMPINGHAM DAM TRIAL BANK

CORRECTION FOR INITIAL MAGNET ELEVATIONS

INCLINOMETER I4 ~ Ch.487

POINT	ELEVATIONS (m AOD)			
	1st. READINGS		CORRECTIONS	CORRECTED INITIAL READINGS
	Magnet	Fill		
V41B	53.150	54.4	0.010	53.160
V42B	55.366	55.8	0.009	55.375
V43B	58.602	59.4	0.028	58.630
V44B	61.708	64.0	0.097	61.805
V45B	64.757	65.0	0.008	64.765

VERTICAL MOVEMENTS
SETTLEMENT MAGNETS

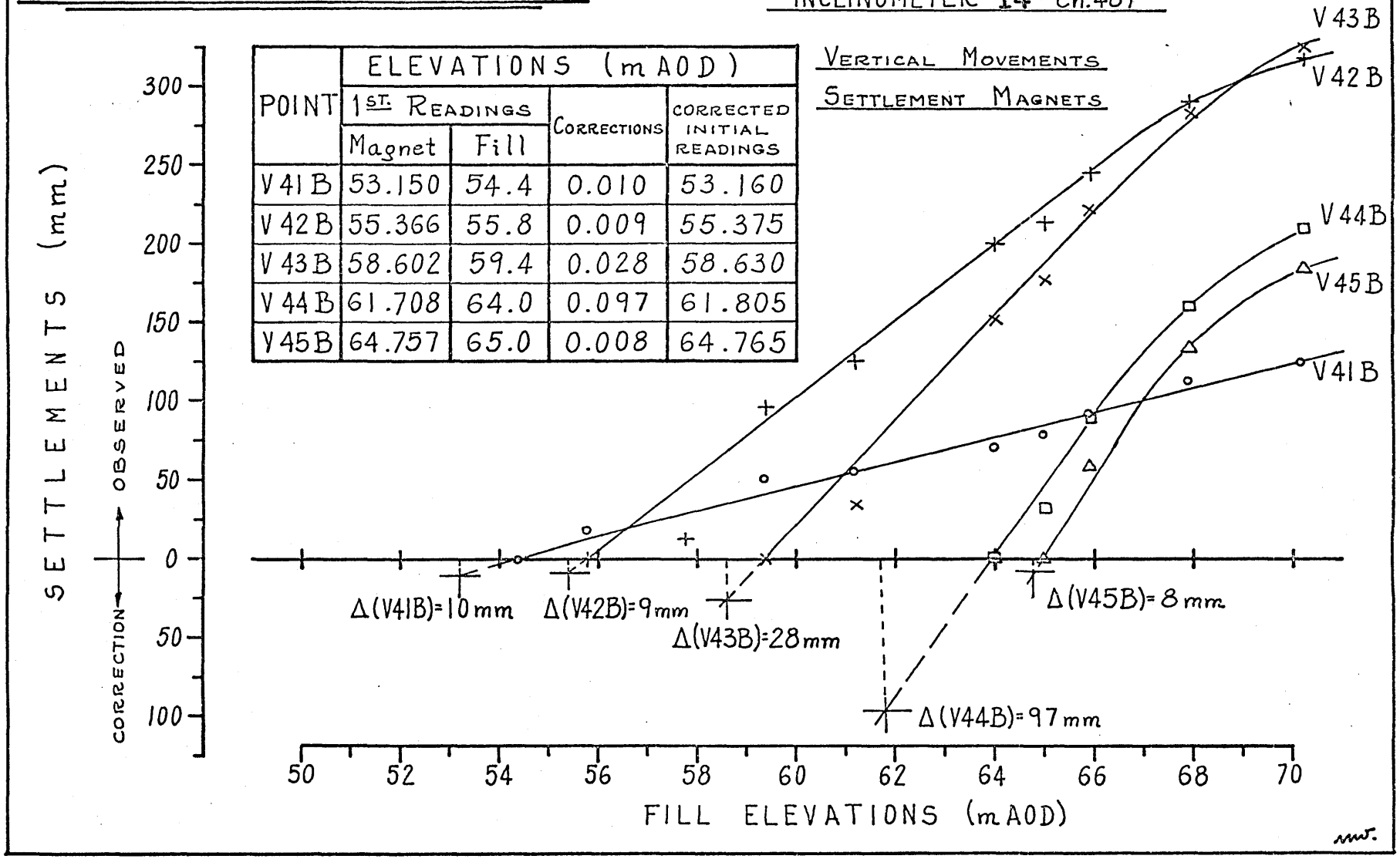
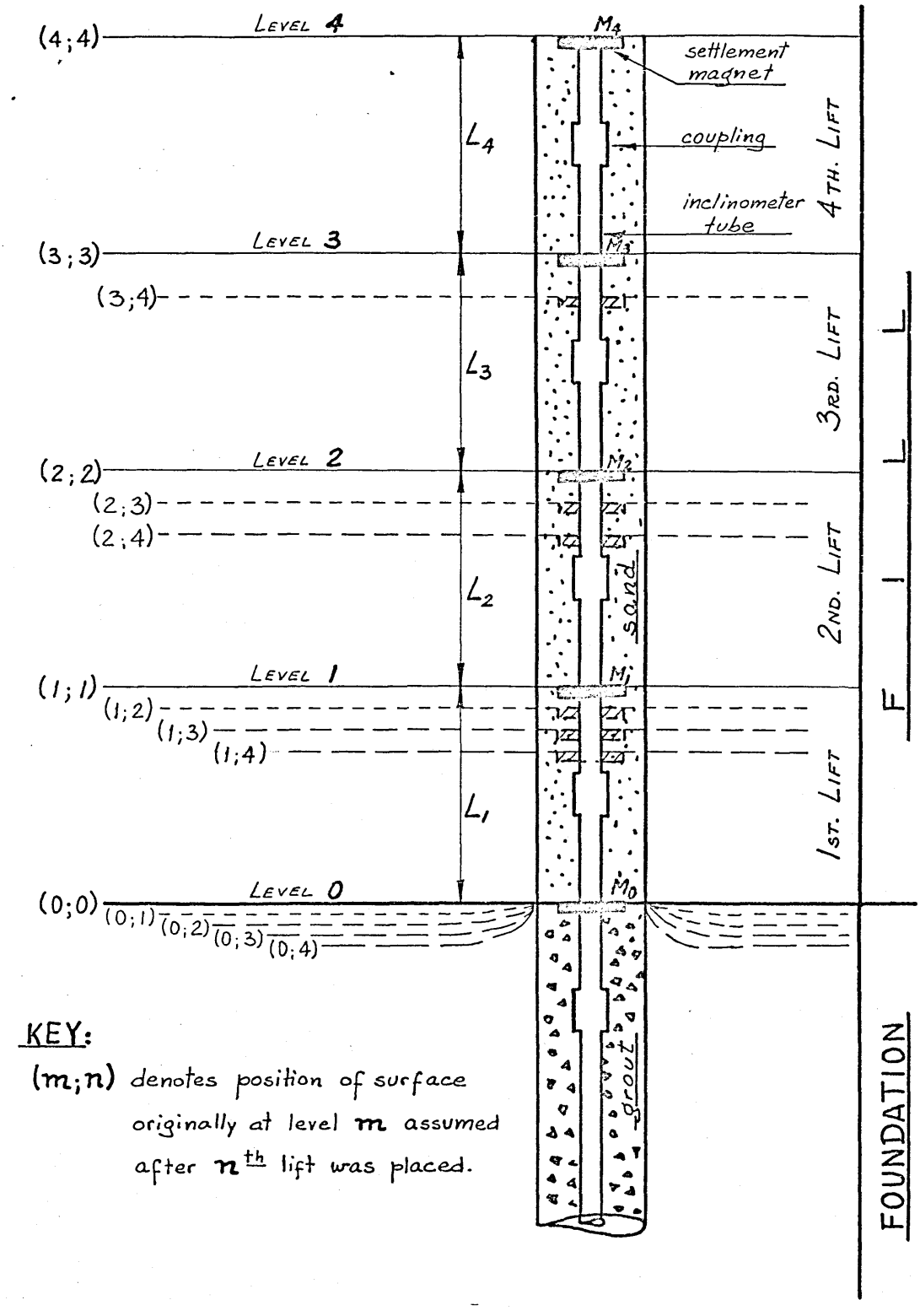


FIG. 6.50

FIG. 6.50

SETTLEMENT MAGNET SYSTEM

EFFECT OF BACKFILLING STIFFNESS



KEY:

(m;n) denotes position of surface originally at level **m** assumed after **n**th lift was placed.

FIG. 6.51

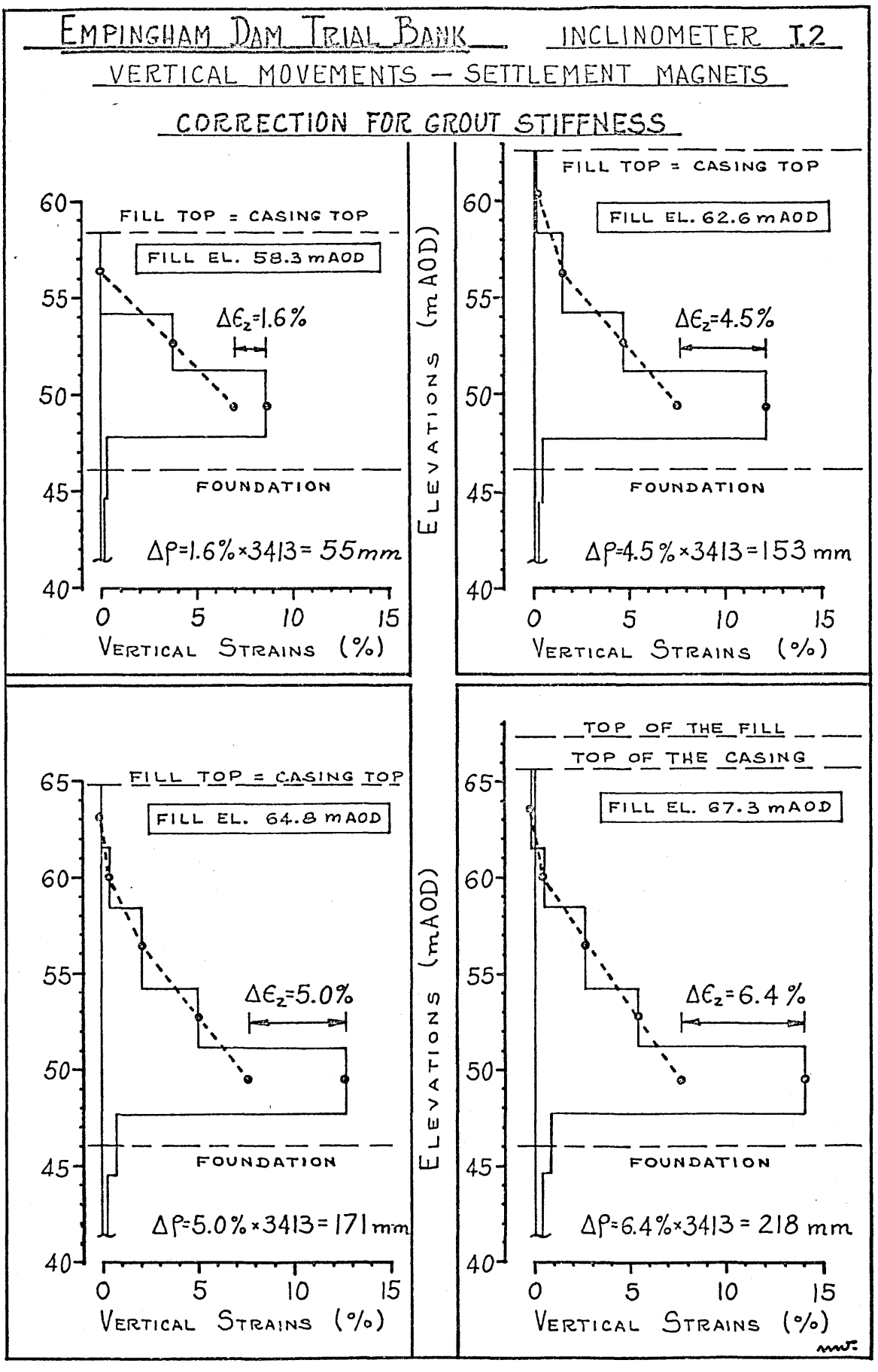

EMPINGHAM DAM TRIAL BANK
INCLINOMETER I.2
VERTICAL MOVEMENTS — SETTLEMENT MAGNETS
CORRECTION FOR GROUT STIFFNESS
FILL TOP = CASING TOP
FILL EL. 58.3 mAOD
ΔE₂=1.6%
FOUNDATION
Δρ=1.6%×3413= 55mm
FILL TOP = CASING TOP
FILL EL. 62.6 mAOD
ΔE₂=4.5%
FOUNDATION
Δρ=4.5%×3413=153 mm
FILL TOP = CASING TOP
FILL EL. 64.8 mAOD
ΔE₂=5.0%
FOUNDATION
Δρ=5.0%×3413=171 mm
TOP OF THE FILL
TOP OF THE CASING
FILL EL. 67.3 mAOD
ΔE₂=6.4%
FOUNDATION
Δρ=6.4%×3413 = 218 mm
ELEVATIONS (mAOD)
VERTICAL STRAINS (%)
0 5 10 15
40 45 50 55 60 65

FIG. 6.52

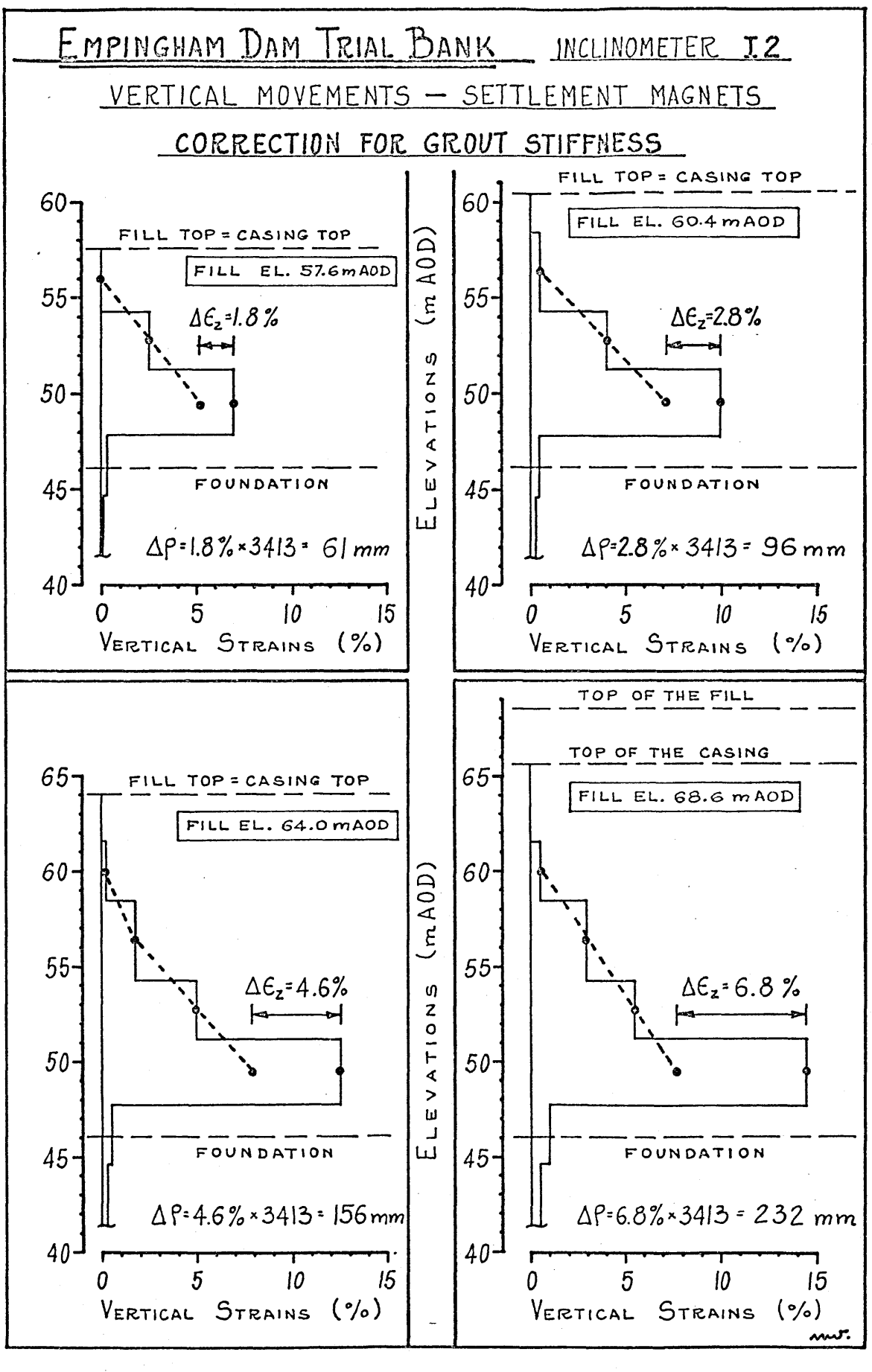

EMPINGHAM DAM TRIAL BANK
INCLINOMETER I2
VERTICAL MOVEMENTS — SETTLEMENT MAGNETS
CORRECTION FOR GROUT STIFFNESS
FILL TOP = CASING TOP
FILL EL. 57.6 m AOD
Δεz=1.8%
FOUNDATION
ΔP=1.8%×3413 = 61 mm
FILL TOP = CASING TOP
FILL EL. 60.4 m AOD
Δεz=2.8%
FOUNDATION
ΔP=2.8%×3413 = 96 mm
ELEVATIONS (m AOD)
FILL TOP = CASING TOP
FILL EL. 64.0 m AOD
Δεz=4.6%
FOUNDATION
ΔP=4.6%×3413 = 156 mm
TOP OF THE FILL
TOP OF THE CASING
FILL EL. 68.6 m AOD
Δεz=6.8%
FOUNDATION
ΔP=6.8%×3413 = 232 mm
VERTICAL STRAINS (%)
0 5 10 15
40 45 50 55 60 65

FIG. 6.53

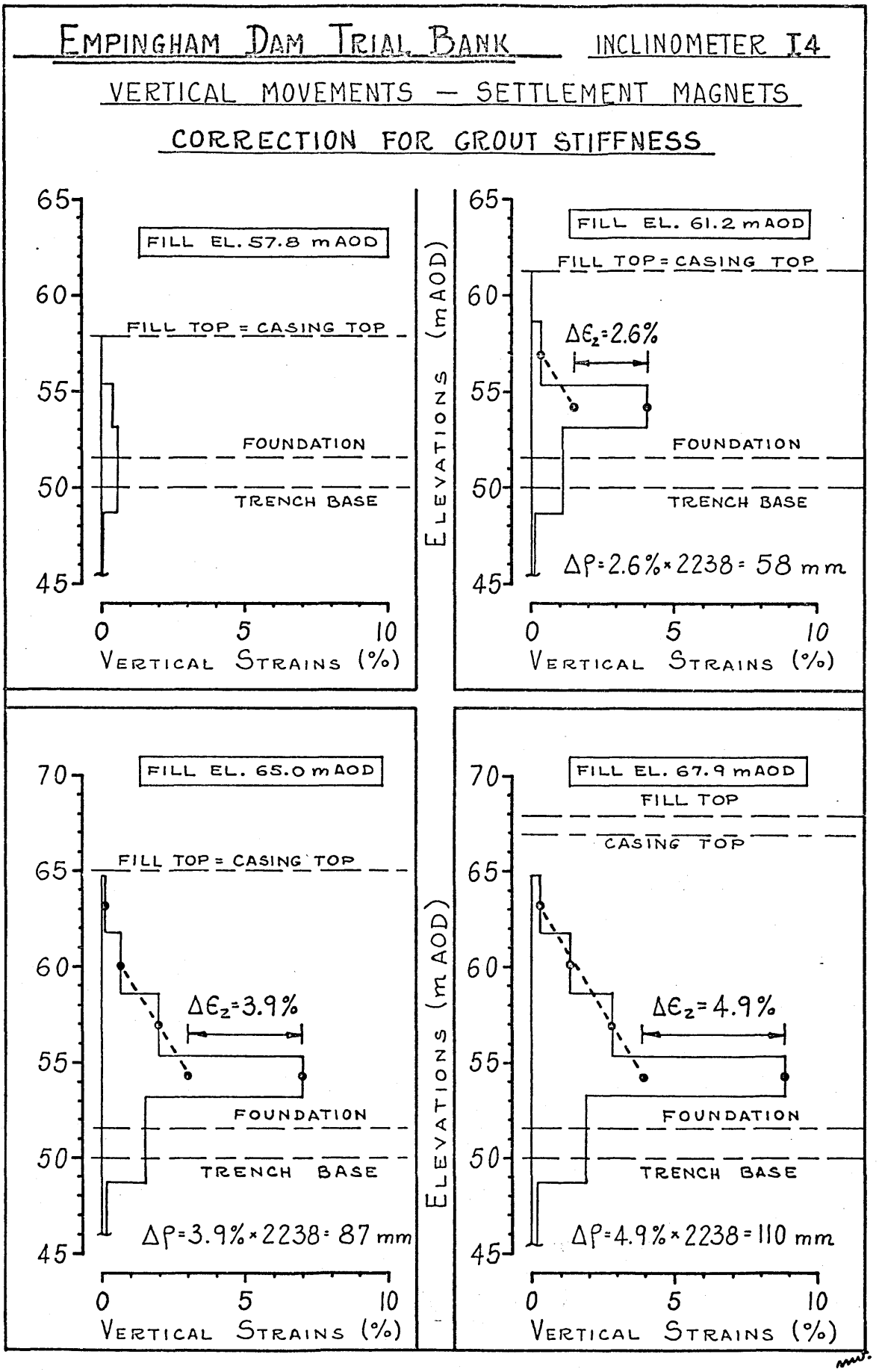

EMPINGHAM DAM TRIAL BANK
INCLINOMETER I4
VERTICAL MOVEMENTS — SETTLEMENT MAGNETS
CORRECTION FOR GROUT STIFFNESS
FILL EL. 57.8 mAOD
FILL TOP = CASING TOP
FOUNDATION
TRENCH BASE
FILL EL. 61.2 mAOD
FILL TOP = CASING TOP
Δε2 = 2.6%
FOUNDATION
TRENCH BASE
Δρ = 2.6% × 2238 = 58 mm
FILL EL. 65.0 mAOD
FILL TOP = CASING TOP
Δε2 = 3.9%
FOUNDATION
TRENCH BASE
Δρ = 3.9% × 2238 = 87 mm
FILL EL. 67.9 mAOD
FILL TOP
CASING TOP
Δε2 = 4.9%
FOUNDATION
TRENCH BASE
Δρ = 4.9% × 2238 = 110 mm
ELEVATIONS (mAOD)
VERTICAL STRAINS (%)
0
5
10
45
50
55
60
65
70

FIG. 6.54

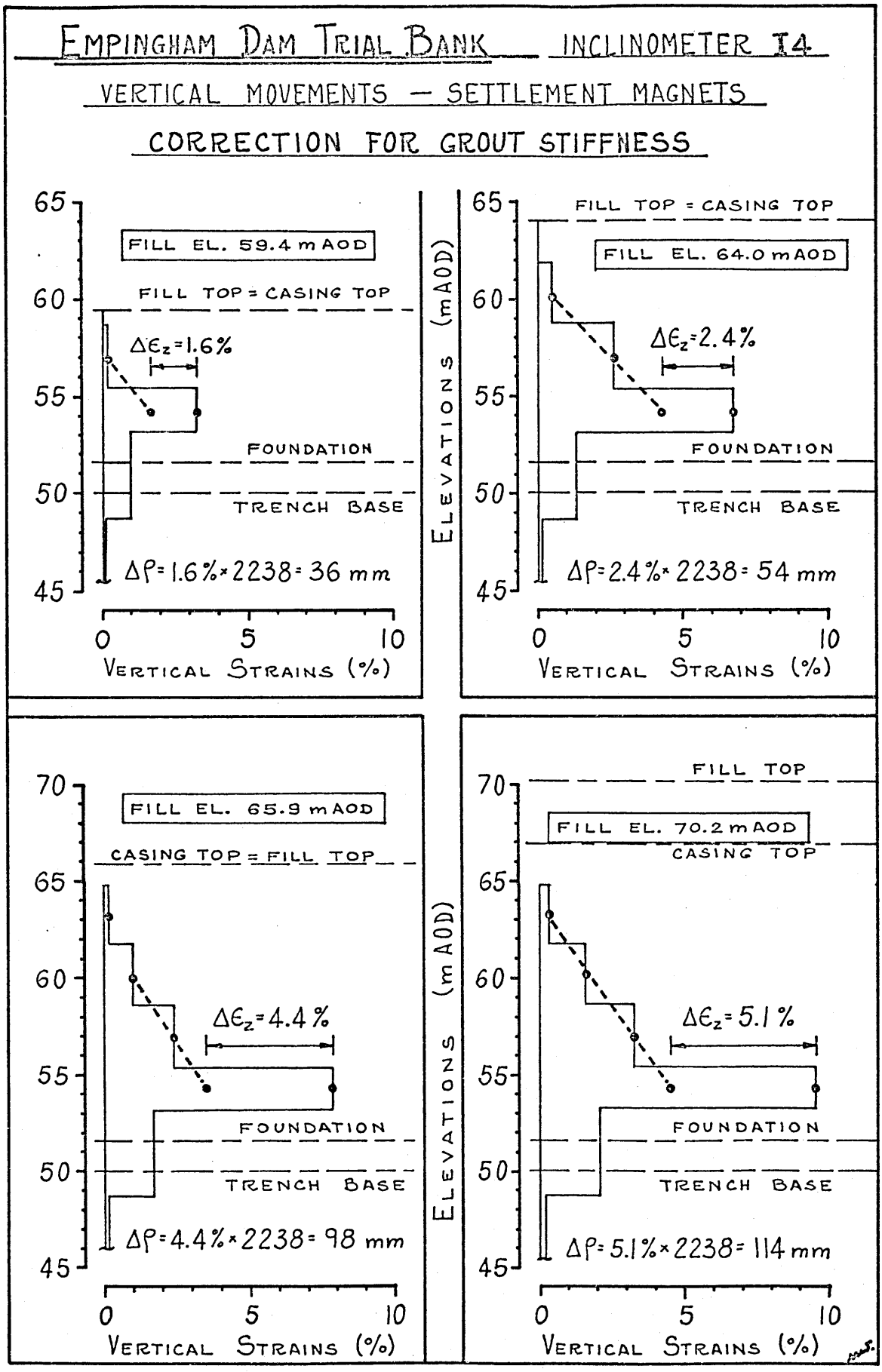
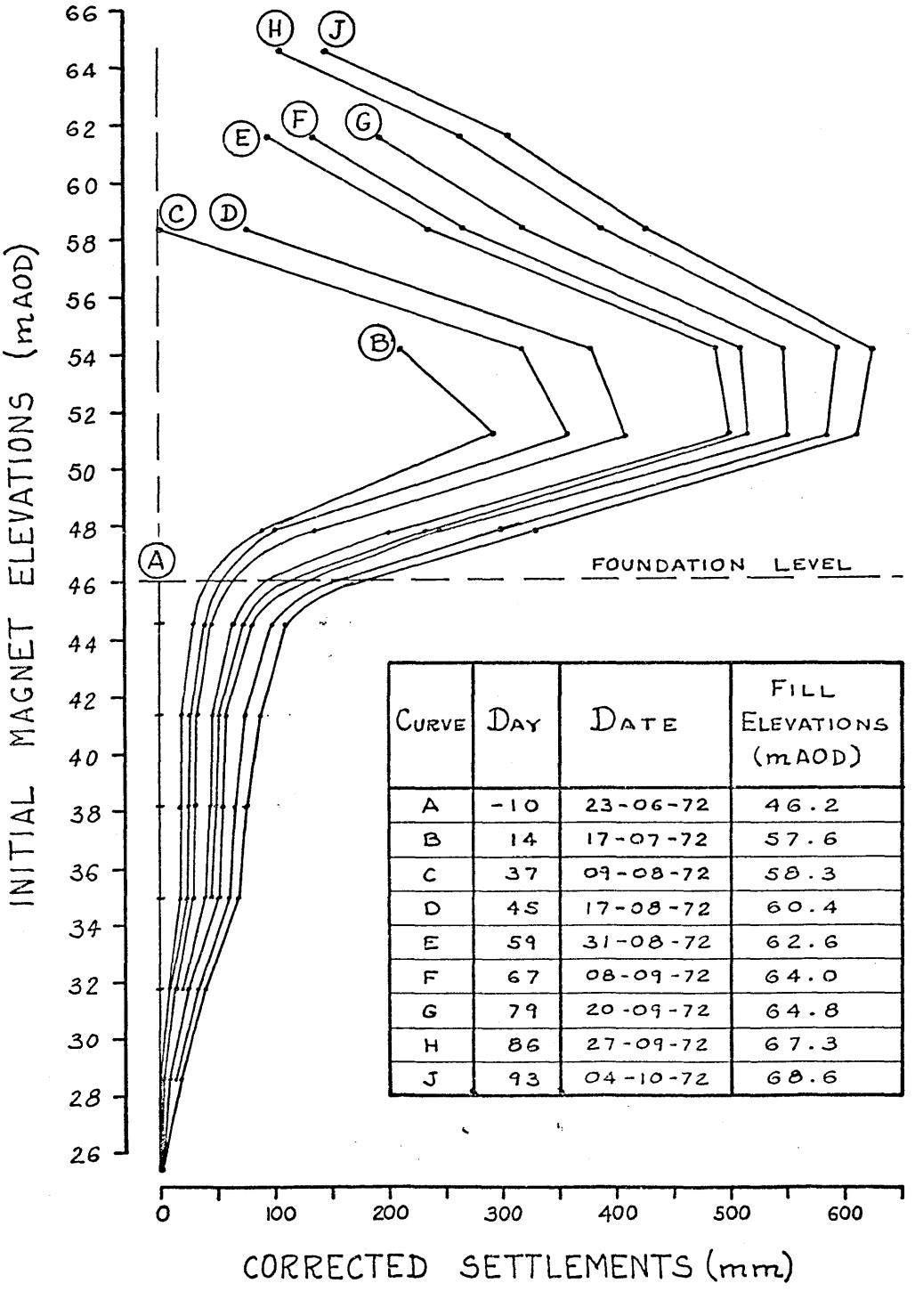

EMPINGHAM DAM TRIAL BANK INCLINOMETER I4
VERTICAL MOVEMENTS — SETTLEMENT MAGNETS
CORRECTION FOR GROUT STIFFNESS
FILL EL. 59.4 m AOD
FILL TOP = CASING TOP
Δεz = 1.6%
FOUNDATION
TRENCH BASE
ΔP = 1.6% × 2238 = 36 mm
FILL EL. 64.0 m AOD
Δεz = 2.4%
ΔP = 2.4% × 2238 = 54 mm
FILL EL. 65.9 m AOD
CASING TOP = FILL TOP
Δεz = 4.4%
ΔP = 4.4% × 2238 = 98 mm
FILL EL. 70.2 m AOD
FILL TOP
CASING TOP
Δεz = 5.1%
ΔP = 5.1% × 2238 = 114 mm
ELEVATIONS (m AOD)
VERTICAL STRAINS (%)
65
60
55
50
45
70
0
5
10

FIG. 6.55

EMPINGHAM DAM TRIAL BANK

INCLINOMETER I2 ~ Ch.537

CORRECTED VERTICAL MOVEMENTS — SETTLEMENT MAGNETS



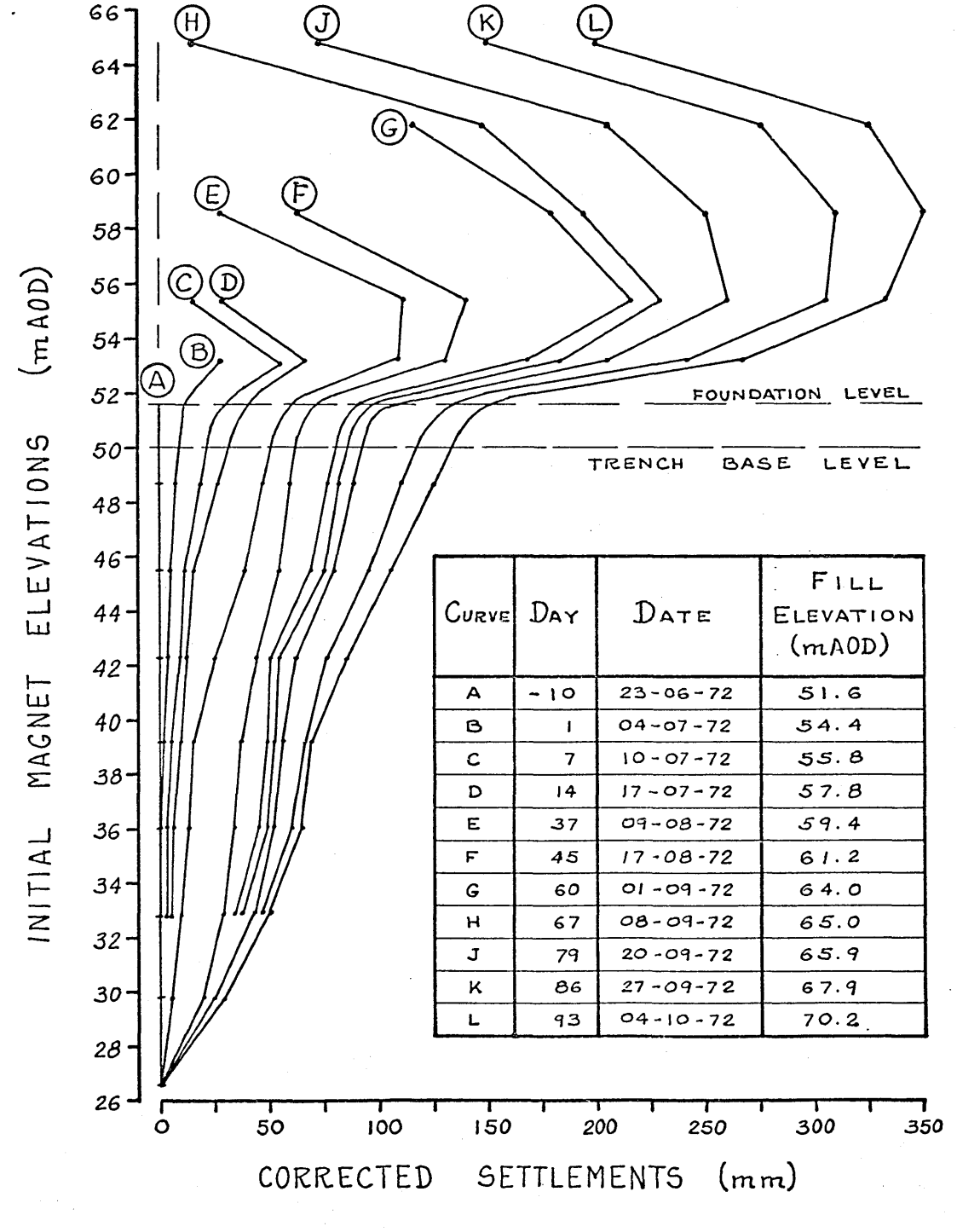
Curve	Day	Date	Fill Elevations (mAOD)
A	-10	23-06-72	46.2
B	14	17-07-72	57.6
C	37	09-08-72	58.3
D	45	17-08-72	60.4
E	59	31-08-72	62.6
F	67	08-09-72	64.0
G	79	20-09-72	64.8
H	86	27-09-72	67.3
J	93	04-10-72	68.6

FIG. 6.56

EMPINGHAM DAM TRIAL BANK

INCLINOMETER I4 ~ Ch. 487

CORRECTED VERTICAL MOVEMENTS — SETTLEMENT MAGNETS



CURVE	DAY	DATE	FILL ELEVATION (mAOD)
A	-10	23-06-72	51.6
B	1	04-07-72	54.4
C	7	10-07-72	55.8
D	14	17-07-72	57.8
E	37	09-08-72	59.4
F	45	17-08-72	61.2
G	60	01-09-72	64.0
H	67	08-09-72	65.0
J	79	20-09-72	65.9
K	86	27-09-72	67.9
L	93	04-10-72	70.2

FIG. 6.57

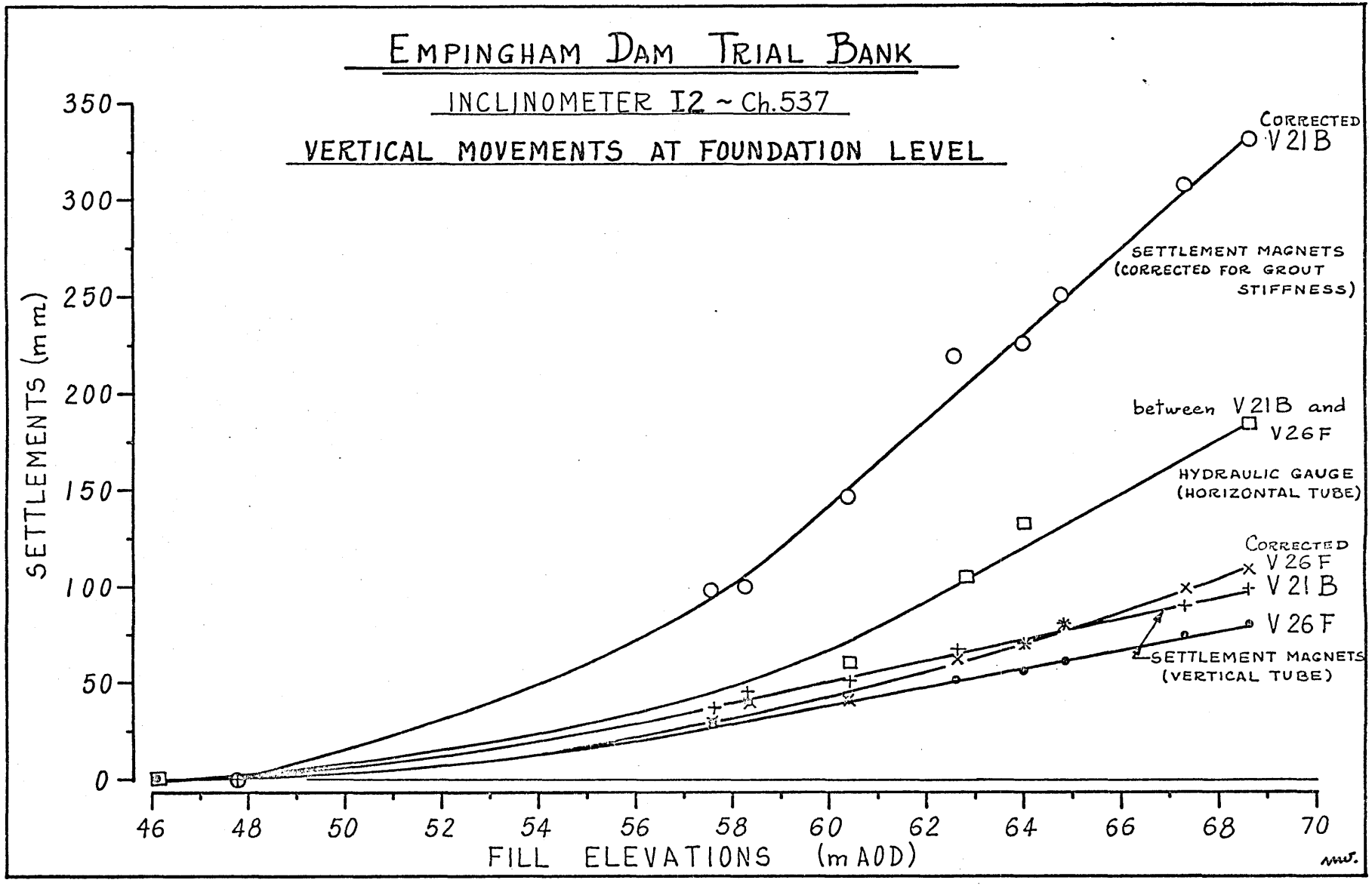


FIG. 6.58

FIG. 6.58

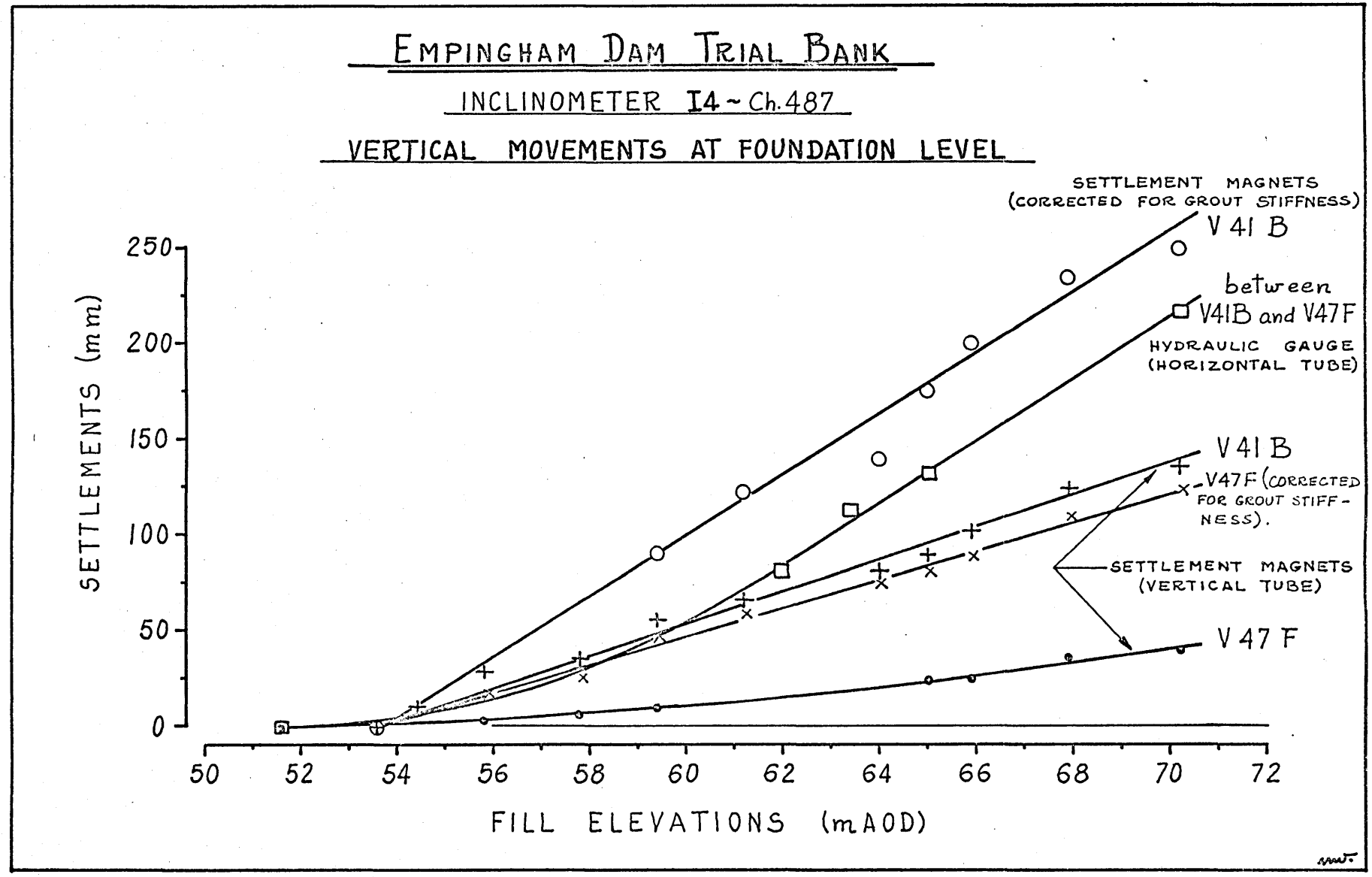


FIG. 6.59

FIG. 6.59

EMPINGHAM DAM TRIAL BANK

VERTICAL MOVEMENTS AT THE TOE — CH 487

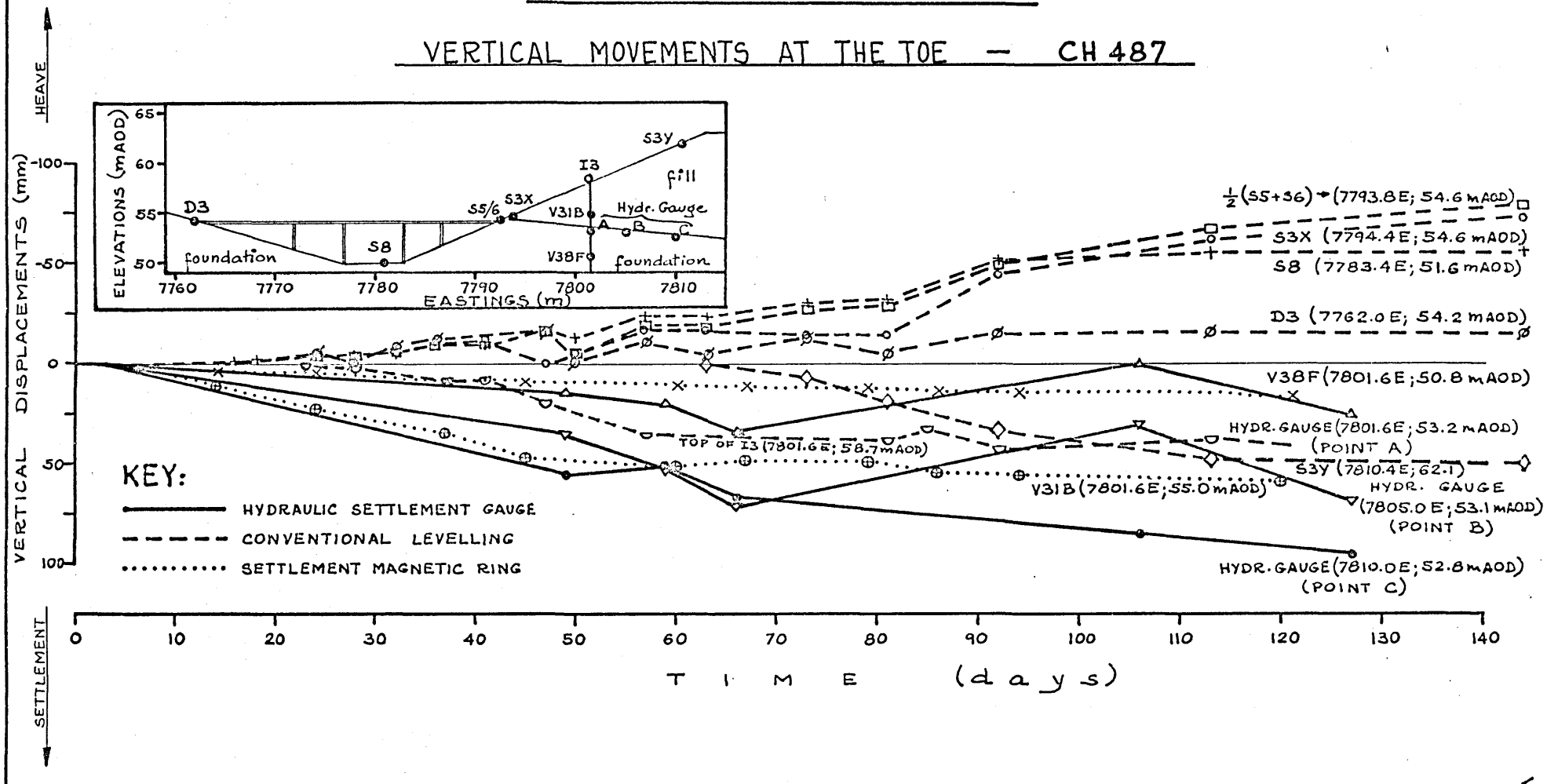


FIG. 6.60

FIG. 6.60

EMPINGHAM DAM TRIAL BANK

VERTICAL MOVEMENTS AT THE TOE — CH 514

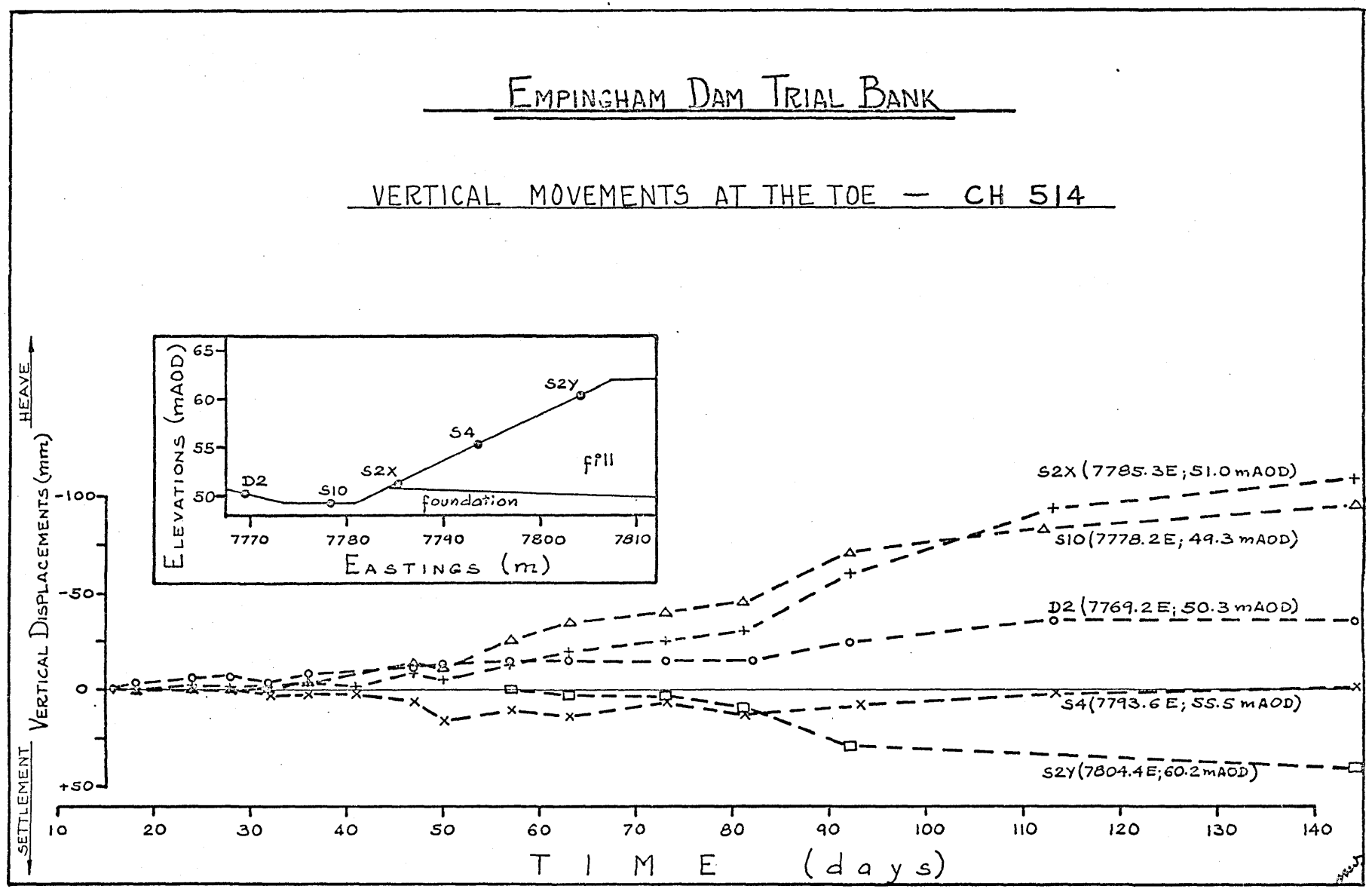
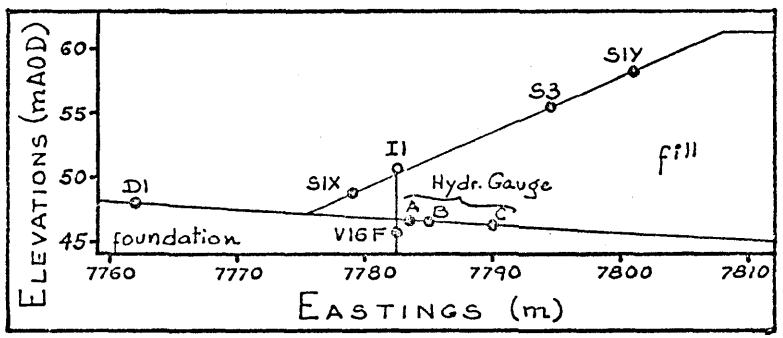


FIG. 6.61

FIG. 6.61

EMPINGHAM DAM TRIAL BANK

VERTICAL MOVEMENTS AT THE TOE – CH 537



KEY:

HYDRAULIC SETTLEMENT GAUGE

CONVENTIONAL LEVELLING

SETTLEMENT MAGNETIC RING

SIX (7780.0E; 48.0 mAOD)

V16F (7782.4E; 45.8mAOD)

TOP OF I1 (7782.4E; 49.2mOD)

Hydr. Gauge (7783.5E; 46.7mAOD) POINT A

Hydr. Gauge (7785.0E; 46.6mAOD) POINT B

D1 (7762.0E; 48.0 mAOD)

SIY (7801.0 E; 58.2 mAOD)

S3 (7794.5 E; 55.6 mAOD)

Hydr. Gauge (7790.0E; 46.4 mAOD) POINT C

VERTICAL DISPLACEMENTS (mm)

HEAVE

SETTLEMENT

+300
+250
+200
+150
+100
+50
0
-50
-100
-150

0 10 20 30 40 50 60 70 80 90 100 110 120 130 140

TIME (days)

FIG. 6.62

FIG. 6.62

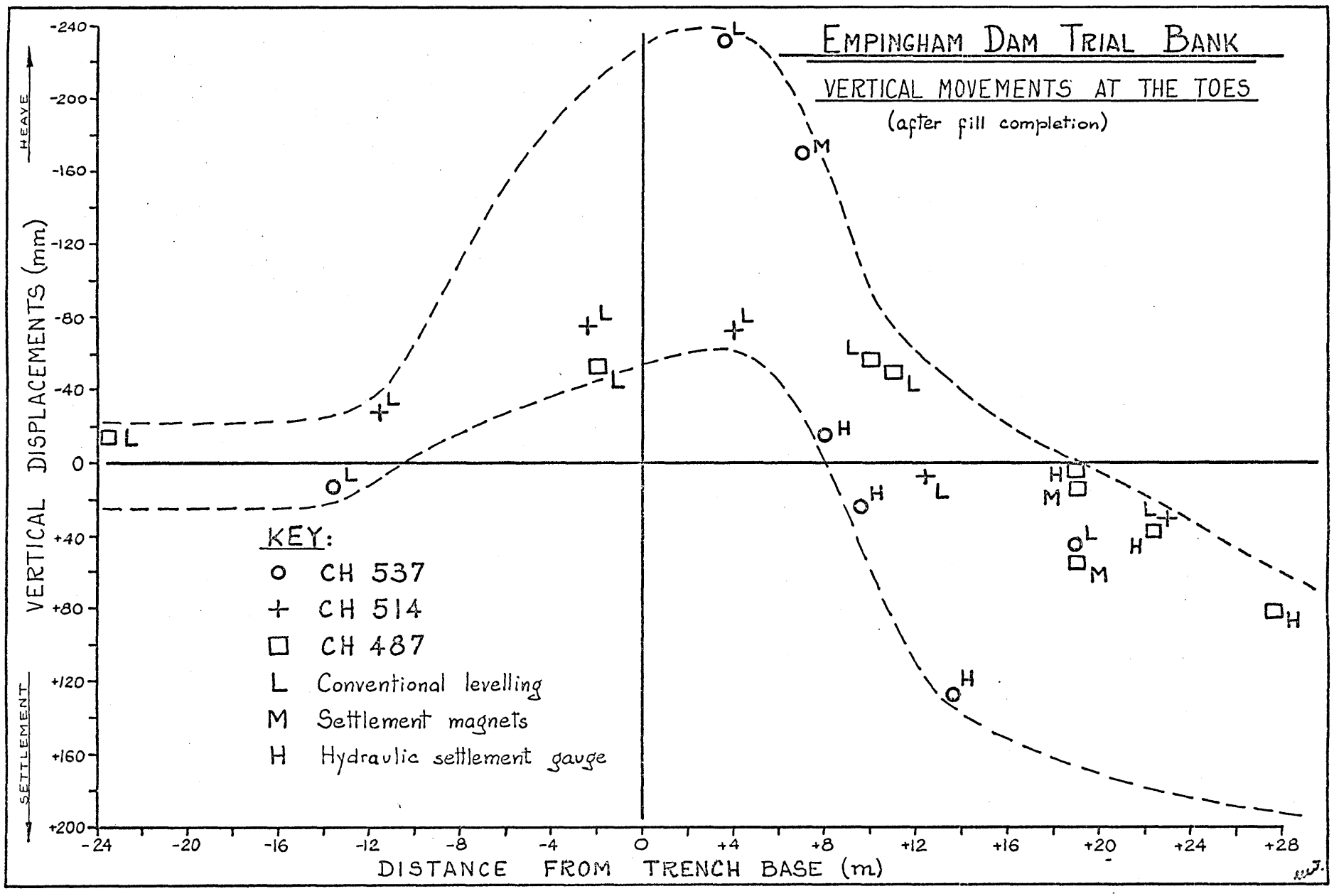


FIG. 6.63

FIG. 6.63

EMPINGHAM DAM TRIAL BANK

VERTICAL MOVEMENTS — HYDRAULIC SETTLEMENT GAUGE

CH 487

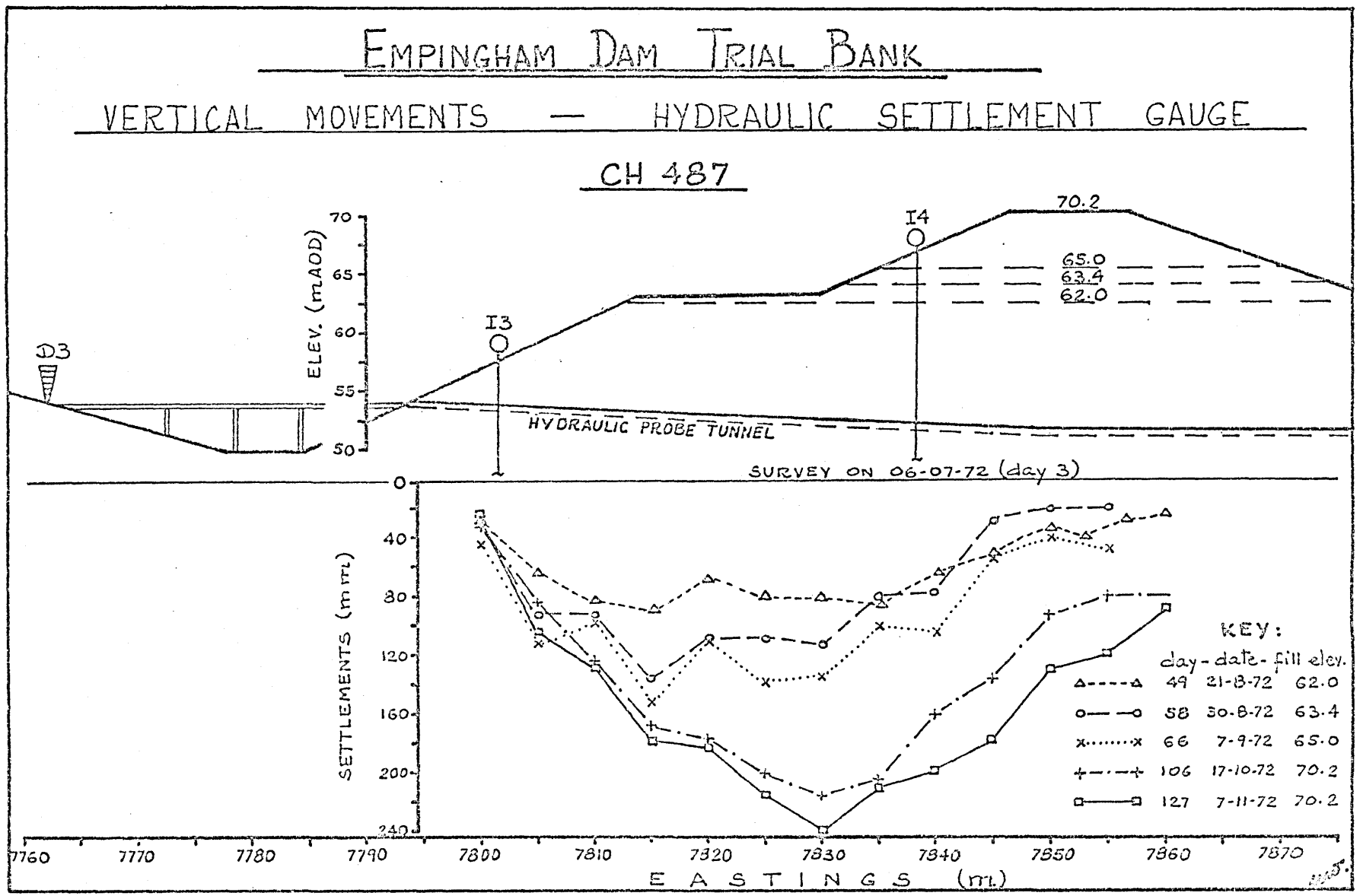


FIG. 6.64

FIG. 6.64

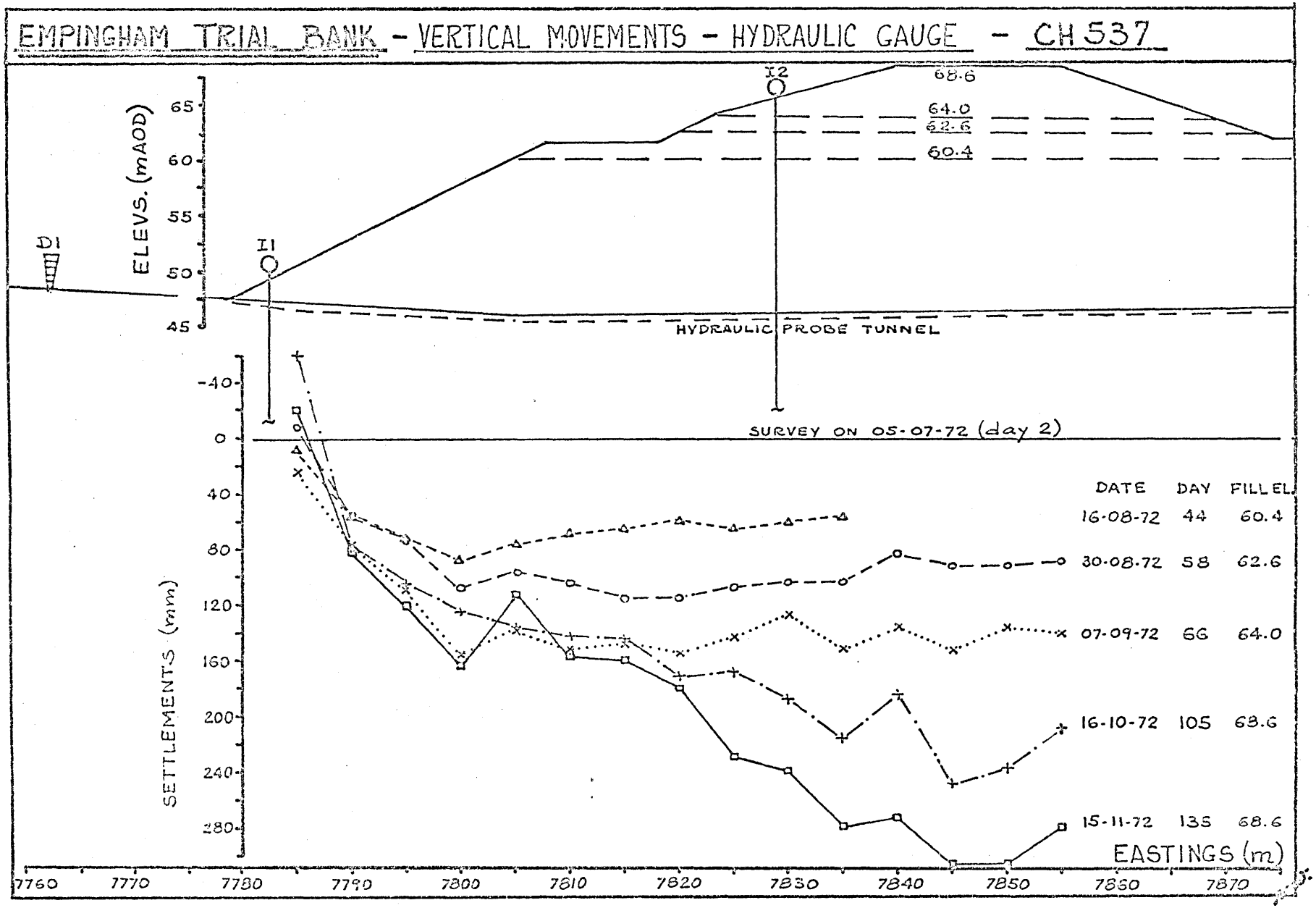


FIG. 6.65

FIG. 6.65

EMPINGHAM DAM TRIAL BANK — VERTICAL MOVEMENTS

SURFACE REFERENCE POINTS

POINT	COORDINATES (m)		
	CHAINAGE	EASTING	ELEVATION
S1	570.0	7801.1	54.6
S2	550.5	7795.8	54.6
S3	534.0	7794.5	55.6
S4	514.5	7793.6	55.5
S5	497.5	7793.8	55.0
S6	478.0	7794.0	54.2
S7	458.2	7795.8	55.2
S8	496.6	7783.4	51.6
S10	477.0	7778.2	49.3
S2X	514.1	7785.3	51.0
S3X	486.9	7794.4	54.6

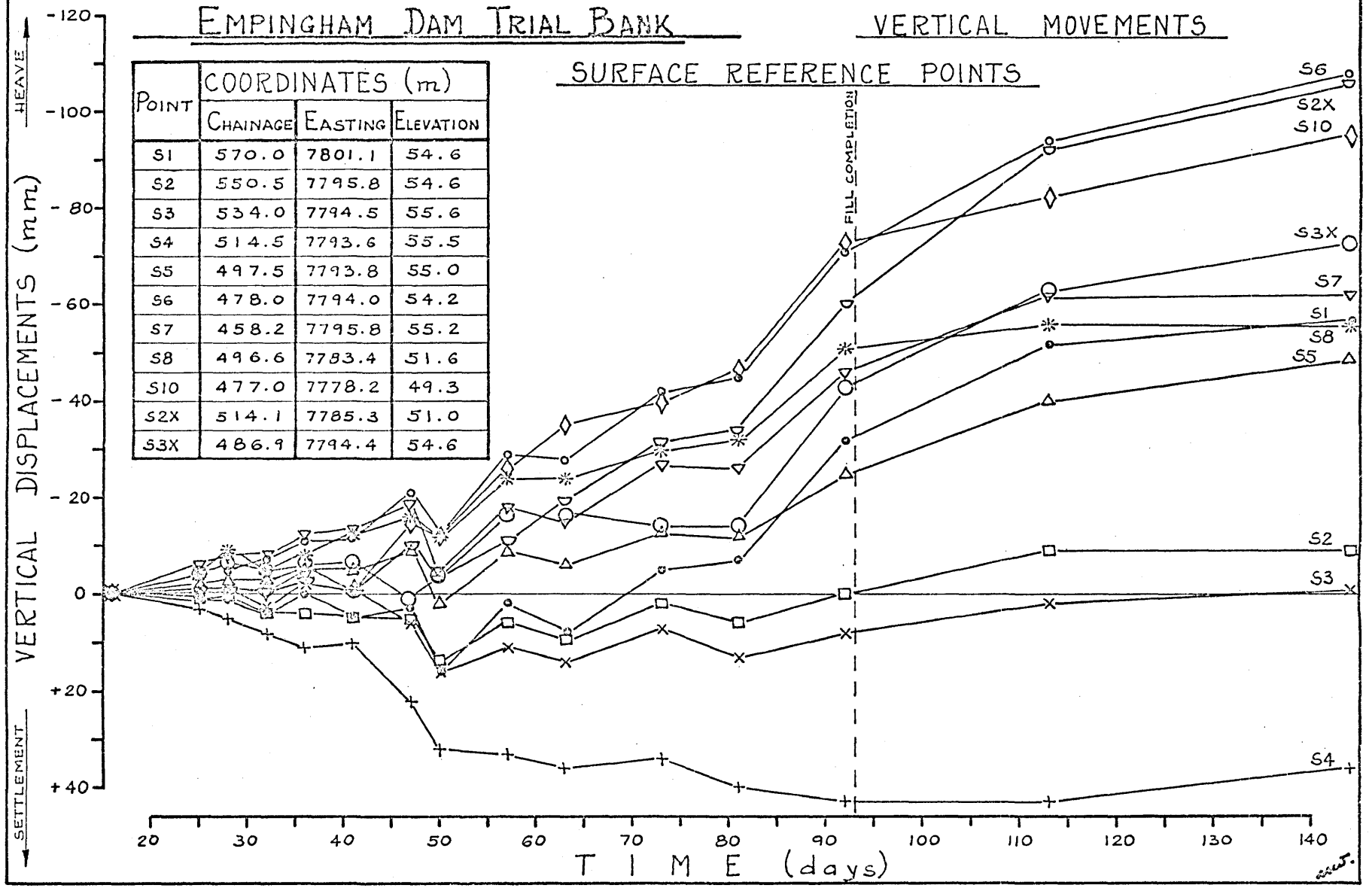


FIG. 6.66

FIG. 6.66

EMPINGHAM DAM TRIAL BANK

VERTICAL MOVEMENTS

SURFACE REFERENCE POINTS

POINT	COORDINATES (m)		
	CHAINAGE	EASTINGS	ELEVATION
S1X	537.0	7780.0	48.0
S1Y	537.0	7801.0	58.2
S2Y	514.1	7804.4	60.2
S3Y	486.9	7810.4	62.1
I1 TOP	539.9	7782.4	49.2
I3 TOP	491.6	7801.6	55.0

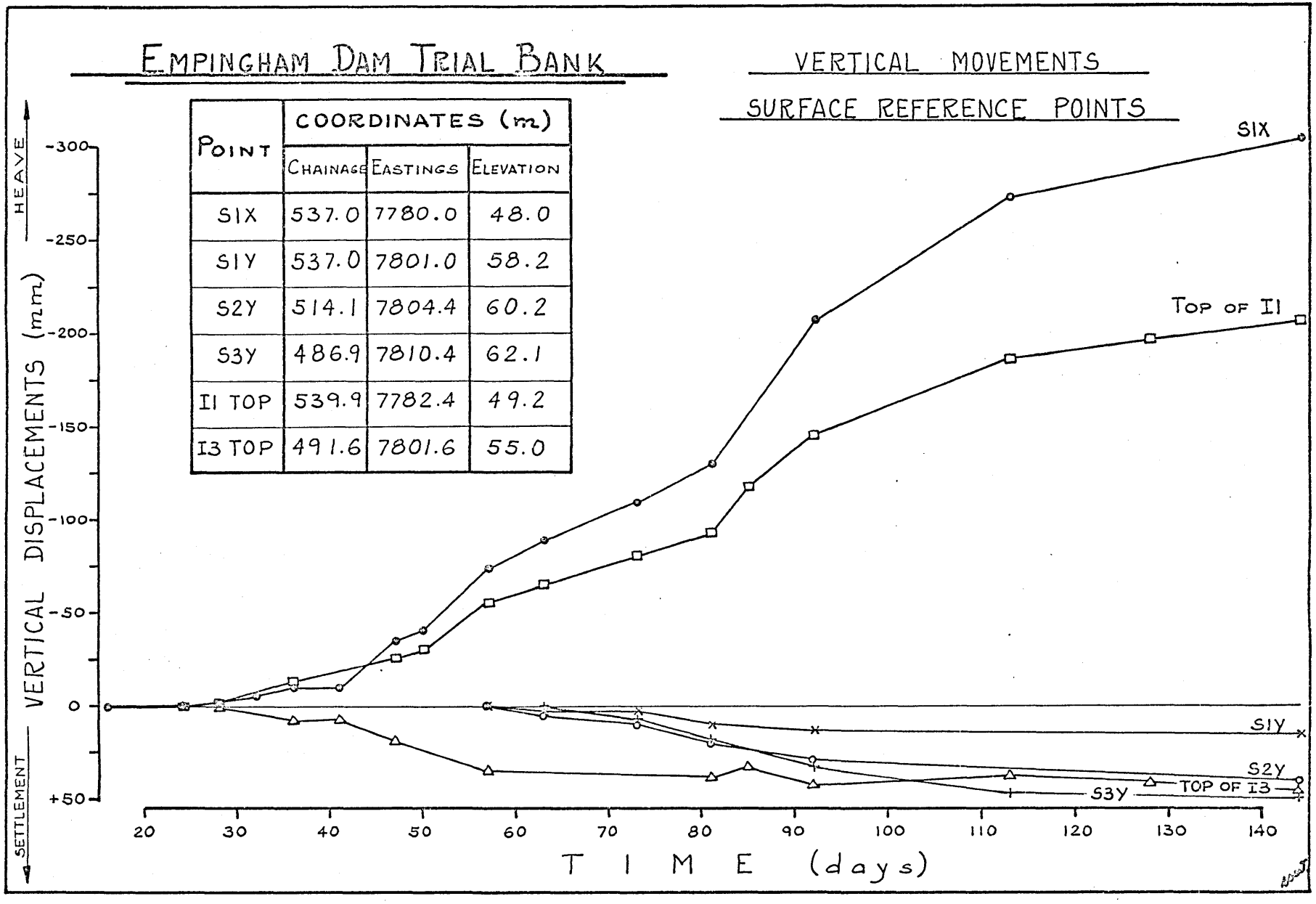


FIG. 6.67

FIG. 6.67

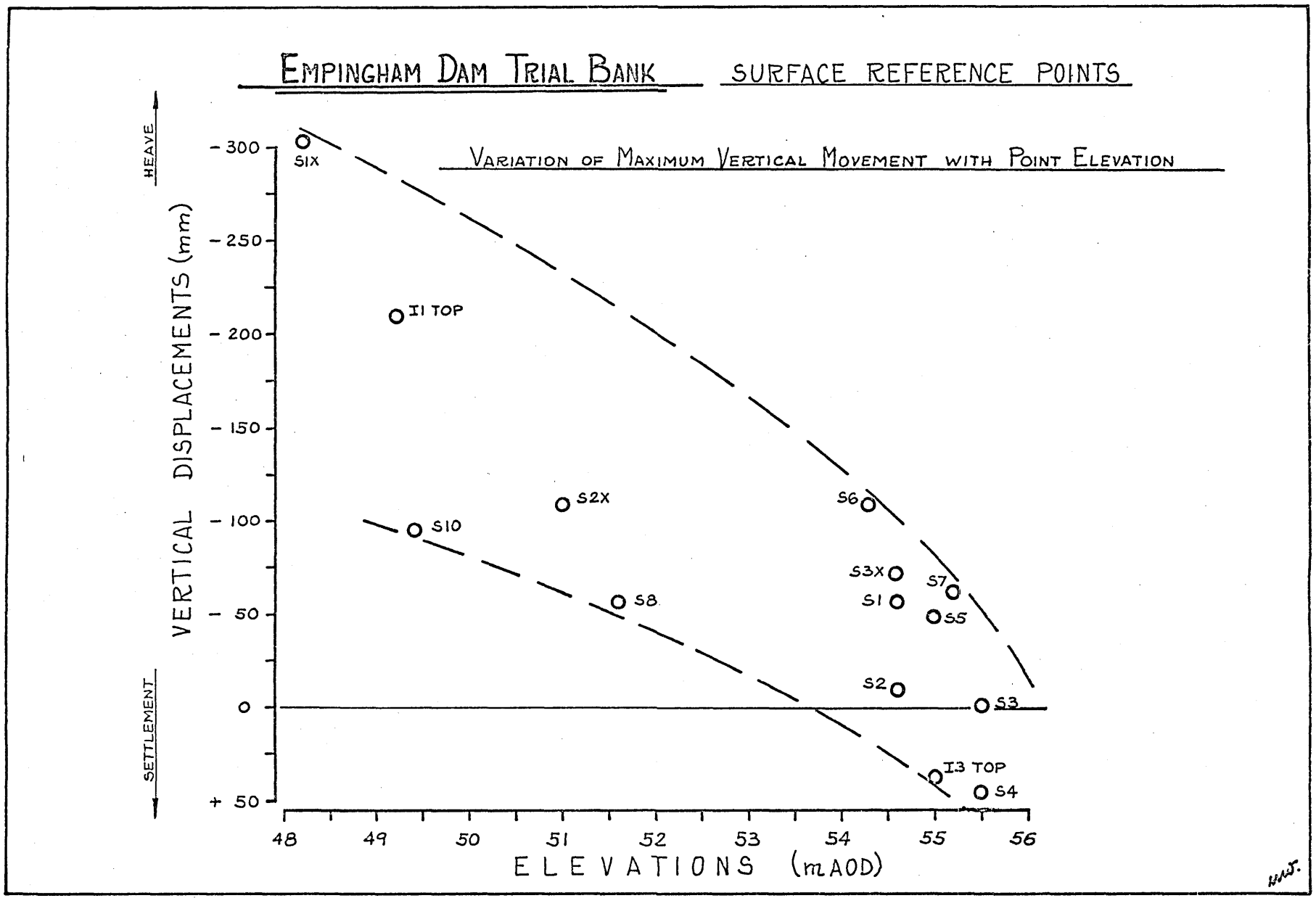


FIG. 6.68

FIG. 6.68

EMPINGHAM DAM TRIAL BANK

MOVEMENTS IN THE FOUNDATION

Ch. 487

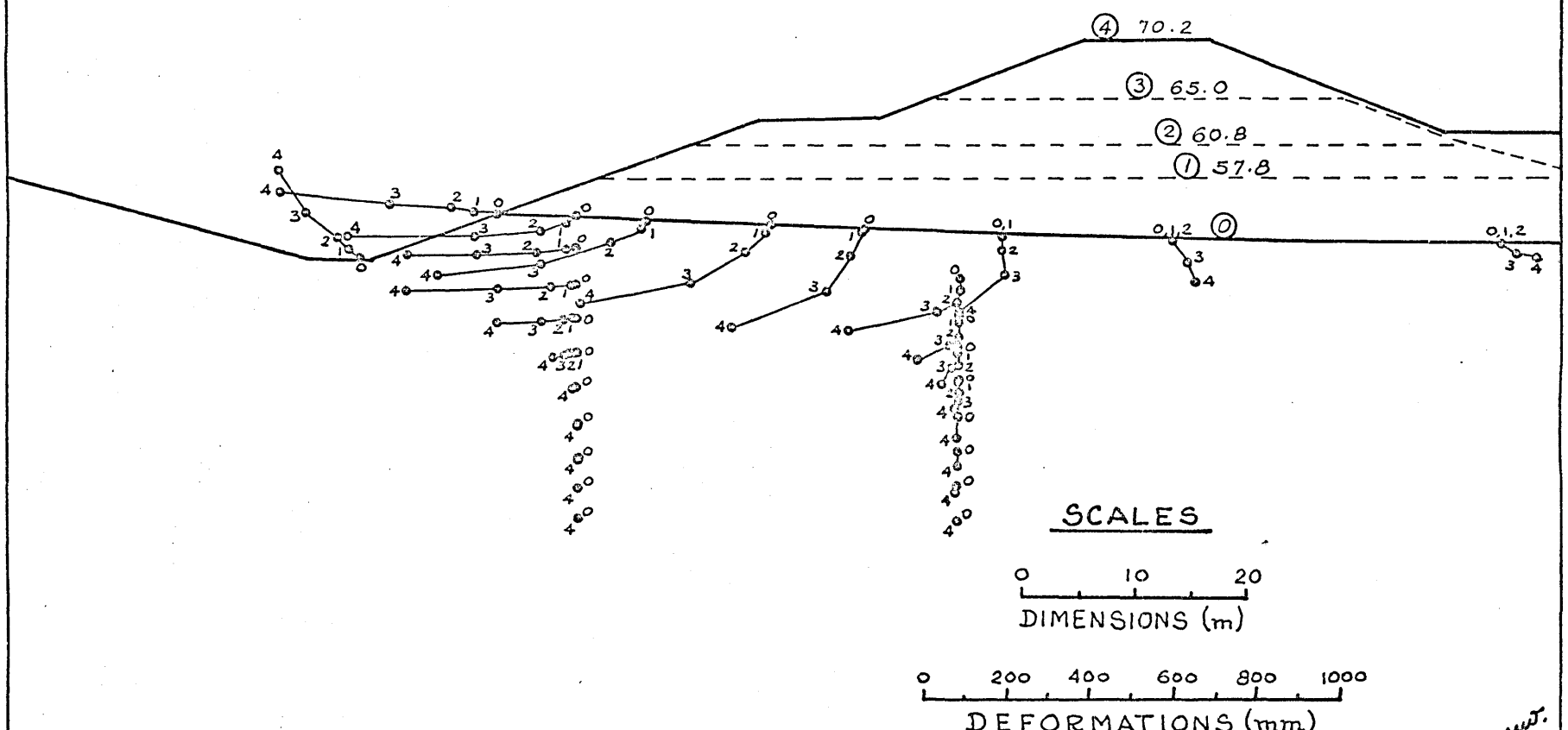


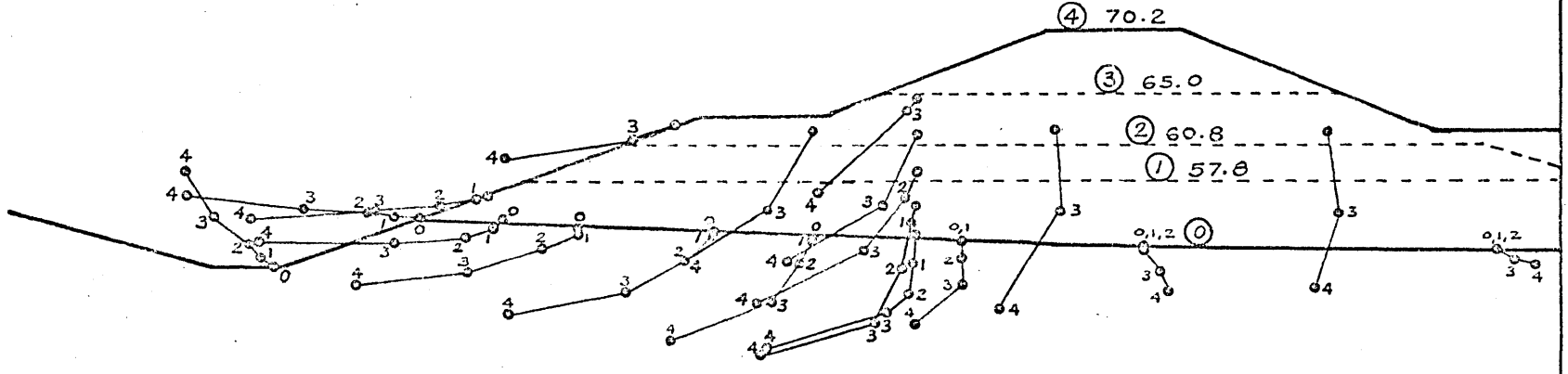
FIG. 6.69

FIG. 6.69

EMPINGHAM DAM TRIAL BANK

MOVEMENTS IN THE FILL

Ch. 487



SCALES

0 10 20

DIMENSIONS (m)

0 200 400 600 800 1000

DEFORMATIONS (mm)

FIG. 6.70

FIG. 6.70

EMPINGHAM DAM TRIAL BANK

MOVEMENTS IN THE FOUNDATION

Ch.537

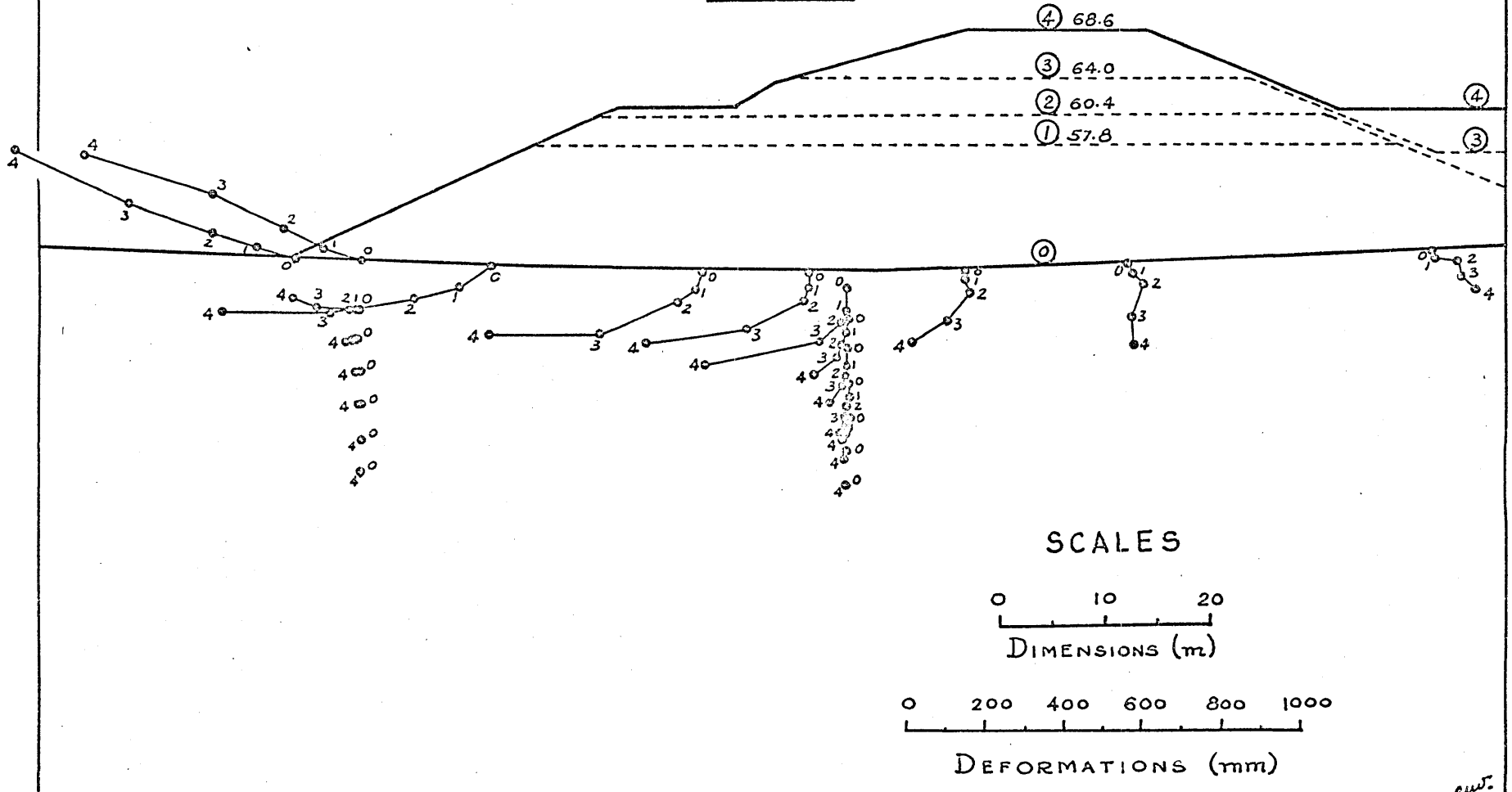


FIG. 6.71

FIG. 6.71

EMPINGHAM DAM TRIAL BANK

MOVEMENTS IN THE FILL

Ch. 537

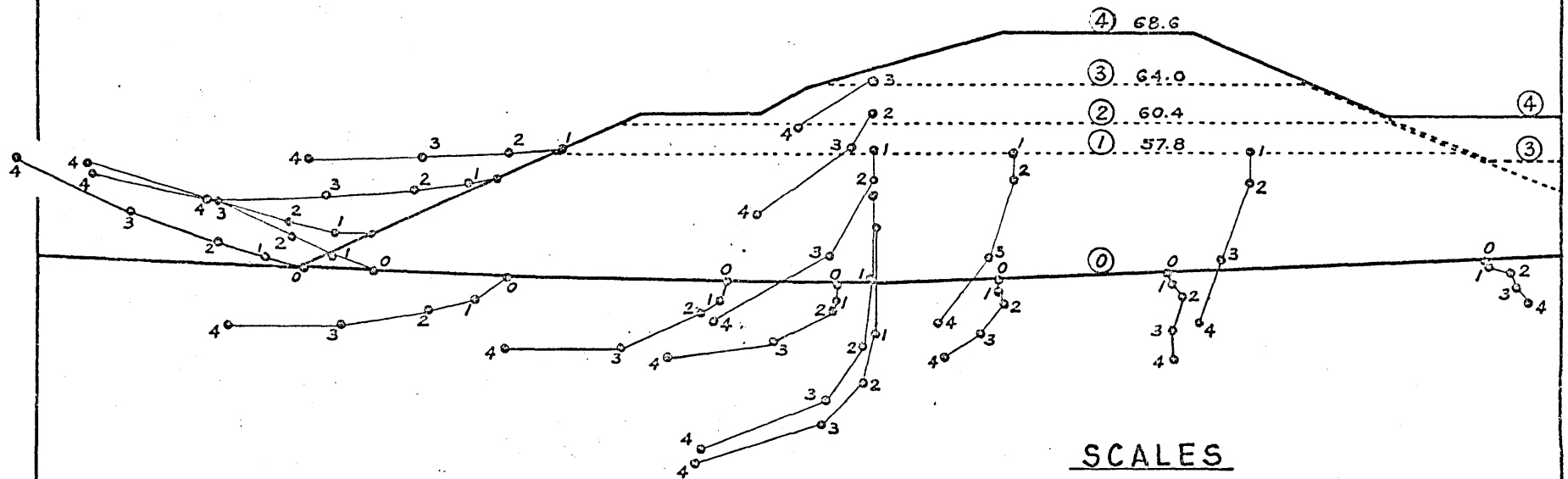


FIG. 6.72

FIG. 6.72

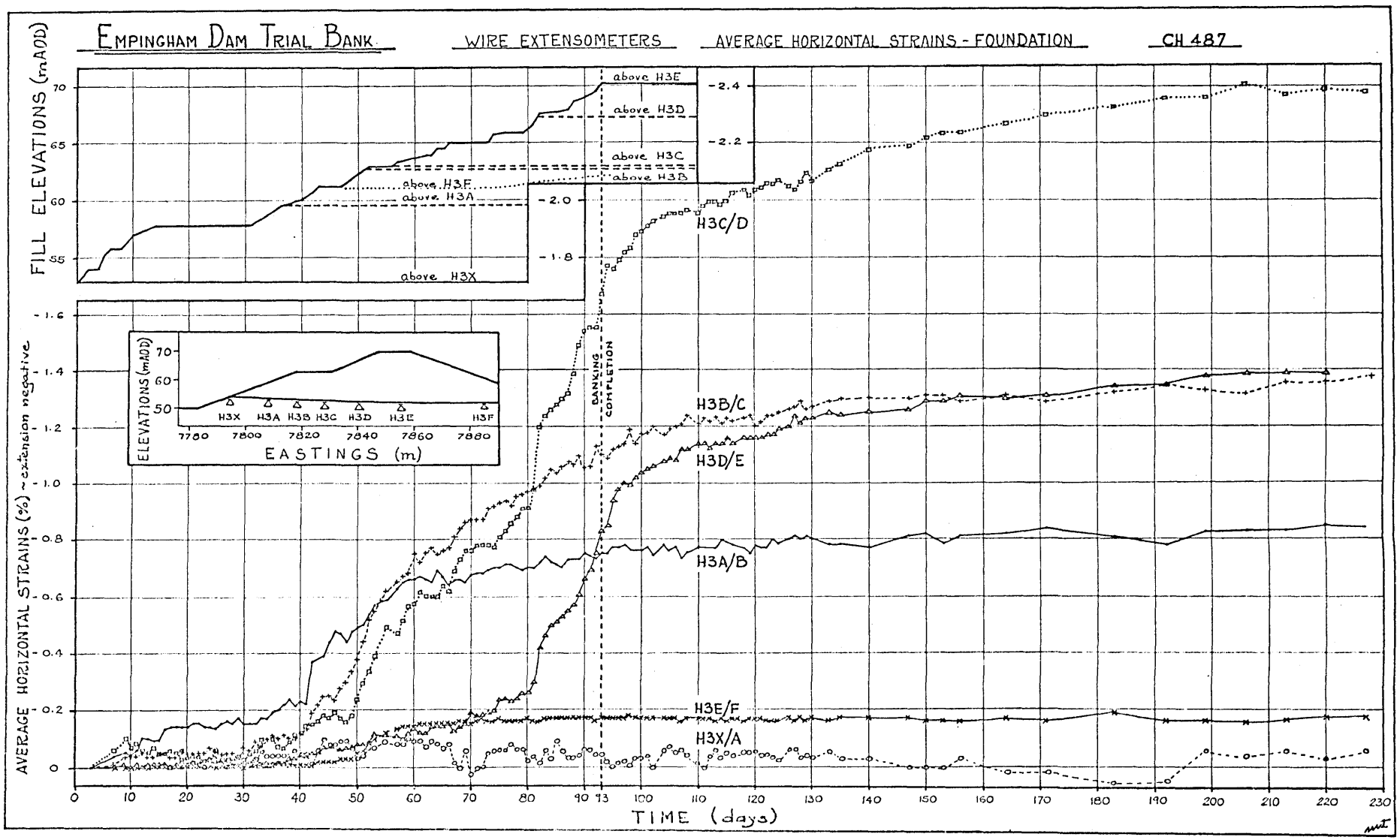

EMPINGHAM DAM TRIAL BANK
WIRE EXTENSOMETERS
AVERAGE HORIZONTAL STRAINS - FOUNDATION
CH 487
FILL ELEVATIONS (mAOD)
above H3E
above H3D
above H3C
above H3B
above H3F
above H3A
above H3X
-2.4
-2.2
-2.0
-1.8
ELEVATIONS (mAOD)
H3X H3A H3B H3C H3D H3E H3F
EASTINGS (m)
AVERAGE HORIZONTAL STRAINS (%) ~ extension negative
BANKING COMPLETION
H3C/D
H3B/C
H3D/E
H3A/B
H3E/F
H3X/A
TIME (days)

FIG. 6.73

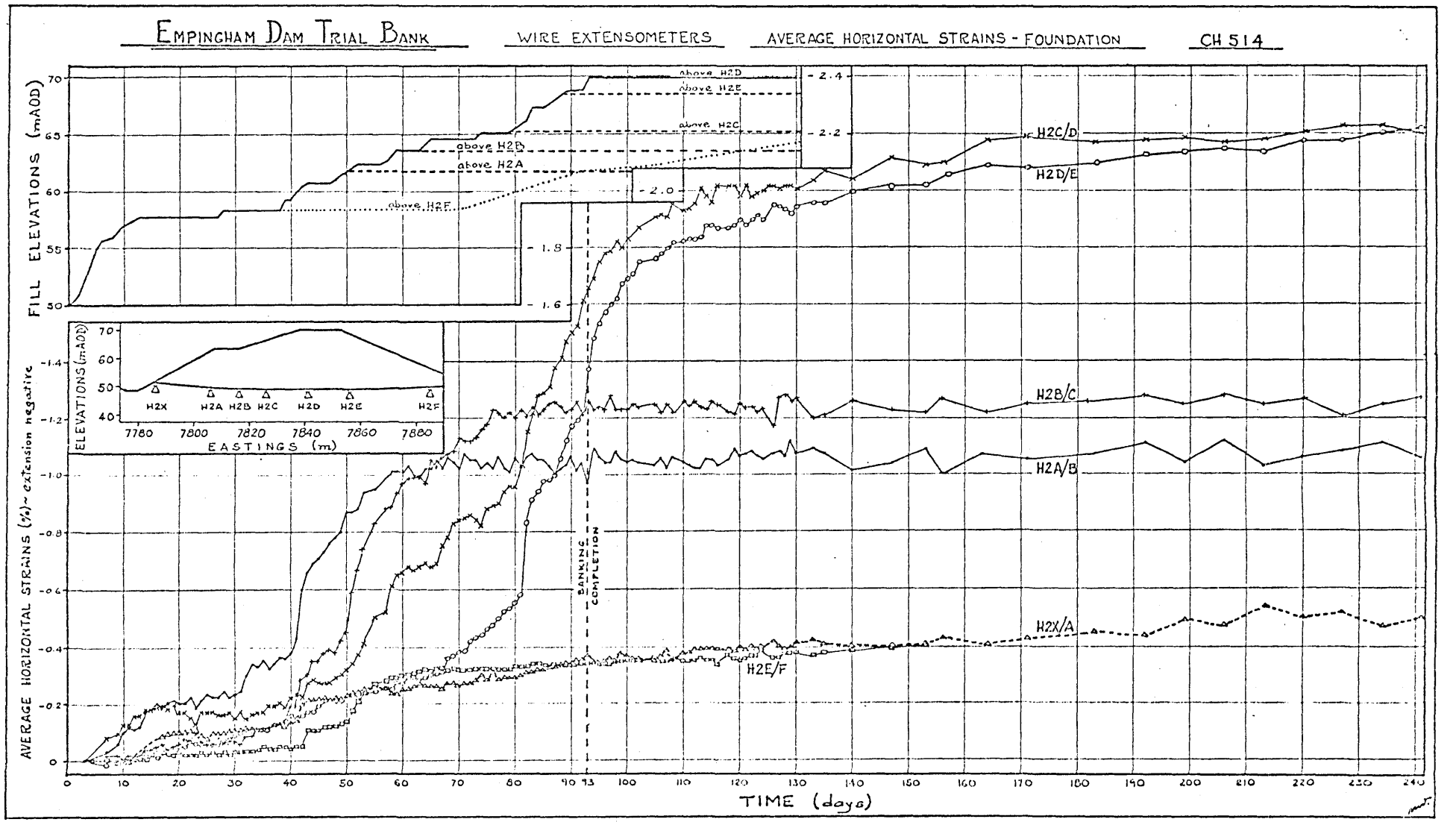

EMPINGHAM DAM TRIAL BANK
WIRE EXTENSOMETERS
AVERAGE HORIZONTAL STRAINS - FOUNDATION
CH 514
FILL ELEVATIONS (mAOD)
above H2D
above H2E
above H2C
above H2B
above H2A
above H2F
- 2.4
- 2.2
- 2.0
- 1.8
- 1.6
ELEVATIONS (mAOD)
H2X H2A H2B H2C H2D H2E H2F
EASTINGS (m)
AVERAGE HORIZONTAL STRAINS (%) - extension negative
H2C/D
H2D/E
H2B/C
H2A/B
H2X/A
H2E/F
BANKING COMPLETION
TIME (days)

FIG. 6.74

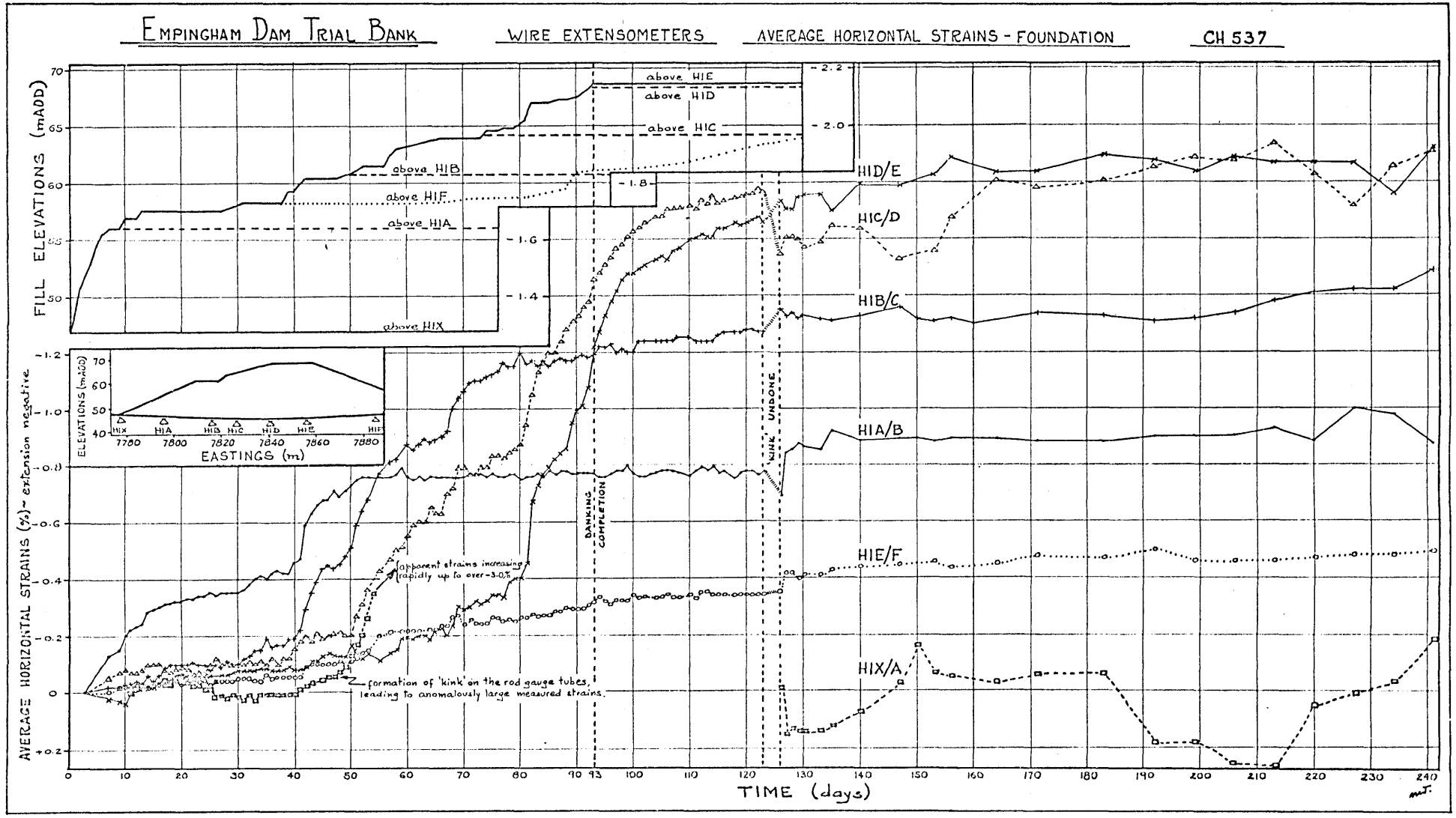

EMPINGHAM DAM TRIAL BANK
WIRE EXTENSOMETERS
AVERAGE HORIZONTAL STRAINS - FOUNDATION
CH 537
FILL ELEVATIONS (mAOD)
above HIE
above HID
above HIC
above HIB
above HIF
above HIA
above HIX
- 2.2
- 2.0
- 1.8
- 1.6
- 1.4
ELEVATIONS (mAOD)
EASTINGS (m)
HIX
HIA
HIB
HIC
HID
HIE
HIF
HID/E
HIC/D
HIB/C
HIA/B
HIE/F
HIX/A
DANKING COMPLETION
KINK UNDONE
apparent strains increasing rapidly up to over -3.0%
formation of 'kink' on the rod gauge tubes, leading to anomalously large measured strains
AVERAGE HORIZONTAL STRAINS (%) - extension negative
TIME (days)

FIG. 6.75

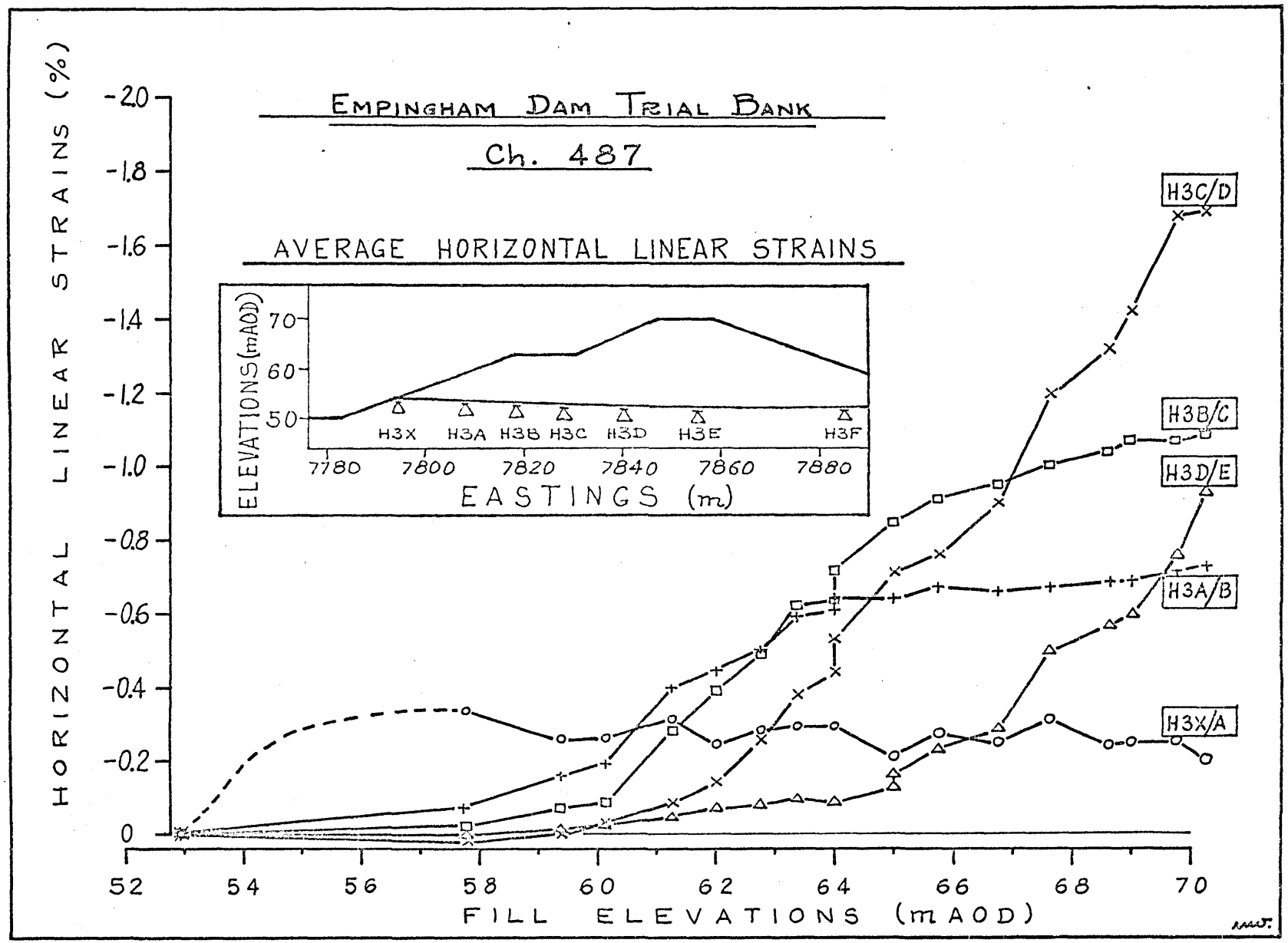


FIG. 6.76

FIG. 6.76

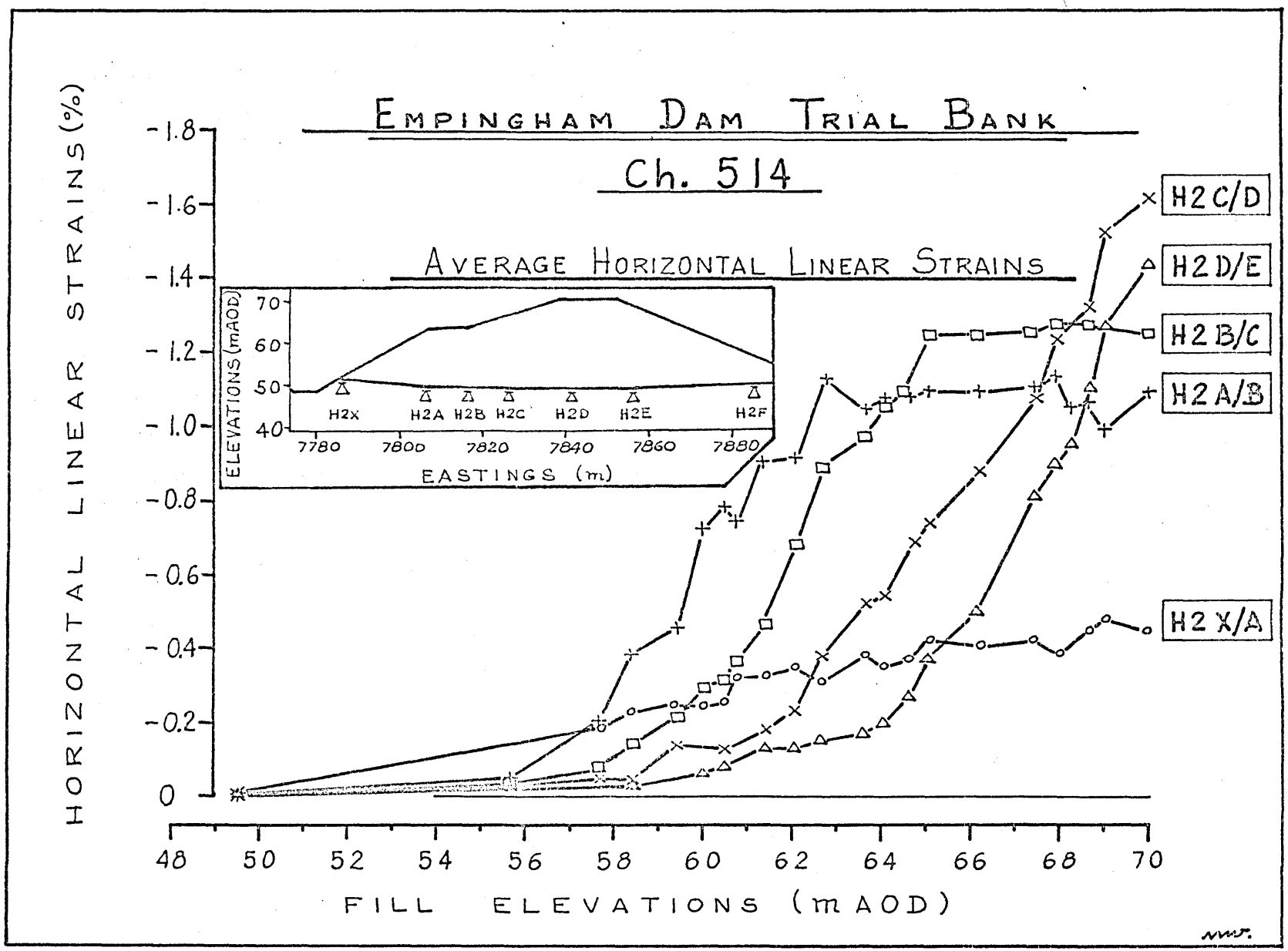


FIG. 6.77

FIG. 6.77

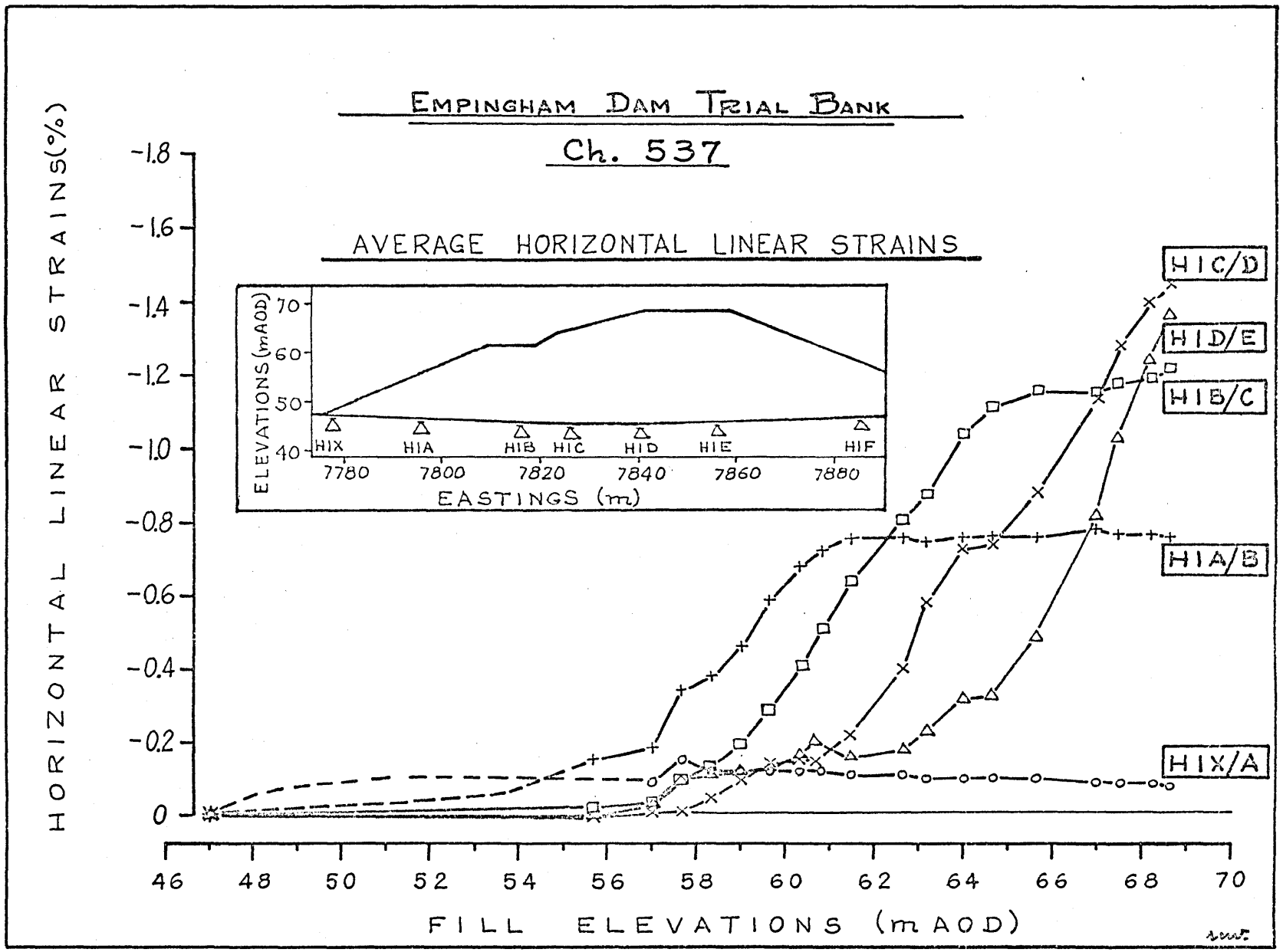


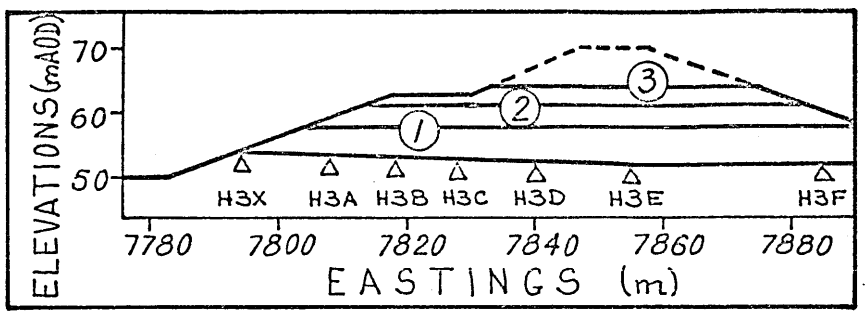
FIG. 6.78

FIG. 6.78

EMPINGHAM DAM TRIAL BANK

HORIZONTAL STRAINS

Ch. 487



KEY: ------ INCREMENTAL STRAINS
——— TOTAL STRAINS

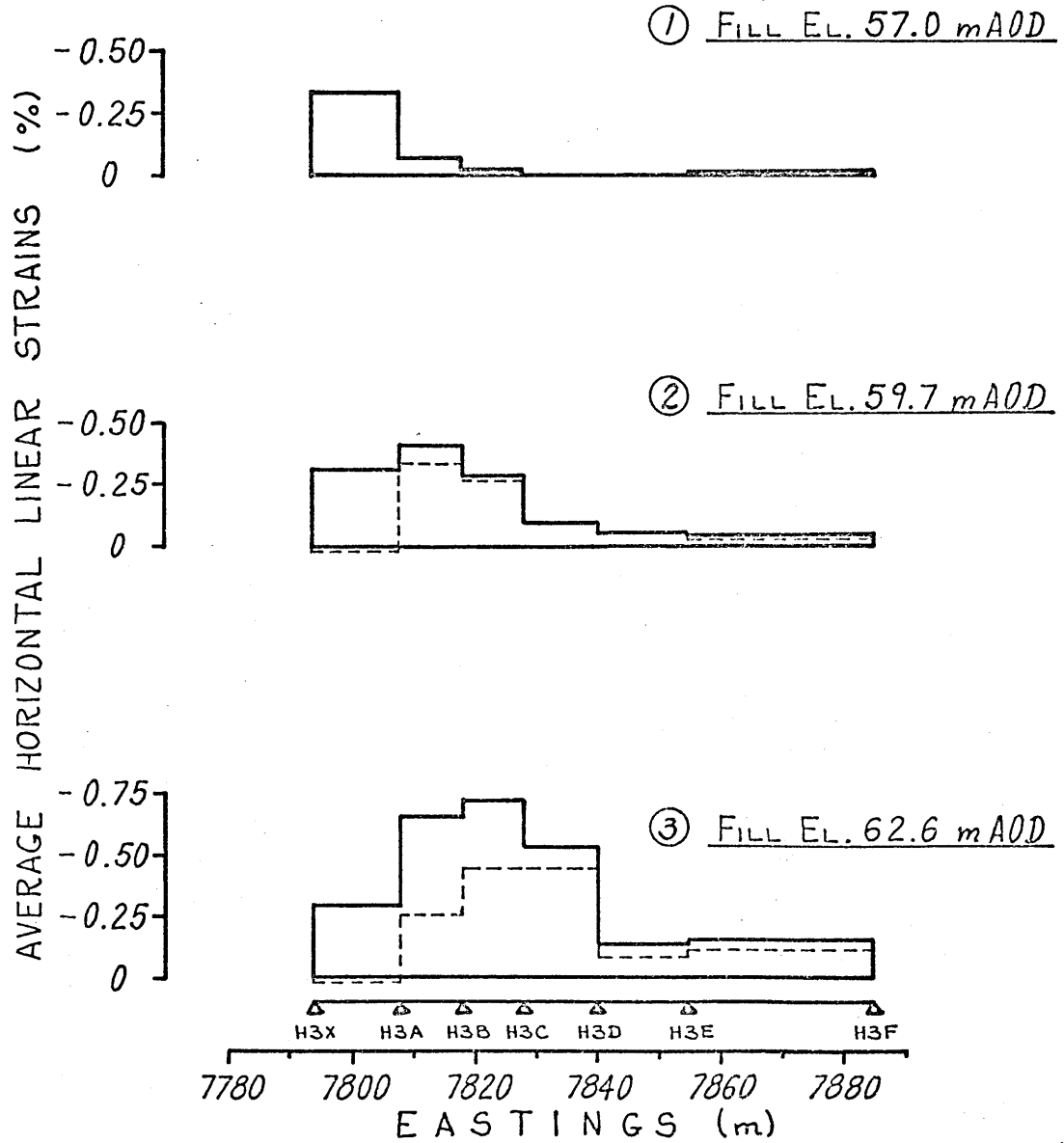
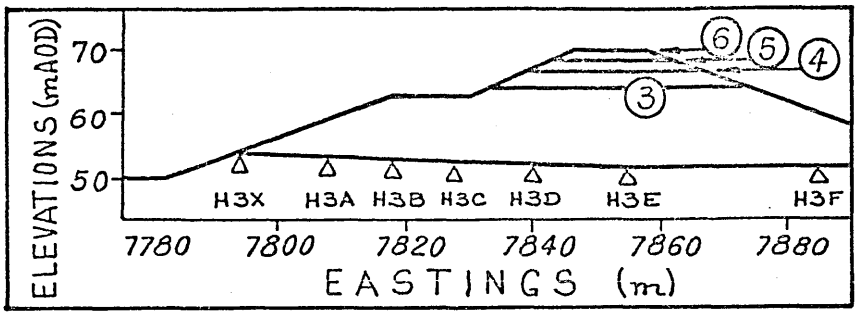


FIG. 6.79

EMPINGHAM DAM TRIAL BANK

HORIZONTAL STRAINS

Ch. 487



KEY: - - - - - - - INCREMENTAL STRAINS
——— TOTAL STRAINS

AVERAGE HORIZONTAL LINEAR STRAINS (%)

-1.00
-0.75
-0.50
-0.25
0

④ FILL EL. 66.7 mAOD

-1.25
-1.00
-0.75
-0.50
-0.25
0

⑤ FILL EL. 68.6 mAOD

-1.50
-1.25
-1.00
-0.75
-0.50
-0.25
0

⑥ FILL EL. 70.2 mAOD

H3X H3A H3B H3C H3D H3E H3F

7780 7800 7820 7840 7860 7880

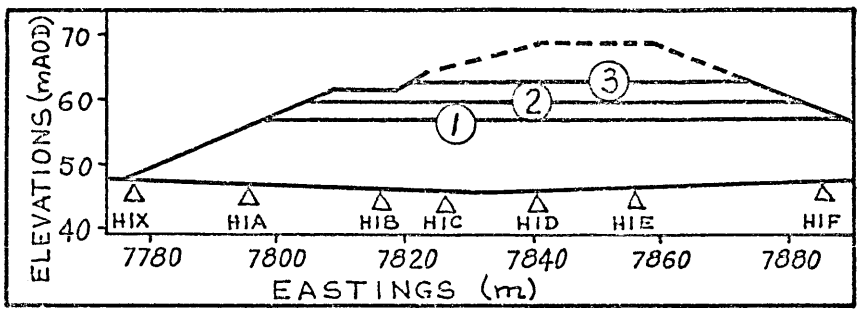
EASTINGS (m)

FIG. 6.80

EMPINGHAM DAM TRIAL BANK

HORIZONTAL STRAINS

Ch.537



KEY: ------ INCREMENTAL STRAINS
——— TOTAL STRAINS

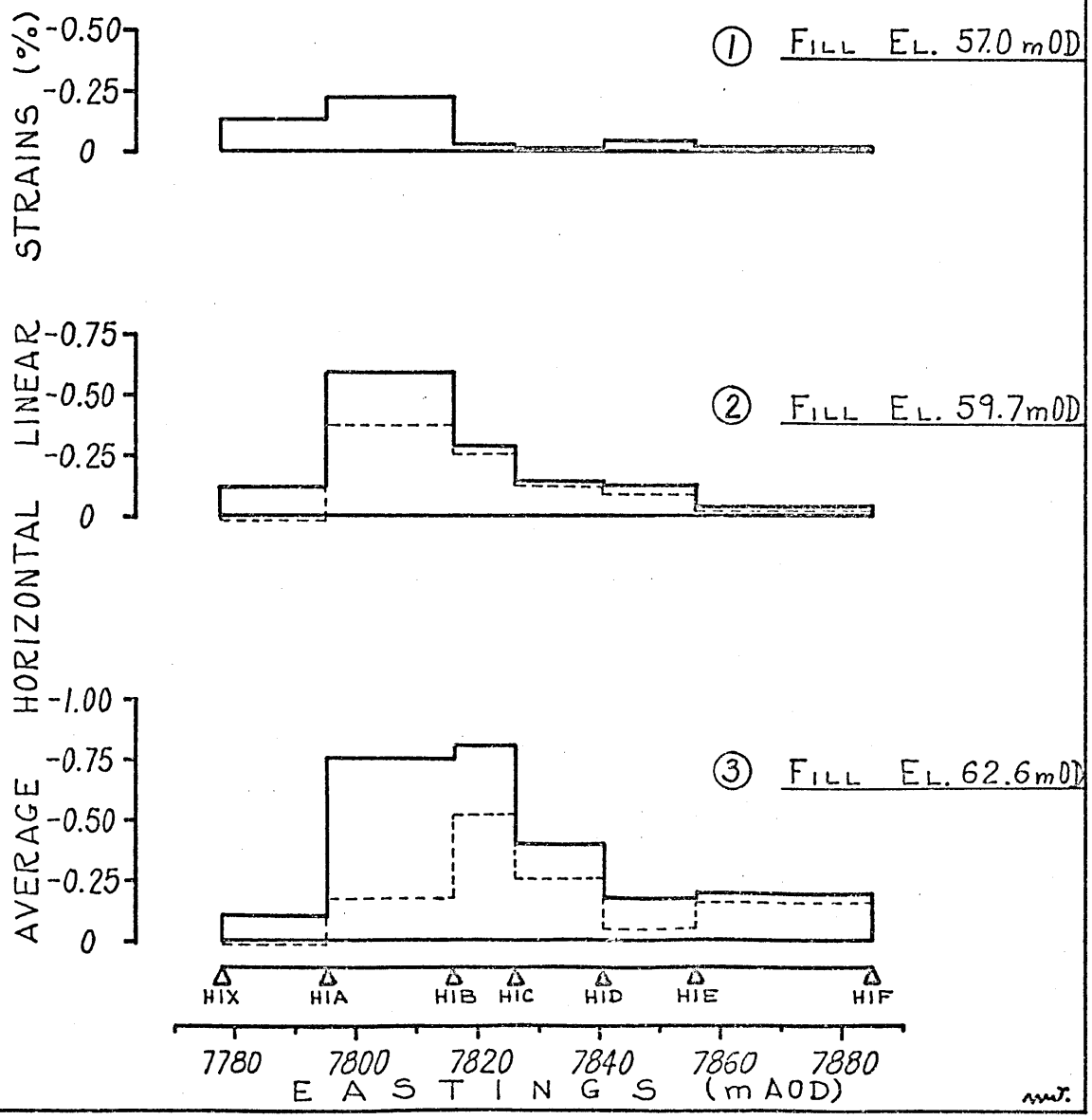


FIG. 6.81

EMPINGHAM DAM TRIAL BANK

HORIZONTAL STRAINS

Ch. 514

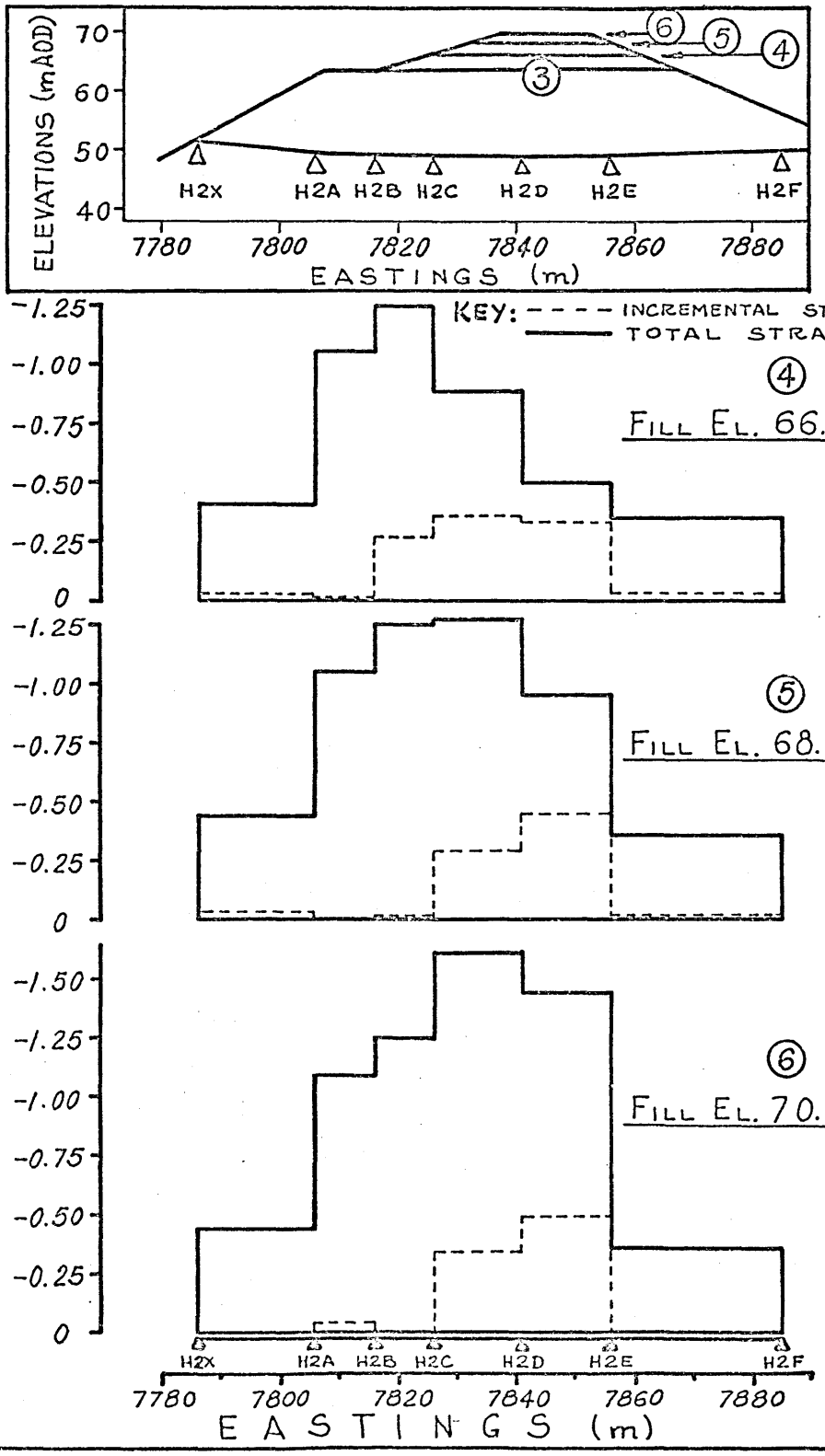
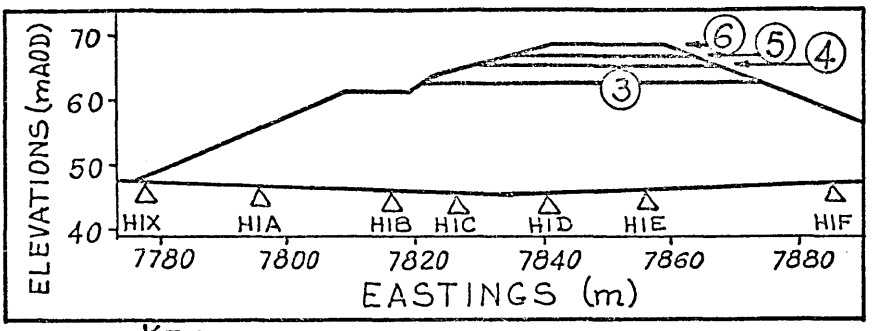


FIG. 6.82

EMPINGHAM DAM TRIAL BANK

HORIZONTAL STRAINS

Ch.537



Key: ----- INCREMENTAL STRAINS
——— TOTAL STRAINS

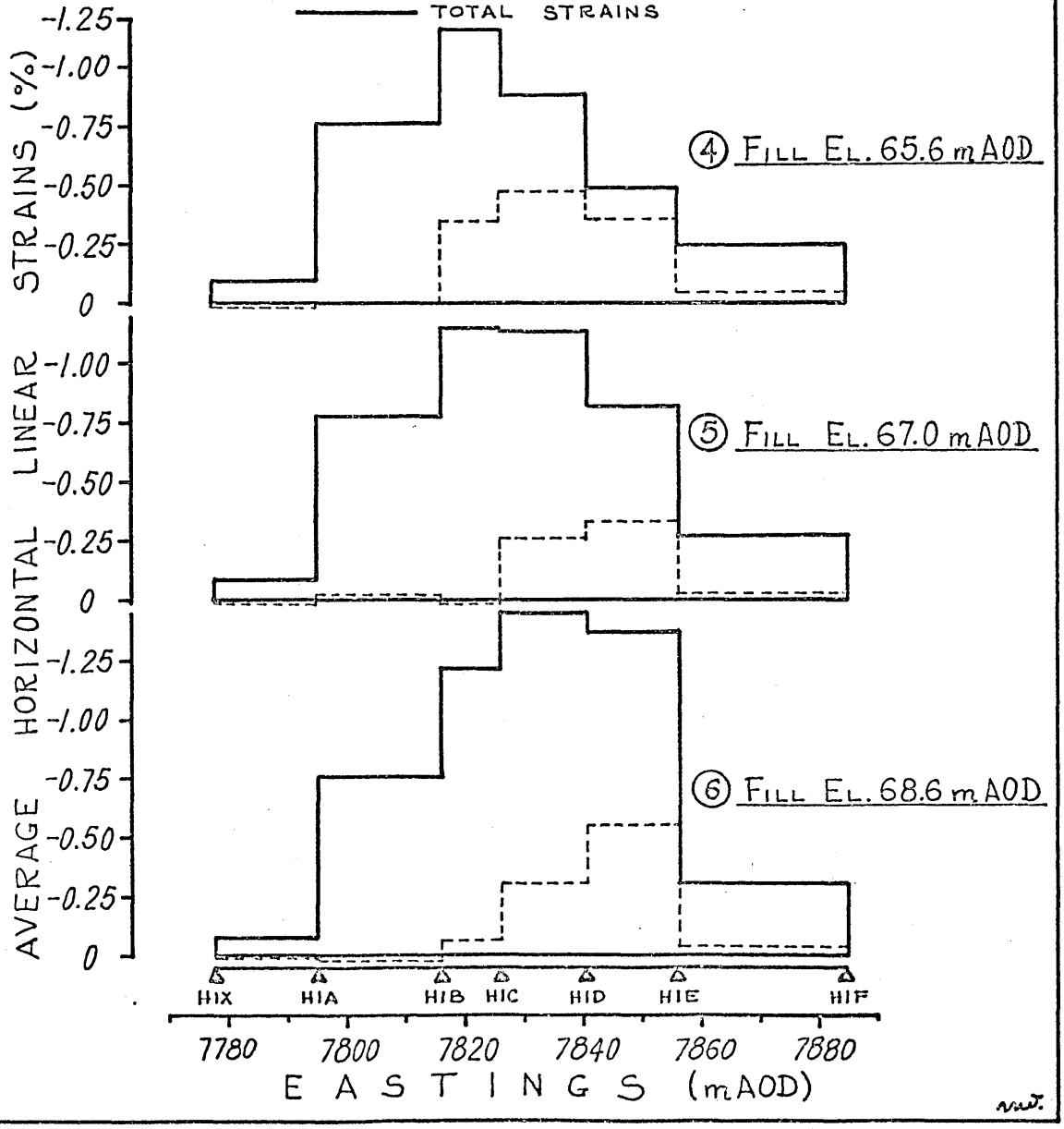
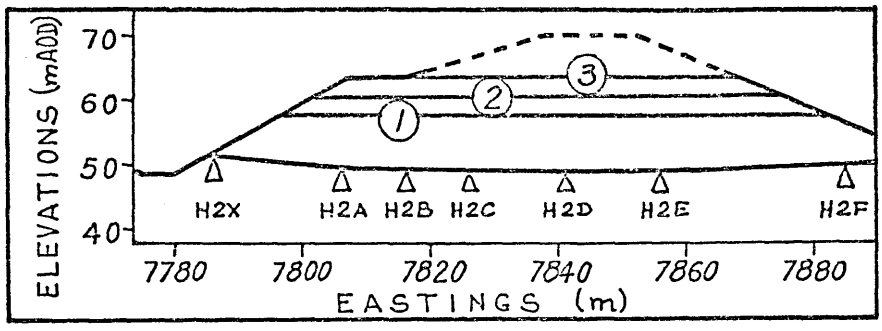


FIG. 6.83

EMPINGHAM DAM TRIAL BANK

HORIZONTAL STRAINS

Ch. 514



KEY: ------ INCREMENTAL STRAINS
——— TOTAL STRAINS

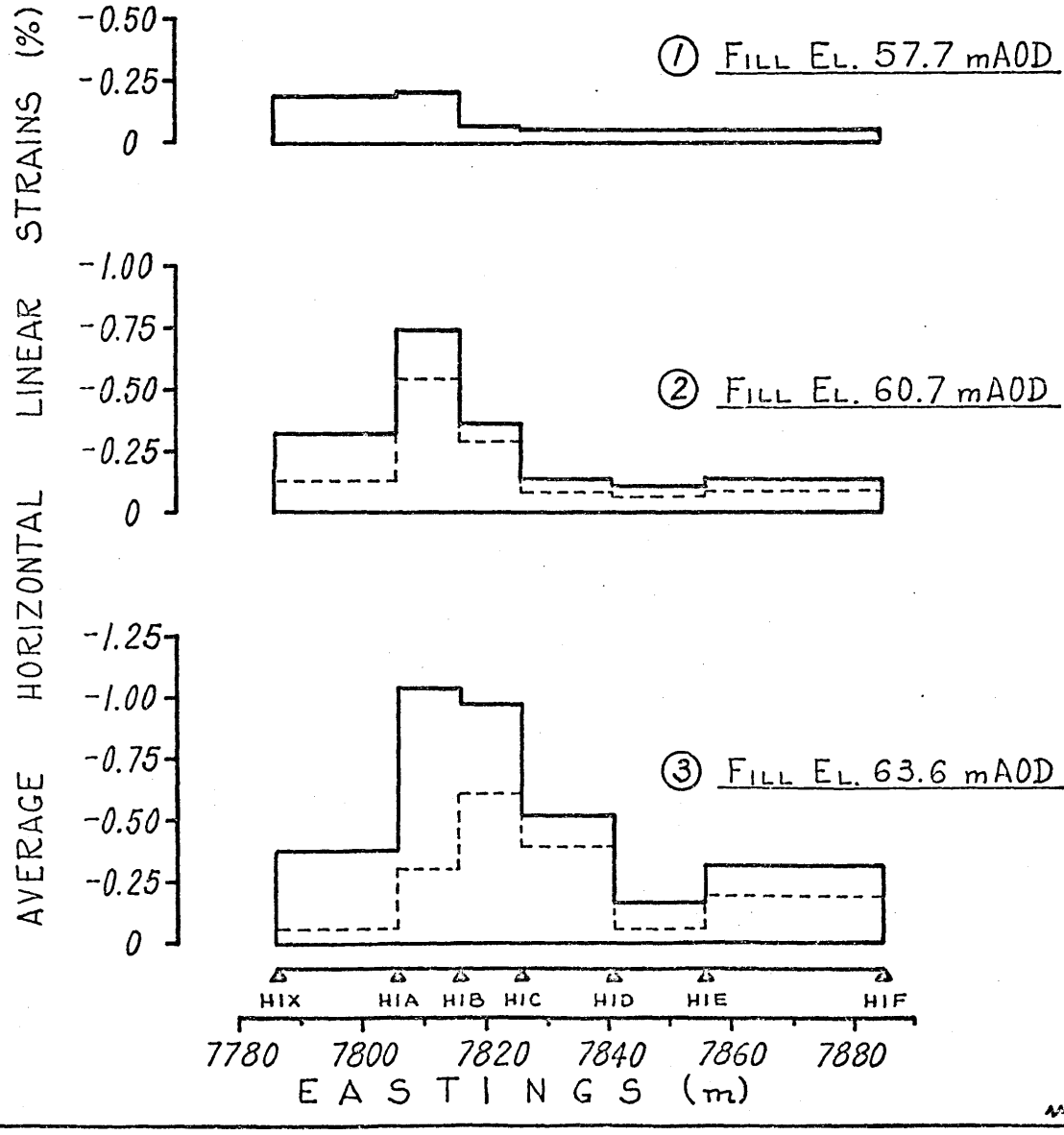


FIG. 6.84

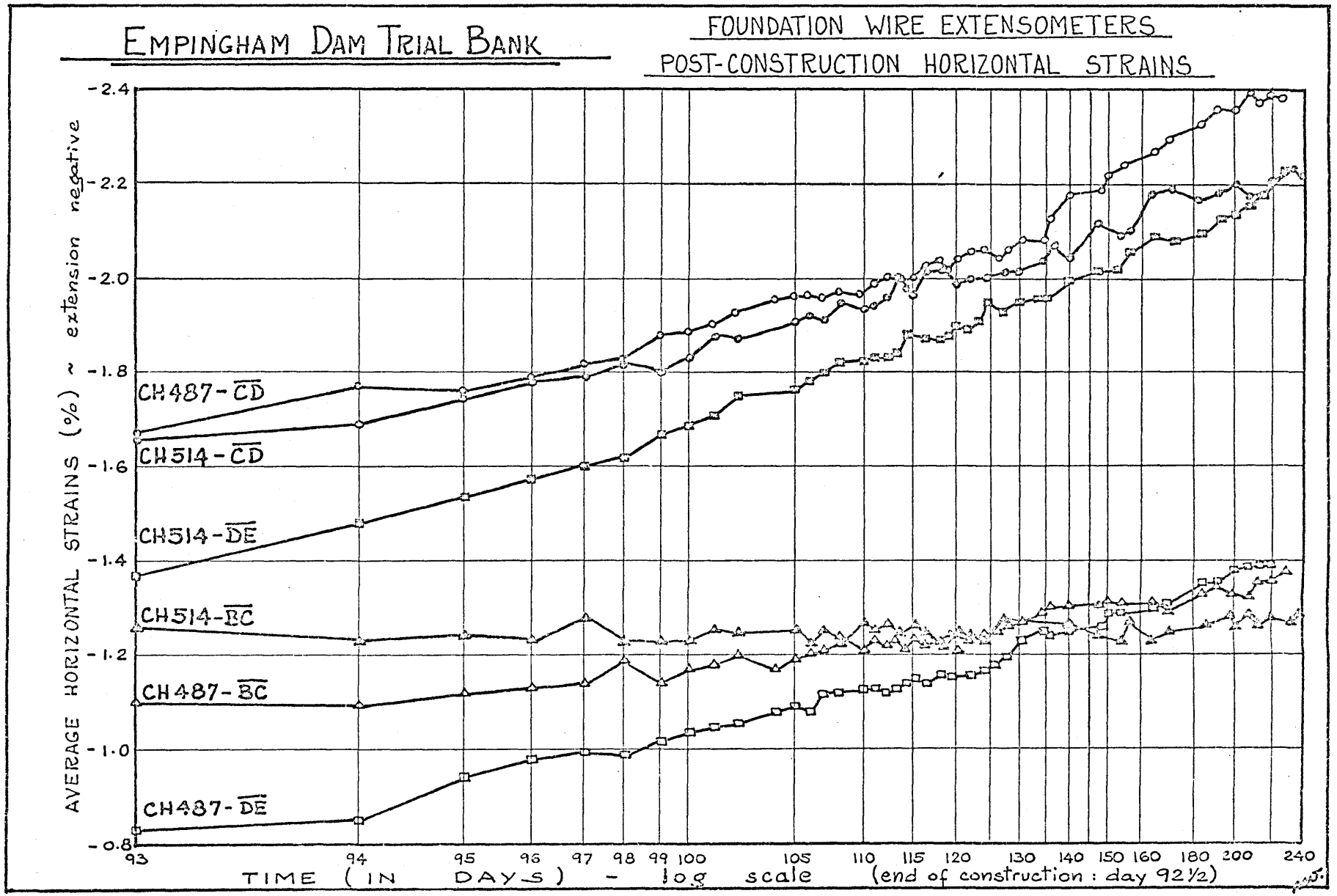


FIG. 6.85

FIG. 6.85

EMPINGHAM DAM TRIAL BANK

WIRE EXTENSOMETERS

AVERAGE HORIZONTAL STRAINS - FILL

CH 487

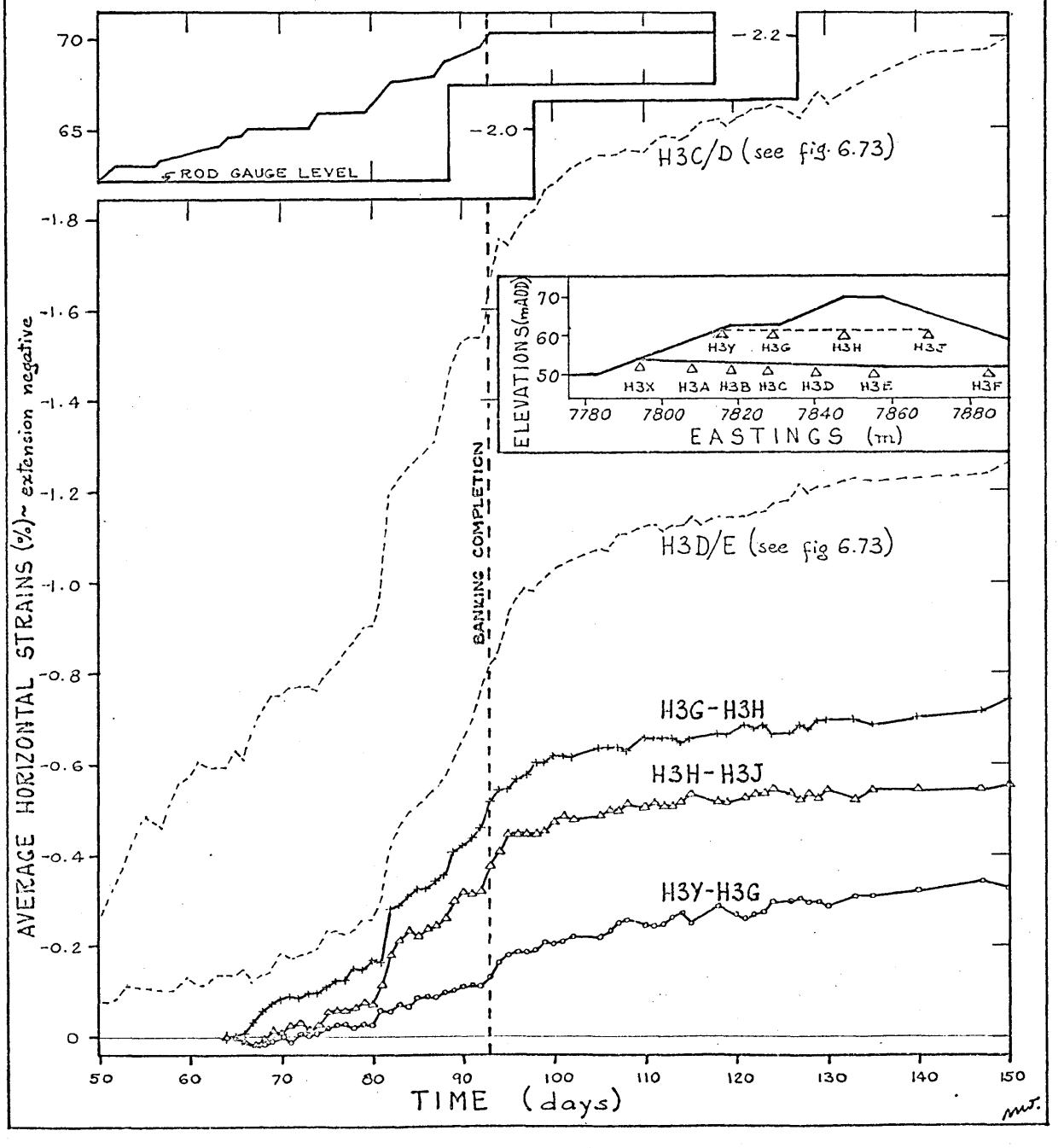


FIG. 6.86

EMPINGHAM DAM TRIAL BANK

WIRE EXTENSOMETERS

AVERAGE HORIZONTAL STRAINS - FILL

CH 514

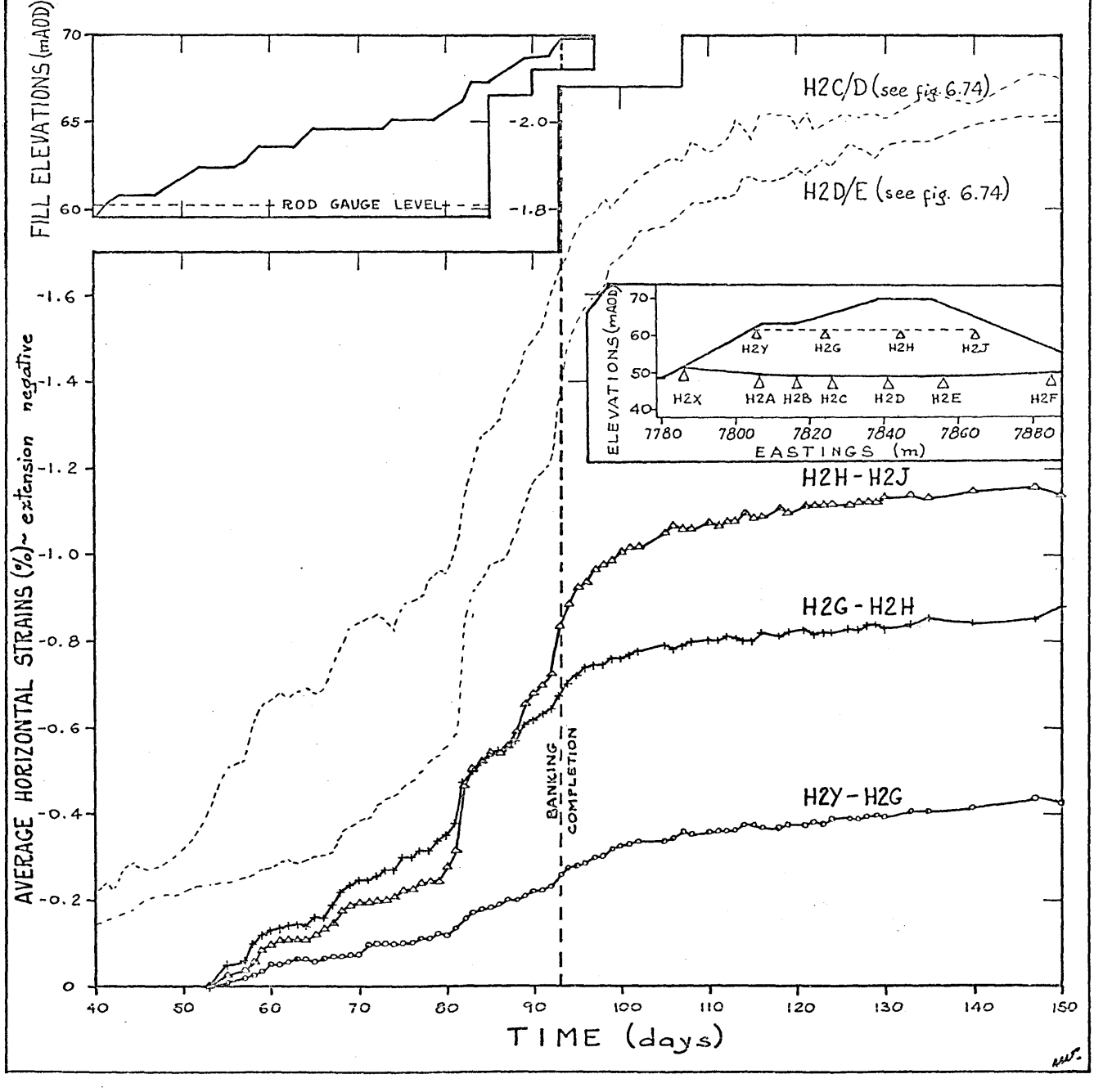


FIG. 6.87

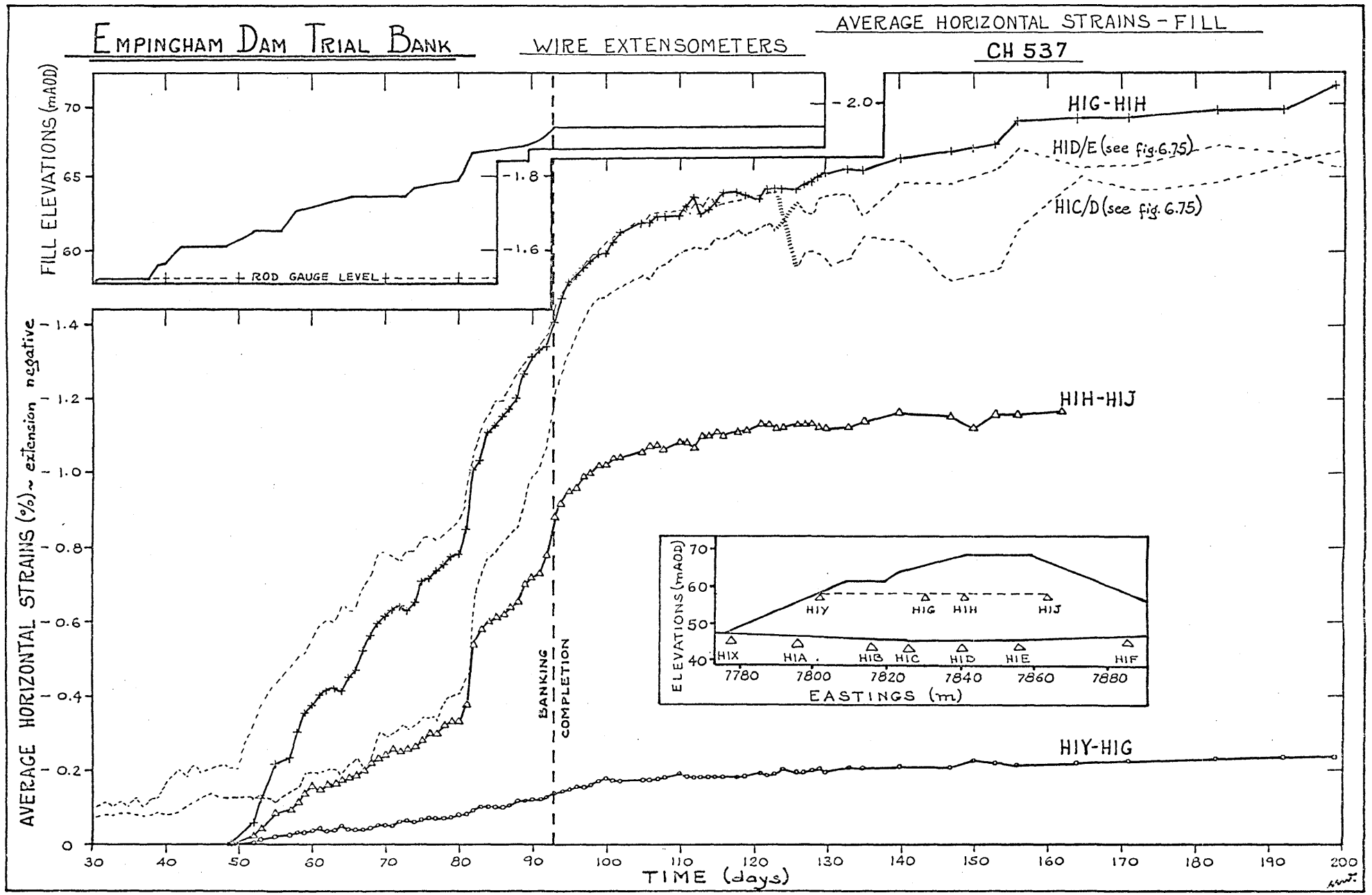

EMPINGHAM DAM TRIAL BANK
WIRE EXTENSOMETERS
AVERAGE HORIZONTAL STRAINS - FILL
CH 537
FILL ELEVATIONS (mAOD)
ROD GAUGE LEVEL
HIG-HIH
HID/E (see fig. 6.75)
HIC/D (see fig. 6.75)
HIH-HIJ
HIY-HIG
AVERAGE HORIZONTAL STRAINS (%) ~ extension negative
BANKING COMPLETION
ELEVATIONS (mAOD)
HIY
HIG
HIH
HIJ
HIX
HIA
HIB
HIC
HID
HIE
HIF
EASTINGS (m)
TIME (days)

FIG. 6.88

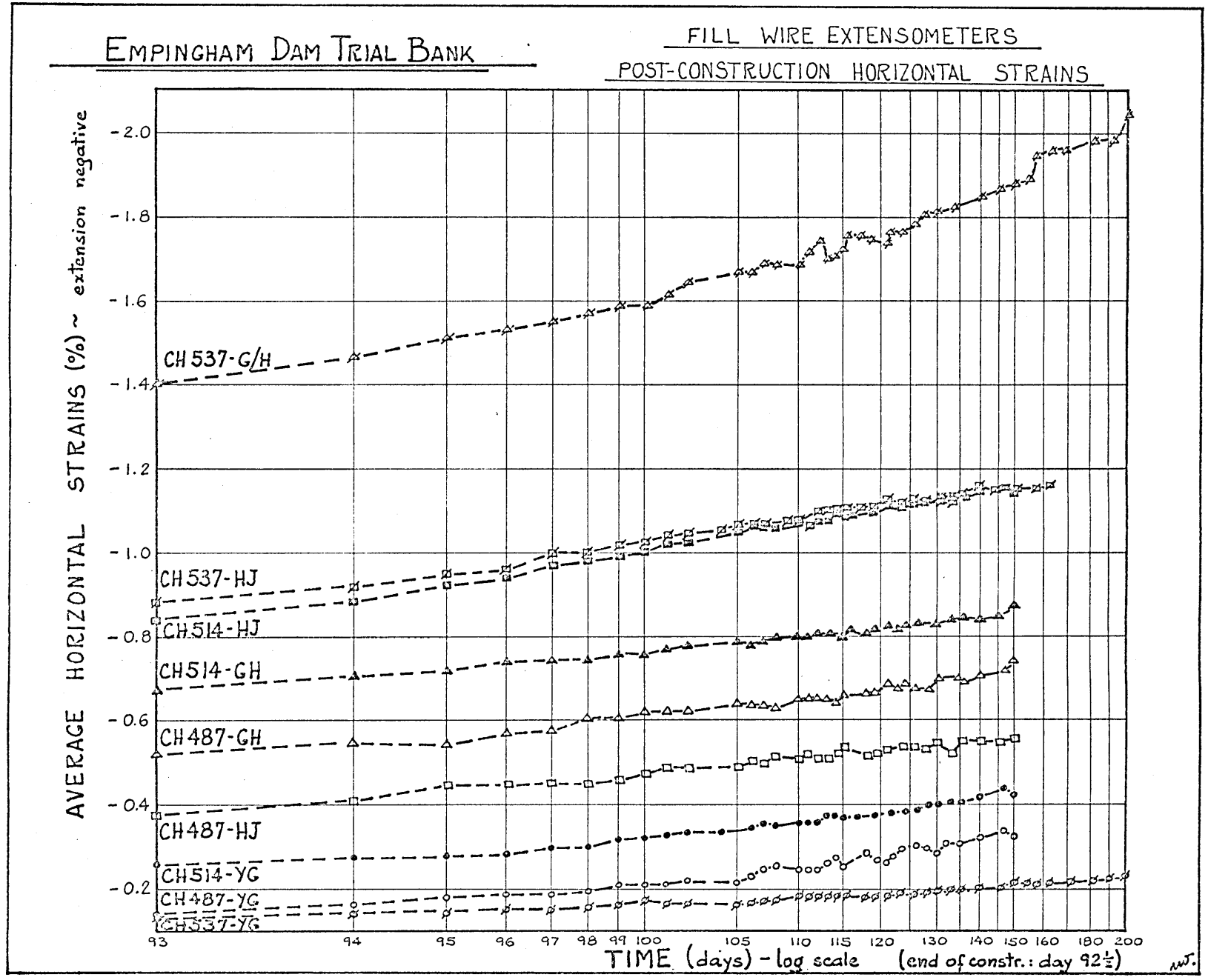


FIG. 6.89

FIG. 6.89

EMPINGHAM DAM TRIAL BANK

WIRE EXTENSOMETERS

HORIZONTAL STRAINS IN THE FILL

CH487

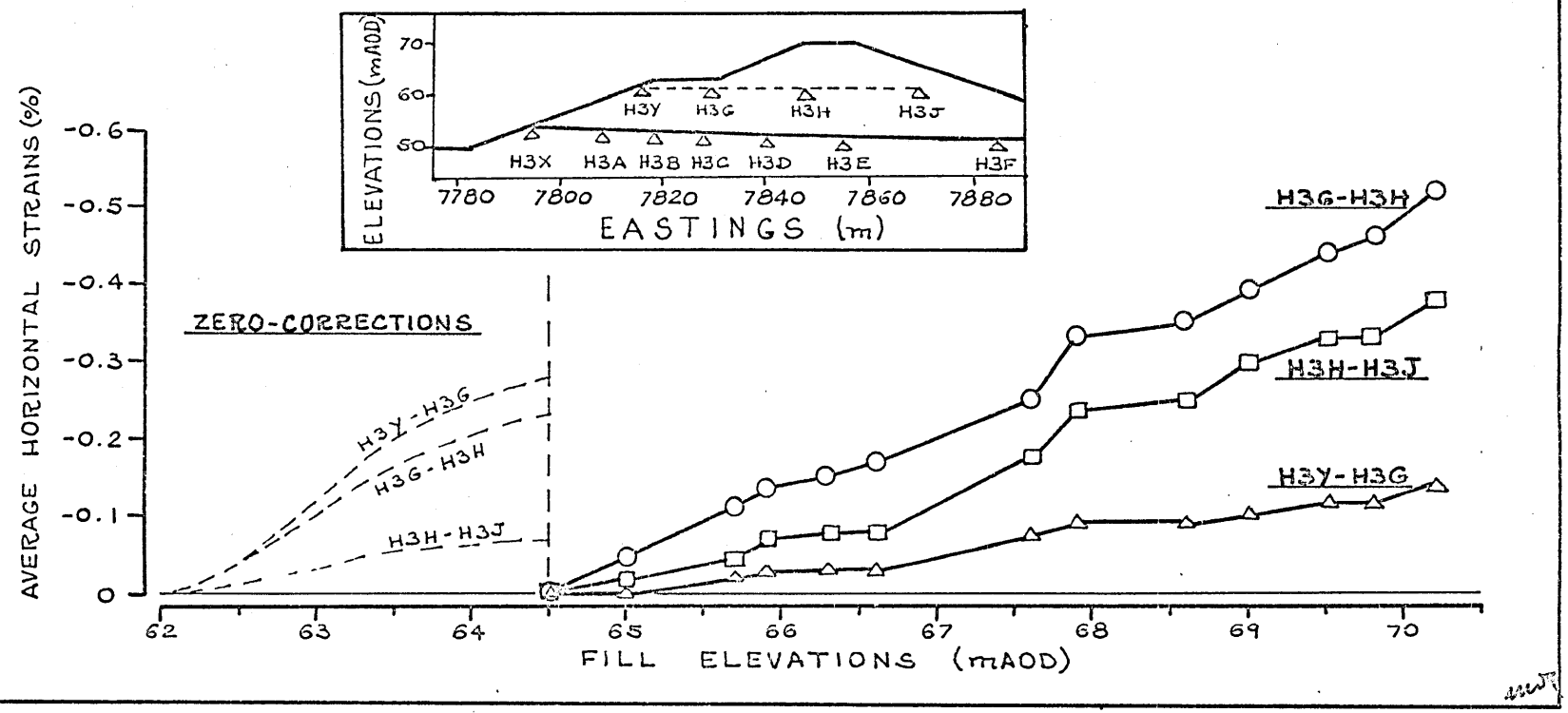


FIG. 6.90

FIG. 6.90

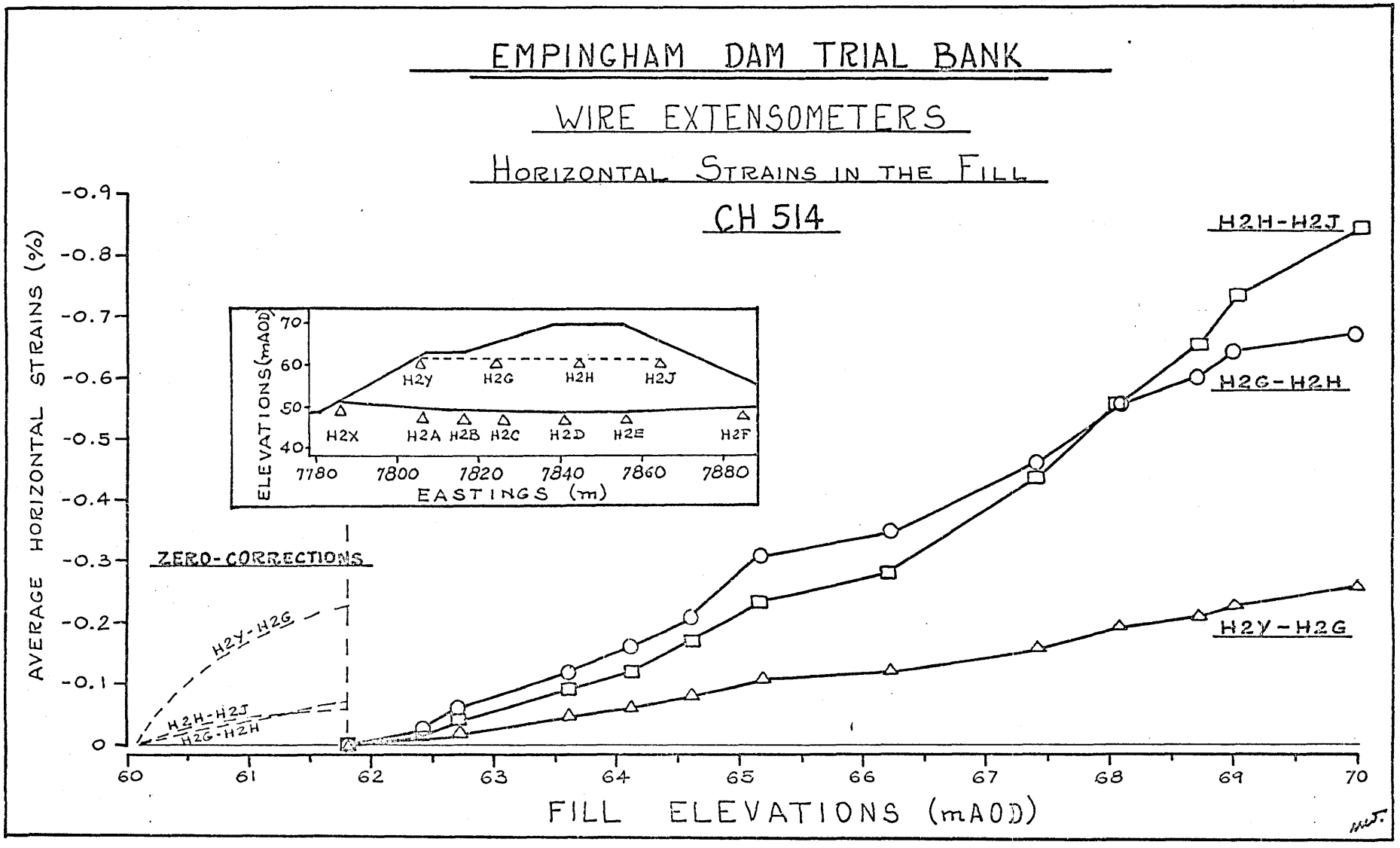


FIG. 6.91

FIG. 6.91

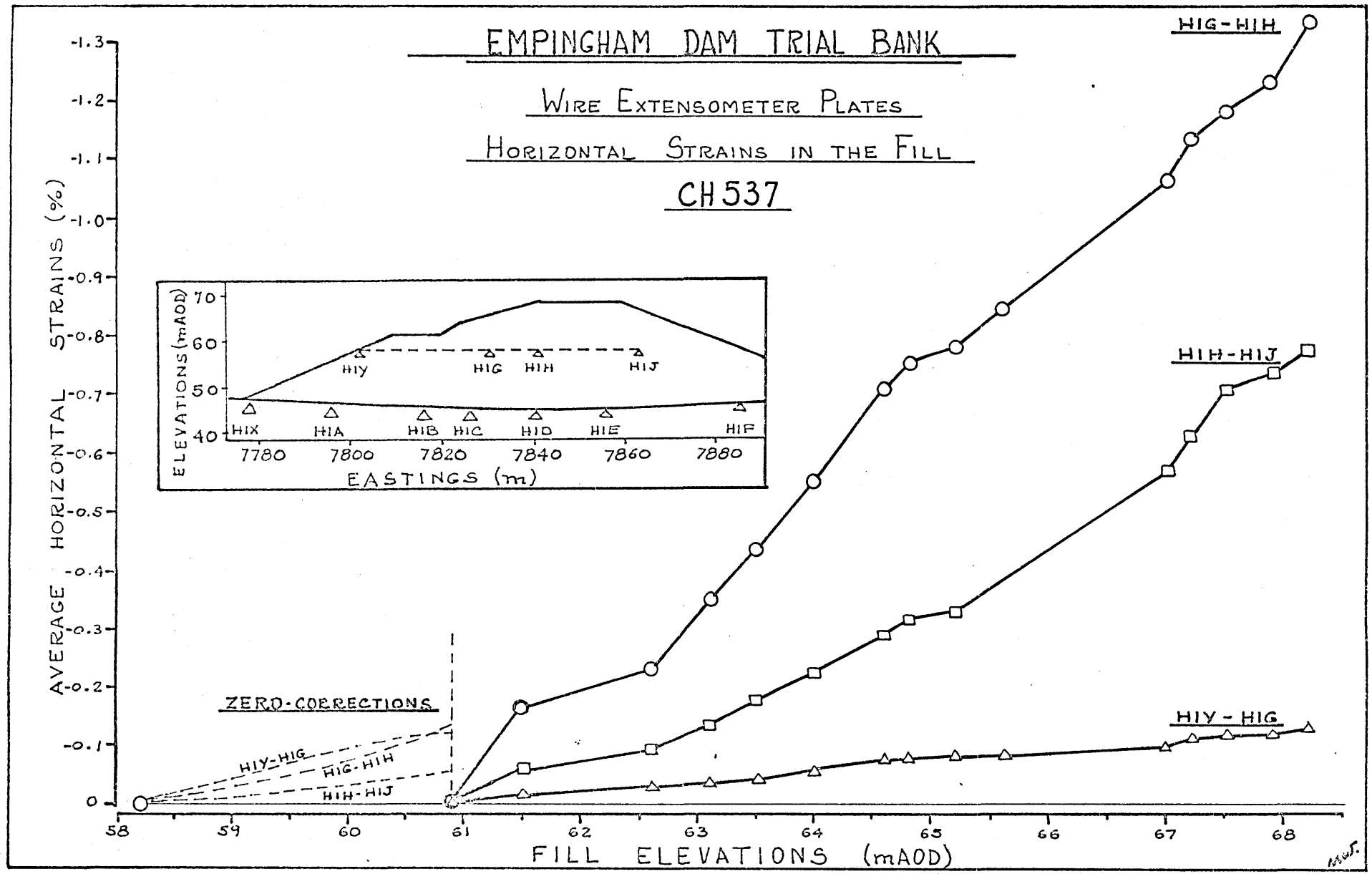


FIG. 6.92

FIG. 6.92

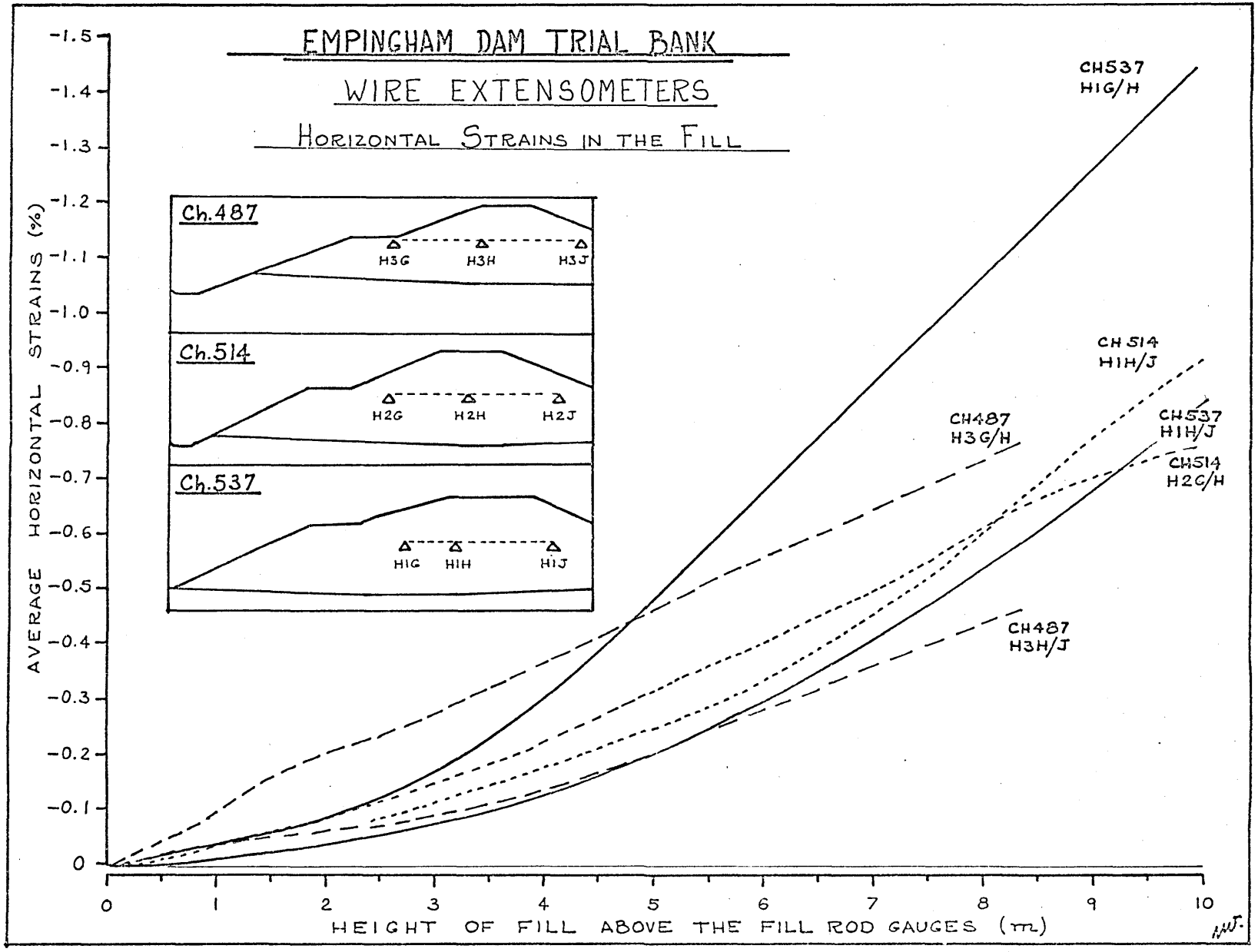


FIG. 6.93

FIG. 6.93

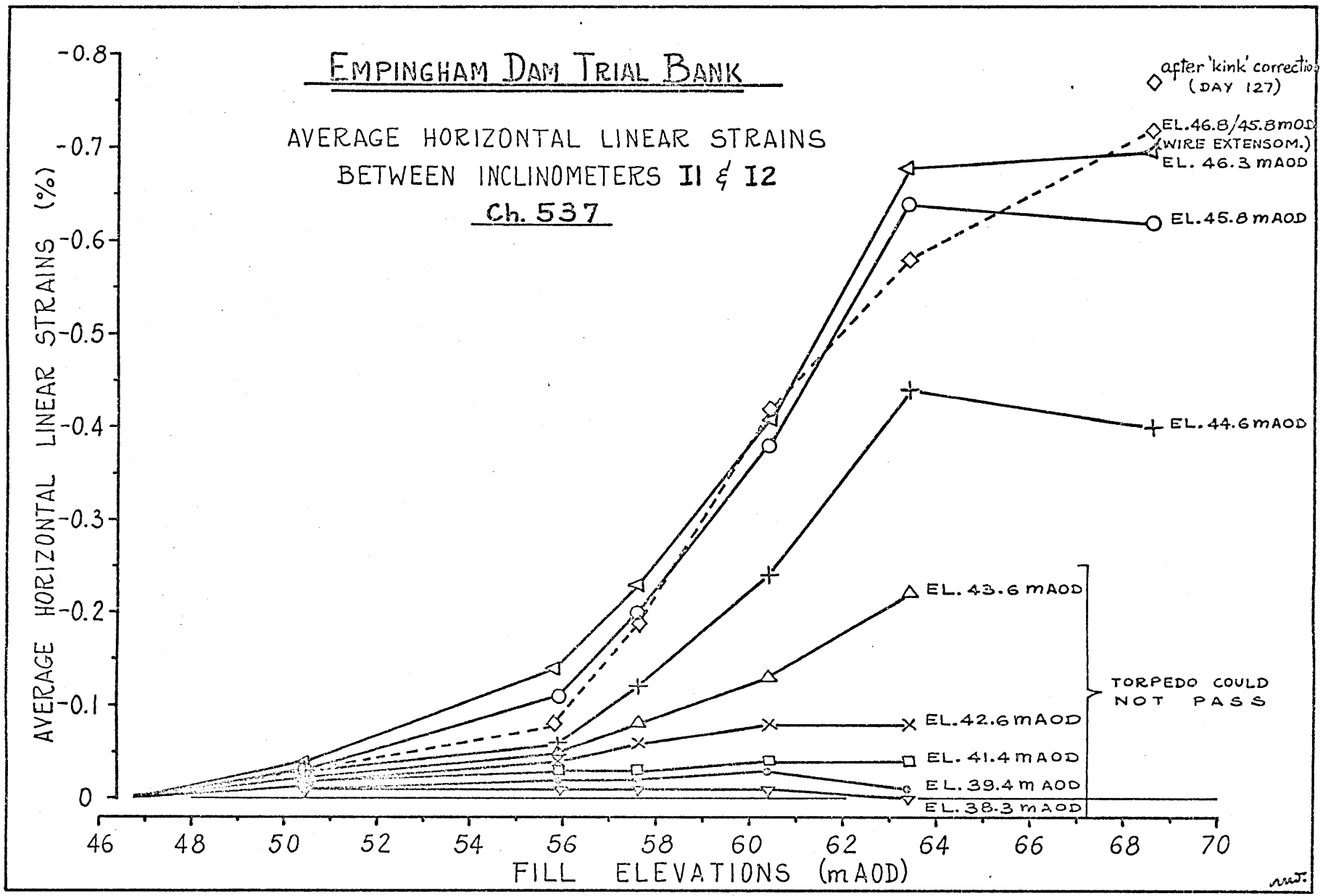


FIG. 6.94

FIG. 6.94

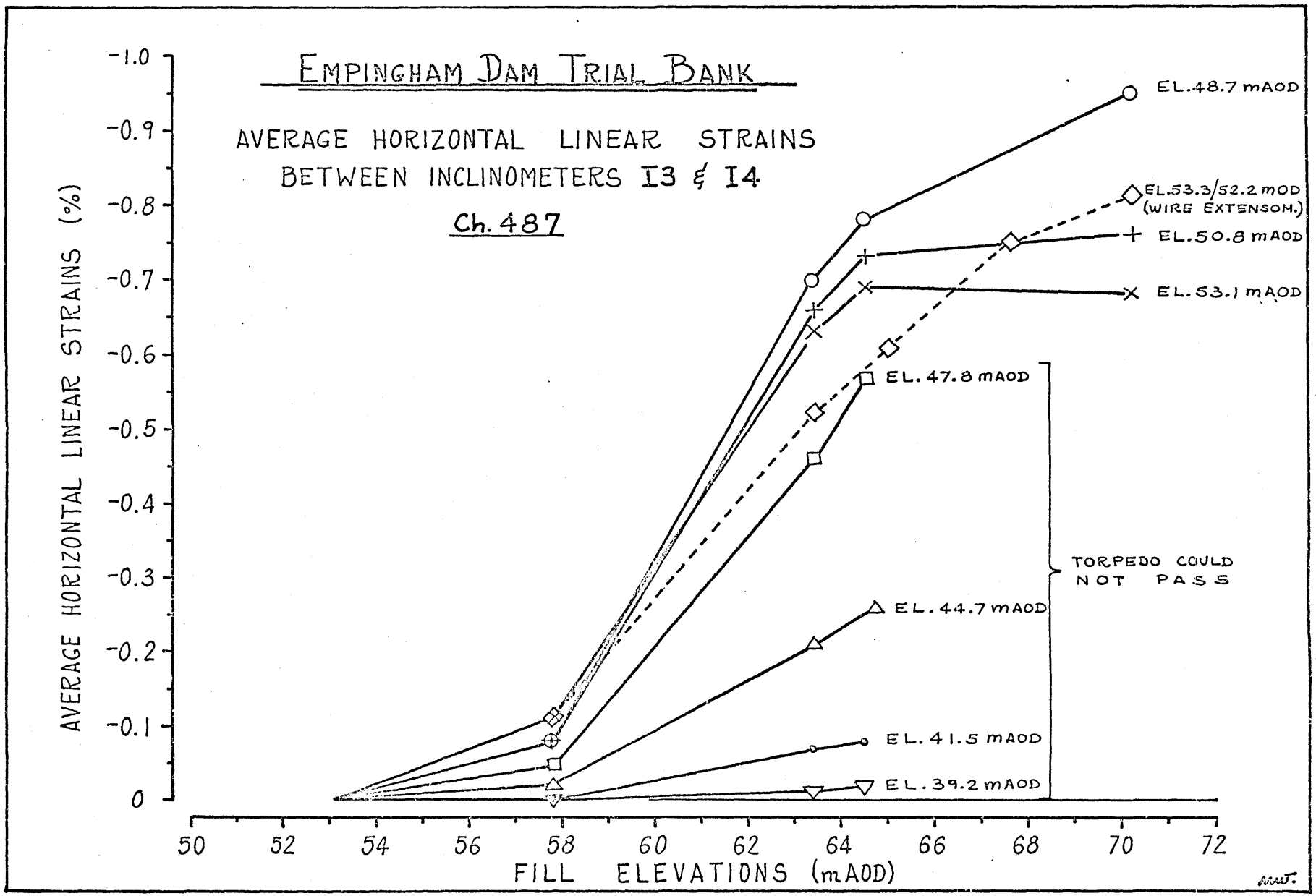


FIG. 6.95

FIG. 6.95

EMPINGHAM DAM TRIAL BANK

CH 487

SETTLEMENT MAGNETS - VERTICAL STRAINS

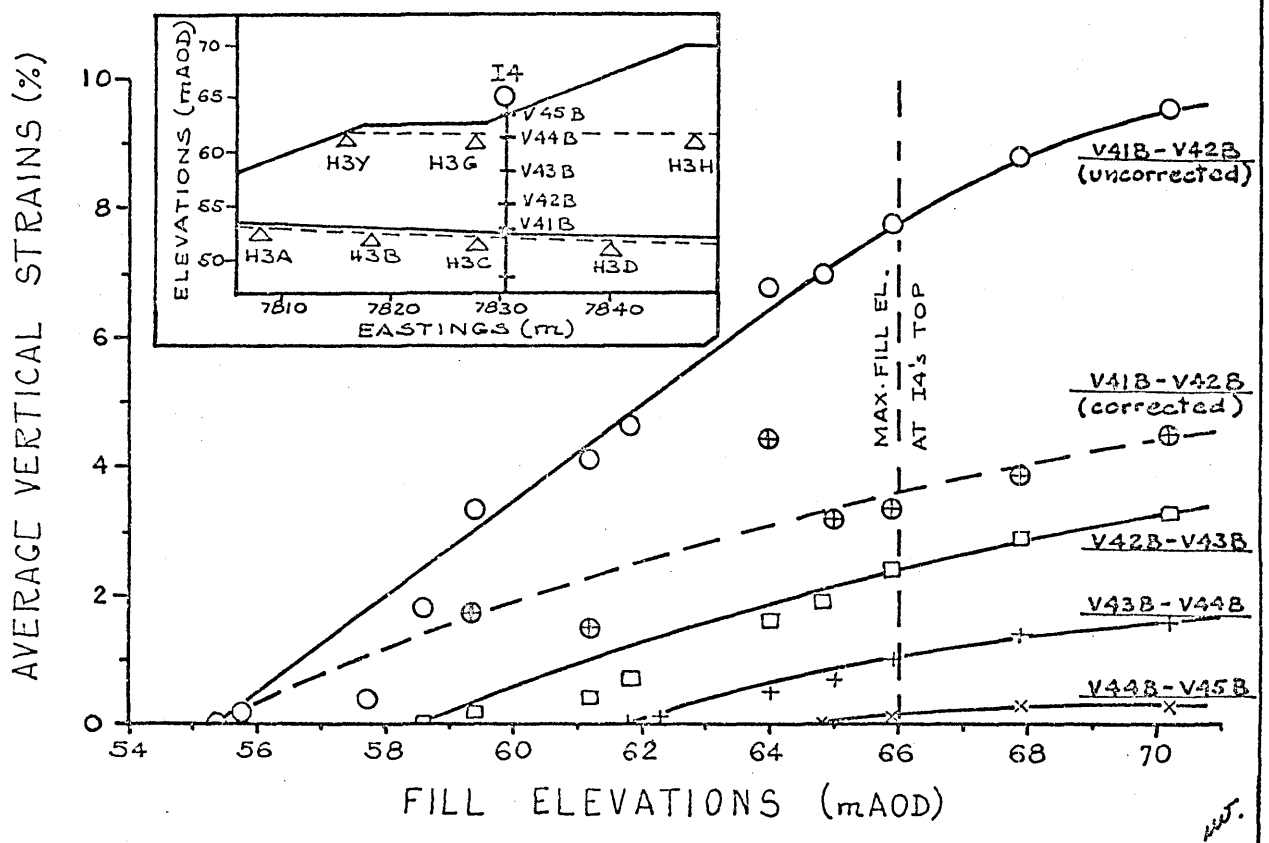


FIG. 6.96

FIG. 6.96

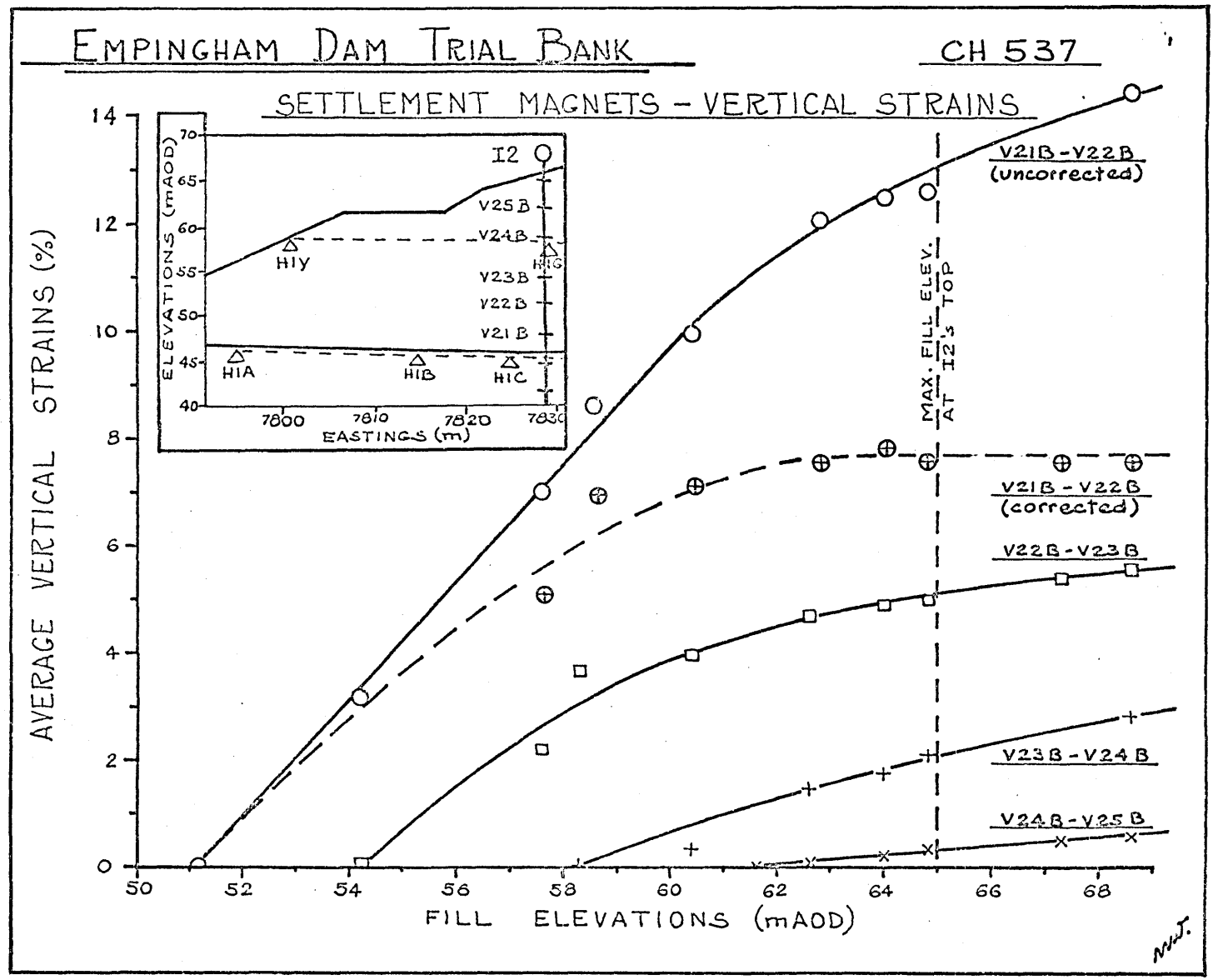


FIG. 6.97

FIG. 6.97

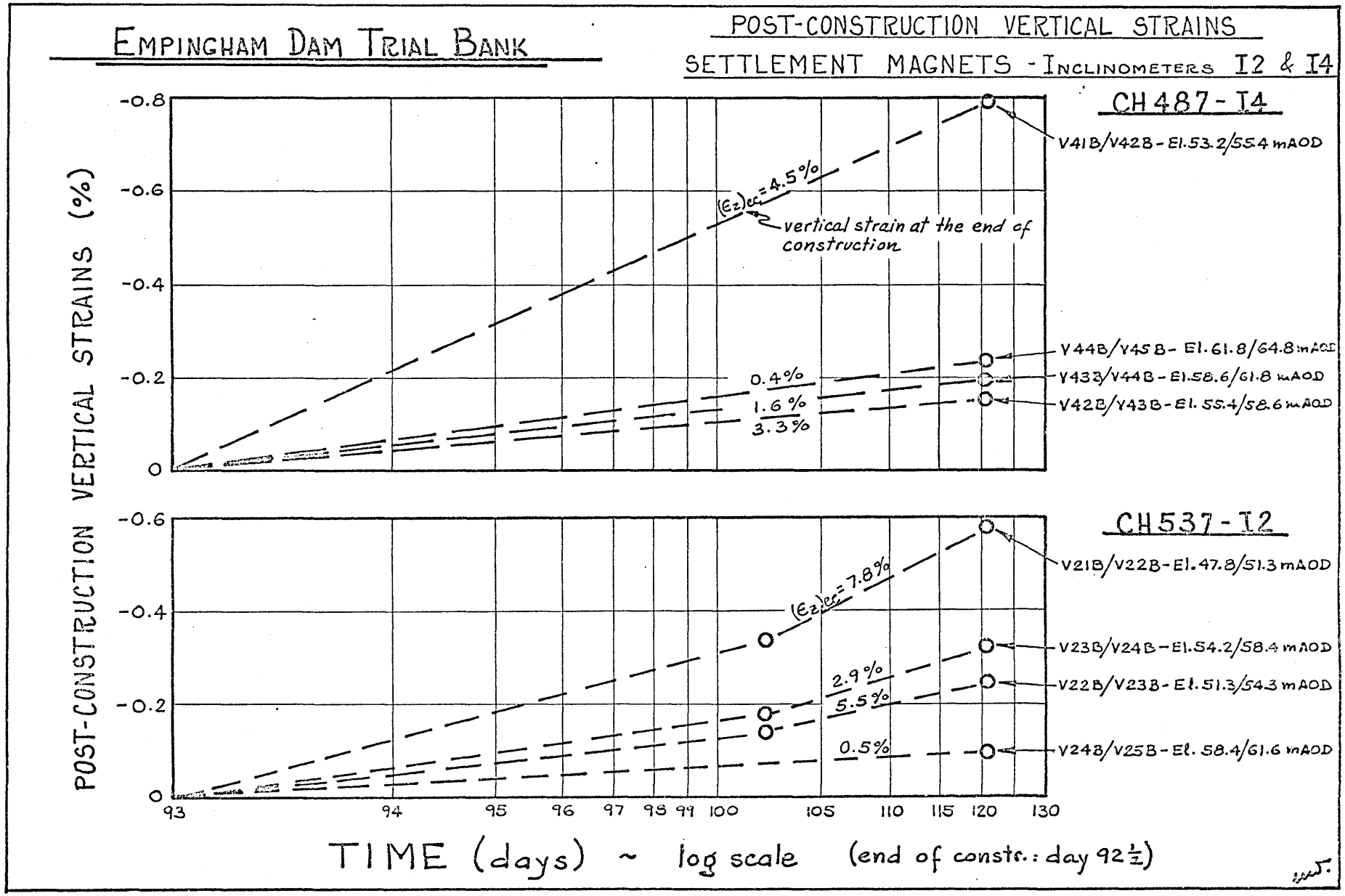


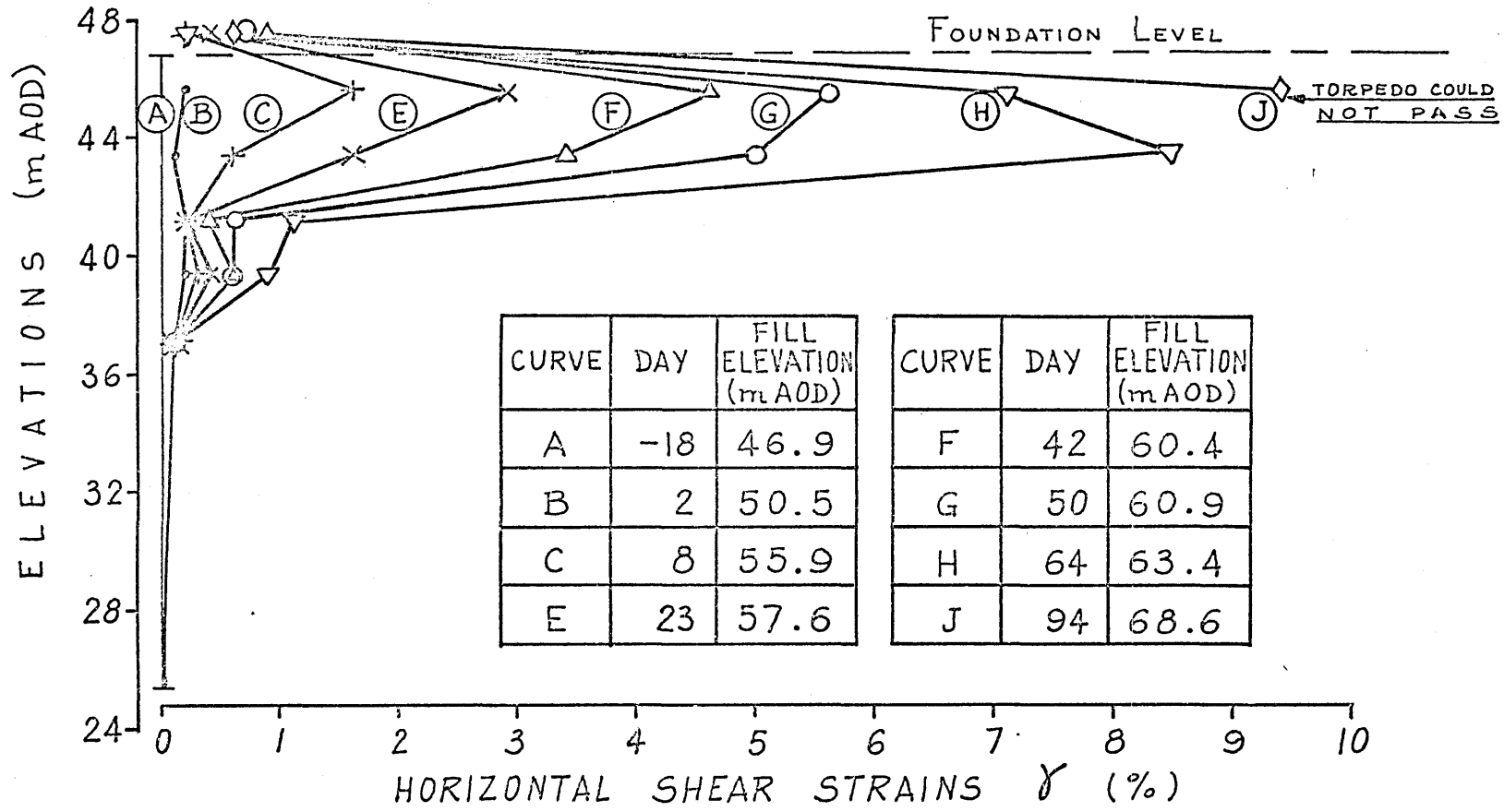
FIG. 6.98

FIG. 6.98

EMPINGHAM DAM TRIAL BANK

HORIZONTAL SHEAR STRAINS

Ch. 537 ~ INCLINOMETER II



CURVE	DAY	FILL ELEVATION (m AOD)
A	-18	46.9
B	2	50.5
C	8	55.9
E	23	57.6

CURVE	DAY	FILL ELEVATION (m AOD)
F	42	60.4
G	50	60.9
H	64	63.4
J	94	68.6

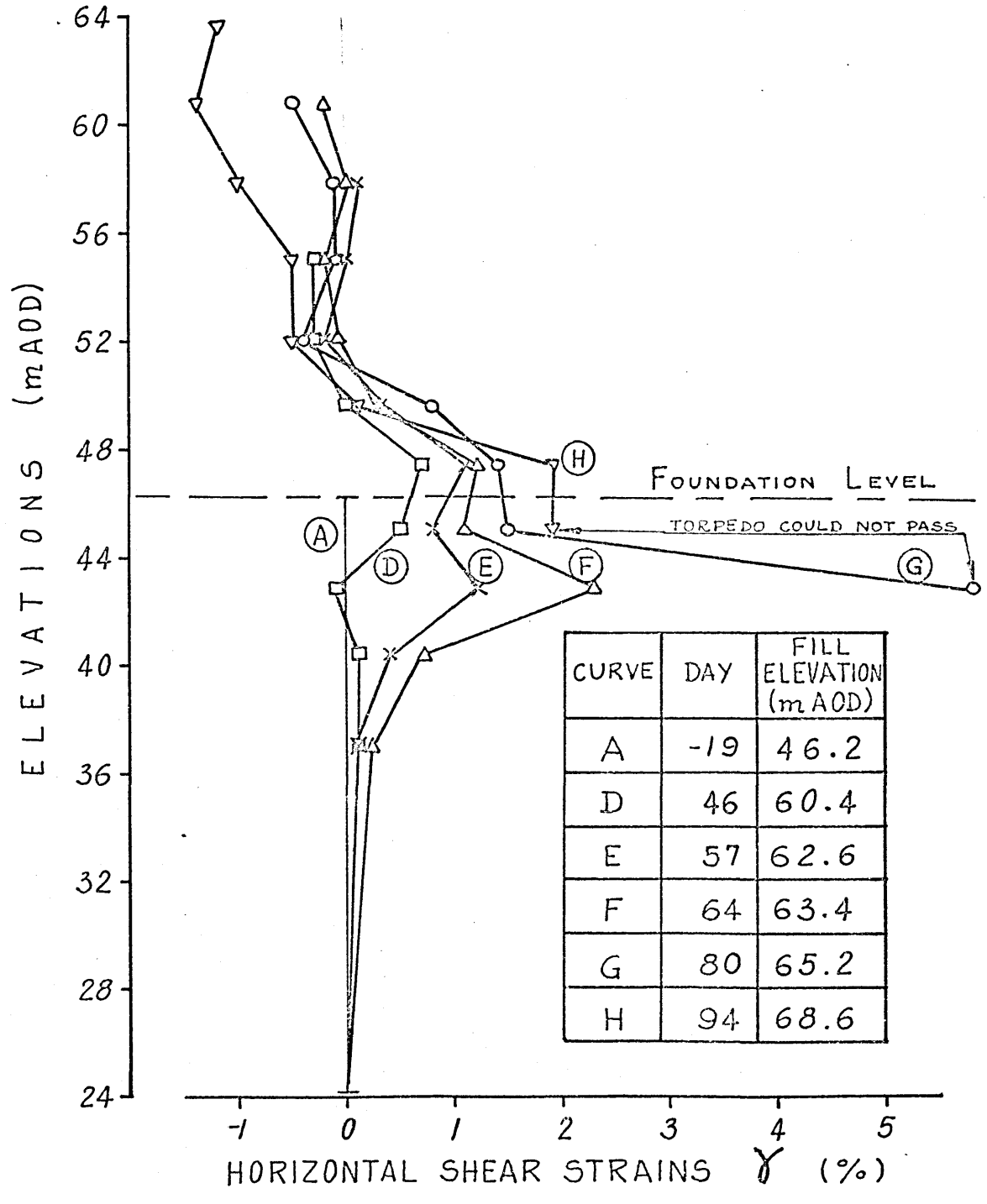
FIG. 6.99

FIG. 6.99

EMPINGHAM DAM TRIAL BANK

HORIZONTAL SHEAR STRAINS

Ch.537 INCLINOMETER I2



CURVE	DAY	FILL ELEVATION (m AOD)
A	-19	46.2
D	46	60.4
E	57	62.6
F	64	63.4
G	80	65.2
H	94	68.6

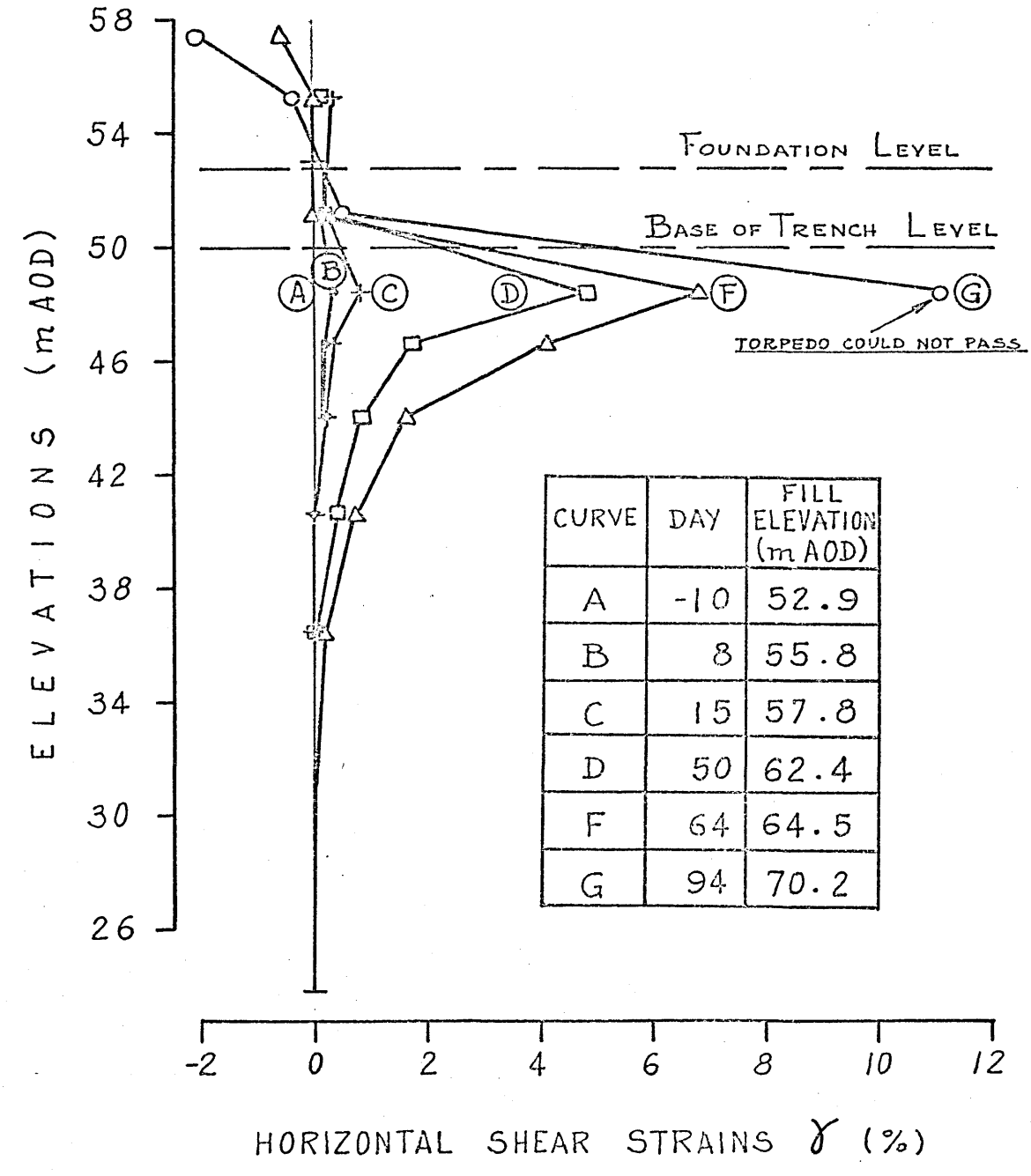
MMJ.

FIG. 6.100

EMPINGHAM DAM TRIAL BANK

HORIZONTAL SHEAR STRAINS

Ch. 487 ~ INCLINOMETER I3



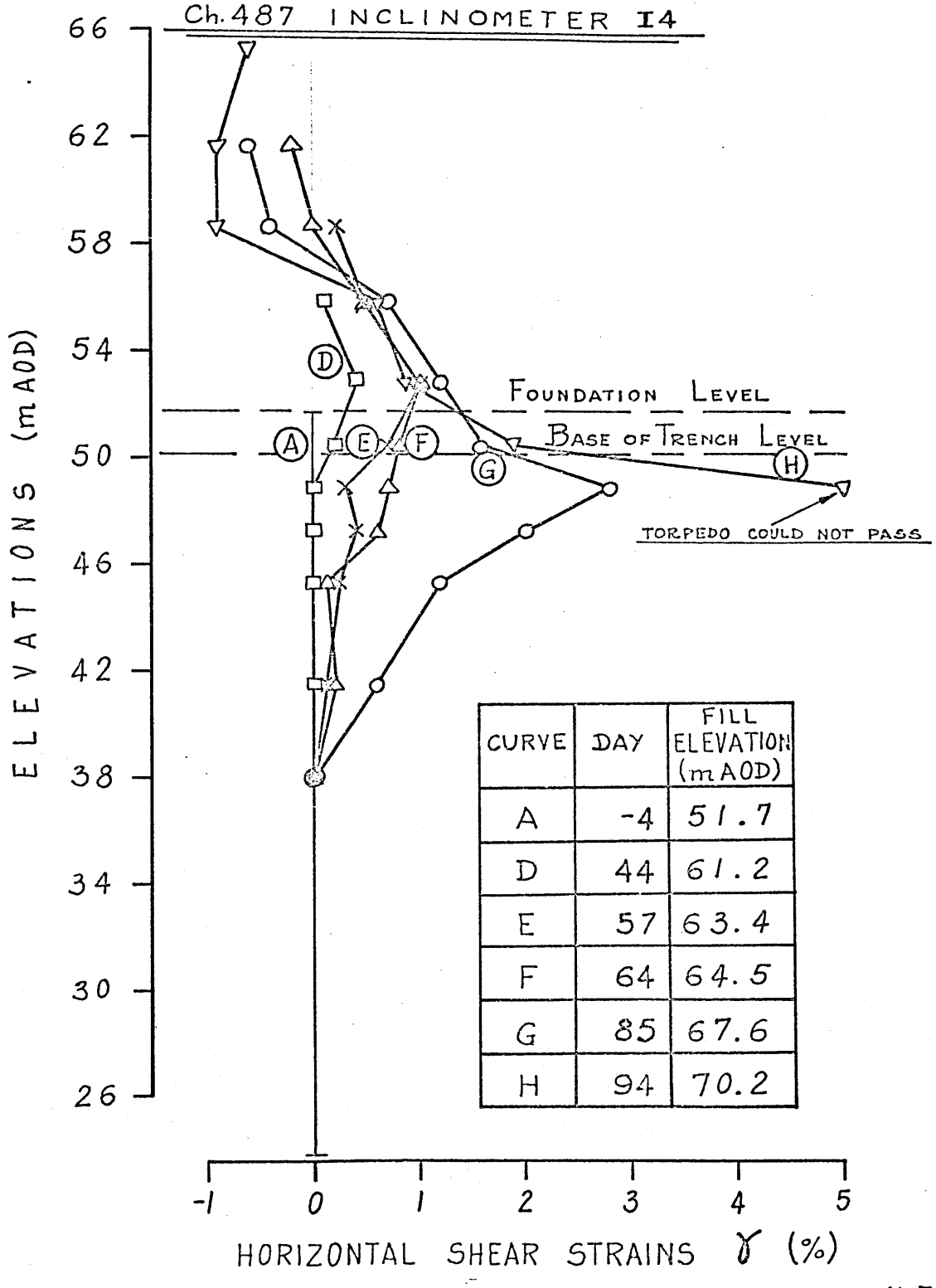
CURVE	DAY	FILL ELEVATION (m AOD)
A	-10	52.9
B	8	55.8
C	15	57.8
D	50	62.4
F	64	64.5
G	94	70.2

FIG. 6.101

EMPINGHAM DAM TRIAL BANK

HORIZONTAL SHEAR STRAINS

Ch. 487 INCLINOMETER I4



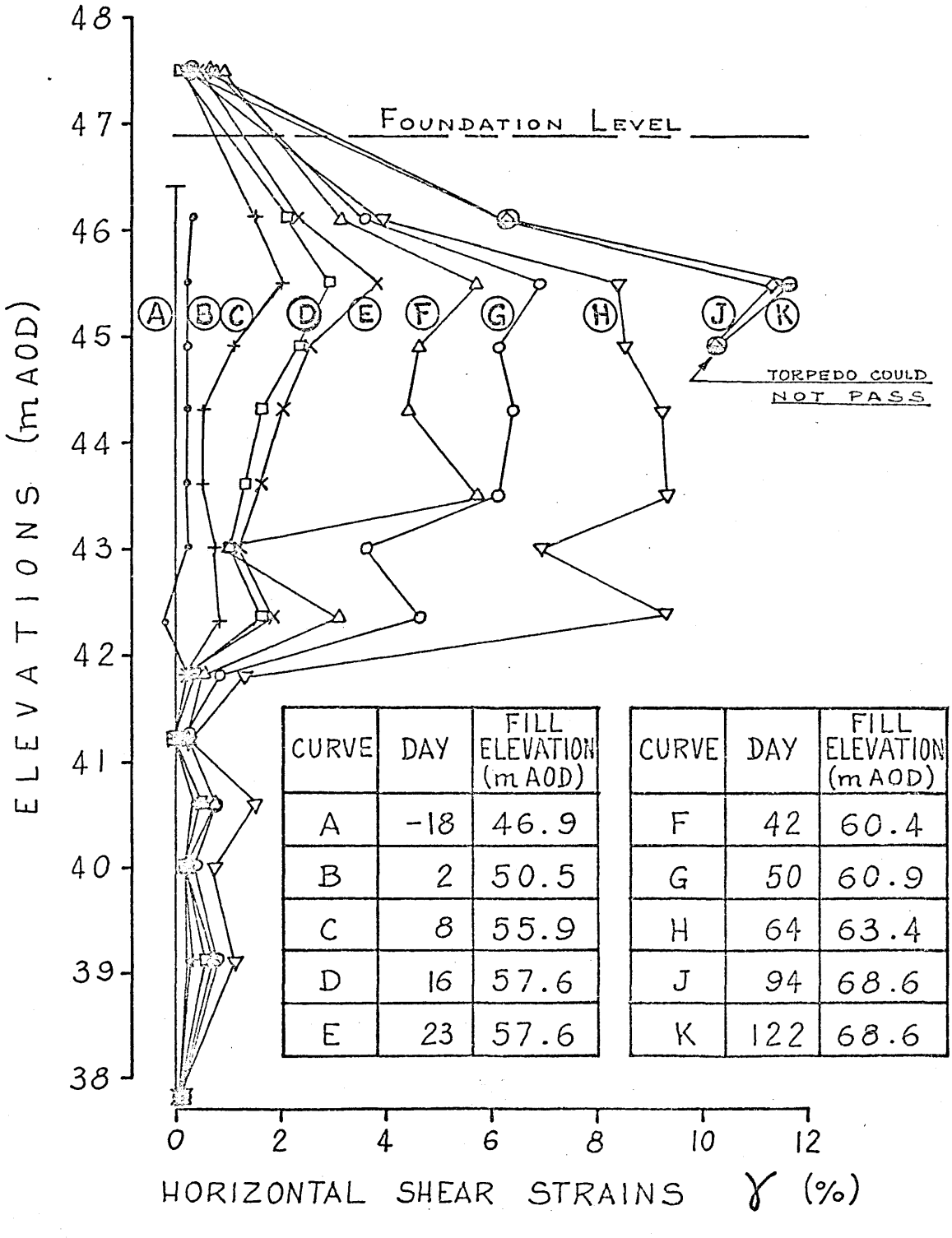
CURVE	DAY	FILL ELEVATION (mAOD)
A	-4	51.7
D	44	61.2
E	57	63.4
F	64	64.5
G	85	67.6
H	94	70.2

FIG. 6.102

EMPINGHAM DAM TRIAL BANK

HORIZONTAL SHEAR STRAINS

Ch. 537 ~ INCLINOMETER II



CURVE	DAY	FILL ELEVATION (m AOD)
A	-18	46.9
B	2	50.5
C	8	55.9
D	16	57.6
E	23	57.6

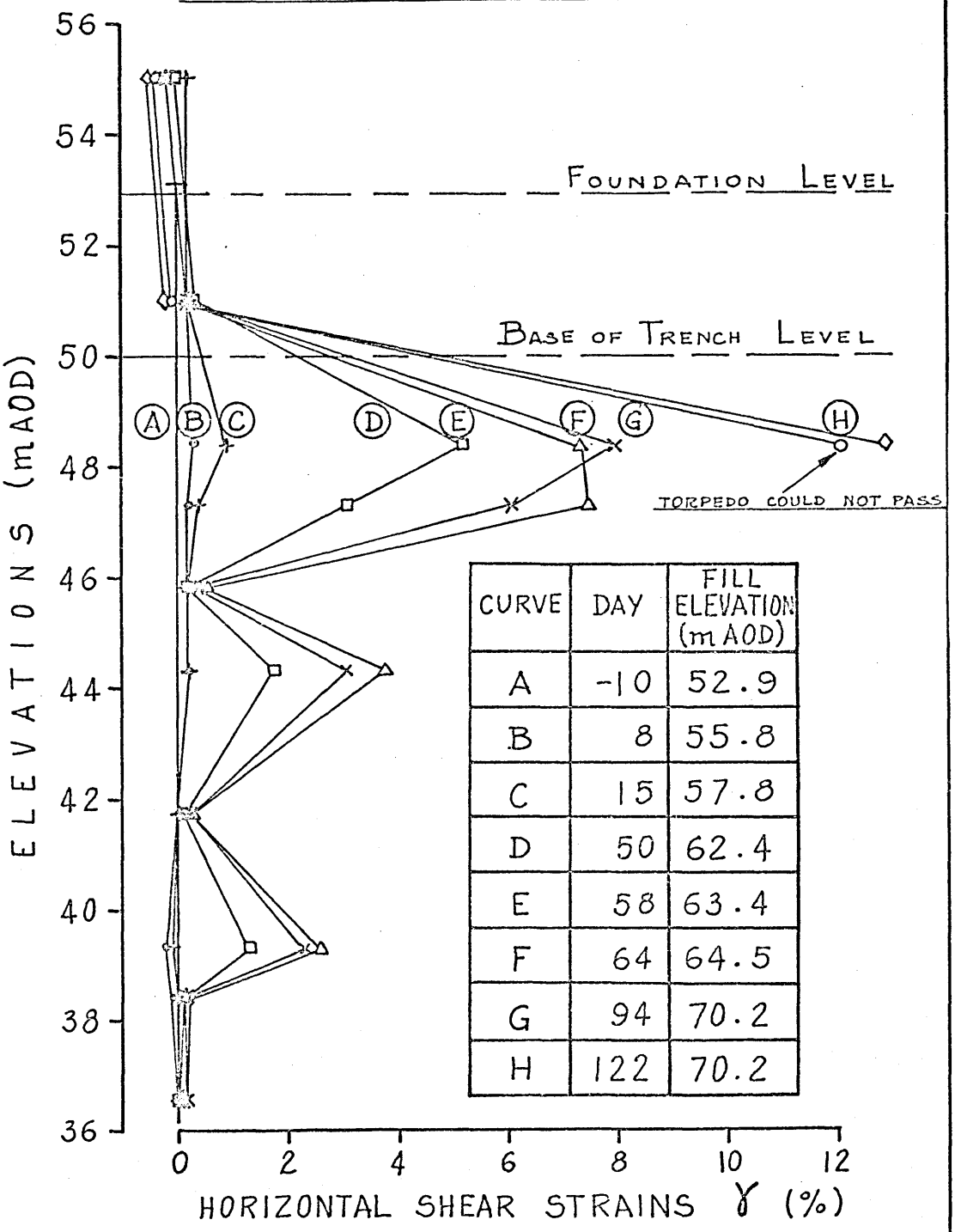
CURVE	DAY	FILL ELEVATION (m AOD)
F	42	60.4
G	50	60.9
H	64	63.4
J	94	68.6
K	122	68.6

FIG. 6.103

EMPINGHAM DAM TRIAL BANK

HORIZONTAL SHEAR STRAINS

Ch. 487 ~ INCLINOMETER I3



CURVE	DAY	FILL ELEVATION (m AOD)
A	-10	52.9
B	8	55.8
C	15	57.8
D	50	62.4
E	58	63.4
F	64	64.5
G	94	70.2
H	122	70.2

FIG. 6.104

EMPINGHAM DAM TRIAL BANK

HORIZONTAL SHEAR STRAINS

Ch. 487

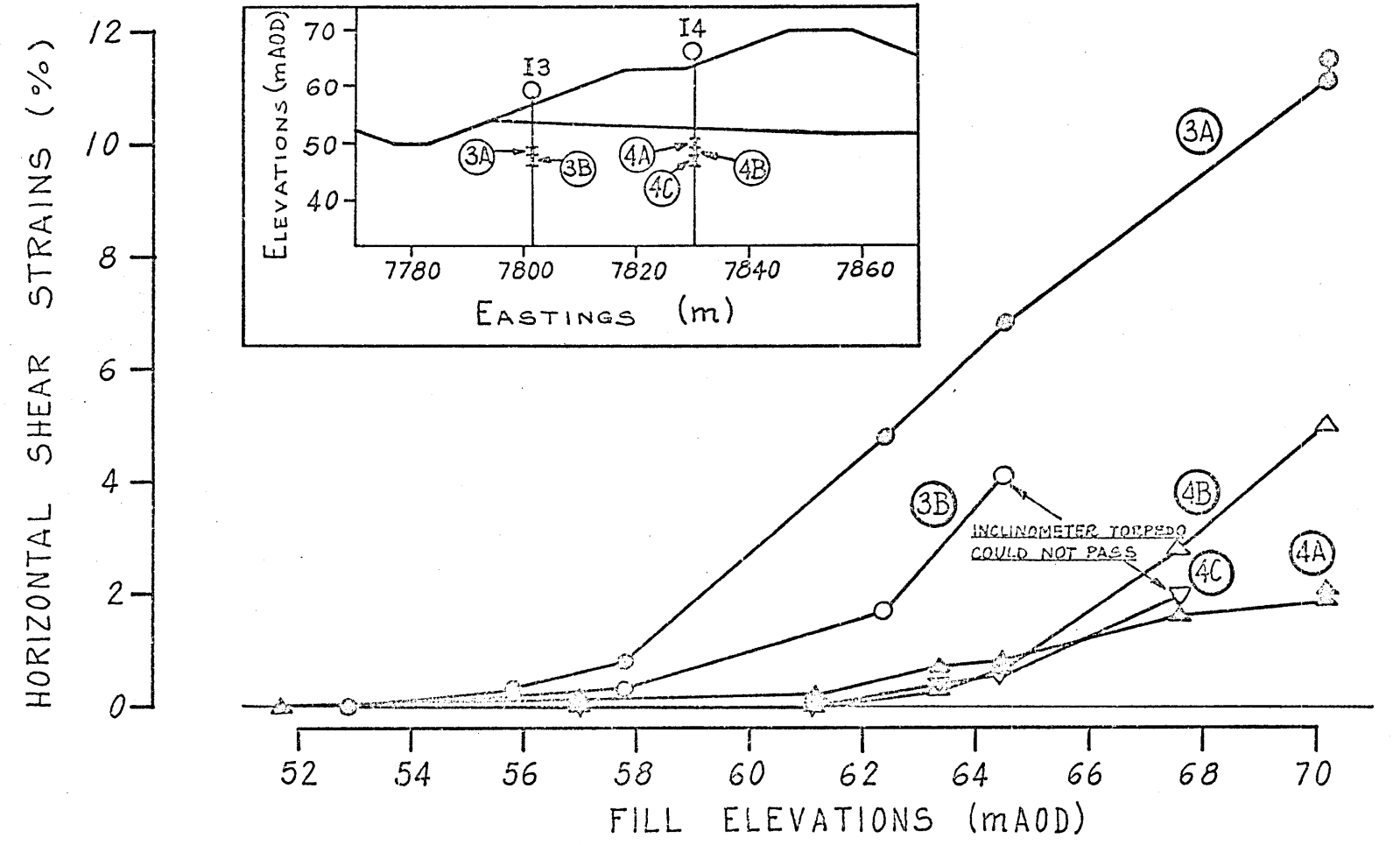


FIG. 6.105

FIG. 6.105

EMPINGHAM DAM TRIAL BANK

HORIZONTAL SHEAR STRAINS

Ch. 537

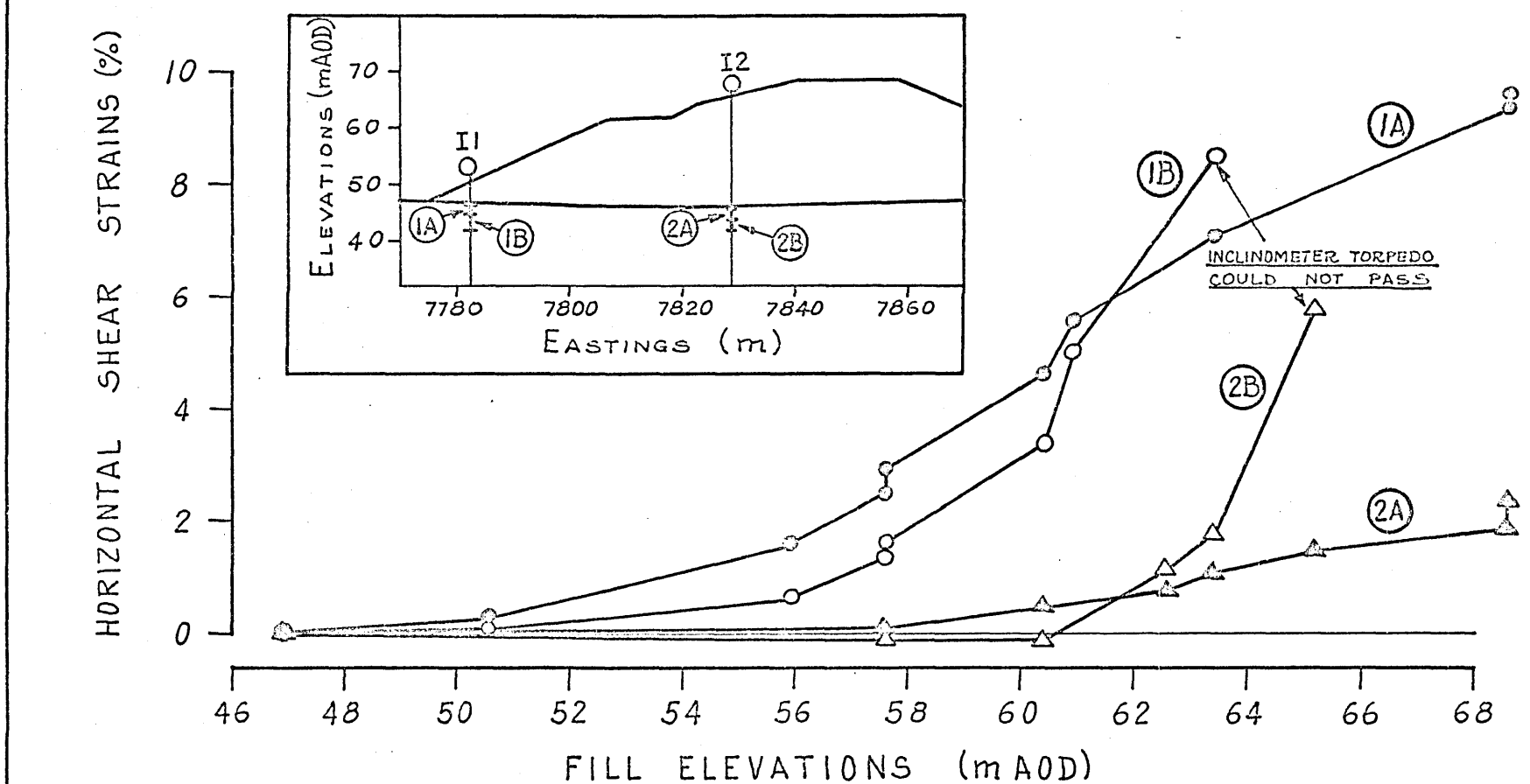
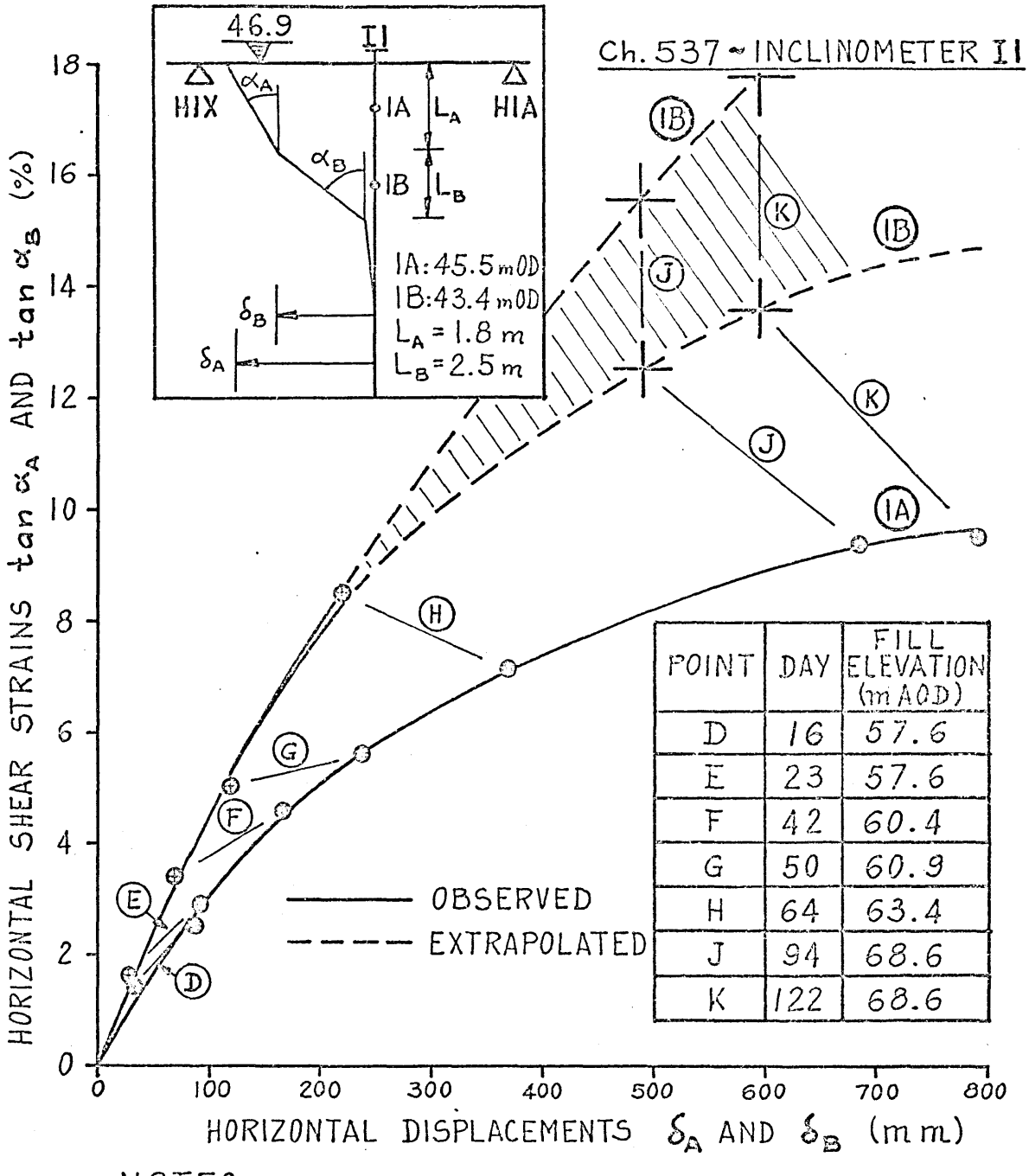


FIG. 6.106

FIG. 6.106

EMPINGHAM DAM TRIAL BANK

ESTIMATIVE OF MAXIMUM HORIZONTAL SHEAR STRAIN



POINT	DAY	FILL ELEVATION (m AOD)
D	16	57.6
E	23	57.6
F	42	60.4
G	50	60.9
H	64	63.4
J	94	68.6
K	122	68.6

NOTES:

(i): δ_A interpolated from displacements at HIX and HIA

(ii): δ_B calculated from δ_A by inclinometer profile

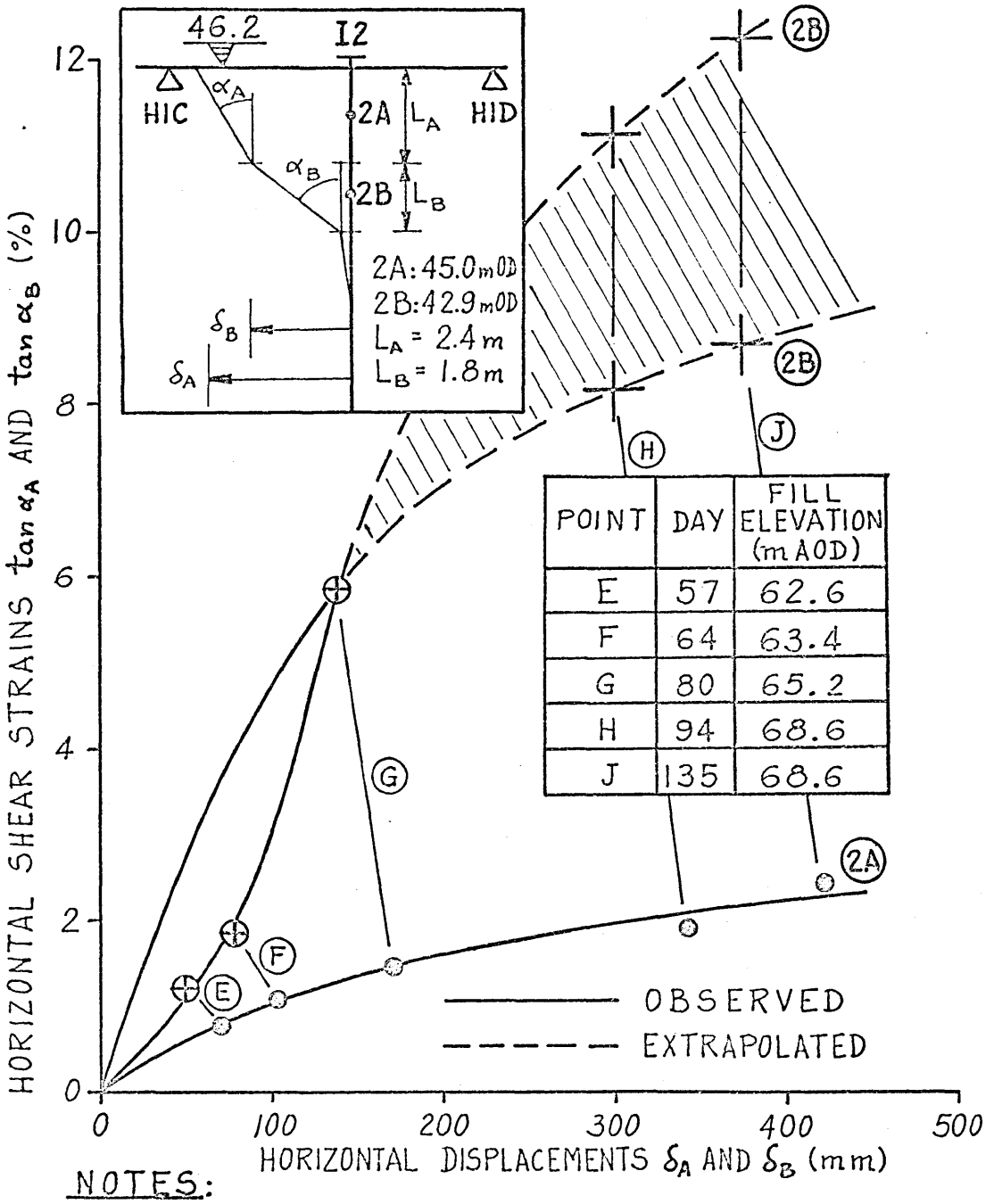
(iii): α_A and α_B from inclinometer profile.

FIG. 6.107

EMPINGHAM DAM TRIAL BANK

ESTIMATIVE OF MAXIMUM HORIZONTAL SHEAR STRAIN

Ch. 537 ~ INCLINOMETER I2



POINT	DAY	FILL ELEVATION (m AOD)
E	57	62.6
F	64	63.4
G	80	65.2
H	94	68.6
J	135	68.6

NOTES:

(i): δ_A interpolated from displacements at HIC and HID

(ii): δ_B calculated from δ_A by inclinometer profile

(iii): α_A and α_B from inclinometer profile

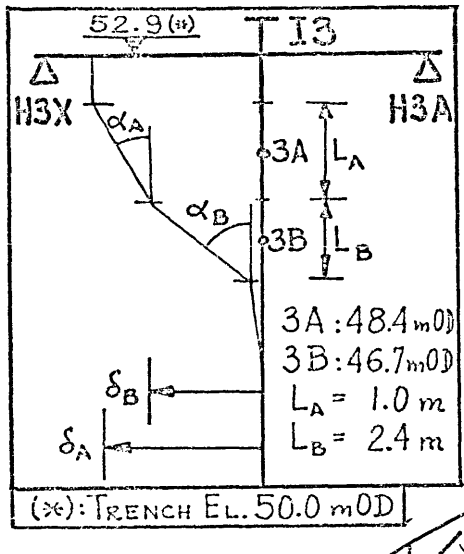
AMJ.

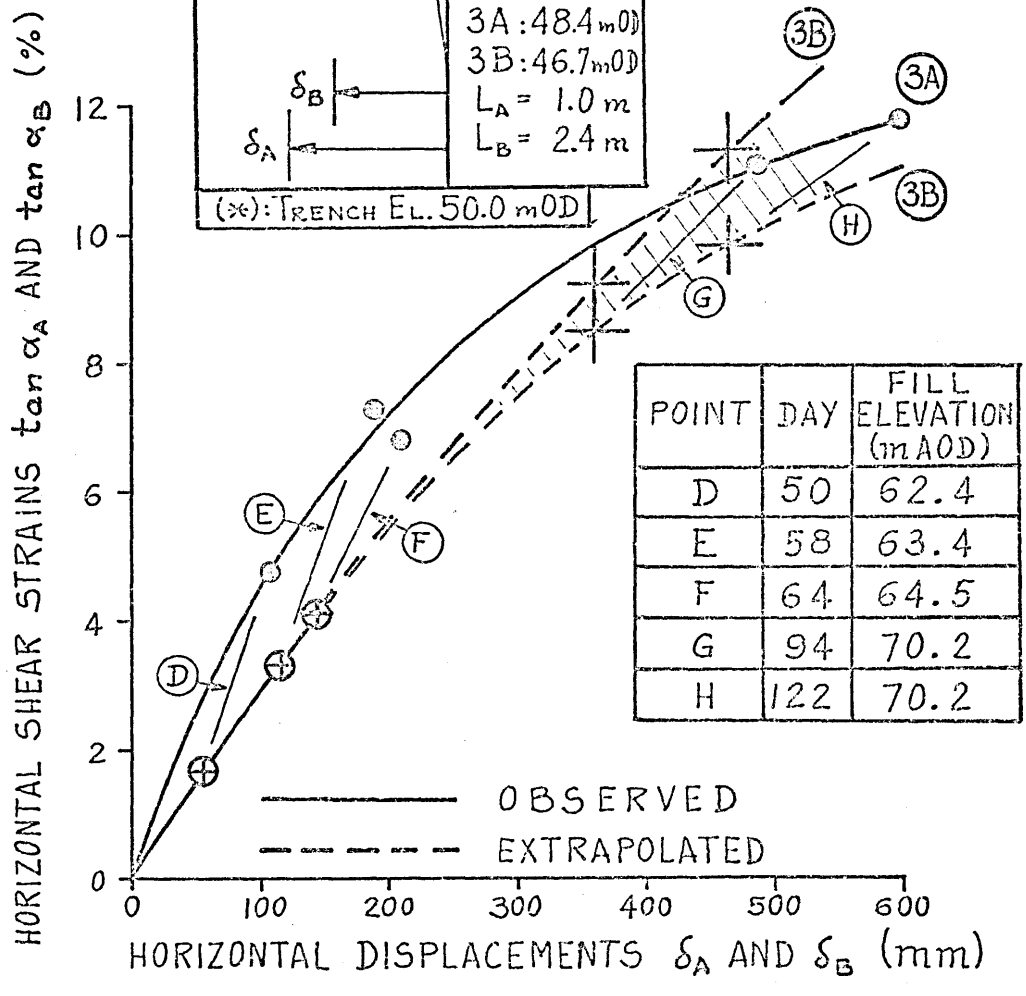
FIG. 6.108

EMPINGHAM DAM TRIAL BANK

ESTIMATIVE OF MAXIMUM HORIZONTAL SHEAR STRAIN

Ch. 487 ~ INCLINOMETER I3





POINT	DAY	FILL ELEVATION (m AOD)
D	50	62.4
E	58	63.4
F	64	64.5
G	94	70.2
H	122	70.2

NOTES:

(i): δ_A interpolated from displacements at H3X and H3A

(ii): δ_B calculated from δ_A by inclinometer profile

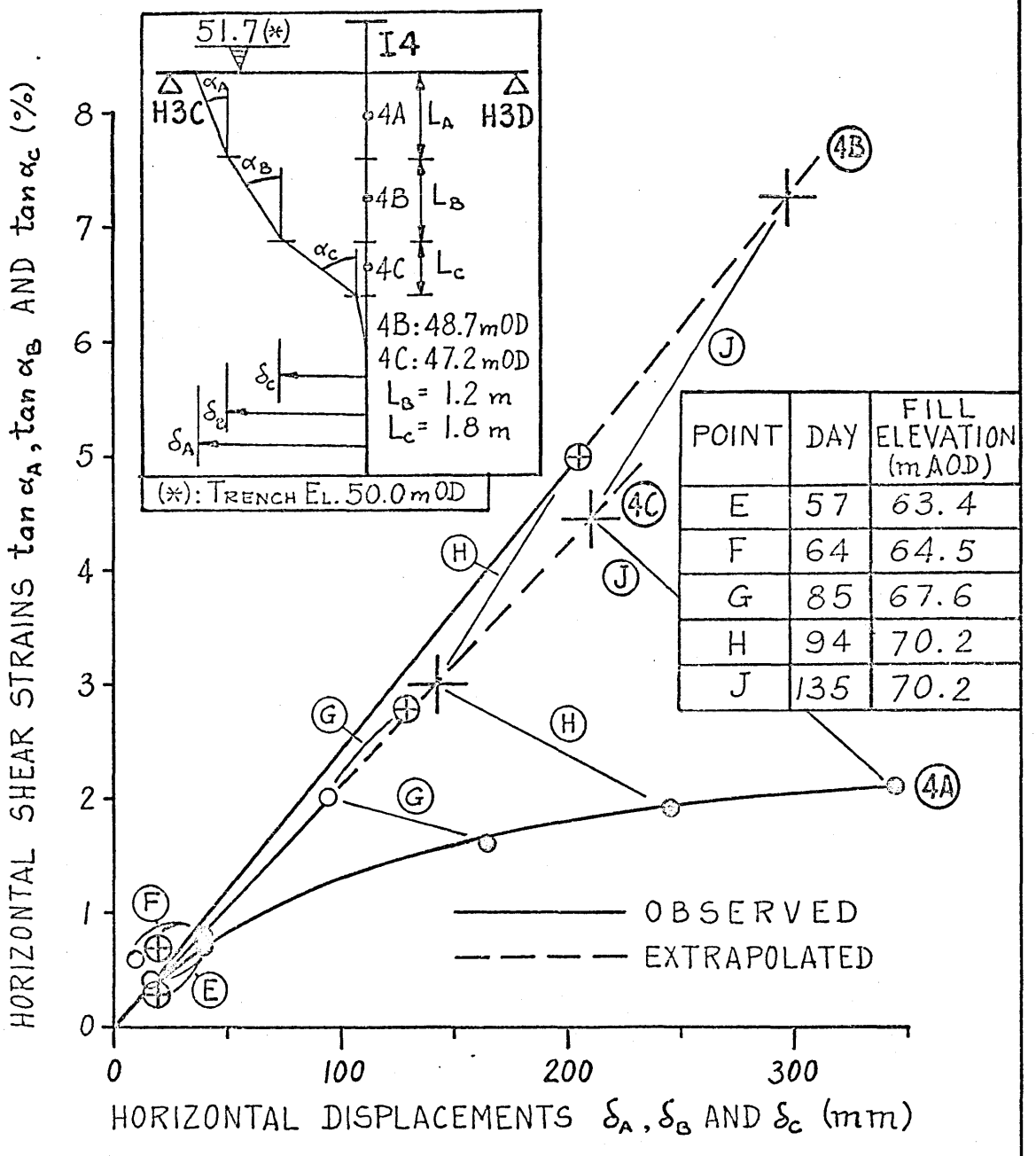
(iii): α_A and α_B from inclinometer profile

FIG. 6.109

EMPINGHAM DAM TRIAL BANK

ESTIMATIVE OF MAXIMUM HORIZONTAL SHEAR STRAIN

Ch. 487 ~ INCLINOMETER I4



POINT	DAY	FILL ELEVATION (mAOD)
E	57	63.4
F	64	64.5
G	85	67.6
H	94	70.2
J	135	70.2

NOTES:

(i): δ_A interpolated from displacements at H3C and H3D

(ii): δ_B and δ_C calculated from δ_A by inclinometer profile

(iii): α_A, α_B and α_C from inclinometer profile

MWS

FIG. 6.110

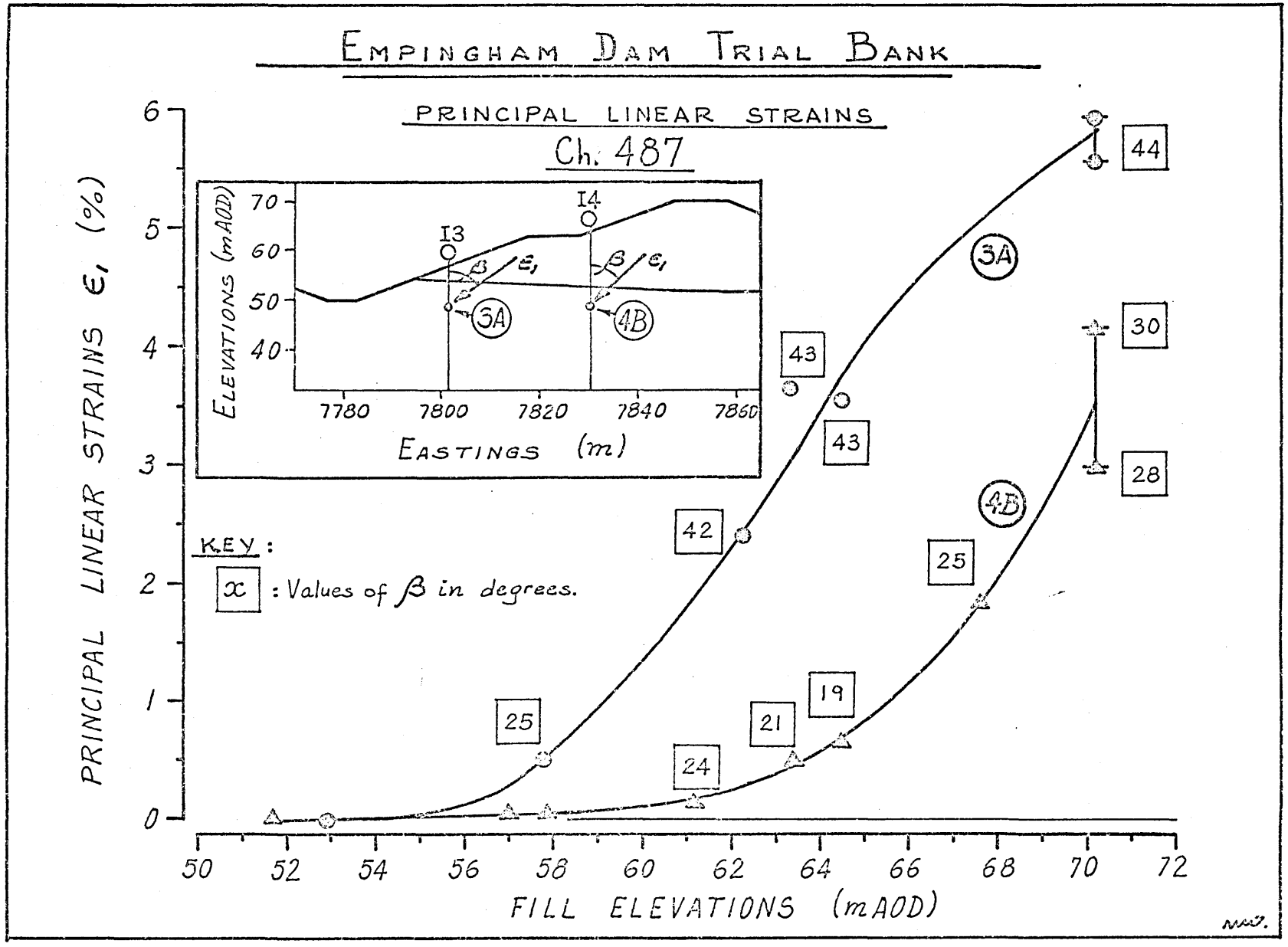


FIG. 6.111

FIG. 6.111

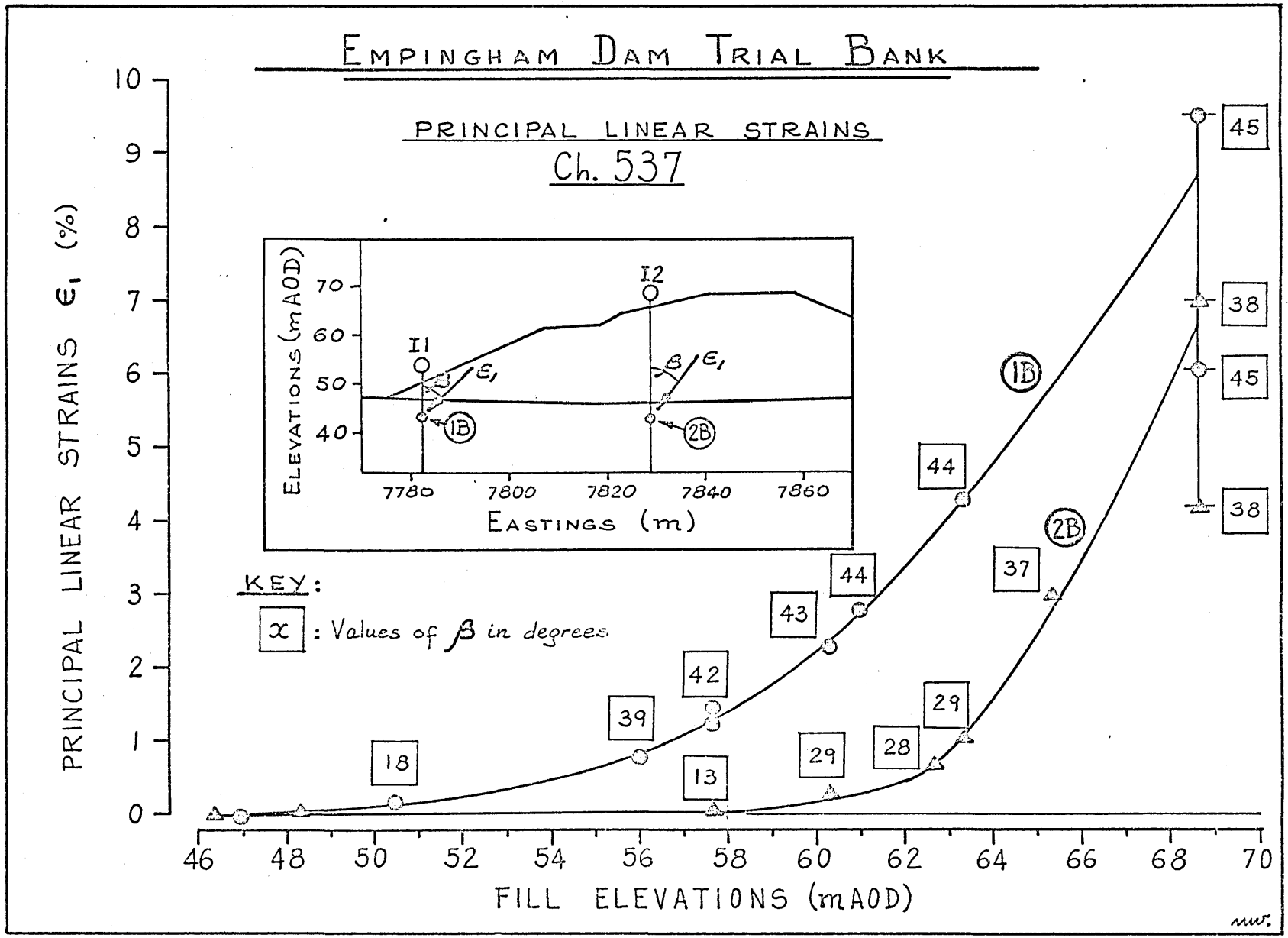

EMPINGHAM DAM TRIAL BANK
PRINCIPAL LINEAR STRAINS
Ch. 537
PRINCIPAL LINEAR STRAINS ϵ_1 (%)
FILL ELEVATIONS (mAOD)
ELEVATIONS (mAOD)
EASTINGS (m)
I1
I2
1B
2B
KEY:
x : Values of β in degrees
18
39
42
43
44
45
13
29
28
29
37
38
45
38

FIG. 6.112

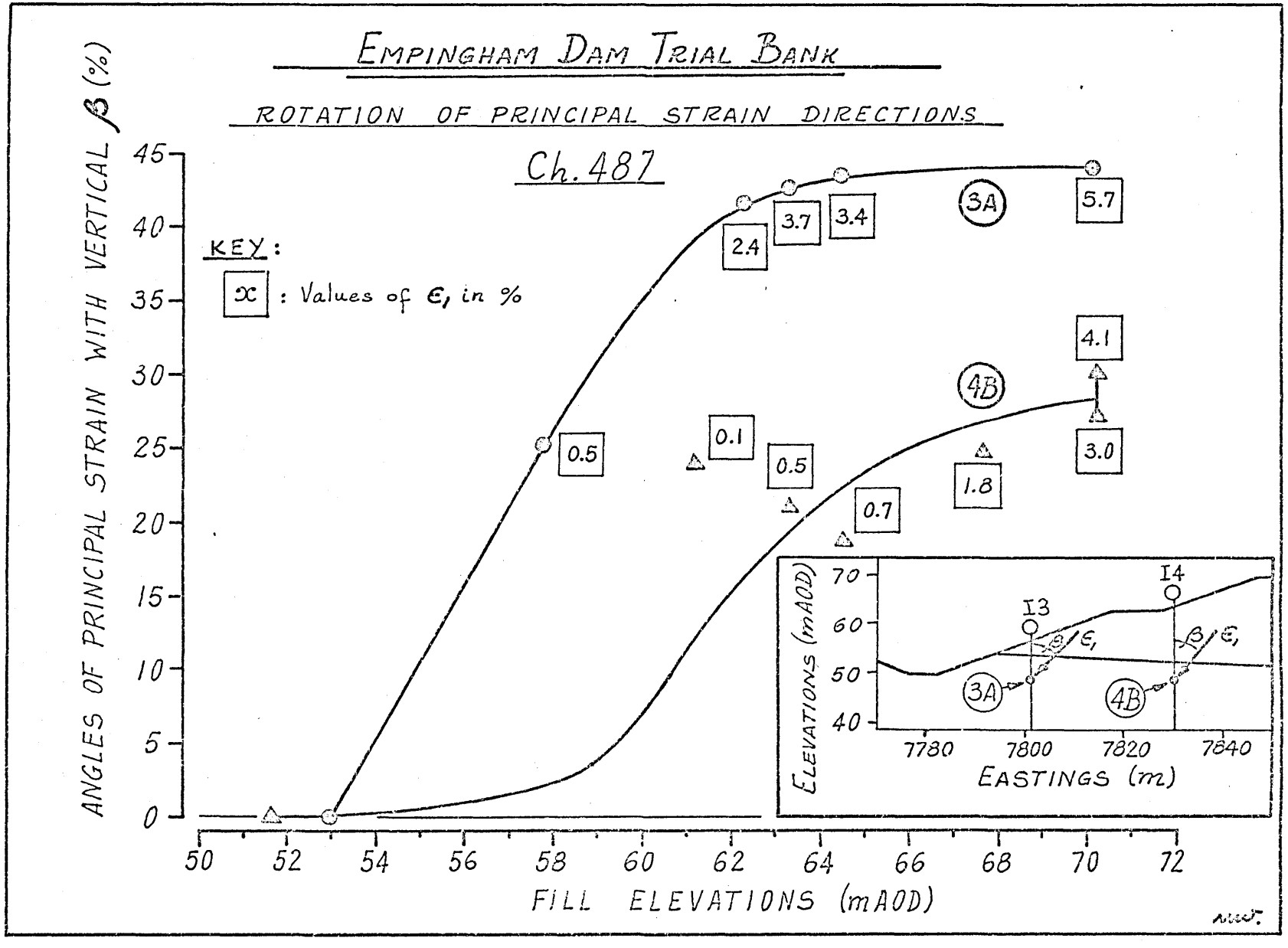


FIG. 6.113

FIG. 6.113

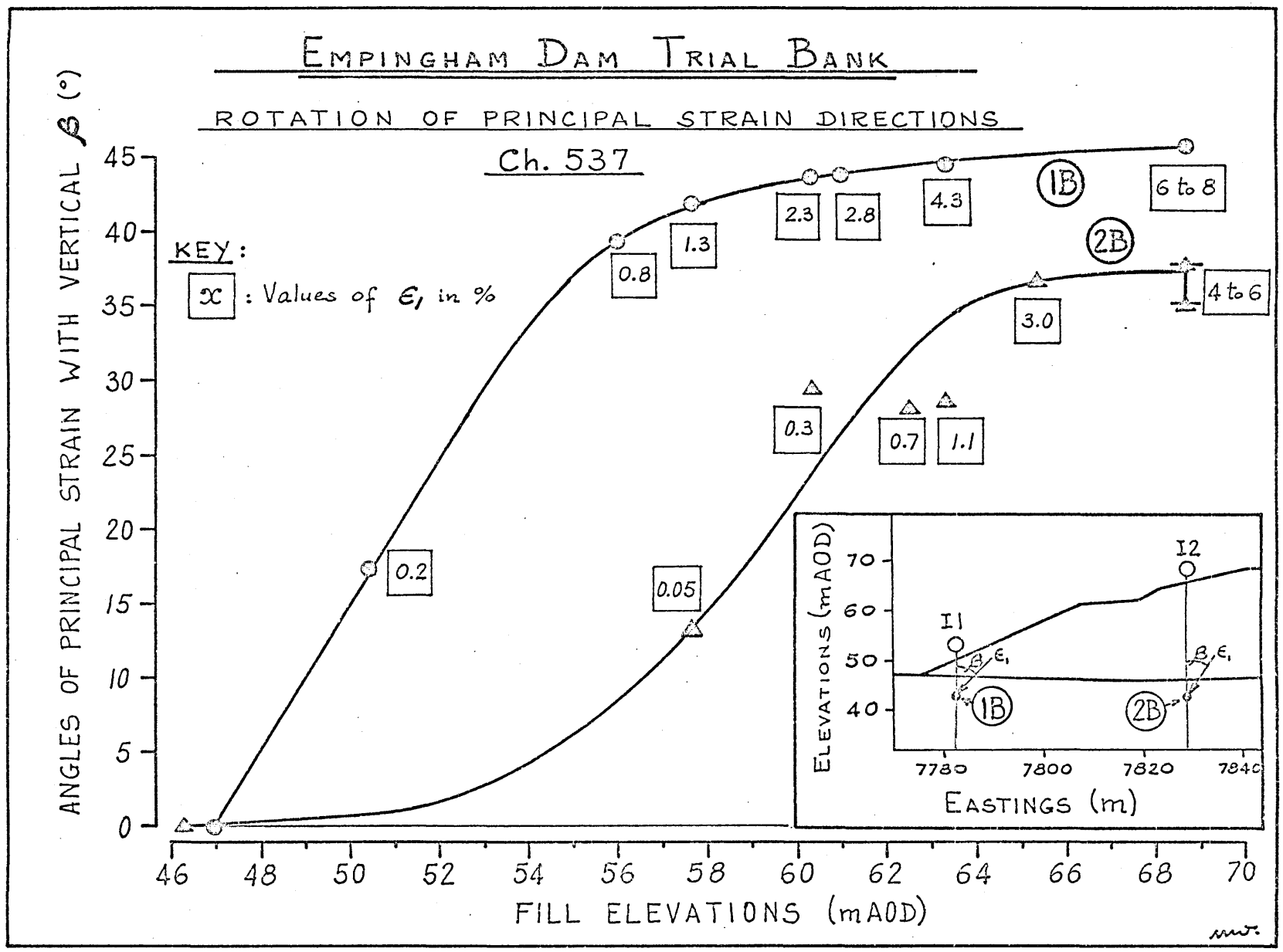

EMPINGHAM DAM TRIAL BANK
ROTATION OF PRINCIPAL STRAIN DIRECTIONS
Ch. 537
KEY:
x : Values of ε1 in %
ANGLES OF PRINCIPAL STRAIN WITH VERTICAL β (°)
FILL ELEVATIONS (mAOD)
0.2
0.8
1.3
2.3
2.8
4.3
6 to 8
1B
2B
3.0
4 to 6
0.3
0.7
1.1
0.05
I1
I2
ELEVATIONS (mAOD)
EASTINGS (m)

FIG. 6.114

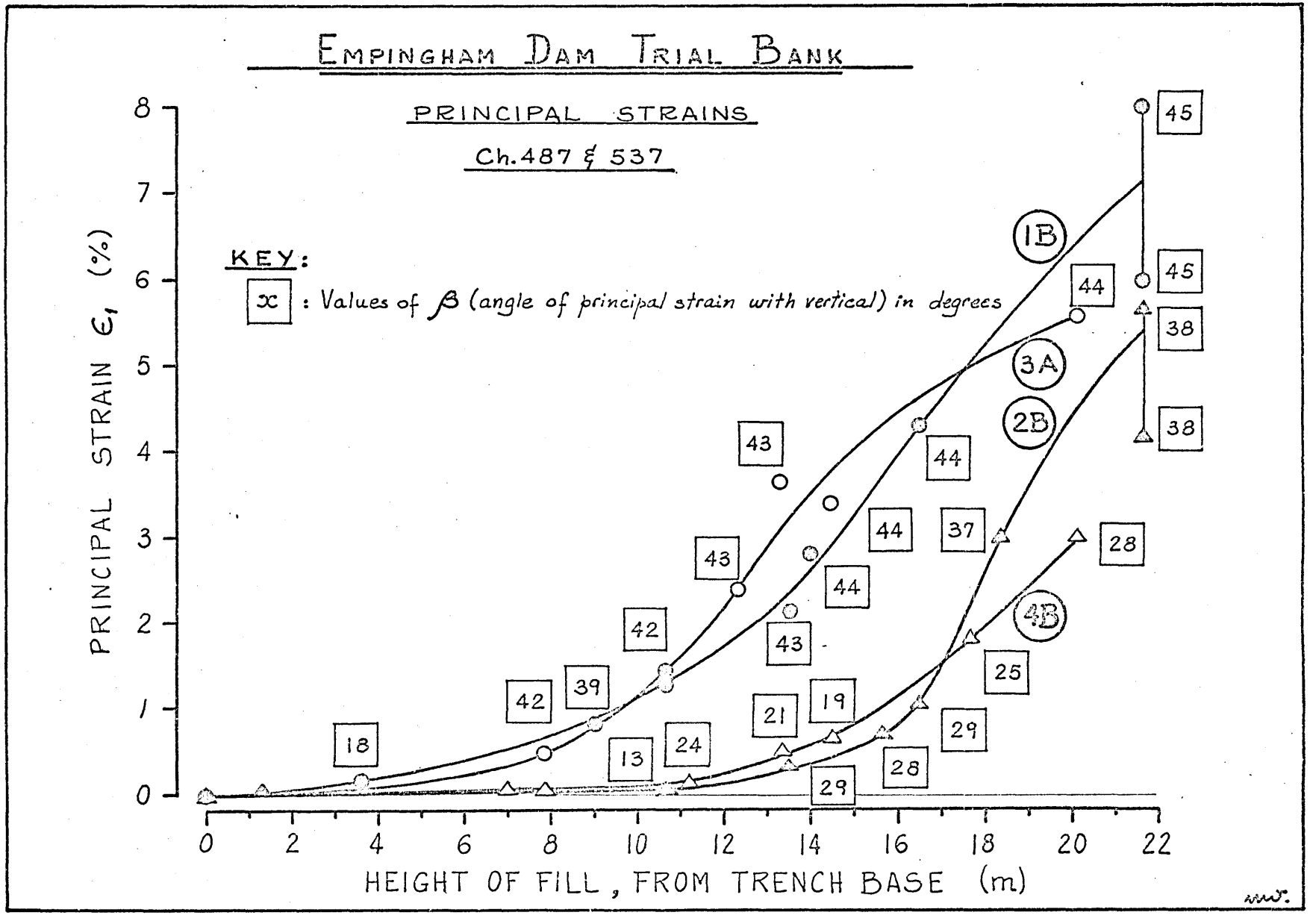


FIG. 6.115

FIG. 6.115

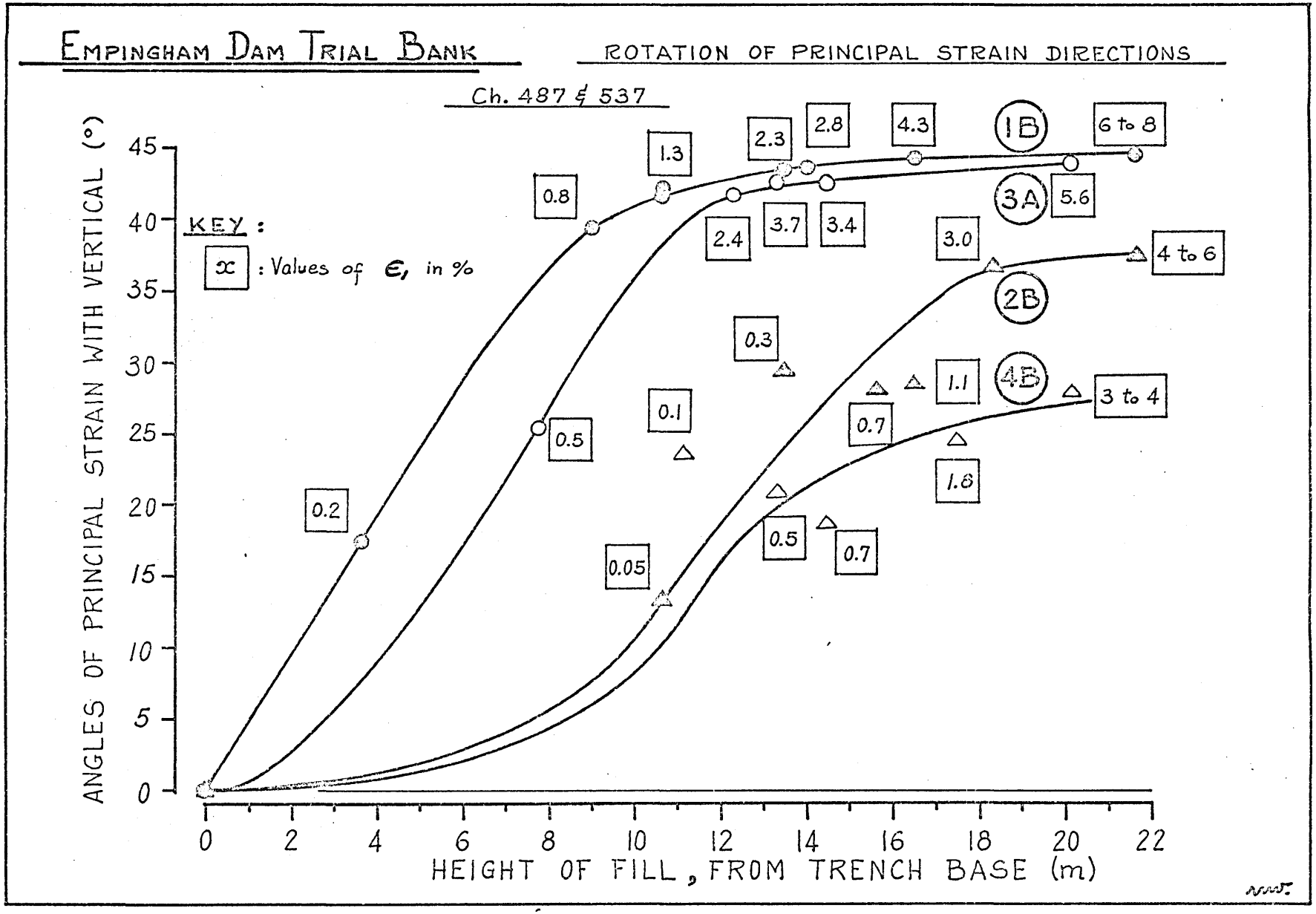


FIG. 6.116

FIG. 6.116

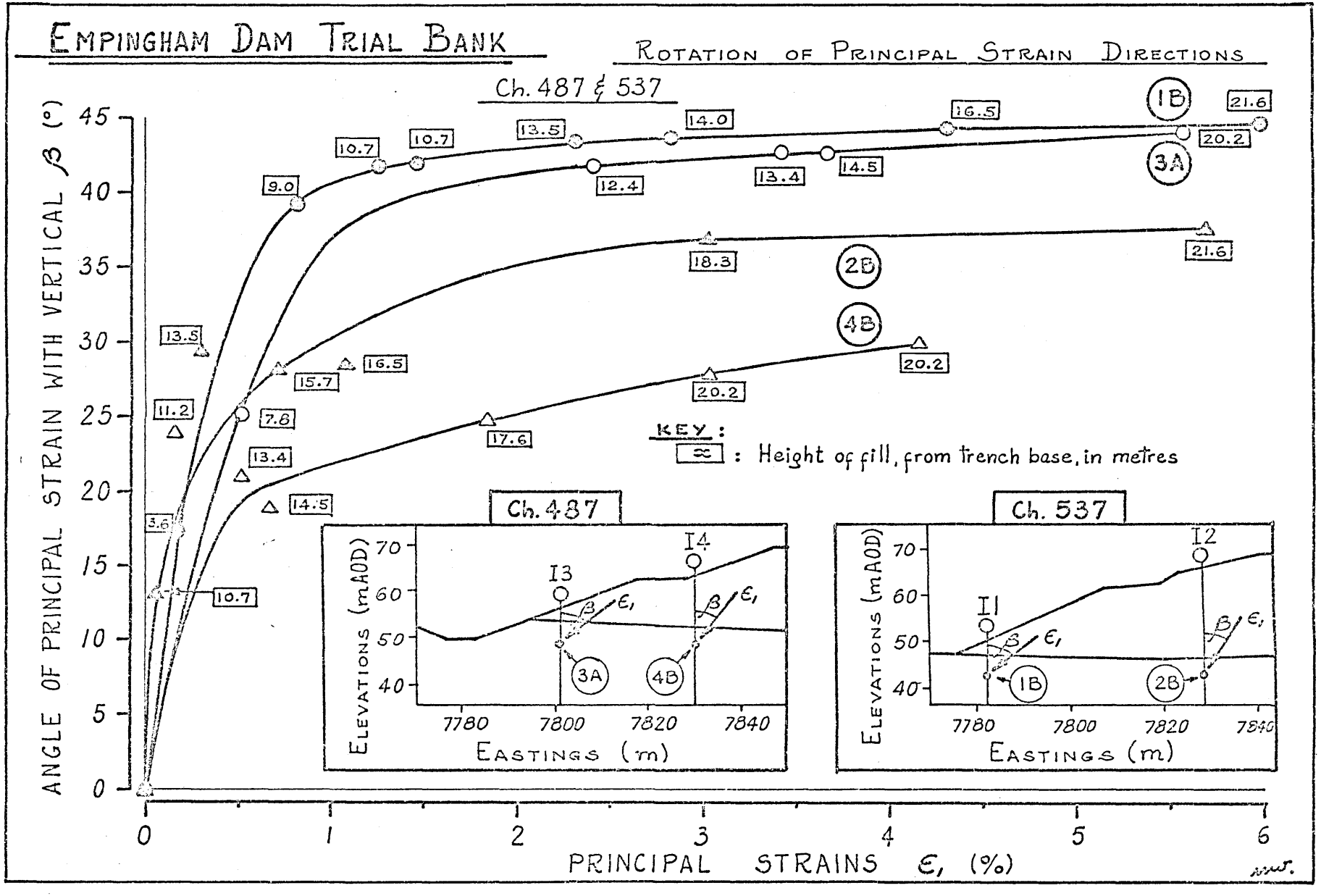

EMPINGHAM DAM TRIAL BANK
ROTATION OF PRINCIPAL STRAIN DIRECTIONS
Ch. 487 & 537
ANGLE OF PRINCIPAL STRAIN WITH VERTICAL β (°)
PRINCIPAL STRAINS ε1 (%)
1B
3A
2B
4B
KEY :
: Height of fill, from trench base, in metres
Ch. 487
Ch. 537
ELEVATIONS (mAOD)
EASTINGS (m)
I1
I2
I3
I4
1B
2B
3A
4B
β
ε1

FIG. 6.117

EMPINGHAM DAM TRIAL BANK

MAXIMUM SHEAR STRAINS

CH 487 – INCLINOMETER I4

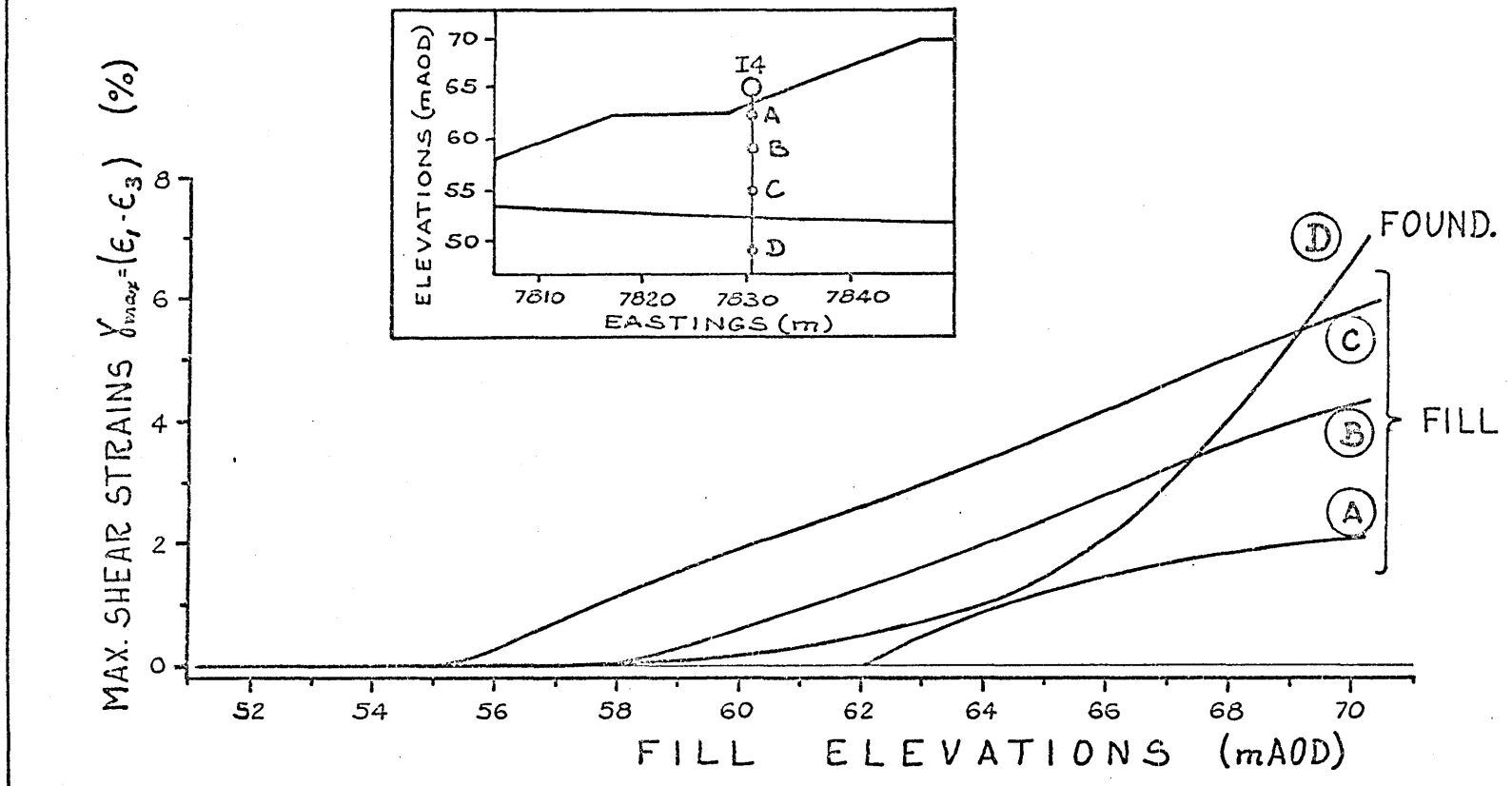


FIG. 6.118

FIG. 6.118

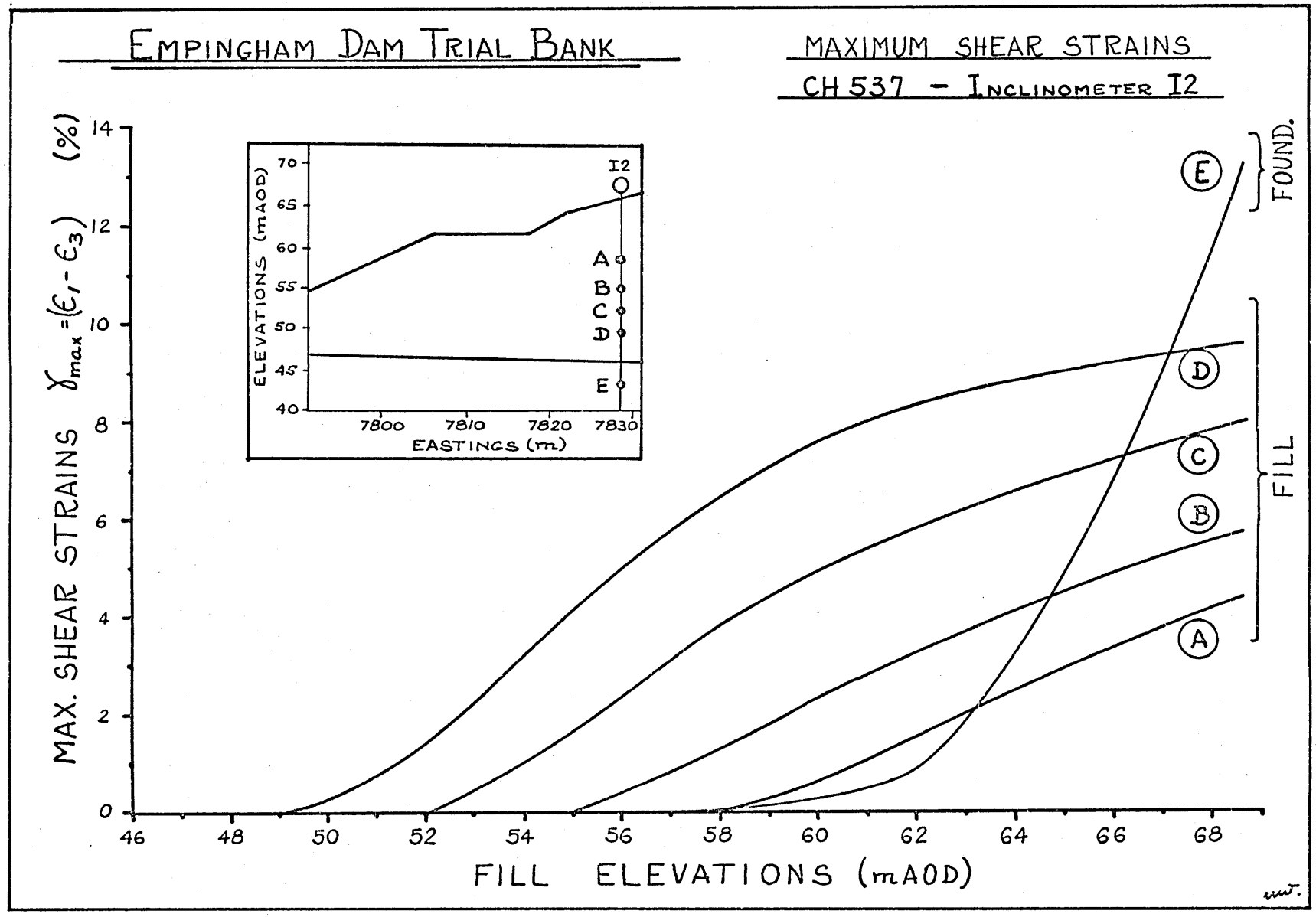


FIG. 6.119

FIG. 6.119

EMPINGHAM DAM TRIAL BANK

CH 487 - INCLINOMETER I4

ROTATION OF PRINCIPAL STRAINS

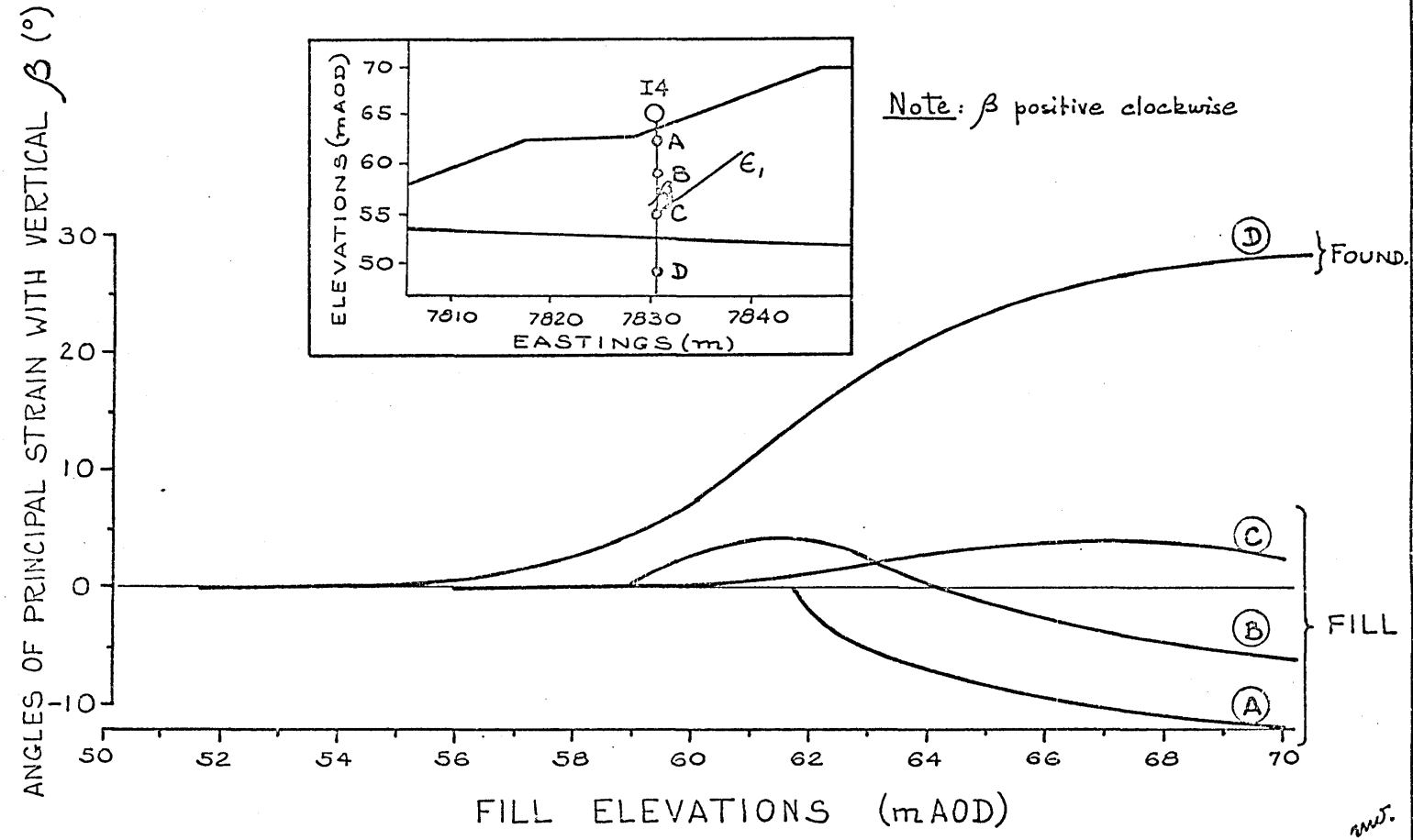


FIG. 6.120

FIG. 6.120

EMPINGHAM DAM TRIAL BANK

ROTATION OF PRINCIPAL STRAINS

CH 537 - INCLINOMETER I2

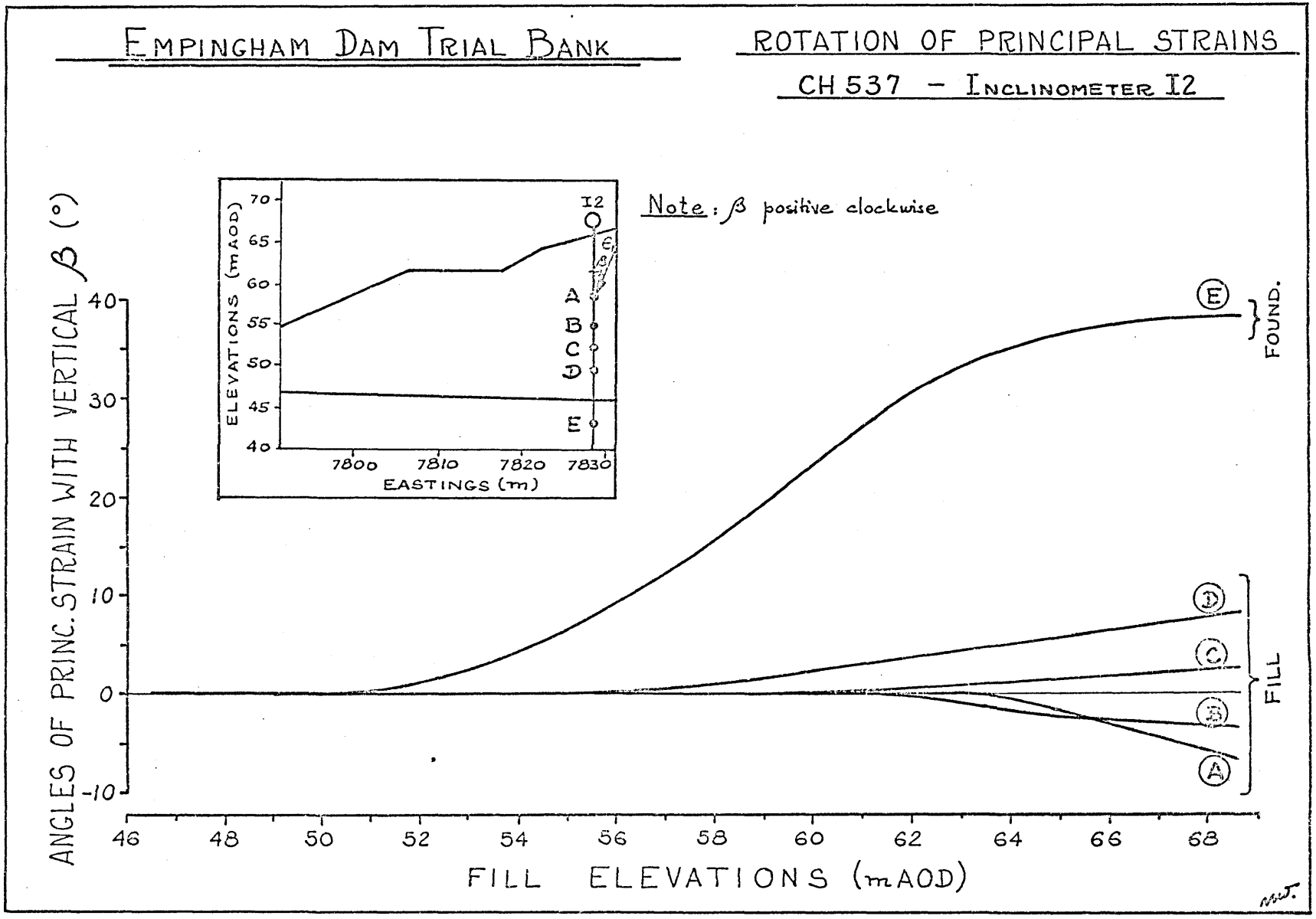


FIG. 6.121

FIG. 6.121

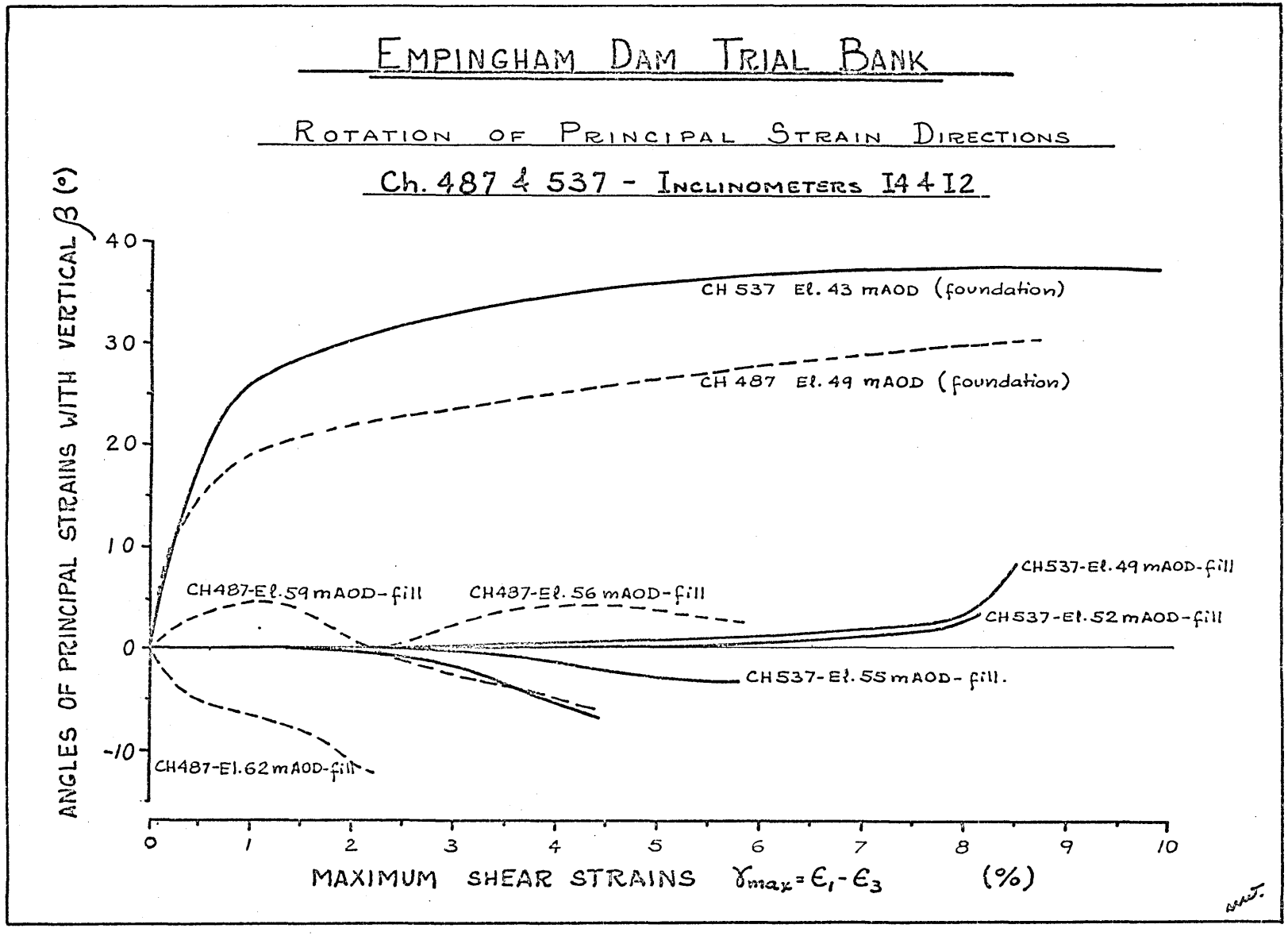


FIG. 6.122

FIG. 6.122

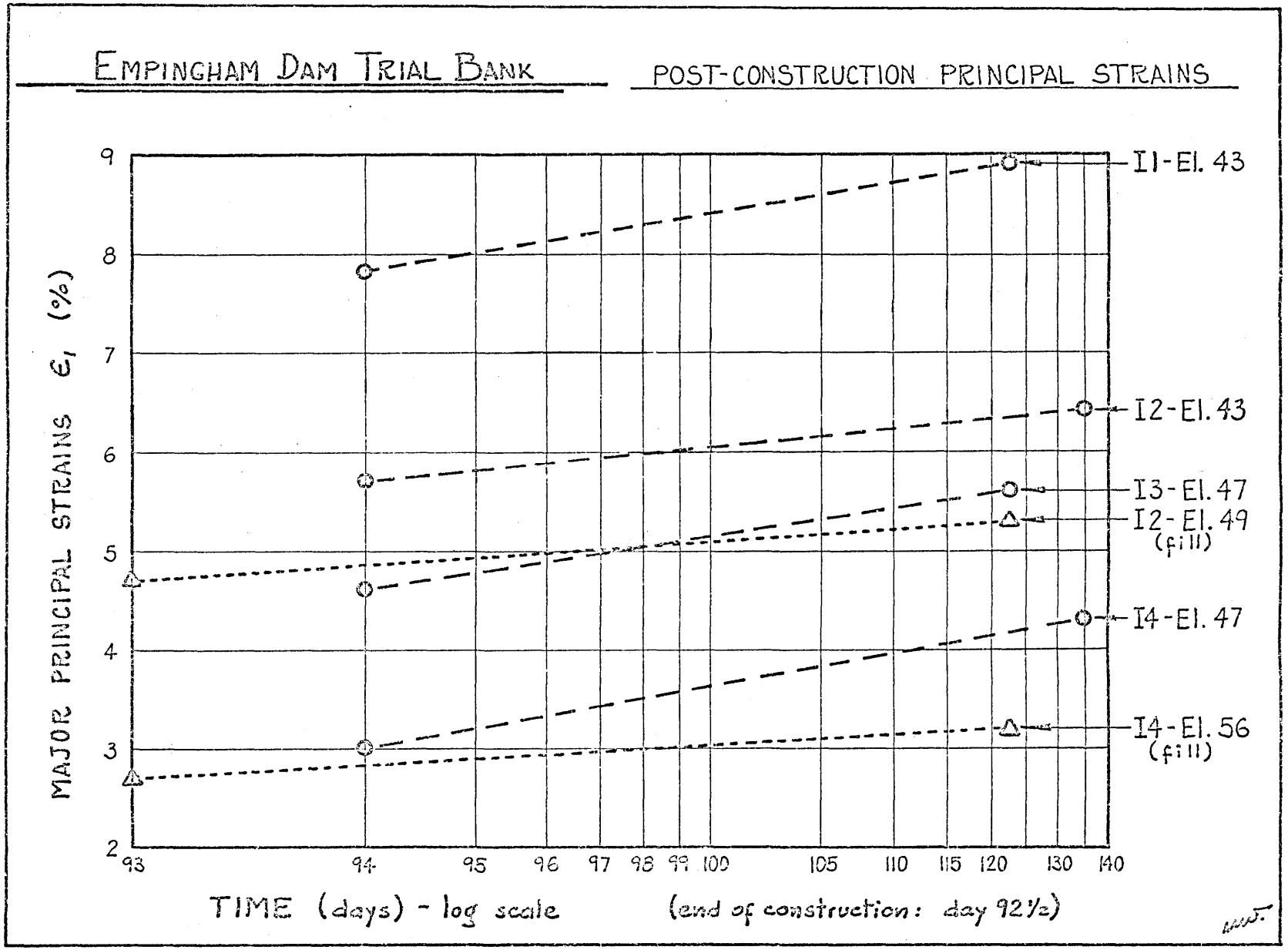


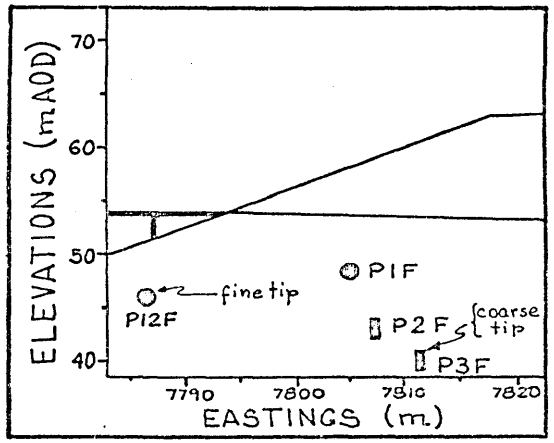
FIG. 6.123

FIG. 6.123

EMPINGHAM DAM TRIAL BANK

PIEZOMETRIC RECORDS - P1, 2, 3 and 12 F

CH 487



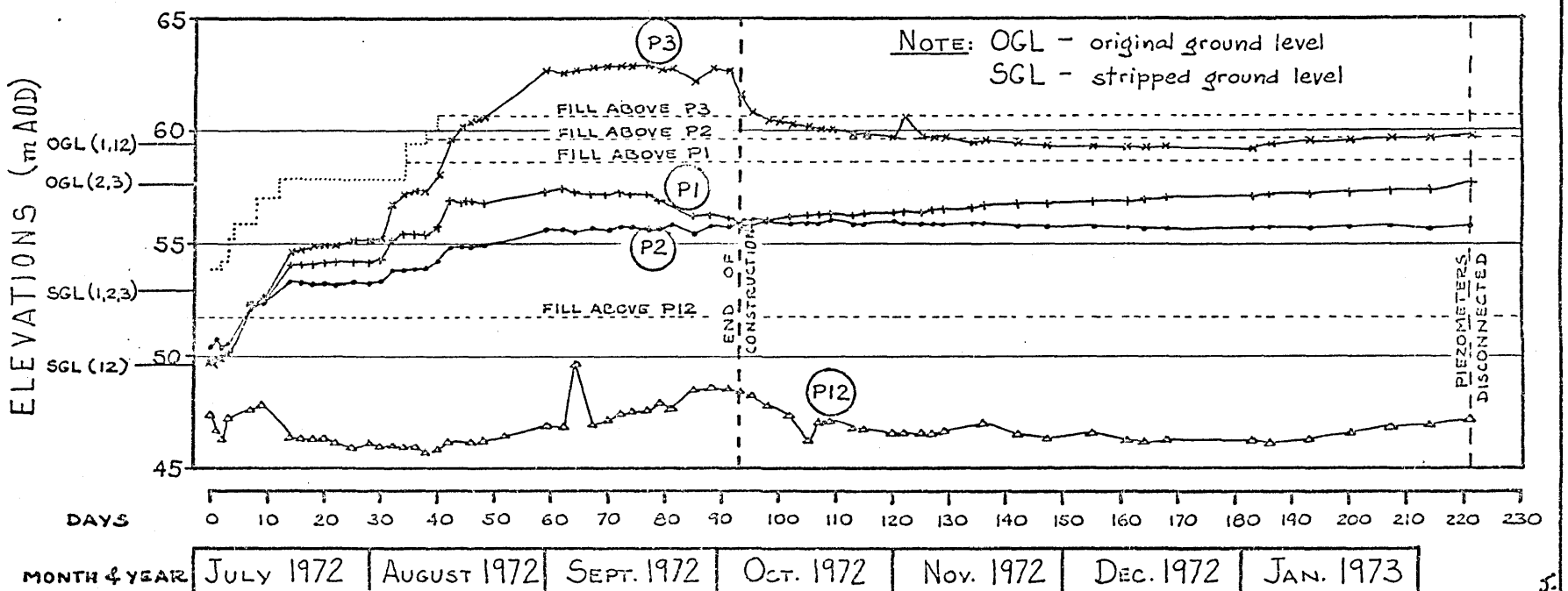


FIG. 6.124

FIG. 6.124

EMPINGHAM DAM TRIAL BANK

PIEZOMETRIC RECORDS - P4,5,6 and 11F

CH 487

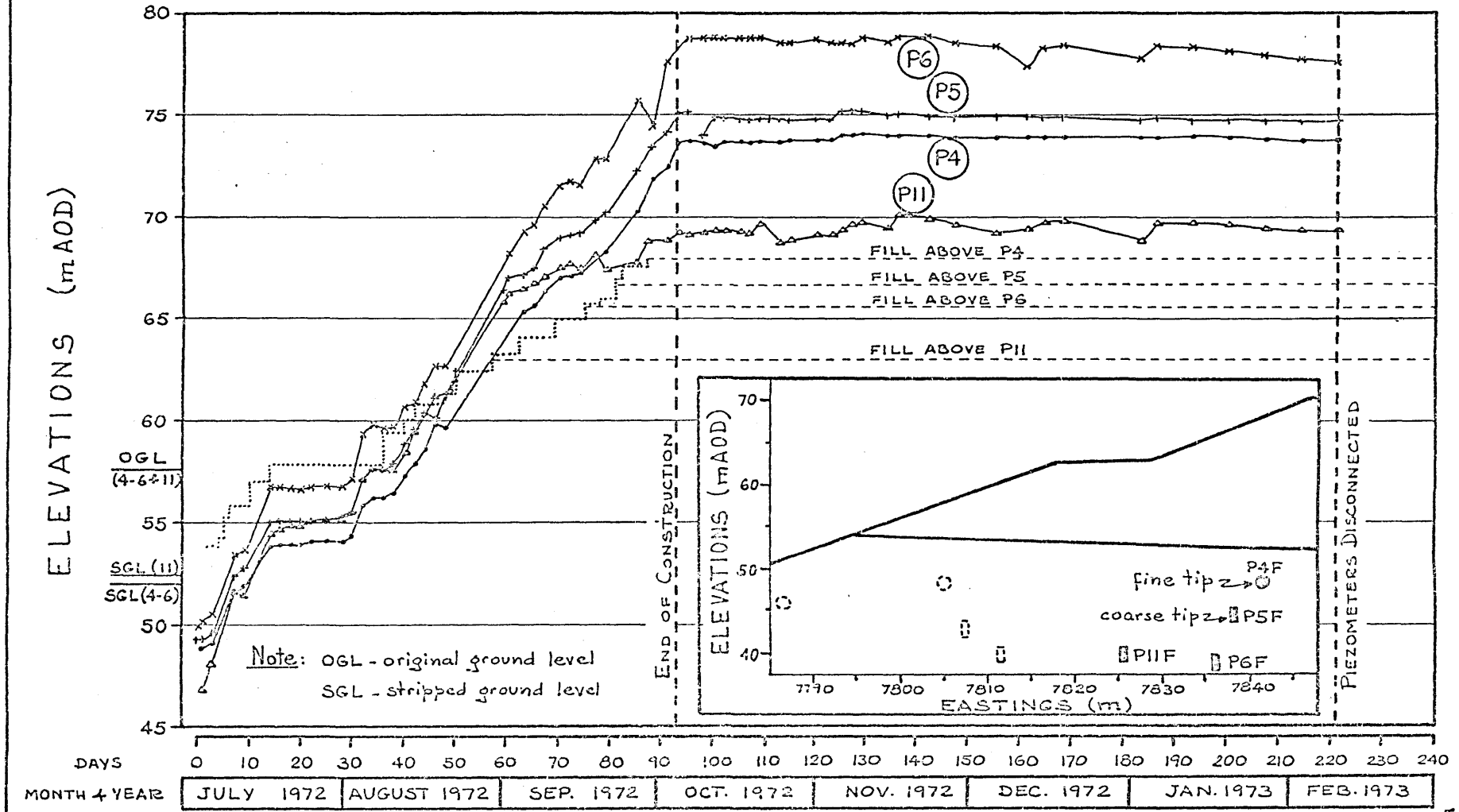


FIG. 6.125

FIG. 6.125

EMPINGHAM DAM TRIAL BANK

PIEZOMETRIC RECORDS - P7,8,9 and 10F

CH 537

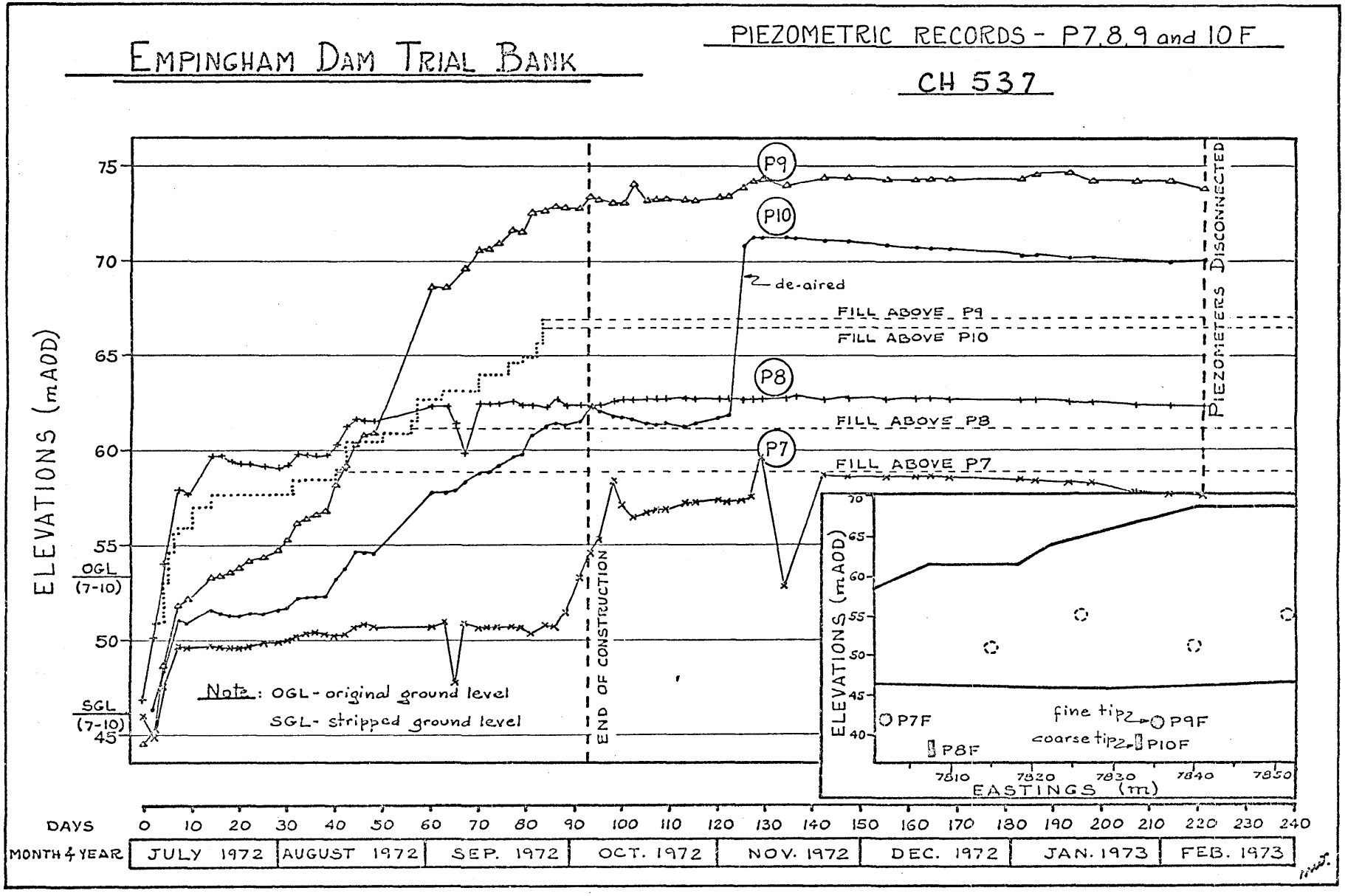


FIG. 6.126

FIG. 6.126

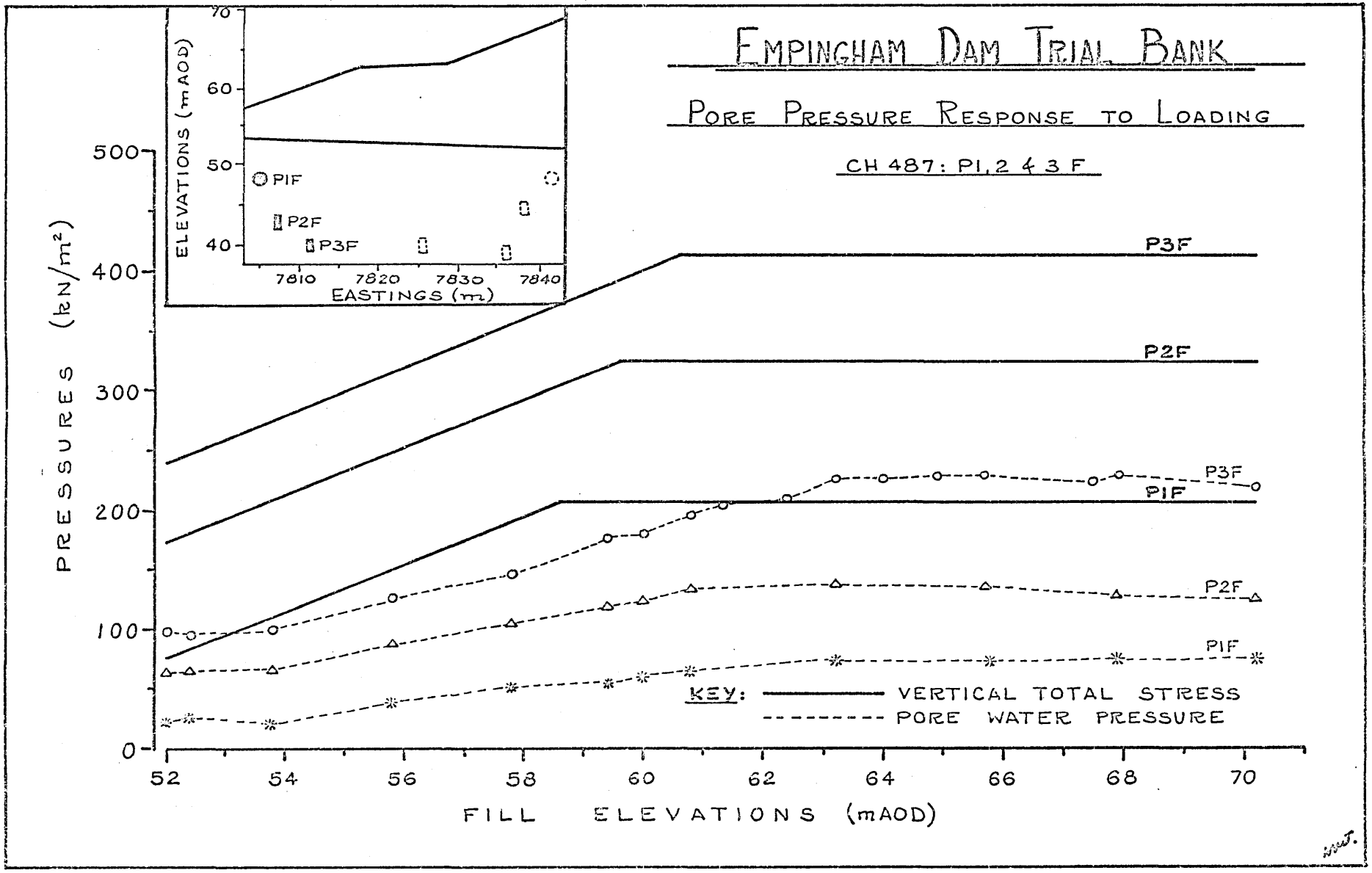


FIG. 6.127

FIG. 6.127

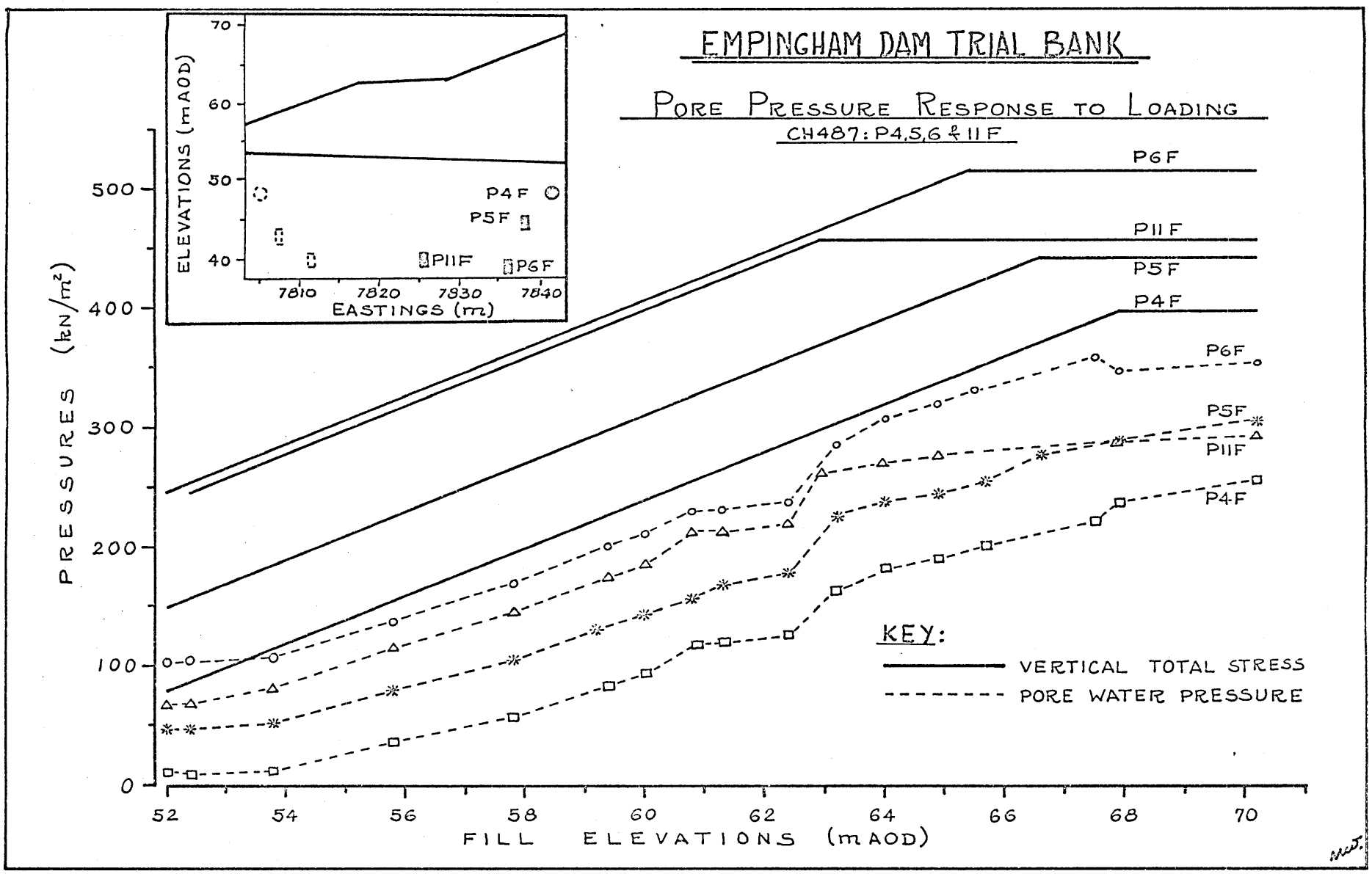


FIG. 6.128

FIG. 6.128

EMPINGHAM DAM TRIAL BANK

PORE PRESSURE RESPONSE TO LOADING

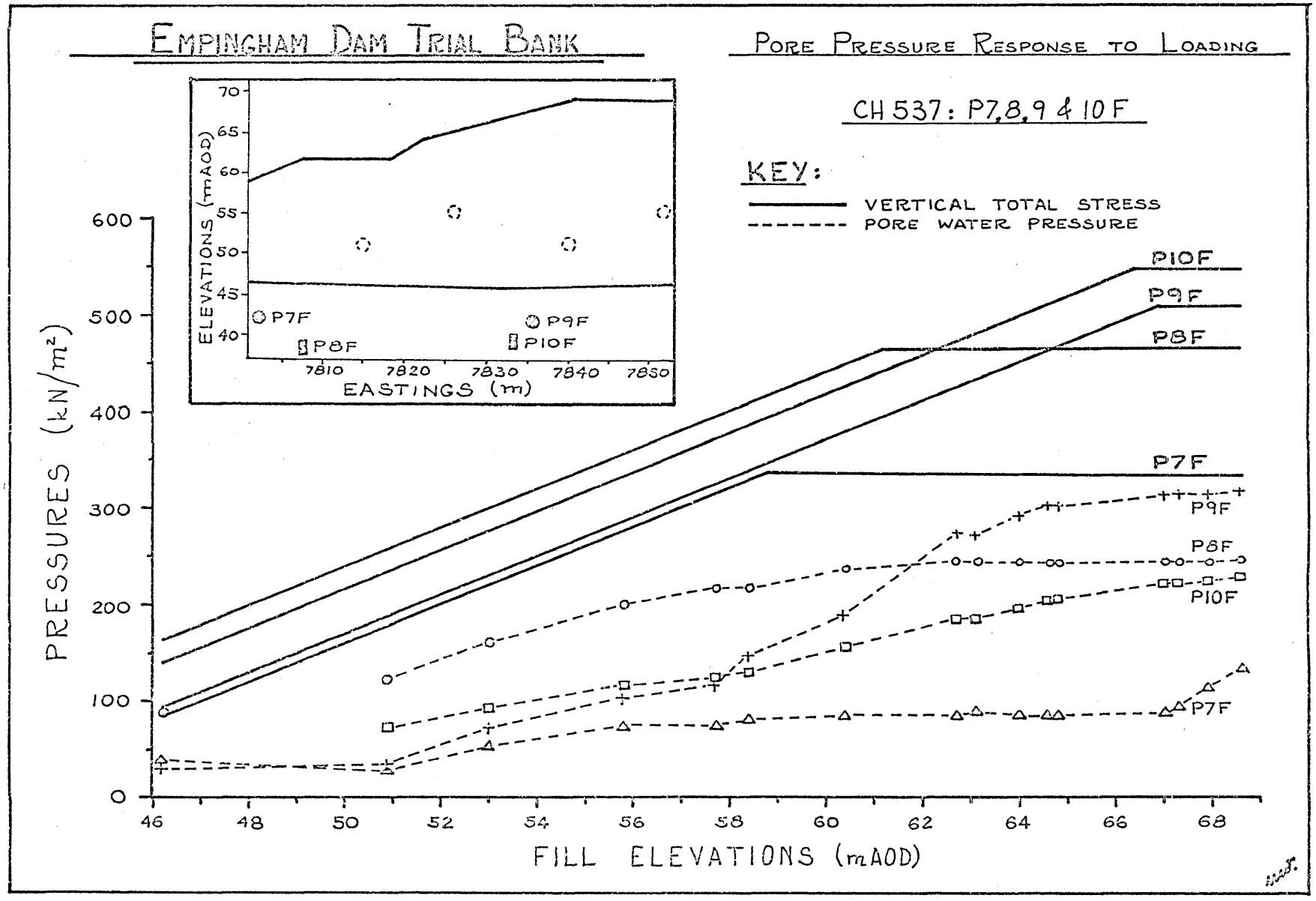


FIG. 6.129

FIG. 6.129

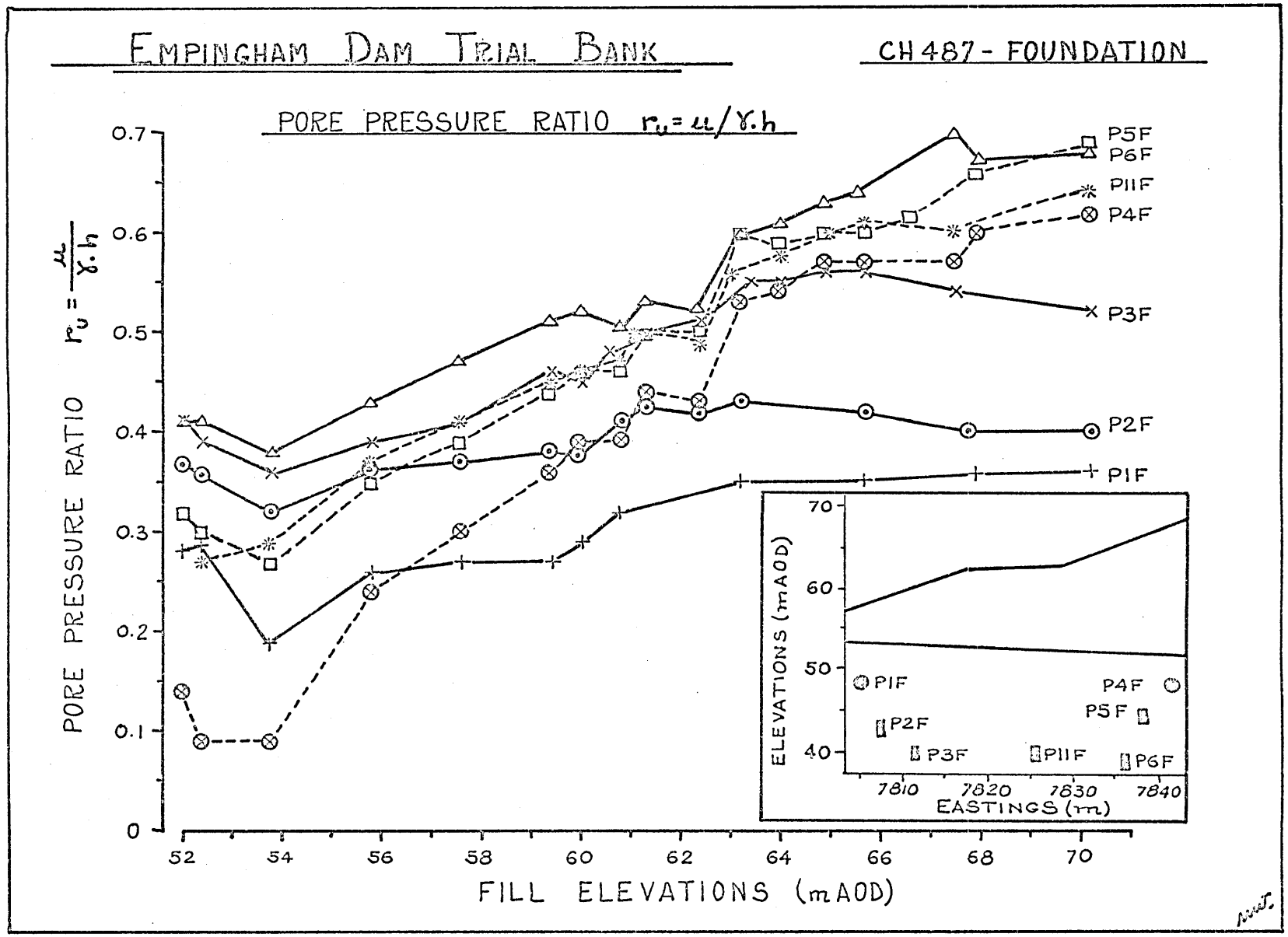


FIG. 6.130

FIG. 6.130

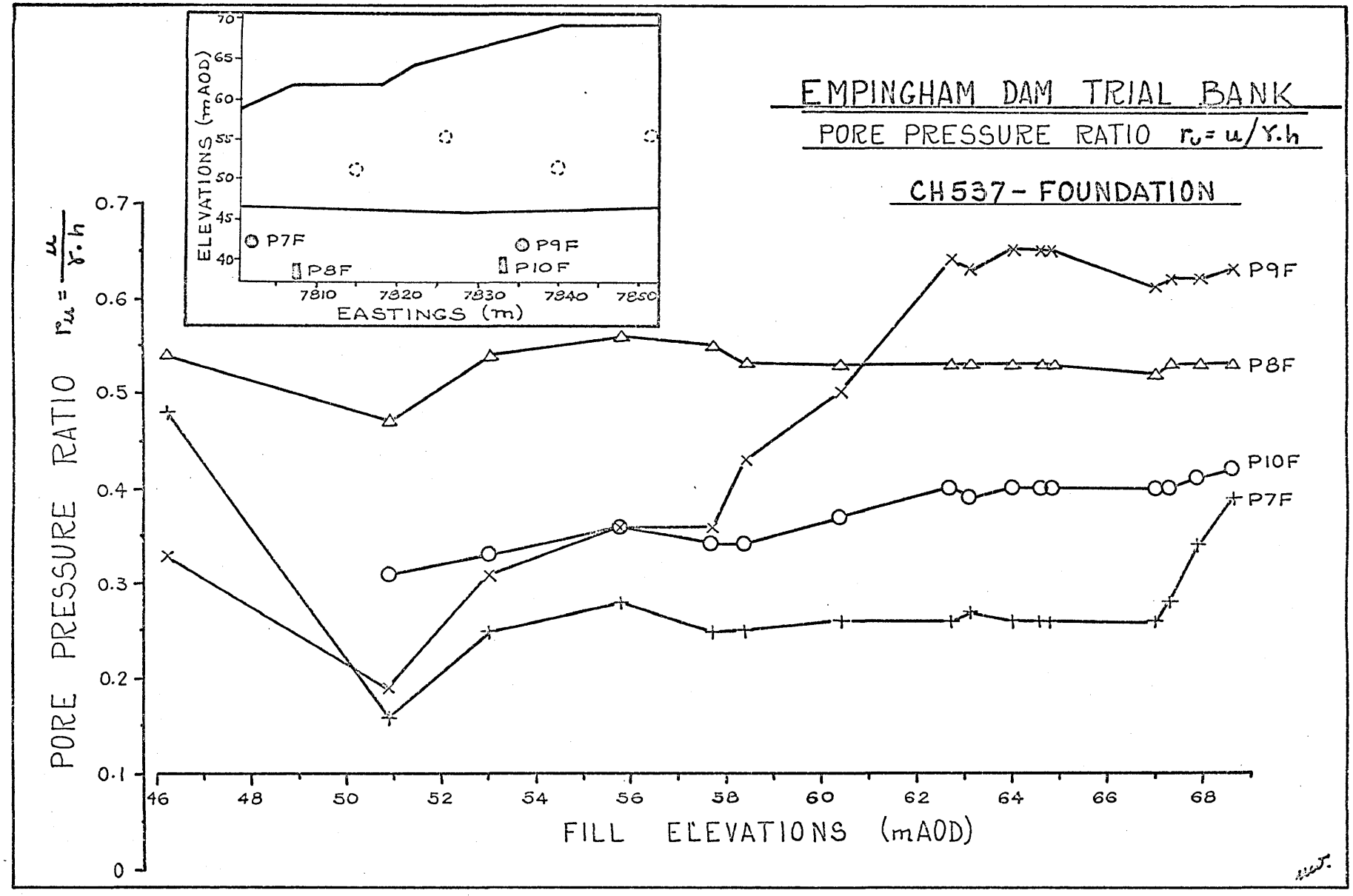


FIG. 6.131

FIG. 6.131

EMPINGHAM DAM TRIAL BANK

PIEZOMETRIC RECORDS - PIEZOS. IN THE FILL: P1, 2, 3 and 4 B

CH 537

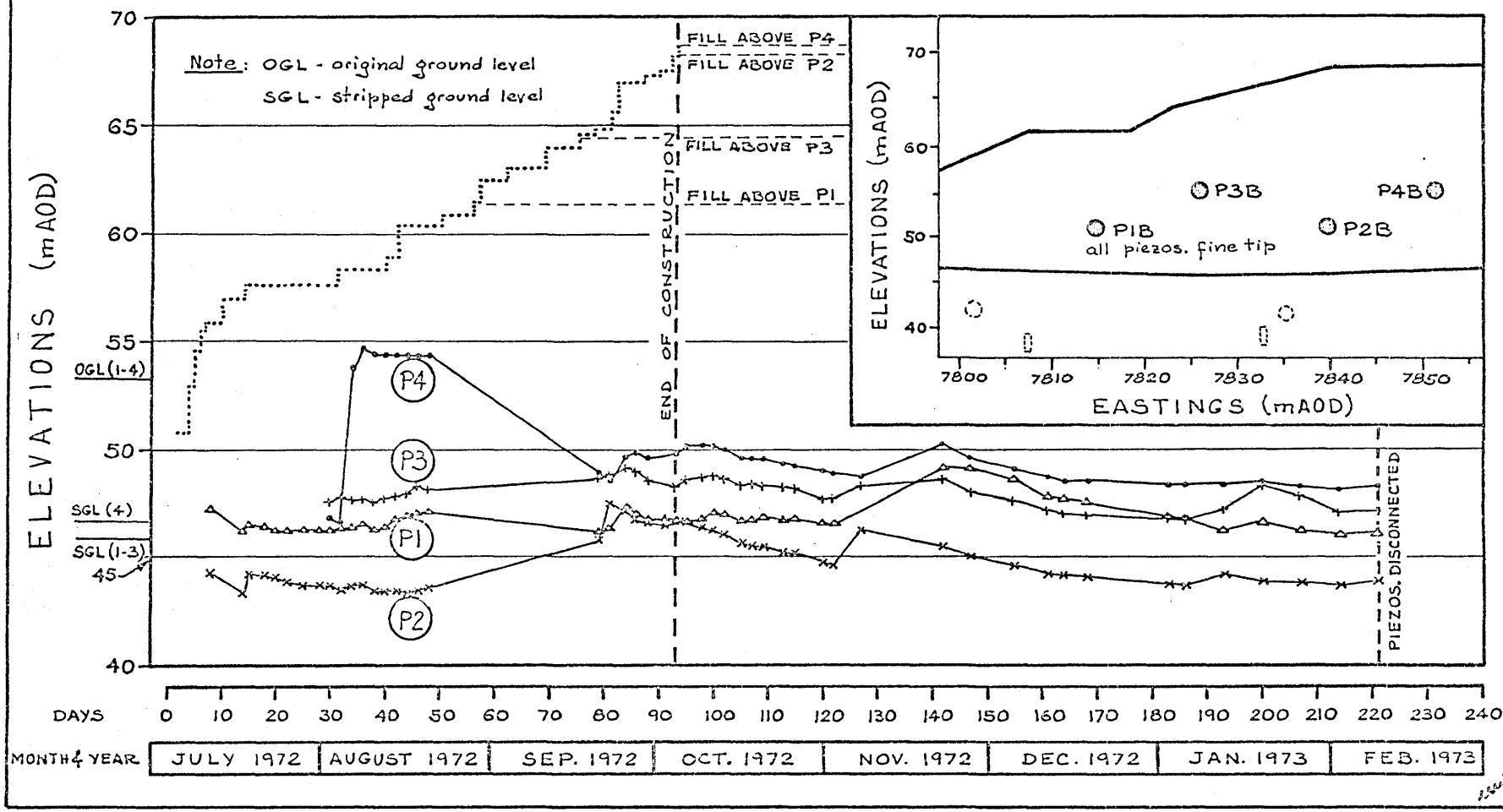


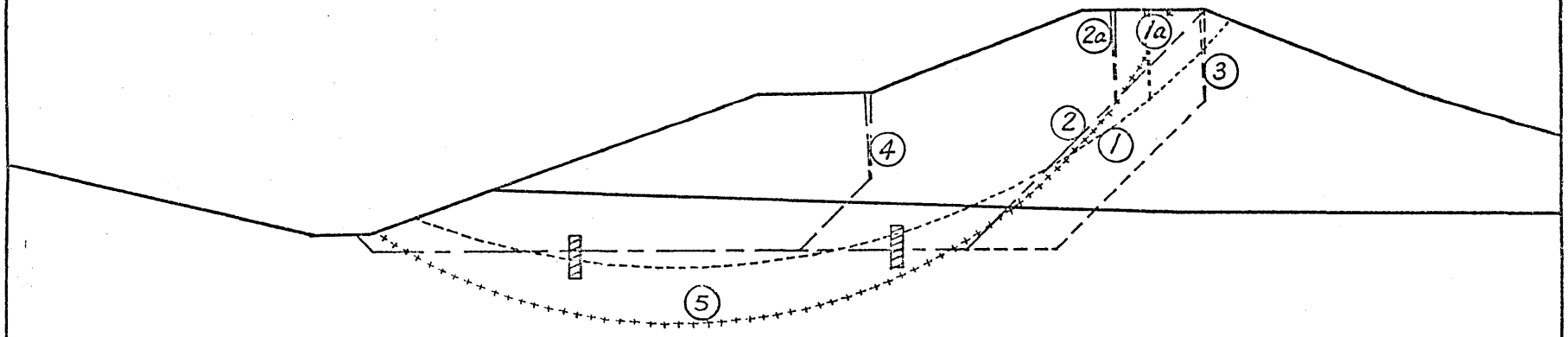
FIG. 6.132

FIG. 6.132

EMPINGHAM DAM TRIAL BANK

$\phi = 0$ STABILITY ANALYSIS

Ch. 487



CURVE	METHOD	Av. MOBILIZED τ_f (kN/m^2)	
		$\tau_b = \tau_f$	$\tau_b = 80\ kN/m^2$
1	slices	44	24
1a	slices	43	30
2	wedge	43	22
2a	wedge	44	35
3	wedge	43	28
4	wedge	25	20

ZONES OF OBSERVED MAXIMUM SHEAR STRAINS

τ_b AVERAGE MOBILIZED SHEAR STRESS (fill)

τ_f AVERAGE MOBILIZED SHEAR STRESS (foundation)

0 10 20

SCALE (m)

(5) critical slip circle for $F_S = 1.0$, $\phi = 0$, $(c_u)_{found}\ (kN/m^2) = 20 + 2.3\,z(m)$, $(c_u)_{fill}\ (kN/m^2) = 43 + 1.9\,h(m)$, and also for $c' = 0$, $(c_u)_{fill}\ (kN/m^2) = 64 + 2.86\,h(m)$, $\phi' = 11.5°$, $F_S = 1.0$ (Bishop)

nwr.

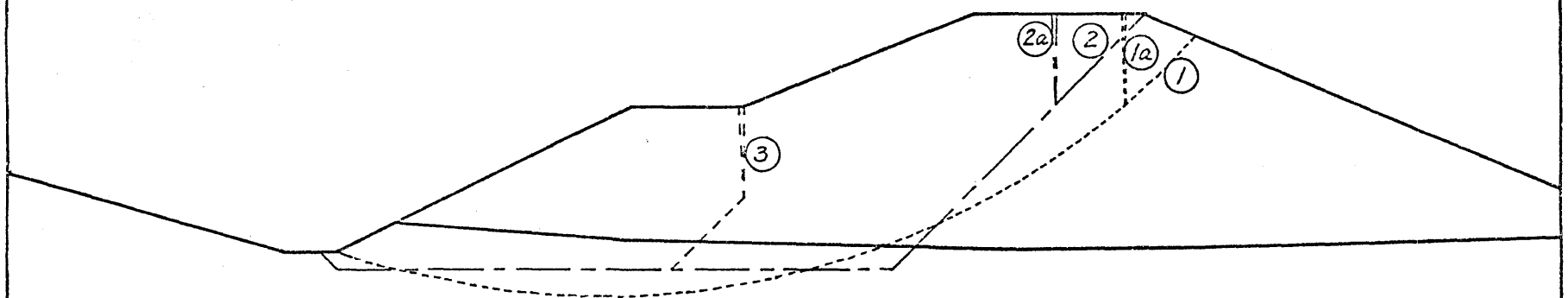
FIG. 7.1

FIG. 7.1

EMPINGHAM DAM TRIAL BANK

$\phi = 0$ STABILITY ANALYSIS

Ch. 514



CURVE	METHOD	Av. MOBILIZED τ_f (kN/m²)	
		$\tau_b = \tau_f$	$\tau_b = 80$ kN/m²
1	slices	54	38
1a	slices	54	42
2	wedge	52	32
2a	wedge	53	37
3	wedge	33	22

τ_b AVERAGE MOBILIZED SHEAR STRESS (fill)

τ_f AVERAGE MOBILIZED SHEAR STRESS (foundation)

0 10 20

SCALE (m)

mvr.

FIG. 7.2

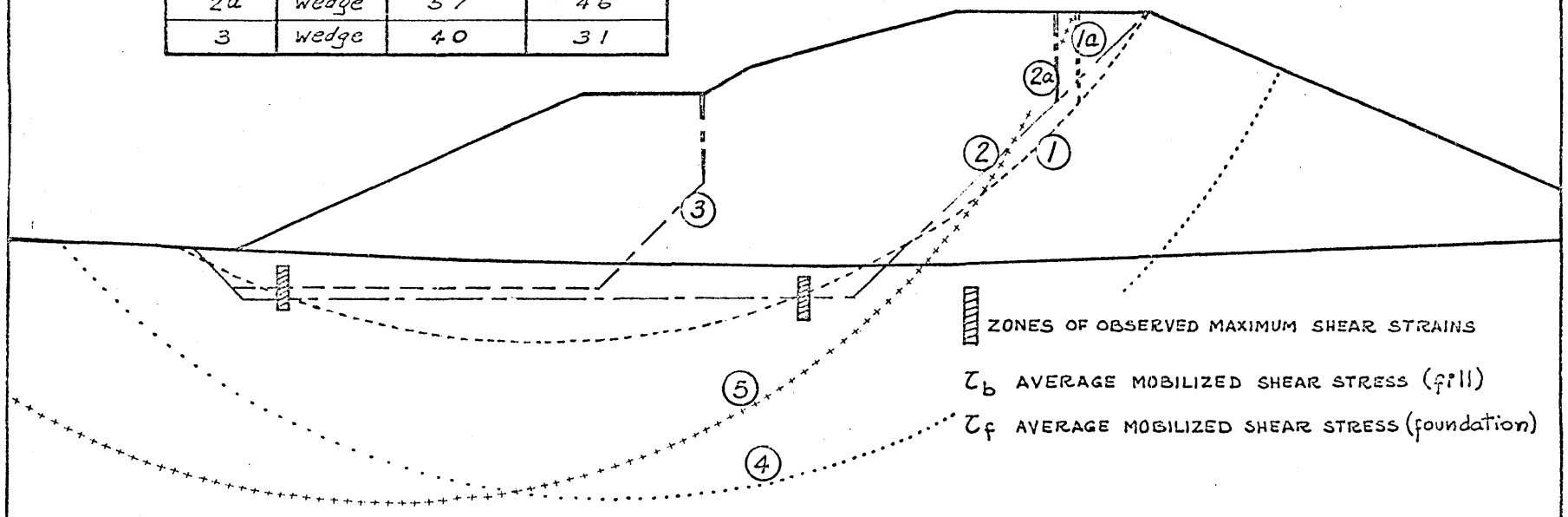
FIG. 7.2

EMPINGHAM DAM TRIAL BANK

ϕ=0 STABILITY ANALYSIS

Ch. 537

CURVE	METHOD	AVERAGE MOBILIZ. τ_f (kN/m²)	
		$\tau_b = \tau_f$	$\tau_b = 80$ kN/m²
1	slices	52	36
1a	slices	54	45
2	wedge	56	40
2a	wedge	57	46
3	wedge	40	31



④ critical circular slip surface for $\phi = 0$, $(c_u)_{found}$ (kN/m²) = 23 + 2.7 z (m), $(c_u)_{fill}$ (kN/m²) = = 50 + 2.2 h (m), $F_s = 1.0$.

⑤ critical slip circle for $c' = 0$, $(r_u)_{found} = 0.5$, $\phi' = 13.5°$, $(c_u)_{fill}$ (kN/m²) = 64 + + 2.86 h (m), $F_s = 1.0$ (Bishop)

0 10 20
SCALE (m)

FIG. 7.3

FIG. 7.3

EMPINGHAM DAM TRIAL BANK

STABILITY ANALYSIS IN TERMS OF EFFECTIVE STRESSES

CH. 487

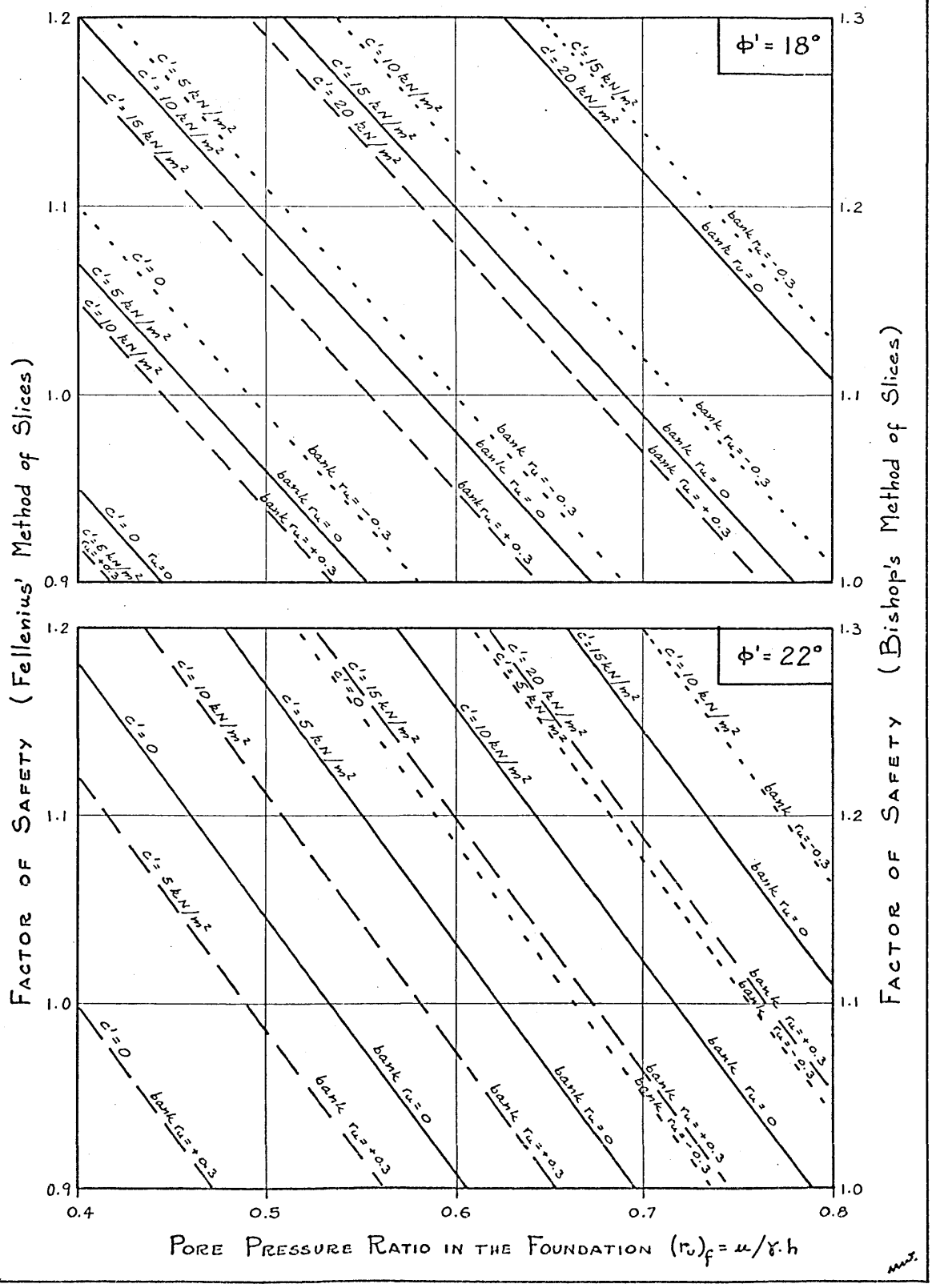


FIG. 7.4

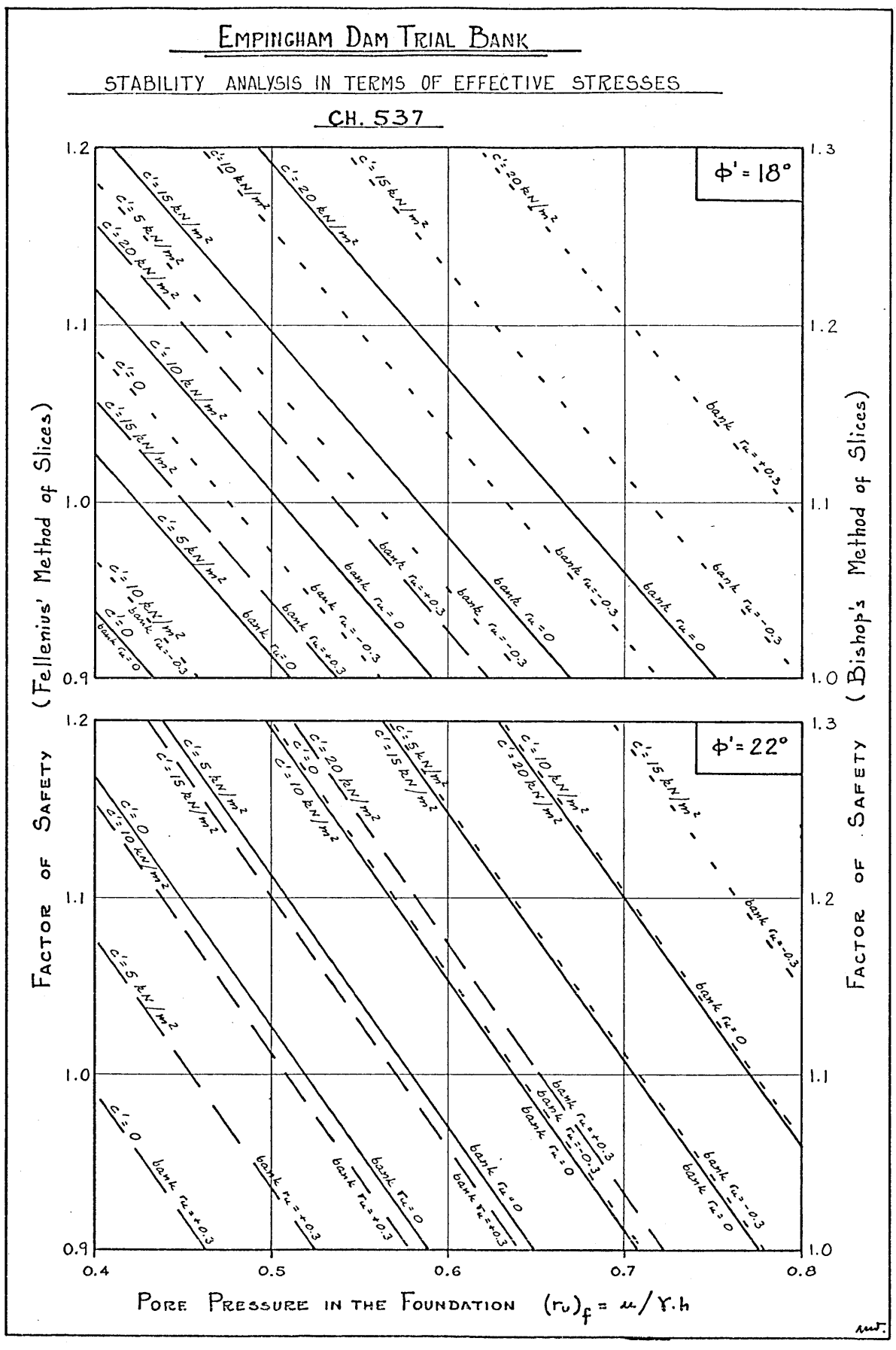
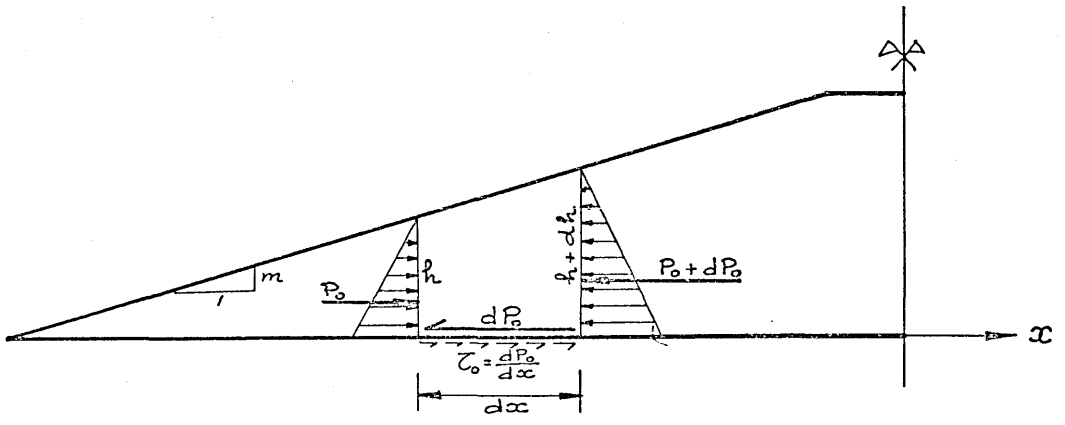

EMPINGHAM DAM TRIAL BANK
STABILITY ANALYSIS IN TERMS OF EFFECTIVE STRESSES
CH. 537
φ' = 18°
φ' = 22°
FACTOR OF SAFETY (Fellenius' Method of Slices)
FACTOR OF SAFETY (Bishop's Method of Slices)
PORE PRESSURE IN THE FOUNDATION (ru)f = u/γ.h
1.2
1.1
1.0
0.9
1.3
1.2
1.1
1.0
0.4
0.5
0.6
0.7
0.8
c' = 10 kN/m²
c' = 15 kN/m²
c' = 20 kN/m²
c' = 5 kN/m²
c' = 0
bank ru = +0.3
bank ru = 0
bank ru = -0.3

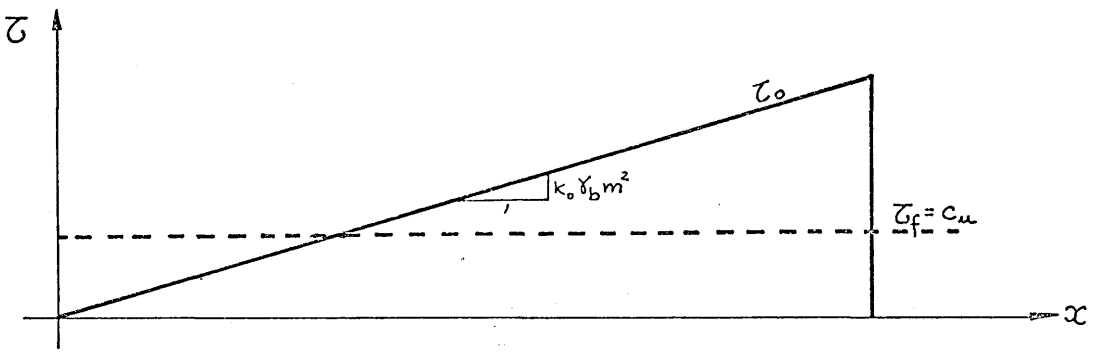
FIG. 7.5

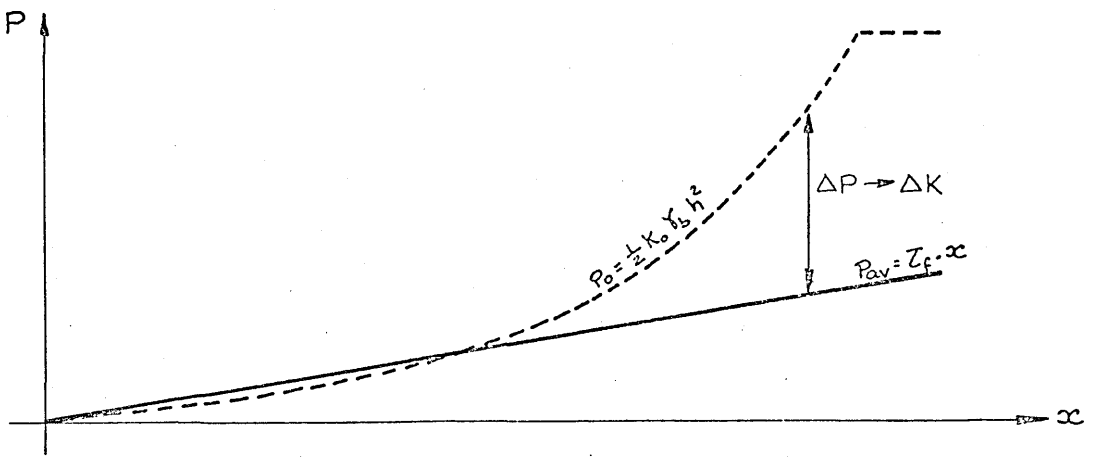
SIMPLE APPROXIMATE DEFORMATION ANALYSIS

PRINCIPAL FEATURES



$P_o=\frac{1}{2}K_o\gamma_b h^2=\frac{1}{2}K_o\gamma_b m^2x^2$ $\quad dP_o=K_o\gamma_b h\,dh=K_o\gamma_b m^2x\,dx$ $\quad \tau_o=\frac{dP_o}{dx}=K_o\gamma_b h m=K_o\gamma_b m^2x$





Linear Isotropic Elasticity (Plane Strain): $(\epsilon_z)_b=\frac{\Delta K}{E_b}(1-\nu_b^2)\gamma_b h=\frac{\Delta K}{E_b}(1-\nu_b^2)\gamma_b m x$

FIG. 7.6

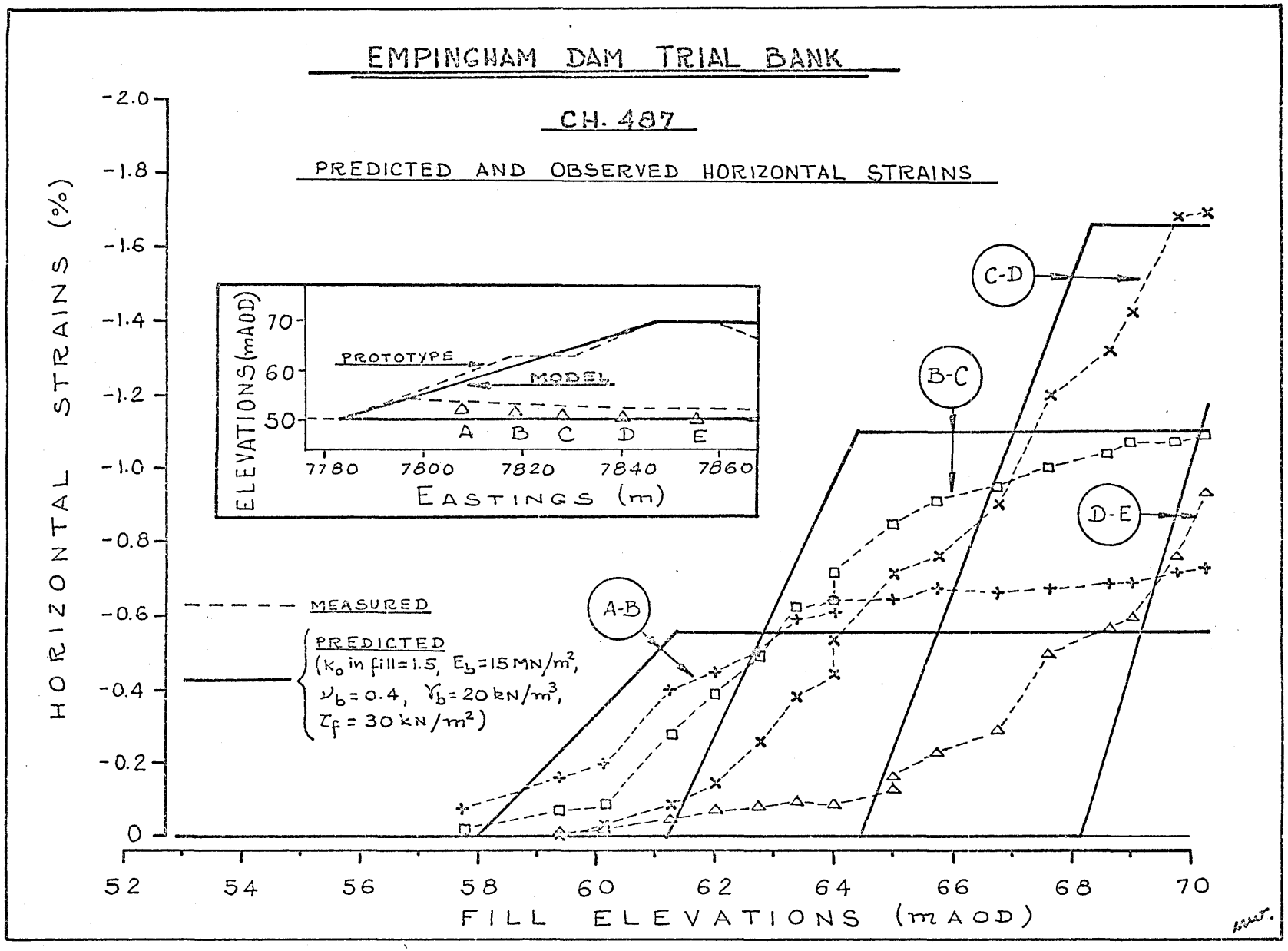

EMPINGHAM DAM TRIAL BANK
CH. 487
PREDICTED AND OBSERVED HORIZONTAL STRAINS
HORIZONTAL STRAINS (%)
-2.0
-1.8
-1.6
-1.4
-1.2
-1.0
-0.8
-0.6
-0.4
-0.2
0
52
54
56
58
60
62
64
66
68
70
FILL ELEVATIONS (mAOD)
ELEVATIONS (mAOD)
70
60
50
PROTOTYPE
MODEL
A
B
C
D
E
7780
7800
7820
7840
7860
EASTINGS (m)
A-B
B-C
C-D
D-E
MEASURED
PREDICTED
(K_o in fill = 1.5, E_b = 15 MN/m², ν_b = 0.4, γ_b = 20 kN/m³, τ_f = 30 kN/m²)

FIG. 7.7

FIG. 7.7

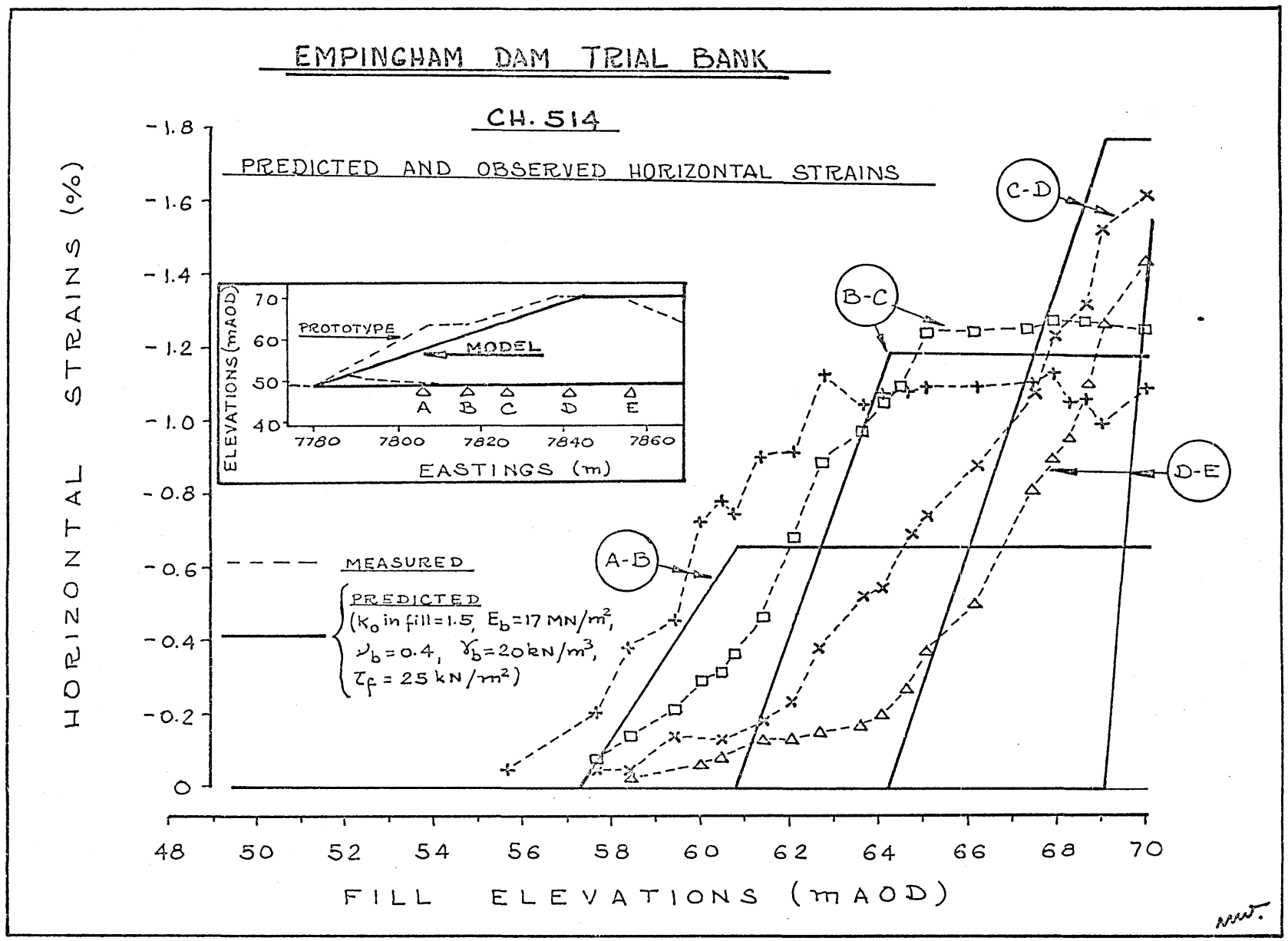

EMPINGHAM DAM TRIAL BANK
CH. 514
PREDICTED AND OBSERVED HORIZONTAL STRAINS
HORIZONTAL STRAINS (%)
-1.8
-1.6
-1.4
-1.2
-1.0
-0.8
-0.6
-0.4
-0.2
0
ELEVATIONS (mAOD)
70
60
50
40
PROTOTYPE
MODEL
A
B
C
D
E
7780
7800
7820
7840
7860
EASTINGS (m)
C-D
B-C
D-E
A-B
MEASURED
PREDICTED
(K_o in fill = 1.5, E_b = 17 MN/m^2,
ν_b = 0.4, γ_b = 20 kN/m^3,
τ_f = 25 kN/m^2)
48
50
52
54
56
58
60
62
64
66
68
70
FILL ELEVATIONS (mAOD)
MMT.

FIG. 7.8

FIG. 7.8

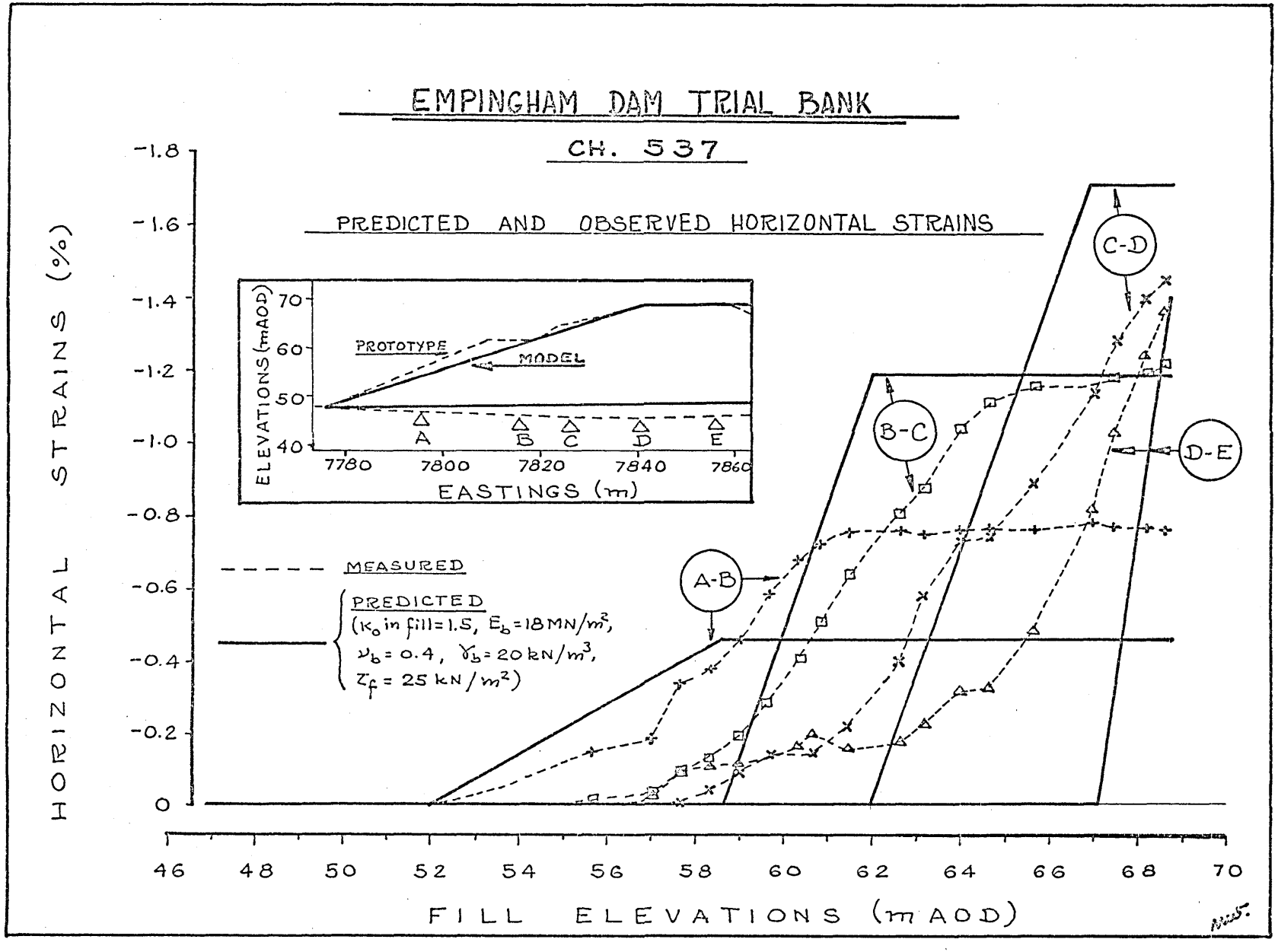

EMPINGHAM DAM TRIAL BANK
CH. 537
PREDICTED AND OBSERVED HORIZONTAL STRAINS
HORIZONTAL STRAINS (%)
-1.8
-1.6
-1.4
-1.2
-1.0
-0.8
-0.6
-0.4
-0.2
0
ELEVATIONS (mAOD)
70
60
50
40
PROTOTYPE
MODEL
A
B
C
D
E
7780
7800
7820
7840
7860
EASTINGS (m)
A-B
B-C
C-D
D-E
MEASURED
PREDICTED
(K_o in fill = 1.5, E_b = 18 MN/m², ν_b = 0.4, γ_b = 20 kN/m³, τ_f = 25 kN/m²)
46
48
50
52
54
56
58
60
62
64
66
68
70
FILL ELEVATIONS (m AOD)

FIG. 7.9

FIG. 7.9

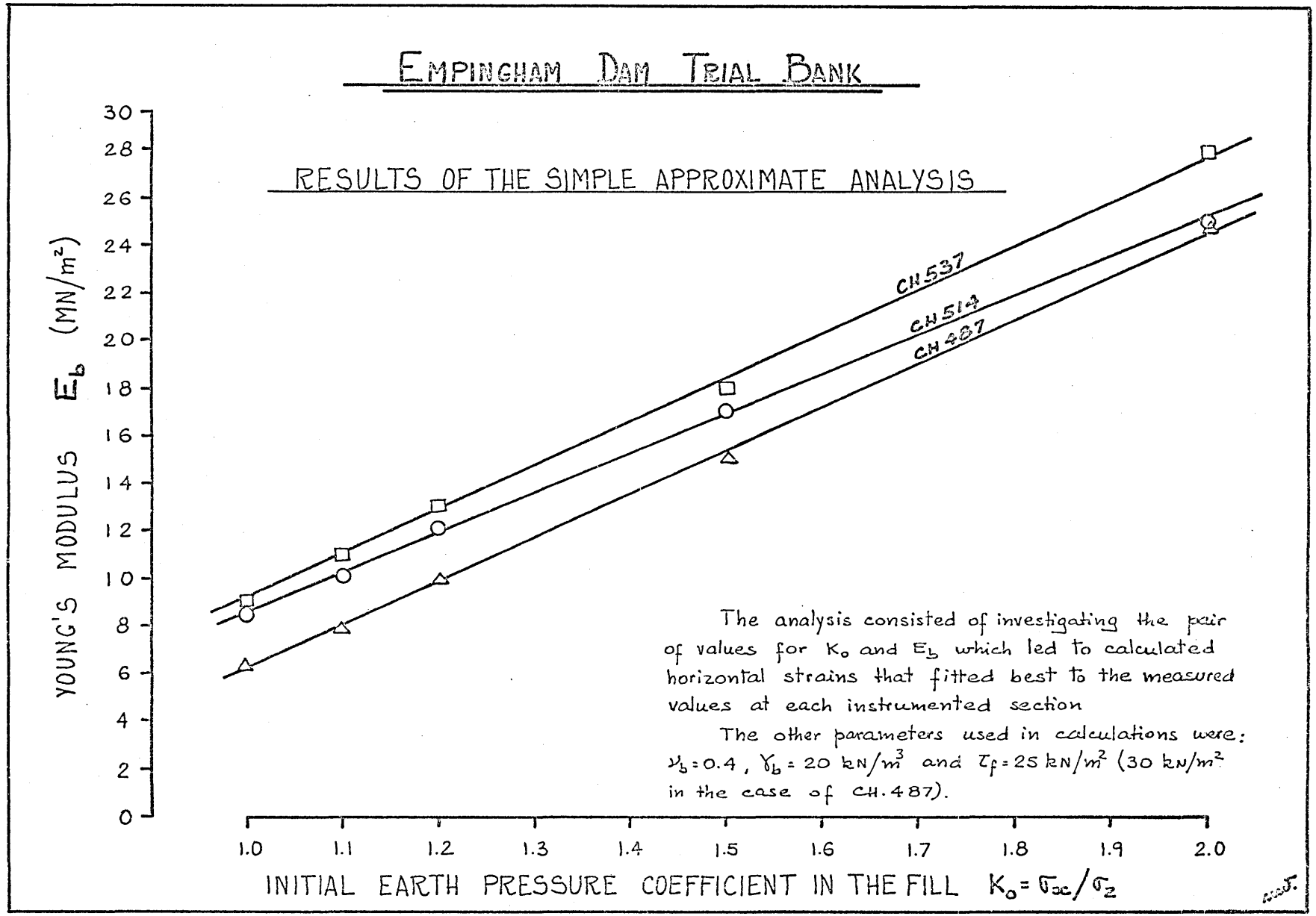


FIG. 7.10

FIG. 7.10

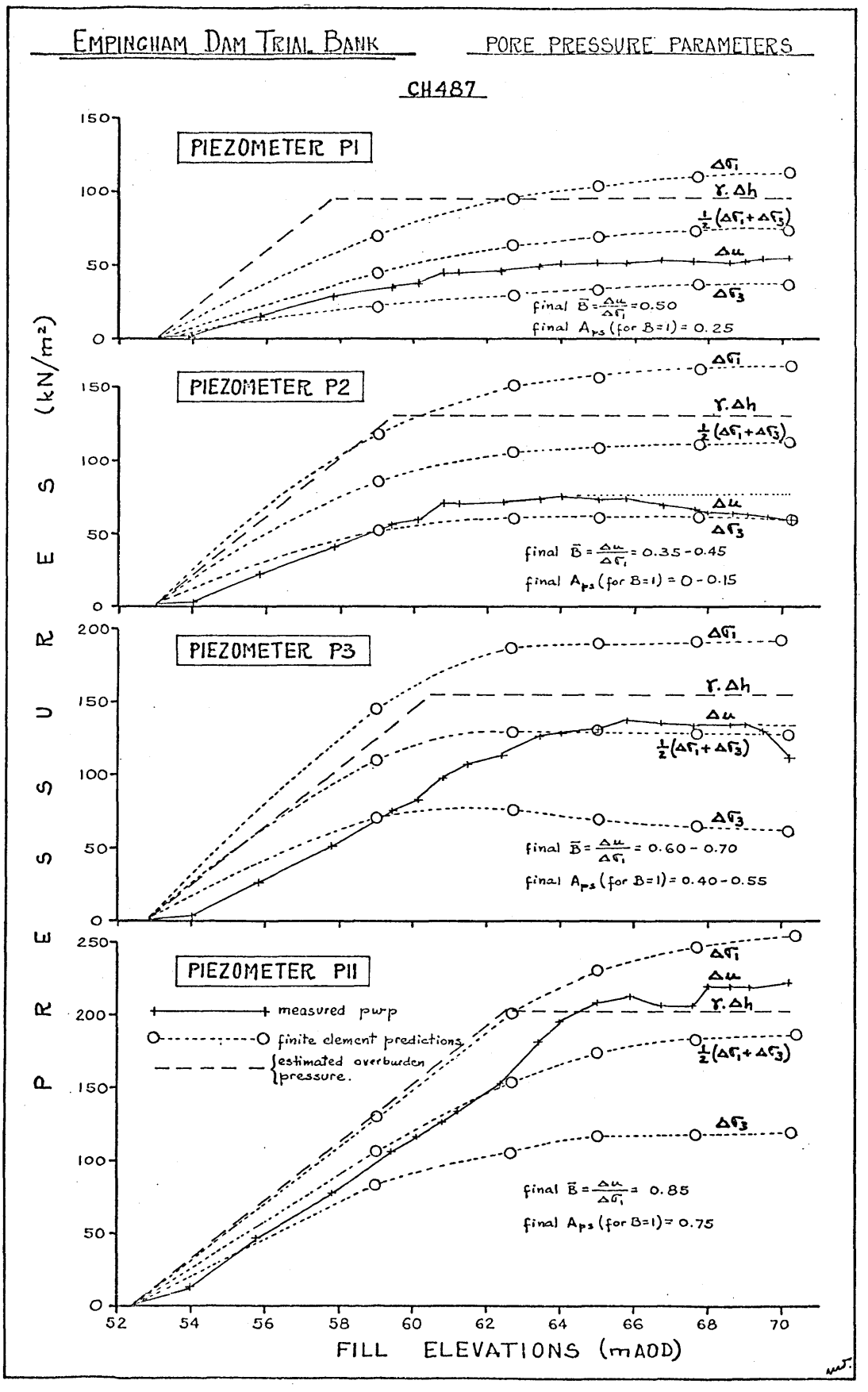

EMPINGHAM DAM TRIAL BANK
PORE PRESSURE PARAMETERS
CH487
PIEZOMETER P1
PIEZOMETER P2
PIEZOMETER P3
PIEZOMETER P11
PRESSURES (kN/m²)
FILL ELEVATIONS (mAOD)
Δσ1
γ.Δh
½(Δσ1+Δσ3)
Δu
Δσ3
final B̄ = Δu/Δσ1 = 0.50
final Aps (for B=1) = 0.25
final B̄ = Δu/Δσ1 = 0.35 - 0.45
final Aps (for B=1) = 0 - 0.15
final B̄ = Δu/Δσ1 = 0.60 - 0.70
final Aps (for B=1) = 0.40 - 0.55
final B̄ = Δu/Δσ1 = 0.85
final Aps (for B=1) = 0.75
measured pwp
finite element predictions
estimated overburden pressure.

FIG. 7.11

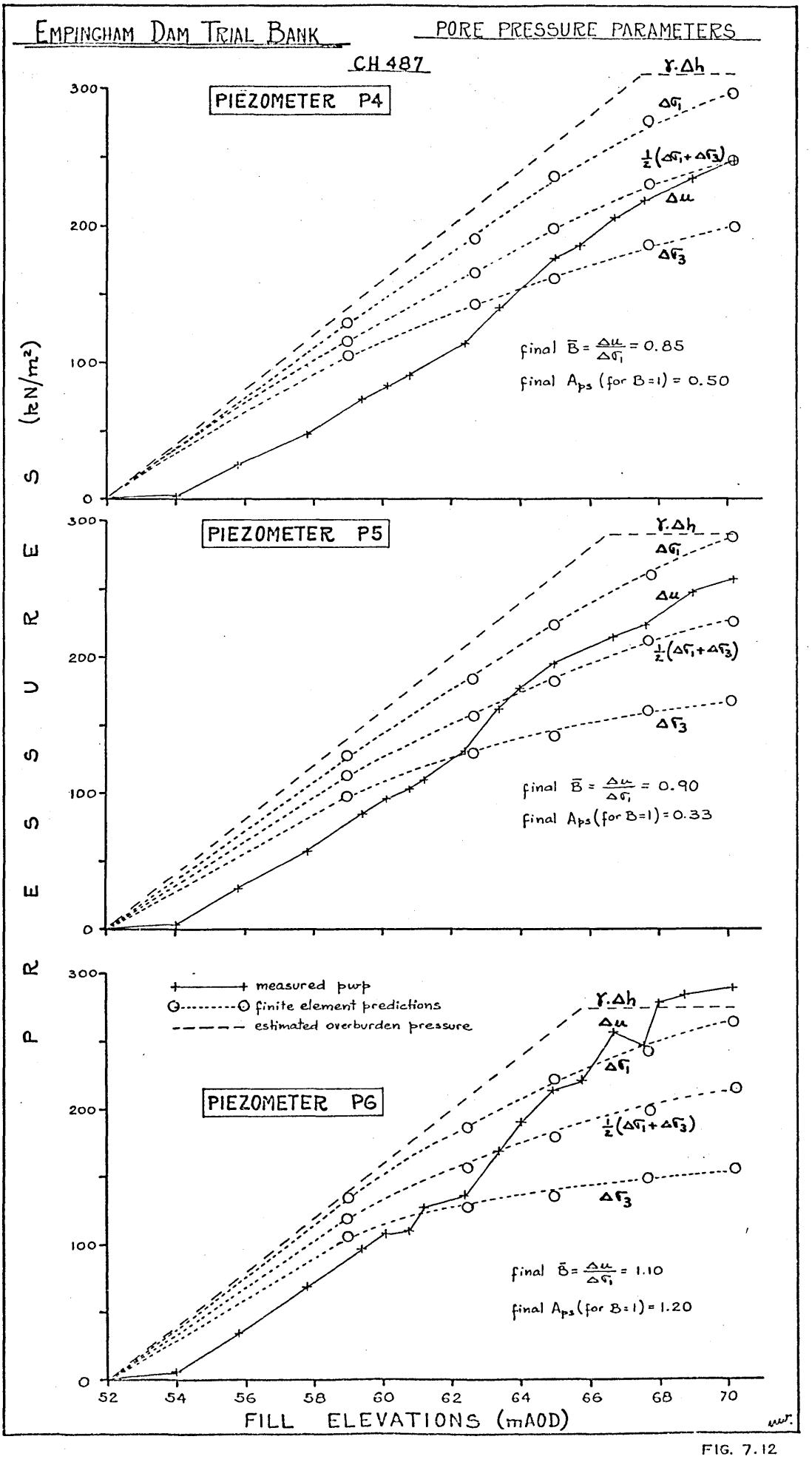

EMPINGHAM DAM TRIAL BANK
PORE PRESSURE PARAMETERS
CH 487
PIEZOMETER P4
PIEZOMETER P5
PIEZOMETER P6
γ.Δh
Δσ1
½(Δσ1+Δσ3)
Δu
Δσ3
final B̄ = Δu/Δσ1 = 0.85
final Aps (for B=1) = 0.50
final B̄ = Δu/Δσ1 = 0.90
final Aps (for B=1) = 0.33
final B̄ = Δu/Δσ1 = 1.10
final Aps (for B=1) = 1.20
measured pwp
finite element predictions
estimated overburden pressure
PRESSURES (kN/m²)
0
100
200
300
52
54
56
58
60
62
64
66
68
70
FILL ELEVATIONS (mAOD)

FIG. 7.12

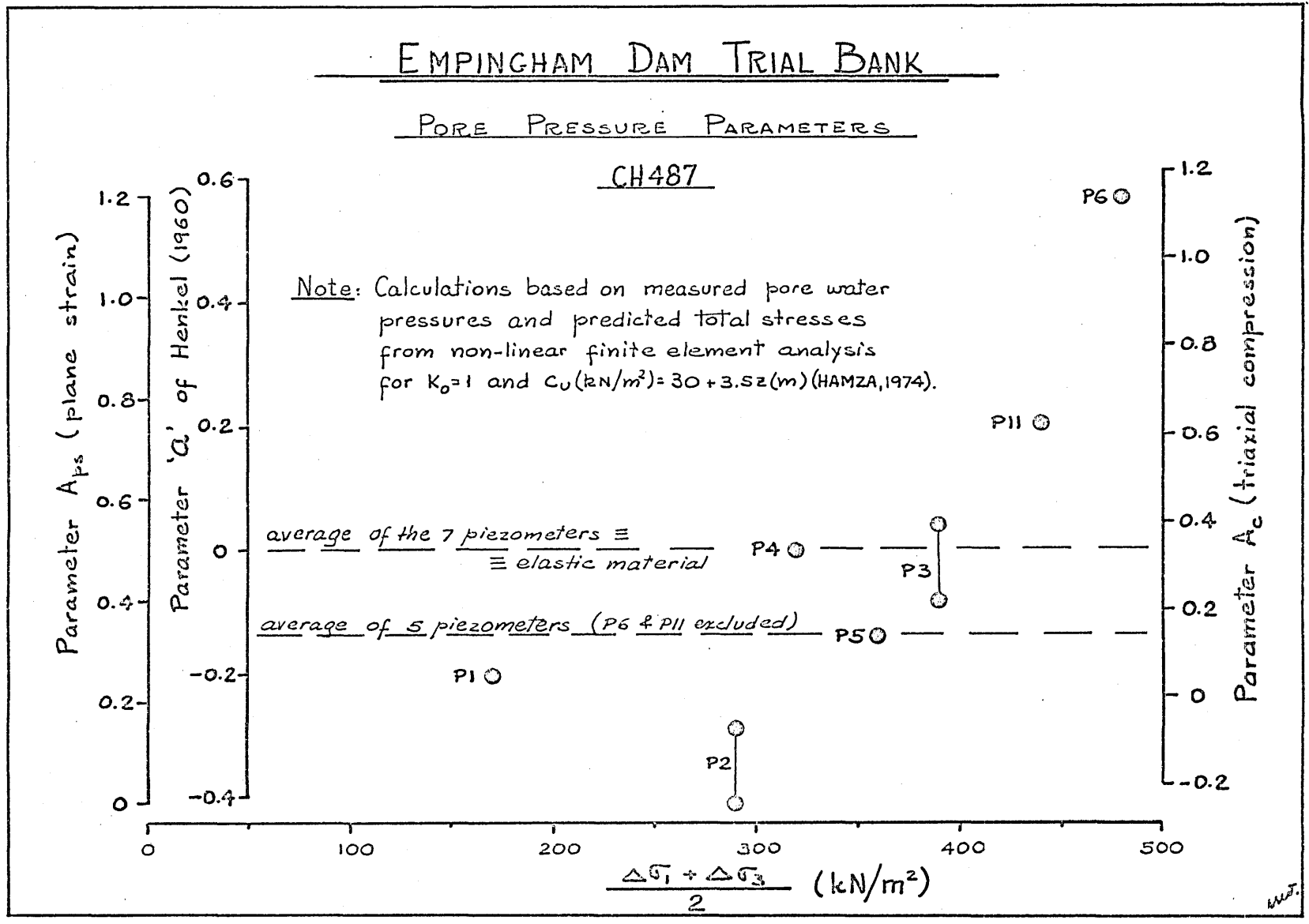
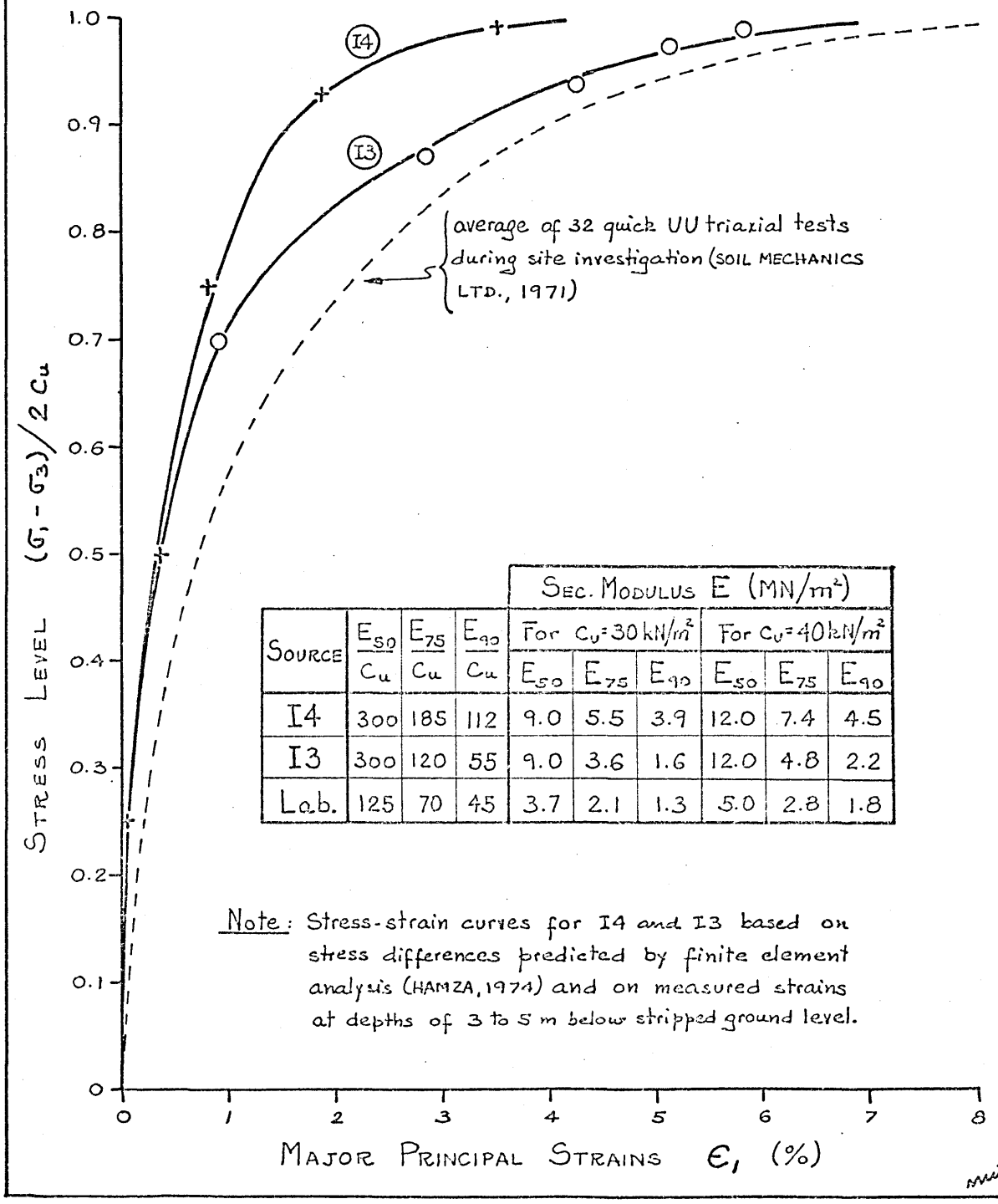


FIG. 7.13

FIG. 7.13

EMPINGHAM DAM TRIAL BANK

STRESS-STRAIN CURVES



SOURCE	$\frac{E_{50}}{C_u}$	$\frac{E_{75}}{C_u}$	$\frac{E_{90}}{C_u}$	SEC. MODULUS E (MN/m^2) For C_u=30 kN/m²			For C_u=40 kN/m²		
				E_{50}	E_{75}	E_{90}	E_{50}	E_{75}	E_{90}
I4	300	185	112	9.0	5.5	3.9	12.0	7.4	4.5
I3	300	120	55	9.0	3.6	1.6	12.0	4.8	2.2
Lab.	125	70	45	3.7	2.1	1.3	5.0	2.8	1.8

Note: Stress-strain curves for I4 and I3 based on stress differences predicted by finite element analysis (HAMZA, 1974) and on measured strains at depths of 3 to 5 m below stripped ground level.

MMT.

FIG. 7.14

EMPINGHAM DAM TRIAL BANK

STRESS-STRAIN RELATIONSHIP

Kondner's Modified Plot

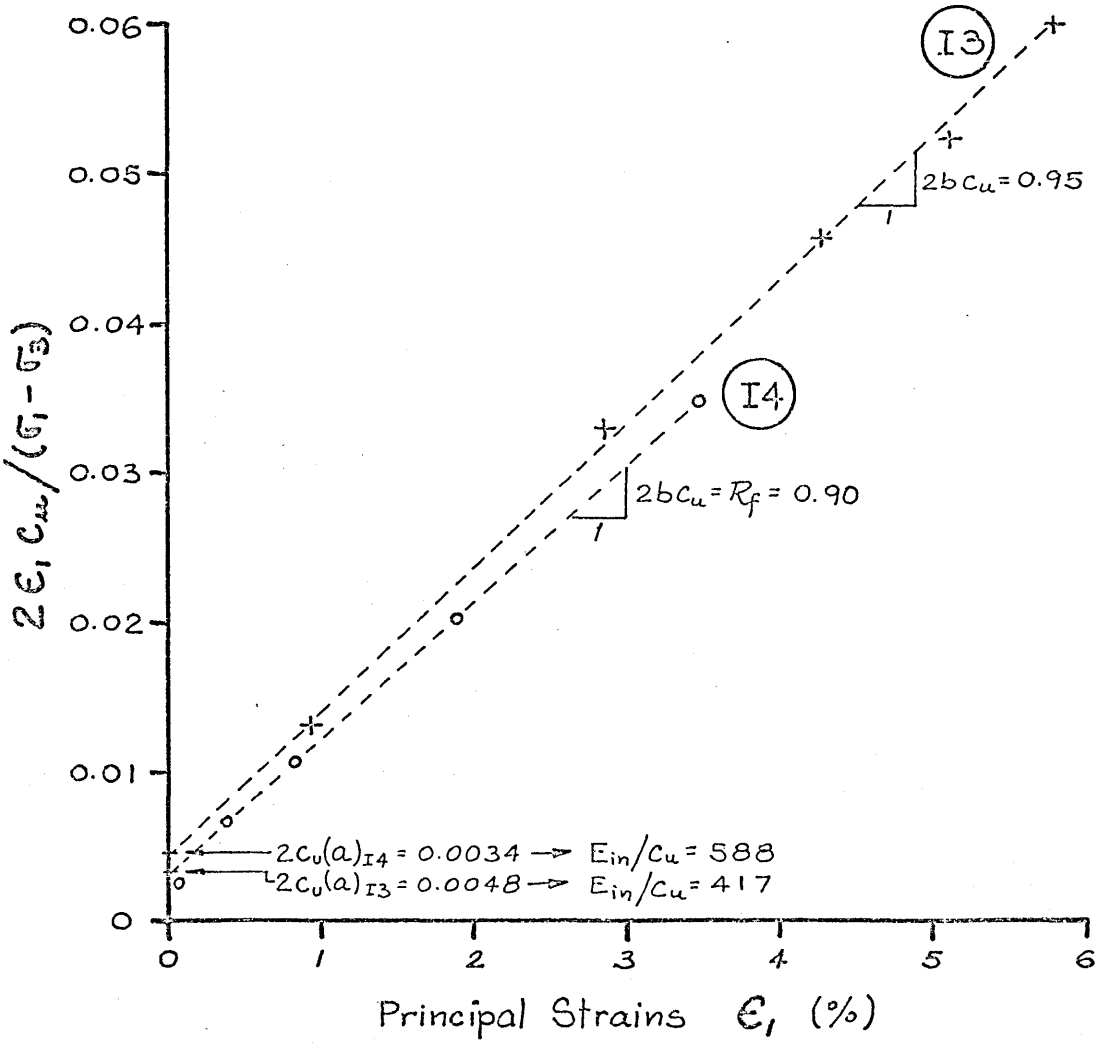


FIG. 7.15

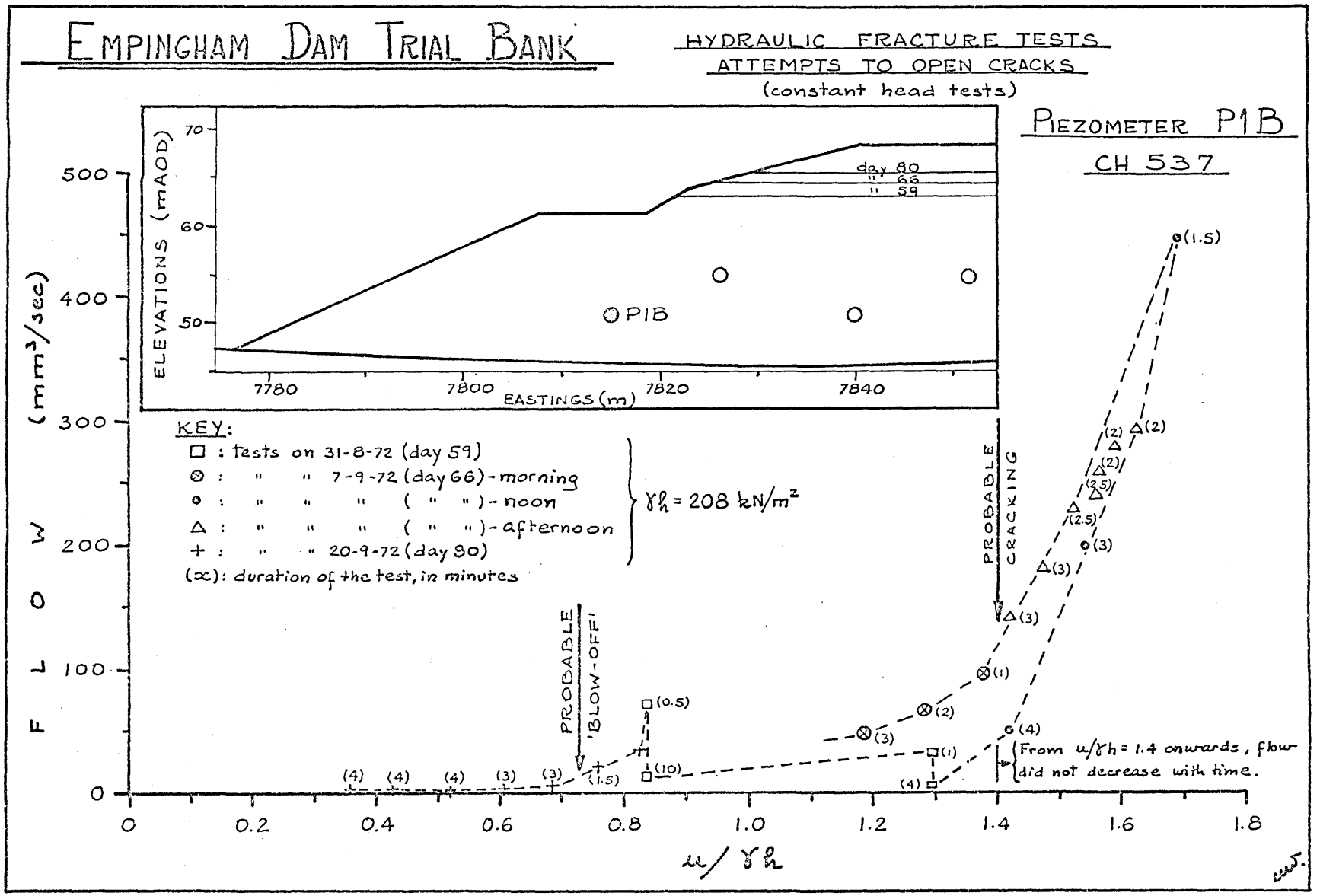

EMPINGHAM DAM TRIAL BANK
HYDRAULIC FRACTURE TESTS
ATTEMPTS TO OPEN CRACKS
(constant head tests)
PIEZOMETER P1B
CH 537
ELEVATIONS (mAOD)
70
60
50
day 80
" 66
" 59
P1B
7780
7800
7820
7840
EASTINGS (m)
KEY:
□ : tests on 31-8-72 (day 59)
⊗ : " " 7-9-72 (day 66) - morning
⊙ : " " " (" ") - noon
△ : " " " (" ") - afternoon
+ : " " 20-9-72 (day 80)
(∞): duration of the test, in minutes
γh = 208 kN/m²
FLOW (mm³/sec)
500
400
300
200
100
0
PROBABLE 'BLOW-OFF'
PROBABLE CRACKING
From u/γh = 1.4 onwards, flow did not decrease with time.
0
0.2
0.4
0.6
0.8
1.0
1.2
1.4
1.6
1.8
u/γh

FIG. 8.1

FIG. 8.1

EMPINGHAM DAM TRIAL BANK

HYDRAULIC FRACTURE TESTS

ATTEMPTS TO OPEN CRACKS

PIEZOMETER P2B-CH.537

(constant head tests)

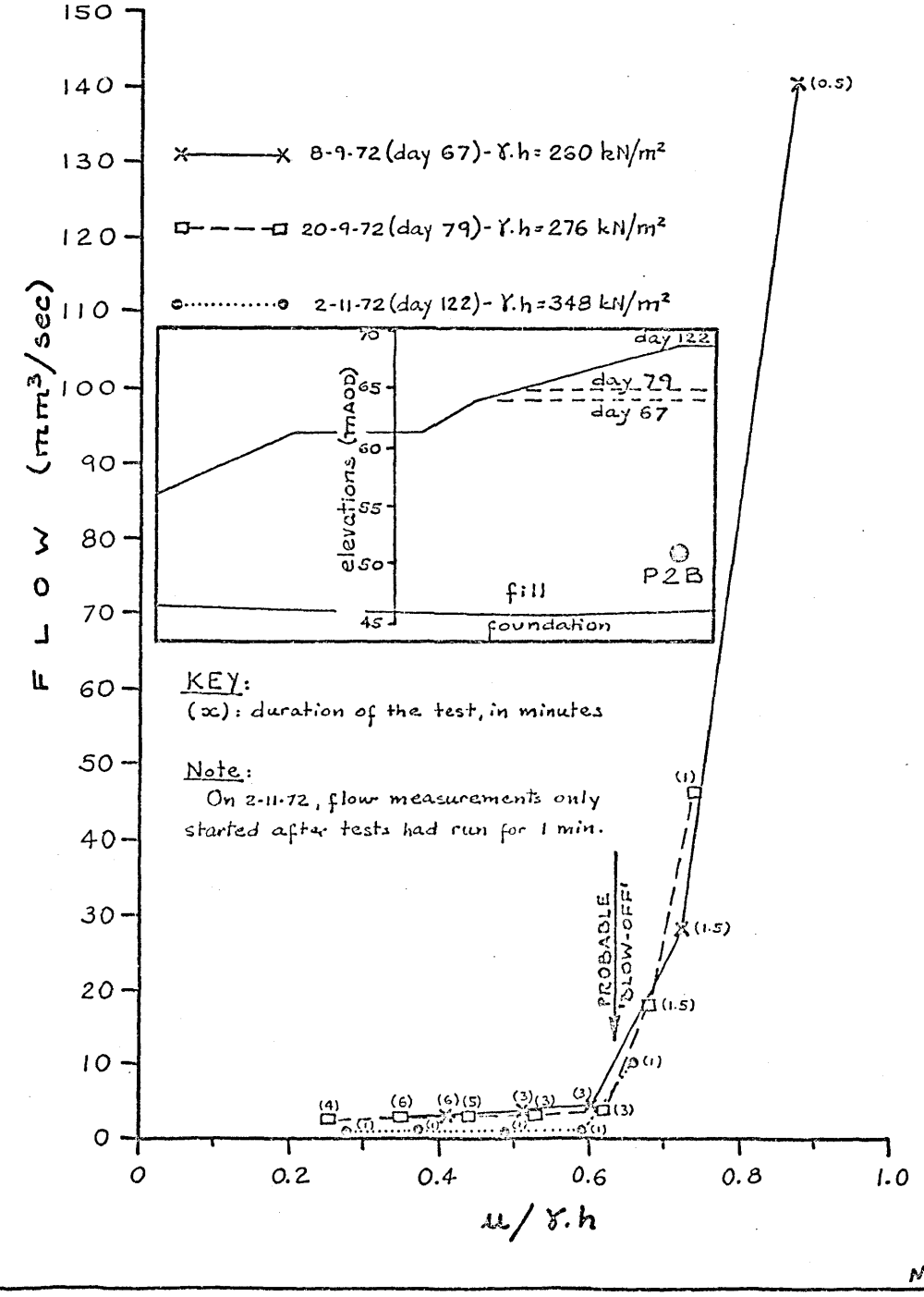


FIG. 8.2

EMPINGHAM DAM TRIAL BANK

HYDRAULIC FRACTURE TESTS

INCREASING CONSTANT HEAD AND FALLING HEAD STAGES

PIEZOMETER P3B

CH 537

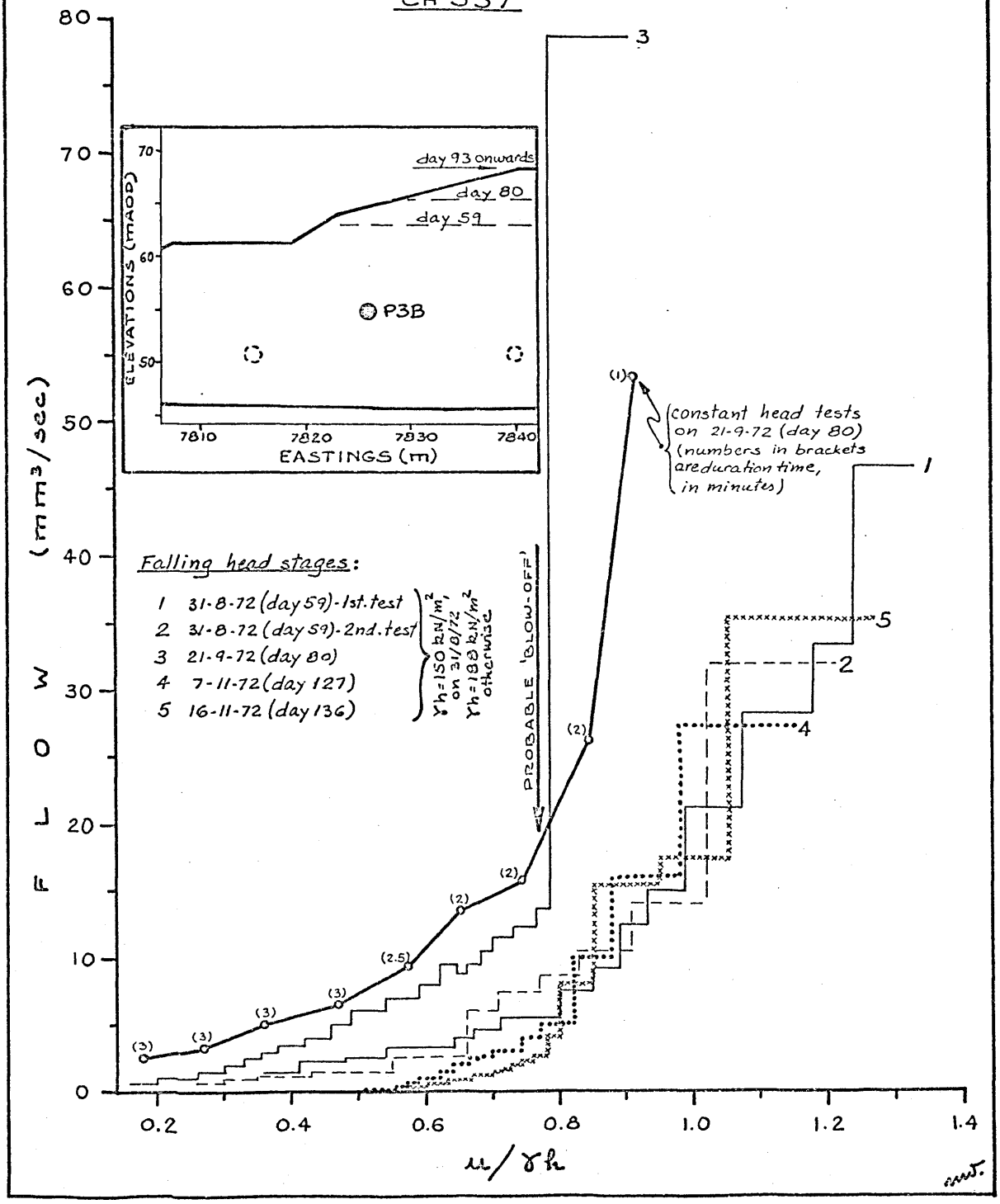


FIG. 8.3

EMPINGHAM DAM TRIAL BANK

HYDRAULIC FRACTURE TESTS ~ FALLING HEAD STAGES

PIEZOMETER PIB

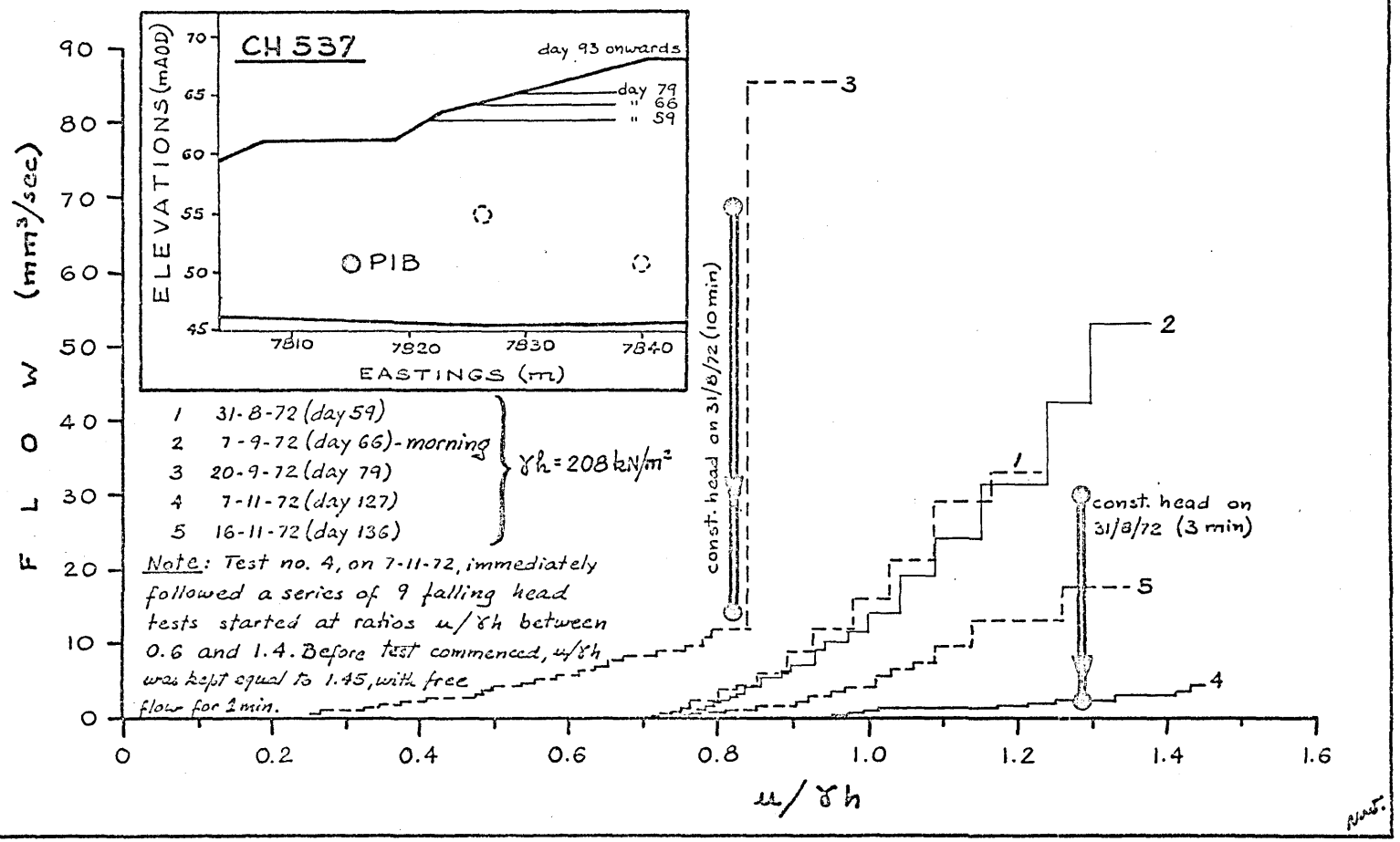


FIG. 8.4

EMPINGHAM DAM TRIAL BANK

HYDRAULIC FRACTURE TESTS

FALLING HEAD STAGES

PIEZOMETER P2B-CH537

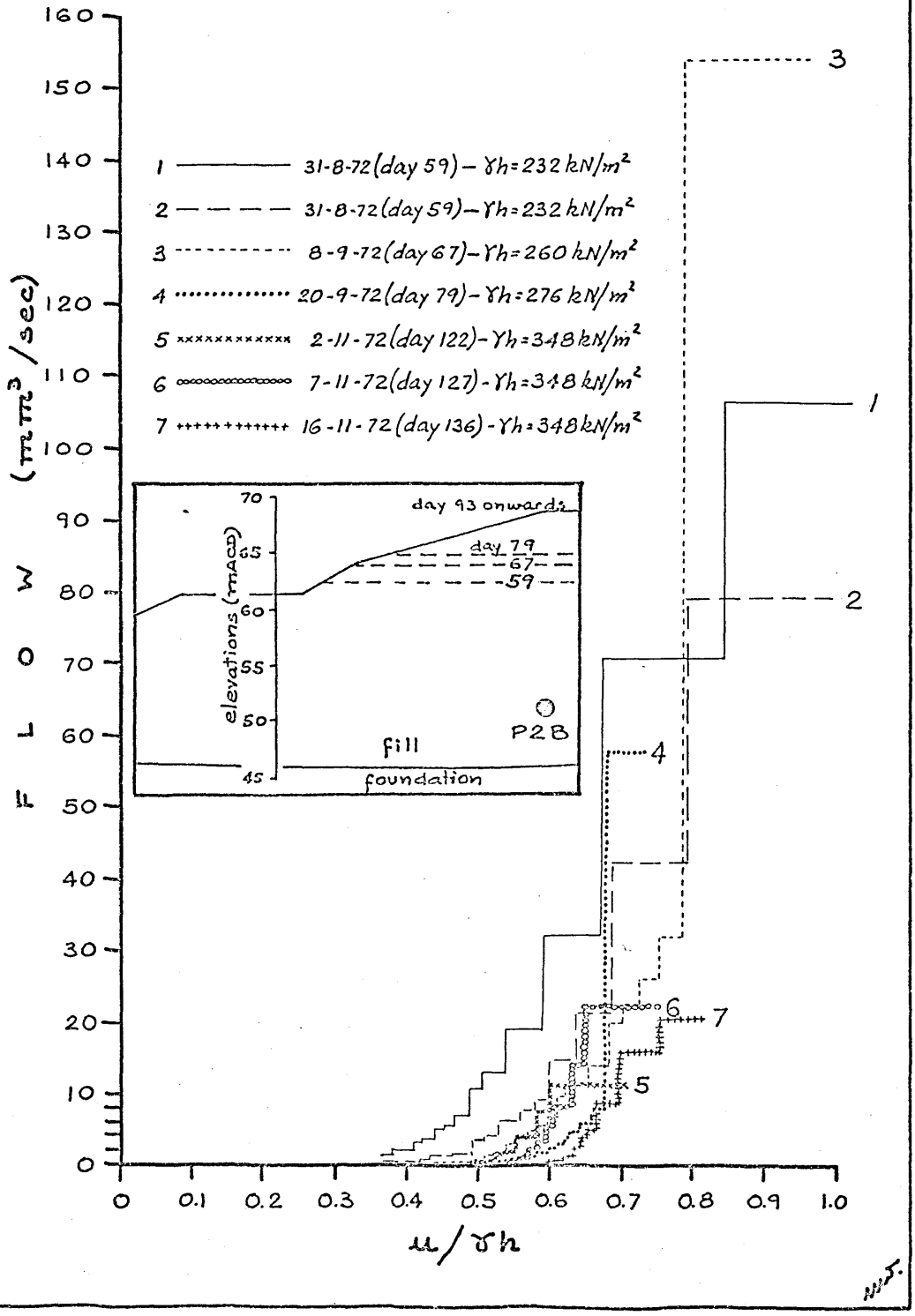


FIG. 8.5

EMPINGHAM DAM TRIAL BANK

HYDRAULIC FRACTURE TESTS

FALLING HEAD STAGES

PIEZOMETER P4B-CH537

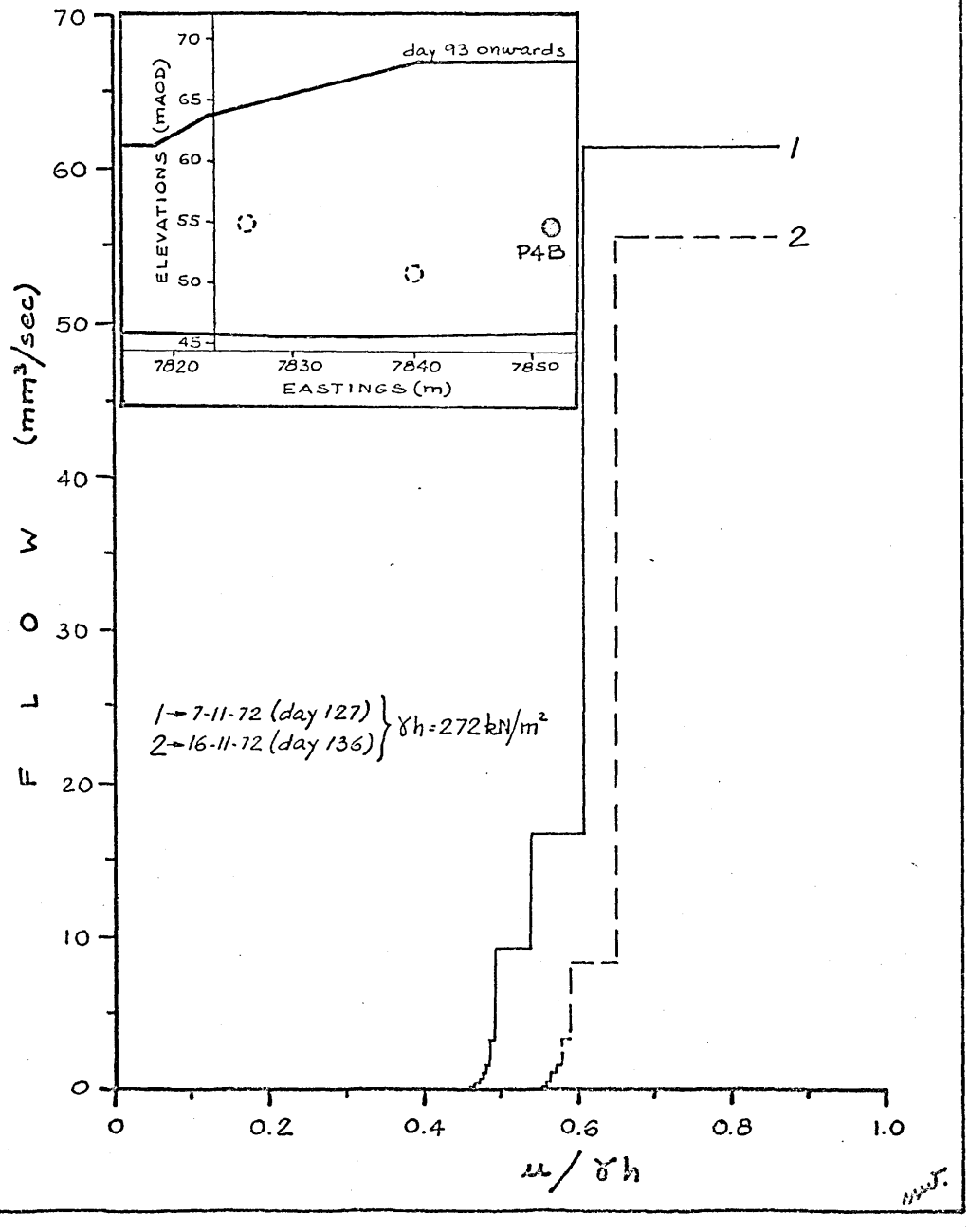


FIG. 8.6

EMPINGHAM DAM TRIAL BANK

PERMEABILITIES MEASURED AT HYDRAULIC FRACTURE TESTS

CH 537

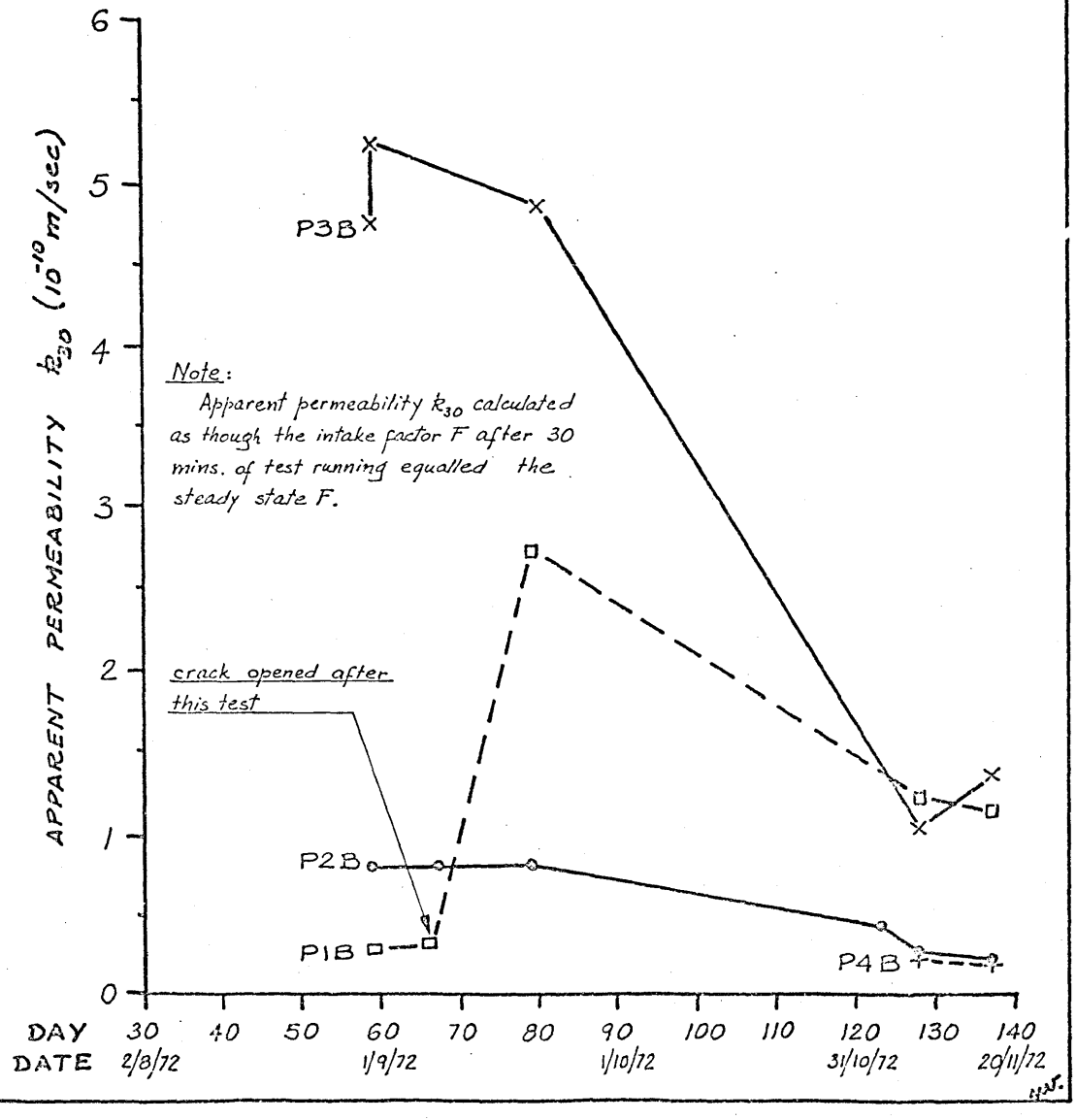


FIG. 8.7